

**Mechanistic Studies on Phosphoric Acid Catalyzed Acetalizations and
Development of Acetal-Containing Ligands for Transition Metal Catalysis**

by

Alonso J. Argüelles

A dissertation submitted in partial fulfillment
of the requirements for the degree of
Doctor of Philosophy
(Chemistry)
in the University of Michigan
2019

Doctoral Committee:

Associate Professor Pavel Nagorny, Co-Chair
Associate Professor Paul Zimmerman, Co-Chair
Associate Professor Jolanta Grembecka
Professor John Montgomery

Alonso J. Argüelles

ajarguel@umich.edu

ORCID iD: 0000-0003-4291-0187

© Alonso J. Argüelles 2019

DEDICATION

I dedicate this work to my little angel, Isabella, whose liveliness fills me with everlasting joy.

ACKNOWLEDGMENTS

I can only take a fraction of the credit for the work described herein. It would not have been possible if not for the valuable interactions that I had throughout these past years. First and foremost, I would like to express my deepest gratitude to my advisors, Dr. Pavel Nagorny and Dr. Paul Zimmerman. Dr. Nagorny has been a true mentor to me, and I am honored to have been part of his group at the University of Michigan. I will greatly miss his perfect combination of openness, exhaustive chemical knowledge, and sincere advice that made me the independent researcher that I am now. I am also extremely grateful to Dr. Paul Zimmerman for his generous and opportune advice when I most needed it. His patience and kindness helped me weather many storms I suffered throughout my graduate studies. I am thankful to both my advisors for allowing me to partake in a successful and enjoyable co-mentored program with no major administrative and scientific hardships. In addition, I would like to extend my gratitude to National Science Foundation CAREER Award (CHE-1350060), National Institute of Health (grants R01GM111476 and U01GM1252740), PPG, Pfizer, and Rackham for their financially supporting my investigations.

I would also like to acknowledge and thank my dissertation committee members, Dr. John Montgomery and Dr. Jolanta Grembecka for their support throughout my graduate studies. I am especially grateful of Dr. Montgomery for his thoughtful comments and insights in my carbohydrate-related projects.

I am indebted with my undergraduate advisor, Dr. Helena Maruenda, for giving me a strong background in organic chemistry and safe laboratory techniques. Your passion for chemistry

inspired me to follow graduate school, and I fear that without your guidance and support I would not be in the position I am today.

I am thoroughly grateful for meeting and befriending so many talented chemists and good friends in the Nagorny and Zimmerman groups. I want to acknowledge my current and former lab mates Dr. Grace Winschel, Dr. Nathan Cichowicz, Dr. Yaroslav Khomutnyk, Dr. Hem Khatri, Dr. Tay Rosenthal, Dr. Bijay Bhattarai, Dr. Jeonghyo Lee, Nicolas Diaz, Zachary Fejedelem, Rami Hourani and Dr. Andrew Vitek for their friendship and scientific advice. I am especially grateful to Brenna Budaitis, Siyuan Sun, Sibin Wang, and Shu Chang for allowing me the privilege of being their mentor, an experience from which I learned immeasurably. I am truly thankful for their sympathy and patience.

I have been truly blessed to have forged strong and invaluable friendships with Michael Robo, Grayson Ritch, and Aaron Proctor. You made my stay in Ann Arbor a true pleasure, and I will miss you greatly. Your constant support and our exciting gatherings helped me stay motivated and sane throughout graduate school.

I want to thank Ebony for her love and support during these last years. Thank you for giving me the best gift of them all, the miracle of life, in Isabella., to whom this thesis is dedicated. I am also grateful to my Ebony's mother, Valerie, for constantly taking care of Bella.

I want to acknowledge and thank the strongest pillar of support in my life, my family. I wish to thank my godmother Anita, my godfather Tomas, and my grandfather Rolando for their love and guidance. I am forever in debt with my parents, Carlos and Sarisa, for the infinite support and unconditional love; and with my brothers, Carlitos and Sebas, for their unwavering kindness and dedication. My love for you knows no bounds, and you will be forever in my heart.

TABLE OF CONTENTS

DEDICATION	ii
ACKNOWLEDGMENTS	iii
LIST OF TABLES	ix
LIST OF FIGURES	xiii
LIST OF SCHEMES	xvii
LIST OF APPENDICES	xxii
LIST OF ABBREVIATIONS	xxiii
ABSTRACT	xxvi
CHAPTER	
1. Introduction	1
1.1 Introduction to transition state theory	1
1.2 Introduction to mechanistic studies: experimental methods	5
1.3 Computational methods in mechanistic studies	11
1.4 Introduction to organocatalysis	14

1.5 Asymmetric organocatalysis	17
1.6 Brønsted acid catalysis and hydrogen-bond catalysis	21
1.7 References	24
2. Direct Interconversion of BINOL and H8-BINOL-Based Chiral Brønsted Acids Using Single-Step Red/Ox Manipulations	28
2.1 Introduction to chiral phosphoric acid catalysis	28
2.2 Results and discussion	36
2.3 References	42
3. Studies on the Mechanism of Phosphoric Acid-Catalyzed Spiroketalizations	44
3.1 Introduction to spiroketals	44
3.2 Introduction to the anomeric effect and conformational aspects of spiroketals	47
3.3 Prior art on spiroketal synthesis	50
3.4 Results and discussion	56
3.5 References	85
4. Design, Synthesis, and Application of Chiral Spiroketal-Containing Ligands	89
4.1 Introduction to asymmetric transition metal catalysis	89

4.2 Results and discussion	95
4.3 References	104
5. Studies on the Mechanism of Phosphoric Acid-Catalyzed Glycosylation of Complex Polyols	107
5.1 Introduction to chemical glycosylation	107
5.2 Mechanism of the CPA-Catalyzed Regiodivergent Glycosylation of 6-deoxy-Erythronolide B	113
5.3 Mechanism of the CPA-Catalyzed Regioselective Acetalization of Sugar-Derived Diols	129
5.4 Mechanism of the CPA-Catalyzed Regio- and Stereoselective Glycosylation of Sugar-Derived Diols	140
5.3 References	155
6. Practical Solid-Phase Glycosylation Using Immobilized Sugar Phosphonates	160
6.1 Introduction	160
6.2 Results and discussion	161
6.3 References	176
7. Studies on the Mechanism of Phosphoric Acid-Catalyzed Epoxide Ring Opening	177
7.1 Introduction	177

7.2 Results and discussion	181
7.3 References	191
8. Closing Remarks	193
APPENDICES	196

LIST OF TABLES

TABLE

1.1.	Relation between reaction rate and E_a for the rotation around the red bond.	4
2.1.	Initial condition screening for the direct partial reduction of a BINOL-derived CPA.	37
2.2.	Substrate scope for the partial hydrogenation of BINOL-derived CPAs.	38
2.3.	Screening of oxidation conditions for the dehydrogenation of H8-BINOL-derived CPAs.	41
3.1.	Initial evaluation of the CPA-catalyzed enantioselective spiroketalization.	58
3.2.	Substrate scope for the CPA-catalyzed enantioselective spiroketalizations.	60
3.3.	Substrate scope for the CPA-catalyzed diastereoselective spiroketalization.	62
3.4.	Intermolecular acetalization with deuterated electrophile.	68
4.1.	Application of SPIRAP, SPIRAP(O), and SPIRAPO in Ir-, Pd- and Rh-catalyzed asymmetric transformations.	101
4.2.	Comparison of 3D structures of SPIRAP diastereomers and SDP.	103

5.1.	Optimization of CPA-catalyzed glycosylation of 6-dEBa.	117
5.2.	Regiodivergent glycosylation of 6-dEB and oleandomycin derivative 5-7 .	124
5.3.	Regioselective acetalization of sugar-based diols.	130
5.4.	C-3 selective acetalization of diols using CPAs.	131
5.5.	Dependence of selectivity on reaction temperature for the (R)-5-4a-catalyzed acetalization of 5-16a .	138
5.6.	CPA-catalyzed glycosylation of diol 5-16a with benzyl protected trichloroacetimidate donor 5-24 .	142
5.7.	CPA-catalyzed glycosylation of diol 5-16b with trichloroacetimidate glycosyl donors.	144
6.1.	Initial promoter screening for the glycosylation of phosphonates.	169
6.2.	Initial promoter screening for the glycosylation of phosphonates.	170
6.3.	Effect of the counterion in the Fe(III) catalyzed glycosylation of phosphonates.	171
6.4.	Evaluation of solvents for the solid-phase glycosylation of phosphonates with menthol.	173
7.1.	Initial control experiments on the intramolecular ERO of 7-1 .	182
7.2.	Catalyst screening for the optimization of endo-selective conditions.	183
7.3.	Catalyst screening for the optimization of exo-selective conditions.	184

B.1.	Calculated values for starting geometries, intermediates, and transition states for the concerted pathway for the [6,6]-spiroketalization catalyzed by DPPA.	204
B.2.	Calculated values for starting geometries, intermediates, and transition states phosphate-mediated pathway for the [6,6]-spiroketalization catalyzed by DPPA.	211
B.3.	Calculated values for starting geometries, intermediates, and transition states phosphate-mediated pathway for the [6,5]-spiroketalization catalyzed by DPPA.	222
B.4.	Calculated values for starting geometries, intermediates, and transition states concerted pathway for the [6,6]-spiroketalization catalyzed by 3-13 .	230
C.1.	Calculated energy values for the described geometries.	300
C.2.	Geometrical parameters for SPIRAP Pd-complexes.	300
C.3.	Crystal data and structure refinement for aa1711	301
C.4.	Crystal data and structure refinement for aa2393	302
D.1.	Calculated energy values for the described geometries.	319
E.1.	Calculated energy values for the BPA-catalyzed acetalization of diols.	330
E.2.	Calculated energy values geometries reoptimized without dispersion corrections.	331
F.1.	Calculated energy values for the BPA-catalyzed acetalization of diols.	348

H.1. Calculated energy values of relevant geometries for the intramolecular
ERO of **7-6**.

367

LIST OF FIGURES

FIGURE

1.1.	Hypothetical reaction of A and B.	2
1.2.	Hypothetical multi-step reaction.	3
1.3.	Hypothetical selective reaction under kinetic control.	4
1.4.	Origin of the KIE.	9
1.5.	Simplified process flow for GSM.	14
1.6.	Role of a catalyst in the kinetics of a reaction.	15
2.1.	Additional substrates for the partial hydrogenation of BINOL-derived CPAs.	40
2.2.	Additional substrates for the oxidation of H8-BINOL-derived CPAs.	41
3.1.	Spiroketal are common amongst insect pheromones.	45
3.2.	Structure of (+)-spongistatin 1.	46
3.3.	Structure of ivermectin and tofogliflozin, spiroketal-containing drugs.	47
3.4.	Geminal dialkoxyalkanes are more stable than their non-acetal diether isomers.	47

3.5.	Structure of pectenotoxin 2.	49
3.6.	Hammett studies for the phosphoric acid-catalyzed spiroketalizations of enol ether of hydroxy enol ethers.	71
3.7.	Concerted asynchronous mechanism for the ring closure of the model system.	75
3.8.	Anomeric phosphate mechanism for the model system.	76
3.9.	Molecular dynamics on the TS of the concerted pathway for the model system.	78
3.10.	Comparison of the activation barriers for the (<i>R</i>)- and (<i>S</i>)- 3-13a -catalyzed spiroketalizations.	81
3.11.	Comparison of TS _{<i>S</i>} and TS _{<i>R</i>} .	82
3.12.	Key steric interactions at TS _{<i>R</i>} between the phenyl groups on the alcohol appendage of the enol ether and the ortho and para substituents of the aryl substituents of (<i>R</i>)- 3-13 .	83
4.1.	Interactions between tertiary phosphines and metal centers.	91
4.2.	Spiroketal-based analogs of SPINOL.	94
4.3.	A. Acetal and spiroketal-containing commercial phosphine ligands. B. Pseudoenantiomeric SPIROL-based ligands.	96
4.4.	Comparison of (<i>R,S,S</i>)-SPIRAP, (<i>S,S,S</i>)-SPIRAP, and SDP complexes of PdCl ₂ .	103

5.1.	Selection of sugar-containing natural products.	108
5.2.	Regioselective glycosylation of 6-dEB.	115
5.3.	Theoretical studies on the mechanism of phosphoric acid-catalyzed glycosylations.	125
5.4.	Preparation and characterization of the covalently linked phosphate intermediates 5-10 and 5-12 .	128
5.5.	Energy diagram for the CPA-catalyzed intermolecular acetalization of 6-deoxyglucose-derived 2,3-diols.	134
5.6.	Comparison of $\text{TSC}_{\text{C-2}}$ and $\text{TSC}_{\text{C-3}}$	139
5.7.	Formation of glycosyl phosphates from donor α-5-24 .	147
5.8.	Stereochemical assignment of glycosyl phosphates using ^{13}C (H-coupled) NMR	148
5.9.	Phosphate formation in CD_2Cl_2 with different acids.	149
5.10.	Energy diagram for the CPA-catalyzed intermolecular glycosylation of 6-deoxyglucose-derived 2,3-diols.	151
5.11.	Quadrant-based perspective of TSC_2 .	154
6.1.	Hypothesis for the glycosylation of immobilized sugar phosphonates.	162
6.2.	Reaction of phosphonic acid 6-18 with varying equivalents of donor 6-4 .	168
7.1.	Examples of complex structures containing epoxides.	177

7.2.	Ring strain in epoxides.	178
7.3.	Energy diagram for the intramolecular ERO of a truncated mupirocin model.	187
7.4.	Quadrant-based perspective for key TSs.	189
B.1.	Energy diagram for the [6,5]-spiroketalization.	221
D.1.	Energy diagram for the CPA-catalyzed glycosylation of 1,3-diols.	318
E.1.	Energy diagram for the CPA-catalyzed intermolecular acetalization of 6-deoxyglucose-derived 2,3-diols.	329
F.1.	Energy diagram for the CPA-catalyzed intermolecular glycosylation of 6-deoxyglucose-derived 2,3-diols.	347
H.1.	Energy diagram for the intramolecular ERO of a truncated mupirocin model.	367

LIST OF SCHEMES

SCHEME

1.1.	Reference reaction for the Hammett equation.	7
1.2.	Role of isotopic labelling in the discovery of benzyne.	8
1.3.	Examples of normal and inverse α SKIE.	11
1.4.	Two of the earliest examples of organocatalysis.	15
1.5.	Emil Fischer's diastereoselective homologation of glucose.	17
1.6.	Early examples of asymmetric organocatalysis.	20
1.7.	Point chirality and axial chirality.	20
1.8.	A Friedel Crafts acylation.	21
1.9.	Comparison of asymmetric Lewis acid catalysis and hydrogen bond catalysis.	22
1.10.	Specific and general acid catalysis.	23
2.1.	Alkene hydration investigated by Cornforth and coworkers.	29
2.2.	General structure of Cornforth's phosphinic acids.	30

2.3.	BINOL as a chiral auxiliary.	30
2.4.	Noyori's asymmetric hydrogenation of ketones.	31
2.5.	Akiyama's asymmetric Mannich-type reaction.	32
2.6.	Terada's asymmetric Mannich-type reaction.	32
2.7.	Effect of the chiral backbone on the acidity of CPAs.	34
2.8.	Ding's enantioselective Baeyer-Villiger reaction of cyclobutanones.	34
2.9.	Standard synthesis of BINOL and H8-BINOL derived CPAs.	35
2.10.	Direct interconversion of BINOL and H8-BINOL-derived CPAs via single step Red/Ox manipulations.	36
3.1.	Orbital alignment in [6,6] spiroketals allows stabilization by the anomeric effect.	49
3.2.	Spiroketal synthesis by acid-catalyzed dehydration.	50
3.3.	Effect of 1,3-diaxial interactions in the relative stability of spiroketal configurations.	51
3.4.	Examples of thermodynamic acid-catalyzed strategies for nonanomeric spiroketals.	52
3.5.	Deslongchamps's acid-catalyzed spiroketalizations under kinetic control.	53
3.6.	Rychnovsky's reductive spiroketalizations under kinetic control.	54
3.7.	Nagorny's CPA-catalyzed spiroketalizations under kinetic control.	55

3.8.	Catalyst control in spiroketalizations of dihydroxyketones.	57
3.9.	Potential mechanisms of CPA-catalyzed spiroketalizations	66
3.10.	Diastereoselective spiroketalization of deuterium-labeled substrates.	67
3.11.	KIE determination for 3-26 .	67
3.12.	Intermolecular acetalization with deuterated nucleophile.	69
4.1.	Early examples of phosphine ligands used in hydrogenations.	92
4.2.	a. Knowles's asymmetric synthesis of L-DOPA. b. Noyori's asymmetric hydrogenation of ketones.	93
4.3.	C ₂ symmetry is a common feature in privileged structures.	94
4.4.	Highly diastereoselective spiroketalization of benzylic alcohols 4-2 .	97
4.5.	Diol equilibration and chemical resolution of diastereomeric ditriflates.	98
4.6.	Functionalization of scaffold 4-9 into various ligands.	99
5.1.	Simplified biosynthesis of glycogen.	109
5.2.	Examples of regioselective functionalization of polyols.	111
5.3.	Examples of site-selective glycosylation of polyols.	111
5.4.	Debenzylation of 2. .	118
5.5.	Single-pot traceless protection/glycosylation of the C11-position of 6-dEB.	120
5.6.	Glycosylation with anomeric phosphates.	127

5.7.	CPA-controlled acetalizations developed by the Nagorny group.	129
5.8.	One-pot functionalization of diol 5-16a.	132
5.9.	Mechanistic precedents on phosphoric acid-catalyzed intermolecular acetalizations.	133
5.10.	Deuterium labeling studies on the phosphoric acid-catalyzed intermolecular acetalization of alcohols.	136
5.11.	CPA-catalyzed regio- and stereoselective glycosylation of sugar-derived diol 5-16 .	140
5.12.	S_N2 vs. S_Ni mechanism for the phosphoric acid-catalyzed acetalization of alcohols.	150
5.13.	S_Ni mechanism for the glycosylation of sugar-derived 2,3-diols.	153
6.1.	Merrifield solid-phase peptide synthesis method.	161
6.2.	Retrosynthesis of solid-supported phosphonic acid 6-1 .	163
6.3.	a. Synthesis of phosphonic acid-functionalized resin. b. Replication of the solid-phase route synthetic route in solution and determination of the stereochemistry of glycosyl phosphonate 6-9 .	164
6.4.	a. Preparation of phosphonic diacid-functionalized resin. b. Formation of resin bound glycosyl phosphonate.	166
6.5.	Unsuccessful attempt at the TMSOTf-catalyzed glycosylation with resin-bound peracetylated phosphonates.	167

6.6.	Glycosylation of limiting acceptor with 6-11 .	173
6.7.	Proposed mechanism for the FeCl ₃ -catalyzed glycosylation of alcohols with immobilized phosphonates 6-11 .	174
7.1.	Intramolecular ERO leading to endo- or exo-product formation.	179
7.2.	Examples of substrate control strategies in endo-selective intramolecular EROs.	180
7.3.	CPA-catalyzed enantioselective intermolecular ERO.	181
7.4.	Endo and exo concerted cyclizations.	188

LIST OF APPENDICES

APPENDIX

A.	Experimental Information for Chapter 2	196
B.	Experimental Information for Chapter 3	201
C.	Experimental Information for Chapter 4	244
D.	Experimental Information for Chapter 5, Section 5.2	315
E.	Experimental Information for Chapter 5, Section 5.3	327
F.	Experimental Information for Chapter 5, Section 5.4	345
G.	Experimental Information for Chapter 6	357
H.	Experimental Information for Chapter 7	365

LIST OF ABBREVIATIONS

6-dEB	6-deoxy-erythronolide B
Å	angstrom
Ac	acetyl
Acac	acetylacetone
Ad	adamantyl
Aq	aqueous
Ar	aryl
atm	atmosphere (unit)
BINOL	1,1'-bi-2-naphthol
Bn	benzyl
Boc	tert-butyloxycarbonyl
BOM	benzyloxymethyl
Br	broad
BRSM	based on recovered starting material
Bu	butyl
Bz	benzoyl
Calcd	calculated
COSY	correlation spectroscopy
CPA	chiral phosphoric acid
CSA	camphorsulfonic acid
Cy	cyclohexyl
d	days
DBNE	N,N-Dibutylnorephedrine
DBU	1,8-diazabicyclo[5.4.0]undec-7-ene
DCM	dichloromethane
DCE	1,2-dichloroethane
DDQ	2,3-Dichloro-5,6-dicyano-1,4-benzoquinone
DFT	Density Functional Theory
dibm	diisobutyrylmethane

DMAP	4-dimethylaminopyridine
DMF	dimethylformamide
DPPA	diphenylphosphoric acid
dr	diastereomeric ratio
ee	enantiomeric excess
equiv	equivalent
ESI-MS	electrospray ionization mass spectrometry
Et	ethyl
EtOAc	ethyl acetate
FDA	Food and Drug Administration
GSM	growing string method
h	hours
hex	hexanes
HMBC	heteronuclear multiple bond correlation
HOMO	highest occupied molecular orbital
HPLC	high-performance liquid chromatography
HRMS	high resolution mass spectrometry
HSQC	heteronuclear single quantum correlation
Hz	hertz
<i>i</i> Pr	isopropyl
IR	infrared
<i>J</i>	coupling constant
k_{obs}	observed rate
kcal	kilocalorie
LUMO	lowest unoccupied molecular orbital
M	molar
Me	Methyl
mg	milligrams
min	minutes
mL	milliliters
mmol	millimoles
MS	mass spectrometry
MS	molecular sieves
MW	molecular weight
NIH	National Institute of Health
NMR	nuclear magnetic resonance

NOE	nuclear Overhauser effect
NOESY	nuclear Overhauser effect spectroscopy
o/n	overnight
PG	protecting group
Ph	Phenyl
PhMe	Toluene
ppm	parts per million
R	alkyl group (generic)
R ²	coefficient of determination
rac	racemic
Rf	retention factor
RDS	rate determining step
RP-HPLC	reverse phase high-performance liquid chromatography
r.r.	regioisomeric ratio
rt	room temperature
SeIEXSIDE	¹³ C band-selective excitation-sculptured indirect-detection experiment
S _N 1	unimolecular nucleophilic substitution
S _N 2	bimolecular nucleophilic substitution
SPINOL	1,1'-spirobiindane-7,7'-diol
SPOS	solid-phase organic synthesis
t	time
T	temperature
TBDPS	<i>tert</i> -butyldiphenylsilyl
TBS	<i>tert</i> -butyldimethylsilyl
TMSOTf	trimethylsilyl trifluoromethanesulfonate
TBSOTf	<i>tert</i> -butyldimethylsilyl trifluoromethanesulfonate
Ts	<i>p</i> -toluenesulfonyl
TS	transition state
Tf	trifluoromethanesulfonyl
TFA	trifluoroacetic acid
THF	tetrahydrofuran
TLC	thin layer chromatography
TMS	trimethylsilyl
UV	ultraviolet
σ	sigma – Hammett constant
ρ	rho – slope of Hammett plot

ABSTRACT

The field of organic chemistry has evolved exponentially over the last decades. The development of catalysis has played an enormous role in this by allowing access to previously unthinkable targets, controlling the selectivity of challenging reactions, and improving on reaction greenness and efficiency. We often look up to Nature for inspiration on efficient and selective catalysis, but while Nature has found means to regio- and stereoselectively install acetals in complex molecules, finding nonbiological catalyst-controlled alternatives has been challenging. Given that acetals play a fundamental role in numerous natural and man-made products, such as key biological functions in glycosides, new stereoselective reactions to access these is highly desirable. Described herein is the development and mechanistic elucidation of phosphoric acid catalyzed regio- and stereoselective methods for the installation of spiroketals and glycosidic linkages. Inspired by our results on spiroketalizations strategies, we also designed and synthesized novel C₂-symmetric spiroketal-containing ligands for asymmetric transition metal catalysis. Finally, based on mechanistic insights into the phosphoric acid-catalyzed glycosylation, we were able to develop a practical solid-phase glycosylation methodology using solid-supported sugar phosphonates.

Chapter 1 is an introduction to transition state theory and an overview of experimental and computational ways to assess the reaction mechanism. Then, an introduction to organocatalysis is given. This chapter serves to lay a foundation for the mechanistic studies described in the context of organocatalysis for Chapters 3, 5, and 7.

Chapter 2 details our efforts in the development of a practical interconversion of BINOL and H8-BINOL through a single-step Red/Ox manipulation. This chapter also gives an introduction to BIINOL-derived chiral phosphoric acids, which were crucial in the works described later in chapters.

Chapter 3 describes our efforts towards the development of a powerful stereoselective spiroketalization method catalyzed by chiral phosphoric acids. This chapter also describes our work towards the mechanistic elucidation of this reaction using experimental techniques, state-of-the-art quantum chemical reaction path finding tools, and molecular dynamics simulations.

Chapter 4 builds on our acquired knowledge of spiroketal reactivity in Chapter 3 to describe the development of novel acetal-containing C_2 -symmetric ligands for asymmetric transition metal catalysis. Our invention proved to be a very powerful tool in asymmetric catalysis, providing excellent enantiocontrol in a variety of unrelated transition metal-catalyzed reactions.

Chapter 5 describes the application of chiral phosphoric acids to control the regio- and stereoselectivity of intermolecular glycosylations and acetalizations of polyols. The mechanism of these reactions was investigated in depth using spectroscopic and computational techniques.

Chapter 6 encloses research on the development of a novel solid-phase glycosylation method that is based on the mechanistic conclusions drawn out in Chapter 5. The synthesis and characterization of a polystyrene-based resin functionalized with phosphonic acid moieties is described, as well as its application in the formation of solid-supported sugar phosphonates and their subsequent glycosylation with secondary alcohols.

Chapter 7 discloses the application of phosphoric acids as catalysts for the regioselective opening of epoxides. Computational work on the mechanistic elucidation of this reaction is described.

CHAPTER 1

Introduction

“Only those who will risk going too far can possibly find out how far one can go”

T. S. Eliot

1.1 Introduction to transition state theory

Organic chemists use of vast range of reaction conditions when developing, optimizing, and performing different kinds of reactions. Some situations require heating up the reaction to the boiling point of solvent, while in others extreme cooling is appropriate. In many instances, a wide variety of solvents with different properties like dielectric constant, hydrogen bond donor/acceptor capabilities, boiling point, etc. are screened to create a set of circumstances that favor the formation of a desired product with high selectivity in comparison to potential side reactions. The field of reaction kinetics in physical organic chemistry has been developed over the last century to answer how can reaction conditions be chosen in order to favor a particular kind of reactivity.^[1]

While thermodynamics expresses the relative stability of compounds along a reaction pathway, reaction kinetics gives us a quantitative description of chemical reactivity. For a hypothetical reaction where A and B are turned into C and D (Figure 1.1), the fundamental thermodynamic equation that relates the equilibrium constant of the reaction (K) to the Gibbs free energy change of product formation (ΔG) is given in Equation 1.1.^[2]

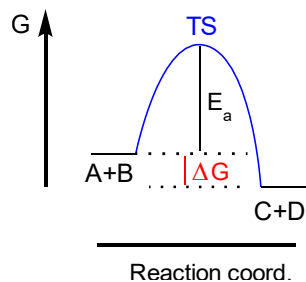


Figure 1.1. Hypothetical reaction of A and B.

Equation 1.1. Fundamental thermodynamic equation.

$$\Delta G = -RT \ln(K)$$

ΔG is the reaction free energy, R is the gas constant, T is the temperature, and K is the equilibrium constant: $K = \frac{[C][D]}{[A][B]}$.

By assuming that an equilibrium exists between reactants and activated complexes, transition state theory (TST) was able to establish a quantitative relationship between the rate constant of an elementary reaction and the difference in free energy between reactants and activated complexes, also known as the energy of activation. This fundamental theory was independently developed by Eyring as well as Evans and Polanyi in 1935,^[3,4] and quickly emerged to become one of the most influential conceptual frameworks in physical organic chemistry.^[5-8] The most common form for the relation between rate constant and the activation barrier is known as the Eyring equation and is depicted in Equation 1.2.

Equation 1.2. Eyring's equation.

$$k = \frac{k_B T}{h} e^{\frac{\Delta G^\ddagger}{RT}}$$

k is the reaction rate constant, k_b is Boltzmann's constant, h is Planck's constant, T is the temperature, R is the gas constant, and ΔG^\ddagger , also represented as E_a is the free energy of activation of the reaction.

Transition state theory offers a powerful solution for the evaluation of reaction kinetics by considering the free energy of transition states and low energy reactants and intermediates. However, the Eyring equation only applies to an elementary reaction, in which reactants form a new species in a single reaction step containing a sole transition state. For this reason, knowledge of the reaction mechanism, or the step-by-step sequence of elementary reactions which comprise the overall transformation, is essential to understand which steps are important in the kinetics of a multistep sequence, and which transition states one should focus on for further reaction optimization. For example, in the hypothetical reaction where A turns into C depicted in Figure 1.2, it is the transformation of B to C which defines the overall reaction rate. This kinetically crucial step is called the rate determining step (RDS). In thinking about optimizing this reaction, one could focus on lowering the energy of TS_2 (transition state effect) or increasing the energy of B (ground state effect) to accelerate the reaction.^[9]

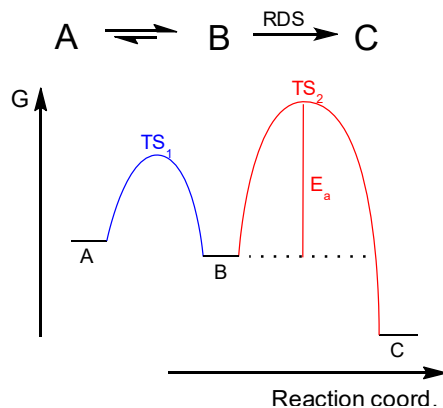


Figure 1.2. Hypothetical multi-step reaction.

Transition state theory is especially useful to understand reaction selectivity. That is, the selection of one reaction pathway over several other competing reactions. Minute amounts of energy are required to achieve almost complete selectivity. In Figure 1.3, $\Delta\Delta G^\ddagger$ need only be 2.8 kcal/mol to achieve 100:1 selectivity for B under standard conditions. As a reference, the strength of hydrogen bonds cover the range of 0.2 to 40 kcal/mol.^[10]

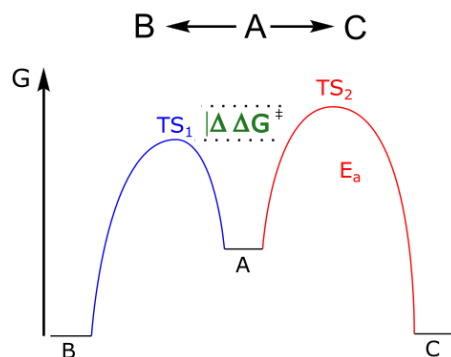


Figure 1.3. Hypothetical selective reaction under kinetic control.

Finally, transition state theory can give us an estimate on the time scale and feasibility of a reaction. Table 1.1 shows the relation between the energy of activation and the half time for different first-order reactions (rotation around the red bond). Due to the exponential nature of the relationship between k and E_a , reactions over 25 kcal/mol are considered very slow and practically unfeasible under standard conditions.

Table 1.1. Relation between reaction rate and E_a for the rotation around the red bond. Adapted from reference [1].

Compound	E_a (kcal/mol)	Approximate k at 298K (s^{-1})	$t_{1/2}$ at 298K
	2.9	5×10^{10}	0.02ns
	10.8	8×10^4	10 μ s
	16.7	3	0.2s
	25.8	7×10^{-7}	11 days
	43.0	2×10^{-19}	10^{11} years

1.2 Introduction to mechanistic studies: experimental methods

Because of the implications of reaction mechanisms in synthetic organic methodology, mechanistic studies of chemical reactions drive research and is a principal point of focus in organic chemistry pedagogy.^{[11],[12]} Fortunately, a multitude of tools have been developed over the past century to interrogate reaction space and clarify even perplexing reactions and results. Among the experimental tools, the main ones are the detection and identification of reaction intermediates, the experimental determination of activation parameters, the experimental determination of the empirical rate law through kinetic analysis, the investigation of linear free energy relationships, and isotopic labeling studies. While not always possible, isolating or identifying *in situ* an intermediate can indicate a reaction profile similar to that depicted in figure 1.3 and reveal additional insights on the reaction mechanism.^{[13],[14]}

By expanding ΔG^\ddagger , and rearranging equation 1.2, one can have:

Equation 1.3. The Eyring plot.

$$\ln\left(\frac{kh}{k_B T}\right) = -\left(\frac{\Delta H^\ddagger}{R}\right)\left(\frac{1}{T}\right) + \frac{\Delta S^\ddagger}{R}$$

ΔH^\ddagger and ΔS^\ddagger , are the enthalpy and entropy of activation.

By performing reactions at different temperatures and then plotting $\ln\left(\frac{kh}{k_B T}\right)$ against $\left(\frac{1}{T}\right)$, one obtains a line where the slope is $-\left(\frac{\Delta H^\ddagger}{R}\right)$ and the intercept is $\frac{\Delta S^\ddagger}{R}$. This type of correlation is called an Eyring plot. Knowing ΔH^\ddagger and ΔS^\ddagger is extremely advantageous in understanding the mechanism involved. For example, a clear break in an Eyring plot strongly suggests a temperature dependent change in the mechanism of the reaction.^[15]

The experimental identification of the empirical rate law can be done through classical kinetic analysis^[15] or more modern and data-driven techniques such as reaction progress kinetic analysis.^[16] This gives invaluable insights on the reaction mechanism. An obvious piece of information obtained from these experiments is the actual rate of the reaction. In addition, only reaction steps that occur before and at the rate determining step are detected in these kinetic studies, so one can make informed inferences about the molecularity and order of events in the mechanism.

Structural information regarding the activated complex can be extracted from a set of similar experiments where one of the reactant's substituents is judiciously modified. By probing the effect of substituent groups on the reactivity, structure-reactivity relationships can be found. Many of these can be expressed quantitatively in ways that allow for both insights on the transition state structure and predictive chemical behavior. The most widely used relationships are the linear free energy relationships, which correlate the energy of activation with a physical parameter that varies depending on the substituent used.^[17] Of these, the Hammett equation is perhaps the most used and well-studied, and is particularly useful in investigating the electronic changes induced by substituents:

Equation 1.4. The Hammett equation.

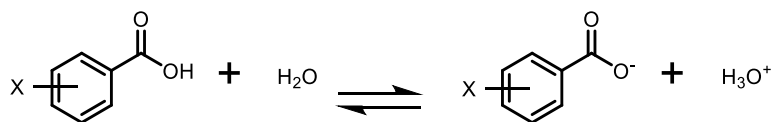
$$\log \left(\frac{K_X}{K_H} \right) = \rho \sigma_X$$

K_X and K_H are the equilibrium constants when the substituent is X or H, respectively, σ_X is the empirical electronic substituent parameter, obtained when calculating $\log \left(\frac{K_X}{K_H} \right)$ for the ionization of substituted benzoic acids in water (Scheme 1.1), ρ is the slope obtained in the Hammett plot.

ρ is the slope obtained in the Hammett plot, and it indicates how the reaction in question compares to the ionization of benzoic acid in water. In other words, ρ reflects the sensitivity of the

reaction to substituents effects. When $\rho > 1$, there is significant build-up of negative charge in the reaction, when ρ is between 0 and 1, the reaction has a slight build-up of negative charge, when $\rho < 0$ there is build-up of positive charge, and when $\rho = 0$, the reaction shows no substituent effects. Other linear free energy relationships are formulated similarly and are just as useful. For example, the Evans-Polanyi equation correlates the reaction enthalpy and is commonly employed in the development of computational methods that can reliably compute reaction enthalpies;^[18] while the Taft equation is excellent at probing the effect of substituent sterics.^[19-21]

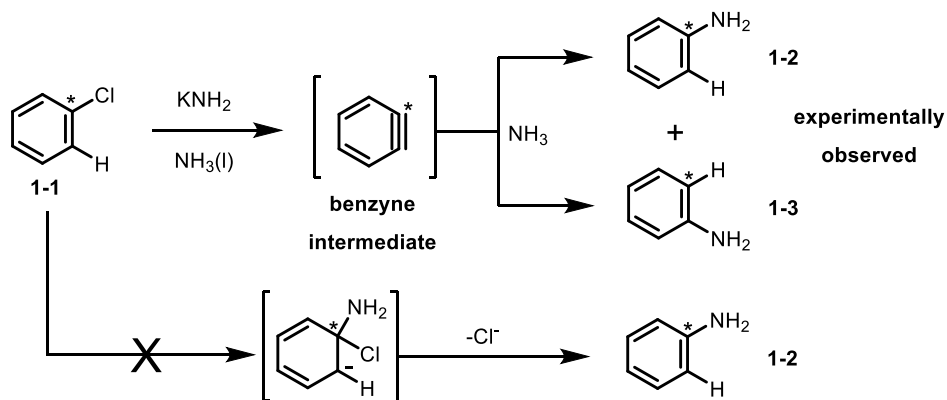
Scheme 1.1. Reference reaction for the Hammett equation.



Another important technique in mechanistic analysis is isotopic labeling. The reactant is labeled by substituting a specific atom by its isotope. This way, the atom can be tracked throughout its reaction. Upon analysis, the isotope can be detected through a variety of techniques including mass spectroscopy (MS), infrared spectroscopy (IR), nuclear magnetic resonance spectroscopy (NMR), among others. This is one of the most powerful ways of distinguishing pathways experimentally, although it has the major drawback that it requires the synthesis of isotopically enriched reactants. One of the most iconic applications of isotopic labeling was John D. Roberts work in the confirmation of the benzyne mechanism in the nucleophilic aromatic substitution of chlorobenzene with dialkyl amides.^[22] Treatment of C¹⁴-labelled chlorobenzene **1-1** with potassium amide in liquid ammonia led to the formation of **1-2** and **1-3** in equal amount, proving the involvement of a benzyne intermediate and discarding traditional mechanisms such as addition-elimination (Scheme 1.2). This had a tremendous impact in the scientific community and

led to the development of countless reactions that invoke a benzyne intermediate and the inclusion of this mechanism in basic organic chemistry textbooks.^[23]

Scheme 1.2. Role of isotopic labelling in the discovery of benzyne.



Another important technique in the experimental mechanistic studies arsenal that also relies in the judicious isotopic substitution of an atom is the kinetic isotope effect (KIE). Although, isotopic substitution does not affect the qualitative reactivity of a compound, it can often have a measurable effect in the reaction rate. KIE is formally defined as the ratio between the rate of the non labelled reactant and the isotopically substituted one, k_H and k_D , respectively, for a H/D substitution (equation 1.5). This technique offers complementary information to the other methods described above. For example, it can indicate which bonds are formed, broken, or rehybridized during the rate determining step. In addition, an advantage of KIEs is that many competent methods exist for their computation. The comparison between experimental and theoretical KIEs is often performed to understand, endorse, or reject a mechanism.^[24,25]

Equation 1.5. Definition of KIE.

$$KIE = \frac{k_H}{k_D}$$

Most KIEs result from the differences in zero-point energy (ZPE) of the reactants and TSs for the labelled and non-labelled systems, which dominates vibrational energy at room temperature (Figure 1.4).^[26]

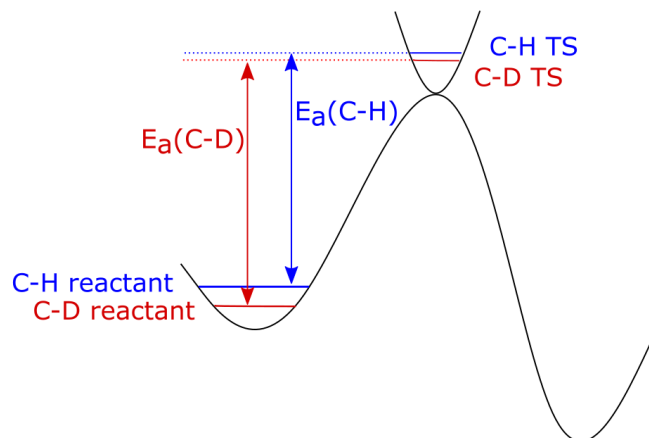


Figure 1.4. Origin of the KIE.

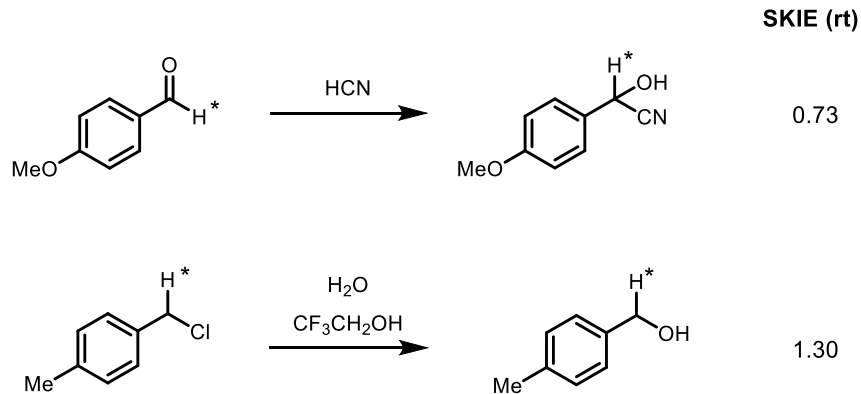
Primary KIEs occur when the rate determining step involves cleavage of isotopically substituted bond. Most KIE experiments consider the H/D substitution atom, since it produces the largest KIEs by a wide margin. This can be easily explained by considering that for a bond formation or bond breaking event, the stretching vibration of that bond is the reaction coordinate. The frequency of this vibrational mode can be modeled using the harmonic oscillator model, and one can promptly conclude that the stretching frequency is inversely proportional to the reduced mass (equation 1.6). For this reason, the H/D substitution offers the largest KIEs, with primary KIEs having theoretical maximum of about 7 at room temperature.^[27,28] In addition, the magnitude of the KIE can give a qualitative indication of how early or late the transition state is. For instance, as small primary KIE indicates that the C-D bond is only slightly weakened at the transition state.

Equation 1.6. Vibrational frequency of a harmonic oscillator. In this equation ν is the vibrational frequency, k_f is the force constant, and μ is the reduced mass.

$$\nu = \frac{1}{2\pi} \sqrt{\frac{k_f}{\mu}}$$

Secondary KIEs (SKIE) arise when bonds with isotopically labeled atom are not formed or cleaved at the rate determining step. They are usually in the range of 0.7-1.5 and are further classified as normal (>1) or inverse (<1), as well as by their position with respect to the bond formation event in the rate determining step (α , β , etc.). In α SKIEs, the isotopic substituted atom is directly connected to the atom involved in bond breaking or bond forming events at the rate determining step. The main use of α KIE is to identify rehybridizations at the TS. In effect, it has been crucial in distinguishing S_N1 and S_N2 mechanisms. This phenomenon arises from the large differences in the frequencies of the out of plane bending modes between sp^3 and sp^2 hybridized atoms, which translates to large differences in the ZPE of the C-H and C-D bonds. Normal α SKIE are expected when rehybridization from sp^3 to sp^2 occurs at the rate determining step, while inverse α SKIE are observed when the reaction involves a rehybridization from sp^2 to sp^3 occurs. The hydrocyanation of *p*-methoxybenzaldehyde^[29] and the hydrolysis of chlorotoluene^[30] shown in Scheme 1.3 are illustrative examples. β SKIE tend to be even smaller and are attributed to hyperconjugative effects.^[31]

Scheme 1.3. Examples of normal and inverse α SKIE.



Fortunately, with the emergence and development of density functional theory (DFT), a vast array of useful and powerful computational methods has been developed to study mechanisms over the past decades. Though there was initial skepticism, these methods have grown to become widely recognized as robust and reliable, and its application has become routine in contemporary synthetic methodology.^[32] A brief overview follows.

1.3 Computational methods in mechanistic studies

(Excerpts of this section were adapted from:

Dewyer, A. L.;* **Argüelles, A. J.**;* Zimmerman, P. M. Methods for exploring reaction space in molecular systems. *WIREs Comput Mol Sci* **2018**, 8:e1354. * equal contribution to this article.)

The area of reaction mechanism discovery simulation has taken considerable strides in recent years. Novel methods that make hypotheses for elementary steps and complementary means for reaction path and transition state (TS) optimization are lowering the amount of chemical intuition and user effort required to explore reaction networks. The resulting networks lead from reactants to reactive intermediates and products; and are becoming closer representations of

physical mechanisms involved in experiments. The powerful methods of this area are designed to locate intermediates, reaction paths, and TSs with as little guidance and effort from the researcher as possible.

First principles, or *ab initio*, simulations of reactant molecules and catalysts provide an important, central viewpoint on how computation can approach reactivity with little or no guidance from experiment.^[33–35] *Ab initio* simulations provide potential energy surfaces (PESs), a multidimensional surface which describes the energy of the system with respect to atomic coordinates. From these, free energy surfaces can be generated, which approximate the true reactive landscapes.^[36] All potential elementary steps may be located by exploring these landscapes, at least in principle. The high dimensionality (approximately $3N$, where N is the number of atoms in the system) of the surfaces, however, means that exhaustive exploration is usually impossible. Some form of search strategy, often coming from a low-dimensional re-envisioning of reaction paths, or chemical intuition, in combination with computationally economical methods, such as DFT, must be employed to locate intermediates and the TSs that connect them.

Locating a pathway for an envisioned reaction often employs local TS finders to optimize saddle points along the path.^[37] The TS structures can be guessed using intuition or approximated using various interpolation tools before optimization.^[38–42] Once a TS is found, intrinsic reaction coordinate (IRC)^[43,44] computations provide the reaction path connecting the TS to its neighboring intermediates. Largely, this method has relied on chemical intuition to designate the TSs that are of interest, as well as the intermediates that have to be found.^[45,46]

Because many of these steps may be costly or fail, constructing full reaction networks becomes hindered by difficulties in optimizing individual reaction paths. Streamlined approaches

for finding reaction paths directly from mechanistic hypotheses therefore have considerable advantages over prior elementary step analysis strategies. For instance, the Zimmerman group has developed methods that systematically generate and follow qualitative reaction coordinates to construct a reaction path, find the TS, and locate an intermediate in a single computation.^[47] In related work, Li and coworkers developed a method that utilizes bond forming and breaking processes to drive reaction exploration.^[48] Both of these methods are designed to find single elementary steps, which reduces the cost of reaction exploration.

Throughout my graduate work at the University of Michigan, I have made extensive use of the methods developed in the Zimmerman group for reaction path finding. Zimmerman and coworkers have developed a single-ended growing string method (GSM), which allows for reaction path searches starting from a single structure and either user-given or automatically generated reaction coordinates.^[47,49-51] The method is developed with user-friendliness as a high priority. Organic chemists can make full use of chemical intuition to accelerate the calculation of relevant pathways by introducing driving coordinates in internal coordinates (bond formation, bond cleavage, angles, and torsions). Briefly, the method works by the sequential addition of nodes distributed along coordinates that follow the driving coordinates from the starting structure. When a node is added, it is optimized in all dimensions except the driving coordinates. After a TS is detected in in reaction path, a two more nodes are added to reach the product. Following optimization of all nodes, an exact TS search is performed using the highest energy node. The created string should then be analyzed by the user. A simplified process flow diagram is depicted in Figure 1.5.

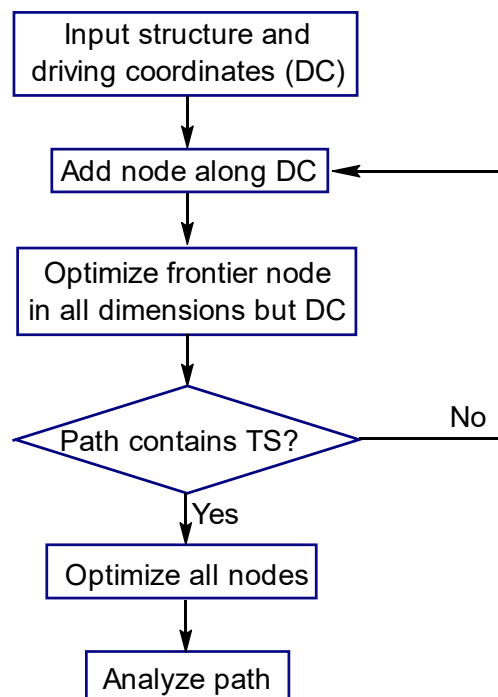


Figure 1.5. Simplified process flow for GSM. Adapted from reference [51].

1.4 Introduction to organocatalysis

Catalysis is an essential phenomenon in both Nature and manmade processes. It is broadly defined as the intervention of a compound that makes a reaction path available with a lower energy of activation (Figure 1.6). Catalysts do not alter the free energy of the reaction (the position of equilibrium, ΔG). However, by lowering of the activation barrier, they allow chemistry that would otherwise be unfeasible. Indeed, most biological reactions occur at rates that enable life thanks to powerful catalysts that Nature engineered. In addition, traditional industries like chemical, petroleum, agriculture, polymer, electronics, and pharmaceuticals depend heavily on efficient catalytic processes. In fact, approximately over 90% of the chemicals rely on catalytic reactions.^[52] Thus, the advancement of the field is of great interest.

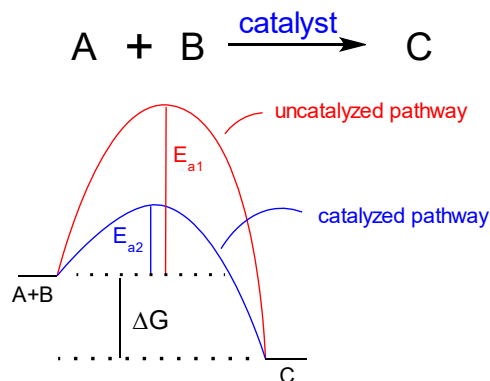
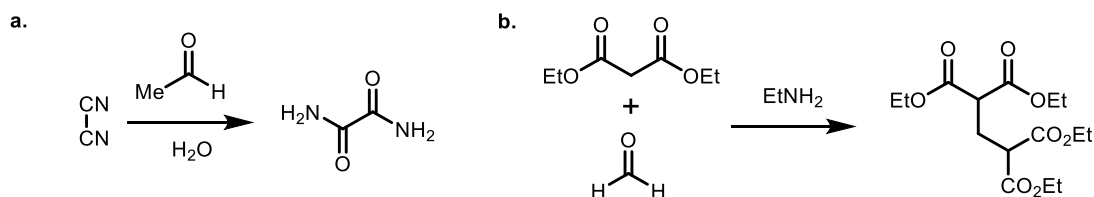


Figure 1.6. Role of a catalyst in the kinetics of a reaction.

Organocatalysis was defined by MacMillan in 2000 as the use of small organic molecules to catalyze organic transformations.^[53] Although this event was very important to the establishment of the field,^[54] the idea of using small organic molecules to activate reactants even in enantioselective fashion already had a long story.^[55] One of the earliest, if not the earliest, reported demonstration of a small organic molecule catalyzing a simple reaction can be attributed to Justus von Liebig, who in 1860 reported the use of aqueous acetaldehyde as a catalyst for the formation of oxamide from dicyan (Scheme 1.4a).^[56] Other sporadic examples of organocatalysis would follow, like Emil Knoevenagel's aldol condensation almost 40 years later, which employed catalytic amounts of an amine base (Scheme 1.4b).^[57]

Scheme 1.4. Two of the earliest examples of organocatalysis.



In 1900, Wilhelm Ostwald, formally classified catalysts somatic, inorganic, and organic catalysts.^[58] He was a German chemist mostly famous for the development of the Ostwald process, a catalytic process which produces nitric acid from ammonia. Later, he would be awarded the

Nobel Prize in chemistry in part for his work in catalysis. The nascent concept of organocatalysis was already recognized.

While other chemical examples of organocatalysis were reported over the last century, they were, in general, few and infrequent. It was not until the late 1990s that the field of organocatalysis blossomed thanks to the pioneering efforts of Yian Shi,^[59] Scott Denmark,^[60] and Dan Yang,^[61] who independently showed that chiral ketones could be used to catalyze the enantioselective epoxidation of simple alkenes. Other significant contributions by Eric Jacobsen,^[62] Elias J. Corey^[63] and Scott Miller^[64] would further captivate the attention of the scientific community and, after Barbas work on proline-catalyzed aldol reactions^[65] and MacMillan definition the term organocatalysis in 2000,^[53] the field rapidly developed into one of the main branches of enantioselective catalysis, alongside enzymatic catalysis and organometallic catalysis. By 2010, over one hundred discrete reactions involving different activation pathways and organic catalysts were published.^[54]

One of the main reasons for the quick growth of the organocatalysis field is that it provides several distinct advantages over other types of catalysis. The strongest fundamental advantages of organocatalysis are their ease of operation and low costs of the catalysts. In contrast to transition metal catalysis, no precious metals like rhodium, palladium, and iridium are required. In addition, these reactions are generally less susceptible to moisture and air, and the methods tend to be safer, as the required organocatalysts are typically non-toxic and environmentally friendly. On the other hand, it compares favorably to enzymatic catalysis in terms of scalability, catalytic scope, robustness, and operational simplicity.

Another advantage about organocatalysis is that it is versatile. Multiple activation modes have been studied and successfully applied, such as, enamine catalysis, iminium catalysis,

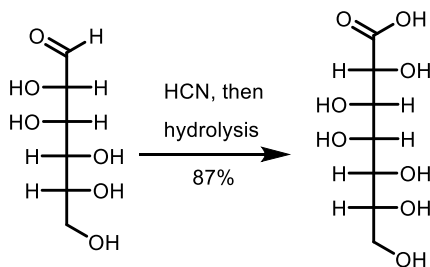
hydrogen-bonding catalysis, singly-occupied molecular orbital (SOMO) catalysis, and counterion catalysis.^[54] For this reason, identifying the mode of operation of the catalyst is often key for the successful reaction development, catalyst design, and optimization studies (see Section 1.3).

1.5 Asymmetric organocatalysis

Since the majority of key molecules in biological systems are chiral, most enantiomers of drugs have markedly different biological properties. Despite this, almost half of the drugs currently used are sold as racemates.^[66] This is in part driven by the difficulties on elaborating an enantioselective route to a drug and reflects the ever-increasing demand for methodologies that help access compounds in enantiopure form. Thus, methods for the enantioselective construction of chiral building blocks are highly desirable.

One can trace the origins of the discipline of stereoselective synthesis (not to be confused with stereoselective catalysis) to Emil Fischer's experiments in the late 1880s regarding the structural characterization of carbohydrates. He observed that addition of HCN to glucose, and subsequent hydrolysis, resulted in the formation of a single diastereomer (Scheme 1.5).

Scheme 1.5. Emil Fischer's diastereoselective homologation of glucose.



We now know that this diastereoselectivity is the result of substrate control. In fact, it may be the earliest example of acyclic substrate control in diastereoselective carbonyl addition

reactions.^[66] Substrate-controlled methods would become the state-of-the-art way of introducing stereocontrol in synthesis. Two techniques became predominant in stereoselective synthesis: 1) chiral pool or Chiron approach, which capitalizes on the use of chiral compounds or fragments as a starting materials; and 2) chiral auxiliary approach, in which a small fragment containing a stereocenter is temporarily introduced in order to affect stereochemical outcome of a key step in the synthesis. The chiral auxiliary approach was developed thanks to the seminal contributions of Evans,^[67] Oppolzer,^[68] Myers,^[69] and Ellman,^[70] among others; and it was crucial in the maturity of the enantioselective synthesis field.

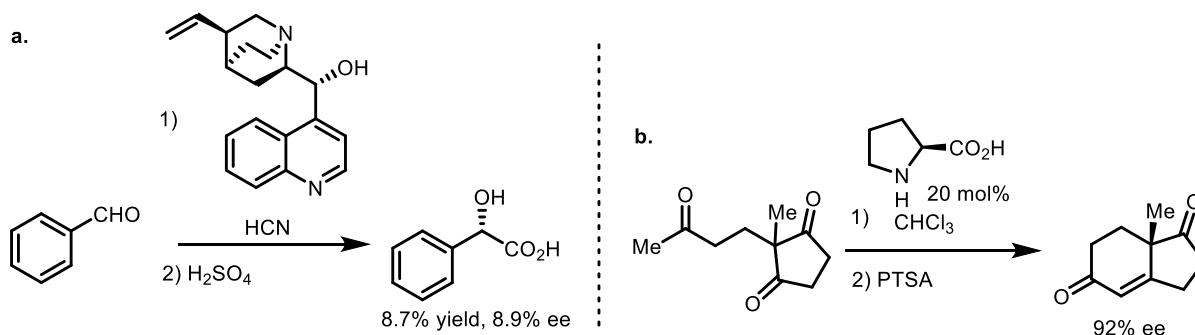
In order to make enantioselective syntheses more robust, dependable, and versatile, nonsubstrate-controlled methods for the construction of chiral molecules was necessary. There are three other main ways of accomplishing this: 1) chiral separation, where a racemic compound is separated into its enantiomers through physical means such as crystallization or chromatography;^[71] 2) chiral reagents, in which stoichiometric amounts of a chiral reagent is utilized in a key step; and 3) chiral catalysis, where catalytic amounts of a chiral molecule is used to control the stereochemical outcome of reaction. While chiral separations are useful in their own right, they are limited in generality and scope, and tend to require expensive equipment like chiral columns for chromatography. The use of stoichiometric amounts of chiral reagents is also often costly and wasteful. The ideal, most atom economical solution to this problem is to employ small, catalytic amounts of a chiral compound to produce a highly enantiomerically enriched product.

The field of asymmetric catalysis has matured over the last century and several important branches are in constant growth and development. The most established and well-studied approaches to asymmetric catalysis are 1) transition metal catalysis, 2) organocatalysis, and 3) enzymatic catalysis. Nature, the world's finest Chemist, through evolution, has developed a

powerful solution to asymmetric catalysis: chiral macromolecular structures built from amino acids. These macromolecular machines, also called enzymes, can superbly control the absolute and relative stereochemistry of an impressive array of reactions. A whole field has developed around the production, manipulation, alteration, and application of enzymes to reactions not exclusive to the portfolio Nature provides. This field is growing rapidly, and has recently been recognized with the 2018 Nobel Prize in Chemistry to Frances H. Arnold for the directed evolution of enzymes.^[72] Although these biocatalysts often make excellent catalysts for asymmetric transformations, they are generally limited in scope, scalability, ease of use, and especially, many enzymes are available only as one enantiomer, so producing both enantiomers of a product may be challenging. These deficiencies are well complemented by asymmetric transition metal catalysis and organocatalysis. An introduction to asymmetric transition metal catalysis is given in Chapter 4.

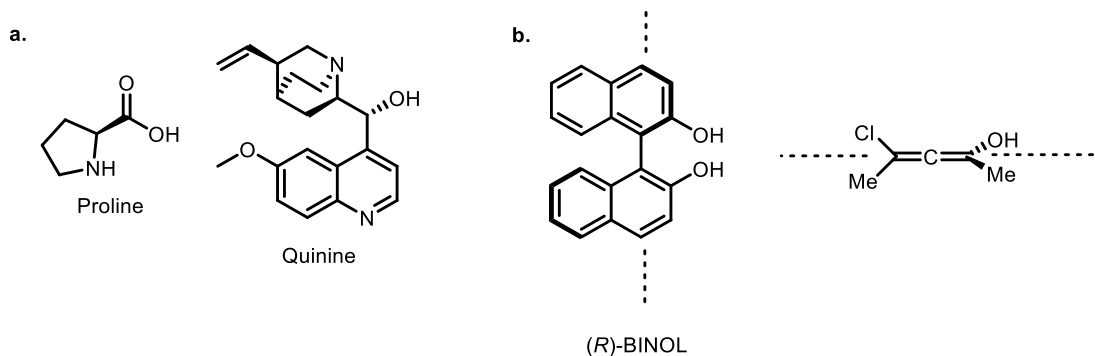
Asymmetric organocatalysis, defined as the use of catalytic amounts of a chiral organic compound to produce an enantiomerically enriched substance, has a long history as well. In 1913, two German chemists Bredig and Fiske reported the use of a cinchona base to catalyze the asymmetric hydrocyanation of benzaldehyde, with dismal but significant enantioselectivities (Scheme 1.6a).^[73] This would be the first asymmetric reaction that would employ cinchona bases,^[74] examples of which are seen in modern chemistry like the Sharpless Asymmetric Dihydroxylation. The usefulness of asymmetric organocatalysis would be established by two independent reports in 1971 by Hajos and Parrish (Scheme 1.6b), a famous and powerful transformation used to this day.^[75]

Scheme 1.6. Early examples of asymmetric organocatalysis.



Originally, asymmetric organocatalysis employed compounds containing chiral sp^3 hybridized stereocenters such as proline or quinine (Scheme 1.7a). This type of chirality based on stereogenic centers is also referred as point chirality. However, chirality can also be present in molecules without stereogenic centers, by possessing an inherent restriction to rotation that does not allow the superimposition of mirror images. An example of these is called axial chirality, and a large number of important catalysts are based on this phenomenon.

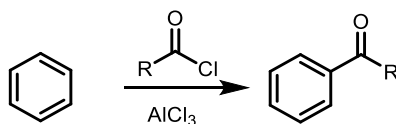
Scheme 1.7. Point chirality and axial chirality **a.** Examples of point chirality. **b.** Compounds containing axial chirality.



1.6 Brønsted acid catalysis and hydrogen-bond catalysis

Until the popularization of chiral phosphoric acids by Akiyama^[76] and Terada,^[77] over the past decades the principal strategy for enantioselective catalysis of polar reactions relied on activation of the electrophile by chiral Lewis acids.^[78] A Lewis acid is defined as any substance that can accept a pair of electrons, i.e., has a low energy lowest unoccupied molecular orbital (LUMO). Following the formation of the dative bond with an electrophile, it would lower its LUMO, making it more susceptible to nucleophilic attack. Application of Lewis acids in organic chemistry is based on the work of Friedel and Crafts, who utilized aluminum chloride catalysts extensively in aromatic acylations and alkylations (Scheme 1.8).^[79]

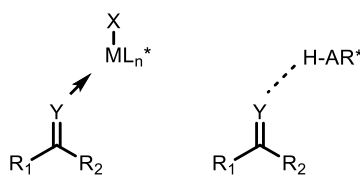
Scheme 1.8. A Friedel Crafts acylation.



Since the 2000s many different types of organocatalyzed transformations have been reported. Among the several different types of activations, Brønsted acid and hydrogen bond catalysis are some of the most important, popular, and well-studied. Brønsted acids or bases are defined as proton donors or acceptors, respectively.^[80] Reactions are catalyzed by acids when, after protonation of a reactant, the conjugate acid of this species is more reactive than the unactivated starting material. Activation of this kind renders the starting material more electrophilic and prone to attack by nucleophilic reactants. At first glance, it may seem that Lewis acids have more advantages over hydrogen bond catalysis given the stronger and more directional interactions with the Lewis base, as well as high tunability of the catalyst such as in the variation of the chiral ligands framework, counterion, and especially the identity of the Lewis acidic element (L_n^* , X, and M in Scheme 1.9, respectively). However, Nature's enzymes rely heavily on hydrogen bond catalysis

and with the advent of organocatalysis, organic chemists have recently learned to harness the latent power of Brønsted acid catalysis and hydrogen bond catalysis, especially in asymmetric catalysis applications.^[81–83]

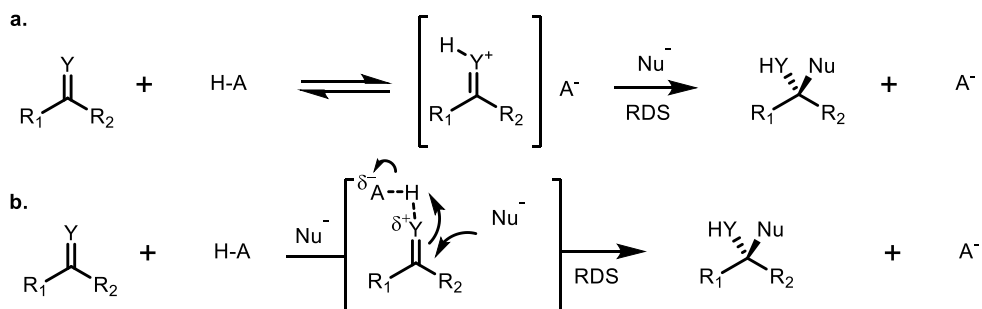
Scheme 1.9. Comparison of asymmetric Lewis acid catalysis and hydrogen bond catalysis.



Strictly speaking, Brønsted acid catalysis can be further categorized into specific acid catalysis and general acid catalysis. In specific acid catalysis the reaction rate is dependent on the equilibrium protonation of a reactant. Thus, such type of acid catalysis is generally independent of the structure of the Brønsted acid catalyst, and its reaction rate is governed by the pH of the solution. However, if the counterion is tightly bound to the electrophile, it can play an important role in the efficiency and stereoselectivity of the reaction. On the other hand, in general acid catalysis, the rate of the reaction depends on the structure and concentration of the Brønsted acid catalyst used (Scheme 1.10).^[2] For convention sake, throughout this text we refer to Brønsted acid catalysis as a specific acid type of catalysis, where a full or almost full proton transfer occurs prior to the transition state. Likewise, we refer to hydrogen bond catalysis to the general acid mechanism case, where there is only a partial interaction through hydrogen bonding in the transition state of the rate-determining step. Although strong acids like triflic acid usually operate through Brønsted acid catalysis and weaker ones like phosphoric acid tend to function through hydrogen bond catalysis, the mechanism is dependent on the reaction conditions and, crucially, the nature and basicity of the reactant being activated. In addition, the variety and tunability of the acid catalysts offers a dynamic and broad range of acid strength, so that there is no clear borderline between Brønsted acid and hydrogen bond catalysis.^[82,84] That being said, an understanding of the

underlying mechanism of Brønsted acid and Hydrogen bond-catalyzed reactions is important in the development of new, more efficient and stereoselective methods.

Scheme 1.10. Specific and general acid catalysis. **a.** Example of specific acid catalysis mechanism (Brønsted acid catalysis). **b.** Example of general acid catalysis mechanism (hydrogen bond catalysis).



This brief introduction gives a hint on the complexity and richness of reaction mechanisms. Thanks to TST we have a clearer understanding on the implication of transition states in reaction reactivity and selectivity. We have described several tools that have been developed to probe reaction mechanisms, and this information can be useful in the development and improvement of synthetic methodology, something that I can attest based on my graduate work. We have used our mechanistic findings to start whole new projects and find explanations to perplexing scenarios. It is my hope the reader finds in these pages the practical utility and intellectual satisfaction of knowing what occurs in the flask at least a little bit better.

1.7 References

- [1] J. Clayden, N. Greeves, S. Warren, *Organic Chemistry 2nd Ed.*, Oxford University Press, **2012**.
- [2] B. E. Norcorss, *Advanced Organic Chemistry: Reactions Mechanisms, and Structure (Mach, Jerry)*, Springer, **2009**.
- [3] H. Eyring, *J. Chem. Phys.* **1935**, *3*, 107–115.
- [4] M. G. Evans, M. Polanyi, *Trans. Faraday Soc.* **1935**, *31*, 875–894.
- [5] K. J. Laidler, M. C. King, *J. Phys. Chem.* **1983**, *87*, 2657–2664.
- [6] D. G. Truhlar, W. L. Hase, J. T. Hynes, *J. Phys. Chem.* **1983**, *87*, 2664–2682.
- [7] D. G. Truhlar, B. C. Garrett, S. J. Klippenstein, *J. Phys. Chem.* **1996**, *100*, 12771–12800.
- [8] P. Pechukas, *Annu. Rev. Phys. Chem.* **1981**, *32*, 159–177.
- [9] F. M. Menger, *Biochemistry* **1992**, *31*, 5368–5373.
- [10] T. Steiner, *Angew. Chemie Int. Ed.* **2002**, *41*, 48–76.
- [11] S. J. Meek, C. L. Pitman, A. J. M. Miller, *J. Chem. Educ.* **2016**, *93*, 275–286.
- [12] K. Bain, M. H. Towns, *Chem. Educ. Res. Pract.* **2016**, *17*, 246–262.
- [13] A. R. Dick, J. W. Kampf, M. S. Sanford, *J. Am. Chem. Soc.* **2005**, *127*, 12790–12791.
- [14] S. E. Denmark, R. F. Sweis, *J. Am. Chem. Soc.* **2004**, *126*, 4876–4882.
- [15] J. Saavedra, H. A. Doan, C. J. Pursell, L. C. Grabow, B. D. Chandler, *The Critical Role of Water at the Gold-Titania Interface in Catalytic CO Oxidation*, University Science Books, **2014**.
- [16] D. G. Blackmond, *Angew. Chemie - Int. Ed.* **2005**, *44*, 4302–4320.
- [17] P. R. Wells, *Chem. Rev.* **1963**, *63*, 171–219.
- [18] S. Roy, S. Goedecker, V. Hellmann, *Phys. Rev. E* **2008**, *77*, 056707.
- [19] R. W. Taft, *J. Am. Chem. Soc.* **1952**, *74*, 2729–2732.
- [20] R. W. Taft, *J. Am. Chem. Soc.* **1952**, *74*, 3120–3128.
- [21] R. W. Taft, *J. Am. Chem. Soc.* **1953**, *75*, 4538–4539.
- [22] J. D. Roberts, H. E. Simmons, L. A. Carlsmith, C. W. Vaughan, *J. Am. Chem. Soc.* **1953**, *75*, 3290–3291.
- [23] H. H. Wenk, M. Winkler, W. Sander, *Angew. Chem., Int. Ed.* **2003**, *42*, 502–528.
- [24] À. González-Lafont, J. M. Lluch, *Wiley Interdiscip. Rev. Comput. Mol. Sci.* **2016**, *6*, 584–603.

- [25] C. Hennig, R. B. Oswald, S. Schmatz, *J. Phys. Chem. A* **2006**, *110*, 3071–3079.
- [26] B. K. Carpenter, *Nat. Chem.* **2010**, *2*, 80–82.
- [27] K. B. Wiberg, *Chem. Rev.* **1955**, *55*, 713–743.
- [28] F. H. Westheimer, *Chem. Rev.* **1961**, *61*, 265–273.
- [29] L. Do Amaral, H. G. Bull, E. H. Cordes, *J. Am. Chem. Soc.* **1972**, *94*, 7579–7580.
- [30] V. J. Shiner, M. W. Rapp, H. R. Pinnick, *J. Am. Chem. Soc.* **1970**, *92*, 232–233.
- [31] K. T. Leffek, J. A. Llewellyn, R. E. Robertson, *Can. J. Chem.* **2006**, *38*, 2171–2177.
- [32] P. H.-Y. Cheong, C. Y. Legault, J. M. Um, N. Çelebi-Ölçüm, K. N. Houk, *Chem. Rev.* **2011**, *111*, 5042–5137.
- [33] T. Sperger, I. A. Sanhueza, I. Kalvet, F. Schoenebeck, *Chem. Rev.* **2015**, *115*, 9532–9586.
- [34] A. T. Bell, M. Head-Gordon, *Annu. Rev. Chem. Biomol. Eng.* **2011**, *2*, 453–477.
- [35] S. M. Bachrach, *Comput. Org. Chem.* **2006**, *109*, 1–478.
- [36] D. J. Wales, T. V. Bogdan, *J. Phys. Chem. B* **2006**, *110*, 20765–20776.
- [37] H. B. Schlegel, in *Mod. Electron. Struct. Theory* (Ed.: D.R. Yarkoni), Singapore: World Scientific Publishing, **1995**, pp. 459–500.
- [38] T. A. Halgren, W. N. Lipscomb, *Chem. Phys. Lett.* **1977**, *49*, 225–232.
- [39] M. J. S. Dewar, E. F. Healy, J. J. P. Stewart, *J. Chem. Soc. Faraday Trans. 2 Mol. Chem. Phys.* **1984**, *80*, 227–233.
- [40] I. V. Ionova, E. A. Carter, *J. Chem. Phys.* **1993**, *98*, 6377–6386.
- [41] C. J. Cerjan, W. H. Miller, *J. Chem. Phys.* **2003**, *75*, 2800–2806.
- [42] P. Maragakis, S. A. Andreev, Y. Brumer, D. R. Reichman, E. Kaxiras, *J. Chem. Phys.* **2002**, *117*, 4651–4658.
- [43] K. Fukui, *Acc. Chem. Res.* **1981**, *14*, 363–368.
- [44] S. Maeda, Y. Harabuchi, Y. Ono, T. Taketsugu, K. Morokuma, *Int. J. Quantum Chem.* **2015**, *115*, 258–269.
- [45] N. Graulich, H. Hopf, P. R. Schreiner, *Chem. Soc. Rev.* **2010**, *39*, 1503–1512.
- [46] B. A. Grzybowski, K. J. M. Bishop, B. Kowalczyk, C. E. Wilmer, *Nat. Chem.* **2009**, *1*, 31–36.
- [47] A. L. Dewyer, P. M. Zimmerman, *Org. Biomol. Chem.* **2017**, *15*, 501–504.
- [48] M. Yang, J. Zou, G. Wang, S. Li, *J. Phys. Chem. A* **2017**, *121*, 1351–1361.
- [49] P. M. Zimmerman, *J. Chem. Theory Comput.* **2013**, *9*, 3043–3050.
- [50] P. M. Zimmerman, *J. Comput. Chem.* **2013**, *34*, 1385–1392.

- [51] P. M. Zimmerman, *J. Comput. Chem.* **2015**, *36*, 601–611.
- [52] C. A. Busacca, D. R. Fandrick, J. J. Song, C. H. Senanayake, *Adv. Synth. Catal.* **2011**, *353*, 1825–1864.
- [53] K. A. Ahrendt, C. J. Borths, D. W. C. MacMillan, *J. Am. Chem. Soc.* **2000**, *122*, 4243–4244.
- [54] D. W. C. MacMillan, *Nature* **2008**, *455*, 304–308.
- [55] F. Liu, *Chirality* **2013**, *25*, 675–683.
- [56] J. von Liebig, *Justus Liebigs Ann. Chem.* **1860**, *113*, 246–247.
- [57] E. Knoevenagel, *Berichte der Dtsch. Chem. Gesellschaft* **1896**, *29*, 172–174.
- [58] O. W., *Z Phys Chem* **1900**, *32*, 509–511.
- [59] Y. Tu, Z. X. Wang, Y. Shi, *J. Am. Chem. Soc.* **1996**, *118*, 9806–9807.
- [60] S. E. Denmark, D. C. Forbes, D. S. Hays, J. S. DePue, R. G. Wilde, *J. Org. Chem.* **1995**, *60*, 1391–1407.
- [61] D. Yang, Y.-C. Yip, M.-W. Tang, M.-K. Wong, J.-H. Zheng, K.-K. Cheung, *J. Am. Chem. Soc.* **1996**, *118*, 491–492.
- [62] M. S. Sigman, E. N. Jacobsen, *J. Am. Chem. Soc.* **1998**, *120*, 4901–4902.
- [63] E. J. Corey, M. J. Grogan, *Org. Lett.* **2002**, *1*, 157–160.
- [64] S. J. Miller, G. T. Copeland, N. Papaioannou, T. E. Horstmann, E. M. Ruel, *J. Am. Chem. Soc.* **1998**, *120*, 1629–1630.
- [65] B. List, R. A. Lerner, C. F. Barbas, *J. Am. Chem. Soc.* **2000**, *122*, 2395–2396.
- [66] R. Breinbauer, *Classics in Stereoselective Synthesis*, Wiley-VCH, **2009**.
- [67] D. A. Evans, J. Bartroli, T. L. Shih, *J. Am. Chem. Soc.* **1981**, *103*, 2127–2129.
- [68] W. Oppolzer, *Tetrahedron* **1987**, *43*, 1969–2004.
- [69] A. G. Myers, B. H. Yang, H. Chen, L. McKinstry, D. J. Kopecky, J. L. Gleason, *J. Am. Chem. Soc.* **1997**, *119*, 6496–6511.
- [70] J. A. Ellman, T. D. Owens, T. P. Tang, *Acc. Chem. Res.* **2002**, *35*, 984–995.
- [71] W. H. Porter, *Resolution of Chiral Drugs*, **1991**.
- [72] F. H. Arnold, *Angew. Chem., Int. Ed.* **2018**, *57*, 4143–4148.
- [73] G. Bredig, P. S. Fiske, *Biochem. Z.* **1913**, *46*, 7–23.
- [74] C. E. Song, in *Cinchona Alkaloids Synth. Catal. Ligands, Immobil. Organocatalysis*, **2009**, pp. 1–10.
- [75] Z. G. Hajos, D. R. Parrish, *J. Org. Chem.* **1974**, *39*, 1615–1621.

- [76] T. Akiyama, J. Itoh, K. Yokota, K. Fuchibe, *Angew. Chem., Int. Ed.* **2004**, *43*, 1566–1568.
- [77] D. Uraguchi, M. Terada, *J. Am. Chem. Soc.* **2004**, *126*, 5356–5357.
- [78] M. S. Taylor, E. N. Jacobsen, *Angew. Chem., Int. Ed.* **2006**, *45*, 1520–1543.
- [79] C. Friedel, J. M. Crafts, *C. R. Hebd. Seances Acad. Sci.* **1877**, *84*, 1450–1454.
- [80] M. Kilpatrick, M. L. Kilpatrick, *Chem. Rev.* **1932**, *10*, 213–227.
- [81] T. Akiyama, *Chem. Rev.* **2007**, *107*, 5744–5758.
- [82] T. Akiyama, J. Itoh, K. Fuchibe, *Adv. Synth. Catal.* **2006**, *348*, 999–1010.
- [83] P. Nagorny, Z. Sun, *Beilstein J. Org. Chem.* **2016**, *12*, 2834–2848.
- [84] M. Fleischmann, D. Drettwan, E. Sugiono, M. Rueping, R. M. Gschwind, *Angew. Chem., Int. Ed.* **2011**, *50*, 6364–6369.

CHAPTER 2

Direct Interconversion of BINOL and H8-BINOL-Based Chiral Brønsted Acids Using Single-Step Red/Ox Manipulations

“Everything should be made as simple as possible but not simpler”

Albert Einstein

2.1 Introduction to chiral phosphoric acid catalysis

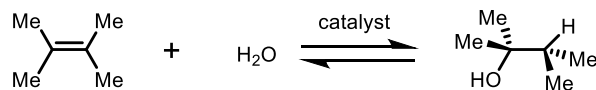
As is highlighted in Chapter 1, the development of methods for the construction of chiral building blocks is of utmost importance in the field of synthetic organic chemistry. Asymmetric Brønsted acid catalysis and hydrogen bond catalysis are branches of asymmetric organocatalysis that have grown considerably over the past decades.^[1] Phosphorous-containing organic compounds have had a massive impact and role in catalysis, and it appears in all major branches of catalysis, including enzymatic catalysis, organocatalysis, and transition metal catalysis. This section gives a brief introduction into chiral phosphoric acid catalysts (CPAs), while the use of phosphorus in asymmetric transition metal catalysis is discussed in the introduction of Chapter 4.

The origins of phosphorus-based acid catalysis can be traced to the works of Sir John Cornforth, an Australian-British chemist and Nobel laureate for his contributions to the stereochemistry of enzyme-catalyzed reactions.^[2] Cornforth was marveled by the mysteriously selective and efficient machinations of nature, and was determined to construct catalysts that could mimic nature as close as possible. Based on the overarching guiding principle that the structure of the catalyst must easily correlate with its activity, in 1978, Cornforth enunciated the following

“prescription” of 9 items for an enzyme-mimicking catalyst for the hydration of an alkene (Scheme 2.1):^[3]

- (1) The catalyst must be acidic.
- (2) The catalyst must work in homogeneous aqueous medium.
- (3) The catalyst must be of definite structure; therefore not a polymer.
- (4) A non-polar cavity in the molecule must fit olefin in the preferred orientation.
- (5) An acidic group must be located precisely in this cavity.
- (6) The cavity must be not too deep, not too rigid, easily variable in detail of shape, potentially chiral, preferably electron-rich and a potential carrier of an oriented nucleophilic group.
- (7) The critical micellar concentration in water must be high.
- (8) Synthesis must be short, feasible on a large scale and variable at a late stage to provide different cavity shapes.
- (9) The acidic group must not be too strong or too weak.

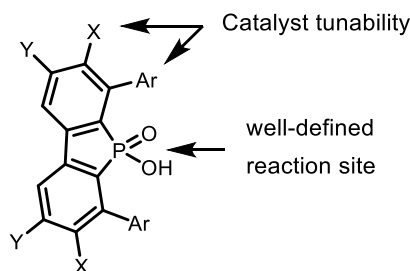
Scheme 2.1. Alkene hydration investigated by Cornforth and coworkers.



With these tenets in mind, Cornforth and coworkers designed a phosphinic acid catalyst with the general as shown in Scheme 2.2, and synthesized a variety of derivatives. Cornforth deserves much credit for his original ideas on catalyst design over 30 years ago, most of which are

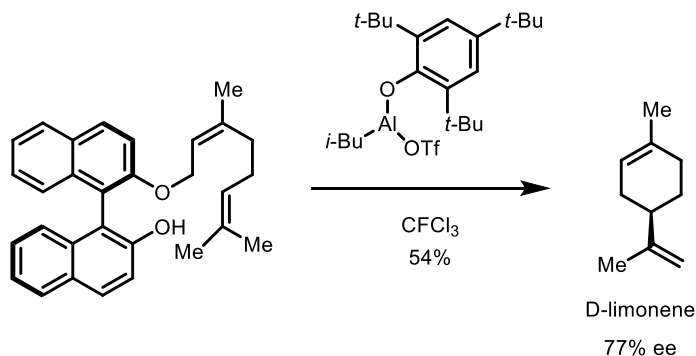
valid to this day, especially those regarding the modularity of the catalyst to control the acidity and steric characteristics at the active site.

Scheme 2.2. General structure of Cornforth's phosphinic acids.



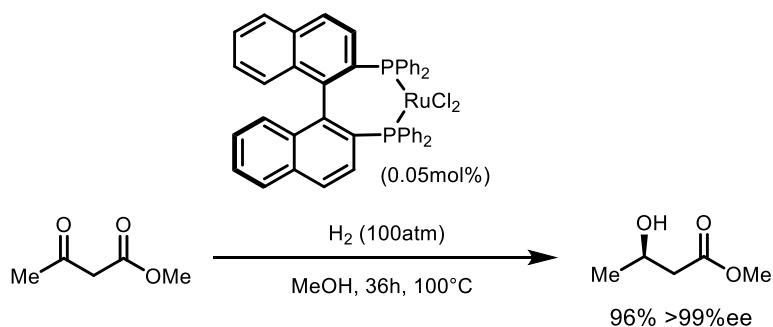
Although Cornforth's phosphinic acids would be effective in their intended role of catalyzing alkene hydration, enantioselective examples were not successful. However, Cornforth was a visionary, tenet number 6 considered the possibility of having a chiral pocket, structurally tuned to its function. Nearly a decade later, chiral atropisomeric 2,2'-disubstituted binaphthyl scaffolds would be discovered to be excellent frameworks for creating the type of chiral environment that Cornforth envisioned.^[4] In 1983, Yamamoto and coworkers showed the high asymmetric induction of the binaphthyl architecture in the enantioselective synthesis of (+)- β -bisabolone in 76% ee and D-limonene in 77% ee from the mono substituted BINOL ether and using an aluminum catalyst (Scheme 2.3).^[5,6]

Scheme 2.3. BINOL as a chiral auxiliary.



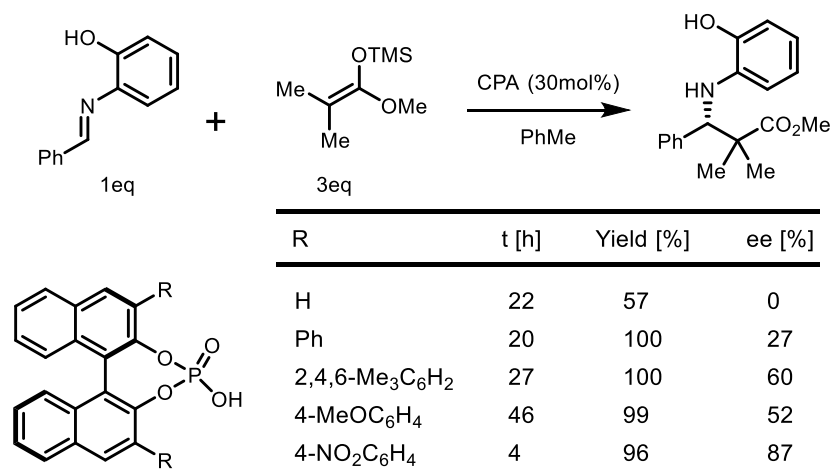
Other 2,2'-disubstituted binaphthyl scaffolds would also find success in asymmetric catalysis. In 1980, Ryoji Noyori reported a reliable synthesis for the atropoisomers (*R*) and (*S*)-BINAP (2,2'-bis(diphenylphosphino)-1,1'-binaphthyl). In a groundbreaking publication in 1987, Ryoji Noyori described the Nobel-prize winning asymmetric hydrogenation of ketones catalyzed by chiral ruthenium catalysts containing BINAP ligands (Scheme 2.4).^[7,8] This reaction would prove so powerful that it would have a drastic influence in modern synthesis. Since it is one of the most reliable ways of introducing chirality, it is taught in most organic chemistry courses and it is used in industry.^[9]

Scheme 2.4. Noyori's asymmetric hydrogenation of ketones.



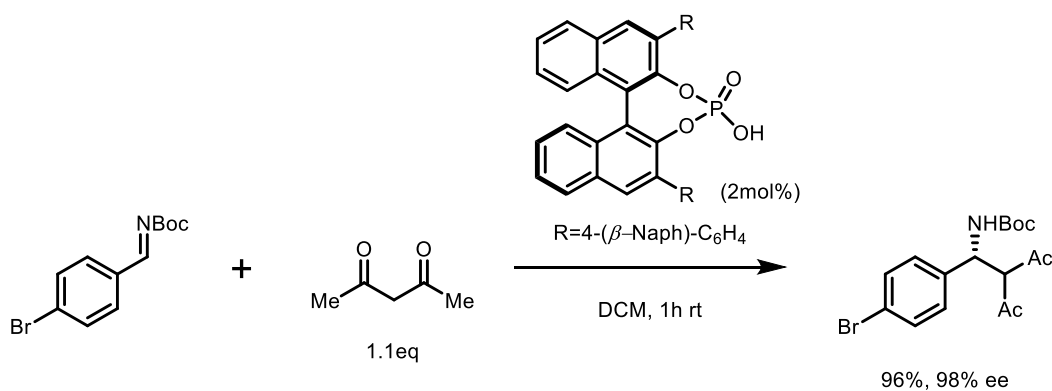
Inspired by these precedents in these precedents, in their seminal works in 2004, Akiyama^[10] and Terada^[11] independently published their applications of BINOL-derived CPAs. The conformationally rigid binaphthyl backbone in combination with substitutions at the 3 and 3' positions led to excellent results in enantioselectivity. Akiyama reported the use of *p*-nitrophenyl substituted CPAs in the Mannich-type reaction of aldimines with silyl enol ethers to obtain chiral amines in excellent yield, diastereoselectivity, and enantioselectivity (Scheme 2.5). The inclusion of nitro substituents in the CPA was essential for both increased reactivity, enantioselectivity and yields.^[10]

Scheme 2.5. Akiyama's asymmetric Mannich-type reaction.



On the other hand, Terada and coworkers developed a CPA-catalyzed Mannich-type reaction of Boc-protected amines with acetyl acetone with excellent yields and enantioselectivities.^[11] They also found that without substitution at the 3 and 3' positions, enantioselectivities were very poor. In their optimized conditions they used *p*-β-naphthylphenyl substituents in CPA (Scheme 2.6).

Scheme 2.6. Terada's asymmetric Mannich-type reaction.

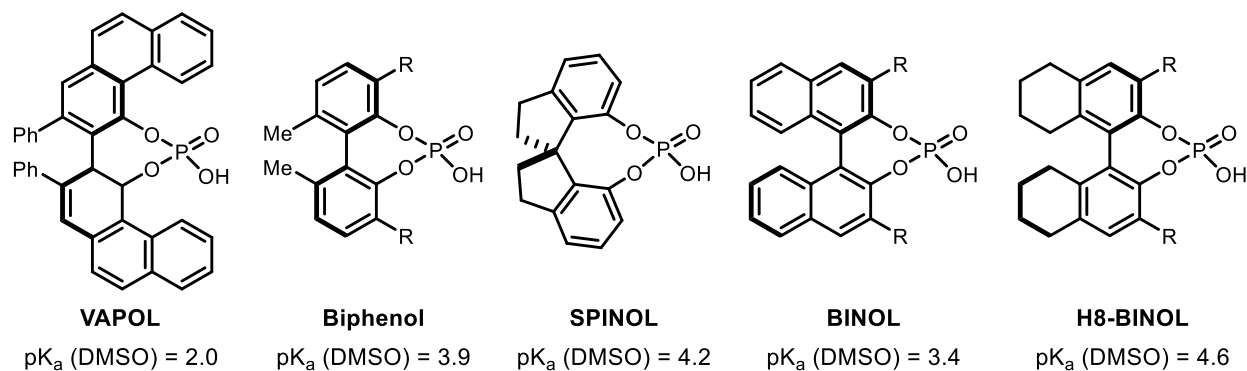


Since these two reports, the popularity of BINOL-derived CPAs grew explosively. As a reference, in 2013, over 100 research articles were published that utilized BINOL derived CPAs.^[12] This family of acid catalysts have several advantages which are responsible for their popularity. In the first place, they are acidic enough to catalyze many reactions efficiently, and

they offer high selectivity due to the strong stereochemical induction of the BINOL rigid and axially chiral framework. Additionally, the reactive site is well defined within the catalyst, and contains both a Lewis basic as well as a Brønsted acidic site. The bifunctional nature of CPAs allow powerful activation modes not available to traditional acids, such as the simultaneous activation of both nucleophiles and electrophiles. In the third place, both the acidity and sterics of the reactive site can be modulated by introducing different groups in place of the phosphoric acid functionality. Importantly, the chiral environment around the reactive site can be modulated in several ways such as by introducing substituents at the 3 and 3' positions or by making alterations in the BINOL backbone. Due to their high degree of tunability and activity, since the introduction of CPAs, these have been applied in a large number of scenarios and are considered a cornerstone in enantioselective organocatalysis.^[1,12-16] This has inspired several theoretical studies in the origin of the efficiency and selectivity of CPA-catalyzed reactions.^[17]

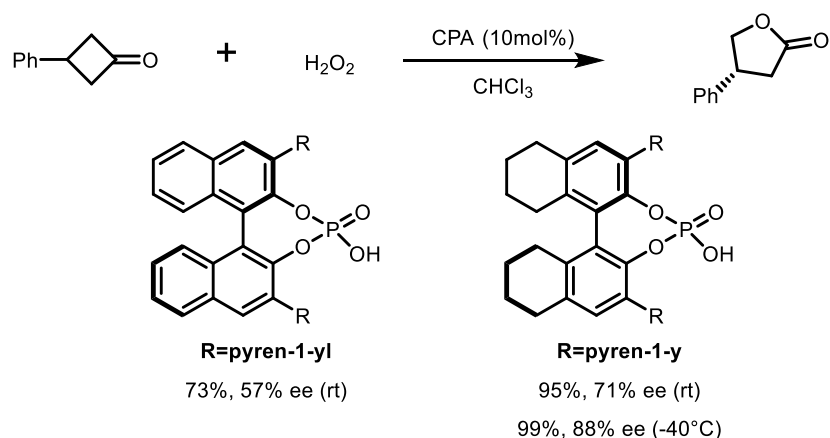
The remarkable efficiency and high degree of tunability of BINOL-derived CPAs led to many experimental and computational investigations into the effect that several structural and electronic parameters have in the acidity of the catalyst.^[18] It was found that the acidity of these catalysts could be modulated by making substitutions on the reactive site, on the substituents on the backbone, or by changing the framework itself. The Nagorny group recently published a comprehensive review that collects most of the conclusions.^[19] In Scheme 2.7, effects of the structure of the chiral backbone on the acidity of the CPA is shown.

Scheme 2.7. Effect of the chiral backbone on the acidity of CPAs. Adapted from reference [19].



In spite of the large success of BINOL-derived CPAs, the use of different backbone scaffolds is scarce, even when such drastic differences in pK_a and sterics are known.^[14,20] A frequently used alternative is the H8-BINOL backbone, which possess a marked difference in solubility, acidity, racemization profile, alternative structural conformations, and bite angle that may prove advantageous to their fully aromatic counterparts.^[12] For example, Ding and coworkers found that H8-BINOL-derived CPAs outperformed their BINOL analogues in the asymmetric Baeyer-Villiger oxidation of substituted cyclobutanones using H_2O_2 (Scheme 2.8).^[21]

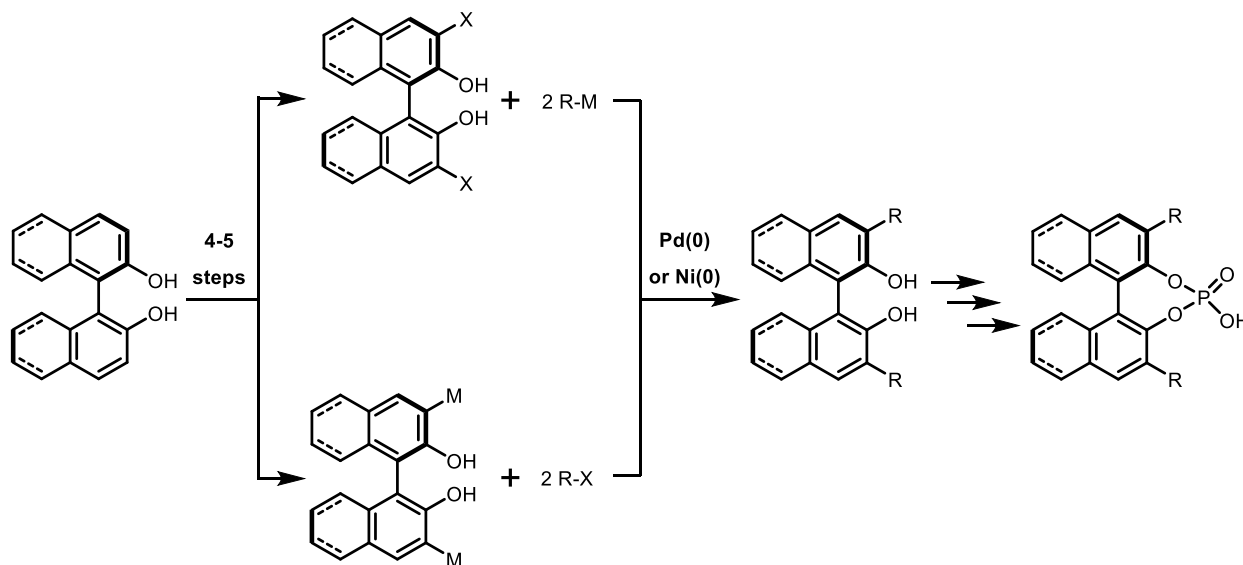
Scheme 2.8. Ding's enantioselective Baeyer-Villiger reaction of cyclobutanones.



H8-BINOL CPAs are often accessed by a similar, yet independent route to BINOL CPAs that starts from partially hydrogenated BINOL (Scheme 2.9).^[12] These synthetic routes depend

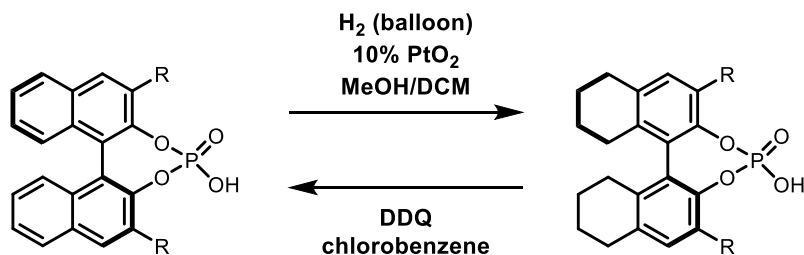
heavily in cross-coupling reactions that require careful optimization and may suffer from lower yields. Therefore, a procedure to obtain H8-BINOL CPAs directly from their fully aromatic counterparts is highly desirable. Conversely, if the independent synthesis of a particular H8-BINOL CPA is higher yielding than the corresponding unsaturated CPA a direct conversion in the opposite direction would be convenient.

Scheme 2.9. Standard synthesis of BINOL and H8-BINOL derived CPAs.



In collaboration with Dr. Tay Rosenthal (Nagorny group), we developed a concise way of interconverting BINOL and H8-BINOL CPAs via single-step redox manipulations (Scheme 2.10).^[22] The synthesis of H8-BINOL CPAs from the BINOL counterparts was accomplished by partial hydrogenation of the latter by heterogenous catalysis with Adam's catalyst. On the other hand, the reverse dehydrogenation was obtained by employing DDQ in chlorobenzene

Scheme 2.10. Direct interconversion of BINOL and H8-BINOL-derived CPAs via single step Red/Ox manipulations.



2.2 Results and discussion

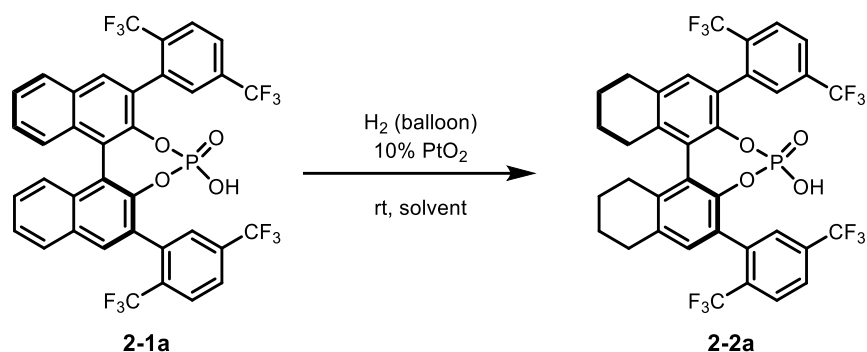
(Excerpts of this subchapter were taken from:

Tay, J. H.; Argüelles, A. J.; Nagorny, P. *Org. Lett.* **2015**, *17*, 3774.

Experimental information can be found in **Appendix A**)

Our studies commenced with investigation of the possibility of hydrogenating chiral phosphoric acid **2-1a** in the presence of PtO₂, previously employed for the conversion of BINOL into H8-BINOL (Table 2.1).^[23] Considering that BINOL-based CPAs display a wide range of solubilities in organic solvents, various solvent systems were investigated (entries 1–7). While **2-1a** is soluble in acetone, DCM, benzene, or DMF, no reduction was observed at rt after 24h (entries 1–4). The reaction in EtOAc resulted in the formation of **2-2** in 26% after 3 days (entry 5), and no reduction of the phosphate or 3,3'-aryl substituents was noted. The corresponding hydrogenations proceeded significantly faster in the presence of the protic solvents such as AcOH or MeOH/DCM (entries 6 and 7) and were accomplished in quantitative yields.

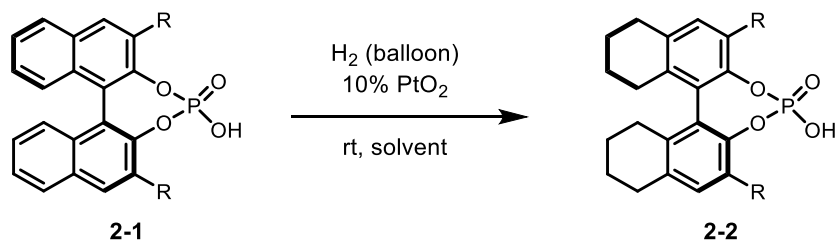
Table 2.1. Initial condition screening for the direct partial reduction of a BINOL-derived CPA. Reactions performed at rt, between 16 to 72h. ^a Yields were determined by NMR ^b Isolated yields. Experiments were performed by Dr. Tay Rosenthal.

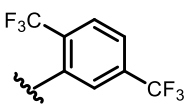
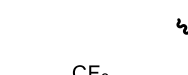
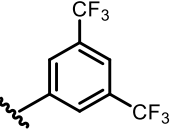
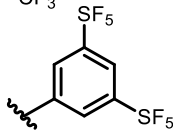
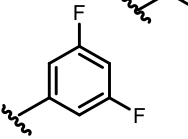
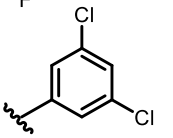
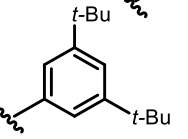
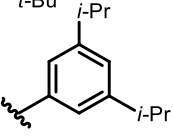
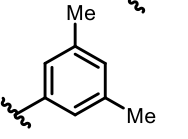
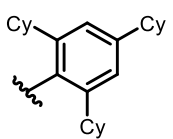
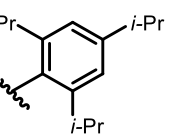


entry	solvent	yield [%]
1	acetone	<5 ^a
2	DCM	<5 ^a
3	benzene	<5 ^a
4	DMF	<5 ^a
5	EtOAc	26 ^a
6	AcOH	98 ^b
7	MeOH/DCM	98 ^b

With the optimal hydrogenation conditions in hand, the scope of this transformation was investigated next (Table 2.2). In order to test the scalability of the hydrogenation, the reduction of 2,5-bis(trifluoromethyl)phenyl-substituted CPA **2-1a** was repeated (entry 1) on a 1.0 g scale (98% yield). Similarly, the reaction with unsubstituted acid **2-1b** proceeded selectively without overreduction of the hydrogen phosphate functionality. Importantly, neither **2-1a** nor **2-1b** was found to racemize under the reaction conditions (see Section 2.3). The acids with electron-withdrawing (entries 3–6) and electron-donating (entries 7–9) substituents in the meta position were examined next. Importantly, the reduction of popular acids such as 3,5-bis(trifluoromethyl)phenyl-substituted acid **2-1c** and 3,5-bis(pentafluoro-*l*-sulfanyl)phenyl-substituted acid **10d** proceeded smoothly and selectively in quantitative yield.

Table 2.2. Substrate scope for the partial hydrogenation of BINOL-derived CPAs. Experiments were performed by Dr. Tay Rosenthal.



entry	R	solvent	yield [%]
1	 2-1a	AcOH	>98
2	 2-1b	MeOH/DCM (2:3)	>98
3	 2-1c	MeOH/DCM (1:1)	>98
4	 2-1d	MeOH/DCM (1:1)	>98
5	 2-1e	MeOH/DCM (2:3)	>98
6	 2-1f	MeOH/DCM (2:3)	-
7	 2-1g	MeOH/DCM (2:3)	96
8	 2-1h	MeOH/DCM (2:3)	>98
9	 2-1i	MeOH/DCM (1:1)	-
10	 2-1j	MeOH/DCM (2:3)	91
11	 2-1k	MeOH/DCM (2:3)	>98

Furthermore, while the reduction of 3,5-difluorophenylsubstituted acid **2-1e** proceeded smoothly, the reduction of 3,5-dichlorophenyl-substituted acid **2-1f** resulted in a mixture of products due to dechlorination followed by the reduction of resultant phenyl rings. Similar to the prior observations, CPAs containing phenyl groups with bulky *t*-Bu- and *i*-Pr-substituents in meta-positions (entries 7 and 8) were selectively reduced to provide the corresponding H8-BINOL acids in excellent yields. However, the 3,3'-aryl substituent diastereomeric overreduction products were obtained for less hindered acid **2-1i**. To our delight, frequently used in asymmetric catalysis catalysts **2-1j** and **2-1k** containing bulky substituents at the ortho- and para positions underwent efficient reduction as well (entries 10 and 11). Considering that the corresponding H8-BINOL-based acids **2-2j** and **2-2k** require challenging syntheses, the described protocol can be used for a single-step preparation of these catalysts from the commercially available catalysts **2-1j** and **2-1k**.

The protonation state of the phosphoric acid had a dramatic effect on the rate of hydrogenation in the aforementioned studies. Thus, a filtration through silica gel produced significantly less reactive form of CPA, probably, due to the formation of Na⁺ and Ca₂⁺ salts that poison the catalyst.^[24] On the other hand, washing the CPA with hydrochloric acid prior to reduction was found to improve the rate of hydrogenation in some cases. To demonstrate that this approach is applicable to the interconversion of other types of Brønsted acids, the formation of H8-BINOL acids **2-3**, **2-4** and **2-5** was investigated (Figure 2.1). The reductions leading to N-triflyl phosphoramidate **2-3** and disulfonimide **2-5** proceeded chemoselectively in excellent yields. However, the formation of the N-triflyl thiophosphoramidate **2-4** was not observed, probably due to catalyst poisoning by sulfur. To our knowledge, the synthesis of **2-5** represents the first synthesis of H8-BINOL-based disulfonimides, and the alternative multistep approach to **2-5** from H8-BINOL is yet to be developed.

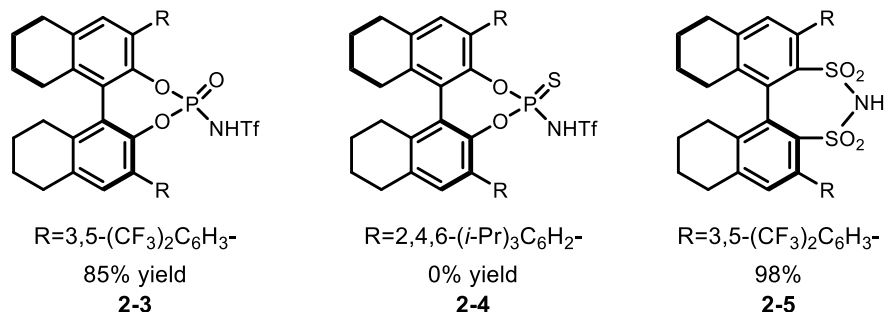


Figure 2.1. Additional substrates for the partial hydrogenation of BINOL-derived CPAs. Experiments were performed by Dr. Tay Rosenthal.

The reverse reaction (i.e., converting H8-BINOL acids to BINOL acids) was investigated next (Table 2.3). The H8-BINOL CPA **2-2a** was subjected to a variety of oxidants known to convert 1,2,3,4-tetrahydronaphthalenes into the corresponding naphthalenes. While the dehydrogenation with Pd/C in refluxing diglyme^[25] resulted in decomposition due to dephosphorylation as well as other pathways (entry 1), the oxidations with V₂O₅^[26] did not result in any reaction, and only starting material **2-2a** was observed (entries 2 and 3). Similarly, the oxidation with DDQ^[27,28] in xylenes at reflux provided no conversion (entry 4), while a similar reaction in 1,4-dioxane resulted in some partial dehydrogenation leading to product 10a (~25%, entry 5). Finally, the oxidation with DDQ (8 equiv) in refluxing chlorobenzene resulted in clean formation of the desired product **2-1a** in 74% isolated yield. Similar to the oxidation of **2-2a**, additional H8-BINOL Brønsted acids (**2-3** and **2-5**) were efficiently converted to the corresponding BINOL derivatives **2-6** and **2-7** (Figure 2.2). To our knowledge, these are the most complex derivatives of H8-BINOL that have been successfully dehydrogenated to date.

In summary, we have developed a new approach that allows a direct reduction of BINOL-based Brønsted acids to the corresponding H8-BINOL-based catalysts. This reduction tolerates various electron-withdrawing and bulky substituents on 3,3'-aromatic rings and could be applied to the

selective formation of chiral phosphates, N-triflyl phosphoramides, and disulfonimides. The reverse transformation allowing the oxidation of H8-BINOL-based catalysts into BINOL-based catalysts has also been demonstrated using DDQ as the oxidant. The outlined strategy would allow a rapid diversification of the existing libraries of Brønsted acids and will expand the availability of BINOL and H8-BINOL-based Brønsted acid catalysts for asymmetric transformations.

Table 2.3. Screening of oxidation conditions for the dehydrogenation of H8-BINOL-derived CPAs.

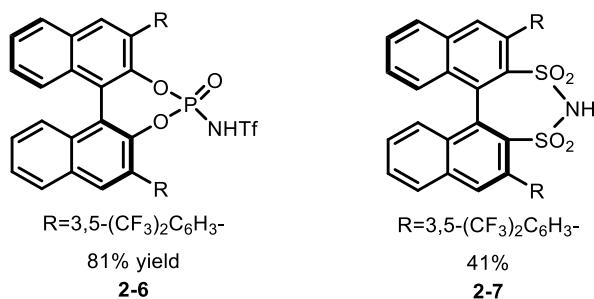
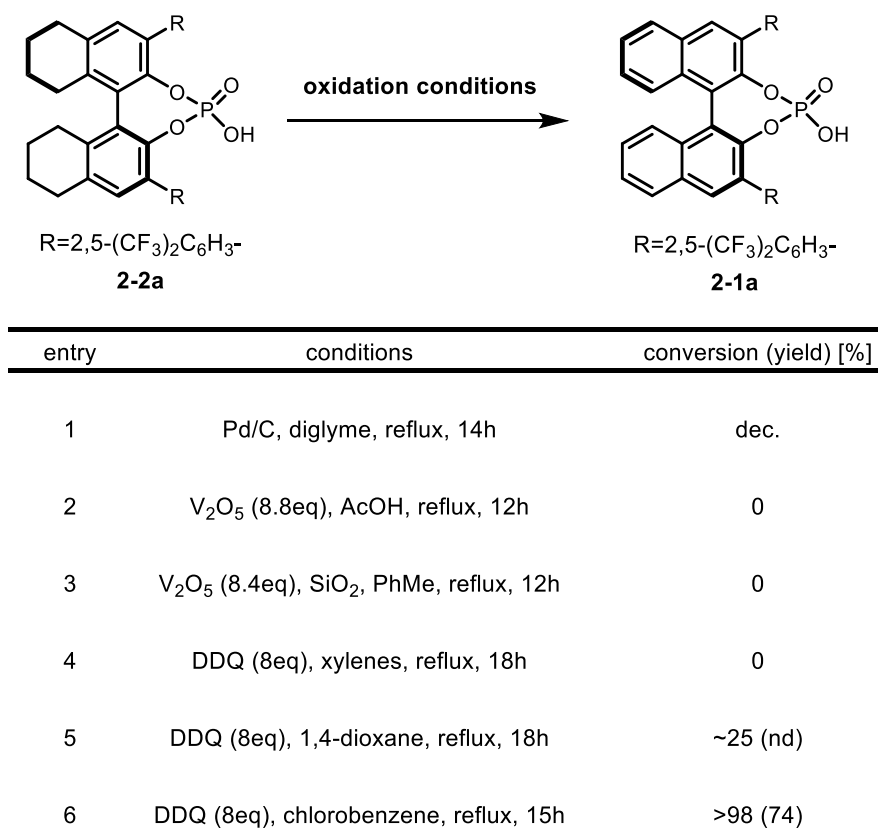


Figure 2.2. Additional substrates for the oxidation of H8-BINOL-derived CPAs.

2.3 References

- [1] T. Akiyama, J. Itoh, K. Fuchibe, *Adv. Synth. Catal.* **2006**, *348*, 999–1010.
- [2] J. Hanson, *Nature* **2014**, *506*, 35–35.
- [3] J. W. Cornforth, *Proc. R. Soc. London. Ser. B. Biol. Sci.* **2006**, *203*, 101–117.
- [4] A. Miyashita, A. Yasuda, H. Takaya, K. Toriumi, T. Ito, T. Souchi, R. Noyori, *J. Am. Chem. Soc.* **1980**, *102*, 7932–7934.
- [5] S. Sakane, J. Fujiwara, K. Maruoka, H. Yamamoto, *J. Am. Chem. Soc.* **1983**, *105*, 6154–6155.
- [6] S. Sakane, J. Fujiwara, K. Maruoka, H. Yamamoto, *Tetrahedron* **1986**, *42*, 2193–2201.
- [7] R. Noyori, T. Ohkuma, M. Kitamura, H. Takaya, N. Sayo, H. Kumobayashi, S. Akutagawa, *J. Am. Chem. Soc.* **1987**, *109*, 5856–5858.
- [8] R. Noyori, H. Takaya, *Acc. Chem. Res.* **1990**, *23*, 345–350.
- [9] R. Noyori, *Angew. Chem., Int. Ed.* **2002**, *41*, 2008.
- [10] T. Akiyama, J. Itoh, K. Yokota, K. Fuchibe, *Angew. Chem., Int. Ed.* **2004**, *43*, 1566–1568.
- [11] D. Uraguchi, M. Terada, *J. Am. Chem. Soc.* **2004**, *126*, 5356–5357.
- [12] D. Parmar, E. Sugiono, S. Raja, M. Rueping, *Chem. Rev.* **2014**, *114*, 9047–9153.
- [13] T. Akiyama, K. Mori, *Chem. Rev.* **2015**, *115*, 9277–9306.
- [14] T. Akiyama, *Chem. Rev.* **2007**, *107*, 5744–5758.
- [15] M. Fleischmann, D. Drettwan, E. Sugiono, M. Rueping, R. M. Gschwind, *Angew. Chem., Int. Ed.* **2011**, *50*, 6364–6369.
- [16] A. Zamfir, S. Schenker, M. Freund, S. B. Tsogoeva, *Org. Biomol. Chem.* **2010**, *8*, 5262–5276.
- [17] R. Maji, S. C. Mallojjala, S. E. Wheeler, *Chem. Soc. Rev.* **2018**, *47*, 1142–1158.
- [18] P. Christ, A. G. Lindsay, S. S. Vormittag, J. M. Neudörfl, A. Berkessel, A. C. O'Donoghue, *Chem. - A Eur. J.* **2011**, *17*, 8524–8528.
- [19] J. H. Tay, P. Nagorny, in *Nonnitrogenous Organocatalysis*, CRC Press, Boca Raton, Florida : CRC Press, [2018] | Series: Organocatalysis Series, **2017**, pp. 39–68.
- [20] A. G. Doyle, E. N. Jacobsen, *Chem. Rev.* **2007**, *107*, 5713–5743.
- [21] S. Xu, Z. Wang, X. Zhang, X. Zhang, K. Ding, *Angew. Chem., Int. Ed.* **2008**, *47*, 2840–2843.
- [22] J.-H. Tay, A. J. Arguelles, P. Nagorny, *Org. Lett.* **2015**, *17*, 3774–3777.
- [23] N. T. McDougal, W. L. Trevellini, S. A. Rodgen, L. T. Kliman, S. E. Schaus, *Adv. Synth.*

- Catal.* **2004**, *346*, 1231–1240.
- [24] M. Klusmann, L. Ratjen, S. Hoffmann, V. Wakchaure, R. Goddard, B. List, *Synlett* **2010**, *2010*, 2189–2192.
- [25] J. Bergman, B. Pelcman, *Tetrahedron* **1988**, *44*, 5215–5228.
- [26] M. Karki, H. Araujo, J. Magolan, *Synlett* **2013**, *24*, 1675–1678.
- [27] E. A. Braude, A. G. Brook, R. P. Linstead, *J. Chem. Soc.* **1954**, *0*, 3569–3574.
- [28] T. Kano, Y. Tanaka, K. Osawa, T. Yurino, K. Maruoka, *J. Org. Chem.* **2008**, *73*, 7387–7389.

CHAPTER 3

Studies on the Mechanism of Phosphoric Acid-Catalyzed Spiroketalizations

“Accuracy of observation is the equivalent to accuracy of thinking”

Wallace Stevens

3.1 Introduction to spiroketals

Spiroketals are cyclic acetals comprised by two rings joined by a single sp^3 -hybridized carbon atom, where the spiro atom is connected to oxygen atoms belonging to each ring. The spiroketal system is a recurrent substructure in a myriad of naturally occurring substances of marine, insect, bacterial, or plant origin.^[1] In addition, although structurally simple and unassuming, this functional motif usually has strong implications on the biological activity of the natural product.^[2,3] This is often attributed to the conformational constraints imposed by the rigidity of these cyclic acetals.^[4]

An illustrative example of the biological importance of even the simplest spiroketals can be made by the sex pheromone of the olive fruit fly, *Bactrocea oleae*. This is the major pest of olives, especially throughout the Mediterranean. In 1980, Baker and coworkers identified the major sex pheromone, the simple [6,6] spiroketal olean **3-1**.^[5] Interestingly, it was later found that the chirality of the spiroketal had a dramatic impact in the biological activity of this pheromone. Mori and coworkers synthesized both enantiomers of **3-1** from (*S*)-malic acid^[6,7] and Haniotakis and coworkers found that (*R*)-**3-1** was active against males while (*S*)-**3-1** was effective against females.^[8] As it turns out, spiroketals are particularly common amongst insect pheromones, such

as (2*S*, 5*R*)-chalcogran **3-2** for the European spruce bark beetle and (5*S*, 7*S*)-conophthorin **3-3** for the navel orangeworm moth (Figure 3.1).^[9] This example highlights the importance of developing enantioselective methods for the construction of chiral spiroketals.

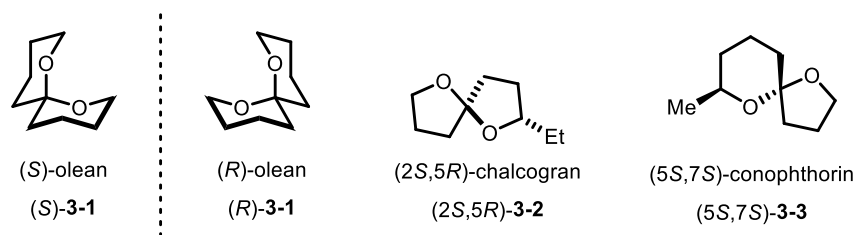


Figure 3.1. Spiroketals are common amongst insect pheromones.

The great relevance of spiroketals in the biological activity of natural products has inspired many chemists to come up with creative and novel solutions for the installation of spiroketals. In addition, spiroketals are extensively studied for being ideal systems to explore the role of the anomeric effect in conformational aspects of heterocyclic systems. Thus, a plethora of synthetic work has been directed towards the synthesis of several more complex spiroketal-containing compounds. For example, spongistatins such as **3-4**, which were discovered in 1993,^[10–12] have shown to be active against a panel of 60 human cancer cell lines from the US National Cancer Institute. Amongst these, spongistatin 1 (Figure 3.2) is one of the most potent tumor cell growth inhibitors reported to date.^[13] The potent biological activity and impressive structural complexity have made spongistatins formidable targets for total syntheses, which have been achieved by several groups such as Evans,^[14–16] Kishi,^[17,18] Smith,^[13,19–22] Paterson,^[23] Crimmins,^[24] Heathcock,^[25] and Ley.^[26]

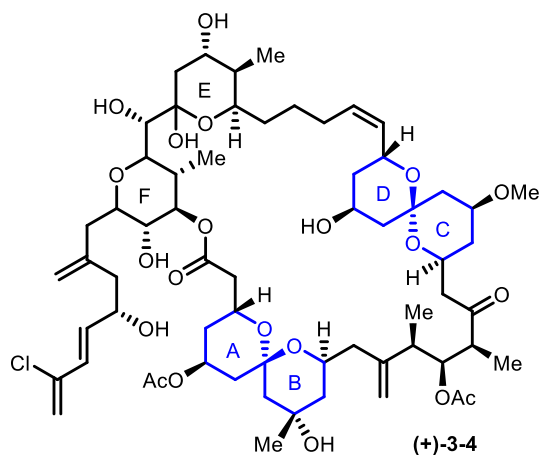


Figure 3.2. Structure of (+)-spongistatin 1.

With the broad range of biological activities that spiroketals display, it comes to no surprise that spiroketal-containing molecules would be tested for medicinal purposes. Ivermectin **3-5**, which some consider a “miracle drug”, is a FDA-approved drug used to treat a broad spectrum of parasitic infestations, including head lice, scabies, river blindness, among others.^[27] It was discovered in 1974, when it was isolated from the bacterium *Streptomyces avermitilis* (later renames *S. avermectinius*).^[28] In fact, Ivermectin is one compound of a family of spiroketals produced by this material called avermectins. Many other avermectins, although not FDA-approved, are used as drugs and pesticides to treat parasites and insect pests.^[29,30] As a different example, Tofogliflozin (**3-6**) is a spiroketal-containing experimental drug for the treatment of diabetes mellitus currently in Phase III clinical trials. It has been demonstrated that tofogliflozin is a highly selective sodium-glucose co-transporter-2 (SGLT2) inhibitor, which is crucial for glucose reabsorption in the kidney.^[31]

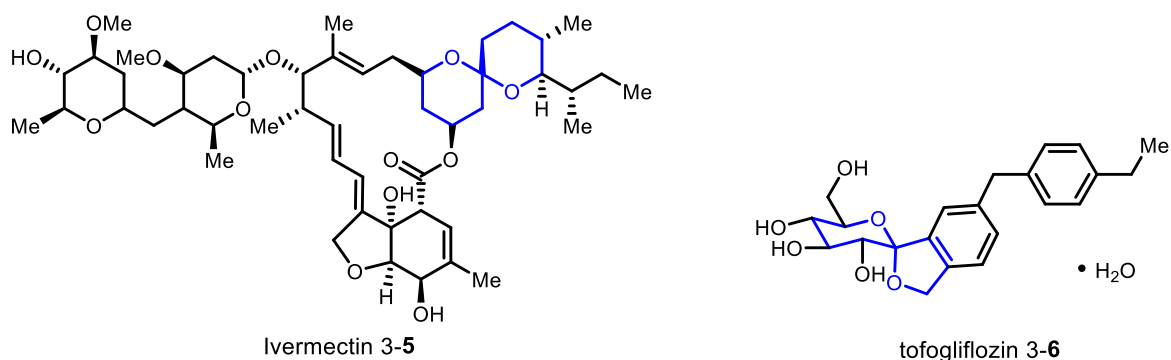


Figure 3.3. Structure of ivermectin and tofogliflozin, spiroketal-containing drugs.

3.2 Introduction to the anomeric effect and conformational aspects of spiroketals

In 1905, chemists were perplexed by the observation that that alkyl pyranosides preferred to adopt the α conformation over their β stereoisomers, contrary to steric demands.^[32] In addition, another important observation made decades ago is that acetals are more stable than their non-acetal, diether isomers. For example, the standard heat of formation (ΔH_f°) in the gas phase of 1,2-diethoxyethane is -98.0 kcal/mol; remarkably less stable than the ΔH_f° of the spiroketal isomer, 1,1-diethoxyethane, which is -108.4 kcal/mol (Figure 3.4a); and ΔH_f° of 1,3-diethoxypropane is 16.8 kcal/mol higher than spirocyclic 2,2-diethoxypropane in the gas phase (Figure 3.4b).^[33]

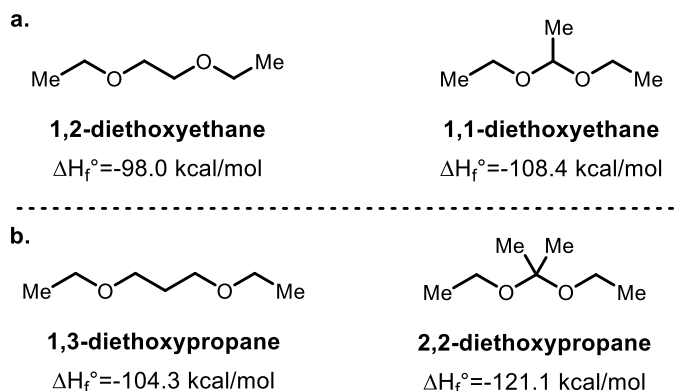


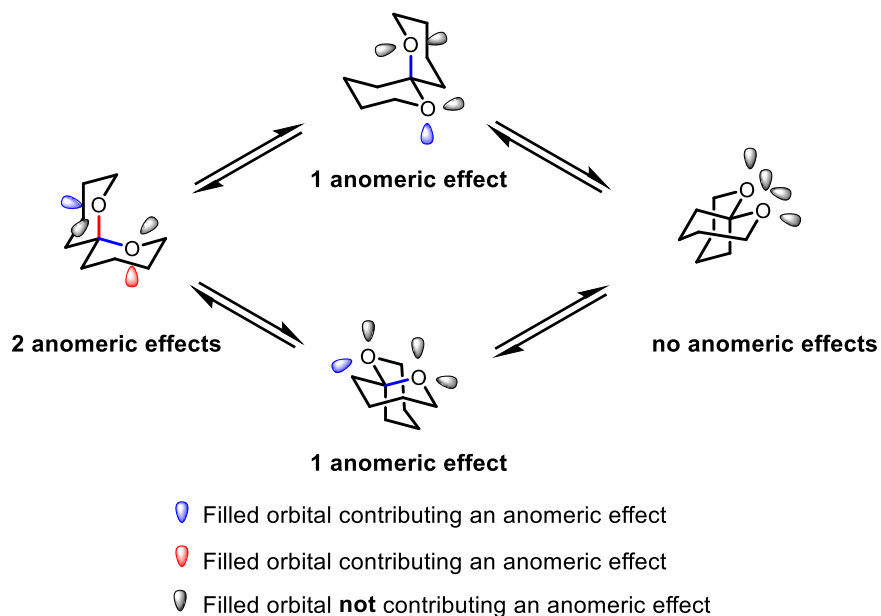
Figure 3.4. Geminal dialkoxyalkanes are more stable than their non-acetal diether isomers.

The stereoelectronic thermodynamic stabilization of geminal dioxy substitution is called the anomeric effect.^[34] It was first formally described by J. T. Edward in 1955 and studied by R. U. Lemieux the same year, which is why the phenomenon is sometimes called the Edward-Lemieux effect.^[35,36] This phenomena alone accounts for both observations noted above.

It is widely accepted that the anomeric stabilization arises from the hyperconjugative interactions of oxygen lone pairs (filled p orbital) with C-O antibonding orbital (unfilled σ^* orbital). The $2p_{(O)} \rightarrow \sigma^*_{(C-O)}$ interaction is strong enough that dictates the conformational preference of acetals. More precisely, each anomeric interaction contributes approximately 1.4-2.4 kcal/mole.^[37] Indeed, another way to define the anomeric effect is that it is the tendency of an electronegative atom at the anomeric carbon of anomeric to assume an axial orientation.^[4] Only by adopting an axial orientation can the orbital overlap between $2p_{(O)}$ filled orbital and the $\sigma^*_{(C-O)}$ unfilled orbital be achieved.

The [6,6]-spiroketal skeleton can adopt four conformations by chair-flipping. Of these, one will possess two axial oxygen atoms, that account for two anomeric interactions, and will tend to be the most thermodynamically stable (*gauche/gauche*), even though it is usually the least favored sterically. Two of the remaining conformations will have a single anomeric effect and will be similarly stabilized (*gauche/anti* and *anti/gauche*). Finally, the remaining conformation will be the least stable since geometrical constrains on orbital overlap don't permit an anomeric effect (Scheme 3.1).

Scheme 3.1. Orbital alignment in [6,6] spiroketals allows stabilization by the anomeric effect. Only certain configurations allow orbital overlap between $2p_{(O)}$ and $\sigma^*_{(C-O)}$. The interacting elements have the same color in this scheme.



Contrary to what might be expected, many natural products contain non-thermodynamic spiroketals. An example is diarrhetic shellfish toxin pectenotoxin 2 (Figure 3.5, PTX2). This natural product was discovered in the late 1980s by Yasumoto and coworkers^[38,39] and was found to be highly toxic to mice and cytotoxic to several cancer cell lines, presumably because of their actin depolymerization capabilities.^[40–42] Despite the biological interest, the complexity of PTX2, especially around the nonthermodynamic spiroketal, has made its synthesis an extraordinary challenge. Only one reported synthesis of PTX2 exists by the Fujiwara group,^[43] though other groups have succeeded in assembling parts of the complex spiroketal.^[44–47]

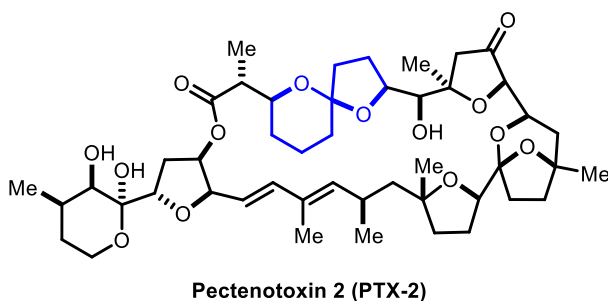


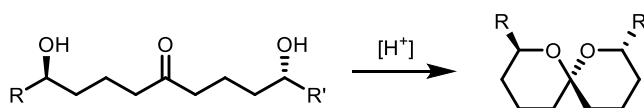
Figure 3.5. Structure of pectenotoxin 2.

These experiences highlight two important and arduous challenges that affront the construction of spiroketal centers: enantioselectivity for asymmetric spiroketalizations, and diastereoselectivity for conformationally locked non-thermodynamic products. The next section delves on the advancements on synthetic methodologies for spiroketal formation.

3.3 Prior art on spiroketal synthesis

The most commonly employed method in the construction of the spiroketal system relies on acid-catalysis spirocyclizations, in many cases accompanied by deprotections. Probably the most used of these methods is the acid-catalyzed dehydration of dihydroxy ketones (Scheme 3.2).^[48] This method has two main drawbacks: 1) it is limited to acid-stable substrates; and 2) it produces a mixture of thermodynamic spiroketals epimers favoring the more stable products. Most spiroketal targets consist of the more thermodynamically stable product, so this method is suitable for the large majority of synthetic needs.

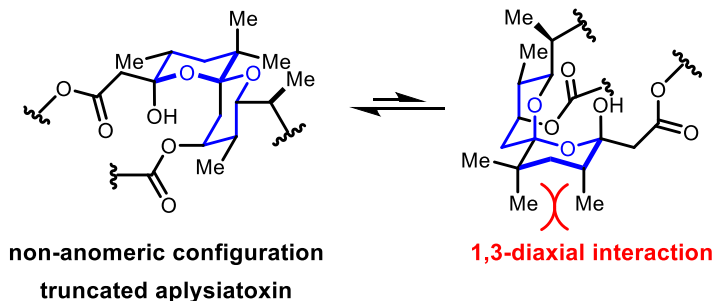
Scheme 3.2. Spiroketal synthesis by acid-catalyzed dehydration.



Although it is known that three and four membered ring systems are abundant in natural products,^[49,50] nearly all spiroketal-containing natural products consist of five and six membered rings. This might lead to the speculation that spiroketals are formed under thermodynamic conditions in nature. However, a considerable number of natural spiroketal structures adopt conformations that aren't the lowest in energy, therefore disproving this generalization. It should be considered that in many cases, the non-anomeric configuration of spiroketals may be stabilized

by additional factors that result in an increased thermodynamic stability in comparison with their anomeric counterpart. These factors include intermolecular hydrogen bonding, geometrical constraints imposed by macrocyclic structures, and unfavorable 1,3-diaxial interactions. For example, Ireland demonstrated that the non-anomeric spiroketal core of aplysiatoxin, a natural product isolated from the sea hare *Stylocheilus longicauda*, is thermodynamically preferred due to the destabilizing effect of 1,3-diaxial interactions between the C4 and C6 methyl groups in the doubly anomeric epimer (Scheme 3.3).^[51]

Scheme 3.3. Effect of 1,3-diaxial interactions in the relative stability of spiroketal configurations.

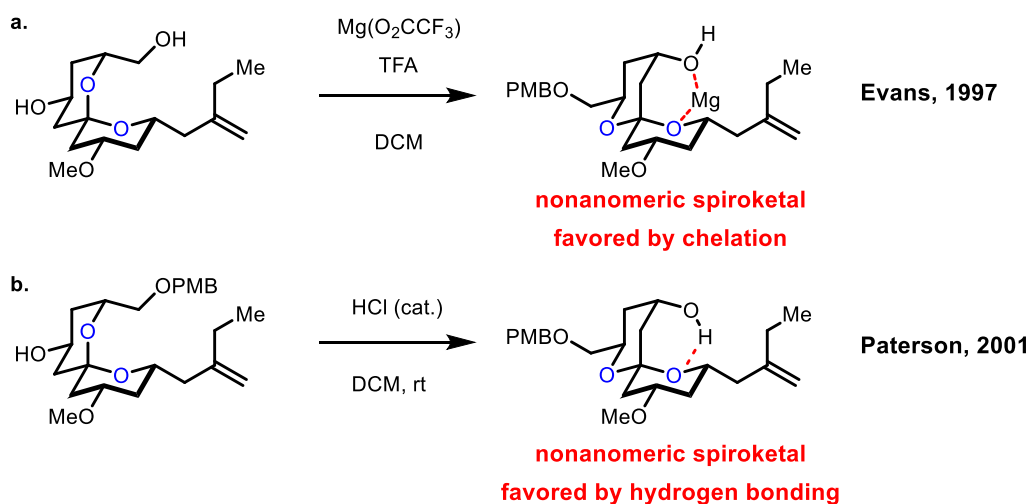


However, many of the non-anomeric spiroketals found in nature are truly not thermodynamically favored and their synthesis is challenging. It should be noted that this anomeric/non-anomeric structural dichotomy is only relevant when two conditions are met. In the first place, there must be a clear difference between axial and equatorial anomeric positions. Six membered rings meet this criterion, while larger and smaller rings do not. For example, five membered rings possess rapid pseudorotation so that non-anomeric relationships cannot be stabilized.^[1] the second criteria is that the ring conformation must be conformationally locked. In other words, ring flipping must be denied, which would otherwise quickly transform non-anomeric structures into their thermodynamic epimers. This is typically accomplished by the inclusion of

aply placed alkyl substituents or by ring fusion. Organic chemists have strived to provide methods for the construction of non-thermodynamic spiroketals, and some strategies are discussed next.

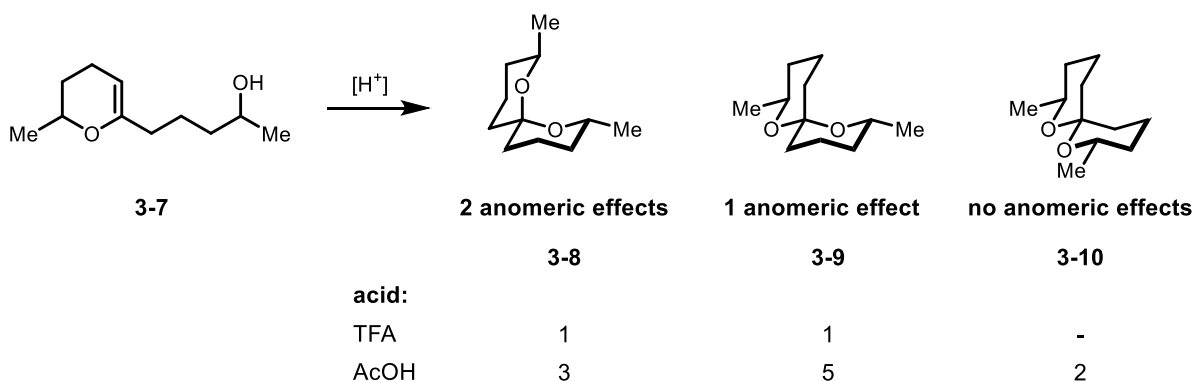
General synthetic strategies for the construction of non-anomeric spiroketals can be classified as thermodynamic or kinetic, depending on whether it relies on thermodynamic equilibration. Accessing the less stable products through thermodynamic means sounds impossible, however the majority of the synthetic approaches for non-thermodynamic spiroketals rely on altering the thermodynamic bias by the utilization of intermolecular hydrogen bonding, chelation effects using different metal salts, substrate specific steric effects, or using some other means. For example, the first total synthesis of spongistatin 1 by the Evans group in 1997 employed a Mg(II) internal chelation strategy to bias the formation of the desired non-thermodynamic spiroketal for the same CD rings (Scheme 3.4a).^[15] Later, in the synthetic route by the Paterson group, the nonthermodynamic CD spiroketal was achieved by allowing the acid-catalyzed thermodynamic equilibration of a spiroketal intermediate which was biased towards the desired single anomeric by an intramolecular hydrogen bond (Scheme 3.4b).^[23]

Scheme 3.4. Examples of thermodynamic acid-catalyzed strategies for nonanomeric spiroketals.



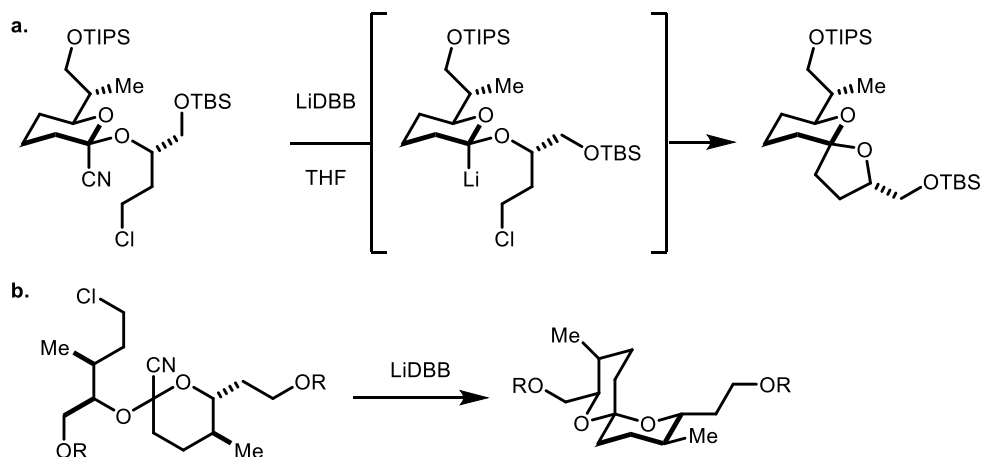
An alternative to the strategies exemplified above is to perform a spiroketalization under non-equilibrating conditions. Acid-catalyzed spiroketalizations under kinetic control have two challenges: 1) the acid catalyst must be strong enough to promote spiroketalizations, and 2) the acid must not be too strong as to allow isomerization of the acid-labile product. Deslongchamps, one of the pioneers of spiroketal chemistry, was the first to discover and report acid-catalyzed spiroketalizations under kinetic control. Treatment of hydroxy enol ethers **3-7** with strong acids such as TFA led to the formation of doubly anomeric **3-8** and singly anomeric **3-9** as a 1:1 mixture. However, exposure to a weaker acid (AcOH), resulted in formation of ~20% of some non-thermodynamic spiroketal **3-10** (Scheme 3.5).

Scheme 3.5. Deslongchamps's acid-catalyzed spiroketalizations under kinetic control.



Most of the synthetic strategies outlined above employ acid catalysts, though several other direct and indirect non acid-catalyzed strategies have been successfully used. For example, Rychnovsky's group was able to construct nonthermodynamic spiroketals by a reductive lithiation followed by a kinetic cyclization sequence. With this method, they were able to access the spiroketal fragment of pectenotoxin 1 (scheme 3.6a),^[47] as well as the CD junction of spirofungin B (Scheme 3.6b).^[52]

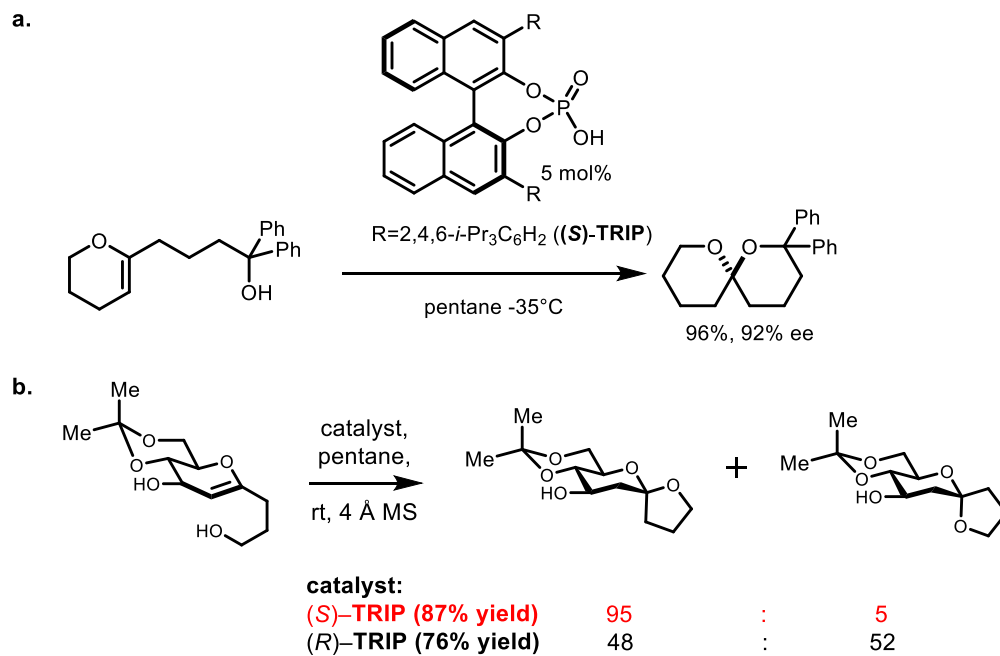
Scheme 3.6. Rychnovsky's reductive spiroketalizations under kinetic control.



As one can imagine, most synthetic methods for the construction of non-thermodynamic spiroketals are highly substrate dependent, since they seek to exploit unique structural features of the synthetic target. A comprehensive review on structure-based synthesis of nonthermodynamic spiroketals was published by the Pihko group.^[1] This highlights the need for the development of general and robust non-thermodynamic spiroketalization strategies.

Contemporaneously with Coric and List,^[53] our group demonstrated that CPAs could be employed as the catalysts for the cycloisomerization of cyclic enol ethers under kinetic control (Scheme 3.7a). In addition, it was observed that non-thermodynamic spiroketals could be obtained in conformationally locked substrates (Scheme 3.7b). However, the substrate scope for this transformation was limited, since tertiary alcohols were required to achieve high enantioselectivities. In collaboration with Dr. Yaroslav Khomutnyk, Grace Winschel, and Zhankui Sun, we sought to unravel the mechanism and origins of enantioselectivity of this CPA-catalyzed spiroketalization, with the hope that the insight provided might contribute to develop more new and better CPA-catalyzed spiroketalizations methods in the future.

Scheme 3.7. Nagorny's CPA-catalyzed spiroketalizations under kinetic control.



3.4 Results and discussion

(This section was adapted from:

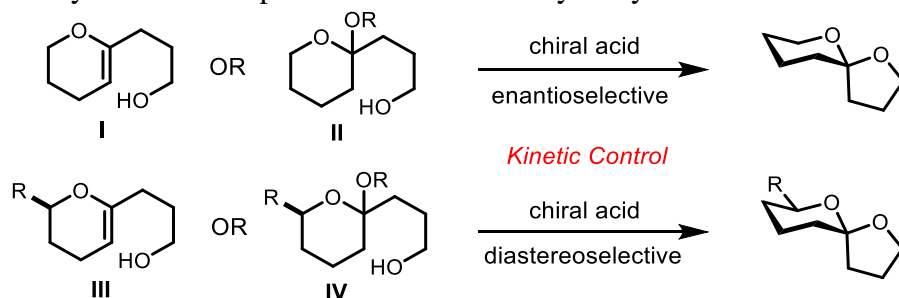
Khomutnyk, Y. Y.; **Argüelles, A. J.**; Winschel, G. A.; Sun, Z.; Zimmerman, P. M.; Nagorny, P. *J. Am. Chem. Soc.* **2016**, *138*, 444.

Experimental information can be found in **Appendix B**)

Initial Optimization Studies.

Although CPAs had been previously employed to catalyze the formation of chiral N,N-,^[54-57] N,O-,^[58] N,S-,^[57,59] and simple O,O-acetals,^[60] no examples of a successful chiral-catalyst-controlled enantioselective or diastereoselective spiroketalization existed at the beginning of these studies. Despite these encouraging precedents, the prospects of using chiral Brønsted acids to promote catalyst-controlled spiroketalizations were unclear considering that spiroketals are significantly more prone to epimerization under acidic conditions. With this in mind, we surmised that the use of cyclic enol ether I or III as the spirocyclization precursor was key in developing this transformation, as the mixed acetal precursors II and IV (Scheme 3.8) are too similar to spiroketals in their ability to ionize under the acidic conditions. Cycloisomerization of enol ethers I and III is easier to achieve under epimerization-free conditions, and the Deslongchamps and Pihko groups had previously utilized weak acids such as acetic acid ($pK_a = 4.7$, H₂O) to promote kinetic spiroketalizations.^[46,61] The same studies also indicated that the reactions catalyzed by stronger trifluoroacetic acid ($pK_a = -0.25$, H₂O) proceeded under thermodynamic control. At the same time, we surmised that the chiral phosphoric acids have intermediate acidities ($pK_a \sim 2$, H₂O) and would be excellent catalysts for kinetic spiroketalizations.

Scheme 3.8. Catalyst control in spiroketalizations of dihydroxyketones.



In order to evaluate the feasibility of this proposal, spiroketalization of substrate **3-11a** to give **3-12a** was investigated (Table 3.1).^[62] Commercially available (*S*)-**TRIP** (**3-13a**) was selected as the initial catalyst for the reaction optimization. In our attempts to optimize the selectivity for the formation of **3-12a**, we encountered significant solvent effects. The reactions conducted in higher-polarity solvents (entries 1–5) resulted in lower levels of stereocontrol, while oxygenated solvents such as tetrahydrofuran (THF) and ethyl acetate significantly retarded the rate of cyclization (entries 2 and 3). At the same time, the spiroketalizations conducted in nonpolar hydrocarbon solvents (entries 7–9) proceeded with higher enantioselectivities and shorter reaction times. The observed solvent effects emphasize the significance of non-covalent interactions between the substrate and chiral phosphoric acid for the productive reaction pathway. More polar, oxygenated solvents (entries 2 and 3) can competitively form hydrogen bonds with the CPA, thereby reducing the complexation with **6a**. At the same time, the less polar solvents favor enhanced hydrogen bonding and other types of non-covalent interactions between **3-11a** and **3-13a**. Other CPAs were screened, but **3-13a** was found superior (entries 9-16). On the basis of these arguments, we surmised that the selectivity for the formation of **3-12a** could be further enhanced at lower reaction temperatures and if the hydrogen-bonding impurities such as water were removed. Although lowering the reaction temperature alone did not significantly affect the

enantioselectivity (entries 17 and 18), the addition of 4 Å MS combined with lowering the temperature to $-35\text{ }^{\circ}\text{C}$ resulted in the formation of **3-12a** with 92% ee (entry 20).

Table 3.1. Initial evaluation of the CPA-catalyzed enantioselective spiroketalization. Experiments were performed by Dr. Yaroslav Khomutnyk.

3-11a $\xrightarrow[\text{solvent, T}]{\text{catalyst 7 (5 mol\%)}}$ **3-12a**

entry	catalyst	solvent	T, $^{\circ}\text{C}$	time, ^b h	ee
1	(S)- 3-13a	CH ₃ CN	rt	0.5	7
2	(S)- 3-13a	THF	rt	12 ^c	10
3	(S)- 3-13a	EtOAc	rt	12 ^c	16
4	(S)- 3-13a	PhH	rt	1	24
5	(S)- 3-13a	Toluene	rt	1	25
6	(S)- 3-13a	CCl ₄	rt	1	40
7	(S)- 3-13a	Hexanes	rt	0.5	63
8	(S)- 3-13a	Cyclohexane	rt	0.5	60
9	(S)- 3-13a	Pentane	rt	0.5	69
10	(R)- 3-13b	Pentane	rt	0.5	-16
11	(R)- 3-13c	Pentane	rt	1	1
12	(R)- 3-13d	Pentane	rt	1	-43
13	(R)- 3-13e	Pentane	rt	1	35
14	(R)- 3-13f	Pentane	rt	1	1
15	(R)- 3-13g	Pentane	rt	1	41
16	(S)- 3-13h	Pentane	0	4	23
17	(S)- 3-13a	Pentane	0	4	73
18	(S)- 3-13a	Pentane, 4 Å MS	-35	40	66
19	(S)- 3-13a	Pentane, 4 Å MS	0	14	84
20	(S)-3-13a	Pentane, 4 Å MS	-35	40	92

3-13a, R = 2,4,6-*i*Pr₃C₆H₂
3-13b, R = 3,5-(CF₃)₂C₆H₃
3-13c, R = 9-anthryl
3-13d, R = 4-(1-Ad)-2,6-*i*Pr₂C₆H₂
3-13e, R = 4-(6-anthryl)-2,6-*i*Pr₂C₆H₂

3-13f, X = NHTf
3-13g, X = OAg

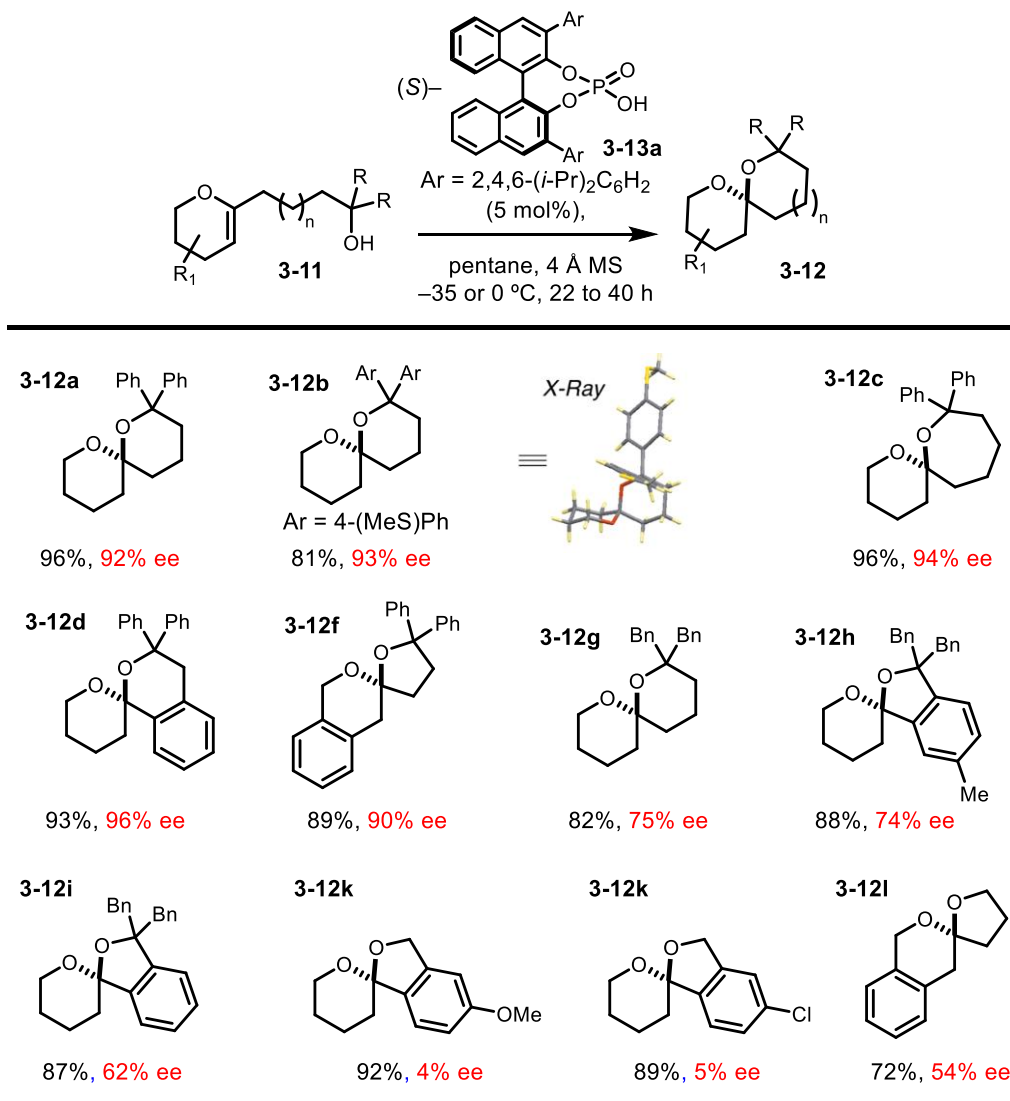
3-13h

^a Phosphoric acids were washed with 6 M HCl after purification by column chromatography. Unless specified otherwise, reactions were performed on a 0.1 mmol scale (0.02 M solution). ^b Time required for the reaction to reach completion. ^c Incomplete conversion.

Enantioselective and Diastereoselective Spiroketalizations.

After the optimal reaction conditions were identified, the scope of the enantioselective spiroketalization was evaluated next (Table 3.2). In addition to the previously evaluated **3-11a**, the cyclic enol ethers **3-11b–k** were synthesized and subjected to the cyclizations leading to **3-12b–k**. The introduction of *p*-MeS substituents on the aromatic rings in **3-11b** and the extension of the tether length in **3-11c** did not affect the reaction yield and selectivity for the corresponding products **3-12c** and **3-12c**. Similarly, the introduction of a fused benzene ring into the side chain (**3-11d**) or into the enol ether ring (**3-11e**) was well-tolerated, and the corresponding products were obtained in excellent selectivities and yields. At the same time, the cyclization of analogous substrates **3-11f–h** containing less rigid Bn substituents at the tertiary alcohol consistently exhibited lower enantioselectivities. Cyclization leading to **3-12g** was found to be more selective (88% yield, 74% ee) than a similar reaction leading to **3-12h** that lacks a methyl group on the aromatic ring (87% yield, 62% ee). These results indicate that further variations in the substrate backbone can potentially enhance the selectivity of the substrates lacking Ph substitution at the nucleophile. This is further reinforced by the observation that primary-alcohol-containing precursor **3-11k** could be cyclized enantioselectively to give **3-12k** (72%, 54% ee) while the reactions with similar substrates **3-11i** and **3-11j** led to almost unselective formation of the corresponding spiroketals **3-12i** and **3-12j**.

Table 3.2. Substrate scope for the CPA-catalyzed enantioselective spiroketalizations. Experiments were performed by Dr. Yaroslav Khomutnyk.



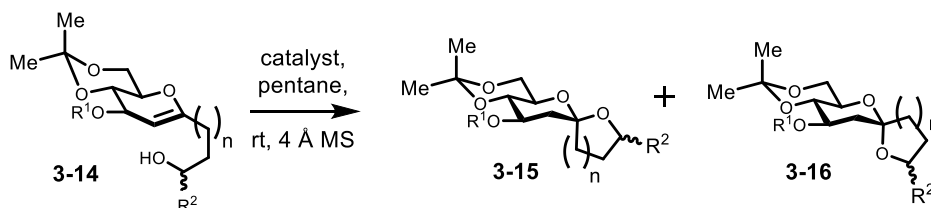
^a Reactions were performed on a 0.1–0.05 mmol scale (0.02 M solution), and the selectivities of these reactions were found to be scale-independent. Catalyst **(S)-3-13a** was used, unless otherwise noted. ^b The reaction was conducted with catalyst **(R)-3-13a**.

The results summarized in Table 3.2 indicate that a chiral catalyst can control the selectivity of the cyclization of achiral substrates **3-11**. However, because the chirality of the substrate may completely override the course of cyclization dictated by the catalyst, the effect of the catalyst on the cyclization of chiral substrates had to be addressed next (Table 3.3).^[62] Since the reactions of carbohydrate-based oxocarbenium ions are highly sensitive to stereoelectronic and steric effects,

conformationally locked D-glucal derivatives (e.g., **3-14a**) were selected for these studies. Upon spiroketalization, these substrates can provide anomericly stabilized thermodynamic products such as **3-16a** or less stable nonthermodynamic spiroketals (**3-15a**). Thus, to evaluate the effect of the chiral catalyst on the course of these cyclizations, substrate **3-14a** was subjected to treatment with (*S*)-**3-13a**, (*R*)-**3-13a**, or the achiral catalyst (PhO)₂PO₂H. Remarkably, the treatment of glycal **3-14a** with catalyst (*S*)-**3-13a** (5 mol %) resulted in a highly diastereoselective cyclization, leading to nonthermodynamic spiroketal **3-15a** (95:5 dr). At the same time, the exposure of **3-14a** to (*R*)-**3-13a** or (PhO)₂PO₂H provided ~1:1 mixtures of nonanomeric and anomeric products **3-15a** and **3-16a**, clearly indicating that the chirality of the catalyst is essential for the selective formation of **3-15a**. Similar trends were observed for other substrates, and catalyst (*S*)-**3-13a** was used for the highly diastereoselective formation of various nonthermodynamic spiroketals (**3-15b–e**) in good yields and diastereoselectivities. Interestingly, the nature of the protecting group at C3 was found to play an important role, and, unlike the formation of **3-15e**, the cyclization leading to **3-15f** was not selective.

The results summarized in Table 3.3 suggest that the cyclizations catalyzed by **3-13a** proceed under kinetic conditions. The non-anomeric spiroketals **3-15** are clearly stable toward both enantiomers of acids **3-13a** for the duration of the reaction (i.e., 14 h). At the same time, when pure **3-15a** was treated with (*S*)-**3-13a** under the reaction conditions, complete epimerization to give **3-11a** was observed after 60 h.

Table 3.3. Substrate scope for the CPA-catalyzed diastereoselective spiroketalization.^a Experiments were performed by Dr. Yaroslav Khomutnyk.



entry	substrate	catalyst	Yield [%]	3-15 : 3-16
1		(<i>S</i>)-3-13a	87 ^b	95 : 5
2		(<i>R</i>)-3-13a	76 ^c	48 : 52
3		(PhO) ₂ PO ₂ H	89 ^c	52 : 48
4		(<i>S</i>)-3-13a	73 ^b	81 : 19
5		(<i>R</i>)-3-13a	83 ^c	33 : 67
6		(PhO) ₂ PO ₂ H	89 ^c	31 : 69
7		(<i>S</i>)-3-13a	85 ^b	90 : 10
8		(<i>R</i>)-3-13a	90 ^c	55 : 45
9		(PhO) ₂ PO ₂ H	80 ^c	45 : 55
10		(<i>S</i>)-3-13a	86 ^b	90 : 10
11		(<i>R</i>)-3-13a	88 ^c	13 : 87
12		(PhO) ₂ PO ₂ H	81 ^c	55 : 45
13		(<i>S</i>)-3-13a	92 ^b	95 : 5
14		(<i>R</i>)-3-13a	90 ^c	23 : 77
15		(PhO) ₂ PO ₂ H	92 ^c	32 : 68
13		(<i>S</i>)-3-13a	42 ^b	51 : 49
14		(<i>R</i>)-3-13a	88 ^c	10 : 90
15		(PhO) ₂ PO ₂ H	91 ^c	43 : 57

^aThe reactions with (*S*)-3-13a (5 mol %) and (*R*)-3-13a (5 mol %) were performed for 14 h, and the reactions with (PhO)₂PO₂H (10 mol %) were performed for 2 h. Longer exposure to (PhO)₂PO₂H (10 mol %) resulted in complete equilibration to give the thermodynamic spiroketals. The cyclizations of 3-14a were performed on different scales without significant variation in selectivity. ^bYield of nonthermodynamic spiroketal 3-15. ^cCombined yield of 3-15 and 3-16.

Mechanistic Considerations.

The above results suggest that **3-13a** is the catalyst of choice for the asymmetric spiroketalization of tertiary-alcohol-containing substrates **3-11** as well as for the diastereoselective cyclization of chiral substrates **3-14** leading to non-anomeric spiroketals **3-15**. Interestingly, the larger size of glycols **3-14** excluded the requirement of using the tertiary-alcohol-based nucleophiles, and **3-13a** could promote the cyclization leading to **3-15** with primary and secondary alcohols as nucleophiles with good-to-excellent selectivities. However, although the aforementioned results provide some crude idea about the scope and limitation of the method, the mechanistic and stereochemical models explaining the origins of the stereocontrol are essential for more general use of these and related transformations.

Despite the fact that CPA-catalyzed transformations invoking oxocarbenium ion intermediates have received significant attention in recent years, very few attempts to understand the mechanisms of such transformations and the factors governing the selectivity have been made.^[63,64] The formation of stable oxocarbenium ion intermediates has been proposed in the recent computational studies of N-triflyl phosphoramidate-catalyzed cyanohydrin ether formation^[63] and CPA-catalyzed Petasis–Ferrier rearrangements.^[64] However, instances where theoretical studies identified alternative mechanisms not involving the formation of oxocarbenium ion intermediates have also been documented. Thus, the recent studies of the acid-catalyzed enantioselective formation of pyrrolidines by the Toste group^[65] and piperidines by our groups^[62] identified alternative pathways involving covalently linked thiophosphate (or phosphate) intermediates rather than the corresponding high-energy carbenium or oxocarbenium ion pairs. The oxocarbenium-based mechanisms for acid-catalyzed acetal formation have indeed received widespread acceptance; however, transformations of this type not involving oxocarbenium ion

intermediates have also been documented. Accordingly, the Tan group observed an S_N2-like concerted (rather than S_N1-like oxocarbenium-based) mechanism for the methanol-promoted spirocyclization of glycal epoxides.^[66] In line with these findings is the theoretical study of the thiourea-catalyzed tetrahydropyranylation reaction by Kotke and Schreiner,^[67] in which a concerted asynchronous addition of alcohol nucleophiles rather than the formation of a discrete oxocarbenium ion intermediate is proposed. Similarly, the true nature of the glycosylation reaction intermediates has been a subject of long-standing debates.^[68] Both the ionic S_N1-like and concerted S_N2-like mechanisms are commonly invoked to explain the outcome of glycosylation reactions, and there is strong evidence that nonionic mechanisms are operational in some instances. For example, the Crich group has provided overwhelming evidence demonstrating that 4,6-O-benzylidenedirected β-mannosylation reactions proceed through covalently bound glycosyl triflates rather than through discrete glycosyl oxocarbenium ion intermediates.^[69,70]

With these prior observations in mind, we considered several different mechanistic pathways for the CPA-catalyzed enantioselective spiroketalization reaction (Scheme 3.9). The reaction mechanisms proceeding through an oxocarbenium ion or covalently linked phosphate intermediate and a concerted mechanism with concomitant C–H and C–O bond formation were viewed as the most prominent options. Both the counterion orientation and the relative stereochemistry of the forming C–H and C–O bonds are crucial for understanding the origins of stereoinduction and developing a stereochemical model. At the same time, these important factors are typically omitted from the mechanistic considerations. Thus, to our knowledge, no information on the selectivity of the C–H/C–O bond addition has been available prior to this work. In theory, the cyclization proceeding via an oxocarbenium ion intermediate can occur through two different modes. In the first mode of cyclization, the C–H and C–O bonds form from different faces of the

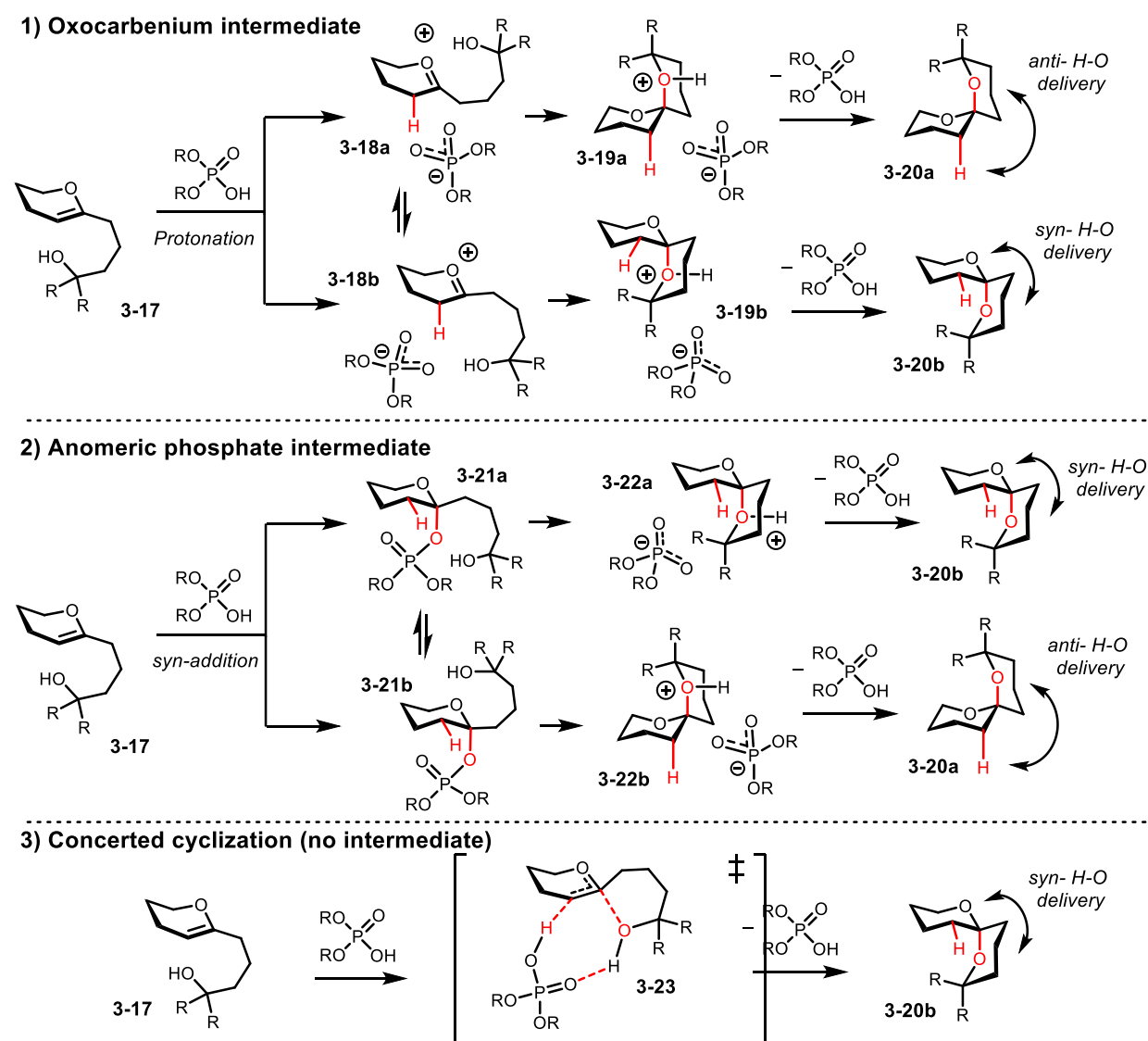
molecule (i.e., the pathway proceeding through **3-18a/3-19a/3-20a**). Alternatively, the pathway proceeding through **3-18b/3-19b/3-20b** and resulting in *syn* protonation/C–O bond formation can be envisioned. Similarly, the reaction proceeding through the anomeric phosphate intermediate conformation **3-21a** or **3-21b** can happen through a retentive or inversive (S_N2 -like) mechanism. An *anti* relationship between the formed C–H and C–O bonds is expected for the inversive mechanism (i.e., the **3-21a/3-22a/3-20a** pathway), and a *syn* relationship between the formed C–H and C–O bonds is expected for the retentive mechanism (i.e., the **3-21b/3-22b/3-20b** pathway). Unlike in the aforementioned mechanistic options that may lead to both selective product formation and mixtures of *syn* and *anti* products, the concerted mechanism, in which the phosphoric acid acts as the bifunctional catalyst, can produce only the *syn* product **3-20b**.

Studies of Diastereoselective Cyclizations.

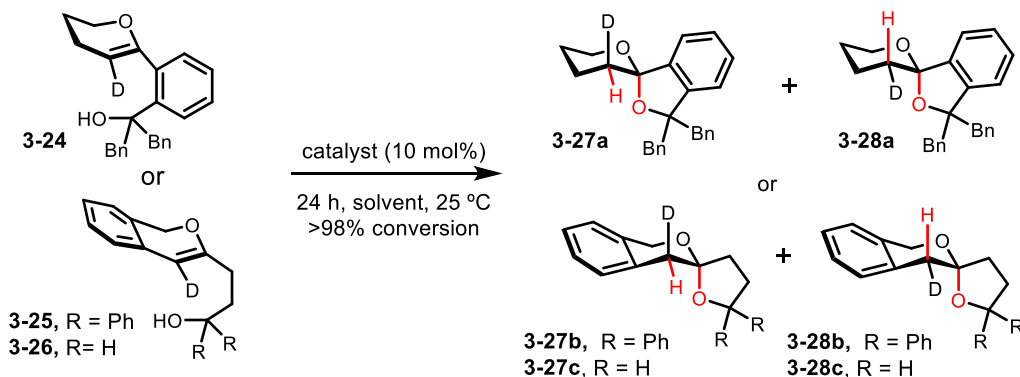
With these considerations in mind, we designed and conducted experiments to distinguish between the diastereodivergent *syn* and *anti* spiroketalization modes (Scheme 3.10). To obtain this information, we generated deuterated cyclic enol ethers **3-24** - **3-26** and subjected them to the cyclization in a nonpolar solvent (i.e., toluene, dichloromethane, or pentane) using (*S*)-**3-13a**, chloroacetic acid, TFA, or *p*-toluenesulfonic acid (*p*-TSA) as the catalyst. The outcomes of these reactions were monitored using ^2H (D) NMR (107 MHz). As per our discussion above (i.e., Scheme 3.9), the cyclization of **3-24** may lead to the *syn* product **3-27a** or the *anti* product **3-28a**. Similarly, the cyclizations of **3-25** and **3-26** may provide the *syn* diastereomers **3-27b** and **3-27c** or the *anti* diastereomers **3-28b** and **3-28c**, respectively. Remarkably, only the *syn* products **3-27a–c** were detected in the experiments with weaker acids (i.e., (*S*)-**3-13a** and $\text{ClCH}_2\text{CO}_2\text{H}$; Scheme 3.10, entries 1–4); however, unselective formation of the *syn* and *anti* products was

detected for the *p*-TSA and CF₃CO₂H-catalyzed reactions (entries 5 and 6). The absence of the selectivity for the *p*-TSA-catalyzed reactions is attributed to rapid epimerization under the cyclization conditions. Thus, subjecting diastereomerically pure **3-27b** to *p*-TSA at -40 °C resulted in rapid isomerization to a 1:1 mixture of **3-27b** and **3-28b** after 15 min. Finally, a substantial inverse kinetic isotope effect (KIE = 0.85) was observed for the cyclization of **3-26c** into **3-27c** (Scheme 3.11).

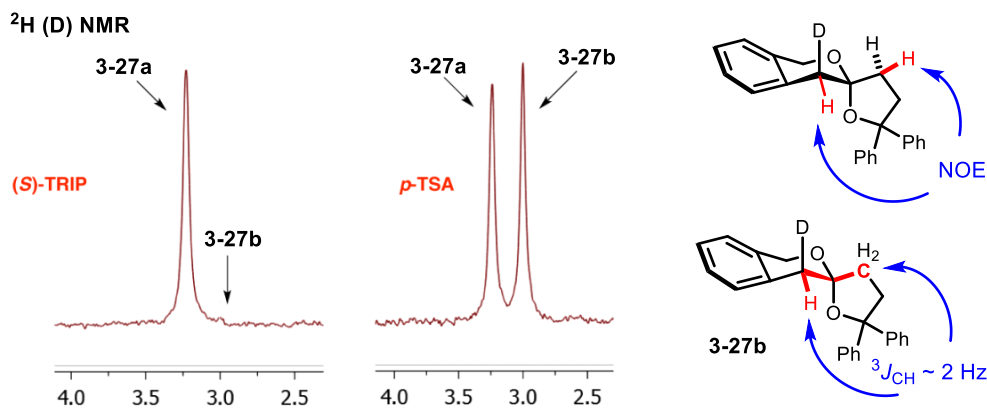
Scheme 3.9. Potential mechanisms of CPA-catalyzed spiroketalizations



Scheme 3.10. Diastereoselective spiroketalization of deuterium-labeled substrates.^a Experiments were performed by Dr. Yaroslav Khomutnyk.

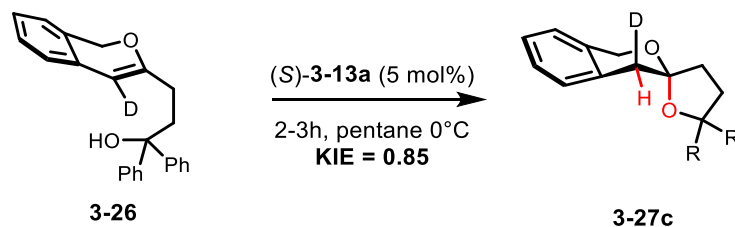


entry	catalyst	solvent	3-27a : 3-28a	3-27b : 3-28b	3-27c : 3-28c
1	(S)-3-13a	toluene	99 : 1	99 : 1	99 : 1
2	(S)-3-13a	CH ₂ Cl ₂	99 : 1	99 : 1	99 : 1
3	(S)-3-13a	pentane	99 : 1	99 : 1	99 : 1
4	ClCH ₂ CO ₂ H ^b	pentane	99 : 1	99 : 1	99 : 1
5	<i>p</i> -TSA ^c	CH ₂ Cl ₂	1 : 1	1 : 1	1 : 1
6	CF ₃ CO ₂ H ^c	pentane	1 : 1	1 : 1	1 : 1



^a The reactions were performed on a 0.5–0.05 mmol scale, and each experiment was reproduced twice. D (²H) NMR spectra were recorded at 107 MHz using a Varian VNMRs-700 spectrometer. The observed diastereoselectivities were found to be conversion-independent. ^b 10 mol % catalyst was employed. ^c The racemization reactions were found to be faster than the cyclization reactions under these conditions.

Scheme 3.11. KIE determination for 3-26. Experiments were performed by Dr. Yaroslav Khomutnyk.



The relative configurations of **3-27a–c** were established using nuclear Overhauser effect (NOE) and two-dimensional heteronuclear NMR studies, including $^3J_{\text{CH}}$ determination by SelEXSIDE,^[71] and some of the key signals are depicted in Scheme 3.10. Despite the numerous studies on the spiroketalization mechanism and the widespread use of spiroketals in organic synthesis, the results in Scheme 3.10 represent the first documented evidence suggesting that the kinetic spiroketalization of cyclic enol ethers in nonpolar solvents proceeds via highly selective *syn* H–O addition. To investigate whether the *syn* addition is more general and could be observed in intermolecular acetalization reactions, the reaction of D-labeled dihydropyran (**3-29**) and *p*-methoxybenzyl alcohol was investigated next (Table 3.4).

Table 3.4. Intermolecular acetalization with deuterated electrophile.^a Experiments were performed by Dr. Yaroslav Khomutnyk.

entry	catalyst	solvent	T [°C]	time [h]	3-30a:3-30b
1	(S)- 3-13a	DCM	rt	12	1:1
2	3-31	pentane	0	48	1:1
3	3-31	benzene	rt	12	1:1
4 ^b	ClCH ₂ CO ₂ H	neat	rt	48	-
5 ^c	3-32	benzene	0	42	1:1

Ar=2,4,6-*i*Pr₃C₆H₂
(S)-3-13a

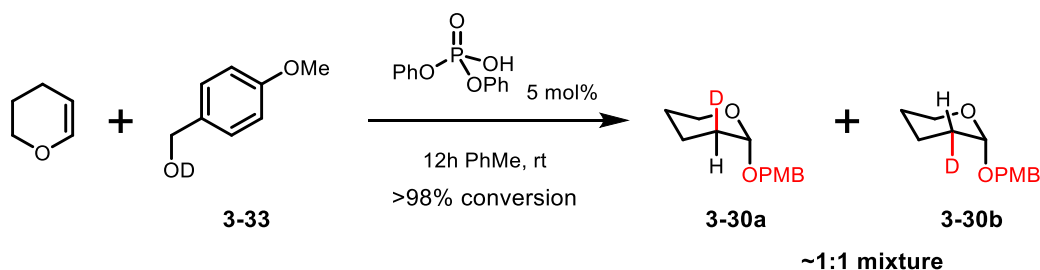
3-31

3-32

^a The reactions were performed on a 0.15–0.59 mmol scale, and each experiment was reproduced twice. D (²H) NMR spectra were recorded at 107 MHz on a Varian 700 spectrometer. The observed diastereoselectivities were found to be conversion-independent. ^b No reaction was observed with 10 mol % catalyst. ^c 2 mol % catalyst **27** was employed.

As in the spiroketalization studies with deuterium-labeled cyclic enol ethers, the formation of two diastereomeric products, *syn*-**3-30a** and *anti*-**3-30b**, is also expected in this case. The phosphoric acids (*S*)-**3-13a**, **3-31**, chloroacetic acid, and Schreiner's thiourea **3-32** were selected as the catalysts. The formation of **3-30** promoted by these catalysts is expected to be irreversible (i.e., kinetic) under most conditions since the tetrahydropyranyl (THP) acetals possess significantly higher stability than typical spiroketals. Interestingly, tetrahydropyranylation reactions were found to be dissimilar to spiroketalization reactions. Thus, the reaction of *p*-methoxybenzyl alcohol with **3-29** produced an approximately 1:1 mixture of products with Brønsted acids (*S*)-**3-13a** and **3-31** (entries 1–3), but no reaction was observed with chloroacetic acid (entry 4). Similar results were observed when unlabeled dihydropyran was reacted with deuterium enriched *p*-methoxybenzyl alcohol (**3-33**) using diphenylphosphoric acid **3-31** as the catalyst (Scheme 3.12).

Scheme 3.12. Intermolecular acetalization with deuterated nucleophile. Experiments were performed by Dr. Yaroslav Khomutnyk.



As before, the nonselective formation of both *syn* and *anti* products was observed in this case. Tetrahydropyranylation of methanol catalyzed by thiourea catalyst **3-32** has been investigated computationally, and the concerted asynchronous addition of methanol proceeding through a polar transition state with oxyanion hole stabilization by **3-32** has been proposed.^[67] Considering that a concerted asynchronous addition of an alcohol to dihydropyran **3-29** should result in the selective formation of *syn*-**3-30a**, we decided to investigate the outcome of the thiourea

3-32-catalyzed formation of **3-30** (Table 3.4, entry 5). Surprisingly, **3-32**-catalyzed acetalization of **3-29** and *p*-methoxybenzyl alcohol produced an equimolar mixture of *syn*-**3-30a** and *anti*-**3-30b** in benzene. Since the formation of *syn*-**3-30a** and *anti*-**3-30b** is not reversible under the reaction conditions, the outcome of the experiments in Table 3.4 is consistent with the formation of a relatively long-lived, solvent-separated (rather than contact), oxocarbenium/stabilized alkoxide ion pair. This ion pair could undergo nonselective association, and both faces of oxocarbenium ion are equally exposed to the reaction with the oxyanion nucleophile.

Hammett Studies.

The above results indicate that the intramolecular and intermolecular acetalization reactions proceed through different mechanisms. To further differentiate between the mechanistic options outlined in Scheme 3.9, a Hammett study was executed for the cyclization of aromatic enol ethers **3-34** leading to spiroketals (Figure 3.6). Thus, the rate constants for the cyclizations of substrates **3-34** with either electron-withdrawing (i.e., X = Cl, F) or electron-donating (i.e., X = CH₃O, CH₃) substituents as well as the unsubstituted substrate (X = H) were measured at low conversion (Figure 3.6A). The obtained $\log(k_{\text{obs}}/k_{\text{H}})$ values for the electronically varied substrates **3-34** displayed an excellent linear correlation ($R^2 = 0.98$) when plotted against the corresponding known σ values. These results allowed for the measurement of ρ value to be -2.9 , which is consistent with a build-up of positive charge in the transition state (TS) of the rate-limiting step ($\rho < -0$, see Chapter 1, section 1.2). It should be noted that the obtained ρ value is lower than the one expected for an S_N1-like mechanism involving rate-limiting formation of a fully charged oxocarbenium ion intermediate. In this regard, the Tan group has investigated the acid-catalyzed epimerization of kinetic D-glucal-derived spiroketals structurally similar to **3-34** and obtained $\rho =$

-5.1, which is more in line with a rate-limiting ionization step than the ρ value obtained in these studies.

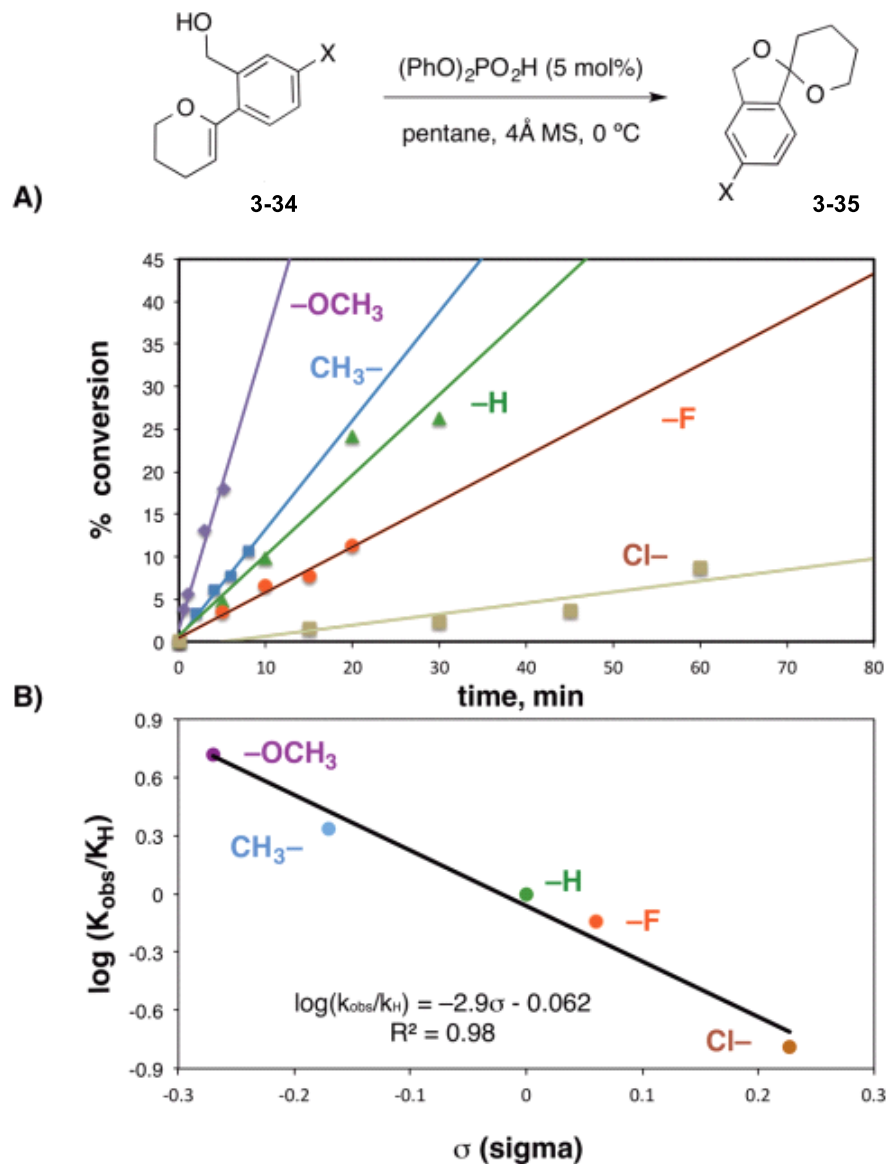


Figure 3.6. Hammett studies for the phosphoric acid-catalyzed spiroketalizations of enol ether of hydroxy enol ethers. Experiments were performed by Dr. Yaroslav Khomutnyk. A. Rates of conversion of **3-34** with $(\text{PhO})_2\text{PO}_2\text{H}$ (5 mol %) as the catalyst in pentane at 0°C. B. Hammett plot exhibiting a linear correlation for the electronically varied substrates **3-34** ($\rho = -2.9$).

The results of the aforementioned studies shed some light on the mechanism of the CPA-catalyzed spiroketalization reactions. Thus, the observed highly diastereoselective *syn* H–O delivery, the significant inverse secondary KIE of 0.85 for substrate **3-26**, indicating that rehybridization happens in the rate-limiting step, and the accumulation of positive charge in the TS of the rate-limiting step observed in the Hammett study all speak against the formation of the covalent anomeric phosphate intermediates **3-21** (Scheme 3.9). This is further reinforced by the fact that *syn* H–O delivery is observed not only for the phosphoric acid catalysts but also for chloroacetic acid. The relatively small ρ value and diastereoselective *syn* H–O delivery are also not consistent with the long-lived oxocarbenium ion intermediates **3-18** but are more in accord with a highly asynchronous concerted mechanism proceeding through the polarized TS **3-23** (Scheme 3.9). At the same time, the scenarios involving the formation of short-lived oxocarbenium/ phosphate contact ion pair **3-18b** or phosphate **3-21** cannot be completely ruled out with the obtained experimental data. These distinctions, however, can be done on the basis of density functional theory (DFT) calculations and molecular dynamics studies that would help to identify the pathway with the lowest energy and provide information on the average lifetime of the TS or intermediate involved. With these considerations in mind, we undertook the studies described in the next section.

Computational Studies

Asymmetric spiroketalization with chiral phosphoric acids may proceed through one or more of the mechanisms depicted in Scheme 3.9, of which the most classical one is mediated by an oxocarbenium intermediate. Experimental analysis of the mechanism provided strong evidence against *anti* H–O delivery (to yield **3-20a**), but the mechanisms resulting in **3-20b** could not be

ruled out. To gain further insight into the mechanism, the transformation was studied in depth using quantum-chemical calculations. Reaction mechanisms in relatively large systems with many flexible degrees of freedom, such as the present catalytic system, are especially difficult to characterize using reaction path optimization tools. To overcome these challenging cases, the Zimmerman group developed the growing string method (GSM) to simultaneously search for reaction paths and transition states (See Chapter 1, section 1.3).^[72–74] By restricting the search to find a transition state within a series of structures along a minimum energy path from reactants to products, GSM can efficiently locate transition states on highly flat energy surfaces. When our tools were applied to the asymmetric CPA-catalyzed formation of piperidines, an accurate description of the reaction selectivity was obtained that invoked a two-step mechanism proceeding through a chiral phosphate acetal intermediate.^[75] In the piperidine formation mechanism and the present spiroketalization, GSM is especially useful in locating challenging asynchronous and concerted transformations because of its flexible treatment of the reaction pathway tangent vector. Prior to the use of GSM to locate reaction pathways, a preliminary study of the diphenyl hydrogen phosphate-catalyzed spiroketalization of a simplified enol ether leading to 1,7-dioxaspiro[5.5]undecane was performed using the Zimmerman group's combinatorial reaction discovery procedure.^[76,77] The results suggested that the concerted pathway could compete with the phosphate-mediated and S_N1-like mechanisms.

Following these preliminary results, more rigorous studies were performed that involved an initial extensive exploration of possible orientations of the catalyst–product complex for three different systems: the diphenyl phosphoric acid **3-31**-catalyzed 6,6-spiroketalization, the **3-31**-catalyzed 6,5-spiroketalization, and the CPA **3-13a**-catalyzed 6,6-spiroketalization. Reaction path exploration and exact transition state searches were performed using GSM for each of the three

types of mechanisms shown in Scheme 3.9. The resultant intermediates and transition states were corrected for thermodynamics and solvent effects (pentane). Reported energies are solvent-phase free energies with thermodynamic corrections at 298 K (diphenyl hydrogen phosphate catalyst system) and 238 K (**3-13** catalyst system) obtained at the ω B97X-D/SMD/6-31G** level. To discriminate between the three mechanisms shown in Scheme 3.9, the transformation leading to a 6,6-spiroketal (substrate **3-11a**) was investigated first using a model diphenyl hydrogen phosphate catalyst. While this initial study did not use a chiral catalyst, the lowest-barrier pathway unveiled by these simulations was further examined with the full catalyst (*vide infra*). Before examining the phosphate-mediated and oxocarbenium pathways, 17 concerted pathways leading to thermodynamic and nonthermodynamic spiroketals were investigated. The most favored pathway produces a nonthermodynamic spiroketal (only one anomeric effect present) that can readily convert to the more stable thermodynamic spiroketal, as shown in Figure 3.7. The reaction pathway is concerted and asynchronous: from the substrate alcohol to phosphate H-bonded complex, an initial protonation of the enol ether occurs at the transition state (TS1). Additionally, the transition state shows a chair-like geometry involving the alcohol oxygen and the electrophilic carbon with a C–O distance of 2.70 Å. After the transition state, synchronous deprotonation and cyclization occur. The initial spiroketal is formed in a chair-boat conformation, which can readily rearrange to a more stable nonthermodynamic chair–chair conformation and ultimately, by a ring flip, to the most thermodynamically stable spiroketal. The Mulliken charges on the enol ether oxygen and electrophilic carbon (provided in Figure 3.7) show a significant buildup of positive charge at TS1 ($\Delta\Sigma Q = 0.247$) that is slightly smaller than the sum of charges of a bare oxocarbenium ion solvated in n-pentane ($\Delta\Sigma Q = 0.271$). The activation barrier for this transformation was 16.0 kcal/mol above the catalyst–substrate complex, which is fully consistent with a mechanism operative at or below

room temperature. It should be noted that the dual function of the phosphoric acid as both a Brønsted acid and a Lewis base is efficiently exploited in this mechanism, as is evident in the rate-determining TS shown in Figure 3.7. Although the product initially formed is predicted to be the nonthermodynamic spiroketal, this is only relevant in conformationally locked systems such as the glucal derivatives shown in Scheme 3.9, since otherwise the thermodynamic spiroketal is readily accessed by a ring flip.

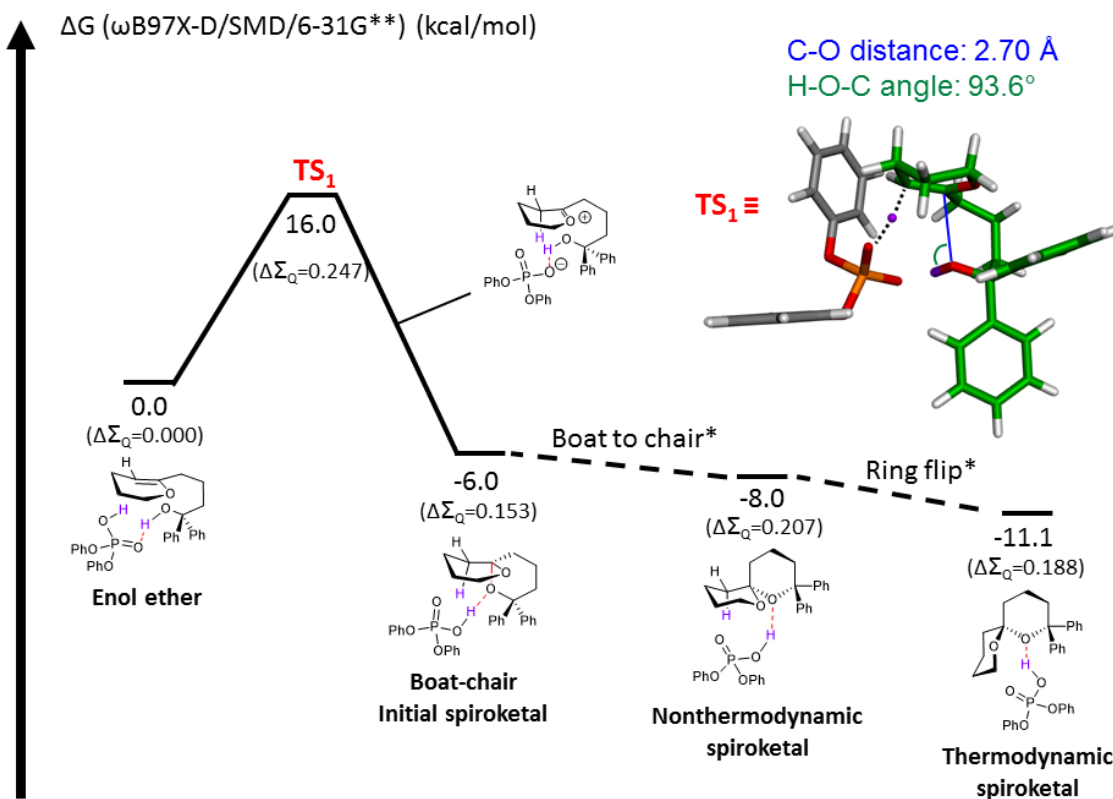


Figure 3.7. Concerted asynchronous mechanism for the ring closure of the model system. The values in parentheses correspond to the differences in the sum of the Mulliken charges on the enol ether oxygen and electrophilic carbon with respect to the starting complex. Barriers indicated by * were not calculated.

The anomeric phosphate-mediated pathway was also examined using the diphenyl catalyst model system, and different orientations of the catalyst were explored for this mechanism. The attack of each phosphate oxygen was examined, and the lowest-energy pathway relevant to this mechanism is depicted in Figure 3.8. The initial orientation of the catalyst is similar to the

concerted pathway described above, but the alcohol is not positioned in such a way that ring closure can readily occur. The formation of the anomeric phosphate intermediate instead proceeds through a concerted asynchronous mechanism. As initial protonation of the enol ether creates an ionic transition state and the alcohol moiety is further away from the electrophilic site, attack of the hydrogen-bonded oxygen of the phosphate can form an axial bond. The formation of the phosphate intermediate has a barrier of 20.6 kcal/mol (TS2), and its *syn* displacement by the nucleophilic alcohol to afford the spiroketal has a barrier of 20.7 kcal/mol (TS3) (the *anti* phosphate displacement likely involves more than one phosphate and was not modeled). Once the phosphate intermediate is formed, there is not a large preference for the immediate formation of a thermodynamic as opposed to a nonthermodynamic spiroketal. In fact, although Figure 3.8 shows the sequence for the formation of the thermodynamic spiroketal, the phosphate could collapse to form a nonthermodynamic spiroketal (TS4) with a barrier of 21.1 kcal/mol.

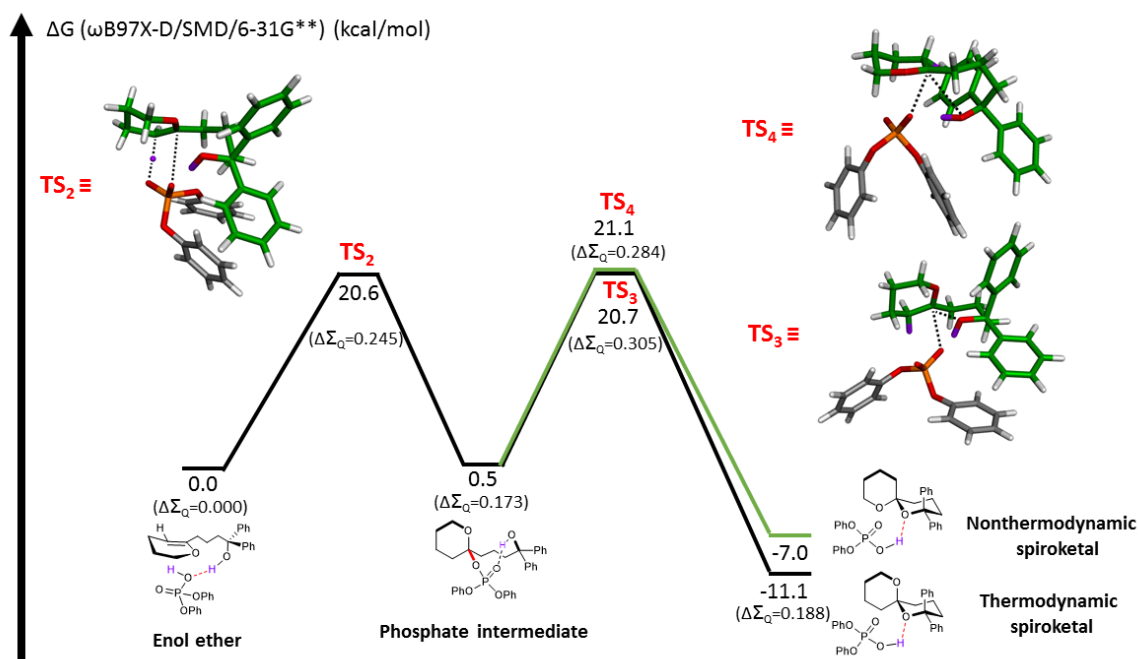


Figure 3.8. Anomeric phosphate mechanism for the model system. The energies of important stationary points are shown in kcal/mol. The values in parentheses correspond to the differences in the sum of the Mulliken charges on the enol ether oxygen and electrophilic carbon with respect to the starting complex.

The difference of 4.6 kcal/mol between the barriers for the concerted and anomeric phosphate mechanisms suggests that the phosphate mechanism is uncompetitive. To determine whether the concerted mechanism was also operative for five membered-ring formation, reactions leading to a 6,5-spiroketal (**3-26c**) were examined. Not surprisingly, the data show that the concerted mechanism ($E_a = 13.8$ kcal/mol) is favored over the anomeric phosphate path ($E_a = 22.9$ kcal/mol for spiroketal formation by *syn* displacement of the phosphate intermediate). The build-up of positive charge on the substrate and the asynchronicity of the changes in bonding are similar to those in the 6,6-spiroketalization. Finally, the KIE of 0.96 calculated for the concerted mechanism was in qualitative agreement with the experimentally measured value of 0.85.

The study of an oxocarbenium-mediated mechanism proved challenging because repeated efforts to optimize stationary points for oxocarbenium intermediates resulted in their collapse to the reactant or product structures. This observation, however, makes sense in light of the proposed concerted mechanism for spiroketalization, where the TS itself is ionic (oxocarbenium-like). Given that an unstable oxocarbenium-like structure is initially formed along the concerted path, we turned to molecular dynamics (MD) simulations to quantify the lifetime of this structure. If a stable oxocarbenium intermediate were possible, it would form after protonation of the substrate and could be identified by MD simulations following the protonation TS. Therefore, trajectories were sampled using quasiclassical initial velocities starting at the concerted TS structure to accurately mimic the experimental conditions. The plot of the C–O distance against time for the product's new C–O connection (Figure 3.9A) shows how most of the 100 MD runs proceed from the TS to the product. After removal of the trajectories that recrossed to the reactant species, Figure 3.9B shows the progression of product-forming trajectories to the ring-closed structures. Of the 71 runs that resulted in product, an average time of 519 fs was required to form the spiroketal. No persistent

oxocarbenium species were formed in any of the trajectories, including seven trajectories that needed to be run to 1.5 ps in order to complete product formation. This short time frame is consistent with the concerted asynchronous mechanism derived by GSM without a stable intermediate along the pathway. Additionally, the trajectories show that the alcohol deprotonation and ring closure occur synchronously, also in agreement with the reaction path from GSM. This occurs as a result of activation of the alcohol by the Lewis basic anionic oxygen of the catalyst, which quenches the buildup of positive charge on the alcohol oxygen by simultaneously deprotonating it while it forms the C–O bond.

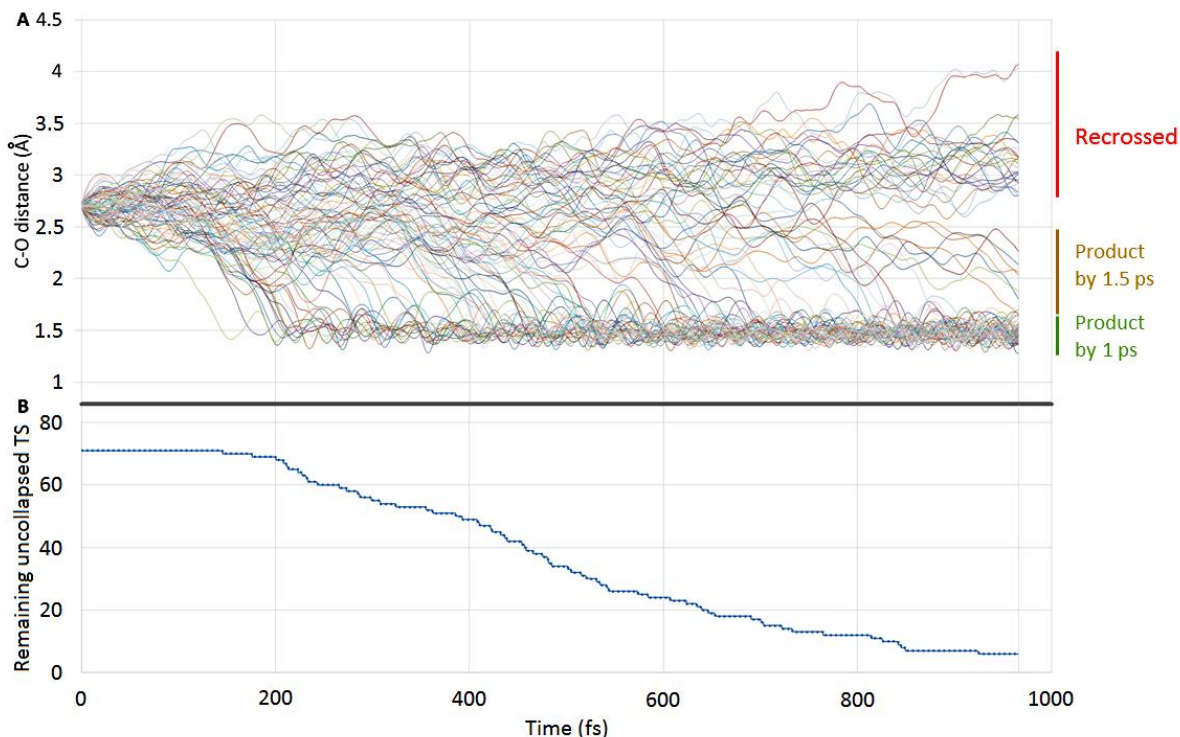


Figure 3.9. Molecular dynamics on the TS of the concerted pathway for the model system. Each line represents one of the 100 independent runs. A. The new ring’s C–O distance is plotted against time. B. The number of productive (71), but yet uncollapsed TSs is plotted against time.

Having established a concerted yet asynchronous mechanism for spiroketalization with the model diphenyl catalyst system, we next studied the reactions of substrate **3-11a** and chiral phosphoric acid **3-13a**. Specifically, formation of the (*R*)-spiroketal was modeled to determine the

key interactions dictating the stereoselectivity of the reaction. Orientations of the catalyst analogous to those in the diphenyl phosphoric acid system were considered. To our delight, we found a 1.5 kcal/mol difference between the lowest computed activation barriers for the (**R**)-**3-13a**-catalyzed and (**S**)-**3-13a**-catalyzed concerted spirocyclizations, with the (**S**) catalyst chirality being favored (see Figure 3.10). Since the (**R**)-spiroketal was the designated simulation product, this result is in agreement with the chirality of the product formed in the experiment. Using a temperature of 238 K, we proceeded to calculate the expected enantiomeric excess, which is given by

$$ee = \frac{\exp\left(\frac{\Delta G^{\text{TS}}}{RT}\right) - 1}{\exp\left(\frac{\Delta G^{\text{TS}}}{RT}\right) + 1}$$

where ΔG^{TS} is the energy gap, R is the gas constant, and T is the absolute temperature. The computed enantiomeric excess is 92%, which exactly matches the experimental result.^[62]

While this is a very promising result, it is only accurate because the intrinsic errors in quantum-chemical simulation have largely canceled one another out. However, this agreement has been seen in other applications of quantum-chemical methods to a number of stereoselective transformations.^[78-80] The extensive study of the PES by careful sampling of the driving coordinates and the end points of the strings, which included five different approaches of the catalyst to produce either thermodynamic (two axial C–O bonds) or nonthermodynamic (two equatorial C–O bonds and both combinations of 1 axial and 1 equatorial C–O bond) spiroketals, as well as the fact that the comparison between the lowest-energy pathways for the two catalyst chiralities gives the proper selectivity, gives us confidence in our method and results.

A description of the predicted mechanism and its associated stereochemical model follows. In the first step of the predicted concerted asynchronous mechanism, the catalyst, irrespective of its chirality, is initially oriented in such a way that the phosphate oxygen can hydrogen-bond with the tertiary alcohol, while the Brønsted acidic hydrogen is aligned to add to the enol ether. As with the diphenyl catalyst model system, protonation of the enol ether occurs at the transition state for both catalyst chiralities. Also coherent with the diphenyl system, there is a considerable buildup of positive charge on the substrate at the TS compared with the enol ether–catalyst complex, in agreement with the experimental data on the mechanism (Hammett and secondary KIE experiments). For both catalyst chiralities, deprotonation of the nucleophilic oxygen and spirocyclization occur simultaneously following protonation, as observed for the diphenyl hydrogen phosphate model system. The cyclization occurs through a six-membered chair geometry to produce an initial boat-chair spiroketal that initially relaxes to a nonthermodynamic spiroketal and finally, by means of a ring flip, to the thermodynamic conformation. The relevant stationary points on the PES, disregarding the boat-chair spiroketal and the later isomerization to a thermodynamic product, are shown in Figure 10. While in this case the conformation of the immediately formed spiroketal is not vital (its equilibration to a more stable conformer is unimpeded), in conformationally locked structures it would be of importance. This mechanism shows how CPA catalysis can be used to form nonthermodynamic spiroketals with kinetic control. A major difference between the TS structures that explains the kinetic origin of the enantioselectivity is the interaction of the 2,4,6-triisopropylphenyl groups at the 3- and 3'-position of **3-13a** with the phenyl rings of the tertiary alcohol of the substrate.

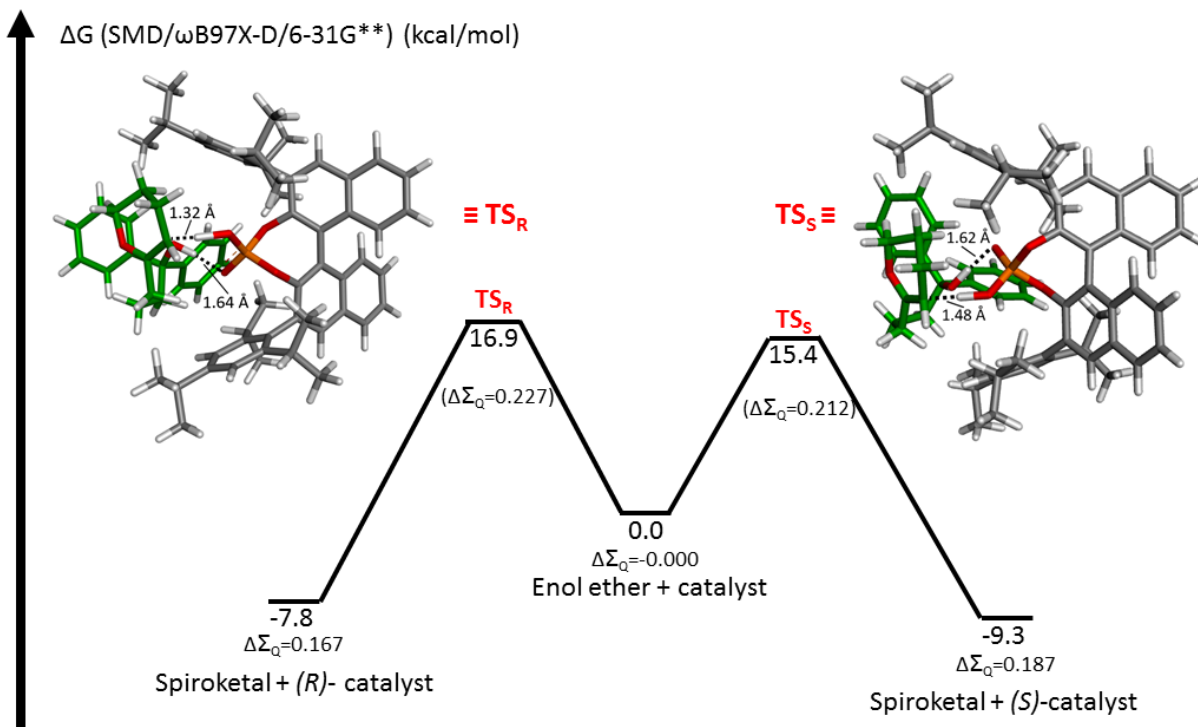


Figure 3.10. Comparison of the activation barriers for the *(R)*- and *(S)*-3-13a-catalyzed spiroketalizations. The insets depict the transition state structures. The values in parentheses correspond to the differences in the sum of the Mulliken charges on the enol ether oxygen and electrophilic carbon with respect to the starting complex.

Figure 3.11 shows the quadrant-based frontal perspective commonly used in stereochemical models involving CPAs and popularized by Himo^[81] and Terada.^[82] From this perspective, the diastereomeric relationship of the substrate-*(R)*-TRIP (TS_R) and substrate-*(S)*-TRIP (TS_S) spiroketalization TS s is made clear. At the TS , the substrate is arranged in such a way that protonation of the enol ether can take place, yet the positive charge being built in the electrophilic carbon is stabilized by its interaction with the alcohol oxygen. This is best achieved when the alcohol appendage adopts a chair-like geometry (Figure 3.11, top left diagram), in preparation for the asynchronous cyclization, and the phenyl rings are not located in the bulky quadrants near the catalytic site. To achieve this, the dihydropyran core is arranged in a different orientation for TS_R and TS_S . The alcohol-containing side chain in TS_R adopts a less ideal chair-like geometry because of unfavorable steric interactions between the phenyl rings of the substrate

and the ortho and para substituents on the aryl groups of the CPA. This is reflected by a longer distance between the nucleophilic oxygen and the electrophilic carbon (2.76 \AA for TS_R vs 2.50 \AA for TS_S) and a less directed angle for electronic interaction (87° H–O–C angle for TS_R vs 117° for TS_S). Figure 3.12 provides a perspective focusing on these key steric interactions in TS_R . Substitution of the phenyl rings on the tertiary alcohol with more flexible benzyl groups would be expected to relieve the steric congestion at TS_R and result in a decreased ee, as observed experimentally.

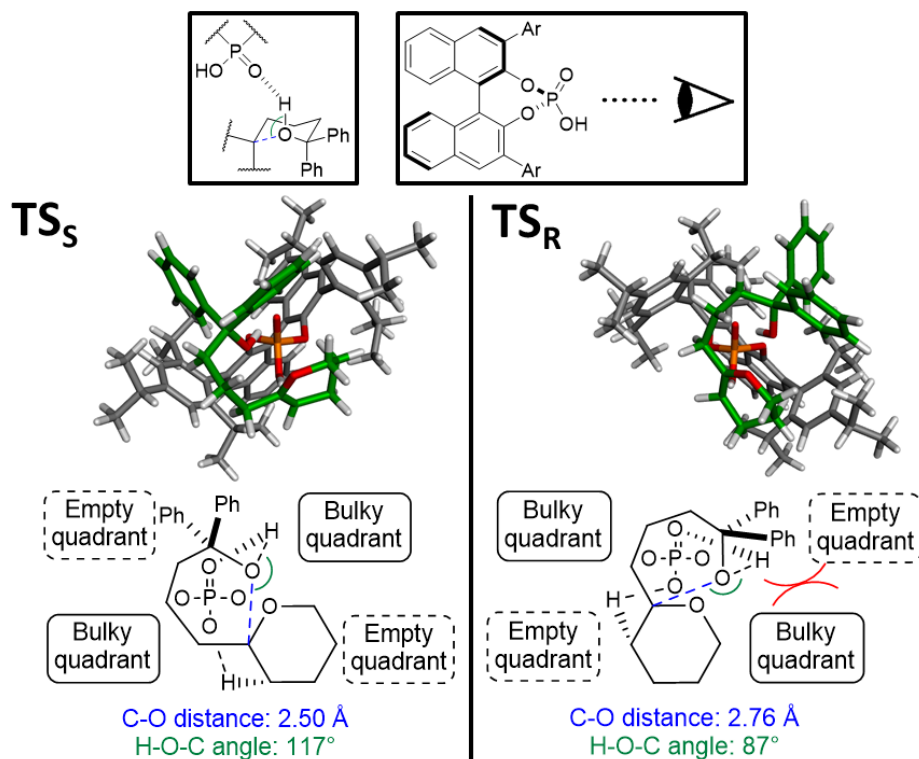


Figure 3.11. Comparison of TS_S and TS_R .

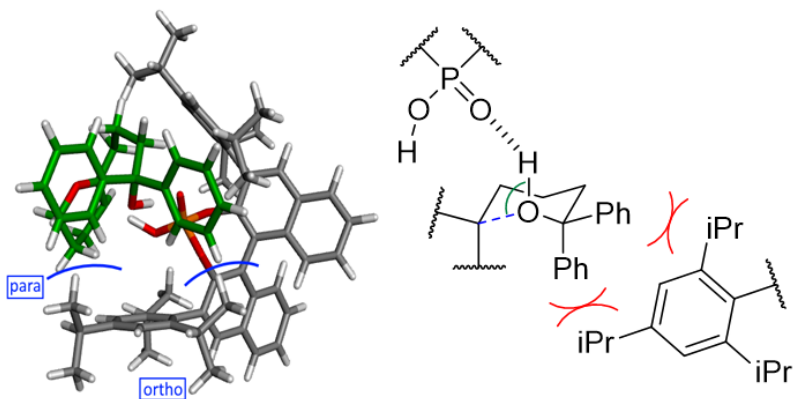


Figure 3.12. Key steric interactions at TS_R between the phenyl groups on the alcohol appendage of the enol ether and the ortho and para substituents of the aryl substituents of (*R*)-**3-13**.

Conclusion

This project describes the development of chiral phosphoric acid-catalyzed stereoselective spiroketalizations as well as mechanistic and computational studies of the mechanistic origins of catalysis. The commercially available TRIP catalysts were found to be effective promoters of the enantioselective formation of chiral spiroketals and diastereoselective formation of non-anomeric spiroketals. The reactions were found to proceed under kinetic control, where nonpolar solvents (i.e., pentane) and anhydrous conditions (4 Å MS as additives) were found to be essential for attaining high levels of stereocontrol. The experimental studies were designed to differentiate between the $\text{S}_{\text{N}}1$ -like, $\text{S}_{\text{N}}2$ -like, and covalent phosphate intermediate-based mechanisms. The CPA-catalyzed spiroketalization of deuterium-labeled cyclic enol ethers revealed a highly diastereoselective *syn*-selective protonation/nucleophile addition, thus ruling out long-lived oxocarbenium intermediates. At the same time, the intermolecular equivalent of these reactions (i.e., tetrahydropyranylation with D₃-labeled dihydropyran) was found to proceed unselectively, presumably by a different (i.e., $\text{S}_{\text{N}}1$ -like) mechanism. Hammett analysis of the reaction kinetics

revealed accumulation of positive charge in the transition state of the rate-limiting step ($\rho = -2.9$), and the KIE for the spiroketalization with D-labeled substrates was determined to be 0.85. The subsequent in-depth computational studies on the phosphoric acid-catalyzed spiroketalization mechanism suggested that a single-step asynchronous mechanism is responsible for the observed experimental data. This mechanism fully exploits the bifunctionality of the catalyst and is novel for this type of transformation. The anomeric phosphate pathway was shown to have higher energy barriers. Additionally, molecular dynamics simulations showed the average lifetime of oxocarbenium structures to be 519 ± 240 fs, which does not support the formation of a stable ionic intermediate. The stereoselectivity of the reaction was examined in a complete system, and the key interactions that favor the experimentally observed results were identified to be linked with the 3,3'-aryl substituents of the CPA and the substituents on the alcohol group of the substrate. This stereochemical model was highly consistent with the observed experimental results in terms of the selectivity and the level of enantiocontrol, and this will allow not only future catalyst design to overcome the procedure limitations and expand its scope, but also the analysis of related reactions, such as intermolecular CPA-catalyzed formation of acetal/aminal/hemiaminal ethers from enol ethers. Finally, the applicability of the growing string method for the analysis of hydrogen-bond organocatalytic transformations involving large systems was demonstrated, as was its usefulness in the proposal of the underlying mechanism and in the explanation of the stereocontrol observed.

3.5 References

- [1] J. E. Aho, P. M. Pihko, T. K. Rissa, *Chem. Rev.* **2005**, *105*, 4406–4440.
- [2] F. M. Uckun, C. Mao, A. O. Vassilev, H. Huang, S. T. Jan, *Bioorganic Med. Chem. Lett.* **2000**, *10*, 541–545.
- [3] S. Mitsuhashi, H. Shima, T. Kawamura, K. Kikuchi, M. Oikawa, A. Ichihara, H. Oikawa, *Bioorganic Med. Chem. Lett.* **1999**, *9*, 2007–2012.
- [4] J. A. Palmes, A. Aponick, *Synthesis.* **2012**, *44*, 3699–3721.
- [5] R. Baker, R. Herbert, P. E. Howse, O. T. Jones, W. Francke, W. Reith, *J. Chem. Soc. Chem. Commun.* **1980**, *0*, 52–53.
- [6] K. Mori, H. Watanabe, K. Yanagi, M. Minobe, *Tetrahedron* **1985**, *41*, 3663–3672.
- [7] K. Mori, T. Uematsu, K. Yanagi, M. Minobe, *Tetrahedron* **1985**, *41*, 2751–2758.
- [8] G. Haniotakis, W. Francke, K. Mori, H. Redlich, V. Schurig, *J. Chem. Ecol.* **1986**, *12*, 1559–1568.
- [9] W. Francke, W. Kitching, *Curr. Org. Chem.* **2005**, *5*, 233–251.
- [10] R. Bai, G. F. Taylor, Z. A. Cichacz, C. L. Herald, J. A. Kepler, G. R. Pettit, E. Hamel, *Biochemistry* **1995**, *34*, 9714–9721.
- [11] N. Fusetani, K. Shinoda, S. Matsunaga, *J. Am. Chem. Soc.* **1993**, *115*, 3977–3981.
- [12] M. Kobayashi, S. Aoki, H. Sakai, K. Kawazoe, N. Kihara, T. Sasaki, I. Kitagawa, *Tetrahedron Lett.* **1993**, *34*, 2795–2798.
- [13] A. B. Smith, T. Tomioka, C. A. Risatti, J. B. Sperry, C. Sfougatakis, *Org. Lett.* **2008**, *10*, 4359–4362.
- [14] D. A. Evans, P. J. Coleman, L. C. Dias, *Angew. Chem., Int. Ed.* **1997**, *36*, 2738–2741.
- [15] D. A. Evans, B. W. Trotter, B. Côté, P. J. Coleman, *Angew. Chem., Int. Ed.* **1997**, *36*, 2741–2744.
- [16] D. A. Evans, B. W. Trotter, P. J. Coleman, B. Côté, L. C. Dias, H. A. Rajapakse, A. N. Tyler, *Tetrahedron* **1999**, *55*, 8671–8726.
- [17] J. Guo, K. J. Duffy, K. L. Stevens, P. I. Dalko, R. M. Roth, M. M. Hayward, Y. Kishi, *Angew. Chem., Int. Ed.* **2002**, *37*, 187–190.
- [18] M. M. Hayward, R. M. Roth, K. J. Duffy, P. I. Dalko, K. L. Stevens, J. Guo, Y. Kishi, *Angew. Chem., Int. Ed.* **2002**, *37*, 190–196.
- [19] A. B. Smith, V. A. Doughty, Q. Lin, L. Zhuang, M. D. McBriar, A. M. Boldi, W. H. Moser, N. Murase, K. Nakayama, M. Sobukawa, *Angew. Chem., Int. Ed.* **2001**, *40*, 191–195.
- [20] A. B. Smith, Q. Lin, V. A. Doughty, L. Zhuang, M. D. McBriar, J. K. Kerns, C. S. Brook,

- N. Murase, K. Nakayama, *Angew. Chem., Int. Ed.* **2001**, *40*, 196–199.
- [21] A. B. Smith, W. Zhu, S. Shirakami, C. Sfougataki, V. A. Doughty, C. S. Bennett, Y. Sakamoto, *Org. Lett.* **2003**, *5*, 761–764.
- [22] A. B. Smith, V. A. Doughty, C. Sfougataki, C. S. Bennett, J. Koyanagi, M. Takeuchi, *Org. Lett.* **2002**, *4*, 783–786.
- [23] I. Paterson, D. Y. K. Chen, M. J. Coster, J. L. Acea, J. Bach, K. R. Gibson, L. E. Keown, R. M. Oballa, T. Trieselmann, D. J. Wallace, *Angew. Chem., Int. Ed.* **2001**, *40*, 4055–4060.
- [24] M. T. Crimmins, J. D. Katz, D. G. Washburn, S. P. Allwein, L. F. McAtee, *J. Am. Chem. Soc.* **2002**, *124*, 5661–5663.
- [25] G. R. Ott, J. Medina, C. H. Heathcock, C. J. Hayes, J. L. Hubbs, M. M. Claffey, G. A. Wallace, R. Scott, M. McLaughlin, *J. Am. Chem. Soc.* **2003**, *125*, 12844–12849.
- [26] M. Ball, M. J. Gaunt, D. F. Hook, A. S. Jessiman, S. Kawahara, P. Orsini, A. Scolaro, A. C. Talbot, H. R. Tanner, S. Yamanoi, et al., *Angew. Chem., Int. Ed.* **2005**, *44*, 5433–5438.
- [27] S. Ōmura, *Int. J. Antimicrob. Agents* **2008**, *31*, 91–98.
- [28] S. Ōmura, A. Crump, *Nat. Rev. Microbiol.* **2004**, *2*, 984–989.
- [29] B. J. Banks, B. F. Bishop, N. A. Evans, S. P. Gibson, A. C. Goudie, K. A. F. Gration, M. S. Pacey, D. A. Perry, M. J. Witty, *Bioorganic Med. Chem.* **2000**, *8*, 2017–2025.
- [30] J. A. Lasota, R. A. Dybas, *Annu. Rev. Entomol.* **2003**, *36*, 91–117.
- [31] Y. Terauchi, M. Tamura, M. Senda, R. Gunji, K. Kaku, *Diabetes, Obes. Metab.* **2017**, *19*, 1397–1407.
- [32] Jungius, C. L. *Z. Phys. Chem* **1905**, *52*, 97.
- [33] S. Favre, P. Vogel, S. Gerber-Lemaire, *Molecules* **2008**, *13*, 2570–2600.
- [34] P. von Ræuë Schlever, E. D. Jemmis, G. W. Spitznagel, *J. Am. Chem. Soc.* **1985**, *107*, 6393–6394.
- [35] E. Juaristi, G. Cuevas, *Tetrahedron* **2002**, *48*, 5019–5087.
- [36] R. W. Franck, *Tetrahedron* **1983**, *39*, 3251–3252.
- [37] P. Deslongchamps, D. D. Rowan, N. Pothier, G. Sauvé, J. K. Saunders, *Can. J. Chem.* **2006**, *59*, 1105–1121.
- [38] T. Yasumoto, M. Murata, Y. Oshima, M. Sano, G. K. Matsumoto, J. Clardy, *Tetrahedron* **1985**, *41*, 1019–1025.
- [39] J. S. Lee, T. Igarashi, S. Fraga, E. Dahl, P. Hovgaard, T. Yasumoto, *J. Appl. Phycol.* **1989**, *1*, 147–152.
- [40] J. S. Allingham, C. O. Miles, I. Rayment, *J. Mol. Biol.* **2007**, *371*, 959–970.

- [41] F. Leiraa, A. G. Cabadoa, M. R. Vieytes, Y. Roman, A. Alfonso, L. M. Botana, T. Yasumoto, C. Malaguti, G. P. Rossini, *Biochem. Pharmacol.* **2002**, *63*, 1979–1988.
- [42] I. Spector, F. Braet, N. R. Shochet, M. R. Bubb, *Microsc. Res. Tech.* **1999**, *47*, 18–37.
- [43] K. Fujiwara, Y. Suzuki, N. Koseki, Y. I. Aki, Y. Kikuchi, S. I. Murata, F. Yamamoto, M. Kawamura, T. Norikura, H. Matsue, et al., *Angew. Chem., Int. Ed.* **2014**, *53*, 780–784.
- [44] J. E. Aho, A. Piisola, K. Syam Krishnan, P. M. Pihko, *European J. Org. Chem.* **2011**, *2011*, 1682–1694.
- [45] P. M. Pihko, J. E. Aho, *Org. Lett.* **2004**, *6*, 3849–3852.
- [46] D. Castagnolo, I. Breuer, P. M. Pihko, *J. Org. Chem.* **2007**, *72*, 10081–10087.
- [47] D. Vellucci, S. D. Rychnovsky, *Org. Lett.* **2007**, *9*, 711–714.
- [48] K. Mead, B. Brewer, *Curr. Org. Chem.* **2005**, *7*, 227–256.
- [49] L. A. Wessjohann, W. Brandt, T. Thiemann, *Chem. Rev.* **2003**, *103*, 1625–1648.
- [50] J. Marco-Contelles, M. T. Molina, S. Anjum, *Chem. Rev.* **2004**, *104*, 2857–2900.
- [51] R. E. Ireland, S. Thaisrivongs, P. H. Dussault, *J. Am. Chem. Soc.* **1988**, *110*, 5768–5779.
- [52] T. E. La Cruz, S. D. Rychnovsky, *Org. Lett.* **2005**, *7*, 1873–1875.
- [53] I. Čorić, B. List, *Nature* **2012**, *483*, 315–319.
- [54] G. B. Rowland, H. Zhang, E. B. Rowland, S. Chennamadhavuni, Y. Wang, J. C. Antilla, *J. Am. Chem. Soc.* **2005**, *127*, 15696–15697.
- [55] Y. Liang, E. B. Rowland, G. B. Rowland, J. A. Perman, J. C. Antilla, *Chem. Commun.* **2007**, *0*, 4477–4479.
- [56] X. Cheng, S. Vellalath, R. Goddard, B. List, *J. Am. Chem. Soc.* **2008**, *130*, 15786–15787.
- [57] M. Rueping, A. P. Antonchick, E. Sugiono, K. Grenader, *Angew. Chem., Int. Ed.* **2009**, *48*, 908–910.
- [58] G. Li, F. R. Fronczek, J. C. Antilla, *J. Am. Chem. Soc.* **2008**, *130*, 12216–12217.
- [59] G. K. Ingle, M. G. Mormino, L. Wojtas, J. C. Antilla, *Org. Lett.* **2011**, *13*, 4822–4825.
- [60] H. Qian, W. Zhao, Z. Wang, J. Sun, *J. Am. Chem. Soc.* **2015**, *137*, 560–563.
- [61] N. Pothier, S. Goldstein, P. Deslongchamps, *Helv. Chim. Acta* **1992**, *75*, 604–620.
- [62] Z. Sun, G. A. Winschel, A. Borovika, P. Nagorny, *J. Am. Chem. Soc.* **2012**, *134*, 8074–8077.
- [63] C. Lu, X. Su, P. E. Floreancig, *J. Org. Chem.* **2013**, *78*, 9366–9376.
- [64] K. Kanomata, Y. Toda, Y. Shibata, M. Yamanaka, S. Tsuzuki, I. D. Gridnev, M. Terada, *Chem. Sci.* **2014**, *5*, 3515–3523.
- [65] N. D. Shapiro, V. Rauniyar, G. L. Hamilton, J. Wu, F. D. Toste, *Nature* **2011**, *470*, 245–

250.

- [66] J. M. Wurst, G. Liu, D. S. Tan, *J. Am. Chem. Soc.* **2011**, *133*, 7916–7925.
- [67] M. Kotke, P. R. Schreiner, *Synthesis*. **2007**, *2007*, 779–790.
- [68] L. Bohé, D. Crich, *Carbohydr. Res.* **2015**, *403*, 48–59.
- [69] M. Huang, P. Retailleau, L. Bohé, D. Crich, *J. Am. Chem. Soc.* **2012**, *134*, 14746–14749.
- [70] M. Huang, G. E. Garrett, N. Birlirakis, L. Bohé, D. A. Pratt, D. Crich, *Nat. Chem.* **2012**, *4*, 663–667.
- [71] C. P. Butts, B. Heise, G. Tatolo, *Org. Lett.* **2012**, *14*, 3256–3259.
- [72] P. M. Zimmerman, *J. Chem. Theory Comput.* **2013**, *9*, 3043–3050.
- [73] P. M. Zimmerman, *J. Comput. Chem.* **2013**, *34*, 1385–1392.
- [74] P. M. Zimmerman, *J. Comput. Chem.* **2015**, *36*, 601–611.
- [75] Z. Sun, G. A. Winschel, P. M. Zimmerman, P. Nagorny, *Angew. Chem., Int. Ed.* **2014**, *53*, 11194–11198.
- [76] P. M. Zimmerman, *Mol. Simul.* **2015**, *41*, 43–54.
- [77] P. M. Zimmerman, *J. Chem. Phys.* **2013**, *138*, 184102.
- [78] S. T. Schneebeli, M. L. Hall, R. Breslow, R. Friesner, *J. Am. Chem. Soc.* **2009**, *131*, 3965–3973.
- [79] C. Allemann, R. Gordillo, F. R. Clemente, P. H. Y. Cheong, K. N. Houk, *Acc. Chem. Res.* **2004**, *37*, 558–569.
- [80] E. H. Krenske, K. N. Houk, *Acc. Chem. Res.* **2013**, *46*, 979–989.
- [81] T. Marcelli, P. Hammar, F. Himo, *Chem. - A Eur. J.* **2008**, *14*, 8562–8571.
- [82] I. D. Gridnev, M. Kouchi, K. Sorimachi, M. Terada, *Tetrahedron Lett.* **2007**, *48*, 497–500.

CHAPTER 4

Design, Synthesis, and Application of Chiral Spiroketal-Containing Ligands

“With respect to chemical reactions, “useful” implies wide scope, simplicity to run, and an essential transformation of readily available starting materials.”

Karl Barry Sharpless

4.1 Introduction to asymmetric transition metal catalysis

Most natural products and other bioactive materials used in pharmaceutical industry possess chirality, a property that is indispensable for a selective interaction between a bioactive compound and its target. For this reason, the demands for methods that can effectively construct chiral building blocks is ever increasing. Amongst the types of the strategies used to produce enantiomerically-enriched materials, the most desirable and challenging is catalytic asymmetric synthesis, since only a small amount of chiral material is required to reproduce chirality in larger amounts of product.^[1] Amid the asymmetric catalysis strategies, enzymatic catalysis, organocatalysis, and transition metal catalysis have emerged as the most popular and successful ways of constructing chiral molecules. Other strategies and their disadvantages are briefly discussed in sections **1.5** and **2.1**.

The formation of carbon-carbon and carbon-heteroatom bonds using transition metal-mediated organic reactions has been the focus of attention of synthetic organic chemists over the past three decades.^[2] Nobel Prize-winning breakthroughs have led to the development of chemistry not possible through enzymatic or organocatalytic methods. In particular, the advent of cross-

coupling reactions in the formation of sp^2 - sp^2 carbon-carbon bonds has revolutionized organic syntheses.^[3-6] Chemists also realized the powerful catalytic properties of metals could be used to activate prochiral substrates and produce products enantioselectively. By the 1990s, several examples of asymmetric hydrogenations, hydrosilylations, and carbon-carbon bond forming reactions were known, and currently it is a powerful tool in the process chemist repertoire.^[1,7]

Based on the powerful capabilities of transition metal chemistry, it is no surprise that vast amounts of effort and energy to spend in the search for catalysts that exhibit improved reactivity, efficiency, and selectivity. Through these studies, it has long been recognized that the characteristics of the ancillary ligands in the coordination sphere of the metal play an essential role in the sterics, electronics, and physical properties of the metal complex, all which define its catalytic activity.^[2] One of the main benefits of transition metal chemistry is that it is extremely versatile in the selection of the ancillary ligands. There is a large variety of ligand types with drastically different properties, such as phosphines, carbenes, carbon monoxide, π -complexing ligands, and N-, O-, and S-based ligands.

Tertiary phosphines and other trivalent phosphorus ligands are arguably the most important and pervasive ligands in homogeneous catalysis. In fact, all transition metals, especially late transition metals, form complexes with trivalent phosphorus ligands. Tertiary phosphines ligands bind to transition metals strongly, forming a Lewis acid-base pair. There are two main reasons for this favorable interaction: 1) the trivalent phosphorus atom is a soft Lewis base, which matches well with the soft Lewis acidity of low valence metals used in transition metal catalysis; and 2) trivalent phosphorus-based ligands can also serve as π -acceptors, so additional stabilization of the metal complex can occur through π - π backbonding. These are the result of filled metal d -orbitals overlapping with unfilled d -orbitals on the phosphorus atom (Figure 4.1), although some studies

suggest that the P-X σ^* antibonding orbital plays a bigger role than the empty d orbital in these backbonding interactions.^[8-10]

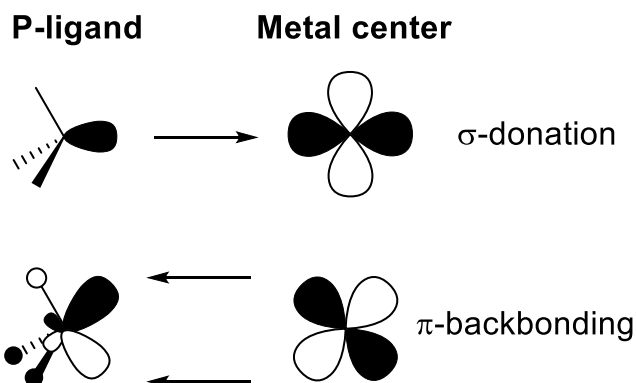


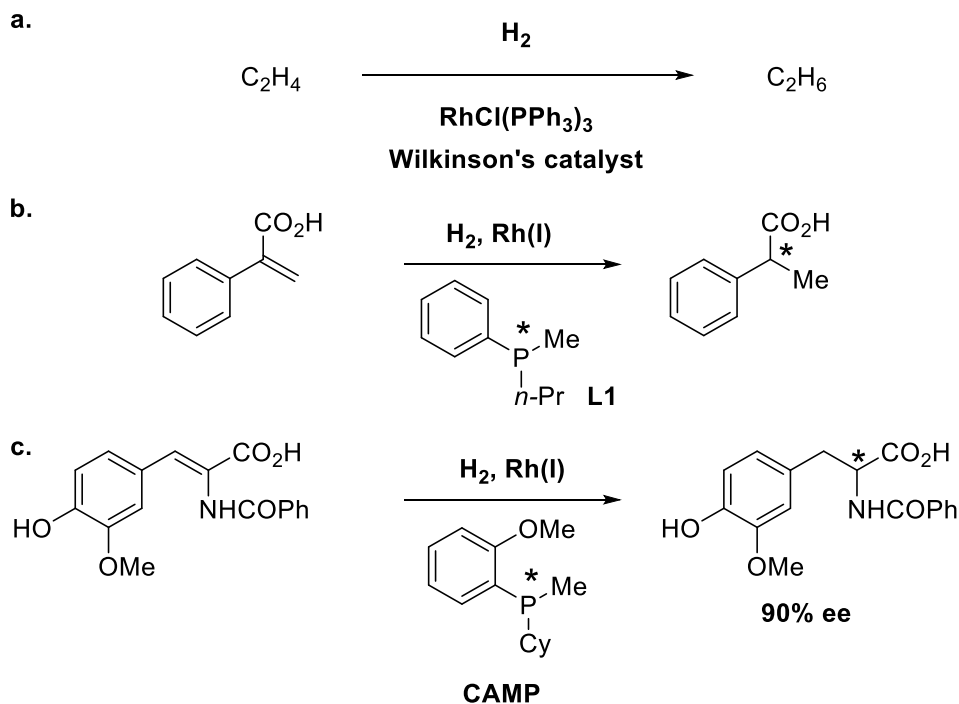
Figure 4.1. Interactions between tertiary phosphines and metal centers.

Because of the reasons outlined above, tertiary phosphines bind better to metals than their tertiary amine counterparts. Another major advantage over amines is that trivalent phosphorus compounds possess a much higher barrier of inversion than nitrogen, typically very slow at room temperature (29-35 kcal/mol),^[11] so P-chiral ligands are isolable and useful. However, a disadvantage over amine ligands is that many P(III) ligands are prone to oxidation, since P(V) is typically a more stable oxidation state.

In 1965, Wilkinson and coworkers were able to achieve higher yielding hydrogenations in homogeneous systems under mild conditions by using a rhodium (I) phosphine complex (Scheme 4.1a).^[12] Three years later, Nobel laureate Knowles would be the first chemist to design and perform a homogeneous catalytic hydrogenation by replacing the PPh_3 ligands in Wilkinson's catalyst with a P-chiral tertiary phosphine ligand **L1**, albeit with low enantioselectivity (Scheme 4.1b).^[13] Subsequent improvements on this method would lead to the development of **CAMP**, a

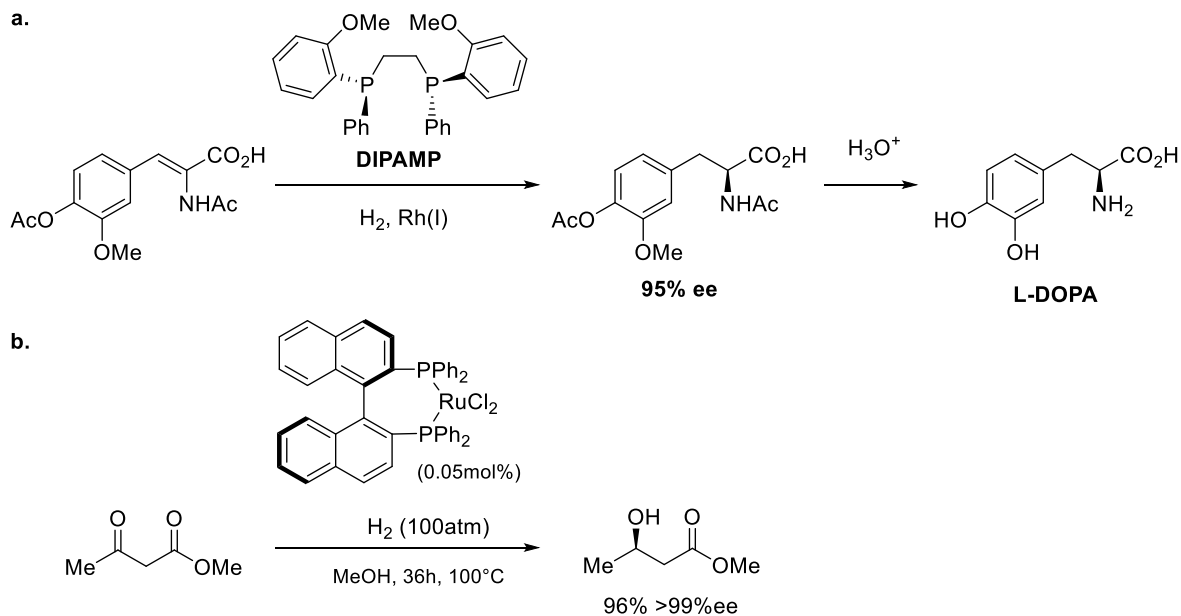
P-chiral ligand that provided the product in 90% ee,^[14,15] a truly remarkable achievement for the time (Scheme 4.1c).

Scheme 4.1. Early examples of phosphine ligands used in hydrogenations.



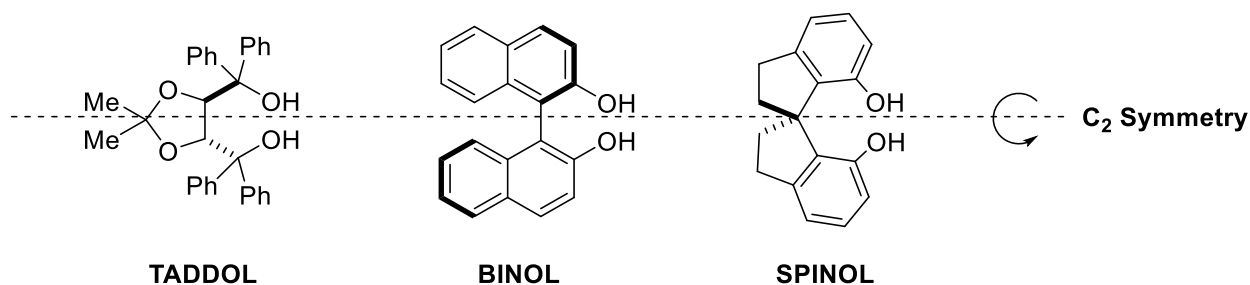
Although the first instances of asymmetric hydrogenation catalyzed by transition metals involved P-chiral ligands, it was not long until Kagan and coworkers made a breakthrough in ligand design by publishing the bidentate phosphine (*R,R*)-DIOP, chiral in the organic framework. It proved to be an excellent ligand in asymmetric hydrogenations.^[16] Inspired by this work, the Knowles group developed DIPAMP in 1975, which was used in the commercial production of L-DOPA (Scheme 4.2a).^[17] Soon after, Noyori would develop BINAP and use it in the asymmetric hydrogenation of ketones, cementing the usefulness and importance of phosphine ligands and earning him the Nobel prize in chemistry (Scheme 4.2b).^[18–22]

Scheme 4.2. **a.** Knowles's asymmetric synthesis of L-DOPA. **b.** Noyori's asymmetric hydrogenation of ketones.



Knowles was a visionary in chiral ligand design. He made a key observation in his Nobel prize lecture: “When we started this work we expected these man-made systems to have a highly specific match between substrate and ligand, just like enzymes. Generally, in our hands and in the hands of those that followed us, a good candidate has been useful for quite a range of applications”.^[23] In other words, he observed that, in many cases, the ligands which were most successful in a particular reaction were more likely to be competent in other unrelated transformations. In modern terms, such structures are called privileged, a term coined by Jacobsen.^[24] TADDOL, BINOL, and SPINOL (Scheme 4.3) are excellent examples of privileged structures. Of the few select privileged structures, a surprisingly large number of them possess C_2 symmetry. This is a desirable feature in asymmetric catalysis because it eliminates the possibility of many isomeric metal complexes, as well as substrate-catalyst conformations.^[25]

Scheme 4.3. C_2 symmetry is a common feature in privileged structures.



In particular, SPINOL-derived ligands, such as 7,7'-bis(diarylphosphino)-2,2',3,3'-tetrahydro-1,1'-spirobiindenes (SDPs),^[26–28] have been used with great success in the past decades (Figure 4.2, left).^[29,30] Although their performance is notable, high prices and tedious preparation methods pose severe limitations to the application of these ligands. Recent efforts of Tan and co-workers focused on addressing some of these problems by developing an optimized synthesis of SPINOL.^[31] However, this approach still suffers from the obligatory use of SPINOL-derived phosphoric acids, which themselves are expensive and commercially unavailable on a large scale. This chapter presents a solution to this problem by the development of useful spiroketal-derived SPINOL analogs which are straightforward to synthesize on large scale (Figure 4.2, right). For an introduction on spiroketal synthesis and conformational properties, refer to sections 3.1 and 3.2.

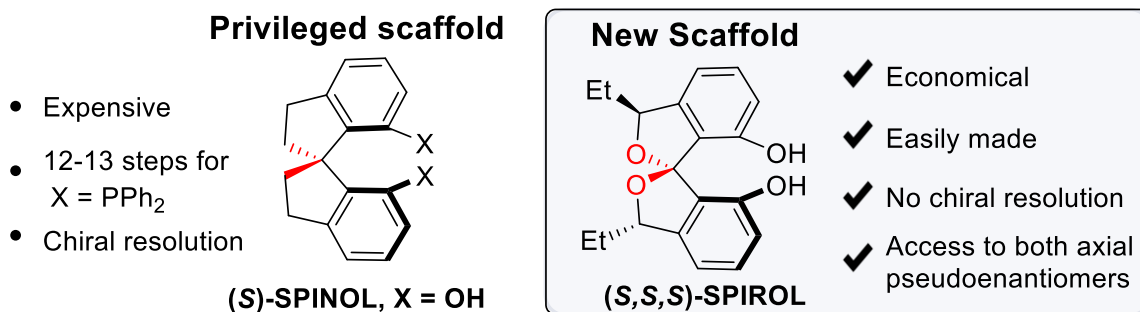


Figure 4.2. Spiroketal-based analogs of SPINOL.

4.2 Results and discussion

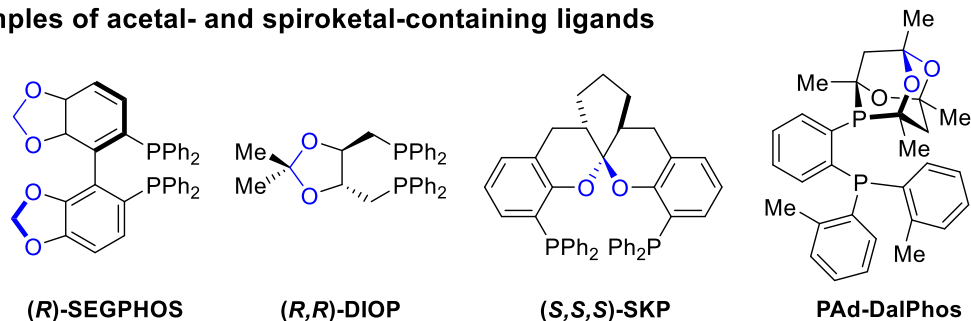
(Excerpts of this chapter were adapted from:

Argüelles, A. J.; Sun, S.; Budaitis, B. G.; Nagorny, P. *Angew. Chem. Int. Ed.* **2018**, 57, 5325.

Experimental information can be found in **Appendix C**)

Based on our prior work on the asymmetric formation of axially chiral spiroketals,^[32–34] we proposed a new easily accessible spiroketal-based C₂-symmetric chiral scaffold termed SPIROL (Figure 4.2, right). While a spiroketal moiety is typically labile under strongly acidic conditions, the majority of the transition metal-catalyzed reactions are not carried out under highly acidic conditions. Due to these reasons as well as their high accessibility, acetal-^[16,35,36] and spiroketal-containing^[37] ligands have proven to be of great value in asymmetric catalysis (Figure 4.3A). We surmised that the introduction of bulky 7,7'-substituents such as R = PPh₂, would render the both axial pseudoenantiomeric diastereomers kinetically stable under a variety of conditions (Fig. 4.3B). Moreover, the additional stereocenters at the benzylic 3,3'-positions would prevent the epimerization of the more stable (*S,S,S*)-diastereomer ($\Delta G^\circ = 2.3$ kcal/mol for SPIRAP) even under equilibrating conditions. This work describes the development of a novel reliable dimerizative condensation that enables rapid access to chiral SPIROL on large scale, and the application of SPIROL-based ligands in various Pd-, Ir-, and Rh-catalyzed asymmetric reactions. These results along with the computational studies carried on Pd(II)-complexes suggest that (*S,S,S*)-diastereomers are structurally and electronically similar to SPINOL-based ligands, whereas their axial pseudoenantiomeric, (*R,S,S*)-diastereomers represent a structurally and electronically different scaffolds. We believe that these features coupled with the ease of preparation and higher level of tunability (i.e. at the 3,3'-benzylic positions) make SPIROL ligands of great value to asymmetric catalysis.

A. Examples of acetal- and spiroketal-containing ligands



B. SPIROL-based pseudoenantiomeric ligands for asymmetric catalysis

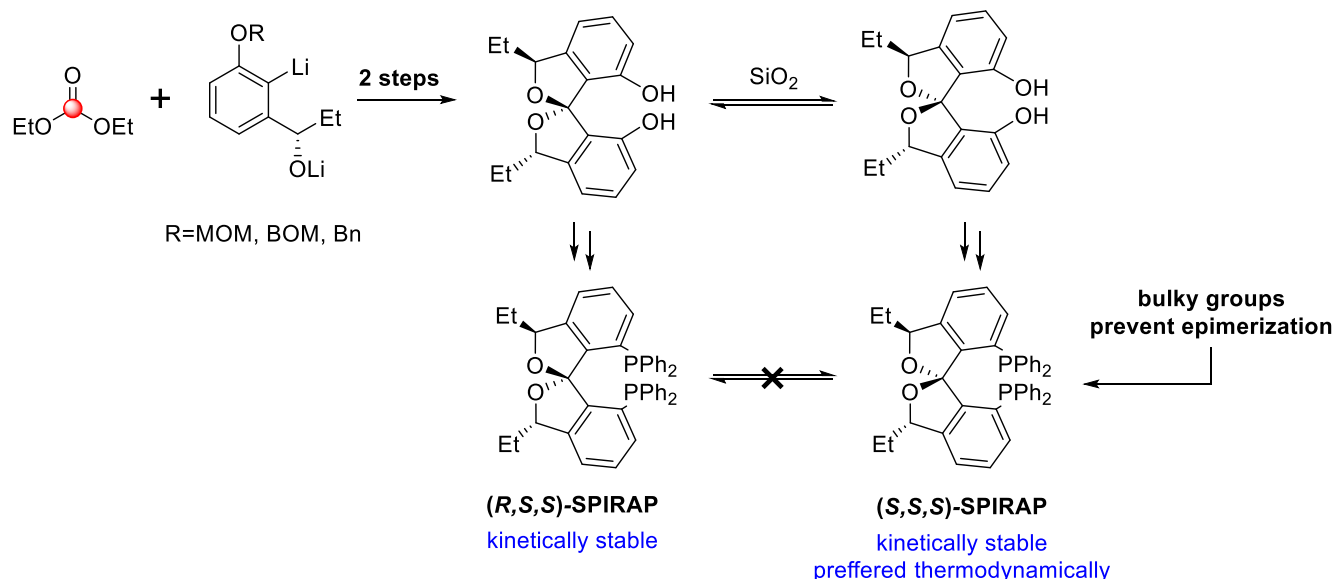
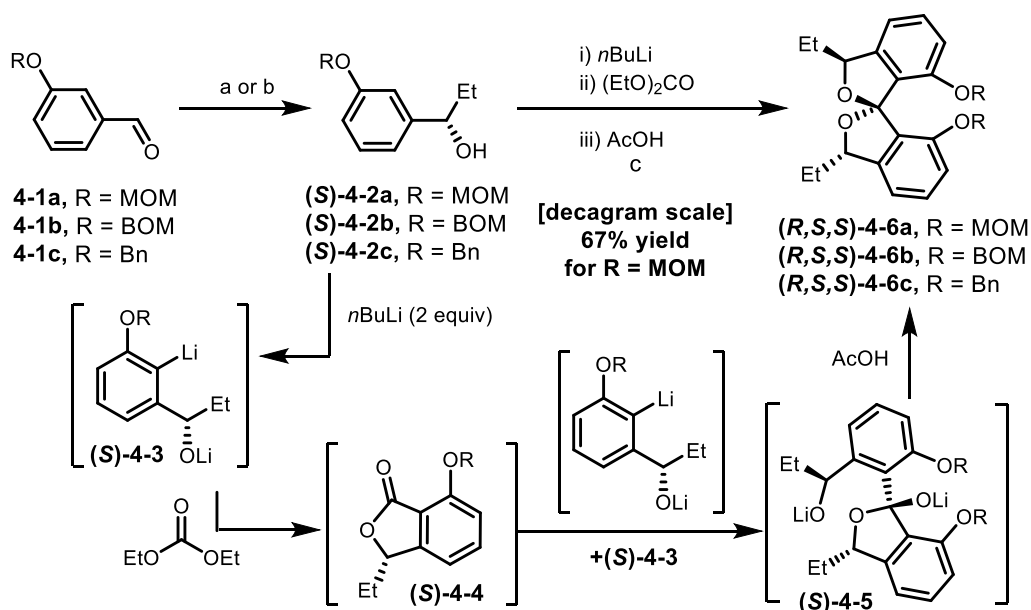


Figure 4.3. A. Acetal and spiroketal-containing commercial phosphine ligands. B. Pseudoenantiomeric SPIROL-based ligands.

Our studies commenced with a highly enantioselective alkylation of protected 3-hydroxybenzaldehyde **4-1** (Scheme 4.4). Although commercially available DBNE could be used to catalyze a highly enantioselective additions to different protected aldehydes (R=MOM, BOM, Bn),^[38] readily available aziridine-based organocatalysts could also be used to attain the desired products **4-2** in a practically enantiopure form.^[39] The treatment of the resulting alcohol **4-2** with two equivalents of *n*-butyl lithium in toluene regioselectively afforded the dilithiated species **4-3**, which is then captured by diethyl carbonate to produce the desired spiroketal **4-6** in good yields and excellent diastereoselectivity. This transformation is proposed to proceed through the

intermediacy of isobenzofuranone **4-4**, and then adduct **4-5** that subsequently collapses to **4-6** upon treatment with acetic acid. This unprecedented dimerization could be carried on a decagram scale and provides quick means for accessing protected SPIROL.

Scheme 4.4. Highly diastereoselective spiroketalization of benzylic alcohols **4-2**.

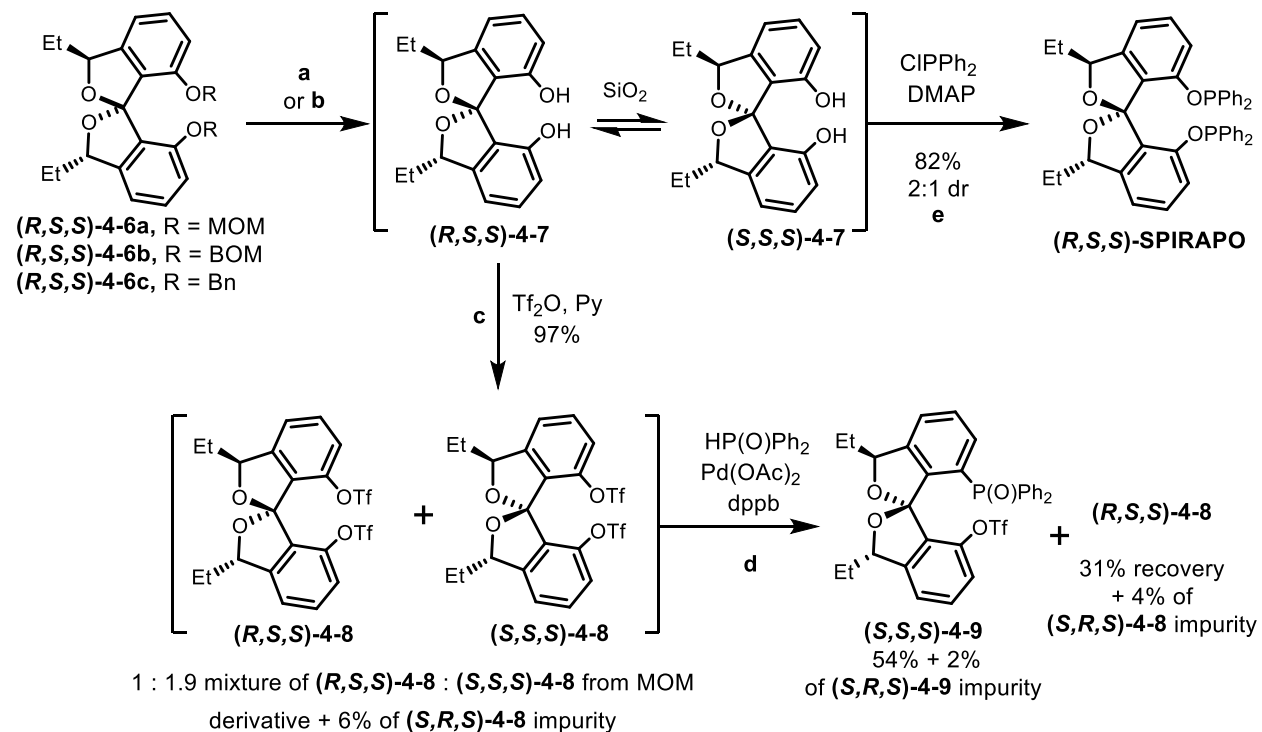


a. For R=Bn/MOM: (-)-DBNE (7 mol%), Et₂Zn (1M in hex, 2.2 eq), hexanes, 0°C; 97% yield, 94% ee (R=MOM); 81% yield, 91% ee (R=Bn); **b.** For R=Bn/BOM/MOM, aziridine diphenyl((R)-1-((S)-1-phenylethyl)aziridin-2-yl)methanol (5 mol%), Et₂Zn (1M in hex, 2.2 eq), PhMe, 0°C; 97% yield, >99% ee (R=MOM); 83% yield, >99% ee (R=BOM); 99% yield, >99% ee (R=Bn); (*S,S*)-aziridine organocatalyst could be used to get (*R*)-**4-2** in excellent ee; **c.** i) *n*-Butyllithium (1 M in hex, 2.0 eq), PhMe, 0°C to rt; ii) diethylcarbonate (0.55 eq), 0°C to rt; iii) AcOH (xs), rt. 67% yield (79% BRSM), >20:1 dr (R=MOM); 54% yield (64% BRSM), >20:1 dr (R=BOM); 42% yield (66% BRSM), >20:1 dr (R=Bn).

The subsequent deprotection of substrates **4-6a-c**, provided the desired SPIROL scaffold (**(R,S,S)-4-7** (Scheme 4.5)). Computational studies showed that the pseudoenantiomeric diol diastereomers (**(R,S,S)-4-7** and (**(S,S,S)-4-7**) had near equal gas-phase energy (1.0 kcal/mol difference, favoring (**(S,S,S)-4-7**), and we therefore surmised that we would be able to equilibrate them under mildly acidic conditions. To our delight, we found that were able to achieve this by stirring the diol in a suspension containing silica, and we furthermore discovered that the

equilibrium could be slightly biased to one of the diastereomers depending on the solvent used (see Appendix C).

Scheme 4.5. Diol equilibration and chemical resolution of diastereomeric ditriflates.

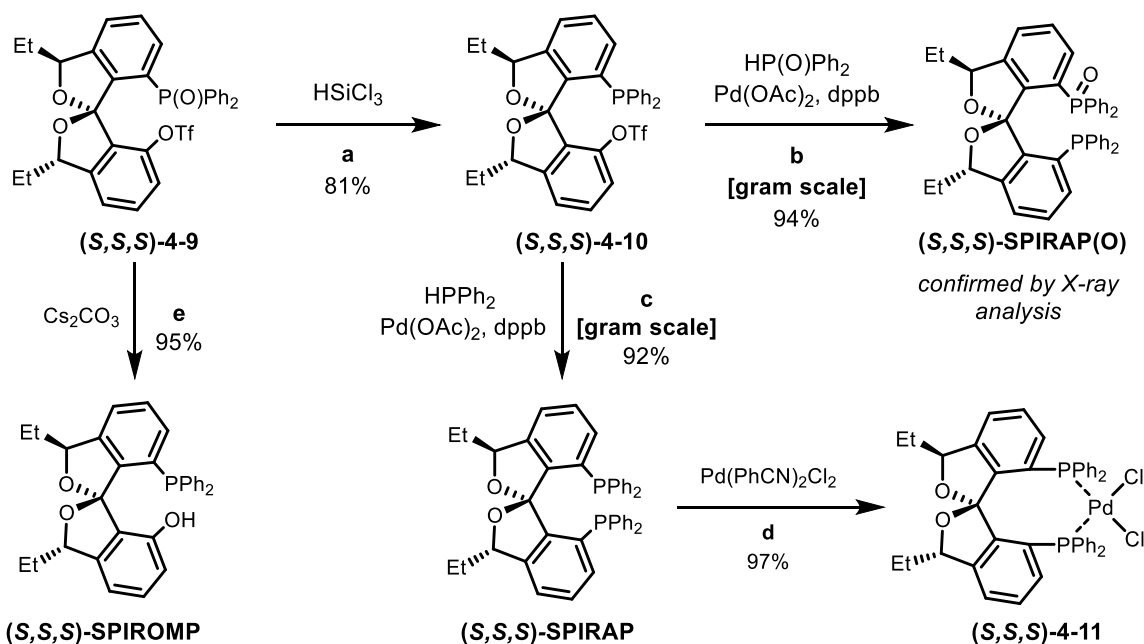


(a) AcCl (2 eq), MeOH, 0°C to rt; for R=MOM, 99% yield; for R=BOM, 98% yield; (b) For R=Bn, H₂ (balloon), NaHCO₃ (9 eq), MeOH, rt; 93% yield; (c) PPh₂Cl (2.5 eq), DMAP (0.1 eq) NEt₃ (4 eq), DCM, 56% yield over 2 steps, 9:1 dr; (d) Tf₂O (2.4 eq), pyridine (5.3 eq), DCM, 0°C to rt; 97% yield, with conserved dr; (e) Quantities with respect to **(S,S,S)-4-8**: HP(O)Ph₂ (1.9 eq), Pd(OAc)₂ (8.8 mol%), dppb (8.8 mol%), DIPEA (4.4 eq), DMSO, 80°C, 94% yield of **(S,S,S)-4-9**, 99% recovery of **(R,S,S)-4-8**. **(R,S,S)-4-7** is the major diastereomer that is initially formed; however, a prolonged exposure to acids, including SiO₂, results in epimerization leading to **(S,S,S)-4-7**.

Although the ditriflate mixture could be separated by the conventional chromatographic techniques, we have identified a more convenient method that takes advantage of the difference in reactivity between these species. Thus, the mixture of **(R,S,S)-4-7** and **(S,S,S)-4-7** was converted to the corresponding configurationally stable ditriflates **(R,S,S)-4-8** and **(S,S,S)-4-8**, which underwent resolution in a Pd-catalyzed coupling with diphenylphosphine oxide at 80°C. We observed that only the **(S,S,S)-4-8** diastereomer reacted in excellent yield to form **(S,S,S)-4-9**,

while (*R,S,S*)-**4-8** diastereomer was recovered almost quantitatively. The phosphine oxide/triflate (*S,S,S*)-**4-9** was then recrystallized in cyclohexane with excellent recovery to obtain enantiopure material. Following this, we were able to elaborate the triflate/phosphine oxide (*S,S,S*)-**4-9** to the respective diphosphine. An initial reduction with trichlorosilane afforded triflate/phosphine (*S,S,S*)-**4-10**, which was then subjected to a second coupling with diphenyl phosphine oxide to obtain phosphine oxide/phosphine (*S,S,S*)-**SPIRAP(O)**, the structure of which was confirmed by X-ray crystallography. In addition, a direct coupling of the phosphine/triflate (*S,S,S*)-**4-10** with diphenyl phosphine provided (*S,S,S*)-**SPIRAP** in excellent yields (Scheme 4.6).

Scheme 4.6. Functionalization of scaffold **4-9** into various ligands.



(**a**) HSiCl_3 (16 eq), DIPEA (40 eq), PhMe, 80°C , 81% yield; (**b**) HP(O)Ph_2 (2 eq), DIPEA (5 eq), Pd(OAc)_2 (5 mol%), dppb (5 mol%) DMSO, 100°C , 94% yield; (**c**) Cs_2CO_3 (5 eq), DMF, 80°C , 95%; (**d**) HPPH_2 (3 eq), DIPEA (6.1 eq), Pd(OAc)_2 (10 mol%), dppb (11 mol%) DMF, 100°C , 92% yield; (**e**) $\text{Pd(PhCN)}_2\text{Cl}_2$ (1.0 eq), benzene, 97% yield.

In line with the aforementioned studies, the ditriflate (*R,S,S*)-**4-8** reacted in good yields with diphenyl phosphine oxide in similar coupling conditions, albeit at 100°C , to provide (*R,S,S*)-**4-9**, which was likewise elaborated to (*R,S,S*)-**SPIRAP(O)** and (*R,S,S*)-**SPIRAP** in good yields.

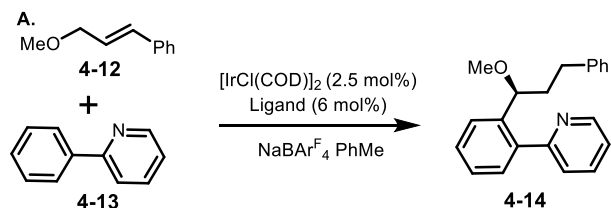
The absolute stereochemistry of (*S,R,R*)-**SPIRAP(O)** obtained by an identical route using (*R*)-**4-2a** was confirmed by X-ray crystallography. In addition, other ligands such as diphosphinite (*R,S,S*)-**SPIRAPO** (Scheme 4.5) and catalysts such as (*S,S,S*)-**SPIROMP** as well as stable PdCl₂ complexes **4-11** (Scheme 5.6) were conveniently generated.

The ligands synthesized above were then tested in various reported asymmetric catalysis applications (Table 4.1). We were pleased to find that (*S,S,S*)-**SPIRAP** is an exceptional ligand in the Ir-catalyzed hydroarylation of methylated cinnamyl alcohol **4-12** and 2-phenyl pyridine **4-13**, which provided better enantiocontrol (entry 4) than the BINAP- (entries 1 and 3) and SEGPHOS-based (entry 2) ligands recently explored by the Nishimura group.^[40] Interestingly, its diastereomer, (*R,S,S*)-**SPIRAP** was not a viable ligand for this reaction, and no product was detected (entry 5). Similarly, excellent performance of (*S,S,S*)-**SPIRAP** was observed in the Pd-catalyzed allylic alkylation of chalcone derivative **4-15** with dimethyl malonate **4-16** to afford chiral diester **4-17** in 94% yield and 97% ee (entry 7), which comparable to commercial (*S*)-**SDP** (entry 6).^[41] Remarkably, the pseudoenantiomeric ligand (*R,S,S*)-**SPIRAP** favored the other enantiomer of the product in 86% ee (entry 8). The phosphine oxide/phosphine ligand (*S,S,S*)-**SPIRAP(O)** was also used with great success in a Pd-catalyzed Heck reaction of 2-vinylphenyl triflate **4-18** with norbornene **4-19** to afford tricycle **4-20** (entry 10).^[42] As before, the diastereomeric complex (*R,S,S*)-**SPIRAP(O)** favored an enantiomeric product albeit with somewhat lower selectivity (entry 11). Finally, diphosphinites (*S,R,R*)-**SPIRAPO** and (*R,R,R*)-**SPIRAPO** were applied in the Rh-catalyzed asymmetric hydrogenations of dehydroalanine derivative **4-21** with excellent results.^[43] The (*R,R,R*)-**SPIRAPO** performed similarly to SPINOL-based ligand (*S*)-**SDP** (entries 15 and 13) while the use of the (*S,R,R*)-diastereomer resulted in

reversal of enantioselectivity (entry 14). In addition, application of SPIROMP organocatalytic aza-Baylis Hillman reaction^[44] has been demonstrated (see Appendix C).

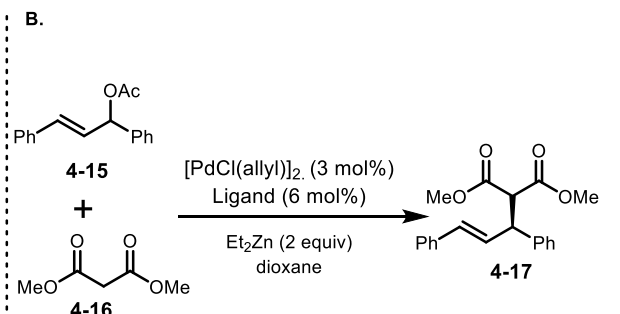
Table 4.1. Application of SPIRAP, SPIRAP(O), and SPIRAPO in Ir-, Pd- and Rh-catalyzed asymmetric transformations.

A.



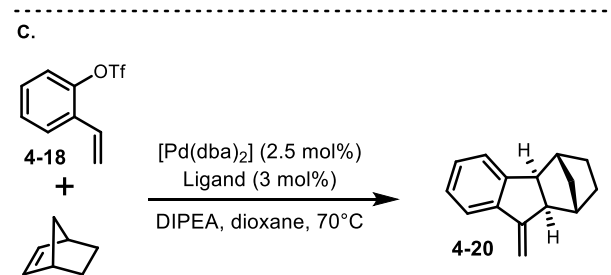
entry	ligand	T [°C]	Yield [%]	ee [%]
1	(<i>R</i>)-BINAP	80	84	88
2	(<i>R</i>)-SEGPHOS	80	7	81
3	(<i>R</i>)-3,5-Xyl-BINAP	80	87	94
4	(<i>R</i>)-SDP	70	82	95
5	(<i>S,S,S</i>)-SPIRAP	70	96	95
6	(<i>R,S,S</i>)-SPIRAP	70	N.R.	–

B.



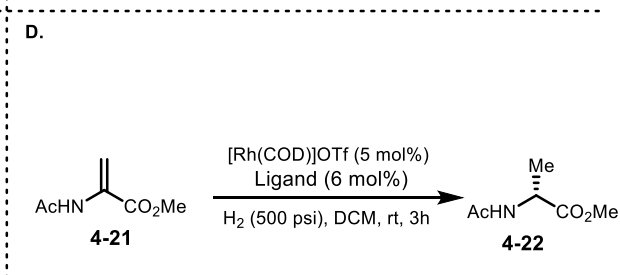
entry	ligand	yield [%]	ee [%]
7	(<i>S</i>)-SDP	97	97
8	(<i>S,S,S</i>)-SPIRAP	94	97
9	(<i>R,S,S</i>)-SPIRAP	98	-83

C.



entry	ligand	yield [%]	ee [%]
10	(<i>R</i>)-3,5-Xyl-SDP(O)	96	99
11	(<i>S,S,S</i>)-SPIRAP(O)	99	-94
12	(<i>R,S,S</i>)-SPIRAP(O)	96	89

D.



entry	ligand	yield [%]	ee [%]
13	(<i>S</i>)-BINAPO	84	89
14	(<i>S</i>)-SDPO	85	-93
15	(<i>S,R,R</i>)-SPIRAPO	87	-90
16	(<i>R,R,R</i>)-SPIRAPO	85	93

(S)-BINAP
Ar = Ph

3,5-Xyl-BINAP
Ar = 3,5-(CH₃)C₆H₃

(S)-SDPO

(S)-BINAPO

(R)-SEGPHOS

(S)-SDP

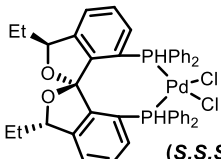
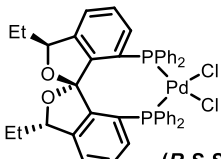
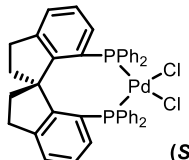
(S)-3,5-Xyl-SDP(O)
Ar = 3,5-(CH₃)C₆H₃

A) [IrCl(COD)]₂ (2.5 mol%), ligand (6 mol%), NaBARF₄ (10 mol%), 2-phenylpyridine (1.07 eq), PhMe; **B)** [PdCl(allyl)]₂ (2.5 mol%), Ligand (6 mol%), dimethyl malonate (2 eq), Et₂Zn (2 eq), 1,4-dioxane; **C)** Pd(dba)₂ (2.5 mol%), ligand (3 mol%), norbornene (4 eq), DIPEA (2 eq), 1,4-dioxane, 70°C **D)** [Rh(COD)]OTf (5.0 mol%), ligand (6.0 mol%), H₂ (500 psi), DCM, rt.

The consistent similar performance of **(S,S,S)-SPIRAP** and **(S)-SDP** and different behavior of **(R,S,S)-SPIRAP** prompted us to do a more thorough comparison between the **(S,S,S)**- and **(R,S,S)**-diastereomers. The density functional theory (DFT)^[45] analysis of diastereomeric Pd(II) complexes of SPIRAP (**4-11**), and commercial **(S)-SDP**, demonstrated that these complexes have similar natural charge at the metallic center. However, while the geometry index parameters τ_4 ^[46] and τ_4' ^[47] showed similar values for **(S,S,S)-4-11** and **(S)-4-23** (entries 1 and 3, Table 4.2), τ_4 and τ_4' for **(R,S,S)-4-11** were found to be considerably different (entry 2, Table 4.2). This implied that, although these three complexes are electronically similar, the **(R,S,S)-SPIRAP** complex is structurally significantly different from **(S)-SDP**, while **(S,S,S)-SPIRAP**, although not identical, is much more similar. The calculated bite angles also demonstrated this trend, with **(R,S,S)-SPIRAP** showcasing a slightly larger angle. This explains the lower performance of **(R,S,S)-SPIRAP** in catalytic applications optimized for SDP. A closer inspection of the three-dimensional structures of these complexes reveals that the ethyl sidechain in **(R,S,S)-SPIRAP** disturbs the π -stacking between the aryl groups of the backbone, leading to a different overall geometry (Figure 4.4). The structural dissimilarities between our spiroketal manifold and the SPINOL core leads us to believe that our catalytic platform could provide a unique solution to new asymmetric methodologies of importance in current organic chemistry. This divergence is reflected in the performance of some of the reactions mentioned above. The ease of preparation, stability, availability of new sites for tuning and outstanding performance of **(S,S,S)-SPIRAP** prompt us to suggest that it could be a widely used and successful ligand in asymmetric catalysis. In addition, easily accessible from the same chiral intermediate **(R,S,S)**- ligands could be used if reversed selectivity is desired. The results obtained with the **(R,S,S)**- ligands are particularly remarkable, as these thermodynamically unstable ligands were found to possess kinetic stability

under a variety of reaction conditions. Further application of our new ligands to novel reactions and chemical processes, as well as the preparation of other catalysts derived from the SPIROL core, are currently underway in our laboratory.

Table 4.2. Comparison of 3D structures of SPIRAP diastereomers and SDP.^a

entry	complex	natural charge at Pd(II)	τ_4	τ_4'	bite angle (°)
1	 (<i>S,S,S</i>)-4-11	0.425	0.113	0.125	94.4
2	 (<i>R,S,S</i>)-4-11	0.425	0.086	0.092	95.3
3	 (<i>S</i>)-4-23	0.427	0.112	0.129	94.2

^a τ_4 and τ_4' are geometry index parameters describe two largest angles at Pd center.

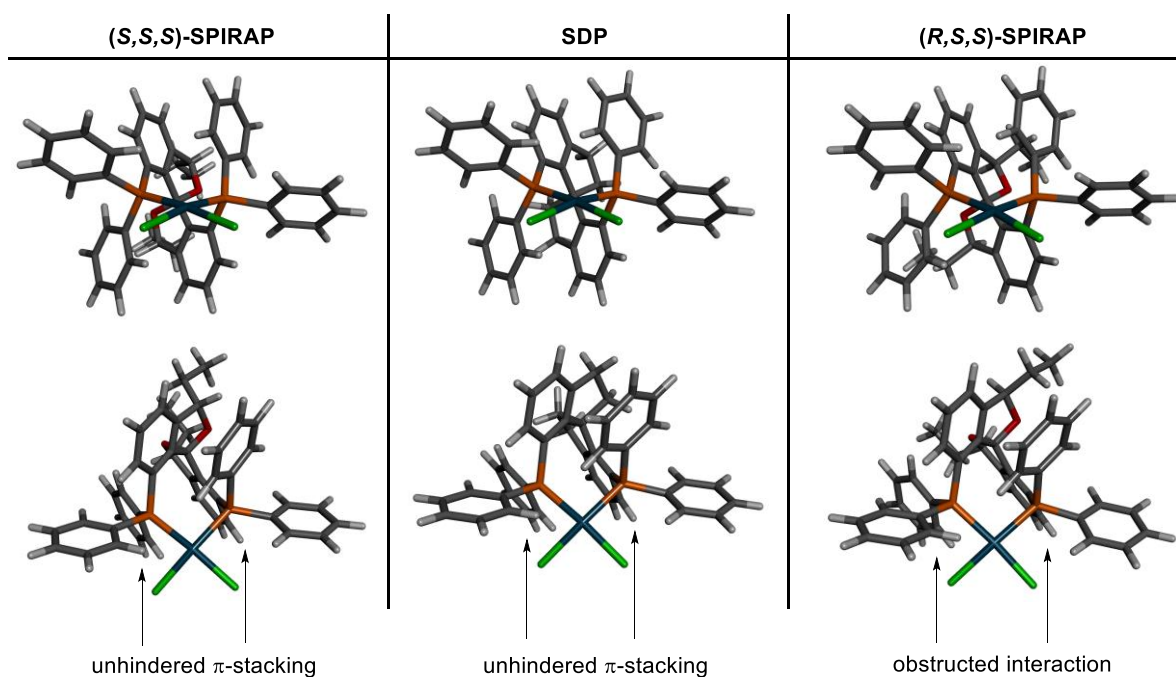


Figure 4.4. Comparison of (*R,S,S*)-SPIRAP, (*S,S,S*)-SPIRAP, and SDP complexes of PdCl₂.

4.3 References

- [1] I. Ojima, N. Clos, C. Bastos, *Tetrahedron* **1989**, *45*, 6901–6939.
- [2] N. G. Andersen, B. A. Keay, *Chem. Rev.* **2001**, *101*, 997–1030.
- [3] M. Kumada, *Pure Appl. Chem.* **2007**, *52*, 669–679.
- [4] J. K. Stille, *Angew. Chem., Int. Ed.* **1986**, *25*, 508–524.
- [5] N. Miyaura, A. Suzuki, *Chem. Rev.* **1995**, *95*, 2457–2483.
- [6] E. ichi Negishi, *Acc. Chem. Res.* **1982**, *15*, 340–348.
- [7] C. A. Busacca, D. R. Fandrick, J. J. Song, C. H. Senanayake, *Adv. Synth. Catal.* **2011**, *353*, 1825–1864.
- [8] J. C. Giordan, J. H. Moore, J. A. Tossell, *Acc. Chem. Res.* **1986**, *19*, 281–286.
- [9] J. A. Tossell, J. H. Moore, J. C. Giordan, *Inorg. Chem.* **1985**, *24*, 1100–1103.
- [10] S. X. Xiao, W. C. Trogler, D. E. Ellis, Z. Berkovitch-Yellin, *J. Am. Chem. Soc.* **1983**, *105*, 7033–7037.
- [11] R. D. Baechler, K. Mislow, *J. Am. Chem. Soc.* **1970**, *92*, 3090–3093.
- [12] J. F. Young, J. A. Osborn, F. H. Jardine, G. Wilkinson, *Chem. Commun.* **1965**, *0*, 131–132.
- [13] W. S. Knowles, M. J. Sabacky, *Chem. Commun.* **1968**, *0*, 1445–1446.
- [14] W. S. Knowles, M. J. Sabacky, B. D. Vineyard, *J. Chem. Soc. Chem. Commun.* **1972**, *0*, 10–11.
- [15] T. Imamoto, J. Watanabe, Y. Wada, H. Masuda, H. Yamada, H. Tsuruta, S. Matsukawa, K. Yamaguchi, *J. Am. Chem. Soc.* **1998**, *120*, 1635–1636.
- [16] T. P. Dang, H. B. Kagan, *J. Chem. Soc. D Chem. Commun.* **1971**, *0*, 481.
- [17] W. S. Knowles, M. J. Sabacky, B. D. Vineyard, D. J. Weinkauff, *J. Am. Chem. Soc.* **1975**, *97*, 2567–2568.
- [18] A. Miyashita, A. Yasuda, H. Takaya, K. Toriumi, T. Ito, T. Souchi, R. Noyori, *J. Am. Chem. Soc.* **1980**, *102*, 7932–7934.
- [19] R. Noyori, T. Ohkuma, M. Kitamura, H. Takaya, N. Sayo, H. Kumobayashi, S. Akutagawa, *J. Am. Chem. Soc.* **1987**, *109*, 5856–5858.
- [20] R. Noyori, H. Takaya, *Acc. Chem. Res.* **1990**, *23*, 345–350.
- [21] R. Noyori, *Angew. Chem., Int. Ed.* **2002**, *41*, 2008.
- [22] M. Berthod, G. Mignani, G. Woodward, M. Lemaire, *Chem. Rev.* **2005**, *105*, 1801–1836.
- [23] W. S. Knowles, *Angew. Chem., Int. Ed.* **2002**, *41*, 1998.

- [24] T. P. Yoon, E. N. Jacobsen, *Science* **2003**, *299*, 1691–1693.
- [25] A. Pfaltz, W. J. Drury, *Proc. Natl. Acad. Sci.* **2004**, *101*, 5723–5726.
- [26] V. B. Birman, A. L. Rheingold, K. C. Lam, *Tetrahedron Asymmetry* **1999**, *10*, 125–131.
- [27] J. H. Zhang, J. Liao, X. Cui, K. B. Yu, J. Zhu, J. G. Deng, S. F. Zhu, L. X. Wang, Q. L. Zhou, L. W. Chung, et al., *Tetrahedron Asymmetry* **2002**, *13*, 1363–1366.
- [28] J. H. Xie, L. X. Wang, Y. Fu, S. F. Zhu, B. M. Fan, H. F. Duan, Q. L. Zhou, *J. Am. Chem. Soc.* **2003**, *125*, 4404–4405.
- [29] J. H. Xie, Q. L. Zhou, *Acc. Chem. Res.* **2008**, *41*, 581–593.
- [30] K. Ding, Z. Han, Z. Wang, *Chem. - An Asian J.* **2009**, *4*, 32–41.
- [31] S. Li, J. W. Zhang, X. L. Li, D. J. Cheng, B. Tan, *J. Am. Chem. Soc.* **2016**, *138*, 16561–16566.
- [32] Z. Sun, G. A. Winschel, A. Borovika, P. Nagorny, *J. Am. Chem. Soc.* **2012**, *134*, 8074–8077.
- [33] P. Nagorny, Z. Sun, G. A. Winschel, *Synlett* **2013**, *24*, 661–665.
- [34] Y. Y. Khomutnyk, A. J. Argüelles, G. A. Winschel, Z. Sun, P. M. Zimmerman, P. Nagorny, *J. Am. Chem. Soc.* **2016**, *138*, 444–456.
- [35] H. Shimizu, I. Nagasaki, K. Matsumura, N. Sayo, T. Saito, *Acc. Chem. Res.* **2007**, *40*, 1385–1393.
- [36] C. M. Lavoie, P. M. Macqueen, N. L. Rotta-Loria, R. S. Sawatzky, A. Borzenko, A. J. Chisholm, B. K. V. Hargreaves, R. McDonald, M. J. Ferguson, M. Stradiotto, *Nat. Commun.* **2016**, *7*, 11073.
- [37] X. Wang, Z. Han, Z. Wang, K. Ding, *Angew. Chem., Int. Ed.* **2012**, *51*, 936–940.
- [38] K. Soai, S. Yokoyama, T. Hayasaka, *J. Org. Chem.* **1991**, *56*, 4264–4268.
- [39] M. C. Wang, Y. H. Wang, G. W. Li, P. P. Sun, J. X. Tian, H. J. Lu, *Tetrahedron Asymmetry* **2011**, *22*, 761–768.
- [40] Y. Ebe, M. Onoda, T. Nishimura, H. Yorimitsu, *Angew. Chem., Int. Ed.* **2017**, *56*, 5607–5611.
- [41] J. H. Xie, H. F. Duan, B. M. Fan, X. Cheng, L. X. Wang, Q. L. Zhou, *Adv. Synth. Catal.* **2004**, *346*, 625–632.
- [42] J. Hu, H. Hirao, Y. Li, J. Zhou, *Angew. Chem., Int. Ed.* **2013**, *52*, 8676–8680.
- [43] R. Guo, T. T. L. Au-Yeung, J. Wu, M. C. K. Choi, A. S. C. Chan, *Tetrahedron Asymmetry* **2002**, *13*, 2519–2522.
- [44] S. Takizawa, K. Kiriyama, K. Ieki, H. Sasai, *Chem. Commun.* **2011**, *47*, 9227–9229.
- [45] P. Geerlings, F. De Proft, W. Langenaeker, *Chem. Rev.* **2003**, *103*, 1793–1874.

- [46] L. Yang, D. R. Powell, R. P. Houser, *Dalt. Trans.* **2007**, 0, 955–964.
- [47] A. Okuniewski, D. Rosiak, J. Chojnacki, B. Becker, *Polyhedron* **2015**, 90, 47–57.

CHAPTER 5

Studies on the Mechanism of Phosphoric Acid-Catalyzed Glycosylation of Complex Polyols

“It is well to remember that most arguments in favor of not trying an experiment are too flimsily based”

Robert Burns Woodward

5.1 Introduction to chemical glycosylation

Throughout the 20th century, it became evident that carbohydrates and glycosylated natural products, were indispensable in biological systems not just as an energy source, but also as key agents in signaling and recognition events of many biological processes.^[1] As examples, oligosaccharides on the cell surface determine human blood groups and play key roles during infection; and several carbohydrate-based vaccines are used to control bacterial disease such as *Haemophilus influenza* type B.^[2] Even today, the role of many glycoconjugates are just being discovered or remain a mystery.^[3] To put things in perspective, according to a survey conducted by Thorson, approximately 20% of bacterial natural products are glycosides.^[4] Thanks to the contributions of the past generation of chemists and biochemists, it is now commonly accepted that carbohydrates play fundamental roles in the development, recognition, growth, function, and survival of living cells and organisms.^[5]

Given the tremendous implications of carbohydrates to biological systems, it is no surprise that even simple carbohydrates are commonly found as powerful scaffolds drug in discovery.^[6,7] In addition, it is well known that glycosylation of drug candidates can result in a drastic

improvement of key properties such as *in vivo* circulatory half-life,^[8] immunogenicity,^[9] selectivity, efficacy, and safety.^[10,11] However the field of glycochemistry has struggled to advance in comparison to other disciplines such as those considering oligonucleotides and proteins.^[5] Several reasons can be given to explain this: 1) the identification of the number of glycan structures in a cell or organism, the “glycome”, is difficult due to the multitude of carbohydrate-containing molecules, variations in sugar identity, and possible glycoforms; 2) the carbohydrate structures themselves are structurally complex, for example glycosides in bacteria can be composed by many monosaccharides connected in a perplexing array of branched structures; and 3) the synthesis of carbohydrates mostly relies on target-specific strategies, only really accessible to synthetic groups with carbohydrate chemistry expertise, in great opposition to the assembly of oligonucleotides and oligopeptides from anomeric building blocks using standardized protocols.^[5,12,13] Figure 5.1 contains a small selection of glycosides which serves to showcase the structural diversity and complexity of some sugar-containing synthetic targets.

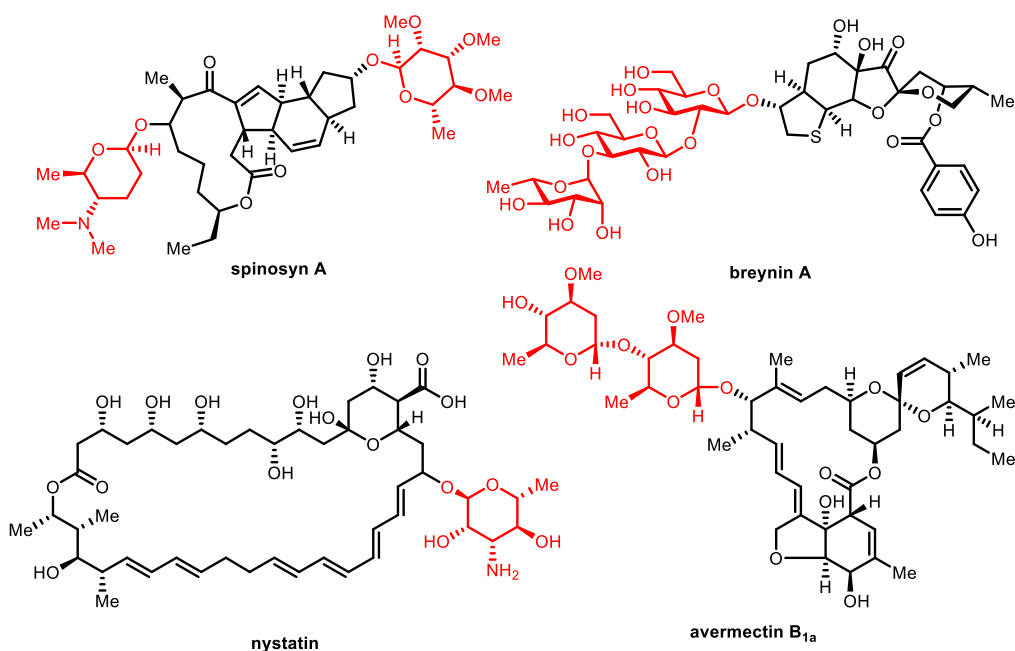
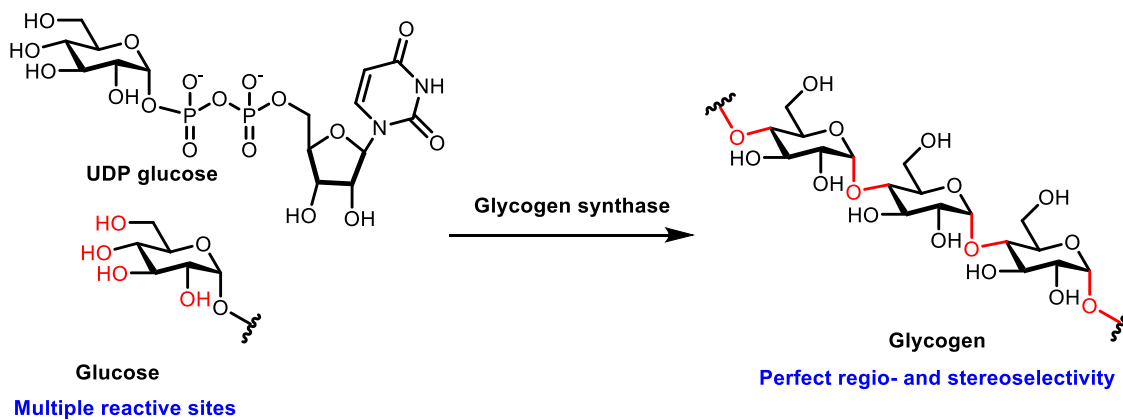


Figure 5.1. Selection of sugar-containing natural products.

The main challenge associated with the synthesis of sugar-containing molecules is the construction of glycosidic linkages between fragments with the correct stereo- and regiochemistry. This is especially true when fragments contain multiple functional groups capable of being glycosylated. The mainstay strategy used to address this relies on multistep protection and deprotection sequences to achieve selective regio- and chemoselective glycosylations of natural products, in conjunction with a judicious choice of a combination of glycosyl donor and glycosyl acceptor to control the stereochemistry of the product.^[14] As it is evident, this strategy represents an *ad hoc* solution tailored to each individual synthetic target. A better alternative would be to forgo the requirement of selective protection and instead rely on the design and implementation of efficient and selective catalysts for the glycosylation step.^[15] We know that this is not only possible, but ideal as it is the modus operandi of nature. Indeed, nature utilizes enzymes to perform glycosylations with exquisite regio- and stereocontrol. For instance, glycogen synthase, a class of glycosyltransferase enzymes, catalyzes the selective formation of $\alpha(1\rightarrow4)$ glycosidic bonds between glucose monomers to produce glycogen, an essential form of energy storage in mammals and other living species (Scheme 5.1).^[16]

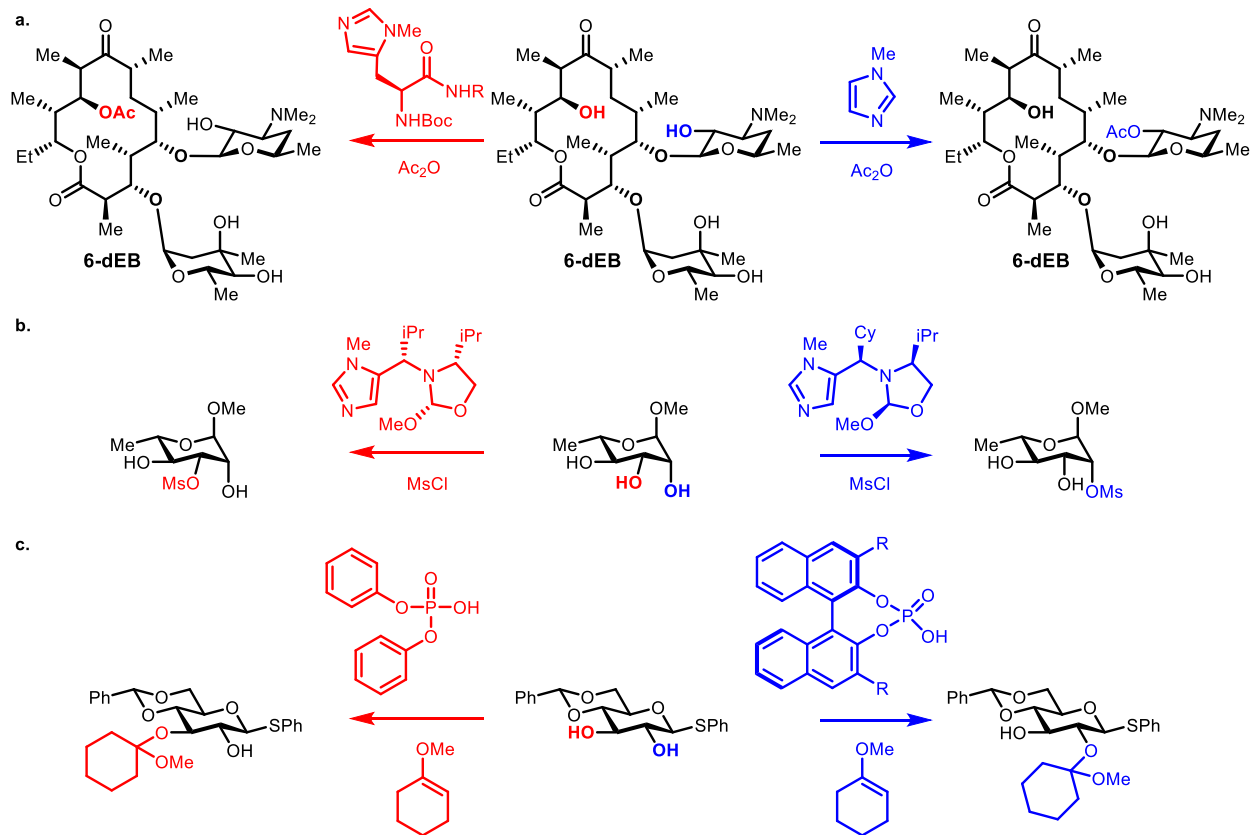
Scheme 5.1. Simplified biosynthesis of glycogen.



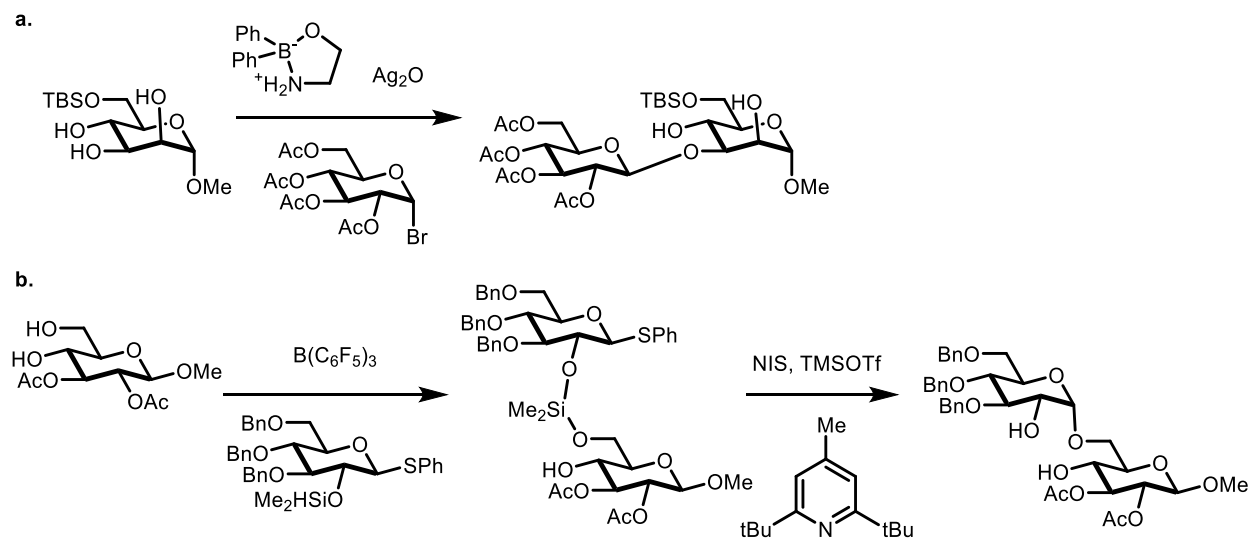
Although nature is very successful in derivatizing molecules with excellent control, replicating such degrees of selectivities in a flask remains a formidable challenge. However, thanks to the contributions of many research groups, remarkable advances in the site-selective functionalization of polyols have been made, some of which are mentioned next. Miller, one of the pioneers in this field, used a peptide derived organic catalyst to regioselectively install sugar moieties in complex polyols such as erythromycin,^[17] vancomycin,^[18–20] and apoptolidin A^[21] (Scheme 5.2a). In 2013, the Tan group reported the regiodivergent glycosylation of unprotected monosaccharides using a chiral amine base as an organocatalyst (Scheme 5.2b).^[22] As a final example, contemporaneously to the Tan group we published our work in the chiral phosphoric acid catalyzed regioselective acetalization of monosaccharides-derived diols (Scheme 5.2c, see section **2.1** for an introduction to phosphoric acid catalysts).^[23]

The inherent selectivity bias that bulky and chiral sugar donors impose as well as the stereochemistry in the formation of the glycosidic bond, make site-selective glycosylation of natural products even more challenging than the functionalization of natural products with simple groups such as those examples shown in Scheme 5.2. However, chemists have come up with many inventive solutions to accomplish chemical site-selective glycosylations of unprotected polyols.^[14] For example, in 2011 the Taylor group reported the use of borinic acids as catalysts in the highly rigid selective glycosylation of unprotected monosaccharides (Scheme 5.3a).^[24] In addition, indirect glycosylation strategies have also been reported such as the work by the Montgomery group on an intramolecular aglycone delivery in the synthesis of 1,6-disaccharides (Scheme 5.3b).^[25]

Scheme 5.2. Examples of regioselective functionalization of polyols.



Scheme 5.3. Examples of site-selective glycosylation of polyols.



Another hurdle in the development of powerful and general glycosylation methodologies is that disproportionately small amounts of information are known about the mechanistic details of glycosylations, even though this is the most important reaction in the field of glycoscience. The lack of mechanistic insight results in an unnecessarily high degree of empiricism that slows down the development of next-generation catalysts for glycosylations. An explanation to this is that glycosylation reactions are immensely detailed and complicated, and a wide spread of competing mechanisms ranging from S_N1 to S_N2 are invoked.^[26–29] Insights in glycosylation mechanisms, therefore, are greatly needed.

The Nagorny group has a long-standing interest in the development of powerful glycosylation reactions. To this end, Dr. Tay Rosenthal (Nagorny group) studied the CPA-controlled stereo- and regioselective glycosylation of complex polyols. Given our experience and success in the application of the growing string method to the mechanistic elucidation of CPA-catalyzed spiroketalizations (See Chapter 3), a collaboration to uncover the finer mechanistic details of CPA-catalyzed glycosylations was undertaken and is described section 5.2. In addition, in 2013 the Nagorny group reported that CPAs and enol ethers could be used to regioselectively protect sugar pyranosides bearing unprotected hydroxyl groups at the C2 and C3 positions. Our computational mechanistic investigations into this related transformation are detailed in section 5.3. Finally, given our success in the regioselective acetalization of diols in sugar frameworks (section 5.3) and in regio- and stereoselective glycosylation of 6-dEB (section 5.2), we hypothesized that we could employ CPAs to glycosylate D-glucose-derived diols with stereocontrol and site-selectivity. Computational work revealed mechanistic details of these efforts, which are expanded in section 5.4.

5.2 Mechanism of the CPA-Catalyzed Regiodivergent Glycosylation of 6-deoxy-Erythronolide B

(This section was adapted from:

Tay, J. H.; Argüelles, A. J.; DeMars, M.; Zimmerman, P. M.; Sherman, D.; Nagorny, P. *J. Am. Chem. Soc.* **2017**, *139*, 8570.

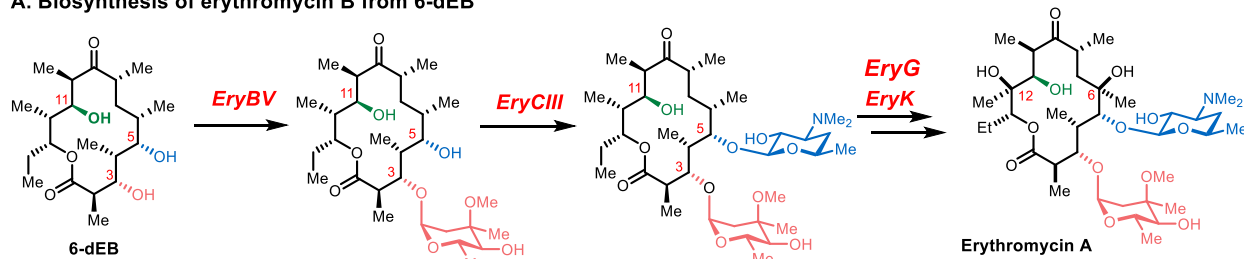
Experimental information can be found in **Appendix D**)

While some remarkable examples of stereo-, chemo-, or regioselective glycosylation reactions have recently emerged,^[24,25,48–51] the available synthetic tools have limited versatility, and many challenges for the selective glycosylation of polyols remain unaddressed. One of such challenges is achieving regiodivergent selective formation of glycosylated isoforms from the same initial polyol by judicious selection of catalysts or reaction conditions. Inspired by the seminal work of Miller and coworkers^[17,21,43] and believing that the problem of regiocontrol could be addressed with the use of chiral catalysts that would change the environment around the glycosyl donor and affect the default reactivity pattern exhibited by the acceptor,^[23] our groups pursued studies focused on developing and applying such transformations.^[52–55] In order to demonstrate the power of this approach in a complex settings medicinally important 14-membered triol, 6-deoxyerythronolide B (6-dEB), was selected as our initial target.

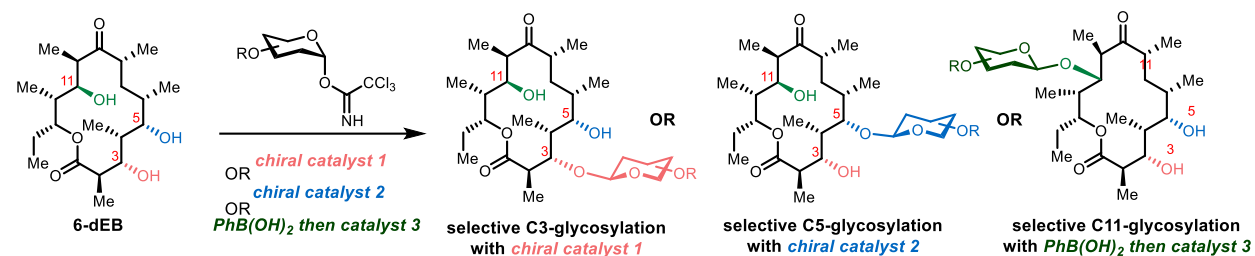
6-dEB is a biogenic precursor to 14-membered macrolide antibiotics erythromycins A and B.^[56] Once produced, 6-dEB undergoes sequential glycosylations first at the C3 and then at the C5 position, which is an essential requirement for both the subsequent oxygenation at the C12 position, as well as for the antibiotic activity exhibited by erythromycins (Figure 5.2A). While recombinant techniques provide access to non-glycosylated 6-dEB,^[57,58] the selective installation of sugars enzymatically represents a significant challenge.^[59,60] To address this challenge and to

demonstrate that chemical catalysis could serve as a powerful tool for the regioselective glycosylation of complex natural polyols, we initiated studies directed to discovery of new methods that would allow direct and selective formation of all three regioisomeric glycosides from unprotected 6-dEB (Figure 5.2B). In particular, we were interested in identifying chiral catalysts that could mimic the function of EryBV and accomplish selective installation of the sugar at the C3 position in the presence of other functionalities. Indeed, our subsequent studies revealed that chiral acids such as chiral phosphoric acids (CPAs)^[61-67] or chiral disulfonimides could promote regiodivergent introduction of different sugars at both the C5 or C3 positions of 6-dEB and oleandomycin-derived 14-membered macrolides. In addition, conditions based on temporarily *in situ* masking of the C3/C5 diol as a cyclic boronate and subsequent glycosylation of the C11 position followed by unmasking the diol upon work up have been developed. These protocols have been used to generate various isomeric glycosides of 6-dEB with 6-deoxysugars, a task that cannot be easily accomplished with existing achiral catalyst-based glycosylation or enzymatic methods. Remarkably, the mechanistic and theoretical studies contradict the traditionally proposed oxocarbenium ion-based reaction mechanism and are in line with the formation of covalently linked anomeric phosphate reaction intermediates (Figure 5.2C). This work represents the first example of chiral catalyst-controlled regioselective glycosylation, and the methods developed in this study hold great potential for the non-enzymatic generation of glycosylated isoforms of complex natural polyols.

A. Biosynthesis of erythromycin B from 6-dEB



B. Accessing glycosylated 6-dEB by mimicking glycosyltransferases with chiral catalysts (this work)



C. Chiral phosphoric acids as the catalysts for regioselective glycosylation reaction

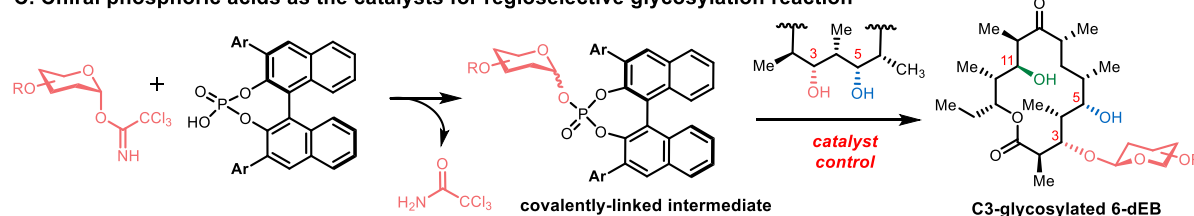
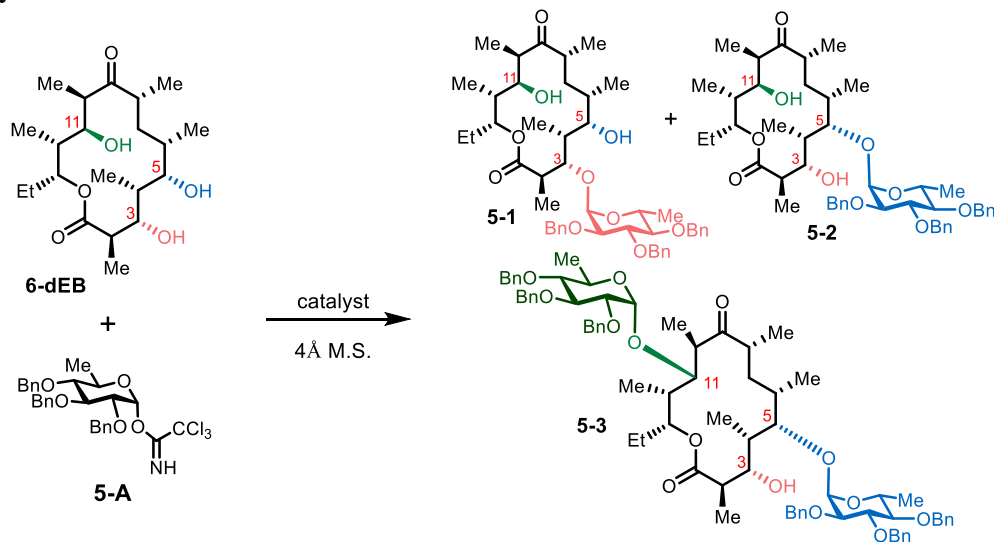


Figure 5.2. Regioselective glycosylation of 6-dEB.

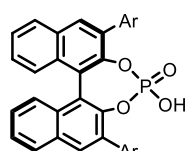
To acquire sufficient amounts of 6-dEB for our studies, we employed an *E. coli* strain that had previously been engineered and optimized for high-level production of this biosynthetic intermediate.^[58] Although the original study reported 6-dEB production titers as high as 129 mg/L in shake flask fermentation experiments, we were unable to reproduce these yields under the same conditions, typically acquiring ~5 mg/L of isolated material. Furthermore, quantification of 6-dEB production by LC-MS prior to culture extraction revealed that the low isolated yields were not due to loss of material from downstream workup, isolation, and purification procedures. After testing several alternative culturing conditions, we established a protocol that could reliably furnish 20–25 mg/L of the purified macrolactone. Thus, 200 mg of pure 6-dEB for glycosylation studies could be obtained in a facile manner following purification from a standard 9 L-scale fermentation.

Our studies commenced with investigating selective glycosylation of 6-dEB with 6-deoxyglucose derivative **5-A** (Table 5.1). To establish the inherent reactivity of the C3, C5, and C11 hydroxyls, control experiments where the reaction between 6-dEB and **5-A** was catalyzed by achiral catalysts (TMSOTf, (PhO)₂PO₂H, anhydrous *p*-TsOH and BF₃•OEt₂) were carried out (entries 1–5). The reaction with TMSOTf resulted in exclusive formation of the α -C5 product **5-2** (50% yield) along with the formation of *bis*-glycosylated product **5-3** (7% yield). The reaction with diphenylphosphoric acid (50 mol%) in dichloromethane and toluene (entries 2 and 3) proceeded with low conversion and provided the C5-glycoside (**5-2**) as the major product (24% and 30% yield respectively) along with minor quantities (5-6% yield) of the corresponding C3 product **5-1**. Despite its higher acidity, anhydrous *p*-TsOH was not an effective catalyst for the glycosylation of 6-dEB and only trace amounts of products **5-1** and **5-2** (< 10%, 17:83 r.r.) was detected by NMR. Finally, the reaction catalyzed by BF₃•OEt₂, (entry 5), a standard promoter for the glycosylation with trichloroacetimidates, proceeded in 59% yield to provide products **5-2** and **5-1** in 66:34 d.r. While all of the previous control reactions (entries 1-4) resulted in clean formation of the α -anomers, the reaction with BF₃•OEt₂ as the catalyst led to the mixture of diastereomers of the C5-product **5-2** (α : β = 2.9:1). It should be noted that thus produced glycosides contain perbenzylated sugars, which can be converted in one step to the fully deprotected macrolide glycosides by hydrogenolysis over Pd/C as exemplified by the debenylation of **5-2** to **5-2A** (Scheme 5.4).

Table 5.1. Optimization of CPA-catalyzed glycosylation of 6-dEB^a. Experiments were performed by Dr. Tay Rosenthal.

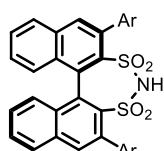


entry	activator (mol%)	solvent (conc.)	T (°C)	t (h)	yield	1 : 2 : 3
1	TMS-OTf (20)	PhMe (0.05 M)	-20	17	57%	0 : 88 : 12
2	PhO ₂ PO ₂ H (50)	CH ₂ Cl ₂ (0.05 M)	r.t.	26	30%	21 : 79 : 0
3	(<i>R</i>)-5-4a (20)	CH ₂ Cl ₂ (0.05 M)	r.t.	30	13%	13 : 87 : 0
4	(<i>R</i>)-5-4b (20)	CH ₂ Cl ₂ (0.05 M)	r.t.	30	13%	17 : 83 : 0
5	(<i>R</i>)-5-4c (20)	PhMe (0.10 M)	r.t.	24	57%	25 : 75 : 0
6	(<i>R</i>)-5-4d (20)	CH ₂ Cl ₂ (0.05 M)	r.t.	26	50%	50 : 50 : 0
7	(<i>S</i>)-5-4d (20)	PhMe (0.20 M)	r.t.	30	98%	1 : 99 : 0
8	(<i>R</i>)-5-5d (20)	PhMe (0.10 M)	r.t.	24	71%	1 : 99 : 0
9	(<i>R</i>)-5-4e (20)	PhMe (0.10 M)	r.t.	24	80%	52 : 48 : 0
10	(<i>R</i>)-5-4f (20)	CH ₂ Cl ₂ (0.05 M)	r.t.	48	51%	69 : 31 : 0
11	(<i>R</i>)-5-6f (20)	PhMe (0.10 M)	r.t.	48	75%	7 : 93 : 0
12	(<i>S</i>)-5-6f (20)	PhMe (0.10 M)	r.t.	48	54%	60 : 40 : 0
13	(<i>S</i>)-5-6f (20)	PhCF ₃ (0.10 M)	r.t.	64	83%	63 : 37 : 0
14	(<i>S</i>)-5-6f (20)	CH ₂ Cl ₂ (0.10 M)	r.t.	64	57%	71 : 29 : 0
15	(<i>S</i>)-5-6f (30)	CH ₂ Cl ₂ (0.10 M)	r.t.	72	82%	73 : 27 : 0



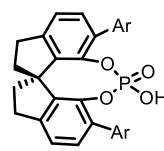
(*R*)-5-4

a : Ar = 2,6-*i*Pr₂-4-Ad-C₆H₂
 b : Ar = 2,4,6-*i*Pr₃-C₆H₂

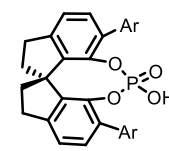


(*R*)-5-5

c : Ar = C₆F₅
 d : Ar = 3,5-CF₃-C₆H₃



(*R*)-5-6

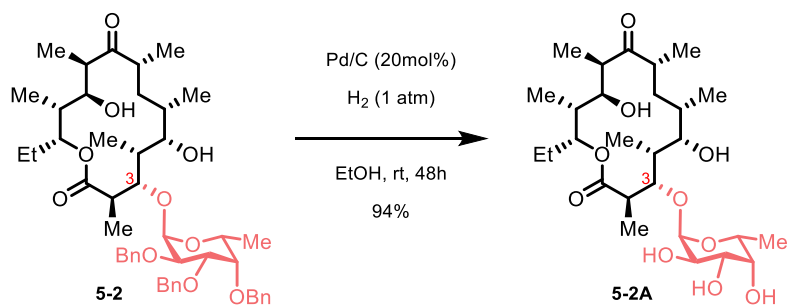


(*S*)-5-6

e : Ar = 3,5-Cl-C₆H₃
 f : Ar = 3,5-F-C₆H₃

^aConditions: 6-dEB (1 equiv.), A (1.2 equiv.), 4 Å M.S., solvent (0.20–0.05 M). Reactions were run on 0.02 mmol scale. ^bObtained as the 2.9:1 mixture of α : β diastereomers.

Scheme 5.4. Debenzylation of **2**. Experiments were performed by Dr. Tay Rosenthal.



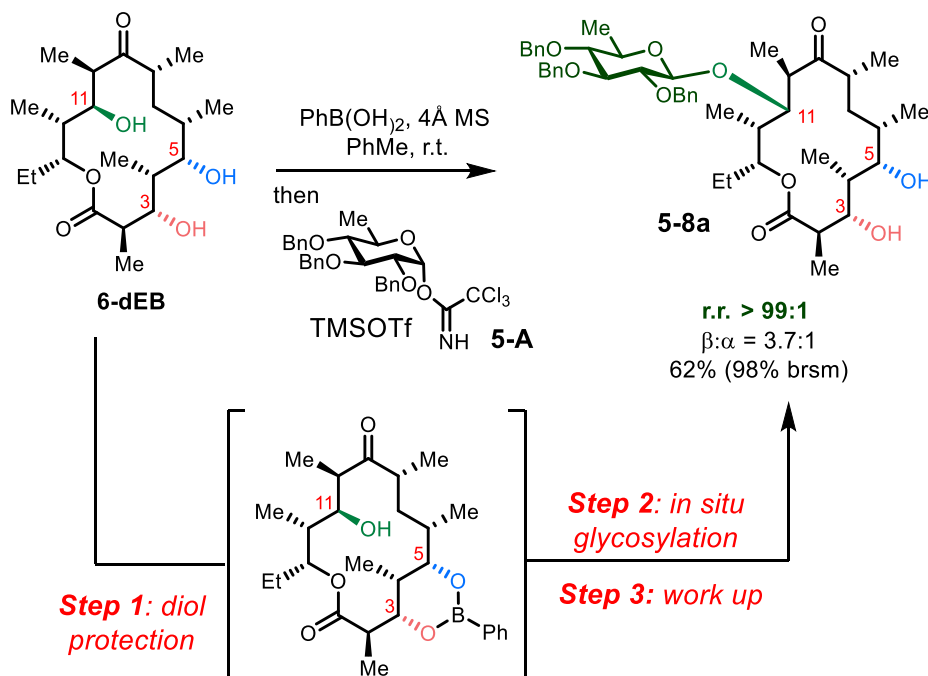
With these results in hand, our subsequent studies were focused on evaluating various chiral catalysts (entries 6–12) with the objective of increasing the selectivity and yield of the C5-glycoside **5-2**. The evaluation of catalysts **5-4a-d** in nonpolar solvents (entries 6–11) helped to identify catalyst **(S)-5-4d** as the catalyst of choice (entry 11) that promoted the formation of α -C5 glycoside **5-2** in an excellent yield and selectivity (98% yield, 99:1 r.r.) and without the formation of *bis*-glycoside **5-3**. In addition, commercially available *bis*-sulfonimide **(R)-5-5d** could also promote highly selective formation of **5-2** albeit in lower yield (71% yield, entry 12). The biosynthesis of Erythromycin A from 6-dEB involves initial selective glycosylation at the C3 position catalyzed by EryBV.^[68–71] However, our results indicate that the non-enzymatic version of this transformation is not accessible as the C5 hydroxyl of 6-dEB is inherently more reactive than the C3 position. Therefore, one of the important objectives in our following studies was to discover a catalyst that could mimic EryBV function and promote a C3-selective glycosylation directly from 6-dEB. The aforementioned studies indicated that the use of catalyst **(R)-5-4d** with DCM as the solvent (entry 9) resulted in ~1:1 C5:C3 selectivity and thus we decided to explore structurally similar catalysts with the objective of enhancing selectivity for the formation of **5-1** (entries 13–19). Considering that **(R)-5-4d** possesses 3,3'-aryl substituents functionalized at the 3,5-positions of the phenyl ring (i.e. 3,5-(CF₃)₂Ph–), BINOL-based catalysts **5-4e** and **5-4f** with similar substitution of the phenyl ring were examined (entries 13 and 14). To our delight, catalyst

(R)-5-4f (Ar = 3,5-F-Ph) indeed promoted the selective formation of **1** for the first time (51% yield, 69:31 r.r.). In further attempts to optimize the reaction yield and selectivity, SPINOL-based catalysts **5-6** were examined (entries 15–19). Such catalysts possess a less flexible backbone with a different angle between substituents, which may result in a better differentiation of the diastereomeric transition states and hence higher selectivities in comparison to the BINOL based catalysts.^[72] Gratifyingly, catalyst **(S)-5-6f** (with a stereochemical configuration identical to **(R)-5-4f** and Ar = 3,5-F-Ph) promoted selective formation of the C3 glycoside **5-1** in higher yield and selectivity (82% yield, 73:27 r.r.) when the reaction was carried in dichloromethane at room temperature (entry 19). In addition, the use of enantiomeric catalyst **(R)-5-6f** resulted in a selectivity switch and enhanced formation of the C5-glycosylated product **5-2** (entry 11, 75% yield, 93:7 r.r.). These results strongly indicate that the chiral catalyst configuration plays a determining role for whether the C5 (entry 11) or C3 (entry 19) position of 6-dEB is functionalized. Although with lower selectivity than observed in nature with EryBV, catalyst **(R)-5-6f** overrides the inherent preference for the C5 glycosylation exhibited by 6-dEB and directs glycosylation to proceed at the C3-position.

The optimization studies depicted in Table 5.1 led to the development of selective reactions between 6-dEB and 6-deoxyglucose derivative **5-A** that resulted in the C3-product **5-1** (73:27 r.r., >99:1 α : β , 82% yield) or the C5-product **5-2** (99:1 r.r., >99:1 α : β , 98% yield). In order to demonstrate that regiodivergent glycosylation of 6-dEB leading to all possible regioisomeric forms is possible, the development of a protocol allowing single step generation of the C11 glycoform of 6-dEB (**5-8a**) was pursued next (Scheme 5.5). Based on the prior glycosylation studies (Table 5.1), the C11 hydroxyl appeared to be the least reactive hydroxyl functionality in 6-dEB. We surmised that since the C3 and C5 hydroxyls are in 1,3-*syn* relationship, they could be selectively

masked to form a cyclic boronic acid ester, which, in theory, could be formed *in situ* and cleaved upon work up without introducing additional steps. While such strategy has been successfully implemented in carbohydrate synthesis,^[73–75] we are unaware of its use for the single-pot selective glycosylation of 14-membered macrolides or other non-carbohydrate-based natural products. Upon careful selection of the reaction conditions, the traceless *in situ* protection of 6-dEB with phenylboronic acid followed by glycosylation with **5-A** was accomplished to provide the corresponding C11 glycoside. This single pot sequence was completed by peroxide work up that cleaved boronate and resulted in **5-8a** in 62% yield (99:1 r.r., 3.7:1 β : α).

Scheme 5.5. Single-pot traceless protection/glycosylation of the C11-position of 6-dEB. Experiments were performed by Dr. Tay Rosenthal.



With selective methods for the introduction of sugar at all three positions of 6-dEB leading to glycosylated macrolides **5-1**, **5-2**, and **5-8a** (Table 5.2) in hand, the scope and limitations of these methods were investigated. To demonstrate that catalysts (*S*)-**5-4d** and (*S*)-**5-6f** could promote the reactions with other 6-deoxysugars, the reaction of 6-dEB and *D*-fucose derivative 5-

B using chiral catalyst-controlled glycosylation (conditions I and II, Table 5.2) was examined. As before, in the control experiment with TMSOTf as the promoter, the highly selective formation of C5 product **5-8c** was observed in 69% yield along with significant amounts (31% yield) of *bis*-glycosylated product. This strongly contrasts with the (*S*)-**5-6f**-catalyzed reaction (conditions I) that allowed achieving the formation of the C3 product **5-8b** that was not observed in the control experiment (56:44 r.r., >99:1 α : β , 87% yield). As before, applying the BINOL-based catalyst (*S*)-**5-4b** resulted in exclusive formation of the C5 glycoside **5-8c** (>99:1 r.r., 1.7:1 α : β , 82% yield) with no *bis*-glycosylation product observed in the reaction mixture.

Our studies turned next to demonstrating that the methods identified in Table 5.2 could be applicable to the glycosylation of macrolides other than 6-dEB. Thus, we identified a related 14-membered macrolide **5-7** as a substrate that is structurally similar to 6-dEB, yet displays a dissimilar reactivity pattern due to the variant functionalities at the C8 position. In addition, this readily accessible oleandomycin derivative was selected due to its stability to spontaneous hemiacetalization documented for other deglycosylated oleandomycin derivatives.^[70,76] Interestingly, macrolide **5-7** exhibited a markedly different reactivity profile in comparison to 6-dEB in reactions with achiral and chiral catalysts. When exposed to TMSOTf (conditions IV), macrolide **5-7** and donor **5-A** reacted to produce the mixture of the C5 product **5-8d** (99:1 r.r., 1.6:1 = α : β , 31% yield), and hemiacetalized C3 side product **5-8e** (99:1 r.r., 1.6:1 = α : β , 31% yield). These results suggest that the C3 and C5 hydroxyls are equally reactive, and that an unselective glycosylation is followed by hemiacetalization of the C3 product to form **5-8e**. Similarly, the reactions catalyzed by CPAs followed a different trend as both (*R*)- and (*S*)-CPA catalysts were found to be C3-selective. The highest selectivity for the reaction of **5-7** and **5-A** was observed for the catalyst (*R*)-**5-6f**, while its enantiomer (*S*)-**5-6f** also promoted a C3-selective glycosylation of

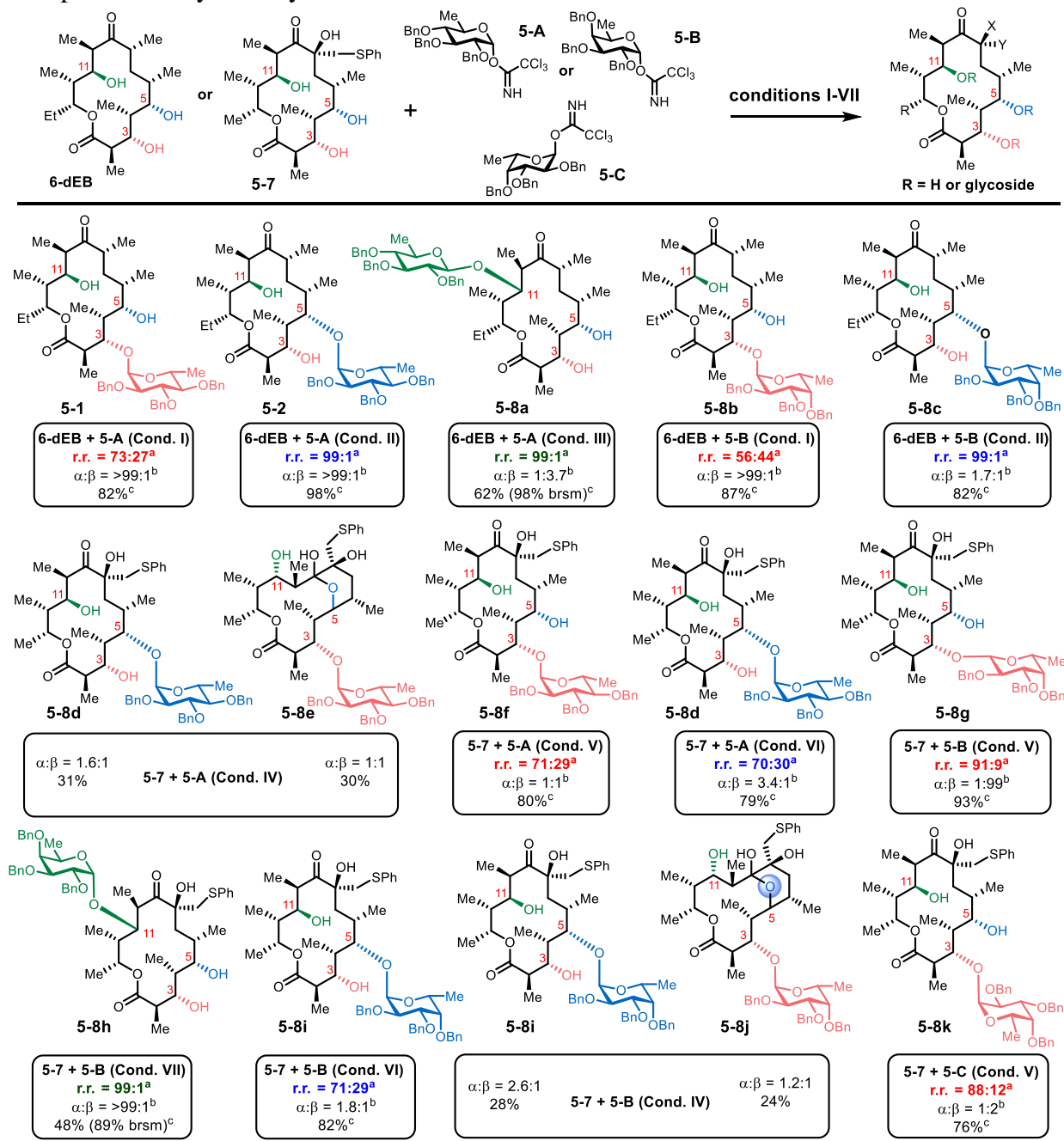
5-7; albeit with lower regioselectivity. Thus, the use of (**R**)-**5-6f** led to regioselective formation of the C3 glycoside **5-8f** (71:29 r.r., 1:1 = α : β , 80% yield), while the reaction with (**R**)-**5-6f** provided 39% of **5-8f** (3.4:1 = α : β) and 21% of C5-glycosylated product **5-8d** with no hemiacetalization side product **5-8e** observed. In attempts to accomplish selective C5 glycosylation, catalysts (**S**)-**5-4d** and (**R**)-**5-5d** were explored, and (**R**)-**5-5d** catalyzed the selective formation of the C5 product **5-8d** (70:30 r.r., 3.4:1 = α : β , 79% yield). Similar trends were observed for the glycosylation of **5-7** with fucose derivative **5-B**. In a control reaction, macrolide **5-7** provided equimolar mixture of C5-glycosylated product **5-8i** along with the hemiacetalized C3-glycosylated product **5-8j**. The use of catalyst (**S**)-**5-6f** resulted in a highly selective formation of the corresponding C3 product (91:9 r.r., 1:99 = α : β , 93% yield). Using our prior findings, the formation of the C5-glycosylated product **5-8i** was accomplished with catalyst (**R**)-**5-5d** (71:29 r.r., 1.8:1 = α : β , 82% yield). Additionally, we demonstrated that, in analogy to 6-dEB, macrolide **5-7** could also be glycosylated at the C11 position to provide compound **5-8h** (99:1 r.r., 99:1 α : β , 48%, 89% brsm) yield) using traceless *in situ* protection with methylboronic acid prior to glycosylation (conditions V). Finally, to assess the effect of sugar chirality, the reactions of **5-7** with enantiomeric *L*-fucose derivative **5-C** were investigated. The control experiments with **C** where TMSOTf was used as the catalyst resulted in essentially the same outcome as the *D*-fucose derivative **5-B**. Similarly, the (**R**)-**5-6f**-catalyzed reaction of **5-7** and **5-C** proceeded with high levels of regioselectivity and provided the corresponding C3 glycoside **5-8k** (88:12 r.r., 1:2 α : β , 76% yield). In summary, while the change in the macrolide structure may require reevaluation of a preselected group of catalyst (i.e. (**R**)- and (**S**)- enantiomers of **5-4d**, **5-5d** and **5-6f**), the overall regioselectivity trends hold for a given macrolide and are not affected by minor changes in the donor structure.

To rule out the possibility of deglycosylation pathways that may affect the observed

selectivities, NMR studies of the reaction was employed to monitor the reaction of **5-7** and **5-B** leading to selective formation of the C3-glycoside **5-8h** at different conversions, and no changes in the product composition were observed. In addition, the overnight exposure of the C5-glycoside **5-8i** to catalyst (*R*)-**5-6f** did not lead to any isomerization products or formation of hemiacetal **5-8j**. However, the overnight treatment of the C3-glycoside **5-8h** with TMSOTf at $-20\text{ }^{\circ}\text{C}$ led to the slow formation of hemiacetalization product **5-8j**. These observations suggest that the selectivities observed in Tables 5.1 and 5.2 are due to the catalyst control and are not due to the decomposition or isomerization reactions.

In order to further understand the mechanism and stereoselectivity of the aforementioned reactions, a combined experimental and computational mechanistic investigation was undertaken (Figure 5.3). Based on a similar system,^[52–55] we hypothesized an oxocarbenium intermediate could be formed by Brønsted acid activation and departure of the trichloroacetimidate moiety. In this scenario, the chiral environment of the CPA/oxocarbenium ion pair would provide stereocontrol. To probe this mechanism a simplified model system was developed (Figure 5.3A) and modern reaction path searching algorithms developed by the Zimmerman group were used.^[77–80] This assessment surprisingly found the formation of β -anomeric phosphate **5-9B** via a $\text{S}_{\text{N}}2$ -like displacement of the α -trichloroacetimidate **5-9A** (**TS**₁, Figure 5.3B) was facile, at a 12.1 kcal/mol barrier. Following an exchange with 2,4-pentadiol (**5-9C**), a second, rate-determining (**TS**₂, 20.7 kcal/mol), $\text{S}_{\text{N}}2$ -like reaction affords the α -glycoside **5-9D**. Interestingly, the *syn*-1,3 diol moiety plays a role in the glycosylation step, as it is more geometrically suited to do an inversion on the anomeric center. This step involves a proton shuttle mechanism akin to enzymatic reactions, where one hydroxyl group protonates the leaving phosphate and simultaneously deprotonates the proximal attacking hydroxyl group.

Table 5.2. Regiodivergent glycosylation of 6-dEB and oleandomycin derivative **5-7**. Experiments were performed by Dr. Tay Rosenthal.



Condition I: 6-dEB (1 equiv.), donor (1.2 equiv.), (*S*)-**5-6f** (30 mol%), 4Å M.S., CH₂Cl₂ (0.10M), r.t.; **Condition II:** 6-dEB (1 equiv.), donor (1.2 equiv.), (*S*)-**5-4d** (20 mol%), 4Å M.S., PhMe (0.20M), r.t.; **Condition III:** 6-dEB (1 equiv.), PhB(OH)₂ (1 equiv.), 4Å M.S., PhMe, r.t.; then **5-A** (3 equiv.), TMS-OTf (0.2 equiv.); -20 °C, work-up with H₂O₂ and NaHCO₃; **Condition IV:** **5-6** (1 equiv.), donor (1.2 equiv.), TMSOTf (0.2 equiv.), 4Å M.S., PhMe (0.05 M), -20 °C; **Condition V:** **5-6** (1 equiv.), donor (1.2 equiv.), (*R*)-**5-6f** (20 mol%), 4Å M.S., PhMe (0.30M), r.t.; **Condition VI:** **5-6** (1 equiv.), donor (1.2 equiv.), (*R*)-**5-5d** (20 mol%), 4Å M.S., PhMe (0.20 M), r.t.; **Condition VII:** **6** (1 equiv.), MeB(OH)₂ (1 equiv.), 4Å M.S., PhMe, r.t.; then **5-B** (3 equiv.), TMS-OTf (0.5 equiv.), -20 °C; work-up MeOH. All reactions were carried on 0.02 mmol scale with the exception of **5-8g**, which was formed on both 0.02 and 0.1 mmol scales without erosion in yield and selectivity. ^a Only C₃ and C₅ glycosides were observed. ^b The $\alpha:\beta$ selectivity for the major regioisomer ^c Isolated yield for the mixture of regioisomers

While these steps are labeled S_N2-like, the first step has a much earlier TS (**TS₁**: C-O_{formed} 2.63 Å vs C-O_{broken} 2.23 Å) compared to the second (**TS₂**: C-O_{formed} 2.09 Å vs C-O_{broken} 2.62 Å), which indicates that the latter is more dissociative in nature.^[28,81] In comparison, reactions in which the phosphate departed to form an intermediate oxocarbenium were found to be less favorable (> 26 kcal/mol). Finally, in order to discount the possibility of an uncatalyzed background reaction, an analogous S_N2-like displacement of α-trichloroacetimidate by the diol was modeled but found to be implausible (TS₃ in SI, 34.8 kcal/mol). Finally, it should be noted that trichloroacetamide (CCl₃CONH₂) released throughout the reaction might serve as an inhibitor by forming a hydrogen bond complex with chiral phosphoric acid or phosphate intermediate.^[82,83] Therefore further optimization of the glycosyl donor leaving group might lead to improved catalyst loading often observed for the other acetalization reactions.

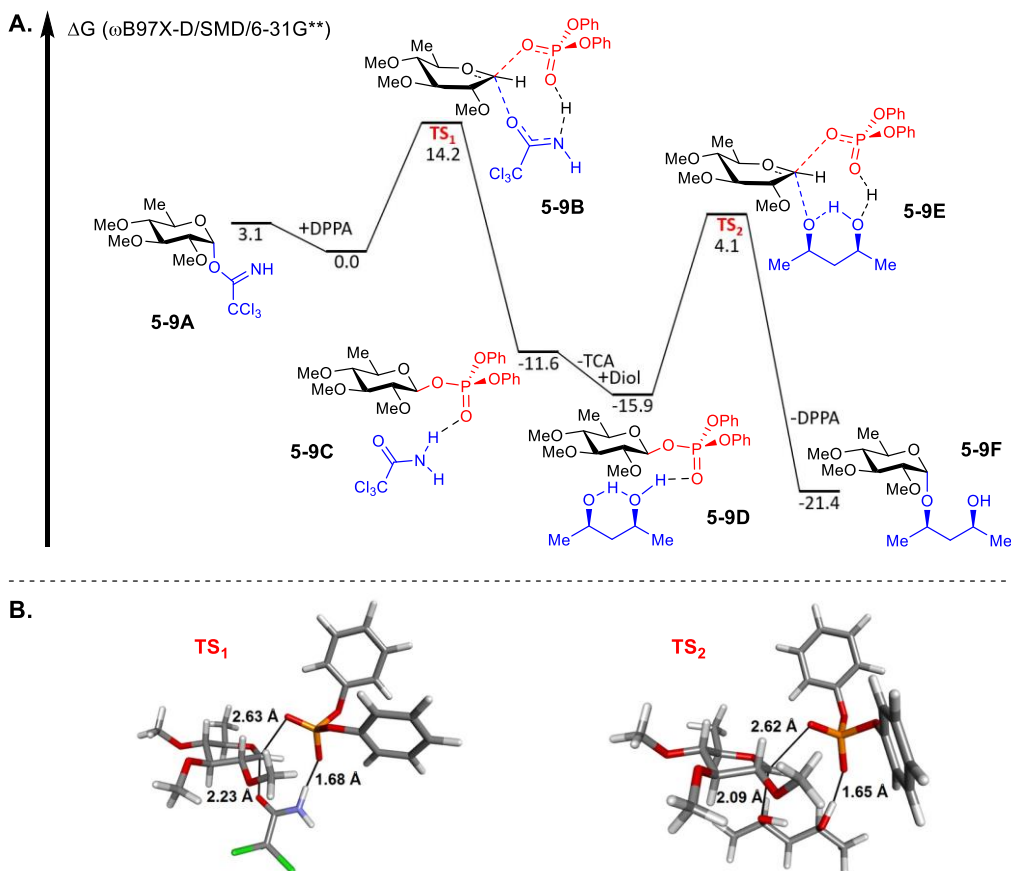
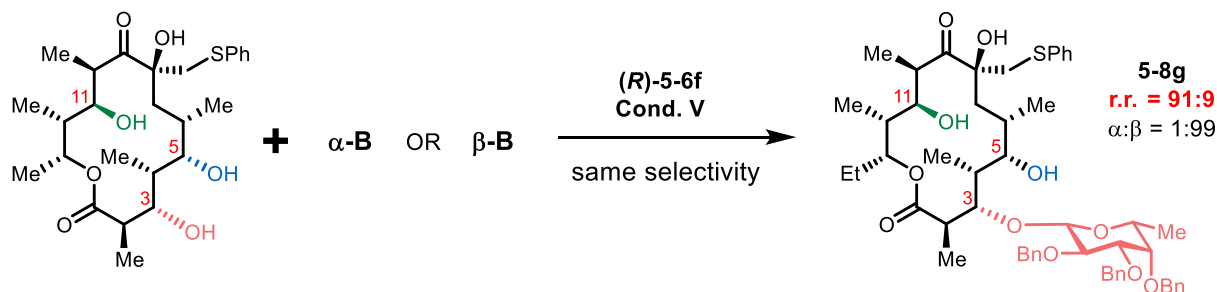


Figure 5.3. Theoretical studies on the mechanism of phosphoric acid-catalyzed glycosylations.

As the proposed mechanism is fundamentally different to proposals on similar systems,^[28,52,84] experimental support was sought. Since the phosphate intermediate was predicted to be relatively stable, efforts were directed to detect the formation of **5-9B**. Indeed, when monosaccharide **5-A** is combined with (*R*)- **5-6f**, anomeric phosphate **β-5-10** was observed by NMR (Figure 5.4). When combined with CD₃OD, **β-5-10** underwent a facile S_N2-like displacement forming product **α-5-11**. Likewise, when a similar investigation was carried on sugar derivative **C** (Figure 5.4), the formation of an α-phosphate (**α-5-12**) was observed. This intermediate underwent stereoselective S_N2-like reaction with CD₃OD to provide the corresponding β-fucose derivative (**β-5-13**). In line with these experiments, the reaction between sugar **5-B** and (*R*)- **5-6f** produced anomeric phosphate **α-5-14** that was observed by NMR. When combined with macrolide **5-7**, phosphate **α-5-14** produced C3-glycosylation product **5-8g** (67% yield, 73:27 r.r., 99:1 α:β). Although the formation of the C3-glycoside **5-8g** for this control experiment was less selective than what was observed under conditions **V** (Table 5.2), we believe that this result is nonetheless consistent with the mechanistic proposal outlined in Figure 5.3 as some discrepancy in selectivity is expected based on the absence of molecular sieves as well as difference in concentration, and presence of larger quantities of trichloroacetimidate that may inhibit hydrogen bonding between **α-5-14** and macrolide **5-7**. Finally, a reaction of **β-B** and **5-7** lead to the formation of **5-8g** in the same selectivity as for the α-trichloroacetimidate **5-B** (Scheme 5.6), which is consistent with the formation of the same reaction intermediate such as anomeric phosphate from both α- and β-donors **5-B**. Altogether, these results along with the computational studies and precedents by the Schmidt group^[85-87] suggest that the mechanisms for the formation of the anomeric phosphates from trichloroacetimidates may vary and are not always S_N2-like, especially with axial alkoxy substituents in the C3 position. In addition, these results strongly

imply that the α : β selectivity for the final glycosylation step is determined by the stereoselectivity for the anomeric phosphate formation step (Scheme 5.6). It also should be noted that the proposed involvement of the covalently linked to catalyst intermediates is consistent with the mechanistic proposals made by our group for the CPA-catalyzed reactions of acetals^[88–90] and for the related transformation by Toste,^[91] List,^[92] Luo^[93] and Takasu^[94] groups.

Scheme 5.6. Glycosylation with anomeric phosphates. Experiments were performed by Dr. Tay Rosenthal.



Conclusion

In summary, this work describes the first example of chiral catalyst-controlled regioselective glycosylation of complex chiral polyols. These transformations were found to be particularly useful for the preparation of isomeric glycosides of 6-dEB and oleandomycin B derivative **5-7** with 6-deoxysugars, a task that cannot be easily accomplished with existing achiral catalyst-based or enzymatic methods. Chiral phosphoric acids and sulfonimides were used to promote regiodivergent introduction of the sugars at both the C5 or C3 positions of 6-dEB and **5-7** in a complementary manner. In addition, the conditions based on temporarily *in situ* masking of the C3/C5 diol as a cyclic boronate with a subsequent glycosylation of the C11 position followed by unmasking the diol upon work up have been developed and applied to directly form C11 glycosides **5-8a** and **5-8h** in excellent regioselectivities. While the change in the macrolide structure required re-optimization of the catalyst, the methods developed for specific macrolides tolerated changes in donor structure. Mechanistic and theoretical studies have been carried to

elucidate the mechanism by which phosphoric acids promote these transformations. These studies lend support to a mechanism with the formation of covalently linked anomeric phosphate intermediates, and more detailed mechanistic studies directed to understand the observed selectivity are currently underway. This work represents the first example of chiral catalyst-controlled regioselective glycosylation, and the methods developed in this study hold great potential for the non-enzymatic generation of glycosylated isoforms of complex natural polyols.

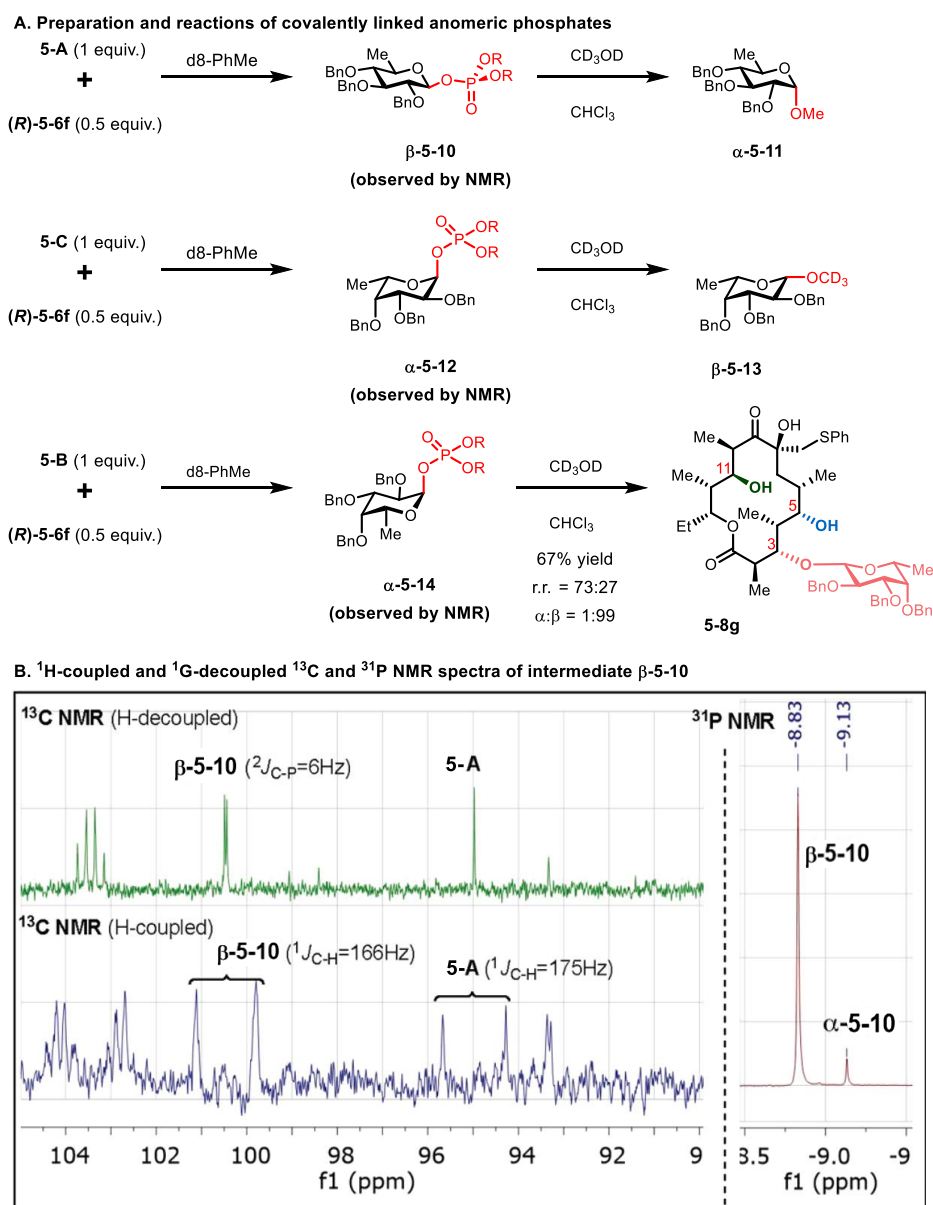


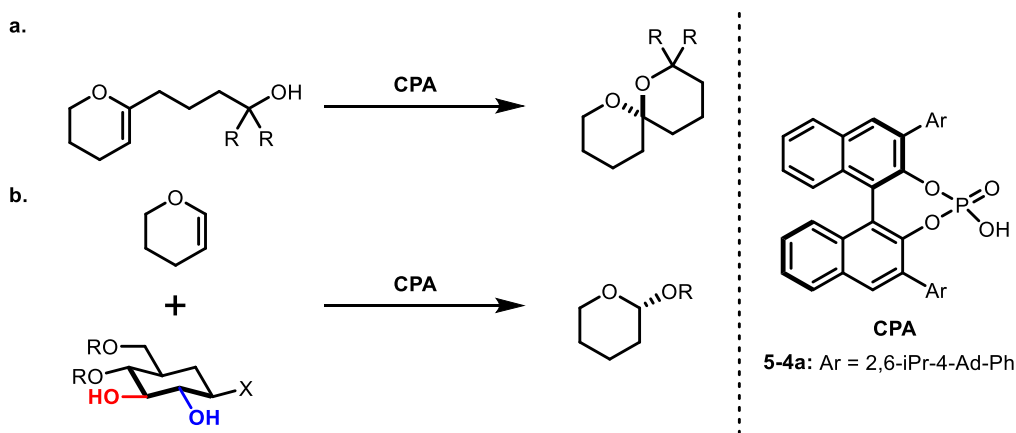
Figure 5.4. Preparation and characterization of the covalently linked phosphate intermediates **5-10** and **5-12**. Experiments were performed by Dr. Tay Rosenthal.

5.3 Mechanism of the CPA-Catalyzed Regioselective Acetalization of Sugar-Derived Diols

(Experimental information can be found in **Appendix E**)

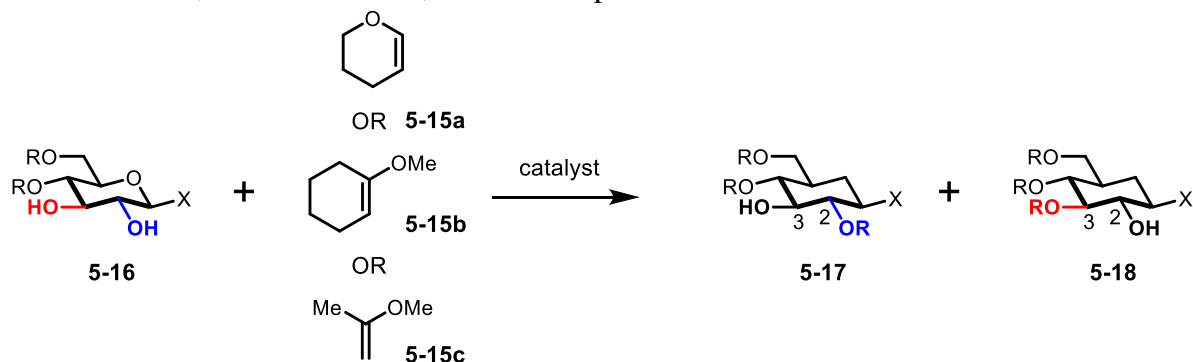
In 2012, the Nagorny group demonstrated that BINOL-derived CPAs could be used to control the stereo- and enantioselectivity of spiroketalizations (Scheme 5.7a).^[95] These promising results showed that CPAs could control the course of intramolecular acetalizations, although the precise mechanism of this transformation would not be studied until later on (see Chapter 3).^[96] Given the impact of CPAs in intramolecular acetalizations, it was surmised that these chiral Brønsted acid catalysts could be used to impart selectivity in intermolecular acetalizations. Indeed, in 2013 the Nagorny group would extend the application of CPAs to the regioselective acetalization of carbohydrate-based diols (Scheme 5.7b).

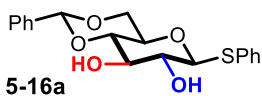
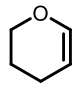
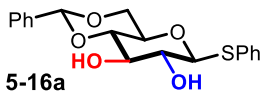
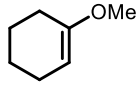
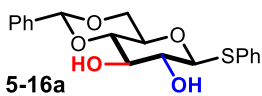
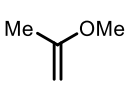
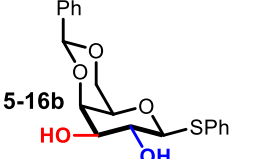
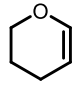
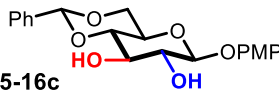
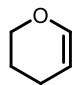
Scheme 5.7. CPA-controlled acetalizations developed by the Nagorny group.



After an extensive optimization of the reaction conditions, it was found that enol ethers **5-15** and (*R*)-4-(1-adamantyl)-2,6-*i*-PrC₆H₂-CPA (**5-4a**) could be used to revert the inherent substrate regioselectivity of diols **5-16** and favor the formation of C2-functionalized products **5-17** with high regioselectivities (Table 5.3, entries 1, 4, 7, 10, 13). Moreover, the reaction was found to have a broad scope in both the monosaccharide-derived diol and also the protecting group that was installed. Some of examples reported are shown in Table 5.3.

Table 5.3. Regioselective acetalization of sugar-based diols.^a Experiments were performed by Enoch Mensah, Nicole Camasso, and Will Kaplan.



entry	diol	PG	catalyst	Yield [%] (conv.)	5-17 : 5-18 ^b
1	 5-16a		(<i>R</i>)- 5-4a	86 (87)	11:1
2			(<i>S</i>)- 5-4a	nd (15)	1:2
3			(PhO) ₂ PO ₂ H	43 (48)	1:2.2
4	 5-16a		(<i>R</i>)- 5-4a	95 (97)	>25:1
5			(<i>S</i>)- 5-4a	nd (79)	1:1.7
6			(PhO) ₂ PO ₂ H	62 (67)	1:1.3
7	 5-16a		(<i>R</i>)- 5-4a	72 (95)	>25:1
8			(<i>S</i>)- 5-4a	nd (69)	1:2.7
9			(PhO) ₂ PO ₂ H	39 (79)	1:1.7
10	 5-16b		(<i>R</i>)- 5-4a	74 (85)	8.4:1
11			(<i>S</i>)- 5-4a	nd (62)	2.9:1
12			(PhO) ₂ PO ₂ H	69 (70)	1.3:1
13	 5-16c		(<i>R</i>)- 5-4a	54 (58)	6:1
14			(<i>S</i>)- 5-4a	nd (31)	1:2.6
15			(PhO) ₂ PO ₂ H	31 (nd)	1:1

^a Reactions performed on 0.05 mmol scale and 5h. ^b Determined by ¹H NMR.

This work represented the first example of chiral catalyst-controlled regioselective acetalization of diols. Importantly, it selectively protected the C2 hydroxyl group of the 2,3-diol system, a result which is synthetically complementary to the borinic-acid catalyzed methods developed by the Taylor group^[97–99] and substrate-controlled transformations such as those relying on organotin reagents.^[100,101] However, as a limitation, this method was not useful in obtaining

C3-acetylated products in high selectivity. Based on these hallmarks, we believed that this work merits further development and understanding. To this end, in collaboration with Dr. Jeonghyo Lee, this work was expanded upon to extend the applicability of this methodology and to obtain some insights into the reaction mechanism.

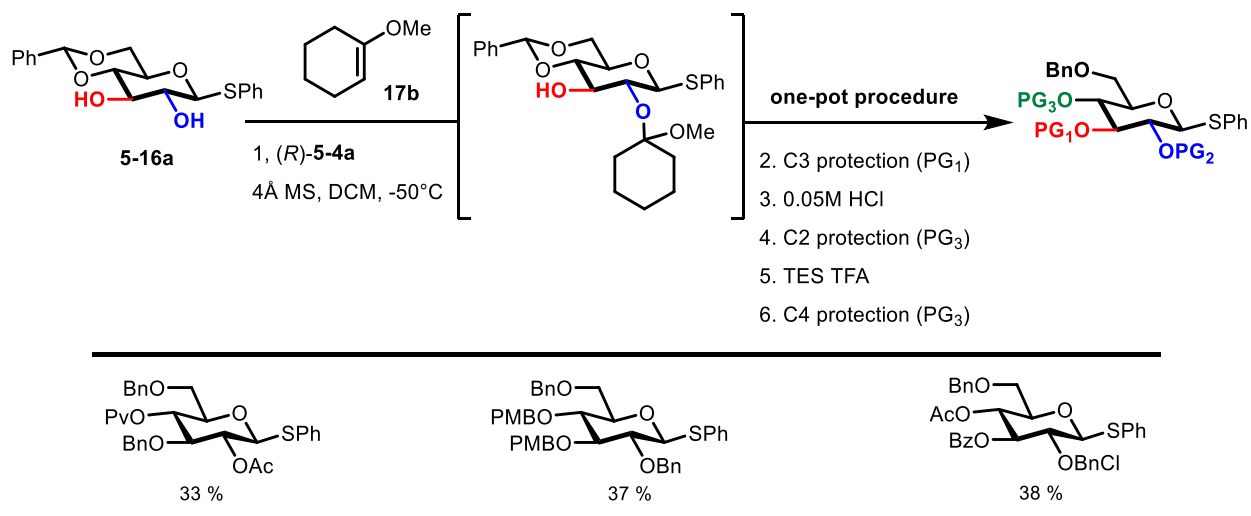
In yet unpublished work, Dr. Jeonghyo Lee has furthered this method in several aspects. In the first place, he demonstrated that, as opposed to the original reported work, it is in fact possible to obtain high C3 selectivity by using (*S*)-**5-4a** and **5-15b**, provided that ortho-disubstituted thioglycosides are employed (Table 5.4, entry 5). In addition, he has shown that the method is amenable to an impressive number of single-pot multi-step sequences that further functionalize C2-protected products in diverse patterns. A few examples are depicted in Scheme 5.8.

Table 5.4. C-3 selective acetalization of diols using CPAs.^a Experiments were performed by Dr. Jeonghyo Lee.

entry	Ar	catalyst	Conv [%]	5-17 : 5-18 ^b
1		(<i>R</i>)- 5-4a	92	>25:1
2		(<i>S</i>)- 5-4a	88	1:1.5
3	5-16d	BPA	89	1:1.1
4		(<i>R</i>)- 5-4a	90	22:1
5		(<i>S</i>)- 5-4a	71	1:5.6
6	5-16e	BPA	93	1:1.1

^a Reactions performed on 0.04 mmol scale and 5h. ^b Determined by ¹H NMR.

Scheme 5.8. One-pot functionalization of diol **5-16a**. Experiments were performed by Dr. Jeonghyo Lee.

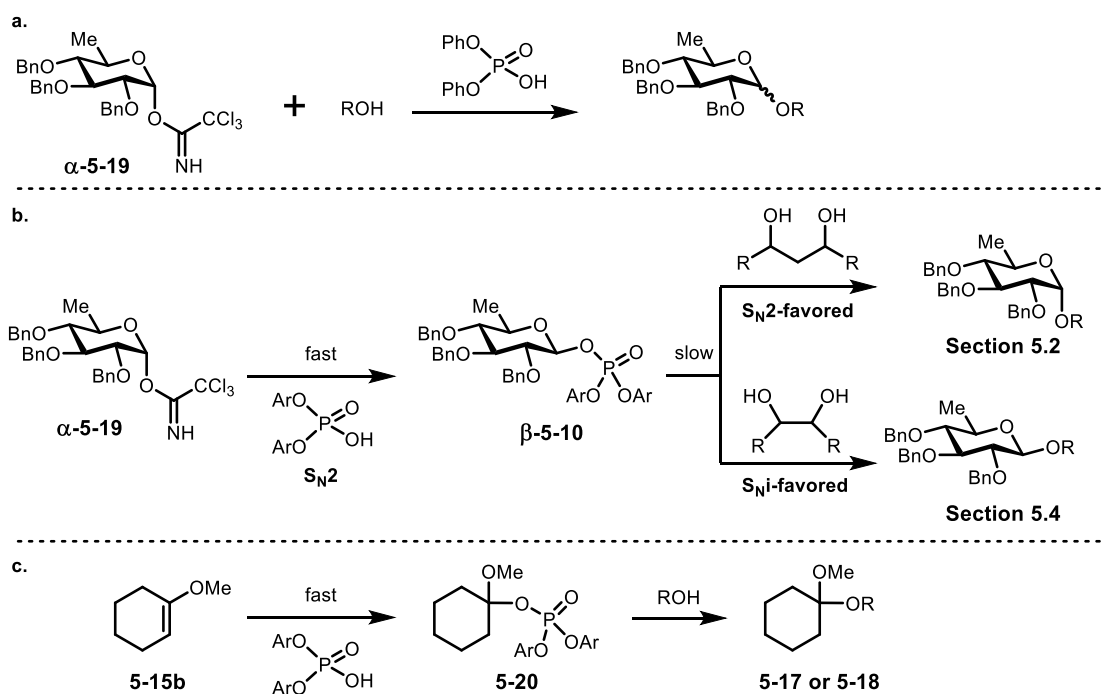


With all of these experimental results, there remained several open-ended inquiries. For example, on the reason why these reactions are much faster than their glycosylating analogs (Section 5.2 and Section 5.4), occurring smoothly at -50°C; on the importance of maintaining this low temperature for achieving high degrees of regiocontrol; and on the origin of the stereo- and regioselectivity of this reaction. To answer some of these questions, we sought to investigate the reaction mechanism. Nevertheless, computational methods to describe the reaction mechanism in systems with many degrees of freedom, such as this, is a daunting task to even modern approaches. Fortunately, new and powerful methods on reaction path finding have emerged over the last decade.^[102] To uncover mechanistic details on this transformation, a computational study was carried out employing state-of-the-art reaction path finding tools developed by the Zimmerman group.^[77–80] In past and contemporary work, we have found success in using this method to detail the mechanism of other phosphoric-acid catalyzed transformations (See Chapter 3, Chapter 7, and Sections 5.2 and 5.4 of this Chapter), thus we were confident that employing the single-ended growing string method could shed light on some of the questions regarding the intermolecular

CPA-catalyzed acetalization of sugar-derived 2,3-diols.

To study this reaction, we considered a model system consisting of glucose-based diol **5-16a**, enol ether **5-15b**, and biphenyl phosphoric acid (**BPA**). In our mechanistic accounts on intermolecular CPA-catalyzed glycosylations of polyols (Section 5.2 and 5.4, Scheme 5.9a), we proposed that the reactive intermediate was likely a covalent phosphate **5-10**, a species arising from the reaction of phosphoric acid with reactive trichloroacetimidate donor α -**5-19** (Scheme 5.9b). We surmised that a similar phosphate intermediate **5-20** could arise from the addition of BPA to enol ether **5-15b** (Scheme 5.9c), and that a phosphate-mediated pathway should therefore be considered and contrasted to the more traditional and intuitive pathway involving the BPA-catalyzed direct addition of diol **5-16a** to enol ether **5-15b**. The most relevant stationary points in the potential energy surface calculated at room temperature are shown in Figure 5.5.

Scheme 5.9. Mechanistic precedents on phosphoric acid-catalyzed intermolecular acetalizations. **a.** Phosphoric acid-catalyzed intermolecular glycosylation reaction scheme. **b.** Proposed mechanism. **c.** Possible covalent phosphate-mediated pathway for the analog acetalization of diols.



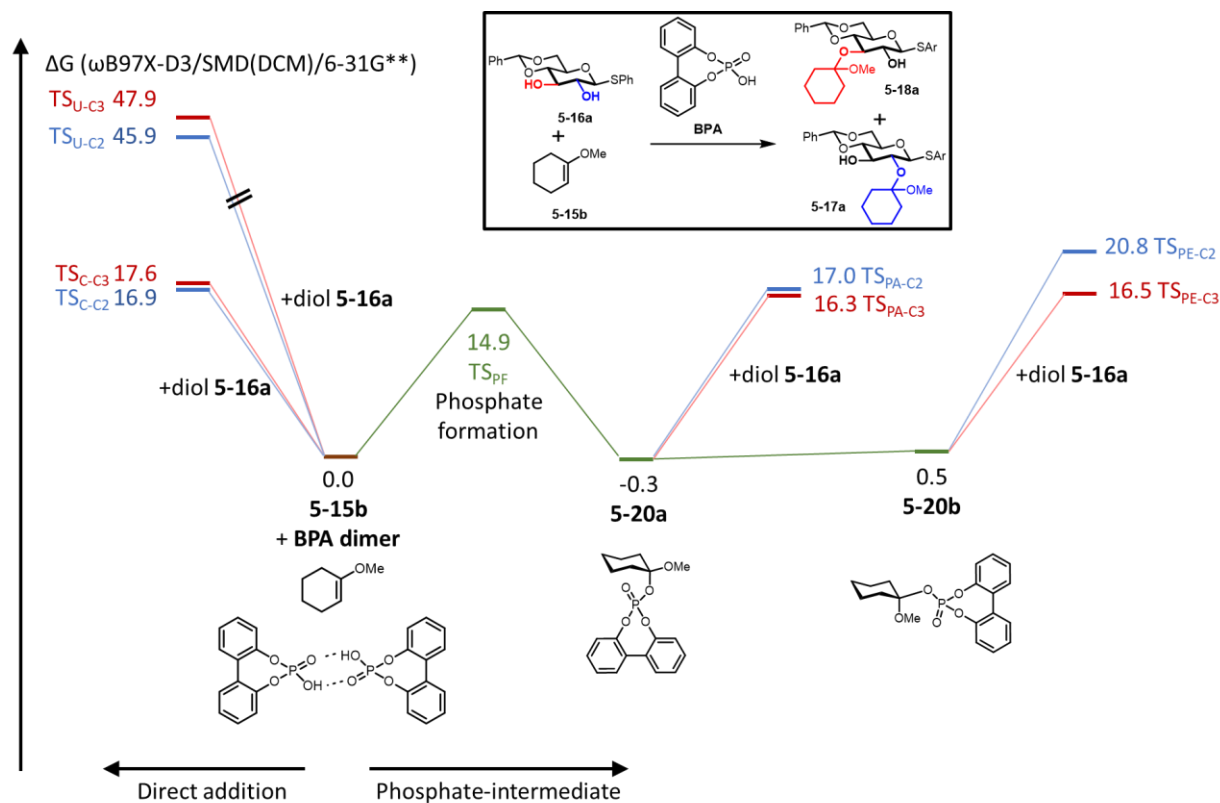


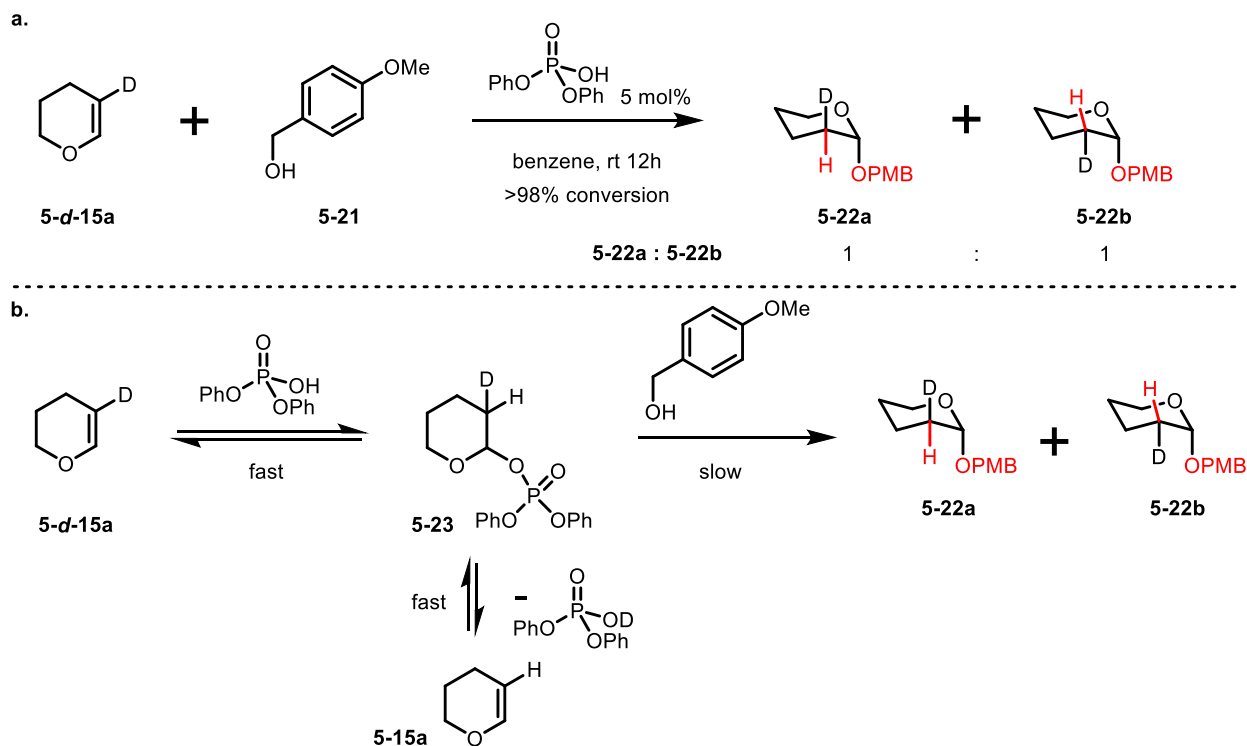
Figure 5.5. Energy diagram for the CPA-catalyzed intermolecular acetalization of 6-deoxyglucose-derived 2,3-diols.

Upon commencing the study of the aforementioned system, a key distinction between the CPA-catalyzed acetalization and glycosylation became immediately apparent. Although the barrier for the formation of axial phosphate was low (14.9 kcal/mol, TS_{PF}), the reaction was not found to be largely exothermic, in stark contrast to the reaction of phosphoric acids with trichloroacetimidate sugar donors such as **5-19** (See sections 5.2 and 5.4). Indeed, covalent phosphates were not detected by ^{31}P NMR at room temperature or lower temperatures (-50 °C). It is possible that the computationally calculated equilibrium constant between enol ether **5-15b** and phosphate **5-20b** is not accurate due to errors in the entropic contributions that would emerge from comparing the thermodynamic properties of **5-15b** and BPA dimer with the covalent phosphates. In support of this, when geometries were reoptimized without dispersion corrections (B3LYP/6-

31G), it was found that the formation of the phosphate intermediate was disfavored by 10.6 kcal/mol, consistent with our failed attempts at detecting this species. The reason why the formation of phosphates from trichloroacetimidates occurs much more readily and exothermically can be attributed to the energetically favored release of trichloroacetamide, an element which is lacking in the **5-15b** system.

While the formation of the phosphate was not as energetically favored as in the systems previously studied, the barrier for its formation was still low, and offers a kinetically feasible platform for the acetalization of alcohols through axial phosphate **5-20a** or equatorial phosphate **5-20b** intermediates. Experimental evidence for the kinetic viability of phosphate formation in the phosphoric acid-catalyzed intermolecular acetalization of alcohols has been shown in deuterium labeling experiments previously reported by our group (See Chapter 3, Table 3.4). Dr. Yaroslav Khomutnyk (Nagorny group) observed that the phosphoric acid-catalyzed acetalization of benzyl alcohol **5-21** with deuterated enol ether **5-d-15a**, proceeded smoothly to give a 1:1 mixture of *syn* and *anti* addition products **5-22a** and **5-22b** (Scheme 5.10a). This could be explained by the rapid equilibration of **5-d-17a** with DPPA to produce phosphate **5-23** (a *syn* addition), which could ring flip and collapse to **5-17a** (Scheme 5.10b). These equilibrations would lead to loss of stereochemical information on the position of the deuterium, which could explain the observed results, provided that such equilibration occurs at a scale that is faster than the acetalization. Our computations support that notion, since TS_{PF} (TS for phosphate formation) is lower than the TS for concerted and phosphate-mediated acetalizations.

Scheme 5.10. Deuterium labeling studies on the phosphoric acid-catalyzed intermolecular acetalization of alcohols. Experiments were performed by Dr. Yaroslav Khomutnyk.



Since phosphate formation for the **5-15b** system is not as favorable as for the trichloroacetimidate **5-19**, the intermediate is higher in energy and offers comparatively lower barriers for reaction with alcohols, a ground state effect. In addition, the concentration of free phosphoric acid is much higher than in the case of glycosylation with trichloroacetimidates, since in the latter all of the initial phosphoric acid is rapidly transformed into non-acidic covalent phosphates and trichloroacetamide. Therefore, in the acetalization system there is more acid catalyst available to undertake the concerted pathway or even catalyze acetalization of phosphate intermediates. These two reasons explain why the phosphoric acid acetalization of alcohols with **5-15b** can be performed even at -50°C and occurs faster and more smoothly than phosphoric acid-catalyzed glycosylations with trichloroacetimidates such as **5-19**.

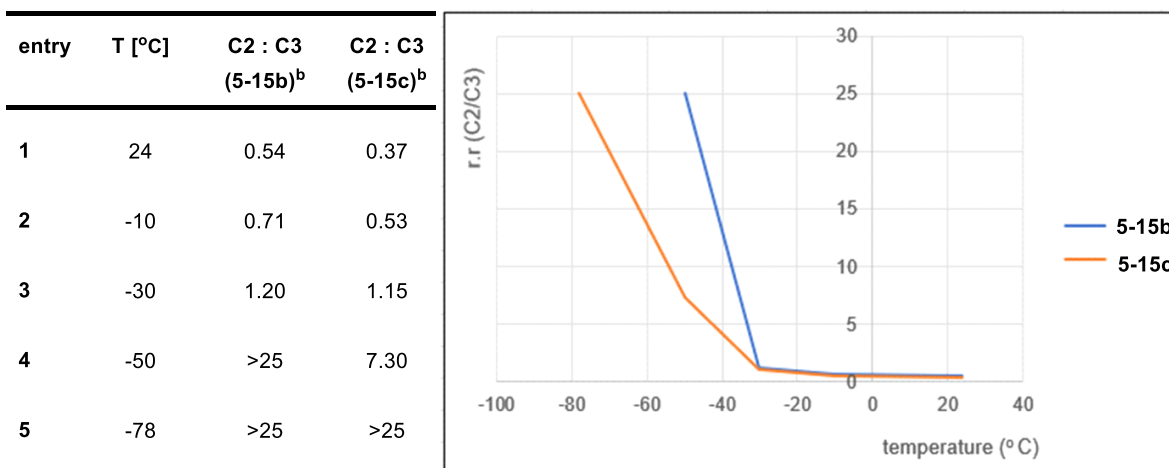
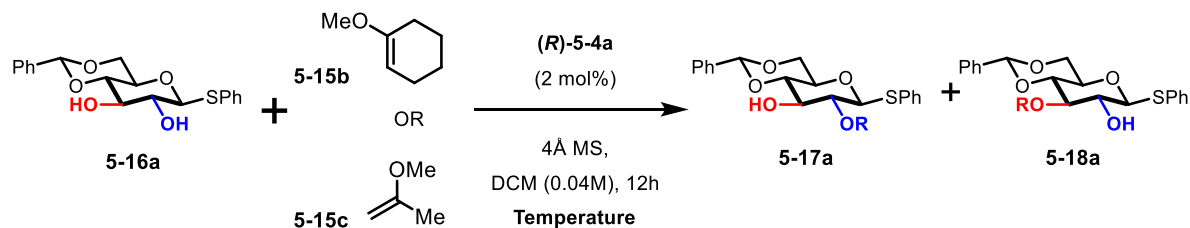
Pathways for the uncatalyzed (**TS_U**) and BPA-catalyzed (**TS_C**) direct addition of diol **5-**

16a to form either C3 (colored red, **5-18a**) or C2 (colored blue, **5-17a**) acetals were readily found using the single-ended growing string method. As expected, BPA-catalysis offers a massive reduction in the activation barrier of the acetalization of nearly 30 kcal/mol. The concerted pathway is calculated to be intrinsically slightly C-2 selective (by 0.7 kcal/mol, **TSC-c3** vs **TSC-c2**), while the phosphate-mediated pathways seem to be naturally slightly C-3 selective (by 0.7 kcal/mol, **TSPA-C3** vs **TSPA-C2**). The pathway mediated by axial phosphate **5-20a** that leads to formation of C3 glycoside is calculated to be slightly kinetically favored overall (**TSPA-C3**). These results suggest that for the BPA-catalyzed system, the principal pathway is likely the one that occurs through axial phosphate **5-20a**. The slight C-3 selectivity that is observed experimentally supports this proposition.

On the other hand, the energy difference between the activation barriers for the concerted and phosphate-mediated mechanisms is narrow and implies that by manipulating reaction conditions one could attain a mechanistic switch from a phosphate-mediated mechanism to a concerted pathway. In line with this hypothesis, studies on the impact of the temperature in the outcome of CPA-catalyzed acetalizations revealed a sudden and drastic change in the regioselectivity of the reaction occurring at roughly -40°C (Table 5.5). While the (*R*)-**5-4a**-catalyzed acetalization of **5-16a** with **5-15b** and **5-15c** occurred with poor C-3 selectivity at room temperature and -10°C (entries 1-2), and almost no selectivity at -30°C (entry 3); excellent C-2 selectivities were found at lower temperatures (entries 4-5). This sudden regioselectivity change is consistent with a mechanism switch, presumably from the inherently C3 selective phosphate mechanism to the C2-selective concerted mechanism, in large agreement with our computational model. To further confirm that the concerted mechanism is predominant at low temperatures, the (*R*)-**5-4a**-catalyzed acetalization of alcohols with deuterium-labelled **d-5-15a** is suggested, since

solely the *syn*-addition product such as **5-22a** would be expected from this mechanism (See Scheme 5.10a).

Table 5.5. Dependence of selectivity on reaction temperature for the (*R*)-**5-4a**-catalyzed acetalization of **5-16a**.^a Experiments were performed by Dr. Jeonghyo Lee.



^a conditions: **5-16a** (1 equiv), **5-15** (1.2 equiv), catalyst (20 mol%), DCM (0.04M). ^b Determined by NMR.

A closer inspection on the minimum energy paths found for the C2 and C3 concerted acetalizations revealed an important difference. While the C3 pathway involved the classical bifunctional activation of the phosphoric acid, where both oxygens participate as Bronsted acid and Lewis base catalysts (Figure 5.6a), in the C2 pathway only the Bronsted acidic site was involved, both serving to protonate the enol ether and to activate the C2-hydroxyl group (Figure 5.6b). Although this is not ideal in terms of the electronic stabilization that the CPA can impart to the TS, this pathway allows the catalyst to approach in a way that minimizes steric interactions at the TS. In this C2-selective pathway, the ortho substituents of the thiophenyl group are in close proximity to the catalyst, which might explain why increased bulk at these positions lowers the C2-selectivity (Table 5.4, entries 4-5).

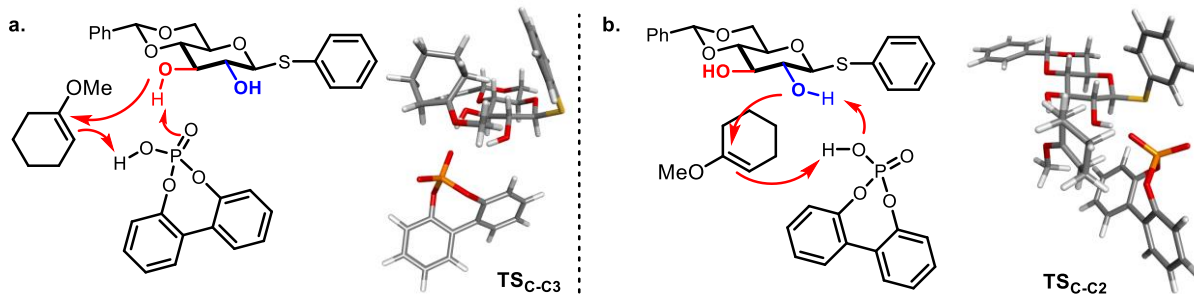


Figure 5.6. Comparison of TSc-c2 and TSc-c3

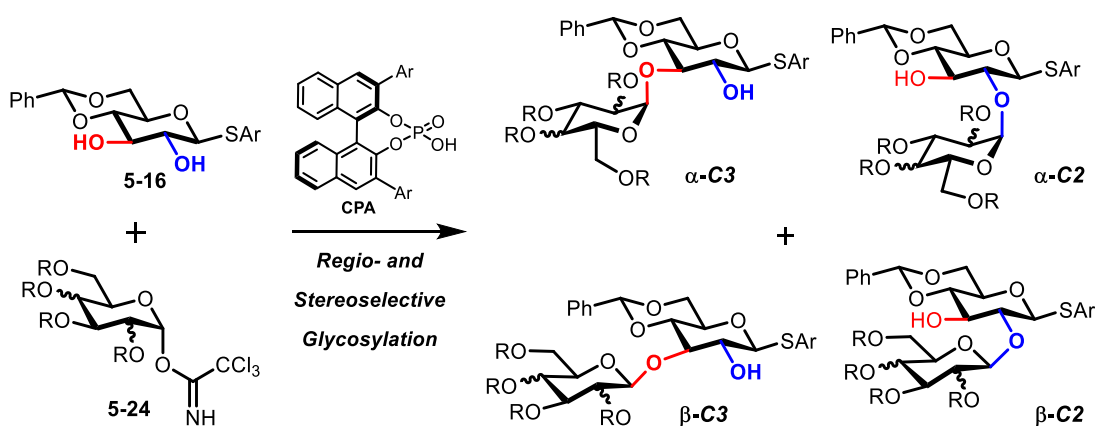
In summary, we have further developed the phosphoric acid-catalyzed intermolecular acetalization of sugar-derived 2,3-diols. Thanks to the efforts of Dr. Jeonghyo Lee, the method has been extended to the construction of both C2 and C3-functionalized of various sugar derivatives. In addition, the method is amenable to single-pot procedures that enable the selective and diverse decoration of sugar-derivatives with different protecting groups in all four positions. Finally, a thorough computational mechanistic study was performed to decipher some of the more enigmatic aspects of this reaction. An explanation to the increased efficiency of this system in comparison to the glycosylation of diols using glycosyl trichloroacetimidate donors is given. In addition, both direct (concerted and uncatalyzed) and phosphate-mediated pathways leading to C2 and C3 glycosides were calculated using the single-ended growing string method developed by the Zimmerman group. The phosphate mechanism was found to be inherently slightly C3 selective and minutely kinetically favoured at room temperature using BPA as the model catalyst, while the concerted pathway was found to be C2 selective. The difference between the activation barriers for these pathways is small and therefore either could be active depending on the catalyst and reaction conditions, in accord to experimental observations. These mechanistic insights cast light upon perplexing experimental observations and will help guide further elaboration of this powerful methodology.

5.4 Mechanism of the CPA-Catalyzed Regio- and Stereoselective Glycosylation of Sugar-Derived Diols

(Experimental information can be found in **Appendix F**)

The work presented in section 5.3 illustrates that acetalization of monosaccharide-derived 2,3-diols are not inherently highly regioselective. However, this was overcome by developing a catalyst-controlled method relying on BINOL-derived CPAs. Indeed, excellent C2 selectivity in the D-glucose system was achieved with (*R*)-**5-4a** as the catalyst. Moreover, in section 5.2 it was demonstrated that CPAs are useful not only in controlling the regioselectivity of glycosylation of a 1,3-diol system, but also its stereochemistry. With these two precedents in mind, we surmised that CPAs could also be useful in controlling the regio- and stereochemistry of glycosylations of monosaccharide-derived 2,3-diols. This is a particularly difficult challenge since in the absence of both regio- and stereocontrol, 4 distinct products can be formed: α -C3, α -C2, β -C3, and β -C2 (Scheme 5.11). This section summarizes experimental efforts in the development of this strategy (performed by Dr. Jeonghyo Lee) as well as accompanying experimental and computational mechanistic work.

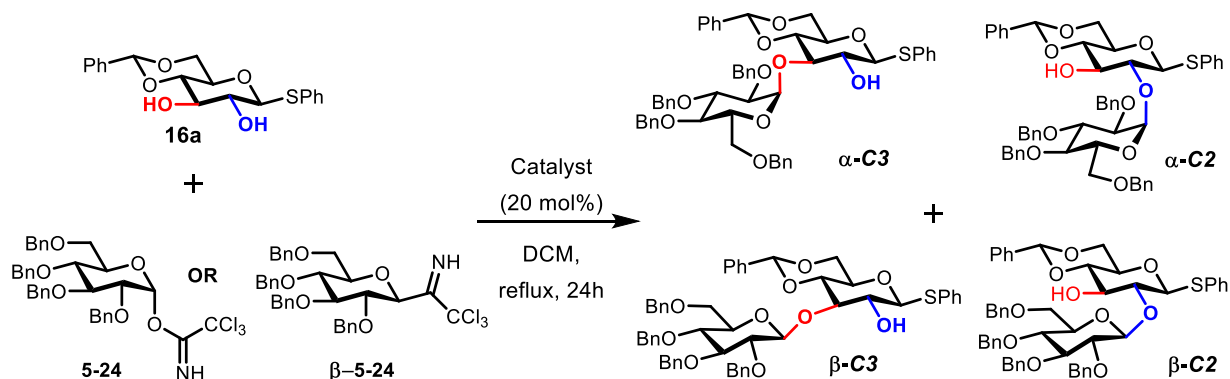
Scheme 5.11. CPA-catalyzed regio- and stereoselective glycosylation of sugar-derived diol **5-16**.



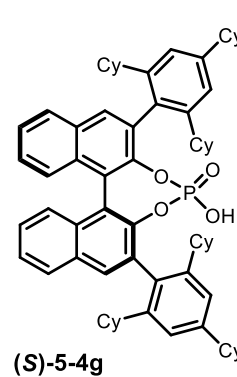
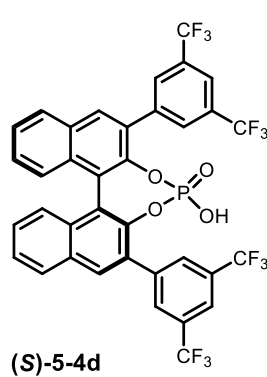
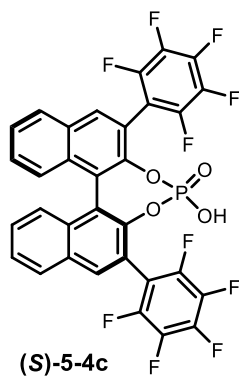
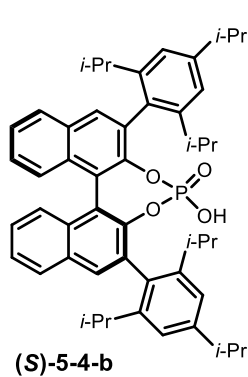
The studies commenced with a thorough screening of catalysts and reaction conditions to survey the possibility of establishing selectivity in the glycosylation of **5-16a** with glucose-derived α -trichloroacetimidate α -**5-24** as glycosyl donors. In contrast to the acetalization of **5-16a** reported in section 5.3, when the glycosylation was attempted 1.5 equivalents of donor α -**5-24** and 20 mol% of CPA (*R*)-**5-4d**, the reaction was found to be slow in DCM at room temperature (low conversion after 24h). Under refluxing conditions, phosphoric acid-catalyzed glycosylations began to yield better conversions. The control reaction with achiral diphenyl phosphoric acid (DPPA) yielded a mixture of the four possible products and revealed a modest inherent β -selectivity (α : β = 36:64) and C3-selectivity (C3:C2 = 70:30) (Table 5.6, entry 1). After screening a number of CPAs, it was found that BINOL-derived CPAs with (*S*) chirality afforded higher C-3 selectivity than their enantiomers, especially highly acidic (*S*)-**5-4d** and (*S*)-**5-4c** (81:19 and 85:15 C3:C2, respectively entries 2 and 4). Surprisingly, popular CPAs such as TRIP (**5-4b**) and TCYP (**5-4g**), which are less acidic and more sterically hindered, failed to promote the reaction (entries 5-7).

A contributing factor for the low reactivity of this system is the limiting solubility of the diol **5-16a** in DCM. After considering some alternative thioglycosides, it was found that 4-*tert*-butyl thiophenol-functionalized diols **5-16b** were well soluble in organic solvents including DCM, and it was hoped that the increased sterics would further enhance the regio- and stereoselectivity of the glycosylation. In accordance to this hypothesis, the **5-16b** system proved to be more reactive, as at least 20% conversion was observed with α -**5-19a** at room temperature in DCM, and the control reactions with DPPA as the catalyst showed that the glycosylation was inherently both β and C3-selective (Table 5.7, entry 1).

Table 5.6. CPA-catalyzed glycosylation of diol **5-16a** with benzyl protected trichloroacetimidate donor **5-24**.^a Experiments were performed by Dr. Jeonghyo Lee.



Entry	Donor	Catalyst [Ar]	Conv [%]	α -C ₃ : α -C ₂ : β -C ₃ : β -C ₂	α : β ^b	C3 : C2 ^b
1	α -5-24	(PhO) ₂ PO ₂ H	41	22.6 : 13.8 : 47.1 : 16.5	36 : 64	70 : 30
2	α -5-24	(S)-5-4d	65	17.3 : 9.1 : 63.6 : 10.0	26 : 74	81 : 19
3	α -5-24	(R)-5-4c	71	7.1 : 4.7 : 67.8 : 20.4	12 : 88	75 : 25
4	α -5-24	(S)-5-4c	55	6.2 : 3.0 : 70.0 : 20.7	9 : 91	85 : 15
5	α -5-24	(R)-5-4b	n.r.			
6	α -5-24	(S)-5-4b	n.r.			
7	α -5-24	(S)-5-4g	n.r.			
8	β -5-24	(PhO) ₂ PO ₂ H	55	40.7 : 41.1 : 10.2 : 8.1	82:18	51:49
9	β -5-24	(R)-5-4d	35	43.2 : 21.7 : 27.7 : 7.5	71:29	65:35
10	α -5-24	(PhO) ₂ PO ₂ H (1.2 eq)	62	46.3 : 31.7 : 10.4 : 11.6	78 : 22	57 : 43

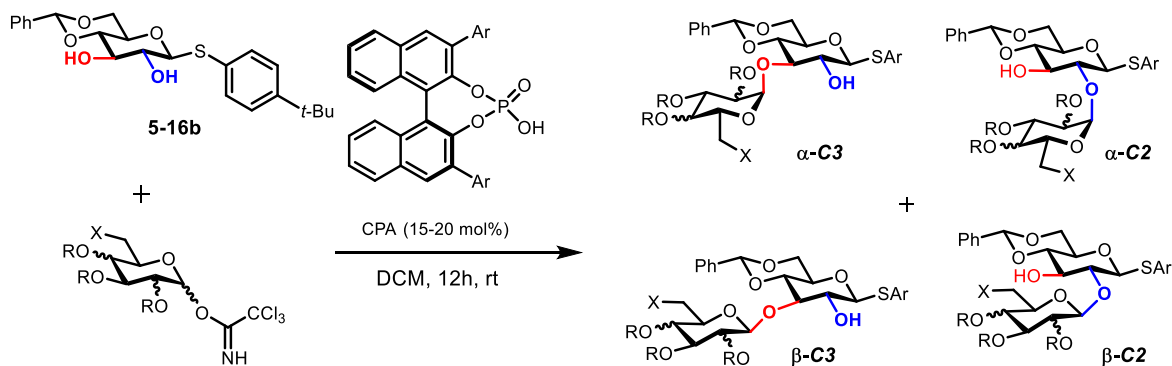


^a conditions: **5-16a** (1 equiv), **5-24** (1.4 equiv), catalyst (20 mol%), DCM (0.04M). ^b Determined by NMR and HPLC.

Our previous results on the glycosylation of 6-dEB demonstrated that 6-deoxy-sugar donors are a more reactive alternative than their oxygenated counterparts. To improve the conversion of our method, the use of deoxy-sugars was investigated next (Table 5.7). To our delight, we found that the glycosylation with 6-deoxy glucose donor **α -5-19a** proceeded efficiently and with high conversion. Control reactions with DPPA revealed that the trends observed in the glucose-based system were maintained (entries 3 and 4). After screening a large number of CPAs, it was found that (*S*)-**5-4c** provided the best C3-selectivity (79:21 C3:C2, entry 5) with high β preference (13:87 α : β). Delightfully, for the first time we were able to identify a catalytic CPA that could form the C2-glycoside preferentially: (*R*)-**5-4b** (25:75 C3:C2, entry 6), a catalyst which was inactive in the oxygenated system (Table 5.6, entry 5).

Given our success with the 6-deoxyglucose system, we sought to extend our methodology to other deoxy-sugar frameworks. Glycosylation using L-rhamnose donor **α -5-19c**, unlike in the prior systems studied, proceeded in exclusive α selectivity (Table 5.7, entries 7-9). The glycosylations were highly efficient, and although the substrate is chiral, it showed no intrinsic preference for the formation of either C2 or C3-glycoside (entry 7). As before, (*S*)-**5-4c** was able to induce regiocontrol in favor of the C3 glycoside (entry 8), while moderate C2-selectivity was observed using (*R*)-**5-4b** as the catalyst.

Table 5.7. CPA-catalyzed glycosylation of diol **5-16b** with trichloroacetimidate glycosyl donors.^a Experiments were performed by Dr. Jeonghyo Lee.



Entry	Donor	Catalyst	Conv [%]	α -C ₃ : α -C ₂ : β -C ₃ : β -C ₂	α : β ^b	C3 : C2 ^b
1	 α -5-24	(R)-5-4-d	20	7.4 : 71.6 : 5.5 : 15.4	13:87	79:21
2	 β -5-24	(R)-5-4-d	20	43.1 : 19.6 : 25.5 : 11.8	63:37	69:31
3	 α -5-19b	(PhO) ₂ PO ₂ H	60	10.73 : 52.66 : 10.61 : 25.99	21:79	63:37
4	 α -5-19b	(PhO) ₂ PO ₂ H (1 equiv)	90	50.19 : 6.70 : 30.48 : 12.61	81:19	57:43
5	 α -5-19b	(S)-5-4-c	60	9.67 : 69.66 : 3.41 : 17.26	13:87	79:21
6	 α -5-19b	(R)-5-4-b	40	2.05 : 23.18 : 2.35 : 72.43	4:96	25:75
7	 α -5-19c	(PhO) ₂ PO ₂ H	20	50 : 50 (α -C ₃ : α -C ₂)	α only	50:50
8	 α -5-19c	(S)-5-4-c	65	71 : 29 (α -C ₃ : α -C ₂)	α only	71:29
9	 α -5-19c	(R)-5-4-b	65	12 : 88 (α -C ₃ : α -C ₂)	α only	12:88
10	 α -5-19d	(S)-5-4-c	95	63.7 : 8.3 : 10.2 : 17.8	72:28	74:26
11	 α -5-19d	(R)-5-4-b	20	17.8 : 3.7 : 4.4 : 74.1	21:79	22:78
12	 α -5-19e	(S)-5-4-c	95	13.3 : 1.33 : 77.5 : 7.9	15:85	91:9
13	 α -5-19e	(R)-5-4-b	20	25.6 : 20.5 : 42.2 : 11.8	45:55	68:32

^a conditions: **5-16a** (1 equiv), donor (1.4 equiv), catalyst (20 mol%), DCM (0.04M). ^b Determined by NMR and HPLC.

Following this, glycosylation with L-fucose donor α -**5-19d** was carried out. While the reactions were efficient, a reversal in stereoselectivity when compared to 6-deoxyglucose substrate was observed, in favor of the α -product (Table 5.7, entries 5 and 10). Gratifyingly, using (*R*)-**5-4b** both the regio- and stereoselectivity were reversed to favor the formation of α glycosides at the C3 position (entry 11), albeit at lower conversions. Finally, we decided to investigate the impact of the chirality of the donor in the selectivity of the glycosylation. Under the optimized reaction conditions with catalyst (*S*)-**5-4c**, diol **5-16b** was smoothly glycosylated by D-fucose donor α -**5-19e** with good stereo- and regioselectivity (15:85 α : β , 91:9 C3:C2, entry 12). However, the intrinsic C3 selectivity could not be inverted using (*R*)-**5-4b** (entry 13). These observations indicate that the chirality of the sugar donor has a significant impact in the regio- and stereoselectivity of CPA-catalyzed glycosylations.

In parallel to this work, a combination of NMR and computational mechanistic studies was undertaken to elucidate mechanistic details and help guide some of the experiments. Based on our mechanistic work on the CPA-catalyzed glycosylation of 6-dEB (Section 5.2), we surmised that the reaction proceeded through the intermediacy of an isolable anomeric phosphate (Figure 5.7). Upon stirring 0.75 equivalents of diphenyl phosphoric acid with 1 equivalent donor α -**5-24** in deuterated benzene at room temperature, immediate formation of β -phosphate β -**5-25a** transpired (Figure 5.7a). Under these conditions, β -**5-25a** partly epimerizes to the more thermodynamically stable α -**5-25a** at room temperature overnight (Figure 5.7b), and this epimerization is greatly accelerated upon addition of excess phosphoric acid (Figure 5.7c). The stereochemistry of the observed phosphates was unequivocally assigned by ^{13}C (H coupled) NMR. The $^1\text{J}(\text{C-H})$ of the anomeric carbon of β -**5-25a** was found to be 167 Hz, consistent with β stereochemistry (Figure 5.8a). On the other hand, the $^1\text{J}(\text{C-H})$ for the same carbon of α -**5-25a** was found to be 176 Hz,

representative of that configuration (Figure 5.8b).

The epimerization of β -**5-25a** occurs more slowly in CD_2Cl_2 , as no α -**5-25a** was found overnight at room temperature with substoichiometric amounts of DPPA (0.75 equiv) (Figure 5.9, left spectra). In contrast to this result, when using more acidic phosphoric acids such as (*R*)-**5-4h**, both α and β phosphates **5-25b** were formed, although in high β preference (1:14.2 α : β , Figure 5.9, center spectra). Moreover, this labile phosphate partly isomerized to its more stable α configuration overnight (1:7.6 α : β). In addition, we found that (*S*)-**5-4h**, had a higher proclivity towards formation of α phosphate α -**5-25c** (1:3.6 α : β , Figure 5.9, right spectra). These results show that the nature of the phosphoric acid used has an impact on the α to β ratio of the intermediate phosphate, and that even changing the chirality of the CPA can provoke substantial alterations in this ratio.

In a similar experience, it was observed that the reaction of donor β -**5-24** with diphenyl phosphoric acid led to the rapid formation of α -**5-25a**. Given that this phosphate is the probable intermediate of the reaction, and that under the reaction conditions shown in Table 5.6, clean formation of the β phosphate is observed, we conjectured that the stereochemistry of the intermediate is essential in the stereochemical outcome of the reaction. As expected, when trichloroacetimidate β -**5-24a** was subjected to the reaction conditions, a reversal of the stereochemical outcome was observed, in favor of the α glycoside (Table 5.6, entries 8-9). In addition, performing the glycosylation with α -**5-24a** and a small excess of DPPA, conditions which we showed lead to epimerization of the intermediate β -**5-25a** into α -**5-25a**, also led to selectivity reversal in favor of the α glycoside (Table 5.6, entry 10). The same trend applied to the 6-deoxyglucose system, as β -**5-19a** led to the preferential formation of α -glycosides (Table 5.7, entry 2). Moreover, Section 5.2 details NMR experiments that show that L-fucose donor α -**5-19d** instantaneously forms α -phosphate at room temperature, presumably through rapid epimerization of the β -phosphate. This explains the

reversal in stereoselectivity when compared to 6-deoxyglucose system (Table 5.7, entries 5 and 10). It is also likely that rapid isomerization to α -phosphate plays a role in the stereoselectivity of the glycosylation using L-rhamnose donor α -5-19c (Table 5.7, entries 7-9). NMR studies to determine the stereochemistry of the rhamnose-based phosphate intermediate are suggested.

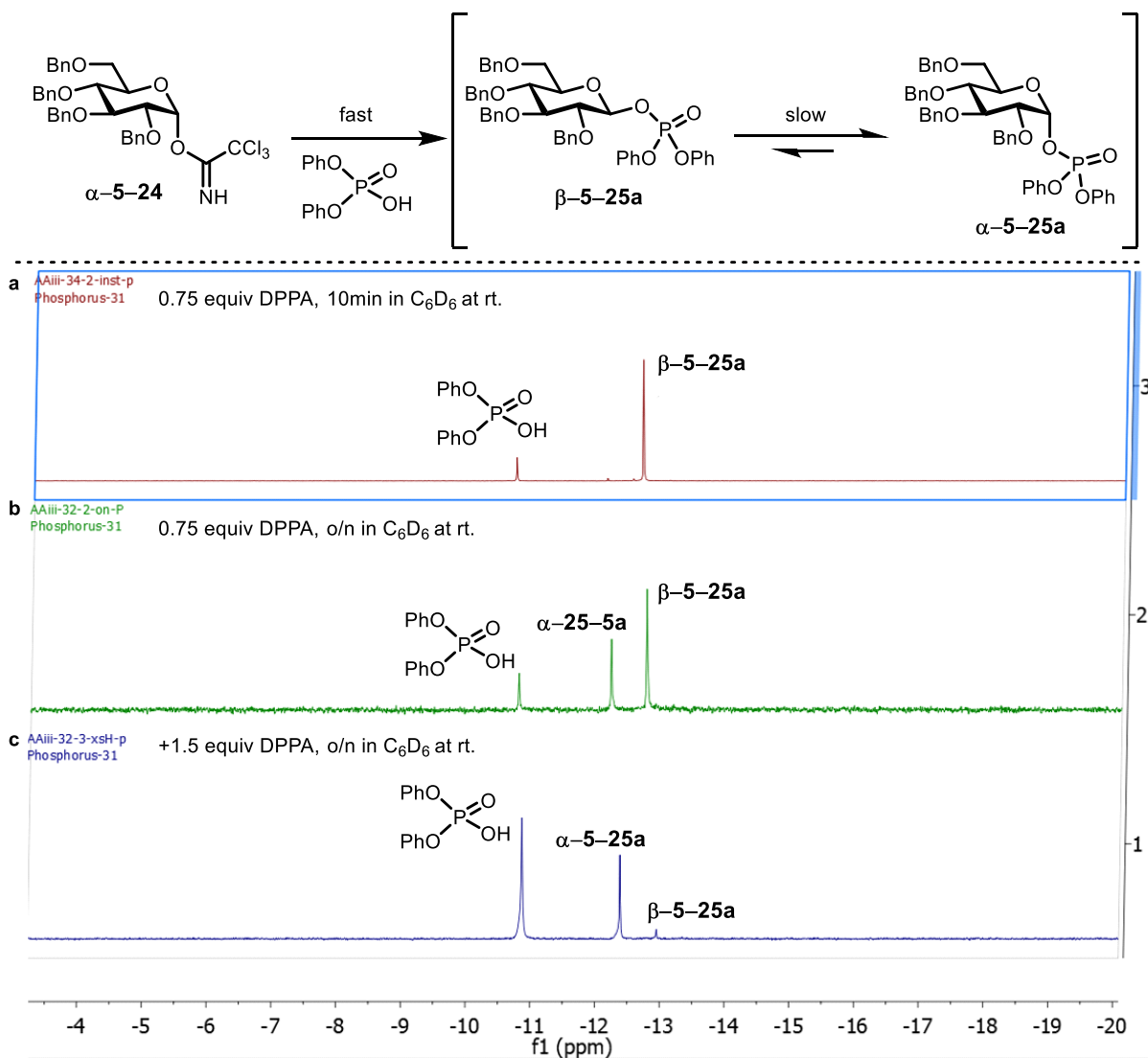


Figure 5.7. Formation of glycosyl phosphates from donor α -5-24. **a.** After 10 minutes of stirring 0.75 equiv. of DPPA with 1.0 equiv of α -5-24. **b.** After overnight stirring of 0.75 equiv. of DPPA with 1.0 equiv of α -5-24. **c.** 10 minutes after the addition of 1.5 extra equiv. of DPPA.

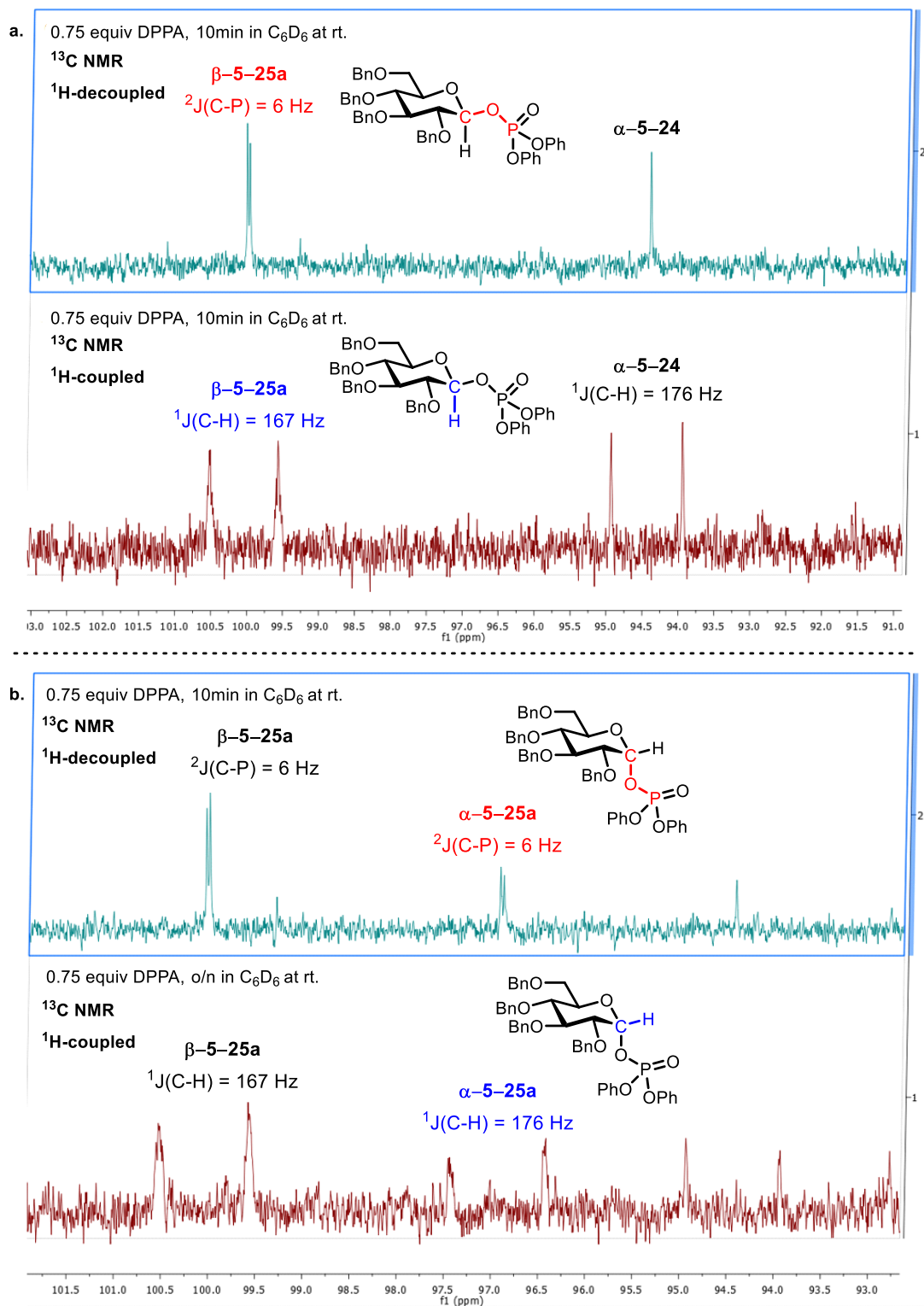


Figure 5.8. Stereochemical assignment of glycosyl phosphates using ¹³C (H-coupled) NMR. **a.** After 10 minutes of stirring 0.75 equiv. of DPPA with 1.0 equiv of α -5-24. **b.** After overnight stirring of 0.75 equiv. of DPPA with 1.0 equiv of α -5-24.

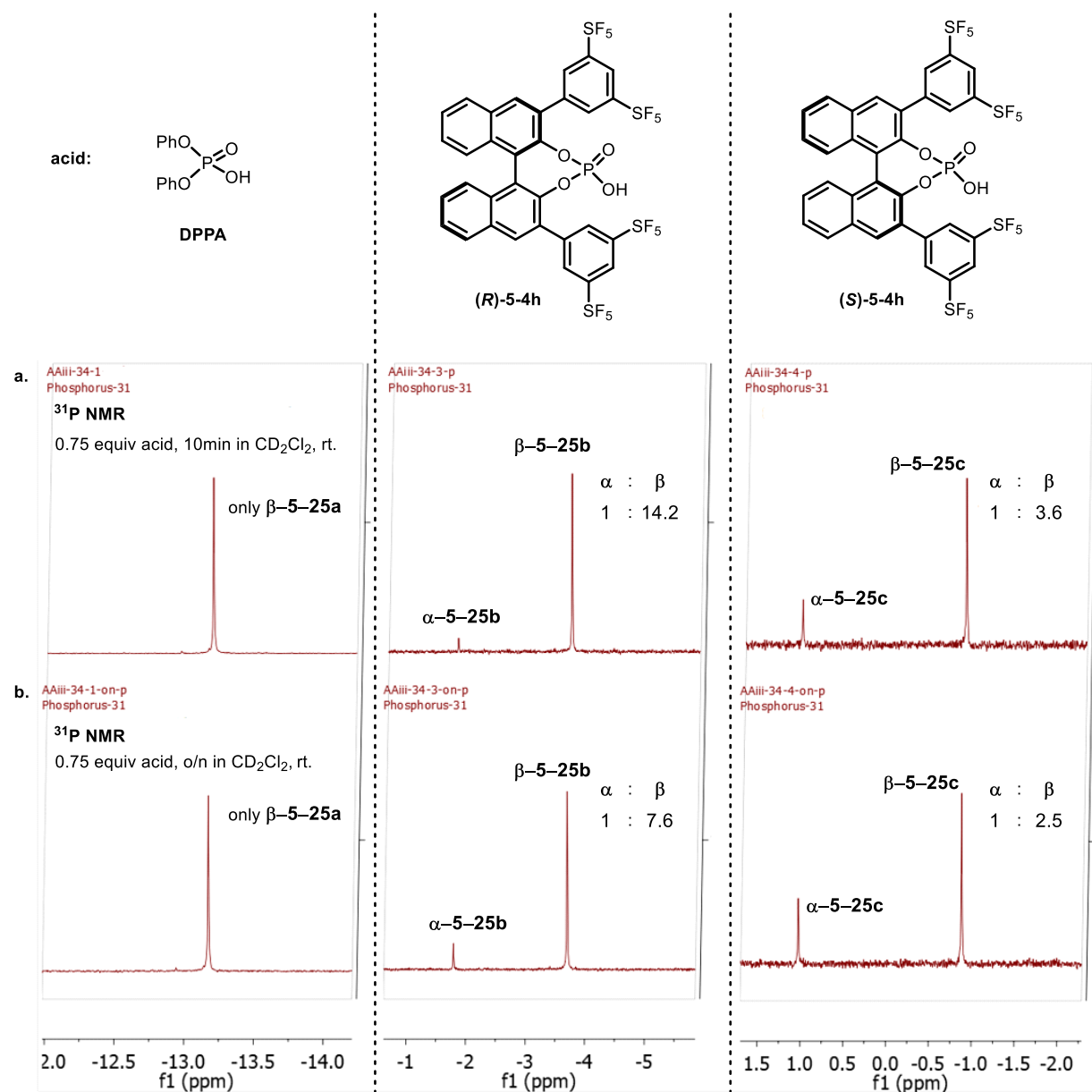
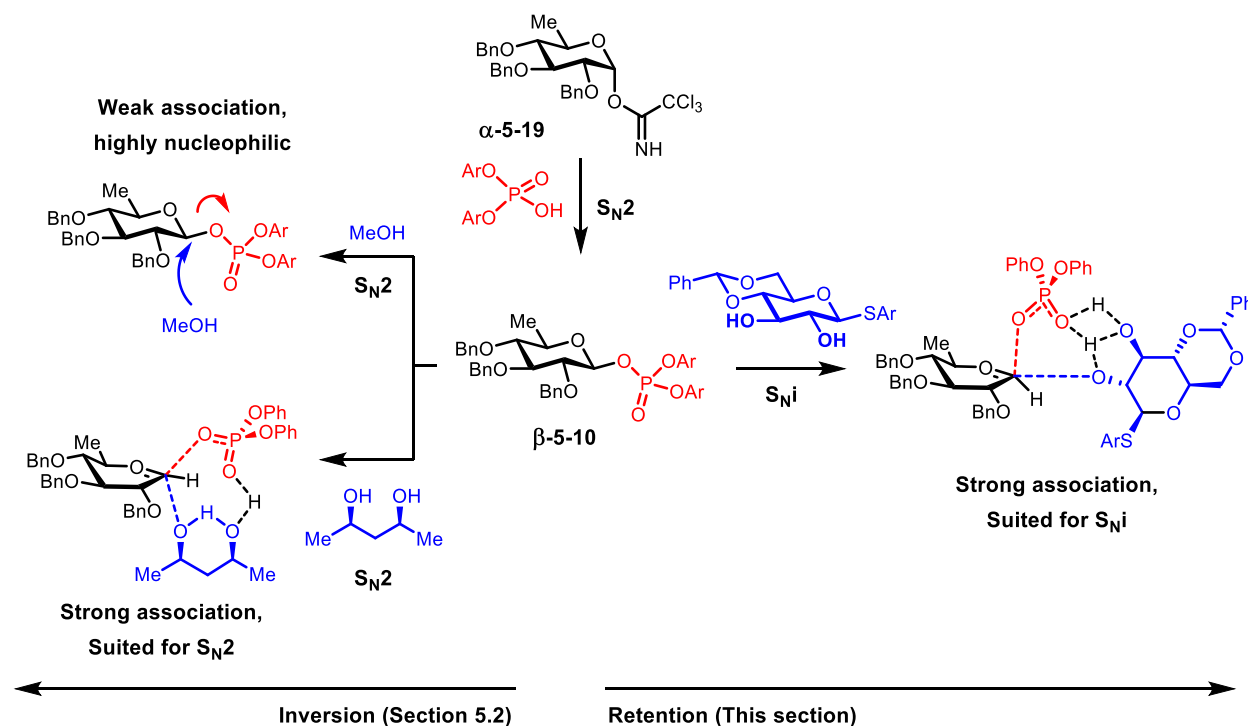


Figure 5.9. Phosphate formation in CD₂Cl₂ with different acids. **a.** After 10 minutes of stirring 0.75 equiv. of acid with 1.0 equiv of α-5-24. **b.** After overnight stirring of 0.75 equiv. of acid with 1.0 equiv of α-5-24.

While these results lend strong support to our mechanistic hypothesis of an intervening phosphate species, it was not entirely clear why α phosphates lead to the formation of α glycosides, and β phosphates favored the formation of β glycosides. In section 5.2 we proposed that these phosphate intermediates undergo S_N2-like substitutions with methanol (Figure 5.4) and with *syn*

1,3-diols, which leads to a selectivity trend opposite to what is reported in this section. Although simple S_N1 / S_N2 mechanistic manifolds do not explain the observed selectivities in Table 5.6 and Table 5.7, the uncommon S_{Ni} mechanism perfectly rationalizes our stereochemical outcomes.^[103] Under this mechanistic regime, nucleophilic substitution occurs with retention of configuration. This requires a strong association of the nucleophile with the leaving group, so that the substitution of the nascent carbenium species is directed by the leaving species. We hypothesize that this is accomplished by strong hydrogen bond association of the 1,2-diol with the glycosyl phosphate. In the case of methanol, the association is weaker due to a lower availability of hydrogen bonds with the phosphate, while for *syn* 1,3-diols the methylene linker enables access to the more kinetically ideal S_N2 mechanism (Scheme 5.12).

Scheme 5.12. S_N2 vs. S_{Ni} mechanism for the phosphoric acid-catalyzed acetalization of alcohols.



In order to validate our mechanistic proposal, we decided to pursue a computational approach. Although methods that accurately describe the reaction mechanism in large systems with flexible substituents remains a formidable challenge, new and powerful strategies on reaction path finding have emerged over the last decade.^[102] In particular, the Zimmerman group has developed an intuitive, influential, and versatile reaction discovery tool based on the growing string method,^[77–80] which we decided to implement to this system with the hope of providing further support to our proposal. To this end, we considered a model system consisting of biphenyl phosphoric acid (BPA), 6-deoxyglucose-derived trichloroacetimidate **α -5-19**, and glucose-based diol **5-16b**. The most relevant stationary points in the potential energy surface calculated at room temperature are shown in Figure 5.10.

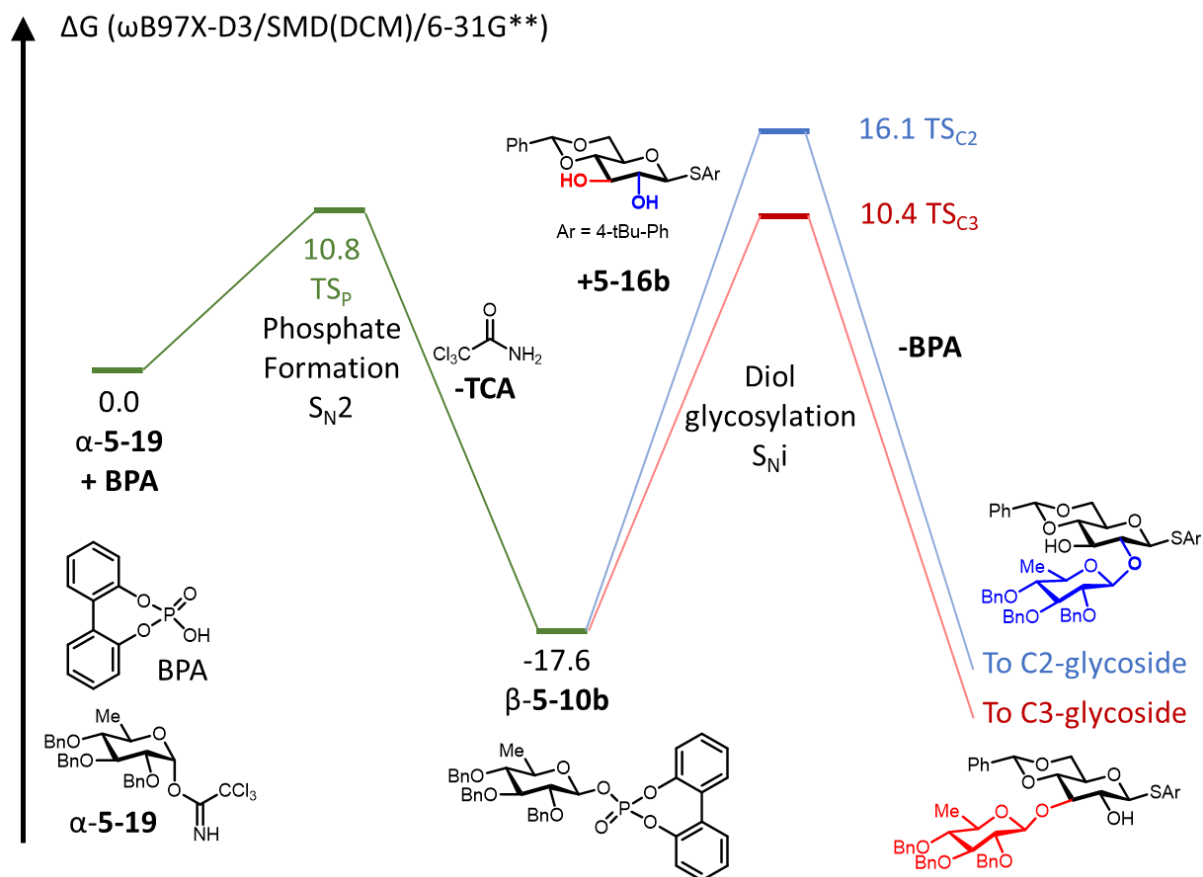


Figure 5.10. Energy diagram for the CPA-catalyzed intermolecular glycosylation of 6-deoxyglucose-derived 2,3-diols.

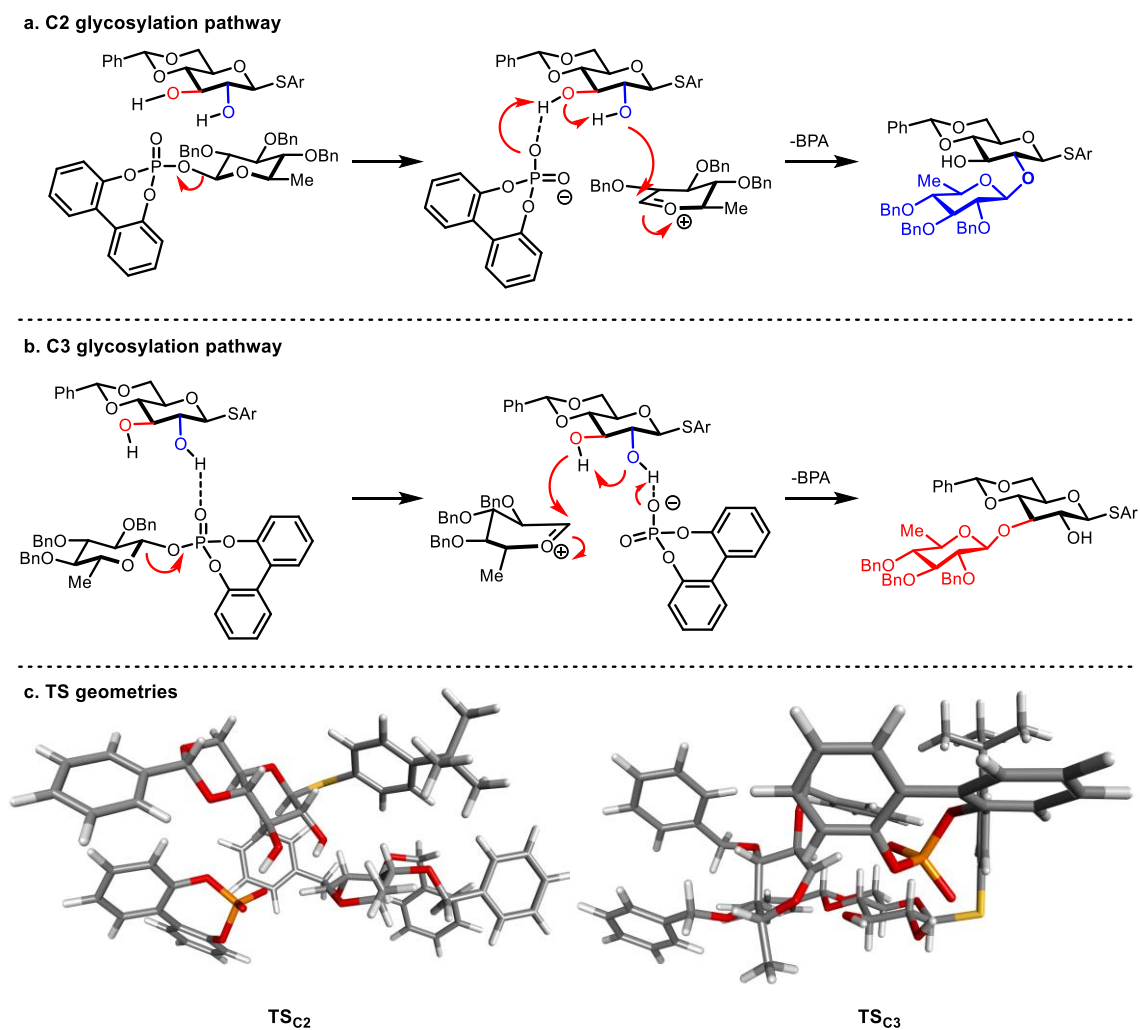
As expected, the barrier for the reaction of trichloroacetimidate donor α -**5-19** with BPA was low, at just 10.8 kcal/mol (**TS_P**). The formation of phosphate occurred in S_N2 fashion, providing β -**5-10b** in a highly exothermic step (17.6 kcal/mol) due to the release of trichloroacetamide (TCA). β -**5-10b** was found to be less thermodynamically stable than its α counterpart by roughly 5 kcal/mol (See Appendix F), in agreement with the experimentally observed favorable epimerization of β -phosphates (Figure 5.9).

Various pathways for the glycosylation of β -**5-10b** with **5-16b** were then explored. In accord with our mechanistic proposal, the pathways with the lowest barriers proceeded through an S_Ni mechanism to deliver either β -C2 glycoside or β -C3 glycoside, with preference for the formation of the C3 glycoside (**TS_{C2}** vs **TS_{C3}**). Our results agree with both the C3 and the β selectivity observed experimentally (Table 5.6). The calculated barriers for the glycosylation are very high (28 kcal/mol for **TS_{C3}** and 33.7 for **TS_{C2}**). While this reflects the relatively long reaction times that are required, it is an overestimation of the real reaction barriers, which should be smaller due to the stabilizing interactions that TCA can provide as a hydrogen bond donor, a parameter that was not taken into consideration in our calculations. The formation of α -glycoside can be attributed to a combination of competing mechanisms, such as unselective S_N1, S_Ni of epimerized phosphate (α -phosphate), and S_N2 mechanisms.

Analysis of the reaction pathways revealed similarities and differences among the C2 and C3-selective glycosylation S_Ni mechanism (Scheme 5.13). In both cases, the glycosylation involves a concerted asynchronous mechanism. The glycosylation is highly dissociative in nature, as just prior to the transition state, the phosphate departs from the sugar forming an oxocarbenium-like species. Following this, both protonation of the phosphate and formation of the new glycosidic bond occur concurrently. Another element in common is that the protonation of the phosphate

involves both hydroxyl groups. The group that is initially hydrogen bonded to the phosphate protonates this species at the TS, while simultaneously abstracting the proton of the vicinal hydroxyl group that gets glycosylated. Therefore, the arrangements required for glycosylation at the C2 or C3 position are mirrored to each other, as is shown in Scheme 5.13.

Scheme 5.13. S_Ni mechanism for the glycosylation of sugar-derived 2,3-diols. **a.** C2-selective pathway. **b.** C3-selective pathway. **c.** Geometry of TS_{C2} and TS_{C3}.



A closer inspection on the C2 pathway and TS revealed that the inflexible 4,6-O-benzylidene acetal is in contact with the phosphoric acid catalyst, especially around the ortho and meta positions of the benzylidene aromatic ring. Therefore, we anticipate that substitution at these positions would enhance C3-selectivity for the glycosylation. In addition, TS_{C2} was examined

using a quadrant-based perspective that has been developed and successfully applied by Himo and Terada to explain the selectivity of BINOL-based CPAs in a range of reactions (Figure 5.11).^[104,105] This perspective helps identify key interactions between the catalyst and the substrate works by juxtaposing the steric profile of (*R*) or (*S*) BINOL-derived CPAs to the reaction model. Figure 11b shows where steric elements of (*R*)-BINOL-derived CPA would be located in comparison to the substrate at TS_{C2}. Based on our model, it is clear that (*R*)-BINOL-based CPAs are matched for this C2-selective pathway, while (*S*) catalysts are severely mismatched. This model is in agreement with the observed results shown in Table 5.6, where it is observed that (*S*)-catalysts are more C3-selective in comparison to catalysts possessing (*R*) axial chirality

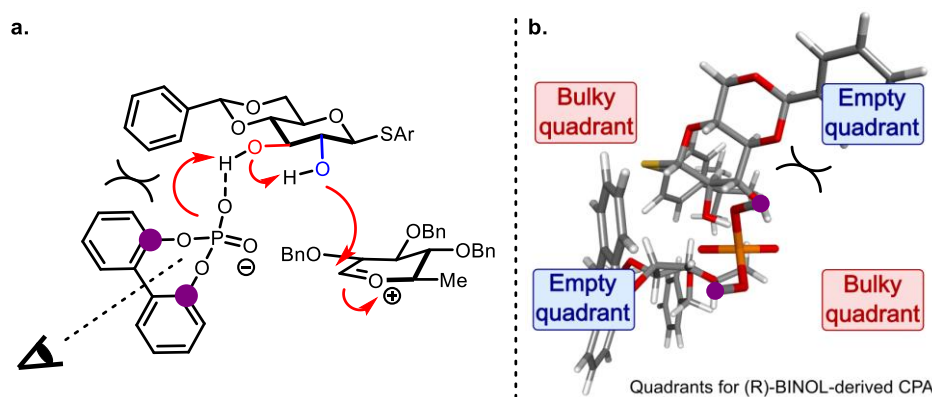


Figure 5.11. Quadrant-based perspective of TS_{C2}. Biphenyl backbone of the catalyst is omitted from the perspective for clarity purposes.

In conclusion, we have summarized our work on the development of a regio- and stereoselective CPA-catalyzed glycosylation of sugar-derived 2,3-diols. In addition, we have reported a thorough mechanistic investigation of this reaction, which supports a mechanism where glycosylation occurs from an anomeric phosphate intermediate through a rare S_Ni mechanism. Through our mechanistic conclusions, we have rationalized the origin of regio- and stereoselectivity for different conditions that can preferentially form α-C2, α-C3, β-C2 or β-C3-glycosides. We hope that the gathered insight into the reaction mechanism will assist in the further development and generalization of this glycosylation strategy.

5.3 References

- [1] A. Varki, *Glycobiology* **1993**, 3, 97–130.
- [2] P. H. Seeberger, *Nat. Chem. Biol.* **2009**, 5, 368–372.
- [3] A. Varki, *Glycobiology* **2017**, 27, 3–49.
- [4] S. I. Elshahawi, K. A. Shaaban, M. K. Kharel, J. S. Thorson, *Chem. Soc. Rev.* **2015**, 44, 7591–7697.
- [5] P. Stallforth, B. Lepenies, A. Adibekian, P. H. Seeberger, *J. Med. Chem.* **2009**, 52, 5561–5577.
- [6] S. A. W. Gruner, E. Locardi, E. Lohof, H. Kessler, *Chem. Rev.* **2002**, 102, 491–514.
- [7] M. C. Galan, D. Benito-Alifonso, G. M. Watt, *Org. Biomol. Chem.* **2011**, 9, 3598–3610.
- [8] A. M. Sinclair, *Biol. Targets Ther.* **2013**, 7, 161–174.
- [9] C. H. Chung, B. Mirakhur, E. Chan, Q.-T. Le, J. Berlin, M. Morse, B. A. Murphy, S. M. Satinover, J. Hosen, D. Mauro, et al., *N. Engl. J. Med.* **2008**, 358, 1109–1117.
- [10] G. Zhang, L. Fang, L. Zhu, Y. Zhong, P. G. Wang, D. Sun, *J. Med. Chem.* **2006**, 49, 1792–1799.
- [11] H. Y. L. Wang, Y. Rojanasakul, G. A. O’Doherty, *ACS Med. Chem. Lett.* **2011**, 2, 264–269.
- [12] R. B. Merrifield, *Angew. Chem., Int. Ed.* **1985**, 24, 799–810.
- [13] M. H. Caruthers, *Science* **1985**, 230, 281–285.
- [14] R. Das, B. Mukhopadhyay, *ChemistryOpen* **2016**, 5, 401–433.
- [15] D.-M. Liang, J.-H. Liu, H. Wu, B.-B. Wang, H.-J. Zhu, J.-J. Qiao, *Chem. Soc. Rev.* **2015**, 44, 8350–8374.
- [16] P. Roach, *Curr. Mol. Med.* **2002**, 2, 101–120.
- [17] C. A. Lewis, S. J. Miller, *Angew. Chem., Int. Ed.* **2006**, 45, 5616–5619.
- [18] T. P. Pathak, S. J. Miller, *J. Am. Chem. Soc.* **2012**, 134, 6120–6123.
- [19] S. Yoganathan, S. J. Miller, *J. Med. Chem.* **2015**, 58, 2367–2377.
- [20] B. S. Fowler, K. M. Laemmerhold, S. J. Miller, *J. Am. Chem. Soc.* **2012**, 134, 9755–9761.
- [21] C. A. Lewis, K. E. Longcore, S. J. Miller, P. A. Wender, *J. Nat. Prod.* **2009**, 72, 1864–1869.
- [22] X. Sun, H. Lee, S. Lee, K. L. Tan, *Nat. Chem.* **2013**, 5, 790–795.
- [23] E. Mensah, N. Camasso, W. Kaplan, P. Nagorny, *Angew. Chem., Int. Ed.* **2013**, 52, 12932–12936.

- [24] C. Gouliaras, D. Lee, L. Chan, M. S. Taylor, *J. Am. Chem. Soc.* **2011**, *133*, 13926–13929.
- [25] J. T. Walk, Z. A. Buchan, J. Montgomery, *Chem. Sci.* **2015**, *6*, 3448–3453.
- [26] P. O. Adero, H. Amarasekara, P. Wen, L. Bohé, D. Crich, *Chem. Rev.* **2018**, *118*, 8242–8284.
- [27] D. Crich, *Acc. Chem. Res.* **2010**, *43*, 1144–1153.
- [28] M. Huang, G. E. Garrett, N. Birlirakis, L. Bohé, D. A. Pratt, D. Crich, *Nat. Chem.* **2012**, *4*, 663–667.
- [29] L. Bohé, D. Crich, *Carbohydr. Res.* **2015**, *403*, 48–59.
- [30] G. Huang, X. Mei, *Curr. Drug Targets* **2014**, *15*, 780–784.
- [31] G. Huang, M. Lv, J. Hu, K. Huang, H. Xu, *Mini-Reviews Med. Chem.* **2016**, *16*, 1013–1016.
- [32] O. Blixt, N. Razi, in *Glycoscience*, Springer Berlin Heidelberg, Berlin, Heidelberg, **2008**, pp. 1361–1385.
- [33] K. M. Koeller, C. H. Wong, *Chem. Rev.* **2000**, *100*, 4465–4493.
- [34] K. W. Fiori, A. L. A. Puchlopek, S. J. Miller, *Nat. Chem.* **2009**, *1*, 630–634.
- [35] Y. Zhao, J. Rodrigo, A. H. Hoveyda, M. L. Snapper, *Nature* **2006**, *443*, 67–70.
- [36] Y. Ueda, T. Furuta, T. Kawabata, *Angew. Chem., Int. Ed.* **2015**, *54*, 11966–11970.
- [37] C. L. Allen, S. J. Miller, *Org. Lett.* **2013**, *15*, 6178–6181.
- [38] J. H. Kim, I. Čorić, C. Palumbo, B. List, *J. Am. Chem. Soc.* **2015**, *137*, 1778–1781.
- [39] B. D. Chandler, A. L. Burkhardt, K. Foley, C. Cullis, D. Driscoll, N. Roy D’Amore, S. J. Miller, *J. Am. Chem. Soc.* **2014**, *136*, 412–418.
- [40] G. Xiao, G. A. Cintron-Rosado, D. A. Glazier, B. Xi, C. Liu, P. Liu, W. Tang, *J. Am. Chem. Soc.* **2017**, *139*, 4346–4349.
- [41] H. Yang, K.-S. Cao, W.-H. Zheng, *Chem. Commun.* **2017**, *53*, 3737–3740.
- [42] B. R. Sculimbrene, Y. Xu, S. J. Miller, *J. Am. Chem. Soc.* **2004**, *126*, 13182–13183.
- [43] C. A. Lewis, J. Merkel, S. J. Miller, *Bioorganic Med. Chem. Lett.* **2008**, *18*, 6007–6011.
- [44] T. P. Pathak, S. J. Miller, *J. Am. Chem. Soc.* **2013**, *135*, 8415–8422.
- [45] S. Han, S. J. Miller, *J. Am. Chem. Soc.* **2013**, *135*, 12414–12421.
- [46] Y. Ueda, T. Kawabata, in *Top. Curr. Chem.*, Springer, Cham, **2015**, pp. 203–231.
- [47] J. Lawandí, S. Rocheleau, N. Moitessier, *Tetrahedron* **2016**, *72*, 6283–6319.
- [48] T. M. Beale, M. S. Taylor, *Org. Lett.* **2013**, *15*, 1358–1361.
- [49] A. Nakagawa, M. Tanaka, S. Hanamura, D. Takahashi, K. Toshima, *Angew. Chem., Int.*

- Ed.* **2015**, *54*, 10935–10939.
- [50] G. Pelletier, A. Zwicker, C. L. Allen, A. Schepartz, S. J. Miller, *J. Am. Chem. Soc.* **2016**, *138*, 3175–3182.
- [51] Y. Park, K. C. Harper, N. Kuhl, E. E. Kwan, R. Y. Liu, E. N. Jacobsen, *Science* **2017**, *355*, 162–166.
- [52] D. J. Cox, M. D. Smith, A. J. Fairbanks, *Org. Lett.* **2010**, *12*, 1452–1455.
- [53] T. Kimura, M. Sekine, D. Takahashi, K. Toshima, *Angew. Chem., Int. Ed.* **2013**, *52*, 12131–12134.
- [54] D. Liu, S. Sarrafpour, W. Guo, B. Goulart, C. S. Bennett, *J. Carbohydr. Chem.* **2014**, *33*, 423–434.
- [55] C. Palo-Nieto, A. Sau, R. Williams, M. C. Galan, *J. Org. Chem.* **2017**, *82*, 407–414.
- [56] J. Cortes, S. F. Haydock, G. A. Roberts, D. J. Bevitt, P. F. Leadlay, *Nature* **1990**, *348*, 176–178.
- [57] B. A. Pfeifer, S. J. Admiraal, H. Gramajo, D. E. Cane, C. Khosla, *Science* **2001**, *291*, 1790–1792.
- [58] H. Zhang, B. A. Boghigian, B. A. Pfeifer, *Biotechnol. Bioeng.* **2010**, *105*, 567–573.
- [59] S. A. Borisova, H. J. Kim, X. Pu, H. Liu, *ChemBioChem* **2008**, *9*, 1554–1558.
- [60] L. Tang, R. McDaniel, *Chem. Biol.* **2001**, *8*, 547–555.
- [61] T. Akiyama, J. Itoh, K. Yokota, K. Fuchibe, *Angew. Chem., Int. Ed.* **2004**, *43*, 1566–1568.
- [62] D. Uraguchi, M. Terada, *J. Am. Chem. Soc.* **2004**, *126*, 5356–5357.
- [63] T. Akiyama, *Chem. Rev.* **2007**, *107*, 5744–5758.
- [64] A. Zamfir, S. Schenker, M. Freund, S. B. Tsogoeva, *Org. Biomol. Chem.* **2010**, *8*, 5262–5276.
- [65] R. J. Phipps, G. L. Hamilton, F. D. Toste, *Nat. Chem.* **2012**, *4*, 603–614.
- [66] M. Mahlau, B. List, *Angew. Chem., Int. Ed.* **2013**, *52*, 518–533.
- [67] D. Parmar, E. Sugiono, S. Raja, M. Rueping, *Chem. Rev.* **2014**, *114*, 9047–9153.
- [68] R. B. Woodward, E. Logusch, K. P. Nambiar, *J. Am. Chem. Soc.* **1981**, *103*, 3215–3217.
- [69] K. Toshima, Y. Nozaki, S. Mukaiyama, T. Tamai, M. Nakata, K. Tatsuta, M. Kinoshita, *J. Am. Chem. Soc.* **1995**, *117*, 3717–3727.
- [70] K. Tatsuta, Y. Kobayashi, H. Gunji, H. Masuda, *Tetrahedron Lett.* **1988**, *29*, 3975–3978.
- [71] Y. Anzai, S. Li, M. R. Chaulagain, K. Kinoshita, F. Kato, J. Montgomery, D. H. Sherman, *Chem. Biol.* **2008**, *15*, 950–959.
- [72] P. A. Champagne, K. N. Houk, *J. Am. Chem. Soc.* **2016**, *138*, 12356–12359.

- [73] T. H. Fenger, R. Madsen, *European J. Org. Chem.* **2013**, 2013, 5923–5933.
- [74] E. Kaji, T. Nishino, K. Ishige, Y. Ohya, Y. Shirai, *Tetrahedron Lett.* **2010**, 51, 1570–1573.
- [75] R. S. Mancini, J. B. Lee, M. S. Taylor, *Org. Biomol. Chem.* **2017**, 15, 132–143.
- [76] K. A. Parker, P. Wang, *Org. Lett.* **2007**, 9, 4793–4796.
- [77] P. M. Zimmerman, *J. Chem. Phys.* **2013**, 138, 184102.
- [78] P. M. Zimmerman, *Mol. Simul.* **2015**, 41, 43–54.
- [79] P. M. Zimmerman, *J. Comput. Chem.* **2015**, 36, 601–611.
- [80] P. M. Zimmerman, *J. Chem. Theory Comput.* **2013**, 9, 3043–3050.
- [81] D. Crich, S. Sun, *J. Org. Chem.* **1997**, 62, 1198–1199.
- [82] M. R. Monaco, B. Poladura, M. Diaz De Los Bernardos, M. Leutzsch, R. Goddard, B. List, *Angew. Chem., Int. Ed.* **2014**, 53, 7063–7067.
- [83] M. R. Monaco, D. Fazzi, N. Tsuji, M. Leutzsch, S. Liao, W. Thiel, B. List, *J. Am. Chem. Soc.* **2016**, 138, 14740–14749.
- [84] Y. Geng, A. Kumar, H. M. Faidallah, H. A. Albar, I. A. Mhkalid, R. R. Schmidt, *Angew. Chem., Int. Ed.* **2013**, 52, 10089–10092.
- [85] R. R. Schmidt, H. Gaden, H. Jatzke, *Tetrahedron Lett.* **1990**, 31, 327–329.
- [86] R. R. Schmidt, B. Wegmann, K. -H Jung, *Liebigs Ann. der Chemie* **1991**, 1991, 121–124.
- [87] R. R. Schmidt, M. Stumpp, J. Michel, *Tetrahedron Lett.* **1982**, 23, 405–408.
- [88] Z. Sun, G. A. Winschel, P. M. Zimmerman, P. Nagorny, *Angew. Chem., Int. Ed.* **2014**, 53, 11194–11198.
- [89] P. Nagorny, Z. Sun, G. A. Winschel, *Synlett* **2013**, 24, 661–665.
- [90] Y. Y. Khomutnyk, A. J. Argüelles, G. A. Winschel, Z. Sun, P. M. Zimmerman, P. Nagorny, *J. Am. Chem. Soc.* **2016**, 138, 444–456.
- [91] N. D. Shapiro, V. Rauniyar, G. L. Hamilton, J. Wu, F. D. Toste, *Nature* **2011**, 470, 245–250.
- [92] L. Liu, M. Leutzsch, Y. Zheng, M. W. Alachraf, W. Thiel, B. List, *J. Am. Chem. Soc.* **2015**, 137, 13268–13271.
- [93] J. Lv, Q. Zhang, X. Zhong, S. Luo, *J. Am. Chem. Soc.* **2015**, 137, 15576–15583.
- [94] Y. Kuroda, S. Harada, A. Oonishi, H. Kiyama, Y. Yamaoka, K. I. Yamada, K. Takasu, *Angew. Chem., Int. Ed.* **2016**, 55, 13137–13141.
- [95] Z. Sun, G. A. Winschel, A. Borovika, P. Nagorny, *J. Am. Chem. Soc.* **2012**, 134, 8074–8077.
- [96] Y. Y. Khomutnyk, A. J. Argüelles, G. A. Winschel, Z. Sun, P. M. Zimmerman, P.

- Nagorny, *J. Am. Chem. Soc.* **2016**, *138*, 444–456.
- [97] L. Chan, M. S. Taylor, *Org. Lett.* **2011**, *13*, 3090–3093.
- [98] D. Lee, M. S. Taylor, *J. Am. Chem. Soc.* **2011**, *133*, 3724–3727.
- [99] D. Lee, C. L. Williamson, L. Chan, M. S. Taylor, *J. Am. Chem. Soc.* **2012**, *134*, 8260–8267.
- [100] S. David, S. Hanessian, *Tetrahedron* **1985**, *41*, 643–663.
- [101] Y. Demizu, Y. Kubo, H. Miyoshi, T. Maki, Y. Matsumura, N. Moriyama, O. Onomura, *Org. Lett.* **2008**, *10*, 5075–5077.
- [102] A. L. Dewyer, P. M. Zimmerman, *Org. Biomol. Chem.* **2017**, *15*, 501–504.
- [103] M. Tanaka, A. Nakagawa, N. Nishi, K. Iijima, R. Sawa, D. Takahashi, K. Toshima, *J. Am. Chem. Soc.* **2018**, *140*, 3644–3651.
- [104] I. D. Gridnev, M. Kouchi, K. Sorimachi, M. Terada, *Tetrahedron Lett.* **2007**, *48*, 497–500.
- [105] T. Marcelli, P. Hammar, F. Himo, *Chem. - A Eur. J.* **2008**, *14*, 8562–8571.

CHAPTER 6

Practical Solid-Phase Glycosylation Using Immobilized Sugar Phosphonates

"As an amateur in the field, I thought there ought to be some way to do this better, some better way to make peptides than the classical methods everybody is using."

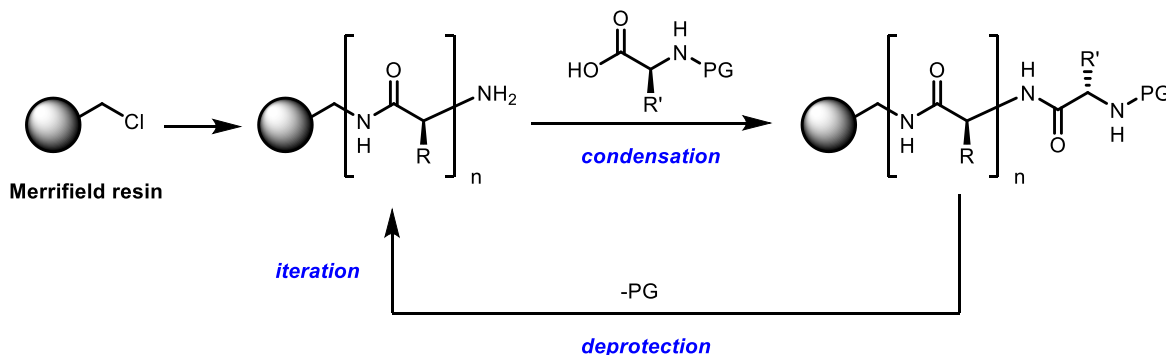
Bruce Merrifield

6.1 Introduction

Since Merrifield's Nobel prize-winning invention and popularization of solid-phase organic syntheses (SPOS) in 1963, the field of solid-phase synthesis exploded in popularity and emerged as a powerful tool in the organic chemist arsenal.^[1,2] The concept of anchoring peptides to insoluble polymeric supports to perform a cascade of chemical reactions and then simply cleave the molecule from the support would facilitate peptide synthesis in such a dramatic way that it would enable an entire new area of chemistry and drug design around synthetic peptides.

The solid-phase synthesis strategy has been in constant growth over the past 50 years, and has been successfully applied in other areas such as the synthesis of oligonucleotides^[3] and oligosaccharides^[4], as well as in the field of small molecule combinatorial chemistry,^[5-7] which in turn led to the dramatic growth in the use of functionalized resins as reagents as catalysts. The main advantage of these solid-phase approach is that the methods allow for the use of excess reagents to drive reactions, simpler workups, and catalyst recyclability.^[8-10]

Scheme 6.1. Merrifield solid-phase peptide synthesis method.



Our group has had long-standing interest in the development of an economic, robust, efficient, and especially simple protocols for the selective chemical glycosylation of alcohols. In line with this, and inspired by our mechanistic insights in the phosphoric acid-catalyzed glycosylations of polyols, where we discovered that these reactions likely proceed through the intermediacy of a reactive covalently bound anomeric phosphate (see Chapter 5, section 5.2),^[11] we sought to commence the development of solid-phase glycosylations based on resins functionalized with glycosyl phosphonates.

6.2 Results and discussion

Experimental information can be found in **Appendix G**)

The vast majority of glycosylation methodologies are based on homogenous catalysis strategies. While these have merits and have contributed brilliantly to the advancement of the field, particularly with regards to selective glycosylations (See Chapter 5), some drawbacks such as the tediousness purification and poor catalyst recyclability might be addressed by a heterogenous approach. Based on our mechanistic conclusions on the phosphoric acid-catalyzed glycosylation of alcohols (Chapter 5, section 5.2 and 5.4), we hypothesized that a phosphonic acid-functionalized

resin could react in a similar way with glycosyl α -trichloroacetimidate donors to form β -phosphonates covalently attached to the solid support. This would enable a solid-phase platform for the glycosylation of various substrates, and since the β -phosphonates is stereoselectively formed, perhaps with the right activator stereoselective glycosylations could be managed (Figure 6.1).

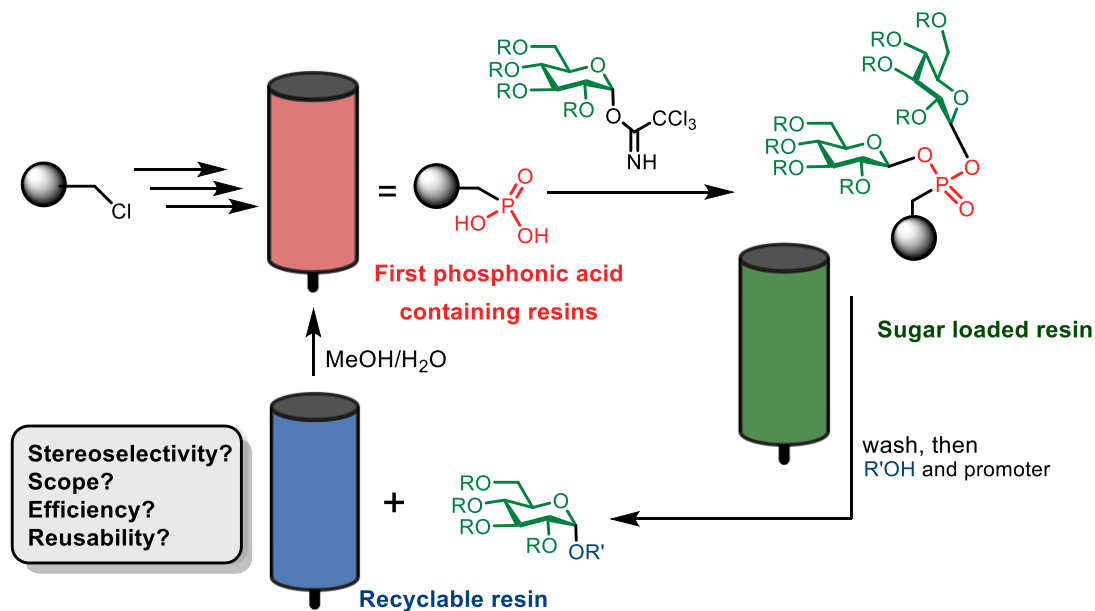
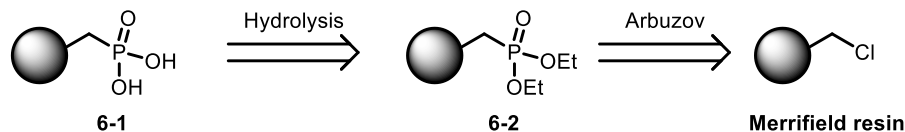


Figure 6.1. Hypothesis for the glycosylation of immobilized sugar phosphonates.

As one of our guiding principles for this project was the development of economic synthetic method, we sought to derivatize the commercially accessible Merrifield resin. Our original retrosynthetic proposal for the preparation of phosphonic acid-functionalized resin **6-1** by the hydrolysis of the phosphonate **6-2**, which in turn could be obtained by an Arbuzov reaction^[12] on the inexpensive Merrifield resin.

Scheme 6.2. Retrosynthesis of solid-supported phosphonic acid **6-1**.

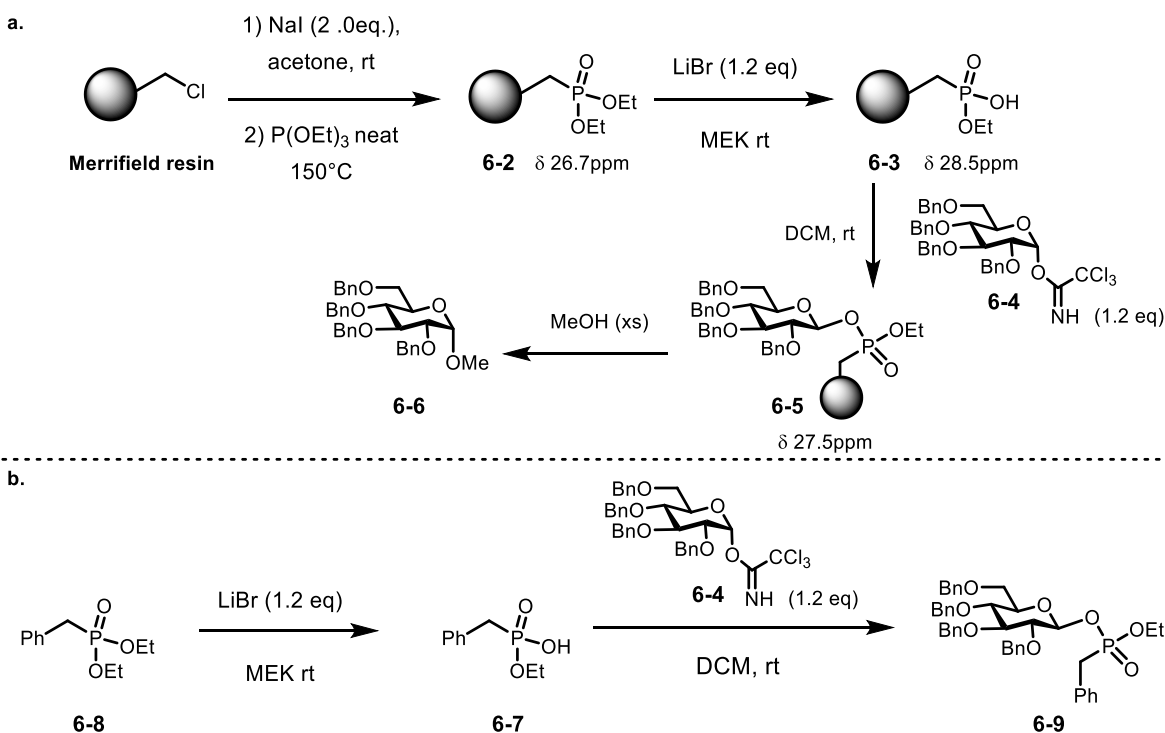


We were comforted to see that the synthesis of **6-2** had been accomplished before,^[13] although not much characterization for this resin was available. We synthesized **6-2** with a slightly modified procedure where we first substituted the benzylic chlorides with iodides using Finkelstein conditions prior to performing the Arbuzov reaction, and then characterized the phosphonate-containing resin using gel ³¹P-NMR (δ 26.7ppm). Our initial attempts at hydrolyzing **6-2** under aqueous acidic conditions ($\text{HCl}_{(\text{aq})}$ 12M) failed, even under refluxing conditions, as did our attempts under basic conditions ($\text{NaOH}_{(\text{aq})}$ 3M with acetone or DMSO as cosolvents). This was not unexpected, as it is known that a swollen polymeric matrix is critical for the reaction to occur, and this requires a different set of solvents, a concept which was remarked by Czarnik in 1998.^[14] While we found that NaI and KI in MEK were unsuccessful, an excess of KOH in organic solvents such as THF could lead to the formation of **6-3**, albeit with a physical alteration of the resin, which became noticeable darker. In contrast, we found that LiBr (1.2 eq) in MEK led to clean formation of **6-3** as a white solid (δ 28.5ppm).

We were delighted to find that α -trichloroacetimidate donor **6-4** in slight excess (1.2 eq) reacted with the solid-supported phosphonate to form immobilized glycosyl phosphonate **6-5** (δ 27.5ppm) (Scheme 6.3a). In addition, washing **6-5** with organic solvents, and then subjecting it to methanol at 80°C led to the selective formation of α -methoxy glycoside **6-6**. To corroborate that the small ³¹P-NMR chemical shift changes were meaningful, the procedure was repeated in a homogeneous scenario using phosphonic acid **6-7**, derived in an identical way from **6-8**. A

diastereomeric mixture of phosphonates **6-9** were observed upon treatment with trichloroacetimidate donor **6-4** (Scheme 6.3b). Importantly, NMR analysis of **6-9** revealed it to be a mixture of diastereomeric β -phosphonates, in accordance to our previous observations.^[11] A diastereomeric mixture is also expected in **6-5**, but the signals are indistinguishable by gel NMR due to the decreased resolution of this technique.

Scheme 6.3. a. Synthesis of phosphonic acid-functionalized resin. **b.** Replication of the solid-phase synthetic route in solution and determination of the stereochemistry of glycosyl phosphonate **6-9**.

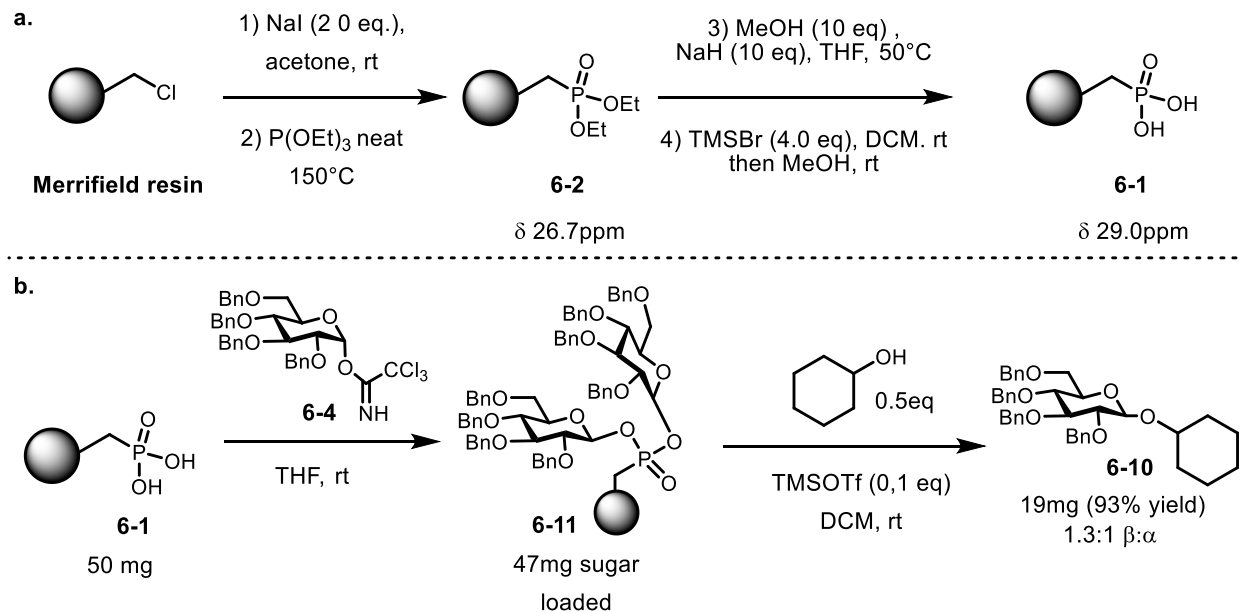


Unfortunately, we found that the reaction of phosphonate **6-9** with secondary alcohols such as cyclohexanol would not occur under neutral conditions. By employing strong Bronsted acid catalysts, such as MsOH, TsOH, and TfOH, the formation of the O-glycoside **6-10** would be observed, albeit with almost no stereoselectivity (1:1 to 1.1:1 β : α). Hydrolyzed starting material would also be frequently observed, as these initial experiments were not performed under strictly

anhydrous conditions. Using anhydrous TBSOTf as a Lewis acid, the desired product was obtained in 1.7:1 β : α selectivity when the reaction was carried out using phosphonate **6-9**. To our delight, when the reaction was performed under anhydrous conditions using resin **6-5**, and excess cyclohexanol (3.0 eq), the product was cleanly formed, although in 1.2:1 β : α . However, it was clear that under our acidic condition and later work-up, the ethyl phosphonate ester would not be stable. Therefore, to provide a more uniform catalyst through several reaction cycles, as well as to have an increased capacity for resin-bound sugar phosphonates, we decided to focus our attention in developing glycosylation strategies for the phosphonic diacid-functionalized resin **6-1**.

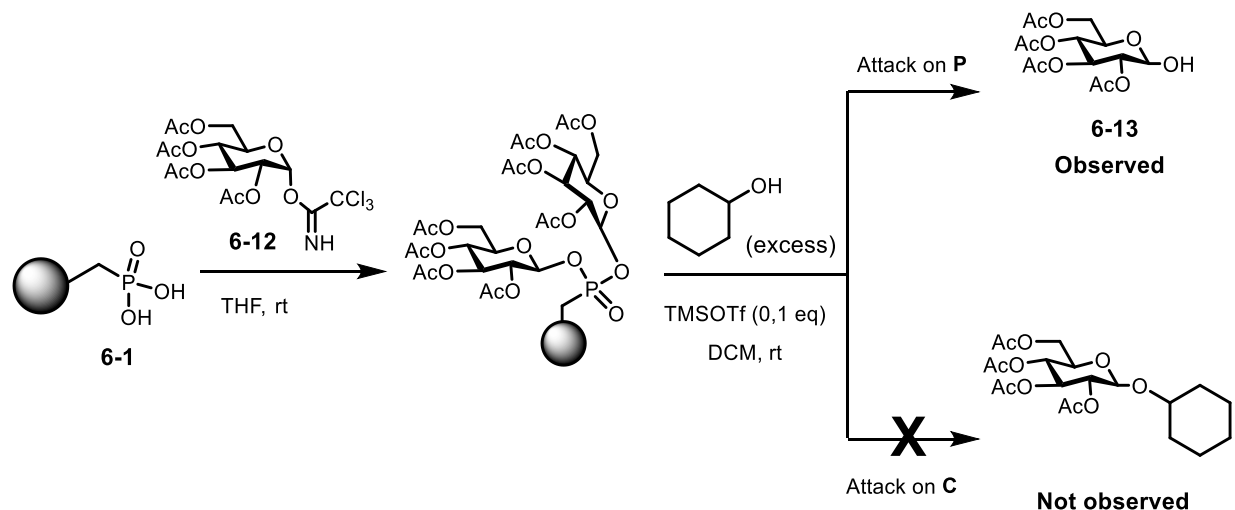
The synthesis of **6-1** was accomplished by methoxide capping of the Arbuzov product **6-6-2**, followed by treatment TMSBr, and subsequent methanolysis of the silylated phosphonate (δ 29.0ppm) (Scheme 6.4a). To the best of our knowledge, this work discloses the first synthesis of solid-phase supported phosphonic mono- and diacids. Glycosyl donor **6-4** could then be loaded to the resin in less than 20 minutes in THF to afford resin-bound diglycosyl phosphonate **6-11** (Scheme 6.4b). TMSOTf catalyzed reaction of **6-11** with excess cyclohexanol (3eq) would yield the desired product in with low stereoselectivity (1.3:1 β : α). To our delight, the reaction with limiting cyclohexanol would yield 93% of product with the same selectivity (Scheme 6.4b). Moreover, the residual resin could be washed and resubjected to the glycosylating reaction conditions to obtain glycoside product in 72% yield and the same selectivity. Importantly, NMR studies of the analog homogenous system revealed that two equivalents of the glycosyl donor reacted with the divalent acid.

Scheme 6.4. a. Preparation of phosphonic diacid-functionalized resin. **b.** Formation of resin bound glycosyl phosphonate.



Glycosyl donors with other protecting groups such as acetyl and benzoyl were also able to be loaded into the resin via a the phosphonic diacid **6-1**. For example, peracetylated glucose trichloroacetimidate donor **6-12** was loaded by stirring it with **6-1** in THF, while perbenzoylated glucose bromide donor formed the phosphonate by using Ag_2CO_3 as a promoter. Unfortunately, TMSOTf-catalyzed reaction of these less active phosphonates would result in decomposition into the unfunctionalized protected sugar **6-13**, presumably because cyclohexanol prefers attacking the P atom instead of the anomeric carbon (Scheme 6.5).

Scheme 6.5. Unsuccessful attempt at the TMSOTf-catalyzed glycosylation with resin-bound peracetylated phosphonates.



To prove that two equivalents of sugar are loaded to phosphonic diacid **6-1**, the reaction of its soluble analog **6-14** with trichloroacetimidate donor **6-4** in THF was conducted and monitored by ^{31}P NMR. As is shown in Figure 6.2, only partial conversion is achieved with 1 equivalent of **6-14**. The ratio of the compounds obtained remains constant from 20min to 1h. However, upon addition of the second equivalent of **6-14**, complete conversion to **6-15** is observed.

Having identified perbenzylated phosphonates as ideal substrates for the glycosylation of secondary alcohols, a number of promoters were screened using the soluble glycosyl phosphonate **6-15** in the search for enhanced stereoselectivities (Table 6.1). Hydrogen-bonding catalysts such as thioureas, squaramides, and thiophosphoramides were not strong enough to catalyze this reaction (entries 1-3). Stronger phosphoric acids such as (*p*-NO₂C₆H₅)₂PO₂H were able to catalyze the glycosylation, although in a nonselective fashion (entry 4). Next, several Lewis acids were tested (entries 5-11), with low to moderate diastereoselectivities.

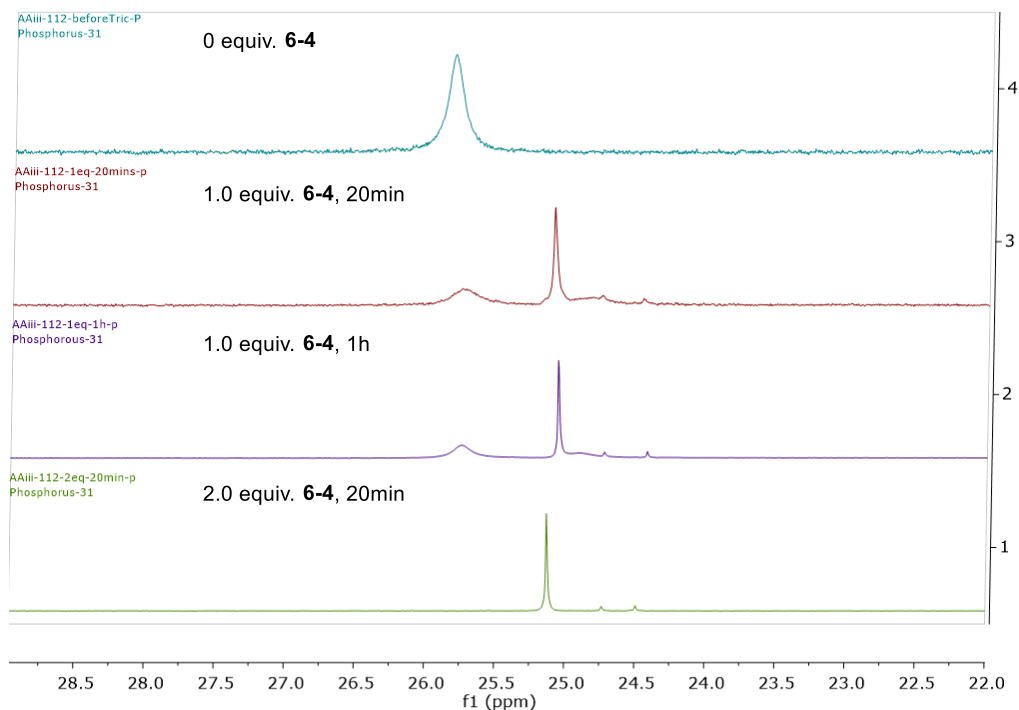
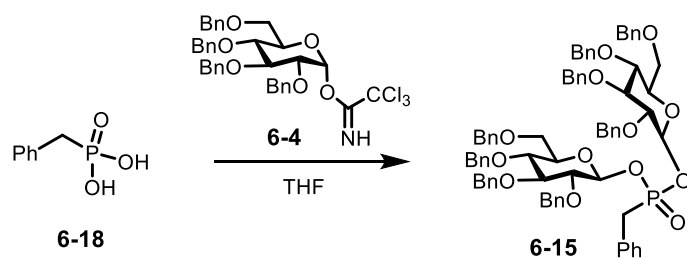
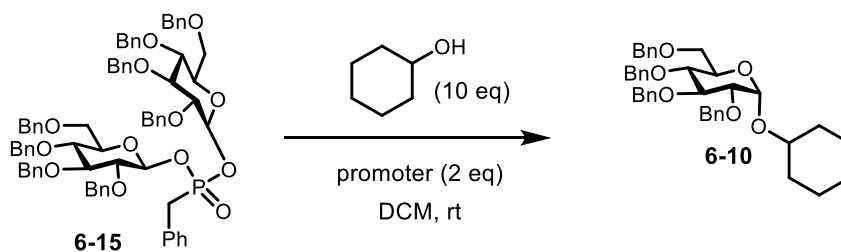


Figure 6.2. Reaction of phosphonic acid **6-18** with varying equivalents of donor **6-4**.

Given the low price of FeCl_3 and the moderate selectivity that it provided (2.3:1 α : β), we decided to further investigate this catalyst (Table 6.2). To our delight, we found that by using substoichiometric amounts of FeCl_3 , and by working up the reaction by directly filtering the reaction mixture through a short SiO_2 plug, good diastereoselectivities were obtained in DCM, DCE, dioxane, and PhMe (Table 6.2, entries 1, 3, 5, and 6). Moreover, with a saturated solution of FeCl_3 in DCM, the reaction was fully complete in 15 minutes, by RP-HPLC analysis.

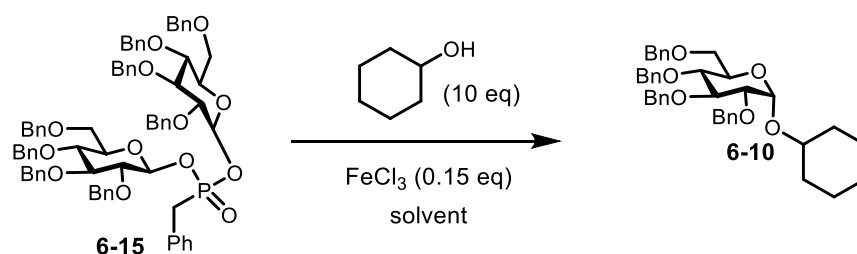
Table 6.1. Initial promoter screening for the glycosylation of phosphonates.^a



entry	promoter	conversion ^b	dr (α : β) ^c
1		trace	--
2		trace	--
3		trace	--
4		major	1:1
5	Cu(OTf) ₂	major	1:1
6	Sc(OTf) ₂	major	3:1
7	Yb(OTf) ₂	major	1:1
8	ZnBr ₂	major	1.6:1
9	ZrCp ₂ Cl ₂	major	1.4:1
10	I ₂	major	2:1
11	FeCl ₃	major	2.3:1

^aGlycosylations performed according to general protocol detailed in Appendix G. ^bTrace product was not observed by TLC, only by RP-HPLC, major indicates product was the major spot in the TLC. ^cDetermined by RP-HPLC.

Table 6.2. Initial promoter screening for the glycosylation of phosphonates.^a



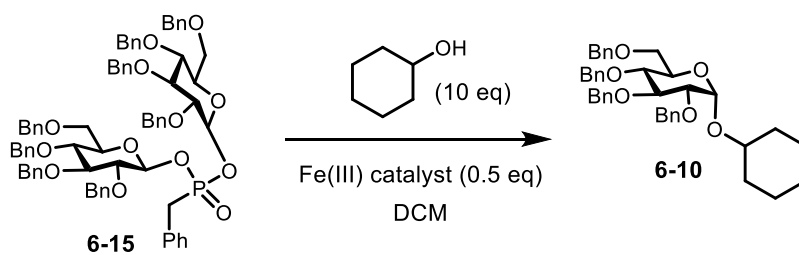
entry	solvent	conversion ^b	dr ($\alpha:\beta$) ^c
1	DCM	major	10.6
2	CHCl_3	trace	--
3	DCE	major	11.0
4	THF	trace	--
5	dioxane	low	10.5
6	PhMe	major	12.5
7	MeCN	trace	--
8	EtOAc	trace	--
9	DMF	trace	--

^a Glycosylations performed according to general protocol detailed in Appendix G. ^b Trace product was not observed by TLC, only by RP-HPLC, major indicates product was the major spot in the TLC, minor indicates product was a significant yet small spot in the TLC. ^c Determined by RP-HPLC.

Additional experiments highlighted the importance of the counterion of the Fe(III) catalyst. Table 6.3 shows the results of different Fe(III) catalysts used. Fe(III) phosphate tetrahydrate, citrate monohydrate, acetylacetonates, and diisobutyrylmethane failed to produce detectable amounts of product, presumably because of their lower Lewis acidity (entries 1-4). Fe(III) triflate did yield the desired product, but in drastically inferior diastereoselectivity and at a much lower reaction rate (entry 5). Fe(III) sulfate provided good diastereoselectivity, but the reaction rate was

even slower than the Fe(III) triflate reaction. Indeed, at 18 hours, only moderate conversion was observed for the Fe(III) sulfate reaction. The excellent diastereoselectivity and reactivity of FeCl₃ speaks for a mechanism involving an anomeric chloride intermediate.

Table 6.3. Effect of the counterion in the Fe(III) catalyzed glycosylation of phosphonates.^a



entry	catalyst	conversion at 5h ^b	dr (α : β) ^c
1	Fe(PO ₄) · 4H ₂ O	--	--
2	Fe(C ₆ H ₅ O ₇) · H ₂ O	--	--
3	Fe(acac) ₃	--	--
4	Fe(dibm) ₃	--	--
5	Fe(OTf) ₃	major	1.1:1
6	Fe ₂ (SO ₄) ₃ · 9H ₂ O	trace	13:1
7	FeCl ₃	full	9:1

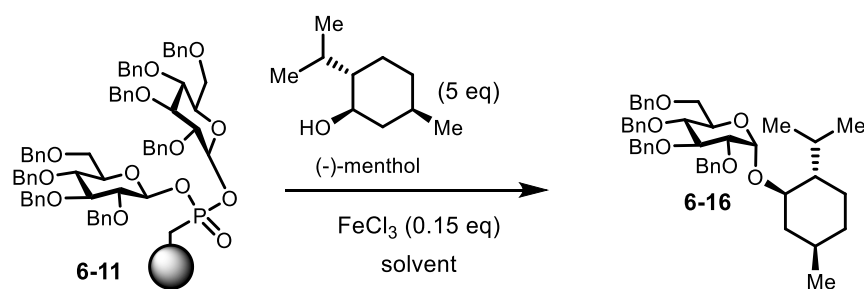
^a Glycosylations performed according to general protocol detailed in Appendix G ^b trace product was not observed by TLC, only by RP-HPLC, major indicates product was the major spot in the TLC, full indicates full conversion by RP-HPLC. ^c Determined by RP-HPLC.

Regrettably, when the optimized conditions in DCM with FeCl₃ were applied to the glycosylation of cyclohexanol with solid-supported phosphonate **6-11**, only a 1.5:1 diastereoselectivity favoring the α epimer was observed. In addition, contrary to the observation made in Table 6.1, entry 4, the use of phosphoric acids such as (*R*)-TRIP were ineffective in catalyzing this reaction. Undeterred, we reevaluated conditions that would better suit the solid-

supported glycosylation. To this end, we attempted the glycosylation of (-)-menthol, a bulkier secondary alcohol compared to cyclohexanol, which might help us notice trends in our method development more easily (Table 6.4). We screened a number of Lewis acids with chloride counterions, such as CoCl_2 , MnCl_2 , NiCl_2 , and VCl_3 , but all of these were either ineffective or drastically inferior to FeCl_3 in their role as catalysts for this reaction. For this reason, we decided to reevaluate conditions for FeCl_3 in this new system. To our relief, we found that the diastereoselectivity could be increased from 3:1 in DCM (Table 6.4, entry 1) to up to 10:1 in 1,4-dioxane (entry 10) in favor of the α diastereomer of the O-glycoside **6-16**. In addition, acetonitrile offers a modest reverse diastereoselectivity, approximately 2:1 favoring the β isomer (entry 7). Finally, we observed that the addition of even hindered Lewis bases in super stoichiometric amounts shuts down this chemistry, for example TEA, DIPEA, lutidine, and even excess benzophenone and external chloride sources such as LaCl_3 .

When we attempted the glycosylation with limiting acceptor, we observed that the reaction suffered from poor conversions when dioxane was used as the solvent. In addition, we detected significant formation of α - glycosyl chloride **6-17** in the solution, as well as hydrolyzed donor **6-18**. After additional optimization, we noticed the reaction occurred more efficiently in toluene, and with the addition of molecular sieves we were able to diminish the amount of hydrolyzed donor. With 0.5 equivalents of FeCl_3 we were able to obtain 41% yield of product **6-16** with very small amounts of residual α - glycosyl chloride **6-17** and hydrolyzed donor **6-18**. (Scheme 6.6).

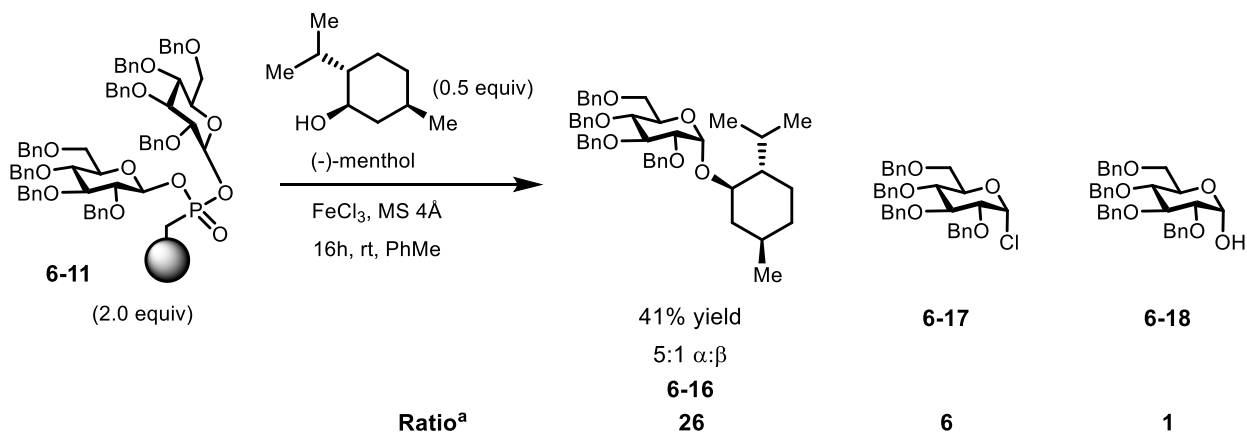
Table 6.4. Evaluation of solvents for the solid-phase glycosylation of phosphonates with menthol.^a



entry	solvent	dr ($\alpha:\beta$) ^b
1	DCM	3:1
2	DCE	2:1
3	Et ₂ O	4:1
4	CyH	5.1:1
5	PhMe	10:1
6	THF	1.9:1
7	MeCN	1:1.9
8	DMF	trace
9	dioxane	10.1:1

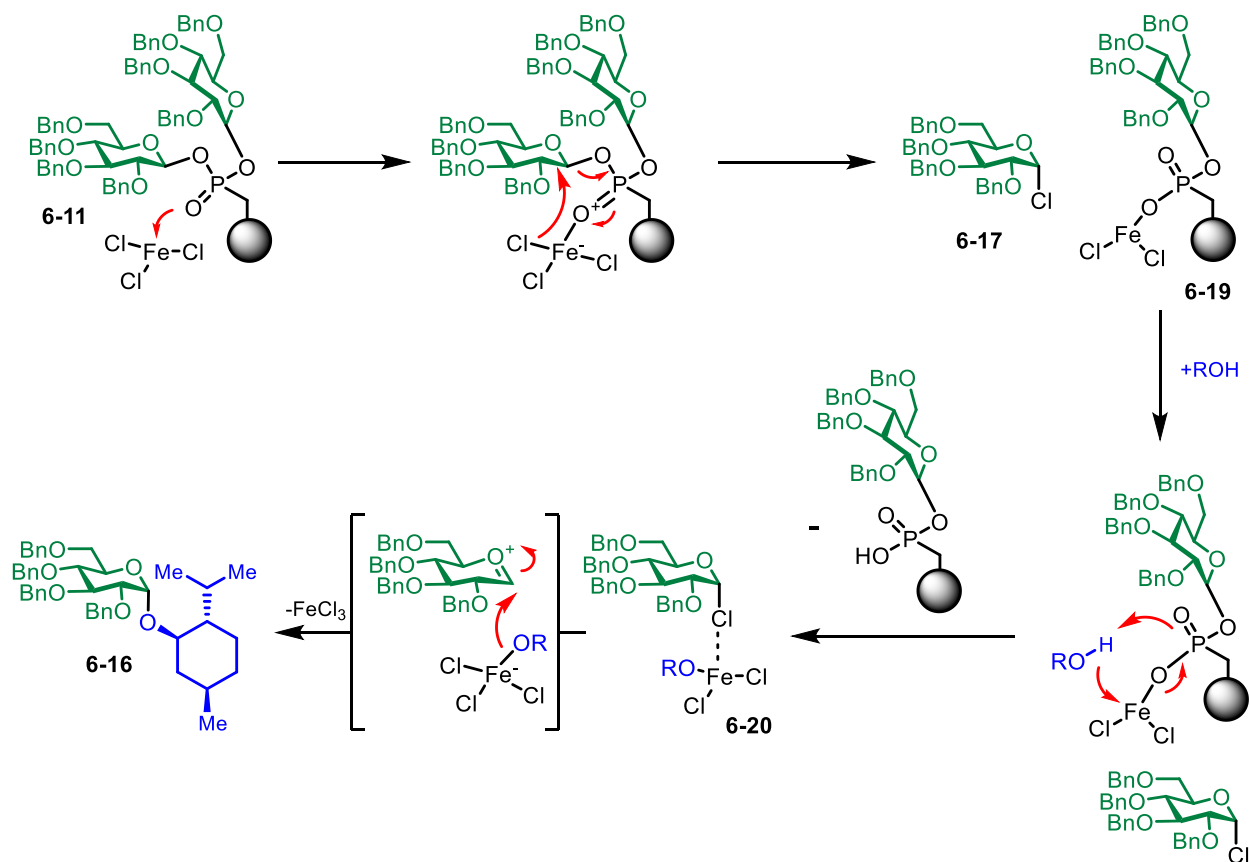
^a Glycosylations performed according to general protocol detailed in Appendix G. ^b Determined by RP-HPLC.

Scheme 6.6. Glycosylation of limiting acceptor with **6-11**. ^a Determined by NMR.



A plausible mechanism for this reaction, based on the observed intermediates and α -selectivity, is shown in Scheme 6.7. Immobilized phosphonate **6-11** could bind to FeCl_3 and then product α -chloride **6-17** and Fe(III)-phosphonate **6-19**. The latter could then bind to the alcohol substrate, and lead to the formation of Fe(III)-alkoxide **6-20** with the release of immobilized phosphonic acid. **6-20** could then bind to the axial chloride of **6-17** and abstract the halide. On the basis of the principle of least motion, the alkoxide would be better suited to attack on the α -face of the transient oxocarbenium species, which would lead to selective formation of **6-16**.

Scheme 6.7. Proposed mechanism for the FeCl_3 -catalyzed glycosylation of alcohols with immobilized phosphonates **6-11**.



In summary, we have developed and characterized the first solid-supported phosphonic acid resins, as well as its application in the glycosylation of secondary alcohols. Our method enables a reliable, fast, and efficient way of covalently linking glycosyl donors to a polystyrene-based solid support. The solid-supported glycosyl phosphonates can then be employed in FeCl₃-promoted glycosylations with primary and secondary alcohols to obtain highly α -enriched O-glycosides. The heterogeneous nature of our method allows for an operationally simple and reliable procedure that does not require expensive instrumentation or tedious work-ups. In a reality where a large fraction of natural products require a glycosidic bond, we envision that our method will be useful to biochemists seeking a practical and expertise-free solution to their glycosylation needs.

6.3 References

- [1] R. B. Merrifield, *J. Am. Chem. Soc.* **1963**, *85*, 2149–2154.
- [2] R. B. Merrifield, *Angew. Chem., Int. Ed.* **1985**, *24*, 799–810.
- [3] R. L. Letsinger, V. Mahadevan, *J. Am. Chem. Soc.* **1966**, *88*, 5319–5324.
- [4] J. M. Frechet, C. Schuerch, *J. Am. Chem. Soc.* **1971**, *93*, 492–496.
- [5] L. A. Thompson, J. A. Ellman, *Chem. Rev.* **1996**, *96*, 555–600.
- [6] J. A. Ellman, *Acc. Chem. Res.* **1996**, *29*, 132–143.
- [7] E. M. Gordon, R. W. Barrett, W. J. Dower, S. P. A. Fodor, M. A. Gallop, *J. Med. Chem.* **1994**, *37*, 1385–1401.
- [8] M. Collot, S. Eller, M. Weishaupt, P. H. Seeberger, *Beilstein J. Org. Chem.* **2013**, *9*, 97–105.
- [9] A. R. Vaino, K. D. Janda, *J. Comb. Chem.* **2002**, *2*, 579–596.
- [10] M. Benaglia, A. Puglisi, F. Cozzi, *Chem. Rev.* **2003**, *103*, 3401–3430.
- [11] J. H. Tay, A. J. Argüelles, M. D. Demars, P. M. Zimmerman, D. H. Sherman, P. Nagorny, *J. Am. Chem. Soc.* **2017**, *139*, 8570–8578.
- [12] A. K. Bhattacharya, G. Thyagarajan, *Chem. Rev.* **1981**, *81*, 415–430.
- [13] M. S. Lukashova, K. N. Belikov, K. Y. Bryleva, S. G. Kharchenko, S. G. Vishnevsky, V. I. Kalchenko, *Funct. Mater.* **2016**, *23*, 111–119.
- [14] A. W. Czarnik, *Biotechnol. Bioeng.* **1998**, *61*, 77–79.

CHAPTER 7

Studies on the Mechanism of Phosphoric Acid-Catalyzed Epoxide Ring Opening

"Chemical synthesis is uniquely positioned at the heart of chemistry, the central science, and its impact on our lives and society is all pervasive."

Elias J. Corey

7.1 Introduction

Among the functional motifs that comprise cyclic ethers, the three membered examples, called epoxides or, less commonly, oxiranes, have several structural and reactivity attributes that set them aside from the rest of cyclic ethers.^[1] For this reason, they are one of the most recurring substructures observed in both manmade applications and biosynthetic routes. In addition, an almost endless number of naturally occurring epoxides with a wide range of interesting biological activities are found in nature, which has further increased the interest of epoxides to biologists, pharmacologists, and synthetic chemists.^[2] A few examples of naturally occurring epoxides are shown in Figure 7.1.

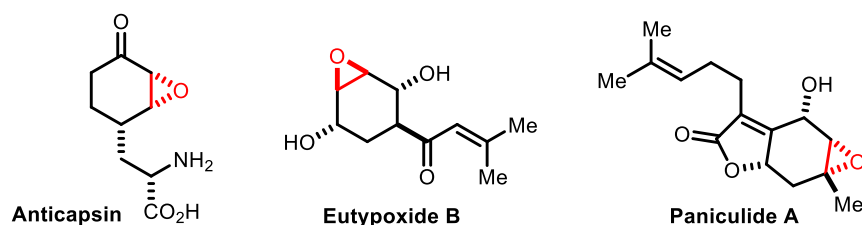


Figure 7.1. Examples of complex structures containing epoxides.

Epoxides are highly strained heterocycles that are relatively easy to synthesize and reasonably stable to handle. Using a combination of experimental and computational techniques, Morgan and coworkers measured gas-phase enthalpy of formation (ΔH_f) and the strain energy of several epoxides. The latter was found to be around 20-25 kcal/mol (Figure 7.2).^[3] Thus, epoxide chemistry is dominated by ring-opening reactions that relieve the vast potential energy that is captured in the ring strain.

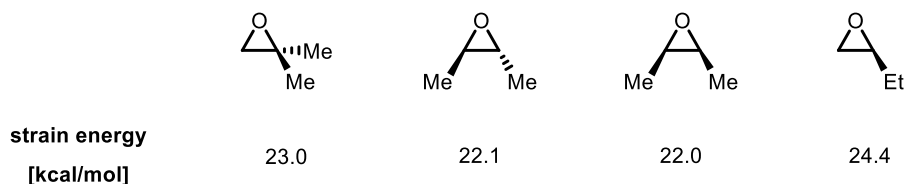


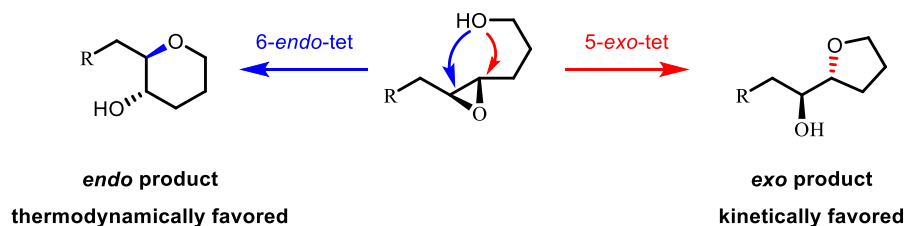
Figure 7.2. Ring strain in epoxides.

Epoxides are powerful and versatile intermediates in synthesis for two main reasons. A contributing factor is the emergence and development of efficient and enantioselective methods for epoxide installation such as the Sharpless asymmetric epoxidation of allylic alcohols,^[4] the Jacobsen epoxidation,^[5,6] and the Shi epoxidation.^[7,8] In addition, there exists a plethora of other methods for the construction of epoxides that have made epoxide-containing chiral building blocks and starting materials readily available.^[1,9]

The second factor is that an immeasurable amount of work has been done in the development of synthetic methods that harness the high reactivity of epoxides for the construction of oxygenated synthetic targets. Given the reactivity of epoxides towards nucleophiles and electrophiles, there exists both acid- and base-promoted epoxide ring openings that one can choose from to achieve a desired regio- and stereochemical outcome with a wide range of substitution patterns for the product.^[1] For this reason, a substantial number of total syntheses rely on the formation and use of an epoxide-containing intermediate.^[9]

While most methods for the functionalization of epoxides focus on the intermolecular epoxide ring opening (ERO) with a nucleophile, the intramolecular variant is a powerful tool for the construction of cyclic products. However, for the latter to be useful in synthesis, effective ways to control the regioselectivity of the ERO is mandatory. Baldwin's rules,^[10] a set of empirical generalizations that help discern kinetically favored intramolecular cyclizations, suggest that the regiochemistry of intramolecular ERO favors *exo* processes that proceed through a spiro transition state. Indeed, with few exceptions, intramolecular ERO leads to the formation of 5-membered rings (*exo*-products) instead of 6-membered rings (*endo*-products) (Scheme 7.1).^[11] For this reason, methods that facilitate *endo* control for intramolecular ERO are of high interest to synthetic chemists.

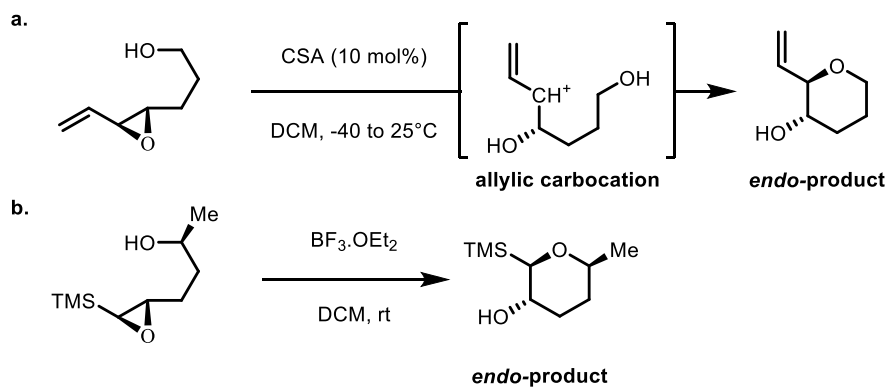
Scheme 7.1. Intramolecular ERO leading to *endo*- or *exo*-product formation.



Most of the strategies developed to control the regiochemistry of intramolecular EROs have relied on the use of directing groups covalently present in the substrates. A variety of modifications have been tried, including alkenyl,^[12–15] alkynyl,^[16] alkyl,^[17,18] and silyl.^[19,20] The majority of these methods justify their regioselectivity in electronic perturbations of the epoxide that stabilize the 6-*endo*-tet TS or disfavor the 5-*exo*-tet TS. For instance, the Nicolaou group, pioneers of the regioselective ERO, used simple vinyl substituents on the epoxide to stabilize the nascent allyl carbocationic intermediate that leads to *endo*-cyclization (Scheme 7.2a).^[14,15] On the

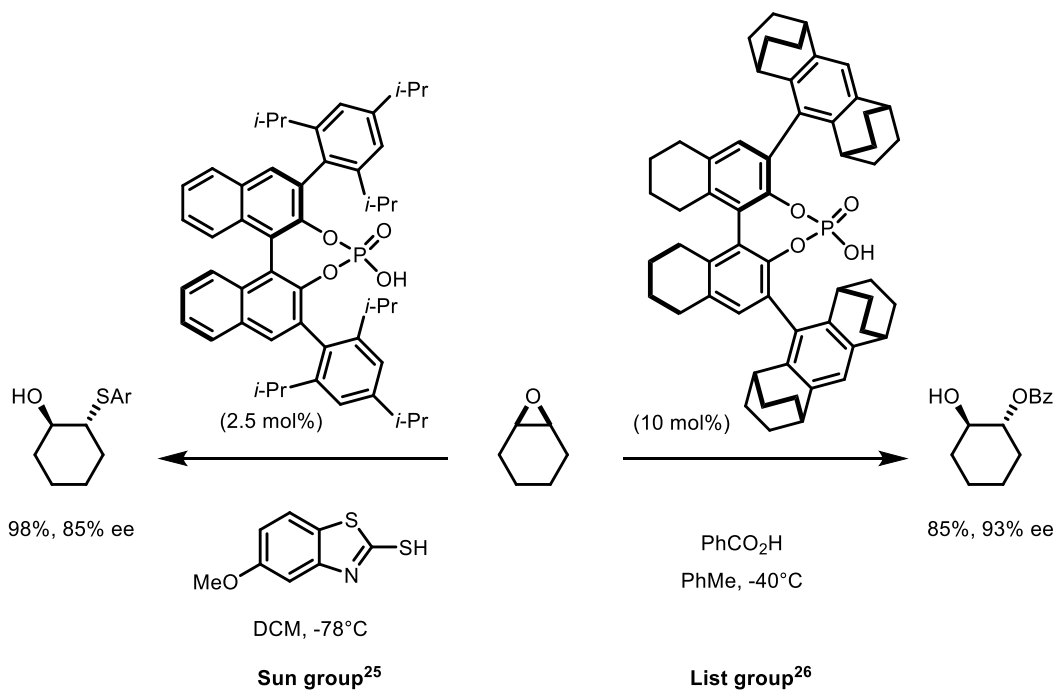
other hand, Schaumann and coworkers achieved a similar stereoelectronic bias by using silyl-substituted epoxides (Scheme 7.2b).^[20]

Scheme 7.2. Examples of substrate control strategies in *endo*-selective intramolecular EROs.



The mentioned substrate-controlled strategies offered a breakthrough in intramolecular ERO. However, the use of covalently linked directing groups as a source of regiocontrol have some evident drawbacks. These methods are restricted in scope and tend to lack generality. On the other hand, catalyst-controlled regioselective intramolecular ERO could provide a more robust method that is applicable across families of substrates. The Nagorny group has ample experience and success in the application of chiral phosphoric acids (CPAs, for an introduction, see Chapter 2), in regio- and stereoselective acetalization reactions, some of which are discussed in this dissertation (Chapters 3 and 5). In collaboration with Sibin Wang, Miyuki Hotta and Dr. Tay Rosenthal (Nagorny group), we sought to extend this strategy to the intramolecular ERO by developing a practical a CPA-controlled methodology to access both *exo*- and *endo*-products. In addition, we sought to understand mechanistic details for CPA selection of either pathway using quantum chemical tools developed by the Zimmerman group.^[21–24] As an encouraging precedent, both the Sun and the List groups independently demonstrated the usefulness of CPAs in desymmetrization intermolecular ERO with thiols and water as nucleophiles, respectively (Scheme 7.3).^[25,26]

Scheme 7.3. CPA-catalyzed enantioselective intermolecular ERO.^[25,26]



7.2 Results and discussion

To test our hypothesis that CPAs could be used to control the regioselectivity of intramolecular ERO in a complex setting, we investigated the cyclization of the methyl ester of natural antibiotic mupirocin **7-1**. The control experiments showed that under a variety of acidic, neutral, and basic conditions, either poor conversion or both *exo* (**7-2**) and *endo* (**7-3**) were formed unselectively (Table 7.1, entries 1-6). However, using catalytic amounts of the acidic phosphoric acid (*p*-NO₂-C₆H₄O)PO₂H, complete conversion of mupirocin methyl ester and a poor *endo*-selectivity was observed (entry 7). This suggests that, contrary to what might be expected by Baldwin's rules, phosphoric acid catalysis has a small inherent *endo*-selectivity for the intramolecular ERO of mupirocin methyl ester, but high selectivity for either **7-2** or **7-3** is unlikely using achiral catalysts.

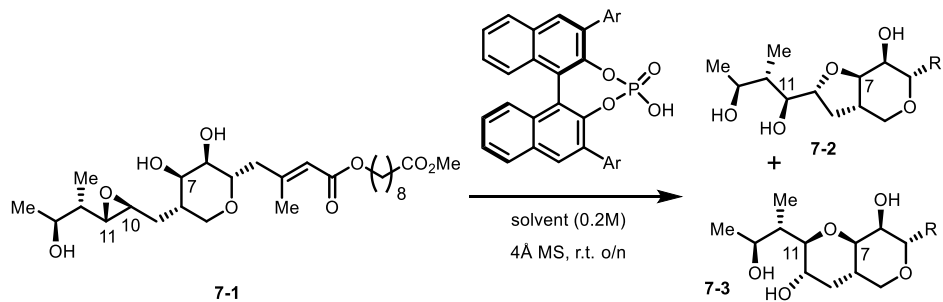
Table 7.1. Initial control experiments on the intramolecular ERO of **7-1**.^a Experiments were performed by Sibin Wang, Miyuki Hotta, and Dr. Tay Rosenthal.

entry	catalyst	Solvent	Time	Conv. [%]	7-2:7-3 ^b
1 ^c	LiCl	DCM	o/n	<5	-
2 ^c	ZnCl ₂	DCM	o/n	82	1.1:1
3 ^d		water	4d	24	1:2.5
4	KH ₂ O ₄ buffer (7 pH)	water	4d	>98	1.1:1
5 ^e	Cs ₂ CO ₃	MeOH	4d	nr	-
6 ^f	LiHMDS	THF	4d	nr	-
7	(<i>p</i> -NO ₂ -C ₆ H ₄ O)PO ₂ H	DCM	5d	>98	1:2.3

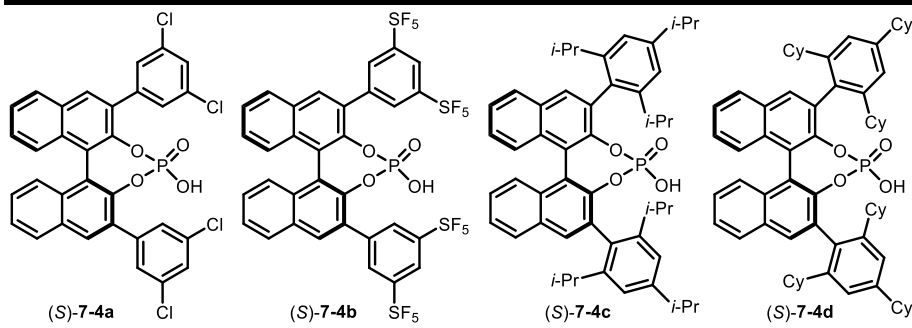
^a conditions: **7-1** (1 equiv), catalyst (20 mol%), DCM (0.2M), rt. ^b Determined by RP-HPLC. ^c DCM (0.01M). ^d 70°C. ^e Cs₂CO₃ (10 equiv.), DCM (0.02M). ^f LiHMDS (3 equiv), DCM (0.01M).

We then evaluated if the use of CPAs could bias or even revert the inherent low *endo*-selectivity for this transformation. To this end, we screened a number of BINOL-derived CPAs. Encouragingly, we found that the axial chirality of the BINOL backbone had a significant impact on the regioselectivity of the transformation, with (*R*) consistently favoring *endo*-product formation more than (*S*) (Table 7.2, entries 1-8). To our delight, for the first time excellent regioselectivity for *endo*-product formation was observed when using (*R*)-**7-4c** and (*R*)-**7-4d** (entries 6 and 8). After screening solvents using (*R*)-**7-4d** as the catalyst (Table 7.2, entries 9-12), we found that the regioselectivity could be further increased to 1:19 (entry 12) by using toluene. Under these optimized conditions, we found that the catalyst loading could be lowered to 5 mol% with minimal detriment to the regioselectivity of the reaction (entries 12-14).

Table 7.2. Catalyst screening for the optimization of *endo*-selective conditions. Experiments were performed by Sibin Wang, Miyuki Hotta, and Dr. Tay Rosenthal.



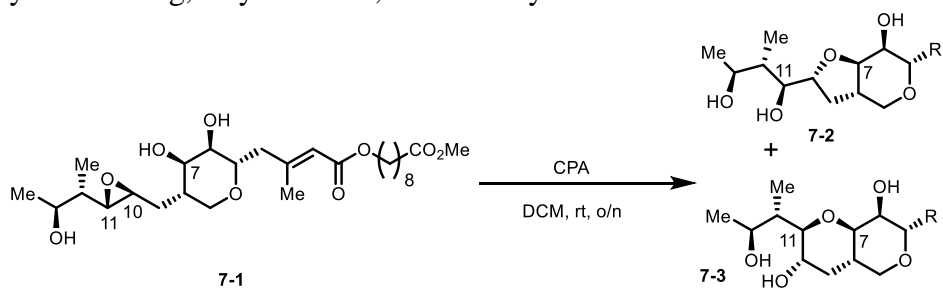
entry	catalyst	Loading [mol%]	Solvent	Conv. [%]	7-2:7-3 ^b
1	(S)-7-4a	20	DCM	>98	1:1.9
2	(R)-7-4a	20	DCM	>98	1:2.8
3	(S)-7-4b	20	DCM	>98	1:1.9
4	(R)-7-4b	20	DCM	>98	1:2.7
5	(S)-7-4c	20	DCM	>98	1:1.3
6	(R)-7-4c	20	DCM	>98	1:13
7	(S)-7-4d	20	DCM	>98	1.2:1
8	(R)-7-4d	20	DCM	>98	1:15.5
9 ^c	(R)-7-4d	20	DCM	67	1:8.7
10 ^c	(R)-7-4d	20	CyH	39	1:3.3
11 ^c	(R)-7-4d	20	PhCF ₃	>98	1:11.5
12 ^c	(R)-7-4d	20	PhMe	>98	1:19
13 ^c	(R)-7-4d	10	PhMe	>98	1:19
14 ^c	(R)-7-4d	5	PhMe	>98	1:18.4



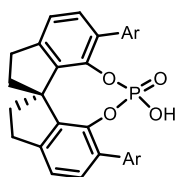
^a conditions: 7-1 (1 equiv), solvent (0.2M), 4Å MS, rt., o/n ^b Determined by RP-HPLC. ^c 4Å MS were not used.

Having been successful in finding conditions for the preparation of the *endo*-product **7-3** with excellent conversion and regioselectivity, we conjectured that through judicious choice of a CPA, we could bias the selectivity towards the formation of *exo*-product **7-2**, especially after having observed that in all cases BINOL derived catalysts with (*S*) chirality gave better *exo*-selectivity than achiral phosphoric acids (Table 7.2, entries 1, 3, 5, 7 compared to Table 7.1, entry 7). To this end, we evaluated SPINOL-derived CPAs as well as BINOL derived CPAs containing functionalities different that aryl substituents at the 3 and 3' position (Table 7.3, entries 1-7). To our delight, we found that the use of 5 mol% of (*S*)-TIPSY resulted in the formation of the *endo*-product in high regioselectivity (5.3:1, Table 7.3, entry 6).

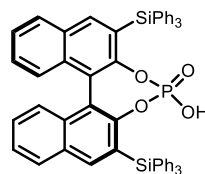
Table 7.3. Catalyst screening for the optimization of *exo*-selective conditions.^a Experiments were performed by Sibin Wang, Miyuki Hotta, and Dr. Tay Rosenthal.



entry	catalyst	Loading [mol%]	Conv. [%]	7-2:7-3 ^b
1	(<i>R</i>)-7-5a	20	>98	1:1.4
2	(<i>R</i>)-7-5b	20	>98	1.1:1
3	(<i>R</i>)-7-5c	20	>98	1.5:1
4	(<i>R</i>)-7-5d	20	>98	1.5:1
5	(<i>S</i>)-7-4e	20	>98	1.9:1
6	(<i>S</i>)-7-4e	5	>98	3:1



(*R*)-7-5a: Ar = 3,5-F₂-C₆H₃
 (*R*)-7-5b: Ar = 3,5-(CF₃)₂-C₆H₃
 (*R*)-7-5c: Ar = 3,5-(SF₅)₂-C₆H₃
 (*R*)-7-5d: Ar = 9-anthryl



(*S*)-7-4e

^a conditions: 7-1 (1 equiv), DCM (0.2M), rt., o/n ^b Determined by RP-HPLC.

Although these results are promising, they are also highly empirical. Further mechanistic details to disclose the high efficiency and modest intrinsic *endo*-selectivity of the phosphoric acid-catalyzed intramolecular ERO of mupirocin methyl ester was therefore highly desirable. However, computational methods to describe the reaction mechanism in relatively large systems, with many degrees of freedom, such as this, constitutes a challenge to even modern approaches.^[27] Fortunately, the Zimmerman group has developed a number of quantum chemical methods to facilitate the accurate and fast search of relevant reactions paths and transition states.^[21–24] This method has been used by the author in the elucidation of fine mechanistic detail of phosphoric acid-catalyzed spiroketalizations and glycosylations (See Chapter 3 and 5).^[28,29] Thus, we employed the single-ended growing string method with the hope to detail the mechanism of phosphoric acid-catalyzed intramolecular ERO.

To save computational cost, a truncated model of the mupirocin methyl ester was used (**7-6**), and biphenyl phosphoric acid (**BPA**) was utilized as the catalyst. Given that CPAs possess both Brønsted acidic and Lewis basic sites in proximity, it is possible that CPAs simultaneously activate the electrophilic epoxide and the nucleophilic alcohol. Several arrangements that allow such concerted operation were modeled. To save time and computational cost, the starting point for the single-ended growing string calculations (GSM) were the products of the reaction **7-7** for the *exo* reaction and **7-8** for the *endo*-reaction, and driving coordinates leading to the reverse reaction to (yielding the epoxide **7-6**) were given. This helps to obtain productive models more easily, since the products have less degrees of freedom, and is a valid strategy due to the principle of microscopic reversibility.

Our computations (Figure 7.3) revealed that the formation of a substrate-BPA complex [**7-6** – **BPA**] was thermodynamically favored by 3.5 kcal/mol, consistent with the formation of 3 hydrogen bonds between C6, C7, and C13 hydroxy groups and the phosphoric acid. In addition, as expected, the *endo*-product **7-7** is preferred thermodynamically by 5.1 kcal/mol and its formation is highly exothermic, 12.6 kcal/mol downhill from the substrate-BPA complex. Concerted pathways for the formation of both *endo*- and *exo*-products were readily found using GSM, and revealed that the preferred regioisomeric pathways, while topologically distinct, shared almost identical activation barriers of around 19.1 kcal/mol. The *endo*-pathway was preferred minutely by 0.16 kcal/mol, a number that, while admittedly within statistic error, agrees with the small intrinsic *endo*-selectivity that is observed with achiral phosphoric acids experimentally (Figure 7.3 TS_{endo} vs. TS_{exo} and Table 7.1, entry 7). Additionally, a mechanism considering an epoxide opening by the phosphoric acid to form a phosphate intermediate was ruled out because the barrier for phosphate formation was substantially higher (~8.3 kcal/mol, TS_P) than the concerted pathways.

The reverse reactions for the concerted mechanism have activation barriers of 36.0 and 32.1 kcal/mol for *endo*- and *exo*-product formation, respectively, indicating an irreversible transformation at room temperature. However, these barriers are not so large that under forcing conditions equilibration to favor *endo*-product formation would not occur. In support of this, when a 1:1 mixture of *exo*- and *endo*-products **7-2** and **7-3** was heated to 80°C overnight in the presence of (S)-TIPSY and Cu(BOX)(SbF₆)₂, the resulting mixture was highly enriched in *endo*-product (>98:1).

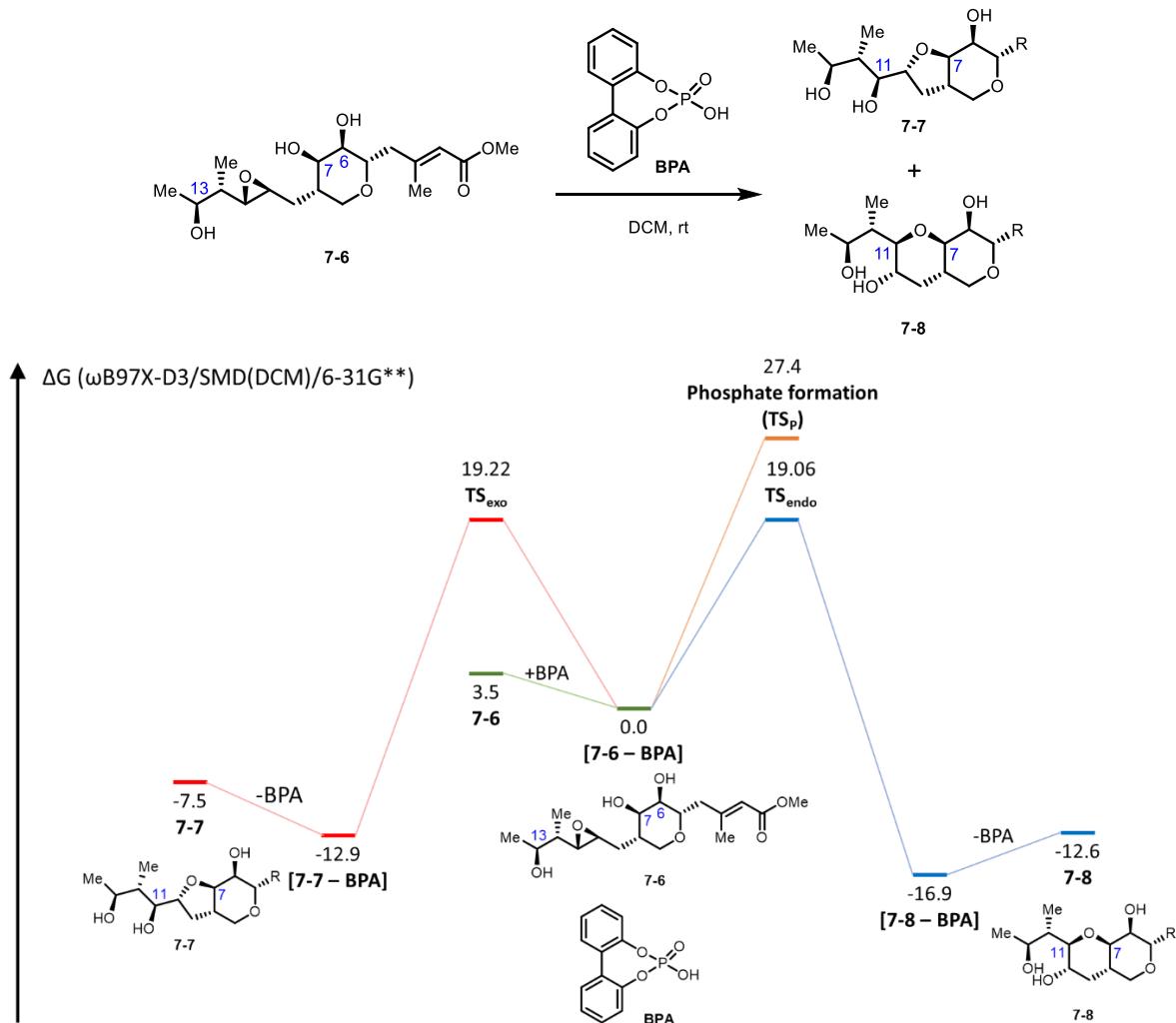
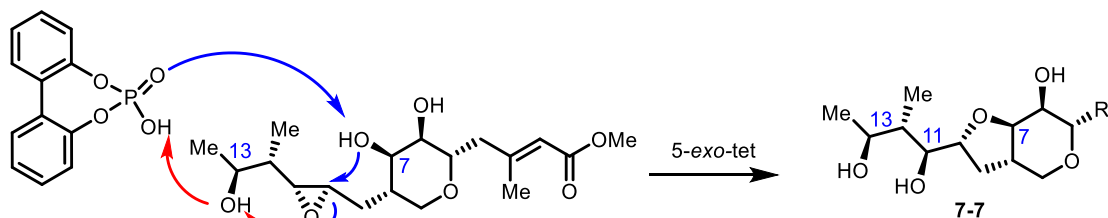


Figure 7.3. Energy diagram for the intramolecular ERO of a truncated mupirocin model.

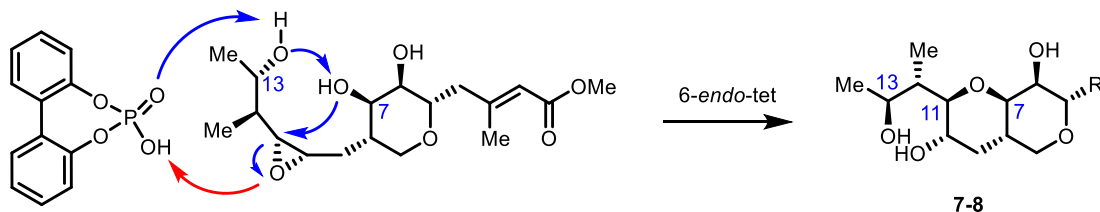
As mentioned earlier, the preferred *endo*- and *exo*-pathways are close in energy and share some features. For instance, in both cases it would be geometrically impossible to have a concerted pathway for this substrate without the hydroxyl group at C13 acting as a relay proton donor and acceptor (Scheme 7.4). Indeed, computational models lacking this aptly placed functional group require a stepwise sequence of events (protonation, rotation, and cyclization) to yield the product, which have a higher activation barrier. Another shared important feature for the concerted pathway is that protonation of the epoxide (red arrows) and cyclization (blue arrows) occur simultaneously in the TS.

Scheme 7.4. *Endo* and *exo* concerted cyclizations.

a. *exo* pathway



b. *endo* pathway



However, there are important and noticeable difference between the *endo*- and *exo*-pathways. The geometrical demands of 5-*exo*-tet cyclizations require a more closed and tight transition state, and the C13 hydroxyl group serves as a relay to protonate the epoxide, while the phosphoric acid activates the C7 alcohol. On the other hand, the 6-*endo*-tet mechanism involves a more open transition state, and the C13 hydroxyl group serves as a relay to activate the C7 alcohol, while the phosphoric acid protonates the epoxide directly.

A quadrant-based analysis has been developed and successfully applied by Himo and Terada to explain the selectivity of BINOL-based CPAs in a number of unrelated reactions.^[30,31] In addition, we have previously used it to explain the origin of enantioselectivity of CPA-catalyzed spiroketalizations (See Chapter 3). This model serves to juxtapose the steric profile of (*R*) or (*S*) BINOL-derived CPAs to reaction models. Figure 7.4b shows that the 6-*endo*-tet pathway leading to **7-8** does not have severe contacts with either (*R*) or (*S*) CPAs, and most of the interactions are with torsionally flexible parts of the substrate, colored blue in Figure 7.4a. This is consistent with the more open and flexible TS compared to the 5-*exo*-tet pathway and suggests that the choice of

chirality of the CPA does not have a drastic impact in the barriers of the 6-*endo*-tet cyclization. On the other hand, the tighter TS of the 5-*exo*-tet mechanism places an inflexible and bulky group (colored in red in Figure 7.4a) in the bottom right quadrant pointing towards the phosphoric acid. This implies that (*R*)-BINOL-derived CPAs would disfavor the *exo*-pathway due to steric clashes in this quadrant. On the other hand, CPAs with (*S*) chirality would not suffer from these interactions and would therefore have lower barriers for the formation of *exo*-product **7-7**. These models are in agreement with the observed tendencies of (*R*) and (*S*) BINOL-derived CPAs in the intramolecular ERO of **7-1** (Tables 7.2 and 7.3).

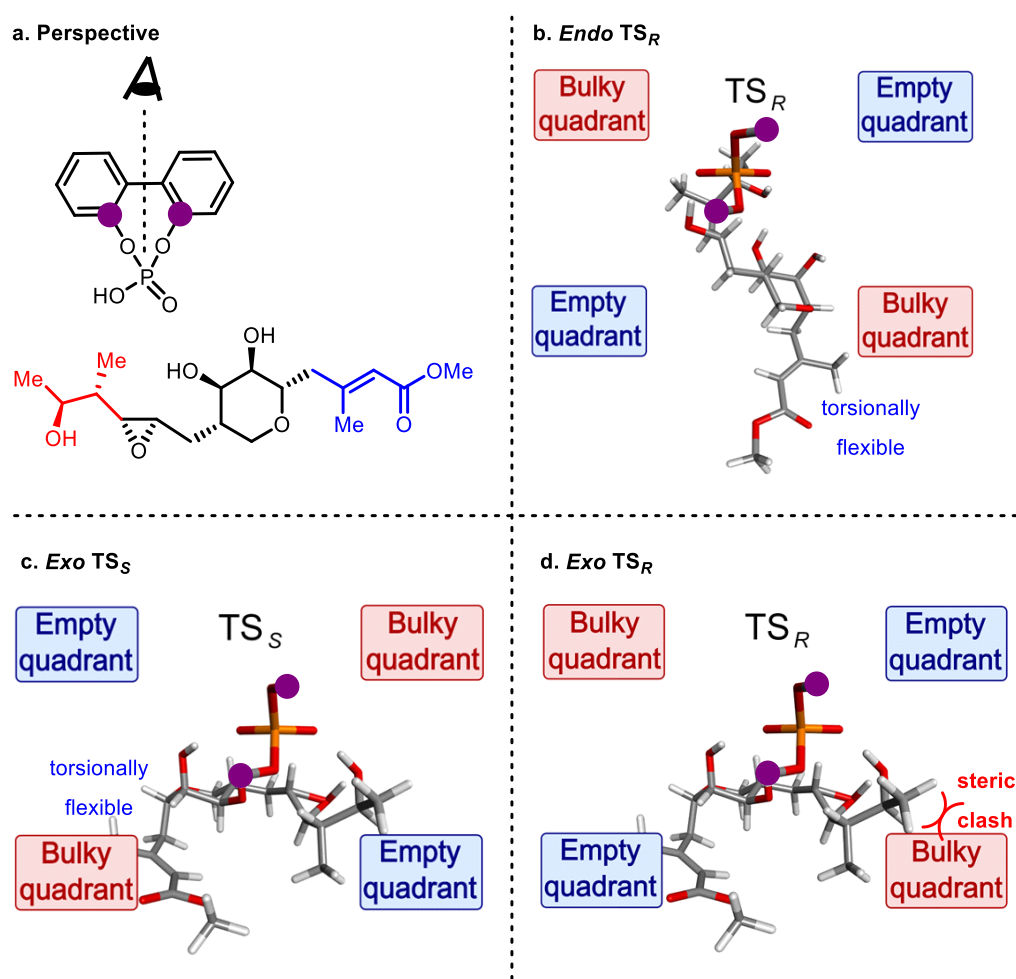


Figure 7.4. Quadrant-based perspective for key TSs. **a.** Perspective taken. **b.** 6-*endo*-tet pathway in a (*R*) CPA quadrant framework. **c.** 5-*exo*-tet pathway in a (*S*) CPA quadrant framework. **d.** 5-*exo*-tet pathway in a (*R*) CPA quadrant framework. Biphenyl backbone of the catalyst is omitted from the perspective for clarity.

In summary, we have developed a catalyst-controlled method for the regioselective intramolecular epoxide ring opening of mupirocin derivatives. After an extensive screening, we found that (*R*)-TCYP could catalyze the formation of *endo*-product in 18.4:1 r.r., while (*S*)-TIPSY yielded the *exo*-product in 3:1 r.r.. Importantly, we investigated the mechanism using state-of-the-art quantum chemical solutions developed by the Zimmerman group. We found that our method could rapidly describe a potential energy surface fully consistent with the experimental observations. On the basis of our results, we postulate that a concerted and highly synchronous mechanism is likely for this reaction. We obtained highly detailed reaction paths for the formation of *exo*- and *endo*-products, that although similar in activation barrier, showed key structural dissimilarities that helped us establish the origin of regiocontrol of these reactions, likely due to steric clashes of the epoxide alkyl substituents with the 3 and 3' substituents of BINOL-derived CPAs with (*R*) chirality. Catalyst-controlled regiodivergent methods for epoxide opening are scarce but synthetically useful and versatile. We hope that our mechanistic insights can assist in developing this methodology further to make it more broadly applicable and useful to the organic chemist.

7.3 References

- [1] A. P. S. Murphree, S. Murphree, *Arkivoc* **2012**, 2006, 6.
- [2] J. Marco-Contelles, M. T. Molina, S. Anjum, *Chem. Rev.* **2004**, 104, 2857–2900.
- [3] K. M. Morgan, J. A. Ellis, J. Lee, A. Fulton, S. L. Wilson, P. S. Dupart, R. Dastoori, *J. Org. Chem.* **2013**, 78, 4303–4311.
- [4] T. Katsuki, K. B. Sharpless, *J. Am. Chem. Soc.* **1980**, 102, 5974–5976.
- [5] S. Chang, J. M. Galvin, E. N. Jacobsen, *J. Am. Chem. Soc.* **1994**, 116, 6937–6938.
- [6] W. Zhang, J. L. Loebach, S. R. Wilson, E. N. Jacobsen, *J. Am. Chem. Soc.* **1990**, 112, 2801–2803.
- [7] Z. X. Wang, Y. Tu, M. Frohn, J. R. Zhang, Y. Shi, *J. Am. Chem. Soc.* **1997**, 119, 11224–11235.
- [8] Y. Tu, Z. X. Wang, Y. Shi, *J. Am. Chem. Soc.* **1996**, 118, 9806–9807.
- [9] B. Das, K. Damodar, in *Heterocycles Nat. Prod. Synth.*, Wiley-VCH Verlag GmbH & Co. KGaA, Weinheim, Germany, **2011**, pp. 63–95.
- [10] J. E. Baldwin, *J. Chem. Soc. Chem. Commun.* **1976**, 0, 734–736.
- [11] I. Vilotijevic, T. F. Jamison, *Angew. Chemie - Int. Ed.* **2009**, 48, 5250–5281.
- [12] H. Matsukura, M. Morimoto, H. Koshino, T. Nakata, *Tetrahedron Lett.* **1997**, 38, 5545–5548.
- [13] T. Suzuki, O. Sato, M. Hiramata, *Tetrahedron Lett.* **1990**, 31, 4747–4750.
- [14] K. C. Nicolaou, C. V. C. Prasad, P. K. Somers, C. K. Hwang, *J. Am. Chem. Soc.* **1989**, 111, 5330–5334.
- [15] K. C. Nicolaou, M. E. Duggan, C. K. Hwang, P. K. Somers, *J. Chem. Soc. Chem. Commun.* **1985**, 0, 1359–1362.
- [16] C. Mukai, Y. I. Sugimoto, Y. Ikeda, M. Hanaoka, *Tetrahedron* **1998**, 54, 823–850.
- [17] Y. Morimoto, Y. Nishikawa, C. Ueba, T. Tanaka, *Angew. Chemie - Int. Ed.* **2006**, 45, 810–812.
- [18] F. Bravo, F. E. McDonald, W. A. Neiwert, B. Do, K. I. Hardcastle, *Org. Lett.* **2003**, 5, 2123–2126.
- [19] T. P. Heffron, T. F. Jamison, *Org. Lett.* **2003**, 5, 2339–2342.
- [20] G. Adiwidjaja, H. Flörke, A. Kirschning, E. Schaumann, *Tetrahedron Lett.* **1995**, 36, 8771–8774.
- [21] P. M. Zimmerman, *J. Chem. Phys.* **2013**, 138, 184102.
- [22] P. M. Zimmerman, *J. Comput. Chem.* **2013**, 34, 1385–1392.

- [23] P. M. Zimmerman, *J. Comput. Chem.* **2015**, *36*, 601–611.
- [24] P. M. Zimmerman, *J. Chem. Theory Comput.* **2013**, *9*, 3043–3050.
- [25] Z. Wang, W. K. Law, J. Sun, *Org. Lett.* **2013**, *15*, 5964–5966.
- [26] M. R. Monaco, S. Prévost, B. List, *Angew. Chemie - Int. Ed.* **2014**, *53*, 8142–8145.
- [27] A. L. Dewyer, P. M. Zimmerman, *Org. Biomol. Chem.* **2017**, *15*, 501–504.
- [28] Y. Y. Khomutnyk, A. J. Argüelles, G. A. Winschel, Z. Sun, P. M. Zimmerman, P. Nagorny, *J. Am. Chem. Soc.* **2016**, *138*, 444–456.
- [29] J. H. Tay, A. J. Argüelles, M. D. Demars, P. M. Zimmerman, D. H. Sherman, P. Nagorny, *J. Am. Chem. Soc.* **2017**, *139*, 8570–8578.
- [30] I. D. Gridnev, M. Kouchi, K. Sorimachi, M. Terada, *Tetrahedron Lett.* **2007**, *48*, 497–500.
- [31] T. Marcelli, P. Hammar, F. Himo, *Chem. - A Eur. J.* **2008**, *14*, 8562–8571.

CHAPTER 8

Closing Remarks

Catalysis is at the heart of chemistry. The acceleration of all kinds of reactions due to catalytic processes has enabled life on Earth to exist and mankind to flourish. The growth and evolution of the general field of catalysis continues to develop at a commendable rate, thus leading to the general advancement of modern organic chemistry. Inspired by the breathtaking efficiency and control of catalytic process that Nature has engineered over thousands of years, organic chemists strive to design and provide artificial catalysts that enable new chemistry and impart selectivity on previously untamed chemistry. The work described herein seeks to add a humble but earnest contribution to this growing field. We have added to the annals of organocatalysts by the elaboration of a synthetic method that interconverts BINOL and H8-BINOL-derived chiral phosphoric acids for asymmetric Brønsted acid and hydrogen bond catalysis (Chapter 2), as well as to the vault of ligands for transition metal catalysis by the development of a novel class of privileged spiroketal-based ligands that enable asymmetric transformations across a variety of unrelated reactions (Chapter 4).

As synthetic methodology progressed, conquering feat after feat, so too have our ambitions and goals. The field is akin to a never-ending upward spiral, continuously seeking to improve yields, perfect the relative and absolute stereoselectivities, and entice even the most unactivated substrates. However, while the complexity of the current topic in organic chemistry has increased dramatically over the past decades, the majority of organic chemists are still armed with the same old qualitative models, such as Valence Bond Theory, to interpret their results and to base their

hypotheses. In other words, although the intricacy of the chemistry has increased, many organic chemists look at it through the same lens as our great predecessors. The need for an updated molecular point of view has been noted in recent years and is reflected by the additional value that computational models impart on an article, as well as the increase in the collaboration between theoretical and organic chemists.

Theoretical chemists have worked on providing a quantitative conceptual framework that can make better sense of the intricacies of current synthetic challenges. In particular, quantum-chemical theories such as wavefunction theory (WFT) and density functional theory (DFT) have emerged as powerful modeling methods to quantify physical and chemical properties of interest. With the advent of powerful computing capabilities, hardware, and software; the use of such methods can be applied to simulate real systems with ever-increasing accuracy and computational efficiency. In particular, the Zimmerman group has developed tools that can rapidly explore reaction landscapes to find reaction pathways and locate transition states. These techniques are fast and reliable, and therefore can be performed in a timeframe that is amenable for collaboration. In the Zimmerman group is at the frontier of reaction space exploration, and we are not only satisfied in explanatory models, but more so in predictive models useful to the experimentalists.

This dissertation describes the application of state-of-the-art quantum chemical techniques in the assessment of different types of powerful and enabling phosphoric acid-catalyzed reactions developed by the Nagorny group. The resulting computational models not only provided a rationale for truly perplexing experimental outcomes but was also used to provide feedback on future experiments in real time and even justify the commencement of a new project (Chapter 6). Thus, the phosphoric acid-catalyzed spiroketalization of enol ether derivatives (Chapter 3), intermolecular glycosylation and acetalization of polyols (Chapter 5), and intramolecular epoxide

ring opening (Chapter 7) were examined using our modern methods, and detail rich reaction mechanism networks were described. It is hoped that these accounts serve to inform the reader of the benefits of enhancing experimental efforts with a sound computational model. The effect is synergistic in both ways, since it was much more facile to construct models with a solid synthetic background. With the advent of powerful and practical reaction path discovery tools and the ever-increasing complexity of synthetic methodology, a collaborative environment with a holistic approach to reaction investigation is therefore highly recommended.

APPENDIX A

Experimental Information for Chapter 2

(Adapted from:

Supporting information for Tay, J. H.; Argüelles, A. J.; Nagorny, P. *Org. Lett.* **2015**, *17*, 3774.)

General information

All reagents and solvents were purchased from Sigma-Aldrich, Fisher Scientific, Corvius Chemicals and were used as received without further purification unless specified. Platinum (IV) oxide was purchased from Sigma-Aldrich with surface area $>75\text{m}^2/\text{g}$ or similar catalysts from Strem. Chiral acids used in these studies were purchased from Sigma Aldrich (**2-1c**, **2-1j**, **2-1k**, **2-7**) or synthesized according to known literature procedures. Heating was achieved by use of a silicone bath with heating controlled by electronic contact thermometer. Deionized water was used in the preparation of all aqueous solutions and for all aqueous extractions. Solvents used for extraction and chromatography were ACS or HPLC grade. Purification of reactions mixtures was performed by flash chromatography using SiliCycle SiliaFlash P60 (230-400 mesh).

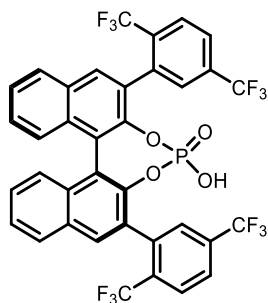
^1H NMR spectra were recorded on Varian vnmrs 700 (700 MHz), Varian vnmrs 500 (500 MHz), Varian INOVA 500 (500 MHz) or Varian MR400 (400 MHz) spectrometers and chemical shifts (δ) are reported in parts per million (ppm) with solvent resonance as the internal standard (CDCl_3 at δ 7.26). Data are reported as (br = broad, s = singlet, d = doublet, t = triplet, q = quartet, m = multiplet; coupling constant(s) in Hz; integration). Proton-decoupled ^{13}C NMR spectra were

recorded on Varian vnmrs 700 (700 MHz), Varian vnmrs 500 (500 MHz), Varian INOVA 500 (500 MHz) or Varian MR400 (400 MHz) spectrometers and chemical shifts (δ) are reported in ppm with solvent resonance as the internal standard (CDCl₃ at δ 77.16). High resolution mass spectra (HRMS) were recorded on Micromass AutoSpec Ultima or VG (Micromass) 70-250-S Magnetic sector mass spectrometers in the University of Michigan mass spectrometry laboratory. Infrared (IR) spectra were recorded as thin film on a Perkin Elmer Spectrum BX FT-IR spectrometer. Absorption peaks were reported in wavenumbers (cm⁻¹).

Optical rotations were measured in a solvent of choice on a JASCO P-2000 or Autopol III digital polarimeter at 589 nm (D-line) and reported as follows $[\alpha]_D^{25}$ (c g/100 mL, solvent).

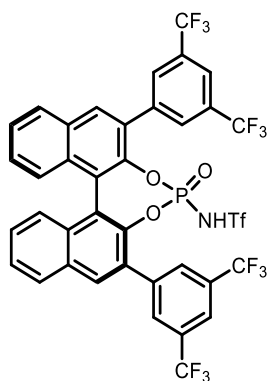
Experiments related to the reduction of BINOL-derived CPAs were performed by Dr. Tay Rosenthal. A complete account of these experiments, as well as characterization data can be found in the Supporting Information for reference [1]. Experiments related to the oxidation of H8-BINOL-based Brønsted acids were done by me and are described next.

Oxidation of H8-BINOL-based Brønsted acid and Characterization of Products, selected examples



(*S*)-3,3'-bis[2,5-di(trifluoromethyl)phenyl]-1,1'-binaphthyl-2,2'-diylphosphoric acid (**2-1a**)

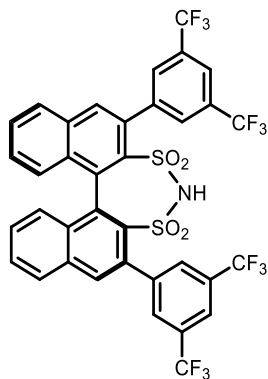
A solution **2-2a** (20 mg, 0.026 mmol) and DDQ (46.5 mg, 0.205 mmol) in 0.5 mL of chlorobenzene (0.05M) was heated in a closed vial at 145°C for 15h. The resulting mixture was diluted with DCM, filtered through a plug of glass wool, and washed with a 1.0 M NaOH_(aq). After extracting the aqueous solution twice with DCM, the organic extracts were combined and concentrated in vacuo. The resulting crude mixture was purified by flash chromatography on SiO₂ (EtOAc/hexanes, 7:3→1:0). The isolated product was washed with 6.0 M HCl_(aq). The aqueous solution was extracted twice with DCM, and the organic extracts were combined and concentrated in vacuo to afford 10a as white solid (14.6 mg, 74% yield). $[\alpha]_D^{25} + 57.8$ (c 0.45, CHCl₃); ¹H NMR (700 MHz, CDCl₃) δ 7.95 (d, J = 8.1 Hz, 2H), 7.89 (s, 2H), 7.82–7.74 (m, 4H), 7.57 (dd, J = 15.5, 8.0 Hz, 4H), 7.40 (t, J = 7.7 Hz, 2H), 7.37 (t, J = 9.6 Hz, 2H); ¹³C NMR (176 MHz, CDCl₃) δ 144.15, 144.10, 136.00, 133.69, 133.50, 132.62, 132.45, 132.05, 130.89, 130.12, 129.61, 128.70, 127.64, 127.07, 126.62, 126.25, 125.43, 124.20, 123.83, 122.64, 122.27, 121.55; ¹⁹F NMR (658 MHz, CDCl₃) δ -59.38, -63.59; ³¹P NMR (283 MHz, CDCl₃) δ 4.03; HRMS (ESI neg.) m/z calcd for C₃₆H₁₇F₁₂O₄P [M-H]⁻ 771.0600, found 771.0594; IR (thin film, cm⁻¹) 2979, 1402, 1313, 1174, 1124, 1088, 1024, 980, 841, 751.



(S)-3,3'-bis[3,5-di(trifluoromethyl)phenyl]-1,1'-binaphthyl-2,2'-diyl-N-triflyl-phosphoramidate (2-

6)

A solution of **2-3** (20 mg, 0.022 mmol) and DDQ (39.8 mg, 0.176 mmol) in 0.5 mL of chlorobenzene (0.4 M) was heated in a closed vial at 145°C for 15 h. The resulting crude mixture was purified by flash chromatography on SiO₂ (hexanes/EtOAc, 6:4) to afford **6** as yellow solid (16.1 mg, 81% yield). [α]D²⁵ +197.4 (c 0.53, CHCl₃); ¹H NMR (700 MHz, CDCl₃) δ 8.23 (s, 2H), 8.18 (s, 2H), 8.07 (d, J = 13.0 Hz, 2H), 8.01 (d, J = 8.2 Hz, 2H), 7.87 (s, 2H), 7.55 (dt, J = 7.9, 4.1 Hz, 2H), 7.45 – 7.31 (m, 4H); ¹³C NMR (176 MHz, CDCl₃) δ 144.53, 144.47, 143.98, 139.39, 139.35, 132.77, 132.65, 131.89, 131.68, 131.59, 131.54, 131.46, 131.35, 131.16, 130.46, 130.31, 128.88, 128.78, 127.68, 127.59, 127.18, 127.11, 126.72, 126.65, 124.40, 124.31, 123.37, 122.95, 122.85, 122.76, 121.45, 120.31. 19F NMR (377 MHz, CDCl₃) δ -63.01, -63.11, -80.95; 31P NMR (162 MHz, CDCl₃) δ 2.49; HRMS (ESI neg.) m/z calcd for C₃₇H₁₇F₁₅NO₅PS [M-H]⁻ 902.0253, found 902.0247; IR (thin film, cm⁻¹) 3442, 2362, 1621, 1474, 1377, 1276, 1173, 1130, 1082, 990, 885, 844.



(*S*)-3,3'-bis[3,5-bis(trifluoromethyl)phenyl]-1,1'-binaphthyl-2,2'-disulfonimide (**2-7**)

A solution of **5** (20 mg, 0.024 mmol) and DDQ (43.8 mg, 0.193 mmol) in 0.5 mL of 1,2-dichlorobenzene (0.05M) was heated in a closed vial at 185°C for 15h. The resulting crude mixture was purified by flash chromatography on SiO₂ (hexanes/EtOAc, 6:4) to afford compound **7** as an orange solid (8.3 mg, 42% yield). ¹H NMR (401 MHz, CDCl₃) δ 7.94 (d, J = 8.2 Hz, 2H), 7.80 (d,

J = 12.8 Hz, 8H), 7.63 (t, J = 7.5 Hz, 2H), 7.36 (t, J = 7.7 Hz, 2H), 7.05 (d, J = 8.6 Hz, 2H).

Characterizations of product match with previously reported data.

References

- [1] J.-H. Tay, A. J. Arguelles, P. Nagorny, *Org. Lett.* **2015**, *17*, 3774–3777.

APPENDIX B

Experimental Information for Chapter 3

(Adapted from:

Supporting information for: Khomutnyk, Y. Y.; **Argüelles, A. J.**; Winschel, G. A.; Sun, Z.;
Zimmerman, P. M.; Nagorny, P. *J. Am. Chem. Soc.* **2016**, *138*, 444.)

The experimental work was done by Dr. Yaroslav Khomutnyk, Grace Winschel, and Zhankui Sun; while the computational studies were done by me. A complete account of the experiments, including the synthesis of substrates as well as characterization data can be found in the supplementary information for reference [1].

Computational Studies

All quantum chemical calculations were performed using a development version of Q-Chem 4.3.^[2] Geometry optimization were evaluated using the B97-D density functional^[3] using double- ζ -quality basis sets with polarization functions, designated 6-31G**.^[4,5] Three-dimensional images of important stationary points were generated in Discovery Studio 4.1 Visualizer.^[6] For the 6,6-spiroketalization (diphenyl hydrogen phosphate and full catalyst), both single and double-ended growing string methods employing B97-D density functional and mixed 6-31G**/6-31G basis sets were used to probe the potential energy profile of the reactions.^[7-9] The larger basis set was used for the phosphoric acid group in the catalyst and all atoms in the substrate

excluding the phenyl rings. On the other hand, only the 6-31G** basis set was used for the 6,5-spiroketalization strings.

For the growing string runs, 7-15 nodes were used, including the end points. During the growth phase, new nodes were added when the perpendicular gradient magnitude on the frontier node was less than 0.10 Hartree/Å for double-ended strings, or when the RMS gradient was less than 0.005 Hartree/Å for single-ended strings. An initial maximum optimization step size of 0.1 was used. When the total perpendicular gradient magnitude over all nodes, F , reached $F < 0.3$, the climbing image search was initiated. When $F < 0.1$, or when the highest energy node had a RMS gradient below double the nodal convergence criterion and $F < 0.2$, the exact transition state search was initiated within the string. The string is considered completely converged when an RMS gradient < 0.0005 Hartree/Å was obtained for the transition state node.

In all cases, the Gibbs free energies and Mulliken charges were computed through solvent corrected (pentane) single point energies using the SMD model^[10] and employing the ω B97X-D exchange functional^[11] with a 6-31G** basis set for all reported starting geometries, intermediates, transition states and final geometries. Frequency computations were performed using the B97-D functional and 6-31G** basis set in order to account for enthalpic and entropic contributions from rotations, translations and vibrations at 298 K for the model diphenyl hydrogen phosphate system and 238 K for the full catalyst system. In the latter case, partial Hessian vibrational calculations involving the 41 most relevant atoms were performed. These were, in the catalyst, the atoms of the phosphoric group, 1, 1', 2, 2', 3, 3', and the carbon atom of the aryl substituents attached to 3 and 3'; and, in the substrate, all atoms except the phenyl rings, but including the carbon directly attached to the alcohol group.

A. Computational studies with the model diphenyl hydrogen phosphate system (6,6-spiroketalization)

A model system consisting of diphenyl hydrogen phosphate and enol ether **3-11a** was utilized to explore different pathways leading to the formation of spiroketal (*rac*)-**3-12a**. The single-ended growing string method employing **3-12a** as the fixed node was run with varying driving coordinates according to each pathway explored. Three mechanisms were modeled: concerted spiroketalization, anomeric phosphate mediated pathway with *syn* displacement of the intermediate, and oxocarbenium mediated spiroketalization. Regarding the mechanism proceeding through the intermediacy of an oxocarbenium species, no DFT-stable oxocarbenium species were found.

A1. 6,6-Spiroketalization: concerted mechanism

12 concerted pathways leading to thermodynamic and nonthermodynamic spiroketals were modeled. The most relevant pathway leads to formation of an equatorial C-O bond during spirocyclization, producing an initial nonthermodynamic spiroketal stabilized by one anomeric effect. This spiroketal can readily rearrange to the thermodynamic spiroketal by a ring flip.

A summary of calculated values including solvent corrected single point energy values, as well as enthalpic and entropic corrections associated with vibrational energy at 298 K are provided in next table.

Table B.1. Calculated values for starting geometries, intermediates, and transition states for the concerted pathway for the [6,6]-spiroketalization catalyzed by DPPA.

	G_{SMD} [kcal/mol] ^a	H_{vib} [kcal/mol] ^b	S_{vib} [kcal/mol] ^b	ΔG [kcal/mol] ^c
Enol ether 3-11a + DPPA complex	-1299501.3	401.2	233.5	0.0
Concerted TS (TS₁)	-1299485.4	397.3	220.4	16.0
Nonthermodynamic chair-chair spiroketal + catalyst complex	-1299513.2	401.9	222.2	-7.7
Thermodynamic spiroketal + catalyst complex	-1299517.4	402.2	220.3	-11.1

^a Solvent-corrected (dichloromethane) electronic energy (ωB97X-D/SMD/6-31G**). ^b Vibrational, rotational, and translational entropic and enthalpic contributions (B97-D/6-31G**) at 298.15 K. ^c Corrected free energy values at 298.15 K

Final corrected free energies, cartesian coordinates, and Mulliken charges for the starting geometry, transition states, and cyclized product are provided below.

• **Enol ether 3-11a + DPPA complex**

Geometry:

75

C 0.66724502	0.94857449	1.35273613	H -1.77349309	-0.23695325	1.95097383
C -0.03145891	2.05784349	0.99409247	H 1.88213748	-2.10660018	-1.60391210
C -1.33249505	2.45920077	1.65275030	H 2.20935411	-0.40899429	-1.93320426
C -1.51239076	1.66943658	2.96450306	H 1.44900145	-1.56287146	0.83098301
C -1.13549173	0.20317164	2.73263344	H 3.08482863	-1.25600219	0.24672037
O 0.24721942	0.05998094	2.30713342	H 2.74386129	0.59036935	1.57667596
O -0.11609735	0.58841972	-1.53833889	H 2.28817664	1.27198760	0.00213042
C 0.13098212	-0.83906546	-1.66669386	C -0.06270032	-1.13417313	-3.16646650
C 1.62056043	-1.08312926	-1.29310995	C -0.78590403	-2.24561016	-3.63408524
C 2.04317910	-0.90545253	0.18224631	H -1.25135969	-2.92827148	-2.92475599
C 1.99797092	0.53645549	0.76625876	C -0.93048835	-2.47401337	-5.01225610
H 0.39608067	2.71087120	0.23256076	H -1.49911258	-3.33954575	-5.35564921
H -0.96659731	1.44195264	-2.44305892	C -0.35748722	-1.59375153	-5.94080075
H -1.32634621	3.54198524	1.84922424	H -0.47339104	-1.77155889	-7.01100889
H -2.17611865	2.27534900	0.96734409	C 0.36209651	-0.47917731	-5.48264488
H -0.86002353	2.08354706	3.74927739	H 0.79567119	0.22508139	-6.19338105
H -2.55126724	1.72289260	3.32347107	C 0.51283077	-0.25634460	-4.10862352
H -1.21129152	-0.39909472	3.64716851	H 1.05397307	0.62211560	-3.76027955
			C -0.85213273	-1.62982020	-0.79540375
			C -0.52361397	-2.91114235	-0.31255932
			H 0.45959617	-3.33124123	-0.51899678
			C -1.45094928	-3.65683931	0.42891244

H -1.17488483 -4.64375389 0.80314662
 C -2.72763216 -3.13491926 0.68806497
 H -3.45043811 -3.71459097 1.26427006
 C -3.06751775 -1.86559912 0.19597764
 H -4.05815049 -1.44789873 0.38090748
 C -2.13789693 -1.11673042 -0.54174324
 H -2.41841358 -0.13221232 -0.91050794
 O -3.37877134 1.88248426 -1.23408385
 P -2.90262367 2.51091146 -2.49942137
 O -1.43262397 2.16551387 -2.99868223
 O -2.93471408 4.16017881 -2.49718785
 C -2.22189098 4.78621729 -1.46338814
 C -0.82247487 4.87215807 -1.52241186
 H -0.29765312 4.42022675 -2.36141282
 C -0.13893416 5.52573463 -0.48580559
 H 0.94935772 5.59498907 -0.52102424
 C -0.84551674 6.09075749 0.58855250
 H -0.30721730 6.59888177 1.38932969
 C -2.24674042 6.00021270 0.62627291
 H -2.80156517 6.43450274 1.45899062
 C -2.94229623 5.34138458 -0.39838161
 H -4.02648930 5.24144364 -0.38384419
 O -3.89121888 2.21540998 -3.75990460
 C -3.41253378 2.29257262 -5.08018813
 C -3.52428886 3.50220038 -5.77533205
 H -3.94066594 4.37200342 -5.26994475
 C -3.08339961 3.55883811 -7.10628602
 H -3.16210016 4.49627345 -7.65873133
 C -2.53957051 2.42065237 -7.72297806
 H -2.19712932 2.47157698 -8.75737589
 C -2.43446261 1.21857981 -7.00451859
 H -2.00354859 0.33160204 -7.46905872
 C -2.87128231 1.14625310 -5.67463730
 H -2.78229465 0.22718628 -5.09841361
 H -0.21248172 0.83735687 -0.58525494

Mulliken charges:

1 C 0.337929
 2 C -0.256307
 3 C -0.244998
 4 C -0.269570
 5 C 0.009222
 6 O -0.527186
 7 O -0.641711
 8 C 0.186913
 9 C -0.211574
 10 C -0.240292
 11 C -0.279393
 12 H 0.130379
 13 H 0.433074
 14 H 0.126690
 15 H 0.162308
 16 H 0.133424
 17 H 0.133954
 18 H 0.138481
 19 H 0.134490
 20 H 0.128783
 21 H 0.127319
 22 H 0.141546
 23 H 0.127009
 24 H 0.151652
 25 H 0.135351
 26 C 0.069700
 27 C -0.147476
 28 H 0.138141
 29 C -0.147752
 30 H 0.141281
 31 C -0.138176
 32 H 0.137349
 33 C -0.136792

34 H 0.141593
 35 C -0.142051
 36 H 0.142331
 37 C 0.033724
 38 C -0.148986
 39 H 0.132915
 40 C -0.147178
 41 H 0.140060
 42 C -0.134439
 43 H 0.139593
 44 C -0.152627
 45 H 0.147709
 46 C -0.142582
 47 H 0.149284
 48 O -0.579187
 49 P 1.249266
 50 O -0.643731
 51 O -0.614453
 52 C 0.292969
 53 C -0.136545
 54 H 0.163740
 55 C -0.146805
 56 H 0.145309
 57 C -0.133966
 58 H 0.141877
 59 C -0.148092
 60 H 0.146582
 61 C -0.128924
 62 H 0.158918
 63 O -0.596509
 64 C 0.303628
 65 C -0.135358
 66 H 0.159207
 67 C -0.148286
 68 H 0.144313
 69 C -0.134991
 70 H 0.138250
 71 C -0.140565
 72 H 0.132112
 73 C -0.118947
 74 H 0.150465
 75 H 0.336609

• **Concerted TS (TS₁)**

Geometry:

75

C 0.066564 -0.660537 -0.842435
 C 0.074765 0.300456 -1.876649
 C 0.180542 1.774124 -1.480855
 C -0.652584 1.956780 -0.198954
 C -0.122152 1.027986 0.888565
 O -0.011714 -0.370806 0.440465
 C 0.212009 -2.132902 -1.127346
 C -0.307503 -3.118856 -0.054353
 C -1.818954 -3.423759 -0.097320
 C -2.793027 -2.257603 0.235522
 O -2.574557 -1.194642 -0.687972
 H -0.224931 2.391072 -2.294037
 H 1.225979 2.082700 -1.309091
 H -1.699816 1.701510 -0.414482
 H -0.612462 2.989885 0.177990
 H -0.786471 0.965691 1.757495
 H 0.891530 1.315501 1.207254
 H -2.025974 -4.271225 0.572940
 H -2.091644 -3.761127 -1.109450
 H -0.251783 -2.325930 -2.104845
 H 1.298111 -2.293680 -1.260244
 C -2.614980 -1.652572 1.636226

C -2.033752 -2.364069 2.705971
 H -1.645697 -3.368009 2.541132
 C -1.942508 -1.789906 3.989138
 H -1.483003 -2.354511 4.801735
 C -2.441155 -0.495666 4.223391
 H -2.374149 -0.051946 5.217601
 C -3.037421 0.217937 3.163570
 H -3.442332 1.216527 3.336667
 C -3.123513 -0.356498 1.883840
 H -3.586285 0.188044 1.063119
 C -4.243074 -2.795168 0.129534
 C -4.688452 -3.801813 1.016061
 H -4.015261 -4.171837 1.790625
 C -5.994158 -4.312060 0.927572
 H -6.321893 -5.086956 1.622461
 C -6.878995 -3.819613 -0.052225
 H -7.893557 -4.213896 -0.123602
 C -6.443470 -2.816101 -0.936535
 H -7.117415 -2.429918 -1.702429
 C -5.134738 -2.304621 -0.846538
 H -4.805199 -1.538032 -1.543144
 H 0.217434 -4.072563 -0.219457
 H -0.013806 -2.764297 0.942530
 H 0.600518 -0.032256 -2.777957
 H -1.136723 0.300753 -2.371570
 P -2.754844 -0.565728 -3.894554
 O -2.225116 0.618134 -3.042968
 O -2.006027 -0.494999 -5.383193
 C -0.599243 -0.501956 -5.310608
 C 0.091861 0.709892 -5.485512
 H -0.477381 1.621000 -5.658163
 C 1.497093 0.713466 -5.413603
 H 2.041519 1.648637 -5.548939
 C 2.199879 -0.482744 -5.161183
 H 3.288700 -0.475176 -5.105601
 C 1.491668 -1.688978 -4.985135
 H 2.031032 -2.617102 -4.792518
 C 0.086005 -1.705209 -5.057841
 H -0.488402 -2.616413 -4.906902
 O -4.295579 -0.248214 -4.350152
 C -4.620904 1.047842 -4.821821
 C -4.956715 2.052304 -3.899504
 H -4.904261 1.835424 -2.834920
 C -5.332949 3.319232 -4.381539
 H -5.593888 4.107779 -3.674956
 C -5.370454 3.570484 -5.767958
 H -5.663550 4.553755 -6.136975
 C -5.027777 2.549492 -6.676442
 H -5.053399 2.740281 -7.749776
 C -4.648741 1.278184 -6.206257
 H -4.369702 0.475576 -6.885297
 O -2.675178 -1.948291 -3.293167
 H -2.614371 -1.575132 -1.602775

Mulliken charges:

1 C 0.525697
 2 C -0.422506
 3 C -0.230221
 4 C -0.283781
 5 C 0.014280
 6 O -0.468424
 7 C -0.310839
 8 C -0.227594
 9 C -0.236078
 10 C 0.182455
 11 O -0.628836
 12 H 0.149260
 13 H 0.129562
 14 H 0.168684
 15 H 0.143330

16 H 0.161757
 17 H 0.153052
 18 H 0.118373
 19 H 0.142752
 20 H 0.170992
 21 H 0.166263
 22 C 0.102931
 23 C -0.159559
 24 H 0.123844
 25 C -0.150090
 26 H 0.135903
 27 C -0.141399
 28 H 0.135200
 29 C -0.149402
 30 H 0.136120
 31 C -0.150283
 32 H 0.146761
 33 C 0.078590
 34 C -0.145369
 35 H 0.119440
 36 C -0.147476
 37 H 0.132375
 38 C -0.140101
 39 H 0.132421
 40 C -0.145961
 41 H 0.138064
 42 C -0.150555
 43 H 0.135094
 44 H 0.129352
 45 H 0.135014
 46 H 0.160314
 47 H 0.365373
 48 P 1.286607
 49 O -0.671955
 50 O -0.621414
 51 C 0.281514
 52 C -0.135408
 53 H 0.158962
 54 C -0.149667
 55 H 0.146197
 56 C -0.139537
 57 H 0.140984
 58 C -0.152544
 59 H 0.145622
 60 C -0.139431
 61 H 0.167524
 62 O -0.610120
 63 C 0.297222
 64 C -0.124286
 65 H 0.155227
 66 C -0.151409
 67 H 0.142646
 68 C -0.134987
 69 H 0.138041
 70 C -0.150215
 71 H 0.143506
 72 C -0.133509
 73 H 0.158097
 74 O -0.659035
 75 H 0.366588

- **Nonthermodynamic chair-chair spiroketal + DPPA complex**

Geometry:

75

C -1.16488148 0.41219989 -0.21711642
 C -1.44830284 1.69875907 -1.01222993
 C -0.13569506 2.42138943 -1.36995306

C 0.64272200 2.69763602 -0.07129436
 C 0.88122264 1.37538277 0.66637197
 O -0.34643278 0.67646410 0.92277888
 C -0.54787212 -0.70617474 -1.08082458
 C -0.50557248 -2.03346911 -0.31028617
 C -1.93595190 -2.39334569 0.11662326
 C -2.55578458 -1.29966957 1.02159482
 O -2.44429188 -0.01134622 0.29877784
 H -0.36335100 3.35829266 -1.89927041
 H 0.47577651 1.80271086 -2.04798428
 H 0.04856144 3.36184437 0.57482732
 H 1.61065524 3.18146966 -0.27743624
 H 1.32178725 1.53382908 1.65984200
 H 1.57205573 0.73854184 0.07956883
 H -1.98963263 -3.36137250 0.63135422
 H -2.57393428 -2.47269735 -0.77672764
 H -1.16163760 -0.81645794 -1.98919185
 H 0.45577748 -0.39488820 -1.40148690
 C -1.91654227 -1.18269118 2.41295753
 C -1.25281829 -2.26173695 3.02177122
 H -1.11198876 -3.19886500 2.48528041
 C -0.75909178 -2.15326270 4.33284703
 H -0.24144940 -3.00101801 4.78488295
 C -0.93251785 -0.96405249 5.05261538
 H -0.55008607 -0.87772172 6.07112034
 C -1.60054204 0.11586350 4.45227855
 H -1.75026110 1.04730225 4.99731491
 C -2.09192345 0.00603718 3.14832318
 H -2.57291794 0.86347033 2.68732903
 C -4.06527298 -1.57500872 1.13599159
 C -4.60146700 -2.21788186 2.26622493
 H -3.95296044 -2.45651195 3.10698085
 C -5.96624732 -2.53583553 2.32643054
 H -6.36279898 -3.03389651 3.21266412
 C -6.82048524 -2.19726916 1.26681317
 H -7.88541573 -2.42694566 1.32248826
 C -6.29138837 -1.56200499 0.13242441
 H -6.94296201 -1.29037939 -0.69909741
 C -4.92288070 -1.27206449 0.06107797
 H -4.51936255 -0.77582436 -0.81968600
 H -0.08448986 -2.82990538 -0.94217379
 H 0.13588954 -1.92385964 0.57616358
 H -2.04328671 1.45040095 -1.90257837
 H -2.03129305 2.36462804 -0.36574071
 O -4.45105734 1.69051994 0.44634055
 P -4.24707759 2.99051216 1.34401727
 O -2.86615634 3.24680361 1.84803464
 O -5.40804514 2.92899905 2.50126288
 C -5.15994570 2.12209475 3.62552586
 C -4.53843823 2.69173572 4.74416663
 H -4.20781805 3.72795067 4.69857181
 C -4.35845925 1.90540007 5.89088008
 H -3.87693255 2.33677784 6.76968749
 C -4.78941122 0.56889229 5.90682397
 H -4.64190995 -0.04189089 6.79807683
 C -5.39814188 0.01626361 4.77055459
 H -5.72172881 -1.02387405 4.77097751
 C -5.58549452 0.78809965 3.61440553
 H -6.04071871 0.36868879 2.71893033
 O -4.91645636 4.11311629 0.36612113
 C -5.05616240 5.43582751 0.81855670
 C -3.93920242 6.18961083 1.20783212
 H -2.95596027 5.72360905 1.21316329
 C -4.13227008 7.52171541 1.60310450
 H -3.27206030 8.11679773 1.91315383
 C -5.41625008 8.08948326 1.59862065
 H -5.55635370 9.12676269 1.90493691
 C -6.51959999 7.31792274 1.19916578
 H -7.52028292 7.75214759 1.19591425
 C -6.34534837 5.98218369 0.80919790

H -7.18399138 5.35739119 0.50468328
 H -3.64995376 1.08170382 0.45568273

Mulliken charges:

1 C 0.550097
 2 C -0.263062
 3 C -0.250188
 4 C -0.250703
 5 C 0.020598
 6 O -0.518897
 7 C -0.232674
 8 C -0.244029
 9 C -0.219376
 10 C 0.191865
 11 O -0.635786
 12 H 0.133662
 13 H 0.116543
 14 H 0.148175
 15 H 0.122544
 16 H 0.143288
 17 H 0.103067
 18 H 0.132562
 19 H 0.128211
 20 H 0.124530
 21 H 0.125362
 22 C 0.076479
 23 C -0.164271
 24 H 0.123609
 25 C -0.149810
 26 H 0.132296
 27 C -0.141838
 28 H 0.131602
 29 C -0.140214
 30 H 0.130302
 31 C -0.084480
 32 H 0.116972
 33 C 0.045723
 34 C -0.132019
 35 H 0.136063
 36 C -0.152563
 37 H 0.137513
 38 C -0.136791
 39 H 0.139852
 40 C -0.144110
 41 H 0.141799
 42 C -0.131238
 43 H 0.137460
 44 H 0.127183
 45 H 0.137870
 46 H 0.129173
 47 H 0.141195
 48 O -0.623129
 49 P 1.300474
 50 O -0.619346
 51 O -0.601378
 52 C 0.273580
 53 C -0.124122
 54 H 0.157834
 55 C -0.153232
 56 H 0.143290
 57 C -0.126756
 58 H 0.138595
 59 C -0.132004
 60 H 0.130639
 61 C -0.114264
 62 H 0.149796
 63 O -0.592289
 64 C 0.299928
 65 C -0.142008
 66 H 0.168134

67 C -0.149452
 68 H 0.145399
 69 C -0.133679
 70 H 0.139846
 71 C -0.146625
 72 H 0.145020
 73 C -0.141472
 74 H 0.157054
 75 H 0.416621

• **Thermodynamic spiroketal + DPPA complex**

Geometry:

75

C 0.93869814 0.48257365 0.17714954
 C 0.96190416 2.02211738 0.03762645
 C -0.24017070 2.74751218 0.67550577
 C -0.52447730 2.17701181 2.07460486
 C -0.69713295 0.66196694 1.95491008
 O 0.50062595 0.03695078 1.43990267
 O 0.05830695 -0.00742487 -0.90565356
 C -0.04591328 -1.46546246 -1.15953843
 C 1.38210878 -2.06991326 -1.21929901
 C 2.29091420 -1.64505109 -0.05913333
 C 2.34021783 -0.11375353 -0.01108925
 H 1.87952655 2.35030019 0.55070322
 H 1.05523230 2.28495759 -1.02448795
 H -0.02338732 3.82510118 0.71874266
 H -1.13686202 2.62464508 0.05663021
 H 0.31098069 2.39374944 2.76057430
 H -1.43949037 2.61624936 2.50292292
 H -0.86380775 0.18125569 2.92747818
 H -1.54604013 0.42599239 1.29502089
 H 1.28543148 -3.16196034 -1.29821260
 H 1.83372676 -1.72277000 -2.16007613
 H 1.91750189 -2.02376270 0.90091572
 H 3.30026583 -2.05354174 -0.21740343
 H 2.96661722 0.24219302 0.81787079
 H 2.74899604 0.28758653 -0.95160215
 C -0.63083795 -1.60391774 -2.57575266
 C -1.42686827 -2.71521661 -2.91258524
 H -1.71411126 -3.42405166 -2.13715945
 C -1.85236880 -2.91066512 -4.23503867
 H -2.47473565 -3.77313657 -4.47850837
 C -1.49222569 -1.99484272 -5.23446321
 H -1.84201925 -2.13527207 -6.25802575
 C -0.69558957 -0.88730896 -4.90525345
 H -0.42871624 -0.15493668 -5.66677691
 C -0.25738463 -0.69867240 -3.58787487
 H 0.35143138 0.16830406 -3.33681769
 C -0.98107888 -2.08506074 -0.11215892
 C -0.61978094 -3.16356559 0.71224652
 H 0.37921565 -3.59155382 0.65449461
 C -1.53803426 -3.70716688 1.62577970
 H -1.23554774 -4.54270638 2.25888258
 C -2.83516801 -3.18558716 1.72203636
 H -3.54674884 -3.61081249 2.43106556
 C -3.21235427 -2.11859203 0.89038095
 H -4.22223755 -1.70939337 0.94478593
 C -2.29567586 -1.58037508 -0.01972755
 H -2.60177315 -0.76255648 -0.66950979
 C -4.70820456 2.06291946 -4.81135442
 C -5.98932154 1.49380081 -4.88141030
 H -6.80941495 2.06876078 -5.31418051
 C -6.21651640 0.19468624 -4.39914249
 H -7.21384198 -0.24306846 -4.45739590
 C -5.15521086 -0.54072675 -3.84732950
 H -5.32000114 -1.55292988 -3.47594423
 C -3.86932246 0.01147992 -3.77331536
 H -3.03629892 -0.54511908 -3.35587738

H -4.50957707 3.07225957 -5.16658896
 C -3.66699603 1.31099573 -4.25480978
 O -2.37586955 1.86715126 -4.24825557
 P -1.68538934 2.38867194 -2.85992647
 O -2.71498647 3.55247754 -2.31958341
 C -3.10186171 4.62949992 -3.12287708
 C -4.44384898 5.02428160 -3.01989918
 C -4.89446133 6.11962440 -3.76915827
 H -5.93760056 6.43006380 -3.69203282
 C -4.01344694 6.80922356 -4.61861739
 H -4.36886225 7.65835616 -5.20334667
 C -2.67366790 6.40014708 -4.70772857
 H -1.98124630 6.93257159 -5.36110236
 H -5.11161478 4.46305437 -2.36792725
 C -2.20255249 5.31298113 -3.95565846
 H -1.16370053 4.99153295 -4.01020954
 O -1.97632313 1.30829646 -1.72913909
 H -1.13380952 0.82152836 -1.41954704
 O -0.27142550 2.78740276 -3.10438411

Mulliken charges:

1 C 0.519328
 2 C -0.266187
 3 C -0.253400
 4 C -0.245215
 5 C 0.016608
 6 O -0.520947
 7 O -0.638527
 8 C 0.198232
 9 C -0.226051
 10 C -0.248077
 11 C -0.232128
 12 H 0.129460
 13 H 0.163342
 14 H 0.130224
 15 H 0.132519
 16 H 0.122951
 17 H 0.128693
 18 H 0.136226
 19 H 0.116190
 20 H 0.134397
 21 H 0.135746
 22 H 0.139659
 23 H 0.129734
 24 H 0.137473
 25 H 0.131744
 26 C 0.027043
 27 C -0.141754
 28 H 0.136679
 29 C -0.149468
 30 H 0.139829
 31 C -0.132553
 32 H 0.141032
 33 C -0.129102
 34 H 0.149417
 35 C -0.160398
 36 H 0.153329
 37 C 0.104016
 38 C -0.150300
 39 H 0.129196
 40 C -0.149445
 41 H 0.138740
 42 C -0.136301
 43 H 0.138744
 44 C -0.146027
 45 H 0.142540
 46 C -0.157600
 47 H 0.142204
 48 C -0.131351
 49 C -0.152914

50 H 0.142552
 51 C -0.133074
 52 H 0.138042
 53 C -0.159238
 54 H 0.141257
 55 C -0.077237
 56 H 0.125926
 57 H 0.150765
 58 C 0.279256
 59 O -0.608581
 60 P 1.310346
 61 O -0.609400
 62 C 0.298275
 63 C -0.149016
 64 C -0.146849
 65 H 0.144189
 66 C -0.136662
 67 H 0.140087
 68 C -0.150218
 69 H 0.147252
 70 H 0.155985
 71 C -0.154981
 72 H 0.175260
 73 O -0.643894
 74 H 0.432266
 75 O -0.589860

• **Bare oxocarbenium (for comparison)**

Geometry:

50

C 4.27373293 -3.27781826 -0.64820620
 C 3.91775194 -4.43904887 0.22412227
 C 4.36604194 -5.80433527 -0.32650746
 C 5.80391962 -5.67323388 -0.85908876
 C 5.85279846 -4.63349739 -1.96580924
 O 5.14487705 -3.34998456 -1.59160700
 C -0.67586231 0.45513388 -1.63016436
 C -0.00200283 -0.92375290 -1.88960362
 C 1.42467697 -0.82849615 -1.24877824
 C 2.23064090 -2.13189300 -1.33535350
 C 3.57081397 -1.98876208 -0.51793486
 H 4.41482634 -4.22615391 1.19091384
 H 4.30707292 -6.55911029 0.46673231
 H 3.68871069 -6.11738155 -1.13509839
 H 6.49069636 -5.39111511 -0.04679707
 H 6.16301421 -6.62251095 -1.28109251
 H 6.86029408 -4.28372078 -2.21284530
 H 5.33035449 -4.94810393 -2.87818695
 H 1.97330978 -0.03012421 -1.76979911
 H 1.32900813 -0.51696490 -0.19676174
 H 1.63736015 -2.96227493 -0.92819450
 H 2.46356796 -2.36122699 -2.38345500
 H 4.16993232 -1.16509619 -0.92587400
 H 3.32456518 -1.80338775 0.53770709
 C 0.19288686 -1.21111402 -3.39371854
 C 0.35762574 -0.16780063 -4.32536329
 H 0.26728624 0.86982952 -4.00813530
 C 0.62738706 -0.43860766 -5.67606981
 H 0.73947871 0.38895540 -6.37750763
 C 0.74347357 -1.76155831 -6.12505408
 H 0.94532678 -1.97066169 -7.17594829
 C 0.58566815 -2.81333474 -5.20916899
 H 0.65865643 -3.84866940 -5.54582134
 C 0.31594672 -2.53809386 -3.86147299
 H 0.17091070 -3.36195078 -3.16286358
 C -0.89654723 -1.97423370 -1.19998668
 C -0.66604815 -2.41350287 0.11916849

H 0.19975135 -2.04922999 0.67375390
 C -1.54670796 -3.30554463 0.75214021
 H -1.34590531 -3.62938207 1.77449719
 C -2.68474504 -3.76952681 0.07819504
 H -3.36970416 -4.46202636 0.56795611
 C -2.93919422 -3.32460823 -1.22877434
 H -3.82767961 -3.66658933 -1.76050122
 C -2.05623153 -2.43595113 -1.85603056
 H -2.25830289 -2.09732875 -2.87184313
 H -0.04052636 1.28871400 -1.96309994
 H -0.85806299 0.57231756 -0.55343761
 H -1.63993423 0.51252370 -2.15265269
 H 2.83944010 -4.38142524 0.43505137

Mulliken charges:

1 C 0.482883
 2 C -0.327430
 3 C -0.261673
 4 C -0.292076
 5 C -0.024700
 6 O -0.400962
 7 C -0.354746
 8 C -0.099282
 9 C -0.207059
 10 C -0.252482
 11 C -0.314833
 12 H 0.229763
 13 H 0.184759
 14 H 0.170286
 15 H 0.172042
 16 H 0.194051
 17 H 0.214481
 18 H 0.209568
 19 H 0.140551
 20 H 0.131255
 21 H 0.144386
 22 H 0.164357
 23 H 0.204638
 24 H 0.193482
 25 C 0.084002
 26 C -0.162263
 27 H 0.133323
 28 C -0.142266
 29 H 0.149176
 30 C -0.137746
 31 H 0.147877
 32 C -0.147275
 33 H 0.141662
 34 C -0.156623
 35 H 0.126108
 36 C 0.084142
 37 C -0.167344
 38 H 0.108171
 39 C -0.146931
 40 H 0.140696
 41 C -0.137706
 42 H 0.148694
 43 C -0.141434
 44 H 0.151268
 45 C -0.148089
 46 H 0.143392
 47 H 0.129114
 48 H 0.136618
 49 H 0.146228
 50 H 0.215945

A2. 6,6-Spiroketalization: covalent phosphate mechanism

12 different orientations of the catalyst with respect to the substrate were modeled for the phosphate mediated mechanism leading to thermodynamic and nonthermodynamic spiroketals. 9 strings were modeled for the formation of a covalently linked anomeric phosphate intermediate were modeled. Attack of either oxygen of the phosphoric acid was considered. The most relevant one has an activation barrier of 20.6 kcal/mol and produces a relatively stable (1 kcal/mol) phosphate intermediate. 24 strings leading to thermodynamic and nonthermodynamic spiroketals by the syn displacement of the phosphate by the alcohol were studied. No significant bias was observed for the formation of a nonthermodynamic (21.1 kcal/mol barrier, axial C-O bond formed) over a thermodynamic (20.7 kcal/mol barrier) spiroketal. A summary of calculated values including solvent corrected single point energy values, as well as enthalpic and entropic corrections associated with vibrational energy at 298 K are provided in next table.

Table B.2. Calculated values for starting geometries, intermediates, and transition states phosphate-mediated pathway for the [6,6]-spiroketalization catalyzed by DPPA.

	G_{SMD} [kcal/mol] ^a	H_{vib} [kcal/mol] ^b	S_{vib} [kcal/mol] ^b	ΔG [kcal/mol] ^c
Enol ether 3-11a + DPPA complex	-1299501.3	401.2	233.5	0.0
Formation of the phosphate intermediate TS (TS₂)	-1299478.4	397.5	228.9	20.6
Phosphate intermediate + catalyst complex	-1299504.9	402.6	222.8	1.0
Syn phosphate displacement leading to thermodynamic product (TS₃)	-1299483.2	399.9	220.7	20.7
Syn phosphate displacement leading to nonthermodynamic product (TS₄)	-1299484.3	400.1	216.5	21.1
Thermodynamic spiroketal + DPPA complex	-1299517.4	402.2	220.3	-11.1
Nonthermodynamic spiroketal + DPPA complex	-1299512.9	402.1	221.2	-7.0

^a Solvent-corrected (dichloromethane) electronic energy (ωB97X-D/SMD/6-31G**). ^b Vibrational, rotational, and translational entropic and enthalpic contributions (B97-D/6-31G**) at 298.15 K. ^c Corrected free energy values at 298.15 K

Final corrected free energies, cartesian coordinates, and Mulliken charges for the starting geometry, transition states, intermediate, and cyclized product are provided below.

• Enol ether 3-11a + DPPA complex

Geometry:

75

C 0.66724502 0.94857449 1.35273613
 C -0.03145891 2.05784349 0.99409247
 C -1.33249505 2.45920077 1.65275030
 C -1.51239076 1.66943658 2.96450306
 C -1.13549173 0.20317164 2.73263344
 O 0.24721942 0.05998094 2.30713342
 O -0.11609735 0.58841972 -1.53833889
 C 0.13098212 -0.83906546 -1.66669386
 C 1.62056043 -1.08312926 -1.29310995
 C 2.04317910 -0.90545253 0.18224631
 C 1.99797092 0.53645549 0.76625876
 H 0.39608067 2.71087120 0.23256076
 H -0.96659731 1.44195264 -2.44305892
 H -1.32634621 3.54198524 1.84922424
 H -2.17611865 2.27534900 0.96734409
 H -0.86002353 2.08354706 3.74927739
 H -2.55126724 1.72289260 3.32347107
 H -1.21129152 -0.39909472 3.64716851
 H -1.77349309 -0.23695325 1.95097383
 H 1.88213748 -2.10660018 -1.60391210
 H 2.20935411 -0.40899429 -1.93320426
 H 1.44900145 -1.56287146 0.83098301
 H 3.08482863 -1.25600219 0.24672037
 H 2.74386129 0.59036935 1.57667596
 H 2.28817664 1.27198760 0.00213042
 C -0.06270032 -1.13417313 -3.16646650
 C -0.78590403 -2.24561016 -3.63408524
 H -1.25135969 -2.92827148 -2.92475599
 C -0.93048835 -2.47401337 -5.01225610
 H -1.49911258 -3.33954575 -5.35564921
 C -0.35748722 -1.59375153 -5.94080075
 H -0.47339104 -1.77155889 -7.01100889
 C 0.36209651 -0.47917731 -5.48264488
 H 0.79567119 0.22508139 -6.19338105
 C 0.51283077 -0.25634460 -4.10862352
 H 1.05397307 0.62211560 -3.76027955
 C -0.85213273 -1.62982020 -0.79540375
 C -0.52361397 -2.91114235 -0.31255932
 H 0.45959617 -3.33124123 -0.51899678
 C -1.45094928 -3.65683931 0.42891244
 H -1.17488483 -4.64375389 0.80314662
 C -2.72763216 -3.13491926 0.68806497
 H -3.45043811 -3.71459097 1.26427006
 C -3.06751775 -1.86559912 0.19597764
 H -4.05815049 -1.44789873 0.38090748
 C -2.13789693 -1.11673042 -0.54174324
 H -2.41841358 -0.13221232 -0.91050794
 O -3.37877134 1.88248426 -1.23408385
 P -2.90262367 2.51091146 -2.49942137
 O -1.43262397 2.16551387 -2.99868223
 O -2.93471408 4.16017881 -2.49718785
 C -2.22189098 4.78621729 -1.46338814
 C -0.82247487 4.87215807 -1.52241186
 H -0.29765312 4.42022675 -2.36141282
 C -0.13893416 5.52573463 -0.48580559
 H 0.94935772 5.59498907 -0.52102424
 C -0.84551674 6.09075749 0.58855250
 H -0.30721730 6.59888177 1.38932969
 C -2.24674042 6.00021270 0.62627291
 H -2.80156517 6.43450274 1.45899062
 C -2.94229623 5.34138458 -0.39838161
 H -4.02648930 5.24144364 -0.38384419
 O -3.89121888 2.21540998 -3.75990460
 C -3.41253378 2.29257262 -5.08018813
 C -3.52428886 3.50220038 -5.77533205
 H -3.94066594 4.37200342 -5.26994475

C -3.08339961 3.55883811 -7.10628602
 H -3.16210016 4.49627345 -7.65873133
 C -2.53957051 2.42065237 -7.72297806
 H -2.19712932 2.47157698 -8.75737589
 C -2.43446261 1.21857981 -7.00451859
 H -2.00354859 0.33160204 -7.46905872
 C -2.87128231 1.14625310 -5.67463730
 H -2.78229465 0.22718628 -5.09841361
 H -0.21248172 0.83735687 -0.58525494

Mulliken charges:

1 C 0.337929
 2 C -0.256307
 3 C -0.244998
 4 C -0.269570
 5 C 0.009222
 6 O -0.527186
 7 O -0.641711
 8 C 0.186913
 9 C -0.211574
 10 C -0.240292
 11 C -0.279393
 12 H 0.130379
 13 H 0.433074
 14 H 0.126690
 15 H 0.162308
 16 H 0.133424
 17 H 0.133954
 18 H 0.138481
 19 H 0.134490
 20 H 0.128783
 21 H 0.127319
 22 H 0.141546
 23 H 0.127009
 24 H 0.151652
 25 H 0.135351
 26 C 0.069700
 27 C -0.147476
 28 H 0.138141
 29 C -0.147752
 30 H 0.141281
 31 C -0.138176
 32 H 0.137349
 33 C -0.136792
 34 H 0.141593
 35 C -0.142051
 36 H 0.142331
 37 C 0.033724
 38 C -0.148986
 39 H 0.132915
 40 C -0.147178
 41 H 0.140060
 42 C -0.134439
 43 H 0.139593
 44 C -0.152627
 45 H 0.147709
 46 C -0.142582
 47 H 0.149284
 48 O -0.579187
 49 P 1.249266
 50 O -0.643731
 51 O -0.614453
 52 C 0.292969
 53 C -0.136545
 54 H 0.163740
 55 C -0.146805
 56 H 0.145309
 57 C -0.133966
 58 H 0.141877
 59 C -0.148092

60 H 0.146582
 61 C -0.128924
 62 H 0.158918
 63 O -0.596509
 64 C 0.303628
 65 C -0.135358
 66 H 0.159207
 67 C -0.148286
 68 H 0.144313
 69 C -0.134991
 70 H 0.138250
 71 C -0.140565
 72 H 0.132112
 73 C -0.118947
 74 H 0.150465
 75 H 0.336609

• **Formation of the phosphate intermediate TS (TS₂)**

Geometry:

75

C 1.652259 1.663080 -0.419432
 C 2.011881 2.971563 -0.849372
 C 1.016144 4.116981 -0.552188
 C 0.018056 3.722267 0.547065
 C -0.572325 2.366806 0.160858
 O 0.489036 1.355982 0.099776
 O -0.854549 -0.576207 -1.354426
 C -0.146939 -1.801149 -1.505990
 C 1.382584 -1.516716 -1.588762
 C 2.022590 -0.923206 -0.300353
 C 2.618571 0.501407 -0.439246
 H 3.068813 3.154717 -0.607895
 H 2.069168 3.050590 -2.155349
 H 1.561078 5.040366 -0.312886
 H 0.441855 4.311708 -1.470799
 H 0.507017 3.641128 1.530781
 H -0.794933 4.458741 0.628627
 H -1.282778 1.956645 0.886380
 H -1.022100 2.387468 -0.840761
 H 1.903838 -2.445304 -1.856758
 H 1.524774 -0.840298 -2.435755
 H 1.300504 -0.943725 0.525794
 H 2.859641 -1.567569 0.005633
 H 3.312378 0.679349 0.402310
 H 3.218344 0.588059 -1.356429
 C -0.608244 -2.535960 -2.795725
 C 0.007455 -3.735905 -3.220075
 H 0.836599 -4.148974 -2.645943
 C -0.456924 -4.421827 -4.356126
 H 0.029988 -5.347766 -4.665812
 C -1.552862 -3.921439 -5.087827
 H -1.917868 -4.455859 -5.965959
 C -2.171725 -2.726864 -4.673769
 H -3.019809 -2.327878 -5.232253
 C -1.703800 -2.042588 -3.536184
 H -2.184418 -1.123975 -3.207909
 C -0.527096 -2.690808 -0.308328
 C 0.355853 -3.667876 0.200300
 H 1.356333 -3.769255 -0.218451
 C -0.035572 -4.515382 1.254117
 H 0.663363 -5.261760 1.635275
 C -1.320773 -4.399019 1.815725
 H -1.625748 -5.055384 2.631948
 C -2.208411 -3.428087 1.315261
 H -3.207679 -3.330219 1.742700
 C -1.816352 -2.583782 0.261406
 H -2.500098 -1.832148 -0.127556
 C 1.151837 0.805449 -6.344547

C 2.060491 0.833597 -7.414584
 C 2.137905 -0.278628 -8.271534
 H 2.844435 -0.268820 -9.101862
 C 1.318673 -1.403171 -8.049462
 H 1.388170 -2.268282 -8.709980
 C 0.411481 -1.409784 -6.971608
 H -0.218376 -2.276548 -6.780834
 H 2.697640 1.705619 -7.550086
 C 0.315696 -0.298727 -6.113304
 H -0.369142 -0.297113 -5.269328
 O 1.100590 1.966058 -5.525609
 P 1.301934 1.813266 -3.904658
 O 2.485338 0.654580 -3.769592
 C 3.716031 0.664172 -4.451667
 C 4.245524 -0.607318 -4.739059
 C 5.478018 -0.707141 -5.405097
 H 5.886107 -1.691758 -5.635049
 C 6.174872 0.458072 -5.786201
 H 7.127971 0.381554 -6.310215
 C 5.633101 1.722182 -5.484756
 H 6.168710 2.627786 -5.772674
 H 3.674407 -1.490526 -4.458251
 C 4.403493 1.839699 -4.809043
 H 3.981772 2.812822 -4.572098
 O 0.118627 1.275451 -3.143650
 H -0.503744 0.045386 -2.031610
 O 1.874017 3.181840 -3.458526

Mulliken charges:

1 C 0.480535
 2 C -0.447832
 3 C -0.231725
 4 C -0.276966
 5 C -0.006796
 6 O -0.424444
 7 O -0.623154
 8 C 0.189412
 9 C -0.253267
 10 C -0.218450
 11 C -0.323192
 12 H 0.177186
 13 H 0.366324
 14 H 0.144529
 15 H 0.155787
 16 H 0.142612
 17 H 0.151772
 18 H 0.171308
 19 H 0.183242
 20 H 0.111303
 21 H 0.155889
 22 H 0.147357
 23 H 0.125700
 24 H 0.173884
 25 H 0.174733
 26 C 0.080699
 27 C -0.147707
 28 H 0.120506
 29 C -0.142829
 30 H 0.134694
 31 C -0.145606
 32 H 0.134456
 33 C -0.139137
 34 H 0.137716
 35 C -0.158580
 36 H 0.138768
 37 C 0.080830
 38 C -0.152263
 39 H 0.118256
 40 C -0.148756
 41 H 0.133318

42 C -0.139933
 43 H 0.133277
 44 C -0.142617
 45 H 0.134261
 46 C -0.143795
 47 H 0.143248
 48 C 0.281481
 49 C -0.135741
 50 C -0.145871
 51 H 0.141798
 52 C -0.139267
 53 H 0.136066
 54 C -0.134140
 55 H 0.130532
 56 H 0.150426
 57 C -0.130318
 58 H 0.151248
 59 O -0.615411
 60 P 1.330721
 61 O -0.662731
 62 C 0.310572
 63 C -0.147318
 64 C -0.145235
 65 H 0.143573
 66 C -0.138704
 67 H 0.137910
 68 C -0.153696
 69 H 0.144347
 70 H 0.152687
 71 C -0.158891
 72 H 0.169635
 73 O -0.652083
 74 H 0.362610
 75 O -0.658753

• **Phosphate intermediate + DPPA complex**

Geometry:

75

C 0.22738980 -0.04904722 -1.39430129
 C 1.51041885 0.65085479 -1.88407936
 C 2.12378932 1.54536922 -0.78686288
 C 1.05345578 2.51569988 -0.25551592
 C -0.16430459 1.71744367 0.21552308
 O -0.69367769 0.90269461 -0.85249291
 C 0.50117803 -1.22413253 -0.42623667
 C -0.66601194 -1.64419479 0.49552097
 C -1.96230473 -2.09367921 -0.22619419
 C -3.24818692 -1.42364381 0.35478484
 O -3.05705181 -0.00128192 0.45057554
 H 2.98273408 2.09540306 -1.19801706
 H 2.50492532 0.92707401 0.04354096
 H 0.74317529 3.20199669 -1.05879965
 H 1.44118483 3.11622658 0.58205242
 H -1.00104770 2.35896597 0.51874500
 H 0.10776526 1.07038306 1.06812381
 H -2.07600951 -3.18364496 -0.15279588
 H -1.92133668 -1.84737713 -1.29145471
 H 0.84608472 -2.06636224 -1.04509571
 H 1.35279019 -0.93539676 0.20878772
 C -3.47632572 -1.95113981 1.78055296
 C -3.98884672 -3.24827890 1.97475496
 H -4.29992046 -3.83355661 -1.10836571
 C -4.11688887 -3.78188684 3.26351793
 H -4.51756276 -4.78867692 3.39456315
 C -3.73870869 -3.02268599 4.38323860
 H -3.84100435 -3.43643048 5.38779515
 C -3.23498460 -1.72726209 4.19834073
 H -2.94315792 -1.12521831 5.06107770

C -3.10332458 -1.19506467 2.90569352
 H -2.71892027 -0.18763624 2.75751466
 C -4.47958034 -1.70137551 -0.53206958
 C -4.54465123 -2.75536117 -1.46108454
 H -3.69592365 -3.42487876 -1.59811783
 C -5.69284954 -2.95114001 -2.24653156
 H -5.71761804 -3.77056576 -2.96735240
 C -6.79335269 -2.09394973 -2.11619810
 H -7.67967317 -2.23803538 -2.73586497
 C -6.73841770 -1.03971799 -1.19099888
 H -7.58153506 -0.35480880 -1.09065233
 C -5.59610915 -0.85207436 -0.40533109
 H -5.54416867 -0.02543814 0.30191315
 H -0.30100743 -2.45022086 1.14857702
 H -0.90827020 -0.80280540 1.15665080
 H 2.21815409 -0.11963895 -2.22355262
 H 1.22800366 1.26977916 -2.74699938
 P -1.45007437 0.24020160 -3.49281231
 O -1.02734143 1.58798617 -3.95263294
 O -1.71772325 -0.87865703 -4.65948325
 C -0.68327021 -1.18109328 -5.56459278
 C -0.20023154 -0.21358918 -6.45606305
 H -0.59015021 0.80098307 -6.40799842
 C 0.79682298 -0.58427737 -7.37086355
 H 1.18544811 0.15951444 -8.06773240
 C 1.29074236 -1.89831758 -7.39566943
 H 2.06272904 -2.17769144 -8.11356106
 C 0.78953976 -2.85163923 -6.49456627
 H 1.17135170 -3.87332173 -6.50784897
 C -0.20160263 -2.49556950 -5.56805968
 H -0.60561631 -3.21125023 -4.85306025
 O -2.83585104 0.11215020 -2.65435242
 C -4.04351927 0.68695555 -3.09119421
 C -4.55108825 1.76814872 -2.36454359
 H -3.98119341 2.16090466 -1.52486010
 C -5.80090636 2.29107892 -2.72447666
 H -6.21320666 3.13115598 -2.16433876
 C -6.52103520 1.73318909 -3.79333204
 H -7.49430063 2.14186168 -4.06716846
 C -5.98988576 0.64686086 -4.50536208
 H -6.55078573 0.20509770 -5.32980560
 C -4.74208532 0.11105904 -4.15652870
 H -4.31755187 -0.74463372 -4.67648435
 O -0.45187032 -0.62062106 -2.54349114
 H -2.53736203 0.26382821 -0.32973140

Mulliken charges:

1 C 0.525268
 2 C -0.239887
 3 C -0.255075
 4 C -0.246456
 5 C 0.014742
 6 O -0.550711
 7 C -0.257783
 8 C -0.229531
 9 C -0.249403
 10 C 0.179040
 11 O -0.613373
 12 H 0.137977
 13 H 0.122425
 14 H 0.145360
 15 H 0.131948
 16 H 0.152800
 17 H 0.121296
 18 H 0.123319
 19 H 0.148059
 20 H 0.144898
 21 H 0.126929
 22 C 0.077264
 23 C -0.146051

24 H 0.124905
 25 C -0.146943
 26 H 0.133858
 27 C -0.139384
 28 H 0.132084
 29 C -0.144397
 30 H 0.131561
 31 C -0.149963
 32 H 0.138450
 33 C 0.074542
 34 C -0.157908
 35 H 0.122328
 36 C -0.151583
 37 H 0.130325
 38 C -0.134357
 39 H 0.129984
 40 C -0.135509
 41 H 0.131150
 42 C -0.134076
 43 H 0.136589
 44 H 0.129127
 45 H 0.129353
 46 H 0.136746
 47 H 0.159311
 48 P 1.303793
 49 O -0.561480
 50 O -0.610011
 51 C 0.293064
 52 C -0.133403
 53 H 0.173005
 54 C -0.150031
 55 H 0.148225
 56 C -0.132641
 57 H 0.141811
 58 C -0.147485
 59 H 0.145911
 60 C -0.139471
 61 H 0.154732
 62 O -0.626692
 63 C 0.311763
 64 C -0.127776
 65 H 0.153552
 66 C -0.149450
 67 H 0.145142
 68 C -0.131263
 69 H 0.139658
 70 C -0.146598
 71 H 0.144587
 72 C -0.124513
 73 H 0.161621
 74 O -0.604397
 75 H 0.359097

- **Syn phosphate displacement leading to thermodynamic product (TS₃)**

Geometry:

75

C 2.687317 -0.262422 -0.316587
 C 3.650580 0.849369 -0.598032
 C 3.009465 2.245507 -0.484744
 C 2.239742 2.328805 0.846310
 C 1.176893 1.239172 0.868350
 O 1.735047 -0.105936 0.535760
 O 0.010799 -0.271219 -1.492325
 C -0.454225 -1.610003 -1.578417
 C 0.734532 -2.606730 -1.759532
 C 1.810903 -2.698627 -0.647288
 C 2.980203 -1.683436 -0.660258

H 4.408832 0.733883 0.205252
 H 4.140313 0.679896 -1.560678
 H 3.792834 3.011157 -0.550944
 H 2.315147 2.394770 -1.322289
 H 2.923258 2.214131 1.702840
 H 1.726185 3.296526 0.953466
 H 0.706626 1.077923 1.843863
 H 0.412648 1.370814 0.093915
 H 0.301730 -3.612643 -1.860420
 H 1.207966 -2.376139 -2.722358
 H 1.343940 -2.711946 0.346687
 H 2.304067 -3.675034 -0.774098
 H 3.695764 -1.991165 0.130421
 H 3.523320 -1.691994 -1.610923
 C -1.411873 -1.762746 -2.788909
 C -2.020862 -3.005202 -3.073648
 H -1.817892 -3.865107 -2.433744
 C -2.913335 -3.137422 -4.152452
 H -3.376871 -4.104218 -4.357488
 C -3.219340 -2.020138 -4.954371
 H -3.914657 -2.117554 -5.789689
 C -2.619331 -0.779850 -4.672568
 H -2.830959 0.085242 -5.297873
 C -1.718713 -0.650011 -3.599604
 H -1.245349 0.309835 -3.401493
 C -1.272404 -1.856126 -0.296441
 C -1.278308 -3.090759 0.388883
 H -0.661082 -3.915537 0.034046
 C -2.079172 -3.279637 1.532597
 H -2.065857 -4.242083 2.046926
 C -2.890424 -2.235341 2.009259
 H -3.512197 -2.380876 2.893442
 C -2.899815 -1.000604 1.326592
 H -3.536498 -0.187165 1.678164
 C -2.102063 -0.816550 0.184594
 H -2.116500 0.131124 -0.352622
 P 2.233581 1.149530 -3.801174
 O 1.160110 2.168155 -3.526339
 O 2.344038 0.736477 -5.410039
 C 1.195349 0.255028 -6.062285
 C 0.308270 1.161860 -6.666793
 H 0.479932 2.229208 -6.546258
 C -0.775733 0.660938 -7.411932
 H -1.466402 1.356286 -7.891537
 C -0.970369 -0.728586 -7.540675
 H -1.815682 -1.110826 -8.114083
 C -0.085921 -1.623262 -6.910519
 H -0.251773 -2.697686 -6.984337
 C 1.003213 -1.135182 -6.166175
 H 1.705721 -1.802638 -5.671401
 O 3.788079 1.758369 -3.660639
 C 4.173032 2.968741 -4.262324
 C 3.466928 4.168976 -4.046561
 H 2.539662 4.143914 -3.480920
 C 3.957854 5.360065 -4.612741
 H 3.412026 6.291276 -4.454485
 C 5.141059 5.358261 -5.377816
 H 5.516545 6.286431 -5.809917
 C 5.834081 4.148764 -5.586426
 H 6.746700 4.136367 -6.183311
 C 5.350728 2.949869 -5.032225
 H 5.863573 2.002648 -5.186871
 O 2.283520 -0.126532 -2.945232
 H 0.652777 -0.115419 -2.225736

Mulliken charges:

1 C 0.506904
 2 C -0.297260
 3 C -0.260909
 4 C -0.280766

5 C -0.014198
6 O -0.390791
7 O -0.629227
8 C 0.191600
9 C -0.234080
10 C -0.231369
11 C -0.301707
12 H 0.180063
13 H 0.210308
14 H 0.155390
15 H 0.176535
16 H 0.142898
17 H 0.166766
18 H 0.179664
19 H 0.209915
20 H 0.115790
21 H 0.150805
22 H 0.135007
23 H 0.136839
24 H 0.180214
25 H 0.196358
26 C 0.072756
27 C -0.151129
28 H 0.118016
29 C -0.147987
30 H 0.130546
31 C -0.141930
32 H 0.128019
33 C -0.120500
34 H 0.130326
35 C -0.165026
36 H 0.148279
37 C 0.091746
38 C -0.163020
39 H 0.121527
40 C -0.149225
41 H 0.134770
42 C -0.140798
43 H 0.134711
44 C -0.145679
45 H 0.135573
46 C -0.146835
47 H 0.144428
48 P 1.255579
49 O -0.664266
50 O -0.620421
51 C 0.301916
52 C -0.131130
53 H 0.155040
54 C -0.152557
55 H 0.137584
56 C -0.131243
57 H 0.130581
58 C -0.136001
59 H 0.138024
60 C -0.138417
61 H 0.147350
62 O -0.653581
63 C 0.320099
64 C -0.148987
65 H 0.160013
66 C -0.150787
67 H 0.138376
68 C -0.140597
69 H 0.133058
70 C -0.147150
71 H 0.138149
72 C -0.155402
73 H 0.145684
74 O -0.707429

75 H 0.363198

- *Syn* phosphate displacement leading to nonthermodynamic product (TS₄)

Geometry:

75

C -0.480881 1.165940 0.285013
O -0.541644 2.445235 0.432500
C -0.026037 3.110519 1.671013
C -0.316121 2.281026 2.914453
C 0.241223 0.858839 2.729384
C -0.297468 0.240622 1.433461
O 1.646824 -0.111972 -1.530362
C 1.334865 -1.501606 -1.555890
C -0.105873 -1.536538 -2.134512
C -1.199470 -0.799386 -1.320956
C -0.997580 0.718479 -1.059589
H -0.534144 4.080733 1.652155
H 1.047238 3.210206 1.471307
H -1.401774 2.265755 3.107247
H 0.167539 2.781008 3.766736
H -0.036931 0.212272 3.573188
H 1.336475 0.890085 2.676359
H -0.434192 -2.576884 -2.285010
H -0.036503 -1.082066 -3.134036
H -1.388344 -1.318225 -0.371232
H -2.129645 -0.891902 -1.901202
H -1.977906 1.227413 -1.125369
H -0.362229 1.179639 -1.827303
C 2.288509 -2.223588 -2.536677
C 2.305834 -3.635230 -2.607793
H 1.677330 -4.214852 -1.930147
C 3.148438 -4.296217 -3.517652
H 3.154841 -5.386783 -3.557167
C 3.994391 -3.551218 -4.364988
H 4.659280 -4.062788 -5.062941
C 3.985581 -2.145767 -4.294585
H 4.648681 -1.559009 -4.931585
C 3.133840 -1.482380 -3.391629
H 3.144652 -0.398376 -3.321397
C 1.452859 -2.159271 -0.171868
C 0.499827 -3.074310 0.331332
H -0.350438 -3.373467 -0.280741
C 0.627045 -3.601141 1.631810
H -0.123616 -4.298949 2.005988
C 1.710579 -3.222631 2.447416
H 1.797097 -3.613717 3.461447
C 2.687067 -2.343369 1.939957
H 3.530687 -2.030566 2.552279
C 2.568601 -1.837674 0.635122
H 3.342565 -1.181504 0.246865
H -1.332998 -0.138813 1.570129
H 0.278209 -0.630841 1.109895
C 7.428605 4.497880 0.362351
H 7.986028 4.984354 -0.439387
C 8.048278 4.243418 1.602263
H 9.087259 4.533704 1.764381
C 7.321957 3.605341 2.628448
H 7.797217 3.399862 3.588457
C 5.981842 3.226437 2.427646
C 5.378812 3.489886 1.182460
O 4.027998 3.172036 0.929177
P 3.519146 1.586795 1.065104
O 4.612523 0.780090 0.081813
C 4.930832 1.140149 -1.233980
C 6.148831 0.621648 -1.716229
C 6.544680 0.885680 -3.036266
H 7.486635 0.478216 -3.405143
C 5.734147 1.671453 -3.878884

H 6.042851 1.877386 -4.904528
C 4.520931 2.186853 -3.384604
H 3.882502 2.793053 -4.029704
H 6.762261 0.018234 -1.049497
C 4.107585 1.926388 -2.066113
H 3.160281 2.301008 -1.695700
O 2.155597 1.613697 0.362450
H 1.992031 0.253178 -0.679437
O 3.672774 1.012471 2.442809
H 5.409199 2.712517 3.195300
C 6.091941 4.119672 0.146008
H 5.600268 4.283299 -0.811011

Mulliken charges:

1 C 0.508022
2 O -0.413593
3 C -0.011217
4 C -0.285071
5 C -0.251249
6 C -0.290012
7 O -0.627183
8 C 0.214941
9 C -0.205573
10 C -0.249350
11 C -0.299406
12 H 0.172717
13 H 0.213102
14 H 0.138690
15 H 0.169289
16 H 0.142975
17 H 0.198431
18 H 0.119783
19 H 0.134456
20 H 0.121578
21 H 0.142607
22 H 0.180170
23 H 0.218906
24 C 0.063219
25 C -0.148474
26 H 0.119121
27 C -0.147343
28 H 0.132221
29 C -0.140241
30 H 0.131267
31 C -0.141263
32 H 0.132238
33 C -0.135810
34 H 0.136654
35 C 0.008211
36 C -0.162666
37 H 0.125725
38 C -0.147496
39 H 0.136787
40 C -0.144188
41 H 0.140044
42 C -0.129338
43 H 0.160998
44 C -0.140472
45 H 0.155402
46 H 0.187156
47 H 0.191203
48 C -0.147425
49 H 0.138037
50 C -0.139461
51 H 0.132614
52 C -0.151194
53 H 0.138812
54 C -0.142014
55 C 0.291871
56 O -0.648258

57 P 1.318339
58 O -0.650331
59 C 0.318121
60 C -0.154020
61 C -0.145278
62 H 0.137843
63 C -0.143859
64 H 0.131075
65 C -0.160615
66 H 0.135972
67 H 0.149911
68 C -0.140099
69 H 0.158461
70 O -0.750588
71 H 0.352371
72 O -0.621597
73 H 0.164449
74 C -0.141424
75 H 0.142320

• **Thermodynamic spiroketal + DPPA complex**

Geometry:

75

C 0.93869814 0.48257365 0.17714954
C 0.96190416 2.02211738 0.03762645
C -0.24017070 2.74751218 0.67550577
C -0.52447730 2.17701181 2.07460486
C -0.69713295 0.66196694 1.95491008
O 0.50062595 0.03695078 1.43990267
O 0.05830695 -0.00742487 -0.90565356
C -0.04591328 -1.46546246 -1.15953843
C 1.38210878 -2.06991326 -1.21929901
C 2.29091420 -1.64505109 -0.05913333
C 2.34021783 -0.11375353 -0.01108925
H 1.87952655 2.35030019 0.55070322
H 1.05523230 2.28495759 -1.02448795
H -0.02338732 3.82510118 0.71874266
H -1.13686202 2.62464508 0.05663021
H 0.31098069 2.39374944 2.76057430
H -1.43949037 2.61624936 2.50292292
H -0.86380775 0.18125569 2.92747818
H -1.54604013 0.42599239 1.29502089
H 1.28543148 -3.16196034 -1.29821260
H 1.83372676 -1.72277000 -2.16007613
H 1.91750189 -2.02376270 0.90091572
H 3.30026583 -2.05354174 -0.21740343
H 2.96661722 0.24219302 0.81787079
H 2.74899604 0.28758653 -0.95160215
C -0.63083795 -1.60391774 -2.57575266
C -1.42686827 -2.71521661 -2.91258524
H -1.71411126 -3.42405166 -2.13715945
C -1.85236880 -2.91066512 -4.23503867
H -2.47473565 -3.77313657 -4.47850837
C -1.49222569 -1.99484272 -5.23446321
H -1.84201925 -2.13527207 -6.25802575
C -0.69558957 -0.88730896 -4.90525345
H -0.42871624 -0.15493668 -5.66677691
C -0.25738463 -0.69867240 -3.58787487
H 0.35143138 0.16830406 -3.33681769
C -0.98107888 -2.08506074 -0.11215892
C -0.61978094 -3.16356559 0.71224652
H 0.37921565 -3.59155382 0.65449461
C -1.53803426 -3.70716688 1.62577970
H -1.23554774 -4.54270638 2.25888258
C -2.83516801 -3.18558716 1.72203636
H -3.54674884 -3.61081249 2.43106556
C -3.21235427 -2.11859203 0.89038095
H -4.2223755 -1.70939337 0.94478593

C -2.29567586 -1.58037508 -0.01972755
H -2.60177315 -0.76255648 -0.66950979
C -4.70820456 2.06291946 -4.81135442
C -5.98932154 1.49380081 -4.88141030
H -6.80941495 2.06876078 -5.31418051
C -6.21651640 0.19468624 -4.39914249
H -7.21384198 -0.24306846 -4.45739590
C -5.15521086 -0.54072675 -3.84732950
H -5.32000114 -1.55292988 -3.47594423
C -3.86932246 0.01147992 -3.77331536
H -3.03629892 -0.54511908 -3.35587738
H -4.50957707 3.07225957 -5.16658896
C -3.66699603 1.31099573 -4.25480978
O -2.37586955 1.86715126 -4.24825557
P -1.68538934 2.38867194 -2.85992647
O -2.71498647 3.55247754 -2.31958341
C -3.10186171 4.62949992 -3.12287708
C -4.44384898 5.02428160 -3.01989918
C -4.89446133 6.11962440 -3.76915827
H -5.93760056 6.43006380 -3.69203282
C -4.01344694 6.80922356 -4.61861739
H -4.36886225 7.65835616 -5.20334667
C -2.67366790 6.40014708 -4.70772857
H -1.98124630 6.93257159 -5.36110236
H -5.11161478 4.46305437 -2.36792725
C -2.20255249 5.31298113 -3.95565846
H -1.16370053 4.99153295 -4.01020954
O -1.97632313 1.30829646 -1.72913909
H -1.13380952 0.82152836 -1.41954704
O -0.27142550 2.78740276 -3.10438411

Mulliken charges:

1 C 0.519328
2 C -0.266187
3 C -0.253400
4 C -0.245215
5 C 0.016608
6 O -0.520947
7 O -0.638527
8 C 0.198232
9 C -0.226051
10 C -0.248077
11 C -0.232128
12 H 0.129460
13 H 0.163342
14 H 0.130224
15 H 0.132519
16 H 0.122951
17 H 0.128693
18 H 0.136226
19 H 0.116190
20 H 0.134397
21 H 0.135746
22 H 0.139659
23 H 0.129734
24 H 0.137473
25 H 0.131744
26 C 0.027043
27 C -0.141754
28 H 0.136679
29 C -0.149468
30 H 0.139829
31 C -0.132553
32 H 0.141032
33 C -0.129102
34 H 0.149417
35 C -0.160398
36 H 0.153329
37 C 0.104016
38 C -0.150300

39 H 0.129196
40 C -0.149445
41 H 0.138740
42 C -0.136301
43 H 0.138744
44 C -0.146027
45 H 0.142540
46 C -0.157600
47 H 0.142204
48 C -0.131351
49 C -0.152914
50 H 0.142552
51 C -0.133074
52 H 0.138042
53 C -0.159238
54 H 0.141257
55 C -0.077237
56 H 0.125926
57 H 0.150765
58 C 0.279256
59 O -0.608581
60 P 1.310346
61 O -0.609400
62 C 0.298275
63 C -0.149016
64 C -0.146849
65 H 0.144189
66 C -0.136662
67 H 0.140087
68 C -0.150218
69 H 0.147252
70 H 0.155985
71 C -0.154981
72 H 0.175260
73 O -0.643894
74 H 0.432266
75 O -0.589860

• **Nonthermodynamic spiroketal + DPPA complex**

Geometry:

75

C -0.87133700 0.40196161 0.32279713
O -1.11653599 1.77572440 0.39236219
C -0.24167651 2.59791118 1.21305565
C -0.01842354 2.02656566 2.61340199
C 0.44992131 0.56611331 2.50428562
C -0.58341895 -0.23342181 1.69861832
O 0.31929701 0.23457795 -0.57929558
C 0.56690791 -1.06012211 -1.24830902
C -0.75215274 -1.58585033 -1.86297025
C -1.90727787 -1.61023631 -0.85494877
C -2.12314624 -0.18141366 -0.34806249
H -0.75012704 3.57068455 1.24872489
H 0.72094848 2.73271939 0.70847634
H -0.95902928 2.07223507 3.18741848
H 0.73772953 2.64218300 3.11847450
H 0.57397287 0.11646703 3.50062812
H 1.43195312 0.53287399 2.01435016
H -0.55633314 -2.57169278 -2.30682243
H -1.01932434 -0.91237077 -2.69024524
H -1.68582325 -2.28685239 -0.01708376
H -2.82305129 -1.97926516 -1.34087737
H -2.94356357 -0.12444629 0.38095335
H -2.37839884 0.47673047 -1.19238712
C 1.51267124 -0.75582514 -2.42386694
C 2.43151269 -1.71851446 -2.87866584
H 2.54445287 -2.65778585 -2.33877984

C	3.21449872	-1.47401653	-4.01652821	14 H	0.114861
H	3.92732142	-2.22922517	-4.35021456	15 H	0.147783
C	3.09828044	-0.25886593	-4.70641722	16 H	0.126948
H	3.71943229	-0.06171211	-5.58159955	17 H	0.117707
C	2.17728820	0.70340581	-4.26225422	18 H	0.133094
H	2.08221494	1.65527364	-4.78637452	19 H	0.135167
C	1.37857911	0.44926914	-3.13996212	20 H	0.124470
H	0.66948549	1.19710725	-2.78958475	21 H	0.133205
C	1.22344716	-2.03590121	-0.25710263	22 H	0.135093
C	0.79934304	-3.36326163	-0.06921170	23 H	0.137168
H	-0.05065891	-3.75394253	-0.62615704	24 C	0.030631
C	1.46422554	-4.20341805	0.84021391	25 C	-0.136230
H	1.11603381	-5.22832784	0.97708548	26 H	0.136698
C	2.56845684	-3.73217576	1.56404149	27 C	-0.148031
H	3.08264094	-4.38711862	2.26867932	28 H	0.138428
C	3.01247751	-2.41422171	1.36583488	29 C	-0.138240
H	3.87797229	-2.02879030	1.90520332	30 H	0.137425
C	2.34534640	-1.58502462	0.46008053	31 C	-0.144291
H	2.69841158	-0.57495032	0.30137776	32 H	0.142660
H	-1.54069520	-0.23312552	2.24509830	33 C	-0.127927
H	-0.27317828	-1.27541945	1.56656663	34 H	0.146256
C	8.11000924	3.61723213	-0.49182344	35 C	0.057303
H	8.94955708	3.40499952	-1.15508895	36 C	-0.158692
C	8.32698078	4.24126791	0.74766444	37 H	0.131237
H	9.33662644	4.52159076	1.05013818	38 C	-0.146401
C	7.24031480	4.49965616	1.59784672	39 H	0.139751
H	7.40165647	4.98296857	2.56244056	40 C	-0.137666
C	5.93631525	4.14506021	1.21895358	41 H	0.141046
C	5.74622370	3.51595952	-0.01900355	42 C	-0.143088
O	4.46503159	3.15406293	-0.47149952	43 H	0.146796
P	3.52795549	2.17856129	0.44444667	44 C	-0.078655
O	4.47605910	0.86849642	0.75315758	45 H	0.070771
C	5.39096933	0.32709968	-0.16399223	46 H	0.121747
C	6.62791653	-0.05570320	0.37165649	47 H	0.129213
C	7.59474258	-0.61354507	-0.47421506	48 C	-0.147049
H	8.56210878	-0.90609664	-0.06375159	49 H	0.144666
C	7.32520022	-0.78409262	-1.84230293	50 C	-0.133500
H	8.08180674	-1.21309778	-2.50034306	51 H	0.140280
C	6.07556433	-0.40569884	-2.35523668	52 C	-0.150829
H	5.84411407	-0.54268130	-3.41127684	53 H	0.147059
H	6.81855994	0.10990178	1.43111347	54 C	-0.143694
C	5.09126197	0.14666521	-1.52112549	55 C	0.282818
H	4.12186028	0.43034083	-1.92193941	56 O	-0.602431
O	2.49301412	1.79413260	-0.70787634	57 P	1.336093
H	1.68977709	1.22786338	-0.49445283	58 O	-0.634022
O	3.00461387	2.70926764	1.73019500	59 C	0.293371
H	5.08096815	4.33253924	1.86606870	60 C	-0.140296
C	6.81585556	3.24684254	-0.88146521	61 C	-0.146747
H	6.62400575	2.73070803	-1.82044546	62 H	0.144125

Mulliken charges:

1 C	0.537456
2 O	-0.539749
3 C	0.009256
4 C	-0.239911
5 C	-0.241667
6 C	-0.224680
7 O	-0.632589
8 C	0.207558
9 C	-0.222212
10 C	-0.249337
11 C	-0.245727
12 H	0.136153
13 H	0.119764
14 H	0.114861
15 H	0.147783
16 H	0.126948
17 H	0.117707
18 H	0.133094
19 H	0.135167
20 H	0.124470
21 H	0.133205
22 H	0.135093
23 H	0.137168
24 C	0.030631
25 C	-0.136230
26 H	0.136698
27 C	-0.148031
28 H	0.138428
29 C	-0.138240
30 H	0.137425
31 C	-0.144291
32 H	0.142660
33 C	-0.127927
34 H	0.146256
35 C	0.057303
36 C	-0.158692
37 H	0.131237
38 C	-0.146401
39 H	0.139751
40 C	-0.137666
41 H	0.141046
42 C	-0.143088
43 H	0.146796
44 C	-0.078655
45 H	0.070771
46 H	0.121747
47 H	0.129213
48 C	-0.147049
49 H	0.144666
50 C	-0.133500
51 H	0.140280
52 C	-0.150829
53 H	0.147059
54 C	-0.143694
55 C	0.282818
56 O	-0.602431
57 P	1.336093
58 O	-0.634022
59 C	0.293371
60 C	-0.140296
61 C	-0.146747
62 H	0.144125
63 C	-0.137636
64 H	0.138555
65 C	-0.145353
66 H	0.132913
67 H	0.156202
68 C	-0.117839
69 H	0.155283
70 O	-0.634249
71 H	0.402997
72 O	-0.569914
73 H	0.174096
74 C	-0.127014
75 H	0.151559

B. Computational studies with the diphenyl hydrogen phosphate system (6,5-spiroketalization)

A model system consisting of diphenyl hydrogen phosphate and non-deuterated enol ether **3-26** was utilized to study different pathways leading to the formation of spiroketal (*rac*)-**3-27**. Single-ended growing string runs employing **3-27** as the fixed node were performed with varying driving coordinates according to the pathway analyzed. 18 different orientations of the catalyst were studied, and both the concerted and phosphate-mediated mechanisms were considered. 42 strings for the concerted pathways and 38 pathways describing the spirocyclization by syn displacement of a phosphate intermediate were modeled. The lowest energy barriers between the concerted spiroketalization and the formation of **3-27** via syn displacement of the phosphate intermediate are compared in the following figure. The considerable difference between these activation energies allowed us to conclude that the phosphate mechanism is uncompetitive without the need of further analysis of the other step of the pathway.

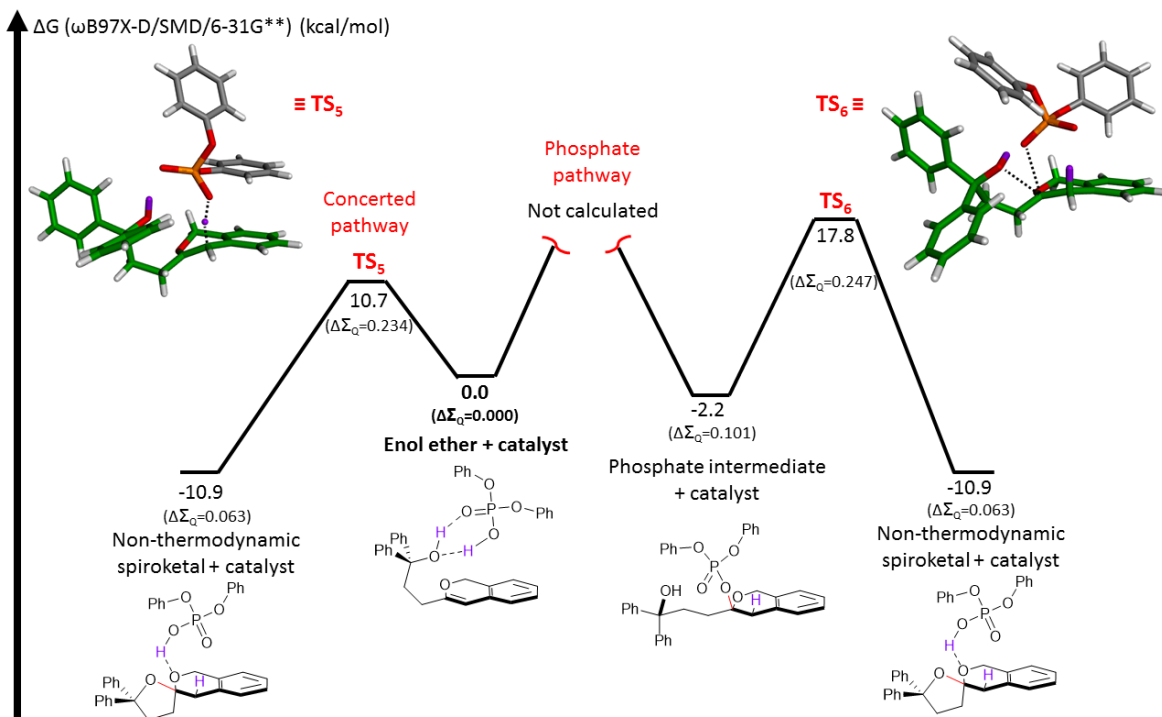


Figure B.1. Energy diagram for the [6,5]-spiroketalization. The values in parenthesis correspond to the difference of the sum of Mulliken charges at the enol ether oxygen and the electrophilic carbon with respect to the starting complex.

A summary of calculated values including solvent corrected single point energy values, as well as enthalpic and entropic corrections associated with vibrational energy at 298 K are provided in the next table.

Table B.3. Calculated values for starting geometries, intermediates, and transition states phosphate-mediated pathway for the [6,5]-spiroketalization catalyzed by DPPA.

	G_{SMD} [kcal/mol] ^a	H_{vib} [kcal/mol] ^b	S_{vib} [kcal/mol] ^b	ΔG [kcal/mol] ^c
Enol ether 3-26 + DPPA complex	-1370455.7	398.8	231.4	0.0
Concerted pathway TS (TS₅)	-1370441.5	395.2	231.0	10.7
Nonthermodynamic spiroketal + catalyst complex	-1370466.2	398.9	233.5	-10.9
Phosphate intermediate	-1370458.4	399.4	232.1	-2.2
Syn Phosphate displacement (TS₆)	-1370438.0	396.0	222.0	17.8

^a Solvent-corrected (dichloromethane) electronic energy (ωB97X-D/SMD/6-31G**). ^b Vibrational, rotational, and translational entropic and enthalpic contributions (B97-D/6-31G**) at 298.15 K. ^c Corrected free energy values at 298.15 K

Final corrected free energies, cartesian coordinates, and Mulliken charges for the starting geometry, intermediate, transition states, and cyclized product are provided below.

• **Enol ether 3-26 + DPPA complex**
Corrected energy: -1370125.9 kcal/mol

Geometry:

76

C -3.23754940 -2.37090578 3.42949345
 C -2.55852016 -3.50333754 2.95274048
 C -2.57921187 -1.12701392 3.46193088
 C -1.26022582 -1.01891612 3.01378710
 C -0.56080674 -2.16227436 2.54706261
 C -1.22878077 -3.40280946 2.51743953
 C -0.52842755 0.30193242 2.92027411
 O 0.89253928 0.17065831 3.21309706
 C 1.51307817 -0.87148086 2.57674606
 C 0.84275164 -1.99208999 2.19437638
 O 1.51008998 0.72334031 0.23607782
 C 2.95581880 0.85873828 0.29507919
 C 3.40050497 0.67766106 1.77122448
 C 2.99587429 -0.65975813 2.43328323
 C 3.31572186 2.24717437 -0.26047985
 C 4.19020267 3.13556810 0.38962377
 C 2.73550251 2.63622932 -1.48491398
 C 4.47357145 4.39210209 -0.17005313
 C 3.88541289 4.77452323 -1.38389373
 C 3.01407214 3.88973127 -2.03979813
 C 3.55795717 -0.25626256 -0.57675148
 C 4.81882526 -0.08056530 -1.17497814
 C 5.39581121 -1.09778865 -1.94914010
 C 4.72027041 -2.31366925 -2.13643521
 C 3.46853199 -2.50330107 -1.53151369
 C 2.89529174 -1.48587052 -0.75495806
 H -4.27191554 -2.45049364 3.76512144
 H -3.06353141 -4.47048928 2.92821888
 H -3.10182143 -0.23814879 3.82163046
 H -0.69774144 -4.28784437 2.16234386
 H -0.90906164 1.03718986 3.64055555
 H -0.61246839 0.72084442 1.90243999
 H 1.39282227 -2.80188945 1.71828875
 H 0.29151298 -0.33277050 -0.17363220
 H 2.97809406 1.50675963 2.35592929
 H 4.49682274 0.75659314 1.80905075
 H 3.44606628 -0.66703673 3.44089893
 H 3.41951363 -1.50924572 1.88070040
 H 4.65068508 2.85931316 1.33657533
 H 2.06583449 1.95160071 -1.99859538
 H 5.15044828 5.07155931 0.35000201
 H 4.10343508 5.75307302 -1.81409646
 H 2.54859212 4.16580006 -2.98611667
 H 5.34119451 0.86857342 -1.05207659
 H 6.37027101 -0.93478866 -2.41208130
 H 5.16522408 -3.10355339 -2.74310332
 H 2.93229807 -3.44472050 -1.66212208
 H 1.92836072 -1.65946235 -0.28991582
 C -3.44780169 -1.98995207 -0.17440387
 H -3.04698823 -1.76441018 0.81004589
 C -3.97820510 -3.25184888 -0.47763711
 H -3.99083485 -4.01871115 0.29737731
 C -4.47899686 -3.52446421 -1.76113380
 H -4.88942062 -4.50871918 -1.99038574
 C -4.44926666 -2.52868221 -2.75114687
 C -3.92222648 -1.26007224 -2.46422843
 H -3.87570197 -0.47175181 -3.21332302
 H -4.83462922 -2.73622388 -3.75029549
 C -3.43230328 -1.01591278 -1.17702274
 O -2.94896377 0.27413074 -0.85975499
 P -1.38819528 0.63942261 -1.06087708
 O -0.58413150 -0.65082153 -0.53921627
 O -1.29605169 0.59483208 -2.70413239
 C -0.04644672 0.77585366 -3.31774953

C 0.93948913 -0.21810712 -3.23732169
 H 0.75557724 -1.11621421 -2.65369633
 C 2.16367381 -0.01770676 -3.89202952
 H 2.94614461 -0.76909852 -3.78806655
 C 2.38492513 1.14775244 -4.64162470
 H 3.33913721 1.29933613 -5.14682575
 C 1.38038074 2.12613601 -4.72435986
 H 1.54749390 3.03595119 -5.30281171
 C 0.16168709 1.95116974 -4.05201991
 H -0.62424996 2.70449052 -4.08340072
 O -0.99062354 1.93498889 -0.43604882
 H 1.06652689 1.59060413 0.25083320

Mulliken charges:

1 C -0.150958
 2 C -0.141663
 3 C -0.165867
 4 C -0.001085
 5 C 0.111230
 6 C -0.175011
 7 C -0.023035
 8 O -0.537337
 9 C 0.388492
 10 C -0.262847
 11 O -0.629740
 12 C 0.219585
 13 C -0.218414
 14 C -0.304204
 15 C -0.000180
 16 C -0.151612
 17 C -0.088889
 18 C -0.148570
 19 C -0.133945
 20 C -0.136093
 21 C 0.076749
 22 C -0.141896
 23 C -0.146685
 24 C -0.140095
 25 C -0.150513
 26 C -0.133085
 27 H 0.137423
 28 H 0.134566
 29 H 0.136996
 30 H 0.132253
 31 H 0.151423
 32 H 0.133634
 33 H 0.126937
 34 H 0.415465
 35 H 0.145334
 36 H 0.131022
 37 H 0.156644
 38 H 0.142186
 39 H 0.133998
 40 H 0.115412
 41 H 0.140635
 42 H 0.140459
 43 H 0.130739
 44 H 0.136236
 45 H 0.141443
 46 H 0.141135
 47 H 0.142776
 48 H 0.117052
 49 C -0.083933
 50 H 0.138083
 51 C -0.148775
 52 H 0.135218
 53 C -0.131663
 54 H 0.139757
 55 C -0.150497
 56 C -0.127865

57 H 0.159911
 58 H 0.145217
 59 C 0.277121
 60 O -0.589753
 61 P 1.287883
 62 O -0.640272
 63 O -0.613334
 64 C 0.286573
 65 C -0.131470
 66 H 0.153285
 67 C -0.125433
 68 H 0.137034
 69 C -0.132959
 70 H 0.142772
 71 C -0.149586
 72 H 0.145556
 73 C -0.139217
 74 H 0.159488
 75 O -0.604182
 76 H 0.362944

• **Concerted pathway TS (TS₅)**

Geometry:

76

C -3.983415 -2.642955 2.952894
 C -3.003126 -3.642155 2.848297
 C -3.623667 -1.293463 2.824045
 C -2.290321 -0.954541 2.568127
 C -1.301504 -1.952086 2.472129
 C -1.662536 -3.300279 2.614799
 C -1.834068 0.459651 2.339832
 O -0.506091 0.694623 2.957821
 C 0.423070 -0.205421 2.729548
 C 0.105373 -1.505357 2.218029
 O 1.132028 1.156630 0.703104
 C 2.392074 1.627009 1.175101
 C 2.236463 1.595600 2.718447
 C 1.791882 0.195305 3.195527
 C 2.645233 3.043975 0.626321
 C 3.014172 4.130754 1.436904
 C 2.532916 3.241894 -0.765260
 C 3.263195 5.394218 0.871794
 C 3.144564 5.582055 -0.511366
 C 2.776433 4.499058 -1.327819
 C 3.564616 0.704564 0.778161
 C 4.888532 1.133694 0.996830
 C 5.969443 0.291915 0.714014
 C 5.744438 -0.995905 0.201820
 C 4.430307 -1.429673 -0.021479
 C 3.342499 -0.586717 0.268155
 H -5.025801 -2.912820 3.124168
 H -3.282579 -4.692074 2.947773
 H -4.380888 -0.510862 2.885176
 H -0.897851 -4.074854 2.536946
 H -2.488524 1.204395 2.803875
 H -1.689881 0.688871 1.274276
 H 0.884791 -2.239969 2.452396
 H 0.190669 -1.517423 0.938724
 H 1.489409 2.343386 3.017586
 H 3.191864 1.843251 3.198875
 H 1.770087 0.177798 4.298814
 H 2.504747 -0.569557 2.862469
 H 3.108352 4.003718 2.514579
 H 2.247779 2.407596 -1.407258
 H 3.547146 6.227512 1.516982
 H 3.335984 6.562818 -0.951410
 H 2.681284 4.634086 -2.407049

H 5.066572 2.142541 1.373111
 H 6.988503 0.644172 0.884743
 H 6.587003 -1.651486 -0.026143
 H 4.241118 -2.424440 -0.426703
 H 2.330807 -0.933368 0.079711
 H -3.840283 1.064388 -0.951772
 C -3.963850 -0.006062 -0.789749
 H -0.384337 0.771196 -6.501108
 H -6.110444 0.065236 -0.585875
 C -5.228029 -0.576899 -0.590712
 O -1.619124 -0.161309 -0.995567
 C -2.824672 -0.827759 -0.807820
 C -0.979257 0.132065 -5.847367
 O 0.757883 0.240615 -1.787882
 H 0.633428 -0.184401 -4.409190
 C -5.360282 -1.963228 -0.414706
 C -0.395031 -0.401485 -4.690014
 H 1.153857 0.951824 -0.267937
 C -2.938850 -2.216158 -0.615753
 H -2.763078 0.262637 -7.072072
 C -2.316683 -0.153084 -6.167339
 H -6.344629 -2.408433 -0.265905
 P -0.180629 -0.885776 -1.442276
 C -4.212698 -2.770642 -0.426753
 H -2.050038 -2.840215 -0.588459
 C -1.173014 -1.218445 -3.857232
 O 0.213634 -1.918432 -0.361382
 H -4.300442 -3.846889 -0.274538
 C -3.078648 -0.971566 -5.319364
 O -0.610260 -1.821043 -2.721081
 C -2.511147 -1.509200 -4.153662
 H -4.120115 -1.190764 -5.559475
 H -3.084812 -2.132030 -3.469131

Mulliken charges:

1 C -0.134064
 2 C -0.136598
 3 C -0.146098
 4 C 0.015539
 5 C 0.105213
 6 C -0.164797
 7 C -0.052946
 8 O -0.448894
 9 C 0.534120
 10 C -0.490197
 11 O -0.630228
 12 C 0.179521
 13 C -0.231235
 14 C -0.312512
 15 C 0.091269
 16 C -0.162413
 17 C -0.152082
 18 C -0.148216
 19 C -0.135278
 20 C -0.147286
 21 C 0.067867
 22 C -0.149009
 23 C -0.145724
 24 C -0.139065
 25 C -0.149171
 26 C -0.146216
 27 H 0.140305
 28 H 0.141993
 29 H 0.140889
 30 H 0.142714
 31 H 0.176783
 32 H 0.197653
 33 H 0.179750
 34 H 0.370804
 35 H 0.151511

36 H 0.141344
 37 H 0.187047
 38 H 0.169242
 39 H 0.123614
 40 H 0.150299
 41 H 0.134968
 42 H 0.135672
 43 H 0.141060
 44 H 0.127181
 45 H 0.135970
 46 H 0.135230
 47 H 0.140436
 48 H 0.124464
 49 H 0.150265
 50 C -0.166538
 51 H 0.142523
 52 H 0.139452
 53 C -0.146757
 54 O -0.641137
 55 C 0.313341
 56 C -0.150256
 57 O -0.640583
 58 H 0.164684
 59 C -0.143422
 60 C -0.128346
 61 H 0.378250
 62 C -0.148062
 63 H 0.136203
 64 C -0.134501
 65 H 0.133198
 66 P 1.328343
 67 C -0.142515
 68 H 0.165144
 69 C 0.283756
 70 O -0.675763
 71 H 0.138916
 72 C -0.149829
 73 O -0.619834
 74 C -0.131673
 75 H 0.141103
 76 H 0.143607

C 7.29748810 -1.14943340 -0.54547815
 C 6.12090948 -1.91067520 -0.50427586
 C 4.90177789 -1.31392802 -0.14634708
 H -3.26000676 -2.61269372 4.44936498
 H -2.26808376 -4.54167333 3.19530607
 H -2.32374348 -0.32692303 4.13896144
 H -0.35379038 -4.15452228 1.64359238
 H 0.26004469 0.75279226 3.52544585
 H -1.04324253 1.16323885 2.37456632
 H 1.58588500 -2.65433511 1.05134322
 H 0.47334834 -1.71725023 0.02463622
 H 2.93125526 1.61293270 2.55528162
 H 4.46464254 0.69635704 2.66466015
 H 2.12071784 -0.49548001 3.50256105
 H 3.22661849 -1.44617877 2.47467429
 H 4.25648341 3.18652066 1.62338261
 H 2.32948664 1.28950851 -1.73772085
 H 3.95415210 5.40452401 0.55397130
 H 2.81946089 5.58148029 -1.66741296
 H 2.00710190 3.50530937 -2.80641798
 H 5.99191812 1.88022956 0.34928371
 H 8.15214325 0.82358362 -0.26622428
 H 8.24412008 -1.61302658 -0.82683528
 H 6.14586644 -2.97227951 -0.75594739
 H 3.98748094 -1.90423367 -0.13358781
 H -4.75157680 1.84746405 0.63978398
 C -4.84391613 0.77292999 0.78888552
 H -3.46026883 5.25677133 -0.65131070
 H -6.95643619 0.79509575 1.23422525
 C -6.06863413 0.17243432 1.11487051
 O -2.49229749 0.60654926 0.38522854
 C -3.71415341 -0.04038010 0.63467998
 C -3.80680628 4.34369200 -1.13760400
 O -0.42800375 1.34504731 -0.77917703
 H -1.86541364 3.35734190 -1.01986749
 C -6.15262215 -1.21971322 1.28186022
 C -2.90260163 3.29021917 -1.34154778
 H 0.10290096 1.08323889 0.03446157
 C -3.77203463 -1.42944646 0.79947188
 H -5.83768445 5.05701828 -1.39564989
 C -5.14210668 4.23296267 -1.55799190
 H -7.10706801 -1.68278528 1.53586541
 P -1.63937333 0.32572701 -0.99563951
 C -5.00523585 -2.01326828 1.12320740
 H -2.86950241 -2.02377392 0.68601375
 C -3.36287552 2.11755305 -1.95739807
 O -1.33767978 -1.09523050 -1.30721857
 H -5.06191831 -3.09397483 1.26000940
 C -5.57605174 3.05823710 -2.19371046
 O -2.52380926 1.01856068 -2.18441074
 C -4.68804731 1.99281138 -2.39451481
 H -6.61081333 2.96384664 -2.52556734
 H -5.00603708 1.06106394 -2.85982590

• **Nonthermodynamic spiroketal + DPPA complex**

Geometry:

76

C -2.41356044 -2.45765902 3.77976650
 C -1.86078053 -3.53737745 3.07168681
 C -1.88492709 -1.17391116 3.60719382
 C -0.80715960 -0.95408002 2.73267423
 C -0.24706825 -2.03328102 2.02223234
 C -0.78581169 -3.32096387 2.20080439
 C -0.24121512 0.44529203 2.58840803
 O 0.68813055 0.58070280 1.49760900
 C 1.65341968 -0.52380311 1.34326948
 C 0.88655327 -1.80533474 1.04074517
 O 2.42669237 -0.16965296 0.23792876
 C 3.53261122 0.70554715 0.64707031
 C 3.46520501 0.71697688 2.21504282
 C 2.62460083 -0.52829816 2.52893339
 C 3.31748243 2.08108783 0.01395243
 C 3.77020223 3.25179843 0.64928738
 C 2.69605877 2.18710640 -1.24440957
 C 3.59849208 4.50687348 0.04563008
 C 2.96308306 4.60587099 -1.20073870
 C 2.51023616 3.44127150 -1.84068837
 C 4.84301858 0.05492131 0.17178895
 C 6.02795643 0.81448226 0.12344618
 C 7.24534272 0.21778430 -0.22989622

Mulliken charges:

1 C -0.136152
 2 C -0.141537
 3 C -0.152591
 4 C 0.017134
 5 C 0.062567
 6 C -0.171448
 7 C -0.014856
 8 O -0.591562
 9 C 0.505552
 10 C -0.294645
 11 O -0.565058
 12 C 0.182024
 13 C -0.255480
 14 C -0.245037
 15 C 0.066507

16 C	-0.161638	C	-1.60902491	-3.06119886	4.09746068
17 C	-0.132622	C	-1.00011324	-2.57632509	2.92763910
18 C	-0.147442	C	-0.30141584	-3.46142562	2.08685022
19 C	-0.136928	C	-0.21397458	-4.82068134	2.43233369
20 C	-0.141730	C	-1.15014171	-1.11412428	2.55107561
21 C	0.078312	O	-0.34718025	-0.69464437	1.42726911
22 C	-0.142567	C	-0.27802688	-1.60533190	0.36942710
23 C	-0.144777	C	0.34988495	-2.93183695	0.82888701
24 C	-0.136623	O	0.47903034	-0.19279563	-3.58158375
25 C	-0.142662	C	0.52480861	0.85080234	-2.59169886
26 C	-0.149443	C	-0.13692493	0.34293501	-1.28143594
27 H	0.139486	C	0.48782536	-0.96612168	-0.78356911
28 H	0.138581	C	-0.18746678	2.10400544	-3.14280755
29 H	0.135429	C	-0.99398429	2.94321711	-2.35397065
30 H	0.136095	C	-0.01670193	2.42105150	-4.50455632
31 H	0.142857	C	-1.62701512	4.06502968	-2.91475139
32 H	0.169417	C	-1.46113049	4.36419379	-4.27412010
33 H	0.140851	C	-0.64754853	3.53726349	-5.06770685
34 H	0.194326	C	2.00411314	1.16480003	-2.32289178
35 H	0.145491	C	2.33673627	2.29086616	-1.54655665
36 H	0.146898	C	3.67065881	2.56493429	-1.21948509
37 H	0.143849	C	4.69409378	1.71442208	-1.66903383
38 H	0.145938	C	4.36911842	0.59161214	-2.44367764
39 H	0.130646	C	3.03115475	0.31440842	-2.76739503
40 H	0.154866	H	-1.97891919	-4.77941345	5.35868090
41 H	0.136558	H	-0.73369717	-6.35741456	3.86242083
42 H	0.136849	H	-2.16237109	-2.37327637	4.74117567
43 H	0.143125	H	0.31335456	-5.50415636	1.76452314
44 H	0.128428	H	-0.83477511	-0.46292741	3.37917023
45 H	0.138570	H	-2.20992451	-0.90104033	2.32824456
46 H	0.137442	H	1.41404563	-2.71081136	1.01225677
47 H	0.138232	H	0.31111365	-3.66750254	0.01491466
48 H	0.135823	H	-1.20860962	0.19283873	-1.47548063
49 H	0.144339	H	-0.04588885	1.10436217	-0.49652276
50 C	-0.127589	H	1.51704971	-0.79025943	-0.44065279
51 H	0.146242	H	0.52753858	-1.69986883	-1.59861889
52 H	0.141864	H	-1.15051401	2.72038298	-1.29976772
53 C	-0.153563	H	0.60287671	1.76550933	-5.11548620
54 O	-0.638195	H	-2.25263363	4.70099892	-2.28574439
55 C	0.281664	H	-1.95419126	5.23441644	-4.71022643
56 C	-0.153342	H	-0.50447727	3.76443406	-6.12564542
57 O	-0.617053	H	1.54178639	2.95869774	-1.21301100
58 H	0.169714	H	3.91186702	3.44307203	-0.61818431
59 C	-0.134091	H	5.73443581	1.92708120	-1.41762882
60 C	-0.142941	H	5.15762750	-0.07544834	-2.79660255
61 H	0.410621	H	2.77567865	-0.56001220	-3.36151211
62 C	-0.101395	H	-3.49794039	-7.97371263	2.11875497
63 H	0.140428	H	-3.13479943	-5.49137897	2.12534006
64 C	-0.137195	C	-3.41905969	-7.43306299	1.17446989
65 H	0.137790	O	-1.70904704	-1.80734211	-0.05769589
66 P	1.279203	C	-3.22333466	-6.04553746	1.19331243
67 C	-0.154870	H	-0.46047775	-0.40998398	-3.70526876
68 H	0.154278	C	-3.50899401	-8.12262228	-0.04535505
69 C	0.295198	C	-3.12091241	-5.35684777	-0.02279035
70 O	-0.563552	H	-4.26712044	0.14459445	-1.30586844
71 H	0.141853	O	-2.96378402	-3.96952890	0.09343806
72 C	-0.147210	H	-3.65767973	-9.20286328	-0.05622724
73 O	-0.605544	P	-2.22874958	-3.00421134	-0.99088125
74 C	-0.138911	O	-3.55780173	-2.33072018	-1.67341028
75 H	0.145565	C	-3.82778143	-0.02437412	-2.28796404
76 H	0.159638	C	-3.40706497	-7.41305527	-1.25149364
		C	-3.21687440	-6.02271440	-1.25321129
		C	-3.37060555	-1.30625013	-2.61725146
		O	-1.25930718	-3.63805016	-1.92631408
		H	-4.01154821	2.01817390	-2.97116220
		C	-3.68766233	1.00988211	-3.22522468
		H	-3.47712304	-7.93890097	-2.20457906
		H	-3.12636668	-5.47361819	-2.18781158
		C	-2.78282731	-1.58042036	-3.86132477
		H	-2.42657959	-2.58591590	-4.07560598

• Phosphate intermediate + DPPA complex

Geometry:

76

C	-1.50975622	-4.41574645	4.44336469
C	-0.80579551	-5.29932742	3.60820304

C	-3.09898505	0.76043561	-4.47420538
C	-2.65210287	-0.53306076	-4.78977974
H	-2.96154116	1.57503778	-5.18341049
H	-2.18972302	-0.73056498	-5.75775919

Mulliken charges:

1 C	-0.143431
2 C	-0.144272
3 C	-0.162157
4 C	0.017795
5 C	0.067244
6 C	-0.160130
7 C	-0.003889
8 O	-0.528312
9 C	0.480574
10 C	-0.303471
11 O	-0.591763
12 C	0.178322
13 C	-0.223629
14 C	-0.234694
15 C	0.065783
16 C	-0.154365
17 C	-0.140051
18 C	-0.152872
19 C	-0.139000
20 C	-0.146754
21 C	0.069009
22 C	-0.141739
23 C	-0.146950
24 C	-0.138351
25 C	-0.143179
26 C	-0.151765
27 H	0.138824
28 H	0.138701
29 H	0.134503
30 H	0.139393
31 H	0.156763
32 H	0.156820
33 H	0.166506
34 H	0.165396
35 H	0.120888
36 H	0.134910
37 H	0.143657
38 H	0.155107
39 H	0.131263
40 H	0.143617
41 H	0.136599
42 H	0.137154
43 H	0.138304
44 H	0.124897
45 H	0.135908
46 H	0.134213
47 H	0.135491
48 H	0.149492
49 H	0.142315
50 H	0.147653
51 C	-0.150545
52 O	-0.593790
53 C	-0.132186
54 H	0.326528
55 C	-0.135302
56 C	0.305735
57 H	0.160379
58 O	-0.581103
59 H	0.139597
60 P	1.309101
61 O	-0.596993
62 C	-0.138628
63 C	-0.151676
64 C	-0.145187

65 C	0.295676
66 O	-0.606932
67 H	0.146742
68 C	-0.133630
69 H	0.146460
70 H	0.163202
71 C	-0.148237
72 H	0.173167
73 C	-0.105583
74 C	-0.184156
75 H	0.143589
76 H	0.157444

• **Syn Phosphate displacement TS (TS₆)**

Geometry:

76

C	-3.243645	-3.217351	3.437016
C	-2.488254	-4.225087	2.815165
C	-2.778285	-1.897670	3.435872
C	-1.565070	-1.582242	2.801062
C	-0.808108	-2.585929	2.177050
C	-1.274373	-3.909910	2.188431
C	-1.101765	-0.150497	2.741139
O	0.343347	-0.015394	2.483126
C	0.993940	-0.894299	1.784969
C	0.418785	-2.195171	1.388339
O	2.591828	-0.295752	-0.983587
C	3.437926	0.597582	-0.278547
C	2.934874	0.727895	1.206285
C	2.473045	-0.649220	1.747043
C	3.446992	1.983323	-0.959244
C	3.696174	3.173655	-0.248666
C	3.205668	2.057374	-2.343360
C	3.708164	4.412068	-0.906709
C	3.466689	4.477218	-2.286355
C	3.212612	3.293959	-3.000451
C	4.853445	-0.009973	-0.280237
C	5.932577	0.699329	0.282175
C	7.217051	0.144353	0.314027
C	7.445837	-1.136295	-0.221921
C	6.378128	-1.845490	-0.789939
C	5.090951	-1.288198	-0.819872
H	-4.192510	-3.458613	3.916087
H	-2.847913	-5.254571	2.811558
H	-3.360923	-1.107632	3.912517
H	-0.693651	-4.685201	1.687065
H	-1.233994	0.365320	3.700207
H	-1.590129	0.418204	1.936961
H	1.215696	-2.952566	1.386958
H	0.079308	-2.114342	0.312213
H	2.110050	1.449628	1.254305
H	3.750737	1.102444	1.837659
H	2.763773	-0.736270	2.809533
H	2.959695	-1.461989	1.196174
H	3.870846	3.142154	0.827245
H	2.982149	1.144635	-2.890294
H	3.896440	5.324616	-0.338190
H	3.466980	5.441117	-2.797787
H	3.001350	3.326551	-4.069618
H	5.766812	1.702529	0.676228
H	8.041451	0.711932	0.749823
H	8.447149	-1.569982	-0.201538
H	6.545266	-2.836241	-1.216164
H	4.263645	-1.829358	-1.273805
C	-3.872028	-1.610687	0.107178
H	-3.059350	-2.150917	0.582314
C	-5.154736	-2.163314	-0.003379
H	-5.345780	-3.153040	0.414766

C -6.183696 -1.456077 -0.646678
 H -7.180494 -1.892065 -0.728674
 C -5.922899 -0.188301 -1.192378
 C -4.643016 0.376619 -1.090788
 H -4.411574 1.355769 -1.508592
 H -6.715085 0.363001 -1.701718
 C -3.633464 -0.338807 -0.434022
 O -2.394742 0.288461 -0.257411
 P -1.027697 -0.283451 -0.999394
 O -1.033036 -1.794107 -1.129446
 O -1.234793 0.479771 -2.458926
 C -0.220079 0.496163 -3.413324
 C 0.667484 -0.577331 -3.611578
 H 0.587645 -1.469327 -2.993691
 C 1.648326 -0.474945 -4.609805
 H 2.344486 -1.301917 -4.754339
 C 1.741103 0.671635 -5.411859
 H 2.506974 0.741978 -6.185069
 C 0.838200 1.729347 -5.209870
 H 0.897834 2.627448 -5.826960
 C -0.141529 1.646777 -4.210637
 H -0.840282 2.462514 -4.027685
 O 0.142780 0.358429 -0.252238
 H 1.674466 0.058755 -0.844138

Mulliken charges:

1 C -0.138198
 2 C -0.134218
 3 C -0.143899
 4 C -0.007098
 5 C 0.070358
 6 C -0.156609
 7 C -0.039732
 8 O -0.415002
 9 C 0.513313
 10 C -0.394180
 11 O -0.635994
 12 C 0.201536
 13 C -0.245375
 14 C -0.298359
 15 C 0.060473
 16 C -0.160162
 17 C -0.118718
 18 C -0.148779
 19 C -0.139205
 20 C -0.133109
 21 C 0.070800
 22 C -0.145880
 23 C -0.147049
 24 C -0.139133
 25 C -0.143510
 26 C -0.153391

27 H 0.150928
 28 H 0.151178
 29 H 0.150046
 30 H 0.150185
 31 H 0.186479
 32 H 0.221961
 33 H 0.189905
 34 H 0.283449
 35 H 0.163685
 36 H 0.134352
 37 H 0.192522
 38 H 0.176088
 39 H 0.118838
 40 H 0.133356
 41 H 0.131780
 42 H 0.131693
 43 H 0.123975
 44 H 0.121296
 45 H 0.135517
 46 H 0.134208
 47 H 0.134453
 48 H 0.148653
 49 C -0.092324
 50 H 0.127727
 51 C -0.155837
 52 H 0.135254
 53 C -0.136451
 54 H 0.134568
 55 C -0.148855
 56 C -0.141768
 57 H 0.152571
 58 H 0.140215
 59 C 0.305086
 60 O -0.631458
 61 P 1.252448
 62 O -0.655887
 63 O -0.607340
 64 C 0.316428
 65 C -0.148079
 66 H 0.166713
 67 C -0.150583
 68 H 0.141041
 69 C -0.141704
 70 H 0.134428
 71 C -0.143466
 72 H 0.137159
 73 C -0.151616
 74 H 0.147691
 75 O -0.705735
 76 H 0.376349

C. Computational studies with (*R*) and (*S*)-**3-13a** (6,6-spiroketalization)

Model systems involving substrate **3-11a** and either (*R*) or (*S*)-**3-13a** catalysts were studied to determine the origin of enantioselectivity. Single-ended growing string runs employing an (*R*)-**3-12a**-catalyst complex as the initial structure were performed with varying driving coordinates according to the pathway explored. Double-ended growing string runs were also performed, using an (*R*)-**3-12a**-catalyst complex and a **3-11a**-catalyst complex (obtained by the optimization of the final node of the single-ended strings) as the endpoints. Due to the fact that very high accuracy is needed to discern enantiomeric pathways, the concerted pathway was thoroughly explored for both of the acid chiralities. 5 major different productive orientations of the catalyst with respect to the substrate were modeled, which could lead to either thermodynamic or nonthermodynamic spiroketals. In total, 188 strings were created (115 for the (*S*)-**3-13a** pathways, the rest for the (*R*) catalyst chirality), of which 155 were single-ended. Additionally, 44 strings were computed to investigate the mechanism involving an oxocarbenium intermediate. However, in the few strings where an apparent oxocarbenium was produced, the structure would collapse to either the enol ether or the spiroketal when its geometry optimization was performed.

After an initial survey of the results of strings from the five productive orientations mentioned, we decided to devote our attention to the favored orientation of the diphenyl hydrogen phosphate model. 86 of the strings constructed had an analogous catalyst-substrate orientation. As specified in the general information about the computational methods, the frequency calculations were performed at 238 K. A difference of 1.5 kcal/mol was found for the enantiomeric concerted pathways, in favor of the (*S*) chirality of the catalyst.

A summary of calculated values including solvent corrected single point energy values, as well as enthalpic and entropic corrections associated with vibrational energy at 238 K are provided

in the following table. The frequency calculation was run using partial Hessian calculations of the 41 most relevant atoms.

Table B.4. Calculated values for starting geometries, intermediates, and transition states concerted pathway for the [6,6]-spiroketalization catalyzed by **3-13**.

	G_{SMD} [kcal/mol] ^a	H_{vib} [kcal/mol] ^b	S_{vib} [kcal/mol] ^b	ΔG [kcal/mol] ^c
Enol ether 3-11a + catalyst complex	-2225385.1	205.0	129.2	0.0
TS_R	-2225366.4	202.1	125.1	16.9
TS_S	-2225367.2	201.7	125.8	15.4
Nonthermodynamic spiroketal + (R)-3-13a complex	-2225395.2	205.8	123.7	-7.8
Nonthermodynamic spiroketal + (S)-3-13a complex	-2225395.4	205.3	126.5	-9.3

^a Solvent-corrected (dichloromethane) electronic energy (ωB97X-D/SMD/6-31G**). ^b Vibrational, rotational, and translational entropic and enthalpic contributions (B97-D/6-31G**) at 298.15 K. ^c Corrected free energy values at 298.15 K

Final corrected free energies, cartesian coordinates, and Mulliken charges for the starting geometry, transition states, and cyclized product are provided below.

• Enol ether 3-11a + catalyst complex

Corrected energy: -2225210.909 kcal/mol

Geometry:

159

C 0.30593744 -1.22546491 -0.28108028
 C 0.21481530 -1.37919451 -1.61863676
 C 0.85763515 -0.42749406 -2.59945462
 C 1.23901510 0.88166521 -1.88395984
 C 1.88892456 0.55755007 -0.53384571
 O 1.02553886 -0.21471925 0.32964652
 C -0.32423334 -2.13618930 0.74721629
 C -1.08991845 -1.44887489 1.92320890
 C -2.62538095 -1.33680977 1.79522436
 C -3.14936347 -0.23777355 0.83481254
 O -2.49473081 -0.45324530 -0.43656874
 H 0.15992160 -0.21632590 -3.41843422
 H 1.74971553 -0.88288330 -3.06569063
 O 0.33557538 1.48910112 -1.72577064
 H 1.93934313 1.48140358 -2.48587839
 H 2.12864023 1.46356248 0.04044558
 H 2.81907220 -0.01777617 -0.69514346
 H -3.03940419 -1.12854438 2.79347433
 H -3.04563766 -2.30276827 1.46843871
 H -0.98090120 -2.84652126 0.22375310
 H 0.49330766 -2.72607667 1.19715381
 C -2.70492809 1.13956761 1.34117082
 C -3.41289087 1.75630805 2.38783379
 H -4.31716255 1.28419908 2.77135019
 C -2.97984975 2.97877188 2.91934473
 H -3.54437753 3.44428578 3.72842765
 C -1.83525810 3.60898945 2.40402813
 H -1.50408376 4.56527997 2.81103257
 C -1.11978428 2.99308012 1.36792293
 H -0.22178439 3.46308504 0.96402688
 C -1.54554958 1.76189351 0.84706465
 H -0.95539531 1.27149731 0.08023284
 C -4.66971612 -0.30424047 0.60801736
 C -5.53385939 -1.02364702 1.45341648
 H -5.14447925 -1.52773864 2.33703137
 C -6.90445823 -1.11600629 1.16206544
 H -7.55939080 -1.67899406 1.82878133
 C -7.42294709 -0.50662457 0.01114183
 H -8.48415768 -0.59404956 -0.22612946
 C -6.56988517 0.22634466 -0.82760757
 H -6.95729931 0.72663948 -1.71307282
 C -5.20925351 0.34279048 -0.52212666
 H -4.56719839 0.94524298 -1.16066436
 H -0.90244556 -2.04306489 2.83028574
 H -0.65706848 -0.45695255 2.11050548
 H -0.38836943 -2.19861846 -2.00431565
 H -2.21925563 0.53415090 -1.59558053
 C -7.11525202 1.87377820 -4.64003882
 C -7.20757909 3.09424829 -3.69545982
 C -6.06857659 3.28525996 -2.68068923
 C -4.68597788 3.40562209 -3.01242170
 C -3.73103796 3.70267982 -2.00460315
 C -2.22688782 4.01815611 -2.16798757
 H -1.73211676 3.39152491 -1.40997505
 C -1.48155373 3.77114780 -3.49669627
 H -0.40373885 3.86617244 -3.29055410
 H -1.65563989 2.77642300 -3.91056562
 H -1.74111830 4.51865751 -4.25732394
 C -1.98097377 5.49696414 -1.76058109
 H -0.90147024 5.71636260 -1.76764643
 H -2.37616437 5.71823711 -0.75997232
 H -2.47134717 6.17253673 -2.47940981
 C -4.18473965 3.80107854 -0.66931933

H -3.45170630 3.98012370 0.11824125
 C -5.53165444 3.70048183 -0.31891379
 C -5.99656683 3.91845214 1.11353313
 H -5.09702071 4.01763256 1.73857526
 C -6.82339192 2.73504287 1.65337437
 H -6.24670139 1.80279845 1.63363797
 H -7.14313185 2.93655984 2.68825501
 H -7.72714994 2.57680165 1.04553237
 C -6.80240970 5.23341714 1.21379872
 H -6.20571986 6.08971328 0.86585676
 H -7.11538071 5.41939056 2.25335046
 H -7.70715331 5.17294579 0.58944004
 C -4.24714631 3.23098125 -4.43026948
 C -4.07599703 4.32311606 -5.26331033
 H -4.30898359 5.31792443 -4.88254862
 C -3.53022443 4.19582259 -6.56827319
 C -3.26427025 5.34609925 -7.36732282
 H -3.54222001 6.32581871 -6.97425528
 C -2.64653218 5.22594462 -8.60009827
 H -2.43943276 6.11238953 -9.20106731
 C -2.26019118 3.94352087 -9.07250675
 H -1.74443571 3.85299048 -10.02939806
 C -2.52166518 2.80467905 -8.32730224
 H -2.20921758 1.83279853 -8.70094757
 C -3.18431627 2.88777245 -7.06616199
 C -3.47669309 1.73103430 -6.25319550
 C -3.21969548 0.35589942 -6.75617840
 C -2.42904791 -0.52097225 -6.01866072
 O -1.93078803 -0.10305379 -4.77497192
 P -2.96209926 -0.02772228 -3.50889692
 O -2.14119620 0.92073596 -2.53711664
 O -3.44694006 -1.30556153 -2.91100919
 H -2.94000771 -1.16929209 -0.93409956
 O -4.21060549 0.83606678 -4.13162887
 C -1.99600154 -1.79024698 -6.49610626
 C -1.20238711 -2.67594070 -5.59611921
 C 0.19929122 -2.48956333 -5.45637635
 C 1.05706547 -1.59513610 -6.36564885
 H 2.05927875 -1.59095491 -5.90663595
 C 0.65773665 -0.10930064 -6.51807142
 H 1.50349970 0.43672696 -6.96381946
 H 0.41765935 0.35161003 -5.55263131
 H -0.20293151 0.01688291 -7.18635168
 C 1.20913944 -2.24517737 -7.76137938
 H 1.94543936 -1.68790176 -8.36228620
 H 1.54315241 -3.28971717 -7.67603773
 H 0.25024028 -2.22830762 -8.29878660
 C 0.89018159 -3.26295301 -4.50888467
 H 1.96698724 -3.12114233 -4.41219160
 C 0.23867663 -4.18753607 -3.68113723
 C 0.98888393 -5.04495551 -2.66925942
 C 2.17932344 -4.32911695 -2.00129459
 H 2.96669638 -4.10846525 -2.73880797
 H 2.62212855 -4.98105626 -1.23315951
 H 1.86268700 -3.38501645 -1.53584187
 C 1.46030935 -6.35317778 -3.34775473
 H 2.18412749 -6.12028843 -4.14460037
 H 1.95320034 -7.01421339 -2.61725803
 H 0.61552647 -6.89311044 -3.80041622
 H 0.26872940 -5.31724515 -1.87847802
 C -1.13728555 -4.37042813 -3.86660274
 H -1.65255928 -5.11324875 -3.25083754
 C -1.88395880 -3.64986509 -4.81931763
 C -3.33313362 -4.13110731 -5.02126766
 H -3.61927090 -4.58309515 -4.05819860
 C -4.46680078 -3.13745931 -5.36314795
 H -4.45547148 -2.26634529 -4.70278750
 H -4.43627647 -2.80497988 -6.40683826
 H -5.42407089 -3.66197810 -5.21461225
 C -3.31493580 -5.27097677 -6.07176429

H -2.58597581 -6.05026320 -5.80504958
H -3.04166516 -4.86701243 -7.05825380
H -4.31321533 -5.72895364 -6.15399904
C -2.38512466 -2.16565316 -7.76979927
H -2.05294605 -3.12503522 -8.16666354
C -3.27631295 -1.37055553 -8.54252142
C -3.75821615 -1.81743535 -9.80720087
H -3.39418230 -2.77079700 -10.19496556
C -4.68275131 -1.07240908 -10.51944461
C -5.17166515 0.14944456 -9.98430480
C -4.71121069 0.61937942 -8.76438182
H -5.09443646 1.55344193 -8.35839206
H -5.92070888 0.72037755 -10.53438930
H -5.04918485 -1.42936504 -11.48281325
C -3.74016777 -0.10988046 -8.01749517
C -3.94588015 1.94140527 -4.95560651
C -6.45563528 3.45724117 -1.34453476
H -7.51607636 3.39089281 -1.09188410
C -7.45758526 4.38578880 -4.50919607
H -6.62774110 4.57206175 -5.20374286
H -7.55847160 5.25542324 -3.84300768
H -8.38214965 4.28629713 -5.09985201
H -8.10998142 2.93289584 -3.08381578
H -6.41994903 2.05156599 -5.46955416
H -6.78934902 0.96954920 -4.10943333
H -8.10840136 1.68657079 -5.07714129

43 H 0.108986
44 H 0.120256
45 H 0.142290
46 H 0.109515
47 H 0.424802
48 C -0.368746
49 C -0.150172
50 C 0.116904
51 C -0.092922
52 C 0.119579
53 C -0.129590
54 H 0.118534
55 C -0.353972
56 H 0.110472
57 H 0.128266
58 H 0.112544
59 C -0.358779
60 H 0.116979
61 H 0.121506
62 H 0.118903
63 C -0.204985
64 H 0.104026
65 C 0.137601
66 C -0.148977
67 H 0.108773
68 C -0.349261
69 H 0.122940
70 H 0.112443
71 H 0.115276
72 C -0.360380
73 H 0.126215
74 H 0.119072
75 H 0.119912
76 C 0.010197
77 C -0.201928
78 H 0.149252
79 C 0.080047
80 C -0.164851
81 H 0.142218
82 C -0.143825
83 H 0.142559
84 C -0.146417
85 H 0.143346
86 C -0.150182
87 H 0.146439
88 C 0.031814
89 C 0.019885
90 C 0.010643
91 C 0.260318
92 O -0.643259
93 P 1.398427
94 O -0.649134
95 O -0.603269
96 H 0.366168
97 O -0.635977
98 C 0.009317
99 C -0.088591
100 C 0.119154
101 C -0.151042
102 H 0.117077
103 C -0.365475
104 H 0.118680
105 H 0.138236
106 H 0.118935
107 C -0.356408
108 H 0.120767
109 H 0.124302
110 H 0.118851
111 C -0.209930
112 H 0.108729

Mulliken charges:

1 C 0.375454
2 C -0.205757
3 C -0.234728
4 C -0.273643
5 C 0.015040
6 O -0.543401
7 C -0.270811
8 C -0.233237
9 C -0.216468
10 C 0.196494
11 O -0.625526
12 H 0.136746
13 H 0.111616
14 H 0.136216
15 H 0.125248
16 H 0.132755
17 H 0.125363
18 H 0.125802
19 H 0.123390
20 H 0.123474
21 H 0.134146
22 C 0.067874
23 C -0.135460
24 H 0.130386
25 C -0.145969
26 H 0.140676
27 C -0.140410
28 H 0.139514
29 C -0.146933
30 H 0.137742
31 C -0.108169
32 H 0.121617
33 C 0.034266
34 C -0.159708
35 H 0.130493
36 C -0.146087
37 H 0.137802
38 C -0.138051
39 H 0.137523
40 C -0.114323
41 H 0.129659
42 C -0.096545

113 C 0.122108
 114 C -0.151465
 115 C -0.369090
 116 H 0.116804
 117 H 0.119066
 118 H 0.128175
 119 C -0.356317
 120 H 0.122888
 121 H 0.121606
 122 H 0.125137
 123 H 0.118033
 124 C -0.218748
 125 H 0.112108
 126 C 0.138439
 127 C -0.146523
 128 H 0.124023
 129 C -0.376711
 130 H 0.154427
 131 H 0.111573
 132 H 0.112932
 133 C -0.352141
 134 H 0.121788
 135 H 0.113652
 136 H 0.121418
 137 C -0.199931
 138 H 0.148343
 139 C 0.077250
 140 C -0.166448
 141 H 0.142440
 142 C -0.143423
 143 C -0.145793
 144 C -0.150508
 145 H 0.147496
 146 H 0.144160
 147 H 0.142911
 148 C 0.021235
 149 C 0.236120
 150 C -0.217419
 151 H 0.110540
 152 C -0.358841
 153 H 0.120717
 154 H 0.123311
 155 H 0.120689
 156 H 0.116389
 157 H 0.119587
 158 H 0.141718
 159 H 0.119127

• TS_r

Geometry:
 159

C -0.121153 -0.209234 -0.158088
 C 0.363520 0.817809 -0.998971
 C 0.552352 2.211104 -0.391431
 C -0.581141 2.415726 0.628955
 C -0.517231 1.314159 1.678794
 O -0.518147 -0.030828 1.083480
 C -0.157451 -1.647272 -0.597859
 C -1.148095 -2.587425 0.124167
 C -2.622505 -2.517461 -0.324457
 C -3.466741 -1.285759 0.119506
 O -2.869990 -0.086848 -0.374099
 H 0.489724 2.965707 -1.187895
 H 1.536315 2.321295 0.096257
 H -1.546170 2.371734 0.107519
 H -0.514505 3.387967 1.137160
 H -1.386047 1.302370 2.347190
 H 0.408650 1.376731 2.270918

H -3.114874 -3.431329 0.034879
 H -2.666996 -2.549556 -1.419578
 H -0.305994 -1.681074 -1.686196
 H 0.864222 -2.022075 -0.406762
 C -3.572632 -1.116967 1.643118
 C -3.376240 -2.178726 2.549599
 H -3.110752 -3.167411 2.178570
 C -3.506880 -1.973892 3.937016
 H -3.344536 -2.806886 4.622902
 C -3.839532 -0.703117 4.437866
 H -3.938101 -0.544338 5.512563
 C -4.053040 0.361253 3.538219
 H -4.326664 1.349564 3.911587
 C -3.925906 0.151952 2.155613
 H -4.099958 0.964905 1.455773
 C -4.905643 -1.431179 -0.447522
 C -5.632046 -2.636975 -0.311545
 H -5.193617 -3.482174 0.219054
 C -6.931159 -2.758056 -0.837623
 H -7.471929 -3.699988 -0.731549
 C -7.532662 -1.667715 -1.493934
 H -8.540382 -1.760062 -1.901621
 C -6.824757 -0.458020 -1.616002
 H -7.279833 0.392885 -2.122285
 C -5.521219 -0.341130 -1.099887
 H -4.964989 0.586396 -1.218091
 H -0.802876 -3.609544 -0.095436
 H -1.066576 -2.446186 1.209936
 H 1.110451 0.459029 -1.718464
 H -0.490851 1.079219 -1.974552
 C -6.314503 2.468098 -3.817834
 C -6.058437 3.691920 -2.900292
 C -4.619598 3.949589 -2.410871
 C -3.491645 4.112855 -3.269476
 C -2.241546 4.549491 -2.741354
 C -0.999110 4.966379 -3.562093
 H -0.153258 4.901942 -2.853060
 C -0.567086 4.148855 -4.808134
 H 0.458205 4.459615 -5.074439
 H -0.558918 3.073793 -4.604099
 H -1.205428 4.345625 -5.677894
 C -1.143277 6.466820 -3.954919
 H -0.208538 6.827632 -4.416030
 H -1.373668 7.090809 -3.076530
 H -1.955715 6.583126 -4.688646
 C -2.148719 4.779527 -1.349735
 H -1.195549 5.121806 -0.938009
 C -3.235013 4.600289 -0.478845
 C -3.109234 4.936070 1.006033
 H -2.039219 5.112362 1.217617
 C -3.597137 3.788448 1.924770
 H -3.049102 2.859222 1.723132
 H -3.457118 4.062170 2.983600
 H -4.669093 3.592840 1.763039
 C -3.881837 6.245037 1.327846
 H -3.516298 7.078578 0.707703
 H -3.765152 6.514761 2.390760
 H -4.955487 6.107457 1.119008
 C -3.578632 3.756842 -4.718230
 C -3.737199 4.707225 -5.715606
 H -3.888552 5.750528 -5.441599
 C -3.622269 4.365552 -7.095096
 C -3.671337 5.368001 -8.112805
 H -3.855422 6.401389 -7.814185
 C -3.464158 5.040350 -9.446767
 H -3.495707 5.813942 -10.214493
 C -3.186669 3.691186 -9.810573
 H -2.991960 3.442541 -10.854211
 C -3.152748 2.690182 -8.846262
 H -2.936149 1.663721 -9.132580

C -3.393419 2.986451 -7.467798
C -3.396105 1.969927 -6.439672
C -3.384841 0.518479 -6.773271
C -2.484457 -0.343417 -6.142340
O -1.537250 0.194128 -5.243949
P -2.067006 0.555640 -3.728665
O -0.957525 1.440022 -3.126264
O -2.499578 -0.634205 -2.919314
H -2.747992 -0.241022 -1.349371
O -3.422700 1.441872 -4.068122
C -2.423237 -1.747072 -6.397246
C -1.606528 -2.619714 -5.498743
C -0.198002 -2.762479 -5.681970
C 0.572386 -2.284054 -6.927982
H 1.628045 -2.550874 -6.739438
C 0.562215 -0.761561 -7.224184
H 1.328106 -0.546834 -7.988589
H 0.781893 -0.173647 -6.323064
H -0.406848 -0.432908 -7.621824
C 0.136024 -3.076728 -8.192452
H 0.811302 -2.842070 -9.032734
H 0.168674 -4.162015 -8.006116
H -0.886844 -2.801490 -8.488587
C 0.539608 -3.496066 -4.730627
H 1.613854 -3.612968 -4.884292
C -0.066604 -4.089829 -3.609440
C 0.735664 -4.935202 -2.621990
C 2.064699 -4.268923 -2.189588
H 2.747187 -4.160665 -3.048312
H 2.572411 -4.887320 -1.431555
H 1.888229 -3.266491 -1.771586
C 1.011530 -6.340655 -3.224494
H 1.628819 -6.247260 -4.133475
H 1.548621 -6.976598 -2.500614
H 0.067128 -6.834874 -3.501272
H 0.111693 -5.074841 -1.719335
C -1.457971 -3.968218 -3.475239
H -1.949804 -4.453601 -2.629242
C -2.256704 -3.255608 -4.399056
C -3.782081 -3.382048 -4.163955
H -3.885512 -3.570692 -3.081502
C -4.750999 -2.211459 -4.468651
H -4.400623 -1.271528 -4.036377
H -4.924086 -2.077874 -5.542900
H -5.718904 -2.455293 -4.000732
C -4.285274 -4.664167 -4.893578
H -3.670547 -5.540336 -4.631708
H -4.240936 -4.521132 -5.985213
H -5.333268 -4.864338 -4.614681
C -3.234016 -2.259659 -7.399316
H -3.188943 -3.323876 -7.627541
C -4.206588 -1.452587 -8.059844
C -5.117085 -2.022539 -9.002683
H -4.995065 -3.073991 -9.268572
C -6.150899 -1.267443 -9.543161
C -6.320467 0.088260 -9.141571
C -5.438663 0.677543 -8.241779
H -5.588673 1.708613 -7.932523
H -7.155954 0.668100 -9.534913
H -6.844707 -1.714467 -10.255633
C -4.339074 -0.056991 -7.697526
C -3.423086 2.389893 -5.104769
C -4.462994 4.193499 -1.031220
H -5.333188 4.086348 -0.380816
C -6.625723 4.978328 -3.567619
H -6.116628 5.167462 -4.525152
H -6.484005 5.854325 -2.914681
H -7.703316 4.855525 -3.768522
H -6.654112 3.518270 -1.985630
H -5.969668 2.650741 -4.844888

H -5.820116 1.563836 -3.443364
H -7.401738 2.285885 -3.860149

Mulliken charges:

1 C 0.516579
2 C -0.439715
3 C -0.235818
4 C -0.270985
5 C 0.013874
6 O -0.457897
7 C -0.312222
8 C -0.222754
9 C -0.239569
10 C 0.185837
11 O -0.647567
12 H 0.145310
13 H 0.130038
14 H 0.166689
15 H 0.137004
16 H 0.161937
17 H 0.152545
18 H 0.108312
19 H 0.150403
20 H 0.178247
21 H 0.165956
22 C 0.106381
23 C -0.160952
24 H 0.121947
25 C -0.148881
26 H 0.134486
27 C -0.142159
28 H 0.133546
29 C -0.146485
30 H 0.132098
31 C -0.139470
32 H 0.135675
33 C 0.073691
34 C -0.152624
35 H 0.122004
36 C -0.146557
37 H 0.132714
38 C -0.142425
39 H 0.132426
40 C -0.129946
41 H 0.126504
42 C -0.146395
43 H 0.134708
44 H 0.122151
45 H 0.132793
46 H 0.181760
47 H 0.376804
48 C -0.363081
49 C -0.156576
50 C 0.118749
51 C -0.076563
52 C 0.136160
53 C -0.146458
54 H 0.113780
55 C -0.376835
56 H 0.108740
57 H 0.159870
58 H 0.115173
59 C -0.352254
60 H 0.121298
61 H 0.120235
62 H 0.115643
63 C -0.221683
64 H 0.105355
65 C 0.126520
66 C -0.157046

67 H 0.109902
68 C -0.356862
69 H 0.121075
70 H 0.119778
71 H 0.127246
72 C -0.358693
73 H 0.129093
74 H 0.121433
75 H 0.124704
76 C -0.005196
77 C -0.196541
78 H 0.145693
79 C 0.069916
80 C -0.165772
81 H 0.140226
82 C -0.145279
83 H 0.141061
84 C -0.146210
85 H 0.142615
86 C -0.150733
87 H 0.146645
88 C 0.020119
89 C 0.011442
90 C 0.014396
91 C 0.251634
92 O -0.635541
93 P 1.361994
94 O -0.656930
95 O -0.655060
96 H 0.388997
97 O -0.648845
98 C 0.014039
99 C -0.094511
100 C 0.121050
101 C -0.156593
102 H 0.115051
103 C -0.356585
104 H 0.114233
105 H 0.139655
106 H 0.119892
107 C -0.359736
108 H 0.119879
109 H 0.122370
110 H 0.121660
111 C -0.228040
112 H 0.109807
113 C 0.119926
114 C -0.154524
115 C -0.363709
116 H 0.125629
117 H 0.123470
118 H 0.116136
119 C -0.357626
120 H 0.124798
121 H 0.121537
122 H 0.129362
123 H 0.114015
124 C -0.218671
125 H 0.107060
126 C 0.159392
127 C -0.135928
128 H 0.111844
129 C -0.363846
130 H 0.148006
131 H 0.106939
132 H 0.109774
133 C -0.355250
134 H 0.117273
135 H 0.113102
136 H 0.122132

137 C -0.198140
138 H 0.146332
139 C 0.067845
140 C -0.166435
141 H 0.140481
142 C -0.142152
143 C -0.146880
144 C -0.150098
145 H 0.146266
146 H 0.142191
147 H 0.141145
148 C 0.030982
149 C 0.277261
150 C -0.218701
151 H 0.114843
152 C -0.356752
153 H 0.120361
154 H 0.122661
155 H 0.121440
156 H 0.117904
157 H 0.118539
158 H 0.145822
159 H 0.114745

• TS_s

Geometry:

159

C 0.986716 1.139248 3.987094
C 0.633099 2.206843 3.162063
C -0.813991 2.701312 3.172427
C -1.715920 1.479941 3.429589
C -1.288494 0.834054 4.742537
O 0.128596 0.464633 4.746431
C 2.423123 0.739918 4.247893
C 2.671738 -0.715262 4.724310
C 2.659980 -1.812621 3.634721
C 1.322731 -2.026292 2.880071
O 1.040578 -0.744540 2.343058
H -1.058221 3.155690 2.202980
H -0.981329 3.468401 3.949123
H -1.608082 0.753878 2.611356
H -2.777730 1.753454 3.494925
H -1.808749 -0.104268 4.958697
H -1.424859 1.532973 5.583701
H 2.985080 -2.766590 4.076219
H 3.396131 -1.555108 2.861601
H 3.001331 0.955959 3.338847
H 2.779322 1.426537 5.036935
C 0.150820 -2.496970 3.767122
C 0.327847 -3.056177 5.050043
H 1.328631 -3.150527 5.469930
C -0.777577 -3.494933 5.807475
H -0.616803 -3.915320 6.801574
C -2.078867 -3.402298 5.283204
H -2.933322 -3.753507 5.863390
C -2.266158 -2.862256 3.994455
H -3.264333 -2.796491 3.561986
C -1.164585 -2.410445 3.249034
H -1.330673 -2.003916 2.253696
C 1.551713 -3.030205 1.728155
C 1.408621 -4.423685 1.904760
H 1.082735 -4.812956 2.869657
C 1.653814 -5.307841 0.837564
H 1.530199 -6.381658 0.987364
C 2.048429 -4.811877 -0.420907
H 2.232855 -5.498146 -1.248843
C 2.208740 -3.425747 -0.594020
H 2.542882 -2.994006 -1.533949

C 1.964226 -2.543349 0.470660
H 2.106364 -1.476664 0.321613
H 3.671926 -0.731910 5.185795
H 1.949898 -0.955768 5.515502
H 1.441253 2.923685 2.983335
H 0.643721 1.720370 1.762322
P -0.270558 0.721277 -0.205883
O 0.504176 1.796400 0.610266
O -1.448252 1.597364 -0.939800
C -2.021129 1.068091 -2.114587
C -3.312609 0.476578 -2.002521
C -3.888229 0.140778 -0.662956
C -4.477497 1.127132 0.182705
C -4.619169 2.637818 -0.110099
H -5.594028 2.916896 0.332091
C -3.543158 3.455190 0.662184
H -3.749247 4.534371 0.563125
H -3.551129 3.193329 1.731810
H -2.544329 3.246133 0.260159
C -4.680539 3.094852 -1.587431
H -5.047687 4.134456 -1.616169
H -5.362278 2.466453 -2.179473
H -3.692960 3.077305 -2.068344
C -5.003601 0.725207 1.428967
H -5.471364 1.482084 2.062477
C -4.963163 -0.607268 1.869490
C -5.565199 -1.013131 3.213379
C -4.812070 -0.347889 4.393694
H -4.926686 0.747867 4.345103
H -5.216096 -0.695410 5.359044
H -3.741744 -0.590260 4.350103
C -7.078696 -0.677885 3.279788
H -7.230346 0.410170 3.190914
H -7.503928 -1.008853 4.241724
H -7.626615 -1.169720 2.460707
H -5.455939 -2.108262 3.313251
C -4.369064 -1.556521 1.025357
H -4.332646 -2.599307 1.350005
C -3.827927 -1.224279 -0.236008
C -3.292229 -2.437919 -1.038610
H -3.020757 -3.176504 -0.262718
C -2.023256 -2.299045 -1.918876
H -1.217987 -1.789435 -1.381478
H -2.216485 -1.779893 -2.865965
H -1.674643 -3.316583 -2.164876
C -4.443561 -3.081421 -1.865728
H -5.336954 -3.246929 -1.242236
H -4.722690 -2.435322 -2.711625
H -4.110570 -4.050495 -2.273722
C -3.959593 0.120664 -3.177875
H -4.965996 -0.291680 -3.125657
C -3.312382 0.208156 -4.444516
C -1.947703 0.688097 -4.518477
C -1.271420 0.602539 -5.775789
H -0.229840 0.906533 -5.837514
C -1.923686 0.132724 -6.910063
C -3.284783 -0.282466 -6.846983
H -3.785081 -0.641991 -7.746500
H -1.384565 0.074326 -7.856059
C -3.959364 -0.251343 -5.633664
H -4.991213 -0.598595 -5.559136
C -1.321014 1.191486 -3.316148
C 0.065283 1.737211 -3.318544
C 0.475976 2.784533 -4.223670
C 1.879033 3.123804 -4.316678
C 2.291623 4.148387 -5.224364
H 3.354498 4.388331 -5.288105
C 1.361396 4.837366 -5.992074
H 1.686091 5.622770 -6.675117
C -0.025101 4.530026 -5.873471

H -0.754501 5.090848 -6.458462
C 2.817565 2.454358 -3.478408
H 3.874397 2.708570 -3.559697
C 2.412726 1.541220 -2.514841
C 3.365494 0.873437 -1.572679
C 3.677811 1.468671 -0.316688
C 3.402019 2.921693 0.148151
H 2.988482 2.825609 1.168344
C 2.436523 3.843929 -0.635633
H 2.242030 4.732525 -0.010930
H 1.477027 3.369394 -0.857480
H 2.887960 4.189261 -1.576211
C 4.770463 3.664862 0.263826
H 4.618060 4.675389 0.678132
H 5.479804 3.121306 0.905742
H 5.221376 3.764299 -0.737476
C 4.403241 0.698084 0.621978
H 4.612558 1.132505 1.602548
C 4.889148 -0.585718 0.342278
C 5.730744 -1.324886 1.382041
H 5.435791 -0.938039 2.375305
C 5.517780 -2.857117 1.382513
H 4.454707 -3.116119 1.482149
H 6.078823 -3.312191 2.215058
H 5.890495 -3.302643 0.445826
C 7.234758 -0.988106 1.178533
H 7.402538 0.099757 1.225522
H 7.848327 -1.478500 1.952764
H 7.570134 -1.344494 0.190095
C 4.644690 -1.112539 -0.938550
H 5.033550 -2.098144 -1.190908
C 3.872824 -0.425839 -1.896581
C 3.726725 -1.117705 -3.271603
C 4.614721 -0.423174 -4.342035
H 4.204613 0.564609 -4.598125
H 5.644217 -0.292649 -3.972667
H 4.641704 -1.033138 -5.260711
C 2.286964 -1.319211 -3.822472
H 1.890184 -0.391467 -4.254201
H 1.596920 -1.655226 -3.036457
H 2.312317 -2.078111 -4.621973
H 4.141061 -2.131728 -3.129060
C -0.456637 3.528043 -5.012058
H -1.517039 3.302637 -4.922347
C 1.024048 1.216313 -2.440404
O -0.775524 -0.497117 0.510676
H 0.301297 -0.790767 1.686073
O 0.640324 0.236857 -1.495950

Mulliken charges:

1 C 0.537279
2 C -0.464744
3 C -0.226617
4 C -0.269280
5 C 0.022040
6 O -0.493097
7 C -0.283040
8 C -0.233941
9 C -0.201618
10 C 0.188301
11 O -0.634903
12 H 0.139903
13 H 0.125035
14 H 0.151778
15 H 0.131560
16 H 0.151539
17 H 0.142026
18 H 0.116419
19 H 0.120497
20 H 0.146940

21 H	0.152539	91 C	-0.190590
22 C	0.104878	92 H	0.146453
23 C	-0.160760	93 C	0.070221
24 H	0.124227	94 C	0.035335
25 C	-0.151483	95 C	-0.151299
26 H	0.134105	96 H	0.145742
27 C	-0.144654	97 C	-0.147492
28 H	0.132818	98 C	-0.143731
29 C	-0.134395	99 H	0.142205
30 H	0.119500	100 H	0.143090
31 C	-0.161100	101 C	-0.165369
32 H	0.145068	102 H	0.141418
33 C	0.043809	103 C	0.018162
34 C	-0.149634	104 C	0.008169
35 H	0.125292	105 C	0.021161
36 C	-0.149506	106 C	0.077534
37 H	0.132260	107 C	-0.166426
38 C	-0.145280	108 H	0.141595
39 H	0.131317	109 C	-0.144094
40 C	-0.116354	110 H	0.142390
41 H	0.112824	111 C	-0.145855
42 C	-0.126587	112 H	0.143808
43 H	0.129818	113 C	-0.200528
44 H	0.122190	114 H	0.147941
45 H	0.134236	115 C	0.001699
46 H	0.158349	116 C	-0.080760
47 H	0.399261	117 C	0.121162
48 P	1.403765	118 C	-0.133016
49 O	-0.641377	119 H	0.114055
50 O	-0.633471	120 C	-0.354458
51 C	0.241452	121 H	0.110163
52 C	0.007206	122 H	0.139564
53 C	-0.086063	123 H	0.111106
54 C	0.107646	124 C	-0.359598
55 C	-0.149976	125 H	0.119991
56 H	0.121468	126 H	0.119687
57 C	-0.361987	127 H	0.122091
58 H	0.116405	128 C	-0.205102
59 H	0.112404	129 H	0.107937
60 H	0.150866	130 C	0.120385
61 C	-0.367373	131 C	-0.148955
62 H	0.119037	132 H	0.111568
63 H	0.123252	133 C	-0.364628
64 H	0.126459	134 H	0.134867
65 C	-0.210695	135 H	0.119138
66 H	0.108939	136 H	0.120493
67 C	0.128701	137 C	-0.359458
68 C	-0.157375	138 H	0.124246
69 C	-0.351852	139 H	0.122153
70 H	0.117712	140 H	0.124807
71 H	0.122186	141 C	-0.210023
72 H	0.118984	142 H	0.113370
73 C	-0.363559	143 C	0.111715
74 H	0.122250	144 C	-0.149125
75 H	0.122551	145 C	-0.359914
76 H	0.130903	146 H	0.119646
77 H	0.115407	147 H	0.123764
78 C	-0.225868	148 H	0.121789
79 H	0.112150	149 C	-0.368488
80 C	0.145535	150 H	0.118765
81 C	-0.148963	151 H	0.142608
82 H	0.126425	152 H	0.120372
83 C	-0.372550	153 H	0.117782
84 H	0.152632	154 C	-0.151045
85 H	0.111689	155 H	0.147193
86 H	0.113930	156 C	0.262417
87 C	-0.353508	157 O	-0.646135
88 H	0.119391	158 H	0.387838
89 H	0.112457	159 O	-0.649771
90 H	0.122265		

• Nonthermodynamic spiroketal + (R)-3-13a

Geometry:

159

C -1.18819304 1.04024598 0.05562871
 C -1.34193568 2.36790725 -0.69066380
 C -0.32914301 3.40326347 -0.16808312
 C -0.48498535 3.56997221 1.35309683
 C -0.35724975 2.19366335 2.01729890
 O -1.29468266 1.25590134 1.46763707
 C 0.08209006 0.25417643 -0.30855141
 C 0.06356343 -1.13123899 0.35525330
 C -1.20859427 -1.89525218 -0.05846134
 C -2.48835580 -1.09918939 0.28894148
 O -2.35509760 0.25046811 -0.30817052
 H -0.48234262 4.35566821 -0.69165483
 H 0.69488970 3.06725765 -0.39880649
 H -1.47757784 3.98930369 1.58117885
 H 0.27749942 4.25055390 1.76510032
 H -0.59292455 2.22548364 3.08985884
 H 0.67677660 1.81809525 1.89906902
 H -1.24289909 -2.88456523 0.41642881
 H -1.20988312 -2.06805171 -1.14318856
 H 0.11901366 0.16650060 -1.40302095
 H 0.96736690 0.82834838 -0.00244040
 C -2.80909498 -0.99494350 1.79290303
 C -2.18187723 -1.79099144 2.76239278
 H -1.38601958 -2.47911192 2.48171961
 C -2.55768441 -1.70076032 4.11378358
 H -2.05316512 -2.32428150 4.85376228
 C -3.56781612 -0.81503515 4.50938864
 H -3.85842385 -0.74487737 5.55868317
 C -4.20882262 -0.02337723 3.54028062
 H -5.00069783 0.66873158 3.83182715
 C -3.83738734 -0.12095423 2.19761426
 H -4.33080633 0.49381319 1.44776986
 C -3.74818819 -1.71232774 -0.34154127
 C -3.99272705 -3.08740419 -0.16023042
 H -3.24415194 -3.70486049 0.33513482
 C -5.20198351 -3.66095148 -0.57236743
 H -5.37138861 -4.72836830 -0.42470148
 C -6.19439886 -2.86327653 -1.16416717
 H -7.13988494 -3.30586180 -1.47982942
 C -5.95385940 -1.49603612 -1.35426940
 H -6.70730597 -0.86613879 -1.82794690
 C -4.73876839 -0.92304783 -0.95218045
 H -4.56275530 0.13960223 -1.10566666
 H 0.95406181 -1.70485172 0.06168342
 H 0.08875264 -1.00698110 1.44673223
 H -1.19928490 2.22557741 -1.76297462
 H -2.36205593 2.72502629 -0.51717634
 C -6.00535651 1.46515119 -3.87870467
 C -6.05801346 3.00884466 -3.81328646
 C -4.88512028 3.65607881 -3.04889483
 C -3.65033898 4.09305723 -3.61404139
 C -2.73056902 4.83776010 -2.82818917
 C -1.42098937 5.47301458 -3.32403438
 H -0.82321427 5.63425919 -2.41135304
 C -0.52118880 4.64690754 -4.26747022
 H 0.48538368 5.09362099 -4.26329238
 H -0.43629455 3.60392859 -3.94321818
 H -0.88215872 4.65759710 -5.30272313
 C -1.67807989 6.88419224 -3.90625593
 H -0.71773721 7.39040940 -4.09167064
 H -2.27286248 7.49950792 -3.21474339
 H -2.21362737 6.82346013 -4.86349522
 C -3.04425240 5.07104980 -1.47469886
 H -2.33957556 5.63996205 -0.86403818
 C -4.19056081 4.55244406 -0.86469728
 C -4.44441738 4.72549033 0.62643791

H -3.57386687 5.25234913 1.05259558
 C -4.57166724 3.35873161 1.33865196
 H -3.65727355 2.75969898 1.24029824
 H -4.77601196 3.50145754 2.41126392
 H -5.40505959 2.78296297 0.90752451
 C -5.70024462 5.58758399 0.88067486
 H -5.61268767 6.56773166 0.38944684
 H -5.84989803 5.74368015 1.96012757
 H -6.59403700 5.08412134 0.48119546
 C -3.32624694 3.70328664 -5.01986003
 C -3.36482974 4.60194197 -6.07248613
 H -3.62137688 5.64116058 -5.87371677
 C -3.07922716 4.20171770 -7.40552888
 C -2.99861024 5.15095339 -8.46617213
 H -3.16145389 6.20485007 -8.23293604
 C -2.70085651 4.74868331 -9.75732622
 H -2.63125401 5.48490680 -10.55915071
 C -2.46879544 3.37460614 -10.03637244
 H -2.20948432 3.06476939 -11.04954054
 C -2.56272737 2.42478684 -9.03191948
 H -2.38206064 1.37376446 -9.24990555
 C -2.87973953 2.80311805 -7.69434732
 C -2.98564251 1.84064220 -6.62680221
 C -3.13598810 0.38325225 -6.90704694
 C -2.39564853 -0.58363267 -6.23376390
 O -1.37007877 -0.20435021 -5.36636150
 P -1.58176510 0.61413375 -3.98412190
 O -0.35327178 1.38270707 -3.65474474
 O -2.09513944 -0.44436663 -2.91162840
 H -2.20248308 -0.08738717 -1.97770394
 O -2.97390913 1.45813800 -4.23773038
 C -2.54510837 -1.98792962 -6.43047697
 C -1.90200759 -2.90609624 -5.44313844
 C -0.54433998 -3.30898135 -5.56465611
 C 0.30014662 -3.11756266 -6.83055155
 H 1.29925012 -3.51120539 -6.58033409
 C 0.51905781 -1.66518795 -7.30752497
 H 1.29296009 -1.66013503 -8.09133328
 H 0.84564818 -1.01429061 -6.48661994
 H -0.39394851 -1.23888715 -7.74188537
 C -0.23846731 -3.99039504 -7.98901879
 H 0.47335458 -3.98071771 -8.82963718
 H -0.38225793 -5.03141415 -7.66350925
 H -1.20037801 -3.60601451 -8.35700470
 C 0.04243926 -4.01173066 -4.50073675
 H 1.08719757 -4.31844741 -4.58758362
 C -0.66537317 -4.32423528 -3.32972401
 C 0.00696403 -5.05022859 -2.17422464
 C 1.25141899 -4.28386258 -1.67848676
 H 2.03076987 -4.26567265 -2.45578736
 H 1.67610400 -4.76203272 -0.78186925
 H 0.99518514 -3.24351847 -1.43738508
 C 0.37465782 -6.49874572 -2.56431771
 H 1.09132852 -6.49893744 -3.40030639
 H 0.83583478 -7.02768926 -1.71547553
 H -0.51765416 -7.05663582 -2.88447131
 H -0.72006939 -5.09385993 -1.34515296
 C -2.01439522 -3.96635155 -3.26378912
 H -2.58768505 -4.22552551 -2.37086905
 C -2.66080168 -3.25951631 -4.29714371
 C -4.16790817 -3.03262677 -4.09486983
 H -4.32377514 -3.12987471 -3.01406004
 C -4.79979566 -1.67718550 -4.46647073
 H -4.23058628 -0.84315057 -4.04900017
 H -4.91415994 -1.53191972 -5.54472997
 H -5.80500876 -1.64480309 -4.02247894
 C -4.95244345 -4.18401171 -4.76636357
 H -4.57960886 -5.16456466 -4.43417352
 H -4.85539312 -4.12956206 -5.86069858
 H -6.02206133 -4.10905645 -4.51332428

C -3.40445336 -2.41080511 -7.42621169
 H -3.52134286 -3.47804162 -7.61362939
 C -4.22787334 -1.49213824 -8.13496808
 C -5.19908680 -1.95942621 -9.06784235
 H -5.22710820 -3.02740346 -9.29255156
 C -6.10673480 -1.08974458 -9.64729950
 C -6.08180174 0.28516012 -9.29642045
 C -5.13344720 0.77505582 -8.41187990
 H -5.14072924 1.83015603 -8.15288810
 H -6.82164681 0.96573243 -9.71979096
 H -6.85323853 -1.46058672 -10.35082985
 C -4.15598362 -0.08322066 -7.82513282
 C -3.05286942 2.33675378 -5.32138633
 C -5.10597118 3.87146523 -1.67904213
 H -6.03919446 3.51359243 -1.23775652
 C -6.35788833 3.58605633 -5.21431057
 H -5.67751099 3.18513816 -5.97538380
 H -6.27762683 4.68239977 -5.22295131
 H -7.38370646 3.30848317 -5.50294373
 H -6.93970912 3.25422851 -3.19790625
 H -5.30191889 1.11627650 -4.64076568
 H -5.70068243 1.03121966 -2.91730848
 H -7.00144811 1.07447210 -4.13986503

Mulliken charges:

1 C 0.527918
 2 C -0.233642
 3 C -0.240755
 4 C -0.243435
 5 C 0.017710
 6 O -0.529203
 7 C -0.245054
 8 C -0.238209
 9 C -0.241298
 10 C 0.165680
 11 O -0.624407
 12 H 0.118136
 13 H 0.123145
 14 H 0.125078
 15 H 0.123208
 16 H 0.140787
 17 H 0.109610
 18 H 0.125523
 19 H 0.142905
 20 H 0.144411
 21 H 0.125707
 22 C 0.146027
 23 C -0.164730
 24 H 0.122838
 25 C -0.150045
 26 H 0.133318
 27 C -0.139982
 28 H 0.133169
 29 C -0.149581
 30 H 0.132693
 31 C -0.107714
 32 H 0.123295
 33 C 0.053593
 34 C -0.135689
 35 H 0.129585
 36 C -0.148456
 37 H 0.139933
 38 C -0.137559
 39 H 0.138314
 40 C -0.130713
 41 H 0.134765
 42 C -0.135341
 43 H 0.143162
 44 H 0.127103
 45 H 0.130354

46 H 0.136384
 47 H 0.126435
 48 C -0.333566
 49 C -0.162545
 50 C 0.119493
 51 C -0.071091
 52 C 0.119157
 53 C -0.148000
 54 H 0.116154
 55 C -0.382803
 56 H 0.113591
 57 H 0.161323
 58 H 0.117447
 59 C -0.353210
 60 H 0.123709
 61 H 0.122526
 62 H 0.112297
 63 C -0.225212
 64 H 0.110368
 65 C 0.129295
 66 C -0.160345
 67 H 0.116236
 68 C -0.362802
 69 H 0.136521
 70 H 0.120728
 71 H 0.119434
 72 C -0.361808
 73 H 0.128911
 74 H 0.123389
 75 H 0.122484
 76 C -0.005599
 77 C -0.191787
 78 H 0.145665
 79 C 0.082608
 80 C -0.165401
 81 H 0.141670
 82 C -0.144216
 83 H 0.142460
 84 C -0.145145
 85 H 0.144076
 86 C -0.146378
 87 H 0.147700
 88 C 0.011441
 89 C -0.002962
 90 C 0.027769
 91 C 0.252336
 92 O -0.603168
 93 P 1.355139
 94 O -0.571943
 95 O -0.609454
 96 H 0.391765
 97 O -0.648781
 98 C -0.002002
 99 C -0.085613
 100 C 0.124038
 101 C -0.156037
 102 H 0.117728
 103 C -0.361124
 104 H 0.116111
 105 H 0.143984
 106 H 0.117620
 107 C -0.359029
 108 H 0.120851
 109 H 0.123823
 110 H 0.118319
 111 C -0.225456
 112 H 0.112078
 113 C 0.129710
 114 C -0.154596
 115 C -0.363080

116 H 0.124222
 117 H 0.120228
 118 H 0.129166
 119 C -0.360659
 120 H 0.123118
 121 H 0.121511
 122 H 0.128841
 123 H 0.111775
 124 C -0.212891
 125 H 0.100409
 126 C 0.140101
 127 C -0.140248
 128 H 0.118955
 129 C -0.340082
 130 H 0.127240
 131 H 0.105153
 132 H 0.101986
 133 C -0.351847
 134 H 0.119865
 135 H 0.112271
 136 H 0.116760
 137 C -0.194316
 138 H 0.149185
 139 C 0.069756
 140 C -0.163576
 141 H 0.141858
 142 C -0.144059
 143 C -0.147206
 144 C -0.146689
 145 H 0.145512
 146 H 0.143029
 147 H 0.142403
 148 C 0.022480
 149 C 0.276148
 150 C -0.214967
 151 H 0.114734
 152 C -0.360788
 153 H 0.122207
 154 H 0.122379
 155 H 0.120999
 156 H 0.122661
 157 H 0.128421
 158 H 0.116670
 159 H 0.115511

• **Nonthermodynamic spiroketal + (S)-3-13a complex**

Geometry:
 159

C -2.24986765 1.86588808 1.04847190
 C -2.46923290 3.28162639 0.50677551
 C -2.58885725 4.29693276 1.66012559
 C -3.70875863 3.85104633 2.61712494
 C -3.45063238 2.41131442 3.08192817
 O -3.28757071 1.51219350 1.97241144
 C -0.85283137 1.67807404 1.66895610
 C -0.60331689 0.21020952 2.03399150
 C -0.76023555 -0.63176606 0.76004321
 C -2.15625018 -0.47800222 0.11061278
 O -2.40447022 0.97772671 -0.07855577
 H -2.79746778 5.29356870 1.24567996
 H -1.63489248 4.36409473 2.20916552
 H -4.67375593 3.88559034 2.09021283
 H -3.77337790 4.51291211 3.49535194
 H -4.30155434 2.00605503 3.64559756
 H -2.55649853 2.38108079 3.73354759
 H -0.55884590 -1.69845127 0.92813108

H -0.03006186 -0.28335131 0.01923885
 H -0.11828421 2.01220959 0.91967695
 H -0.75262632 2.33340012 2.54373664
 C -3.30896027 -1.09853568 0.90656154
 C -3.09742705 -2.03245213 1.93243717
 H -2.08482726 -2.29868501 2.22998660
 C -4.18311405 -2.63133748 2.59302182
 H -3.99793371 -3.35095259 3.39197893
 C -5.49423077 -2.30544348 2.22603042
 H -6.34065359 -2.76637440 2.73742708
 C -5.71210513 -1.38279424 1.18861991
 H -6.73077803 -1.12748977 0.89662671
 C -4.63093019 -0.79018555 0.52920567
 H -4.80223222 -0.07468554 -0.27394420
 C -2.08497128 -1.06975795 -1.30533438
 C -2.65520718 -2.31984319 -1.60853263
 H -3.23683418 -2.84616619 -0.85369663
 C -2.48123918 -2.89325219 -2.87728981
 H -2.93514368 -3.86103440 -3.09570883
 C -1.73434653 -2.22503121 -3.85730261
 H -1.60473429 -2.66383069 -4.84763096
 C -1.16391078 -0.97946875 -3.55932478
 H -0.58098340 -0.44483608 -4.30210079
 C -1.33402459 -0.40707277 -2.29400101
 H -0.88148395 0.55771897 -2.07542679
 H 0.41086185 0.08448816 2.44269243
 H -1.32343429 -0.10658167 2.80159272
 H -1.66403486 3.54064470 -0.19054826
 H -3.40629392 3.28283759 -0.06223331
 P -3.28051067 2.91229548 -3.10422959
 O -2.71087002 4.08522688 -2.39758113
 O -4.60637616 3.33175541 -3.95727901
 C -5.03135340 2.66585646 -5.10450805
 C -6.31278267 2.04359927 -5.02766775
 C -6.94506361 1.90209368 -3.68261973
 C -7.63365239 2.98743077 -3.07548619
 C -8.08604186 4.25114444 -3.82099493
 H -8.63618116 4.84770670 -3.07443022
 C -6.97150200 5.17376960 -4.36164866
 H -7.41889427 6.13672942 -4.65423256
 H -6.19841729 5.35473795 -3.60495921
 H -6.48785727 4.75001206 -5.25028634
 C -9.09990931 3.91509624 -4.93990556
 H -9.52782419 4.84351000 -5.35042528
 H -9.92095517 3.29322901 -4.55270441
 H -8.61285599 3.37404422 -5.76206997
 C -8.00240306 2.88013094 -1.72361298
 H -8.50905381 3.72759730 -1.25795733
 C -7.73636934 1.73066522 -0.96475509
 C -8.00418848 1.66301199 0.53272849
 C -6.80374865 2.26950211 1.29841866
 H -6.68747272 3.32928981 1.02063087
 H -6.97056523 2.21446796 2.38642318
 H -5.86697095 1.74711095 1.06362662
 C -9.31885634 2.34398452 0.95909435
 H -9.27157223 3.43004441 0.78908135
 H -9.49657696 2.18459200 2.03341074
 H -10.17593321 1.94602990 0.39614405
 H -8.07258145 0.59748974 0.80867833
 C -7.13846436 0.64693400 -1.61762568
 H -6.96782354 -0.27369019 -1.05713370
 C -6.71950208 0.69984563 -2.95977022
 C -6.13852000 -0.60804565 -3.52588556
 H -5.86131689 -1.20130288 -2.63967108
 C -4.86674185 -0.56720546 -4.40185269
 H -4.08786332 0.06037775 -3.96193707
 H -5.06522196 -0.22923520 -5.42497004
 H -4.46896666 -1.59013573 -4.46303370
 C -7.25327005 -1.39543977 -4.25733144
 H -8.15099355 -1.49684994 -3.62928613

H -7.53532565 -0.87915933 -5.18565411
H -6.89192985 -2.40123131 -4.52449462
C -6.84349954 1.51056589 -6.18771182
H -7.83619954 1.06123978 -6.16280079
C -6.09008670 1.45296118 -7.39262161
C -4.75764064 2.00673391 -7.42514926
C -3.97689213 1.80200894 -8.60120437
H -2.95353052 2.16865368 -8.62721209
C -4.49759513 1.13493786 -9.69904164
C -5.82707270 0.63627673 -9.68186136
H -6.22658967 0.11885402 -10.55495909
H -3.87411522 0.98544057 -10.58161824
C -6.60225923 0.78940983 -8.54515606
H -7.61532511 0.38517015 -8.50158255
C -4.26247440 2.71174169 -6.26613906
C -2.94283206 3.40177654 -6.28458680
C -2.58820562 4.35823443 -7.30275262
C -1.23016650 4.84104904 -7.37046398
C -0.86986792 5.77110832 -8.38872103
H 0.16369904 6.11997116 -8.42933061
C -1.81084695 6.23590128 -9.29172679
H -1.52572264 6.95298392 -10.06267379
C -3.15744663 5.79158925 -9.20198265
H -3.90272460 6.18106238 -9.89681533
C -0.28011528 4.40075445 -6.40800838
H 0.74797392 4.75790888 -6.47592022
C -0.64316797 3.57767290 -5.35840205
C 0.30165919 3.05618397 -4.32549127
C 0.48059547 3.70938948 -3.07703327
C 0.15160338 5.17263152 -2.72495653
H -0.39305868 5.13194750 -1.76921468
C -0.69800668 6.02821728 -3.68157385
H -0.91835431 6.97955999 -3.17350194
H -1.64709519 5.55024962 -3.93498921
H -0.15148704 6.26115036 -4.60540361
C 1.49397838 5.91758236 -2.48249221
H 1.30086197 6.95084346 -2.15408302
H 2.11375954 5.41925025 -1.72349111
H 2.07208806 5.95563738 -3.41915146
C 1.10005167 2.98173905 -2.03944482
H 1.18914565 3.45568749 -1.05820819
C 1.61318479 1.69124034 -2.21113186
C 2.28556216 0.97760202 -1.04199493
H 1.67709367 1.17754731 -0.14193213
C 2.38186945 -0.55011632 -1.21769375
H 1.40993350 -0.98861541 -1.48446131
H 2.73587696 -1.01614364 -0.28636208
H 3.09882969 -0.80600584 -2.01288479
C 3.68824092 1.57872050 -0.78921901
H 3.62801719 2.66259516 -0.61336510
H 4.16474955 1.10669676 0.08469408
H 4.33024808 1.41199182 -1.66798082
C 1.53410321 1.12835509 -3.49276886
H 1.95786764 0.14033701 -3.67178052
C 0.86957943 1.77052030 -4.54996848
C 0.91328442 1.05558283 -5.91178585
C 1.98564708 1.71313853 -6.81244580
H 1.66872539 2.72464180 -7.10193887
H 2.94918990 1.78787986 -6.28740359
H 2.12909453 1.12261050 -7.73138315
C -0.40104251 0.86838976 -6.71276229
H -0.67496646 1.77460417 -7.26627056
H -1.24729212 0.59184409 -6.07126943
H -0.24586385 0.06304941 -7.44733797
H 1.27274650 0.03760097 -5.68856675
C -3.53618442 4.87473279 -8.23450201
H -4.57105393 4.54579250 -8.16854049
C -1.98923802 3.11095506 -5.30942458
O -3.73797755 1.66138171 -2.24253845
H -3.18998394 1.45858127 -1.42043969

O -2.32999782 2.22872603 -4.27107048

Mulliken charges:

1 C 0.541791
2 C -0.240288
3 C -0.255056
4 C -0.245450
5 C 0.017670
6 O -0.523025
7 C -0.236722
8 C -0.241276
9 C -0.215501
10 C 0.189038
11 O -0.634426
12 H 0.139055
13 H 0.115147
14 H 0.133967
15 H 0.123448
16 H 0.140157
17 H 0.107868
18 H 0.132160
19 H 0.122486
20 H 0.125688
21 H 0.125147
22 C 0.085709
23 C -0.156967
24 H 0.126729
25 C -0.149956
26 H 0.136102
27 C -0.141920
28 H 0.136227
29 C -0.136129
30 H 0.126682
31 C -0.100627
32 H 0.123776
33 C 0.038732
34 C -0.137888
35 H 0.135489
36 C -0.150286
37 H 0.137519
38 C -0.135727
39 H 0.136163
40 C -0.096682
41 H 0.109279
42 C -0.122120
43 H 0.126261
44 H 0.126263
45 H 0.133948
46 H 0.142942
47 H 0.139163
48 P 1.327830
49 O -0.565577
50 O -0.616929
51 C 0.266493
52 C 0.001251
53 C -0.086554
54 C 0.127499
55 C -0.156683
56 H 0.117060
57 C -0.356290
58 H 0.114864
59 H 0.142402
60 H 0.117113
61 C -0.360720
62 H 0.119582
63 H 0.122970
64 H 0.119505
65 C -0.227591
66 H 0.110430
67 C 0.128025

68 C	-0.161518	114 H	0.146320
69 C	-0.352815	115 C	0.010412
70 H	0.121120	116 C	-0.082795
71 H	0.114932	117 C	0.125255
72 H	0.136502	118 C	-0.133644
73 C	-0.369971	119 H	0.136563
74 H	0.122902	120 C	-0.353524
75 H	0.122418	121 H	0.111414
76 H	0.129164	122 H	0.143080
77 H	0.113754	123 H	0.103825
78 C	-0.208958	124 C	-0.361380
79 H	0.096522	125 H	0.120779
80 C	0.145242	126 H	0.116509
81 C	-0.146081	127 H	0.119677
82 H	0.115941	128 C	-0.212504
83 C	-0.358260	129 H	0.111118
84 H	0.140774	130 C	0.113322
85 H	0.109871	131 C	-0.148584
86 H	0.108200	132 H	0.116295
87 C	-0.352242	133 C	-0.371859
88 H	0.121044	134 H	0.129512
89 H	0.112218	135 H	0.123330
90 H	0.119943	136 H	0.124019
91 C	-0.201821	137 C	-0.359007
92 H	0.148480	138 H	0.125814
93 C	0.072158	139 H	0.122153
94 C	0.027180	140 H	0.126812
95 C	-0.149561	141 C	-0.209660
96 H	0.143166	142 H	0.112517
97 C	-0.147660	143 C	0.108884
98 C	-0.144828	144 C	-0.146377
99 H	0.141072	145 C	-0.357443
100 H	0.141628	146 H	0.118984
101 C	-0.164513	147 H	0.125033
102 H	0.140711	148 H	0.122046
103 C	0.020546	149 C	-0.367726
104 C	0.007621	150 H	0.120995
105 C	0.023345	151 H	0.136255
106 C	0.078866	152 H	0.121231
107 C	-0.166806	153 H	0.117736
108 H	0.140478	154 C	-0.147210
109 C	-0.145212	155 H	0.147066
110 H	0.141410	156 C	0.260167
111 C	-0.144382	157 O	-0.622431
112 H	0.142334	158 H	0.425956
113 C	-0.204536	159 O	-0.648553

References

- [1] Y. Y. Khomutnyk, A. J. Argüelles, G. A. Winschel, Z. Sun, P. M. Zimmerman, P. Nagorny, *J. Am. Chem. Soc.* **2016**, *138*, 444–456.
- [2] Y. Shao, Z. Gan, E. Epifanovsky, A. T. B. Gilbert, M. Wormit, J. Kussmann, A. W. Lange, A. Behn, J. Deng, X. Feng, et al., *Mol. Phys.* **2015**, *113*, 184–215.
- [3] A. D. Becke, *J. Chem. Phys.* **1997**, *107*, 8554–8560.
- [4] P. C. Hariharan, J. A. Pople, *Theor. Chim. Acta* **1973**, *28*, 213–222.
- [5] M. M. Francl, W. J. Pietro, W. J. Hehre, J. S. Binkley, M. S. Gordon, D. J. DeFrees, J. A. Pople, *J. Chem. Phys.* **1982**, *77*, 3654–3665.
- [6] Discovery Studio 4.1 Visualizer: Accelrys Software Inc. San Diego, USA, **2015**.
- [7] P. M. Zimmerman, *J. Comput. Chem.* **2015**, *36*, 601–611.
- [8] P. M. Zimmerman, *J. Chem. Theory Comput.* **2013**, *9*, 3043–3050.
- [9] P. M. Zimmerman, *J. Comput. Chem.* **2013**, *34*, 1385–1392.
- [10] A. V. Marenich, C. J. Cramer, D. G. Truhlar, *J. Phys. Chem. B* **2009**, *113*, 6378–6396.
- [11] J. Da Chai, M. Head-Gordon, *J. Chem. Phys.* **2008**, *128*, 084106.

APPENDIX C

Experimental Information for Chapter 4

(Adapted from:

Supporting information for: **Argüelles, A. J.**; Sun, S.; Budaitis, B. G.; Nagorny, P. *Angew.*

Chem. Int. Ed. **2018**, *57*, 5325.)

General information

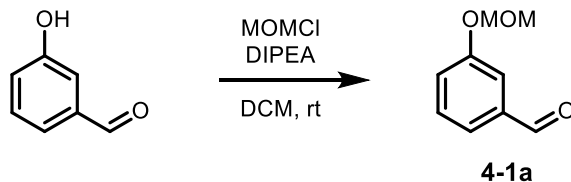
Unless otherwise stated, all reagents were purchased from commercial suppliers and used without further purification. All reactions were carried out under an atmosphere of nitrogen in flame-dried glassware with magnetic stirring, unless otherwise noted. Air-sensitive reagents and solutions were transferred *via* syringe or cannula and were introduced to the apparatus through rubber septa. Reactions were cooled via external cooling baths: ice water (0°C), dry ice-acetone (-78°C), or Neslab CB 80 immersion cooler (0 to -60°C). Heating was achieved using a silicone bath with regulated by an electronic contact thermometer. Deionized water was used in the preparation of all aqueous solutions and for all aqueous extractions. Solvents used for extraction and column chromatography were ACS or HPLC grade. Dry tetrahydrofuran (THF), dichloromethane (DCM), toluene (PhMe), and diethyl ether (Et₂O) was prepared by filtration through a column (Innovative Technologies) of activated alumina under nitrogen atmosphere. Reactions were monitored by nuclear magnetic resonance (NMR, see below) or thin layer chromatography (TLC) on silica gel precoated glass plates (0.25 mm, SiliCycle, SiliaPlate). TLC plate visualization was accomplished by irradiation with UV light at 254 nm or by staining with a potassium permanganate (KMnO₄)

or cerium ammonium molybdate (CAM) solution. Flash chromatography was performed using SiliCycle SiliaFlash P60 (230-400 mesh) silica gel. Powdered 4 Å molecular sieves were pre-activated by flame-drying under vacuum before use.

Proton (^1H), deuterium (D), carbon (^{13}C), fluorine (^{19}F), and phosphorus (^{31}P) NMR spectra were recorded on Varian VNMRS-700 (700 MHz), Varian VNMRS-500 (500 MHz), Varian INOVA 500 (500 MHz), or Varian MR400 (400 MHz). ^1H , ^{13}C , ^{19}F , and ^{31}P NMR spectra are referenced on a unified scale, where the single reference is the frequency of the residual solvent peak in the ^1H NMR spectrum. Chemical shifts (δ) are reported in parts per million (ppm) relative to tetramethylsilane for ^1H and ^{13}C NMR, fluorotrichloromethane for ^{19}F , 85% phosphoric acid for ^{31}P . Data is reported as (br = broad, s = singlet, d = doublet, t = triplet, q = quartet, m = multiplet; coupling constant(s) in Hz; integration). Slight shape deformation of the peaks in some cases due to weak coupling (e.g. aromatic protons) is not explicitly mentioned. High resolution mass spectra (HRMS) were recorded on Micromass AutoSpec Ultima or VG (Micromass) 70-250-S Magnetic sector mass. IR spectra were collected using a Nicolet iS10 spectrometer equipped with a diamond attenuated total reflectance (ATR) accessory. IR absorption peaks were reported in wavenumbers (cm^{-1}). The enantiomeric excesses were determined by GC, SFC, or HPLC analysis employing a chiral stationary phase column and conditions specified in the individual experiment. SFC analysis was carried out in a Waters Investigator SFC instrument. HPLC experiments were performed using a Waters Alliance e2695 Separations Module instrument. GC analysis was done in a Shimadzu GC-2010 Plus instrument. Optical rotations were measured at room temperature in a solvent of choice on a JASCO P-2000 digital polarimeter at 589 nm (D-line).

Synthesis of diphosphine (*S,S,S*)-SPIRAP and Pd(II) complex

3-(methoxymethoxy)benzaldehyde (**4-1a**)



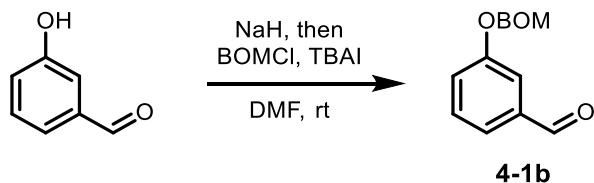
3-hydroxybenzaldehyde (24.0g, 196.5mmol), DCM (500mL), and N,N-Diisopropylethylamine (100mL, 589.6mmol) were cooled to 0°C before adding chloromethyl methyl ether (23mL, 303.6mmol) over 2h with a venting needle to handle the fumes. Reaction mixture was then warmed to room temperature. After 17h at room temperature, reaction mixture was quenched with a saturated aqueous solution of NaHCO₃ (500 mL). After separating the phases, the aqueous layer was extracted DCM twice. Combined organic was washed with brine, dried over Na₂SO₄, and concentrated *in vacuo*. Crude was purified by FCC (SiO₂, 20% EtOAc in hexanes) to obtain the desired product **4-1a** as pale yellow liquid (31.94g, 97.8% yield).

¹H NMR (700 MHz, CDCl₃) δ 9.98 (s, 1H), 7.57 – 7.51 (m, 2H), 7.46 (t, *J* = 7.8 Hz, 1H), 7.32 – 7.28 (m, 1H), 5.24 (s, 2H), 3.49 (s, 3H).

¹³C NMR (176 MHz, CDCl₃) δ 191.96, 157.76, 137.82, 130.11, 123.81, 122.83, 115.93, 94.39, 56.16.

IR (film): ν_{\max} = 2956, 2923, 2849, 2730, 1699, 1585, 1463, 1454, 1389, 1248, 1152, 1077, 1008, 789 cm⁻¹

3-((benzyloxy)methoxy)benzaldehyde (**4-1b**)



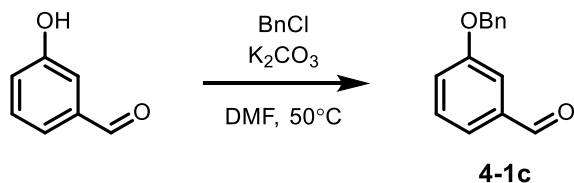
NaH (60% suspension) (2.47g, 61.42mmol) was added to a solution of 3-hydroxybenzaldehyde (5.00g, 40.94 mmol) in DMF (122mL) at 0°C. After 15min, benzyl chloromethyl ether (8.54mL, 61.42mmol) was added dropwise followed by the addition of tetrabutylammonium iodide (826mg, 2.24mmol). After overnight stirring at 0°C, reaction mixture was quenched with water (80mL), and the product was extracted with DCM (4 x 70mL). Combined organic was washed with brine, dried over MgSO₄, and concentrated *in vacuo*. Crude was purified by FCC (SiO₂, 5% EtOAc in hexanes) to afford aldehyde **4-1b** as clear oil (9.62g, 97% yield).

¹H NMR (500 MHz, CDCl₃) δ 9.98 (s, 1H), 7.60 (s, 1H), 7.54 (d, *J* = 7.5 Hz, 1H), 7.46 (t, *J* = 7.8 Hz, 1H), 7.39 – 7.28 (m, 6H), 5.36 (s, 2H), 4.74 (s, 2H).

¹³C NMR (126 MHz, CDCl₃) δ 191.93, 157.83, 137.86, 136.96, 130.14, 128.49, 128.00, 127.98, 123.74, 122.76, 116.16, 92.24, 70.22.

IR (film): ν_{\max} = 2904, 2729, 1699, 1585, 1483, 1454, 1383, 1242, 1157, 1144, 1076, 1013, 989, 736 cm⁻¹

3-(benzyloxy)benzaldehyde (**4-1c**)



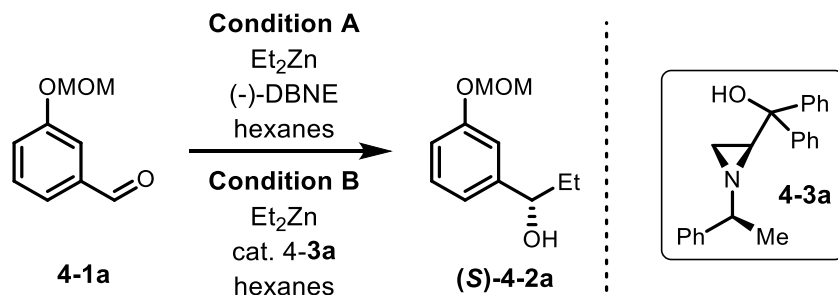
A solution of 3-hydroxybenzaldehyde (13.50g, 110.54mmol) and potassium carbonate (22.90g, 165.82mmol) in DMF (225mL) was treated dropwise with solution of benzylchloride (19mL, 165.82mmol) in DMF (160mL). After 15min at 50°C, reaction mixture was heated to 85°C for 24h. Reaction mixture was cooled to room temperature, diluted with DCM (150mL), and quenched with water (300mL). After separating the phases, the aqueous layer was extracted with DCM (3 x 200mL). Combined organic was washed with brine, dried over MgSO₄, and concentrated *in vacuo*. Crude was purified by FCC (SiO₂, 5% EtOAc in hexanes) to yield aldehyde **4-1c** as a white solid (18.77g, 80% yield).

1H NMR (500 MHz, CDCl₃) δ 9.98 (s, 1H), 7.51-7.43 (m, 5H), 7.40 (t, 7.8 Hz, 2H), 7.37-7.32 (m, 1H), 7.27-7.23 (m, 1H), 5.13 (s, 2H).

13C NMR (126 MHz, CDCl₃) δ 192.02, 159.30, 137.82, 136.30, 130.10, 128.66, 128.19, 127.53, 123.65, 122.17, 113.27, 70.22.

IR (film): ν_{\max} = 2811, 2727, 1693, 1594, 1480, 1443, 1383, 1325, 1255, 1146, 1016, 990, 794, 741, 697 cm⁻¹

(S)-1-(3-(methoxymethoxy)phenyl)propan-1-ol (4-2a)



Alkylations using DBNE as a catalyst were based on a reported procedure.^[1] Those using aziridine catalyst **4-3a** or **4-3b** were based on another report.^[2]

a) Using (-)-DBNE

Aldehyde **4-1a** (31.92g, 192.1mmol), hexanes (370 mL), and N,N-Dibutyl-D-(-)-norephedrine (3.8mL, 13.6mmol) were cooled to 0°C before adding a 1 M solution of diethylzinc in hexanes (430mL, 430mmol) portionwise over 2h. After 27h at 0°C, reaction mixture was quenched with an aqueous solution of HCl 1 M (150mL) and then filtered with DCM washings. Water (400mL) was added to the filtrate. After separating the layers, the aqueous fraction was with DCM twice. Combined organic was washed with brine, dried over Na₂SO₄, and concentrated *in vacuo*. Crude was purified by FCC (SiO₂, 30% EtOAc in hexanes) to obtain (S)-**4-2a** as pale yellow oil (36.5g, 96.8% yield, 94% ee).

¹H NMR (700 MHz, CDCl₃) δ 7.29 – 7.24 (m, 1H), 7.03 (t, *J* = 2.0 Hz, 1H), 6.99 (dt, *J* = 7.4, 1.2 Hz, 1H), 6.96 (ddd, *J* = 8.2, 2.6, 1.0 Hz, 1H), 5.19 (s, 2H), 4.60 – 4.55 (m, 1H), 3.49 (s, 3H), 1.85 – 1.71 (m, 2H), 0.94 (t, *J* = 7.4 Hz, 3H).

¹³C NMR (176 MHz, CDCl₃) δ 157.36, 146.44, 129.44, 119.47, 115.15, 113.91, 94.44, 75.83, 56.01, 31.84, 10.15.

IR (film): ν_{\max} = 3411 (br), 2961, 2932, 1586, 1486, 1451, 1242, 1149, 1077, 1011, 993, 923 cm^{-1}

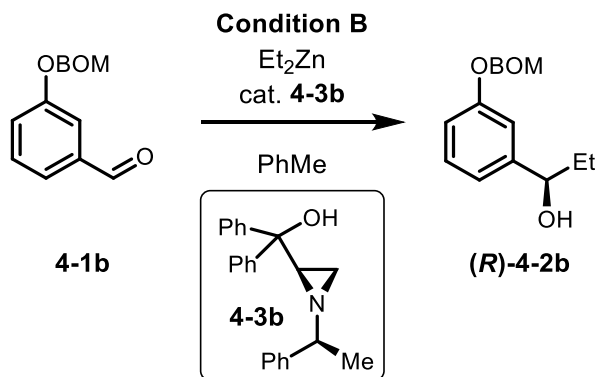
HPLC (Chiralpak IA column, 96:4 hexanes/isopropanol, 1.0 ml/min), t_r = 15.4 min (minor, *R*), 17.0 min (major, *S*)

b) Using aziridine organocatalyst 4-3a:

Hexanes (20mL), and diphenyl((*R*)-1-((*S*)-1-phenylethyl)aziridin-2-yl)methanol **4-3a** (100.0mg, 0.3mmol) were cooled to 0°C before adding a 1 M solution of diethylzinc in hexanes (13.3mL, 13.3mmol) dropwise. Reaction mixture was stirred at 0°C before the addition of aldehyde **4-1a** (1.00g, 6.0mmol) dropwise. After 20h at 0°C and 20h at room temperature, reaction mixture was quenched with a saturated solution of NH_4Cl (20mL). After separating the layers, the aqueous fraction was washed with EtOAc three times. Combined organic was washed with brine, dried over Na_2SO_4 , and concentrated *in vacuo*. Crude was purified by FCC (SiO_2 , 20% EtOAc in hexanes) to obtain (*S*)-**4-2a** (1.14g, 96.7% yield, 99.8% ee) as pale yellow oil.

Identical spectral properties as above.

(*R*)-1-(3-((benzyloxy)methoxy)phenyl)propan-1-ol (4-2b)



Using aziridine organocatalyst **4-3b**:

A solution of Et₂Zn (1M in hexanes) (6 mL) was added dropwise to a cooled (0°C) solution of diphenyl((R)-1-((S)-1-phenylethyl)aziridin-2-yl)methanol **4-3b** (50mg, 0.15mmol) in toluene (0.5mL). After 30min at 0°C, a solution of aldehyde **4-1b** (658mg, 2.71mmol) in toluene (4.5mL) was added dropwise, and the reaction mixture was allowed to slowly warm to room temperature. After 24h, reaction mixture was quenched with a saturated solution of NH₄Cl (8mL), the solid was filtered, and filtrate was extracted with Et₂O (3 x 8mL). Combined organic was washed with brine, dried over anhydrous MgSO₄, and concentrated *in vacuo*. Crude was purified by FCC (SiO₂, 10% EtOAc in hexanes) to alcohol (**R**)-**4-2b** as a clear oil (548mg, 74.0% yield, 98.9% e.e.).

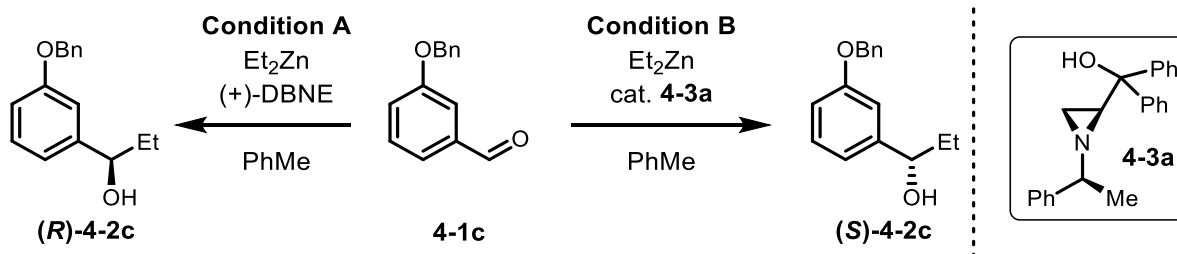
¹H NMR (500 MHz, CDCl₃) δ 7.38 – 7.24 (m, 6H), 7.08 (s, 1H), 7.00 (t, 7.6 Hz, 2H), 5.30 (s, 2H), 4.73 (s, 2H), 4.57 (td, J = 6.6, 3.4 Hz, 1H), 1.96 (d, J = 3.4 Hz, 1H), 1.87 – 1.70 (m, 2H), 0.93 (t, J = 7.4 Hz, 3H).

¹³C NMR (126 MHz, CDCl₃) δ 157.42, 146.43, 137.26, 129.46, 128.43, 128.01, 127.85, 119.51, 115.22, 113.99, 92.30, 75.81, 69.93, 31.84, 10.13.

IR (film): ν_{\max} = 3406 (br), 2962, 2932, 2875, 1585, 1486, 1453, 1237, 1157, 1075, 1015, 993, 785, 736, 696 cm⁻¹

HPLC (Chiralpak IA column, 96:4 hexanes/isopropanol, 1.0 ml/min), t_r = 22.6 min (major, *R*), 24.2 min (minor, *S*)

1-(3-(benzyloxy)phenyl)propan-1-ol (**4-2c**)



a) Using (+)-DBNE

Aldehyde **4-1c** (50mg, 0.24mmol), toluene (3mL), and N,N-Dibutyl-D-(+)-norephedrine (4 μ L, 0.014mmol) were cooled to 0°C before adding a 1 M solution of diethylzinc in hexanes (0.5mL, 0.5mmol) dropwise over 20min. After 20h from 0°C to room temperature, reaction mixture was quenched with a saturated solution of NH_4Cl (5mL). After separating the layers, the aqueous fraction was with EtOAc three times. Combined organic was washed with brine, dried over Na_2SO_4 , and concentrated *in vacuo*. Crude was purified by FCC (SiO_2 , 20% EtOAc in hexanes) to obtain *(R)*-**4-2c** (47mg, 81% yield, 95% B.R.S.M., 91% ee) as pale yellow oil.

^1H NMR (700 MHz, CDCl_3) δ 7.49 (d, $J = 7.2$ Hz, 2H), 7.43 (t, $J = 7.6$ Hz, 2H), 7.37 (t, $J = 7.3$ Hz, 1H), 7.30 (t, $J = 7.9$ Hz, 1H), 7.04 (s, 1H), 6.96 (d, $J = 7.6$ Hz, 1H), 6.93 (dd, $J = 8.1, 2.3$ Hz, 1H), 5.09 (s, 2H), 4.56 (t, $J = 6.6$ Hz, 1H), 2.44 (d, $J = 9.4$ Hz, 1H), 1.87 – 1.80 (m, 1H), 1.80 – 1.73 (m, 1H), 0.96 (t, $J = 7.4$ Hz, 3H).

^{13}C NMR (176 MHz, CDCl_3) δ 158.93, 146.52, 137.08, 129.44, 128.61, 127.99, 127.58, 118.71, 113.80, 112.55, 75.81, 69.99, 31.88, 10.21.

IR (film): $\nu_{\text{max}} = 3366$ (br), 3032, 2962, 2929, 2873, 1583, 1485, 1446, 1250, 1154, 1025, 994, 779 cm^{-1}

HPLC (Chiralpak IA column, 95:5 hexanes/isopropanol, 1.0 ml/min), $t_r = 21.2$ min (*R*), 24.5 min (*S*)

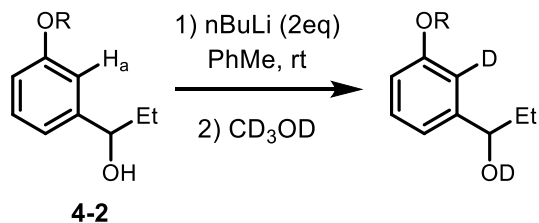
b) Using aziridine organocatalyst 4-3a

Aldehyde **1c** (14.2g, 66.8mmol), toluene (35mL), and diphenyl((*S*)-1-((*S*)-1-phenylethyl)aziridin-2-yl)methanol **4-3a** (1.32g, 4.09mmol) were cooled to 0°C before adding a 1 M solution of diethylzinc in toluene (148mL, 148mmol) dropwise over 6h. Reaction mixture was allowed to warm to room temperature slowly. After 30h, reaction mixture was quenched with a saturated solution of NH₄Cl (150mL). After separating the layers, the aqueous fraction was with EtOAc three times. Combined organic was washed with brine, dried over Na₂SO₄, and concentrated *in vacuo*. Crude was purified by FCC (SiO₂, 20% EtOAc in hexanes) to obtain (*S*)-**4-2c** (16.2g, quant. yield, 98.3% ee) as pale yellow oil.

Identical spectral properties as above.

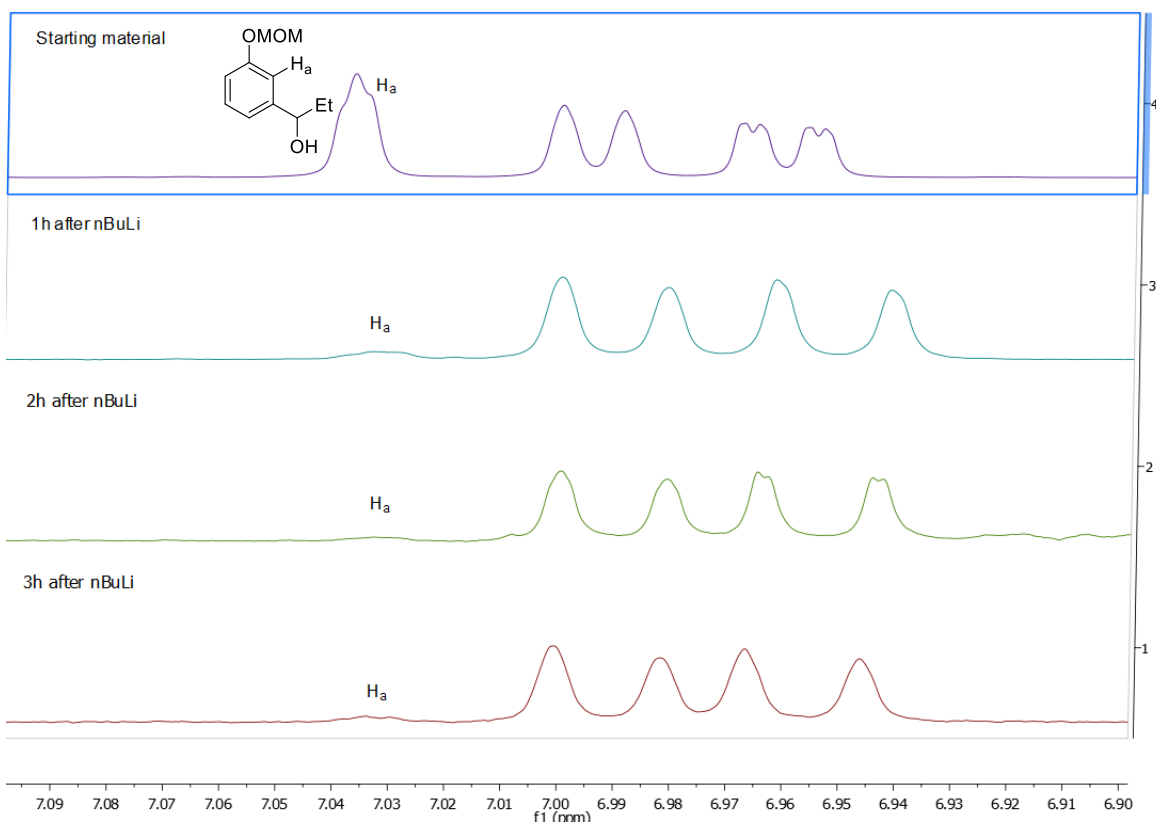
Using organocatalyst **4-3b**, (*R*)-**4-2c** obtained in 97.8% ee.

Lithiation studies

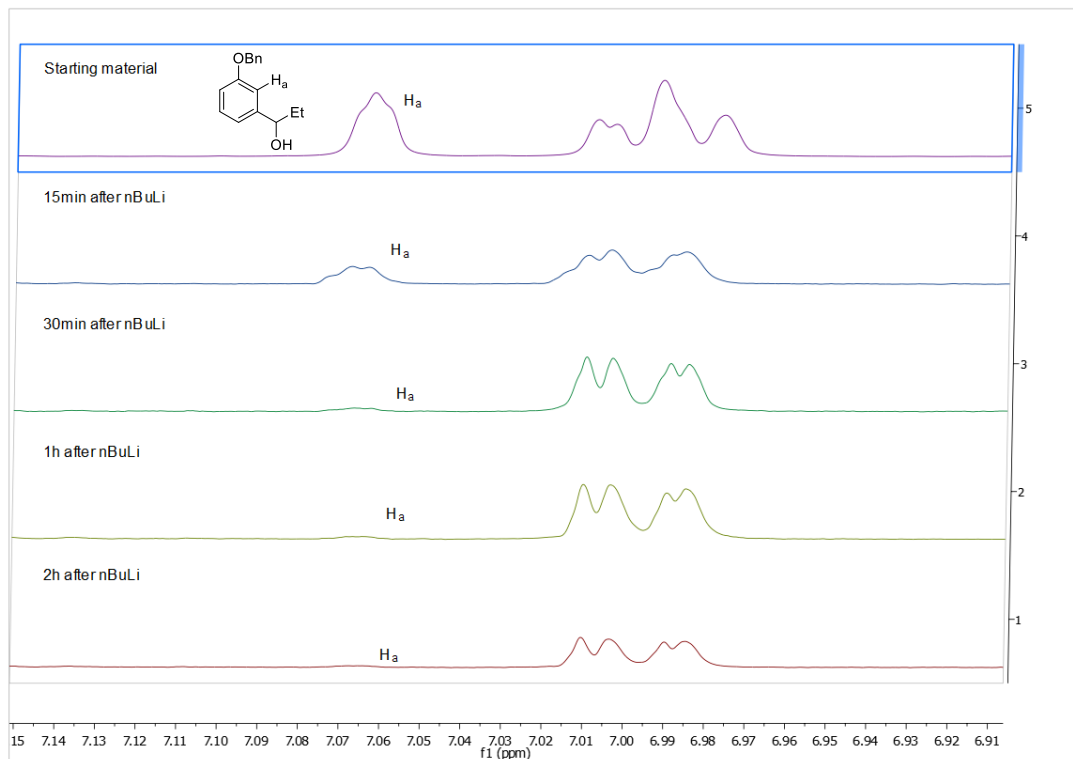


Before optimizing the spiroketalization reaction, we decided to study the selectivity of the *ortho*-lithiation of alcohols **4-2**. After treating **4-2** with 2 equivalents of *n*-butyllithium, aliquots were extracted at time points and then quenched with CD₃OD. After removing the volatiles, the deuterated material was analyzed by NMR. We found that selective and almost quantitative lithiation at the desired position occurred for **4-2a** and **4-2b**, and **4-2c** at around 2-3h in toluene.

For example, for **4-2a**:



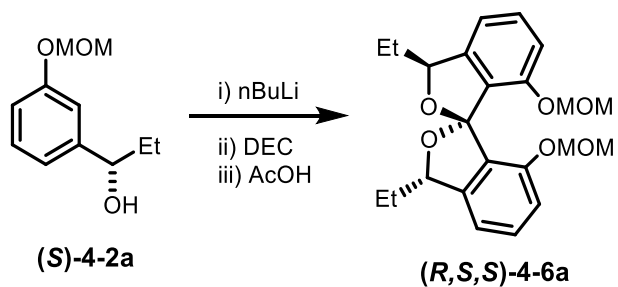
For **4-2c**:



Additionally, using THF as solvent, or TMEDA as additive gave unselective lithiations.

(1*R*,3*S*,3'*S*)-3,3'-diethyl-7,7'-bis(methoxymethoxy)-3*H*,3'*H*-1,1'-spirobi[isobenzofuran]

((*R,S,S*)-4-6a)



Alcohol **(S)-4-2a** (22.84g, 116.4mmol) and PhMe (330mL) were cooled to 0°C before addition of a 2.5 M solution *n*-Butyllithium in hexanes (44mL over 15min, then 50 mL over 1h,

235.0mmol). Reaction mixture was then warmed to room temperature. After 3h, the resulting suspension was dissolved using 12mL of THF and cooled again to 0°C. Diethyl carbonate (7.7mL, 63.5mmol) was incorporated over 2h at 0°C. Reaction mixture was allowed to warm slowly to room temperature overnight (12h). Glacial acetic acid (100mL) was then added slowly at room temperature. After 4h at room temperature, reaction mixture was quenched with 500mL of water, followed by careful addition of 100g of NaHCO₃. After separating the layers, the aqueous fraction was with DCM three times. Combined organic was washed with brine, dried over Na₂SO₄, and concentrated *in vacuo*. The mixture components were purified by FCC (SiO₂): 3.34g of starting material **4-2a** (14.6% recovery) were obtained at 15% EtOAc in hexanes, while 15.65g of desired product **4-6a** (67.2% yield, 78.7% BRSM) were isolated at 25% EtOAc in hexanes as pale yellow oil. Additionally, some intermediate isobenzofuranone **4-4a** (2.43g, 9.4% yield) was obtained at 35% EtOAc in hexanes as pale yellow oil.

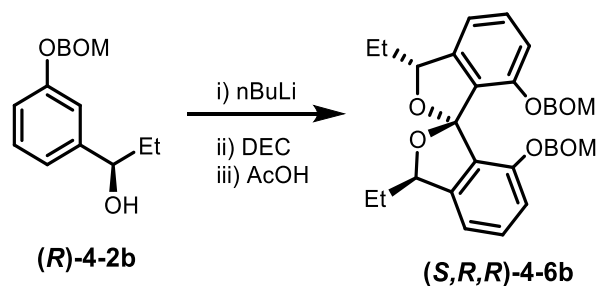
¹H NMR (500 MHz, CDCl₃) δ 7.29 (t, *J* = 7.8 Hz, 2H), 6.88 (dd, *J* = 7.9, 3.6 Hz, 4H), 5.40 (dd, *J* = 7.4, 3.9 Hz, 2H), 4.95 (d, *J* = 6.6 Hz, 2H), 4.82 (d, *J* = 6.6 Hz, 2H), 3.07 (s, 6H), 1.98 (dtd, *J* = 14.8, 7.3, 3.9 Hz, 2H), 1.86 (dq, *J* = 14.3, 7.3 Hz, 2H), 1.04 (t, *J* = 7.4 Hz, 6H).

¹³C NMR (126 MHz, CDCl₃) δ 152.44, 145.61, 130.58, 127.76, 113.99, 112.15, 93.29, 83.15, 55.60, 28.06, 9.74.

ESI-HRMS Calcd. for C₂₃H₂₉O₆⁺ 401.1964 [M+H]⁺, found 401.1958.

IR (film): ν_{max} = 2962, 2934, 1614, 1599, 1479, 1256, 1152, 1002, 960, 928, 734 cm⁻¹

(1*S*,3*R*,3'*R*)-7,7'-bis((benzyloxy)methoxy)-3,3'-diethyl-3*H*,3'*H*-1,1'-spirobi[isobenzofuran]
((*S,R,R*)-4-6b)



Alcohol (**(R)-4-2b**) (210mg, 0.77mmol) and PhMe (4.6mL) were cooled to 0°C before dropwise addition of a 2.5 M solution *n*-Butyllithium in hexanes (690μL, 1.73mmol). Reaction mixture was stirred at room temperature for 90min. Diethyl carbonate (50μL, 0.41mmol) was incorporated over 20min at 0°C. Reaction mixture was allowed to warm slowly to room temperature overnight. After 24h, glacial acetic acid (1mL) was then added slowly at room temperature. After 5h at room temperature, reaction mixture was treated with a saturated solution of NaHCO₃ (8mL). After separating the layers, the aqueous fraction was washed with DCM three times. Combined organic was washed with brine, dried over Na₂SO₄, and concentrated *in vacuo*. The mixture components were purified by FCC (SiO₂, 5% EtOAc in hexanes) to obtain ((***S,R,R***)-**4-6b**) (126mg, 54% yield, 64% B.R.S.M.) as pale yellow oil.

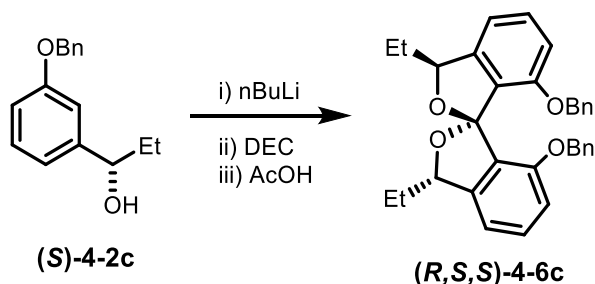
¹H NMR (500 MHz, CDCl₃) δ 7.33 (t, J = 7.9 Hz, 2H), 7.28 – 7.20 (m, 6H), 7.03 (dd, J = 6.5, 2.8 Hz, 4H), 6.97 (d, J = 8.1 Hz, 2H), 6.93 (d, J = 7.5 Hz, 2H), 5.42 (dd, J = 7.4, 4.0 Hz, 2H), 5.04 (d, J = 6.7 Hz, 2H), 4.87 (d, J = 6.8 Hz, 2H), 4.27 – 4.11 (m, 4H), 1.98 (m, 2H), 1.87 (m, 2H), 1.04 (t, J = 7.4 Hz, 6H).

¹³C NMR (126 MHz, CDCl₃) δ 152.53, 145.77, 136.67, 130.73, 128.28, 128.25, 128.16, 127.81, 127.78, 115.94, 114.04, 112.11, 90.33, 83.28, 69.03, 28.13, 9.85.

ESI-HRMS Calcd. for $C_{35}H_{37}O_6^+$ 553.2584 $[M+H]^+$, found 553.2580.

IR (film): ν_{\max} = 2964, 2874, 1599, 1479, 1250, 1155, 1093, 1065, 1002, 958, 734, 697 cm^{-1}

(1*R*,3*S*,3'*S*)-7,7'-bis(benzyloxy)-3,3'-diethyl-3*H*,3'*H*-1,1'-spirobi[isobenzofuran] ((*R,S,S*)-4-6c)



Alcohol **(S)-4-2c** (200mg, 0.83mmol) and PhMe (2.4mL) were cooled to 0°C before addition of a 2.5 M solution *n*-Butyllithium in hexanes (300 μ L dropwise, then 370 μ L over 30min, 1.67mmol). Reaction mixture was stirred at 0°C for 3h. Dimethyl carbonate (38 μ L, 0.45mmol) was incorporated over 30min 0°C. Reaction mixture was allowed to warm slowly to room temperature overnight (12h). Glacial acetic acid (1.2mL) was then added slowly at room temperature. After 6h at room temperature, reaction mixture was diluted with water (20mL) and then neutralized carefully with solid $NaHCO_3$. The product was extracted with DCM three times. Combined organic was washed with brine, dried over Na_2SO_4 , and concentrated *in vacuo*. The mixture components were purified by FCC (SiO_2 , 10% EtOAc in hexanes) to obtain **((R,S,S)-4-6c)** (84.8mg, 42% yield, 66% B.R.S.M.) as white solid, as well as 74.1mg of **(S)-4-2c**.

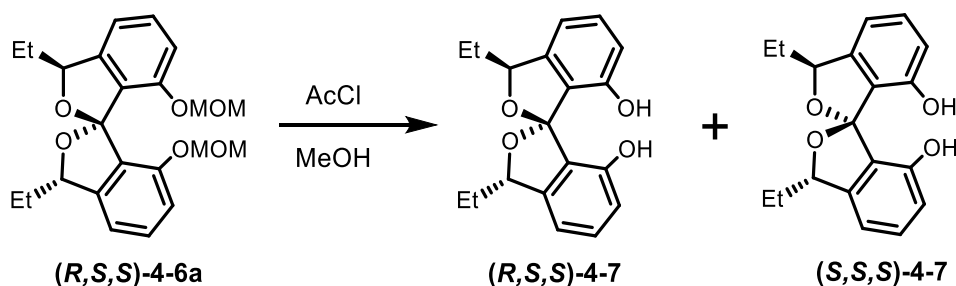
1H NMR (400 MHz, $CDCl_3$) δ 7.38 (t, J = 7.8 Hz, 2H), 7.19 – 7.02 (m, 6H), 6.83 (dd, J = 14.9, 7.8 Hz, 4H), 6.75 – 6.62 (m, 4H), 5.39 (dd, J = 7.2, 4.3 Hz, 2H), 5.00 – 4.80 (m, 4H), 1.87 – 1.59 (m, 4H), 0.86 (t, J = 7.4 Hz, 6H).

^{13}C NMR (100 MHz, CDCl_3) δ 154.21, 145.84, 136.62, 130.52, 127.97, 127.50, 127.15, 126.42, 115.83, 113.51, 110.36, 83.14, 68.86, 27.79, 9.64.

ESI-HRMS Calcd. for $\text{C}_{33}\text{H}_{33}\text{O}_4^+$ 493.2373 $[\text{M}+\text{H}]^+$, found 493.2370.

IR (powder): ν_{max} = 3030, 2963, 2933, 2872, 1735, 1612, 1597, 1480, 1451, 1284, 1267, 1027, 930 cm^{-1}

(*1R,3S,3'S*)-3,3'-diethyl-3H,3'H-1,1'-spirobi[isobenzofuran]-7,7'-diol (*(R,S,S)*-4-7) and (*(S,S,S)*-4-7 diastereomer from 4-6a



The deprotection of the MOM group using AcCl in MeOH was mild enough that after 6h at room temperature the contrathermodynamic diol (*(R,S,S)*-4-7) is the major compound. However, SiO_2 and other acidic conditions epimerize it into (*(S,S,S)*-4-7). These results agree with the calculated ΔG of 1.0 kcal/mol favoring (*(R,S,S)*-4-7). Consequently, neutralizing the acidic conditions after 6h of reaction yields (*(R,S,S)*-4-7) selectively, while performing chromatography after the reaction time gives (*(S,S,S)*-4-7) enriched material, as exemplified below.

(*R,S,S*)-selective deprotection

Spiroketal (*(R,S,S)*-4-6a) (21.9mg, 0.055mmol) and MeOH (0.5mL) were added to a vial. Solution was cooled to 0°C , and then acetyl chloride (8.0 μL , 0.11mmol) was added slowly.

Reaction mixture was warmed to room temperature. After 6h, reaction mixture was quenched with a saturated solution of NaHCO₃. Extracted three times with DCM, and then combined organic was dried with Na₂SO₄, and concentrated *in vacuo* to afford diol **7** (17.0mg, 99% yield, dr ~1:3.1:11.7 of **(S,R,S)-4-7:(S,S,S)-4-7:(R,S,S)-4-7**).

¹H NMR (500 MHz, CDCl₃) δ 7.34 (t, *J* = 7.7 Hz, 1H), 6.86 (d, *J* = 7.5, 1H), 6.77 (d, *J* = 8.0, 1H), 5.41 (dd, *J* = 6.7, 4.1 Hz, 1H), 4.73 (s, 1H), 2.07 (m, 1H), 1.83 (m, 1H), 1.01 (t, *J* = 7.4 Hz, 3H).

¹³C NMR (126 MHz, CDCl₃) δ 151.86, 145.37, 132.30, 123.26, 115.49, 113.62, 83.07, 27.76, 9.18.

ESI-HRMS Calcd. for C₁₉H₂₁O₄⁺ 314.1440 [M+H]⁺, found 314.1435.

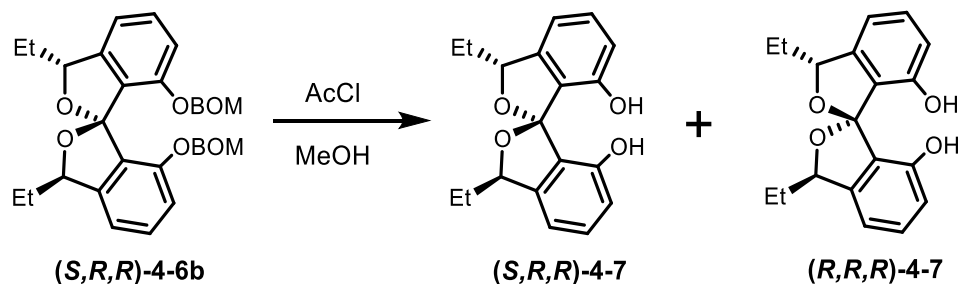
(S,S,S)-selective deprotection

Spiroketal **(R,S,S)-4-6a** (2.82g, 7.04mmol) and MeOH (35mL) were added to a round bottom flask. Solution was cooled to 0°C, and then acetyl chloride (1.0mL, 14.1mmol) was added slowly. Reaction mixture was warmed to room temperature. After 6h, reaction mixture was concentrated *in vacuo*, and purified by FCC (SiO₂, 30%→40% EtOAc in hexanes) to obtain diol **7** (2.15g, 97.5% yield 1:5.7:11.0 dr **(S,R,S)-4-7:(R,S,S)-4-7:(S,S,S)-4-7**).

¹H NMR (500 MHz, CDCl₃) δ 7.31 (t, *J* = 7.8 Hz, 1H), 6.86 (d, *J* = 7.5 Hz, 1H), 6.75 (d, *J* = 8.0 Hz, 1H), 5.27 (dd, *J* = 7.6, 4.4 Hz, 1H), 4.60 (s, 1H), 1.99 – 1.85 (m, 2H), 1.07 (t, *J* = 7.3 Hz, 3H).

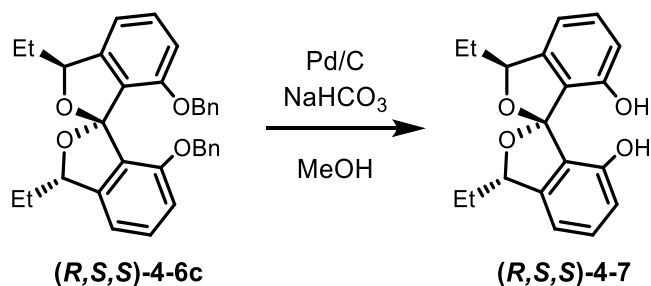
¹³C NMR (126 MHz, CDCl₃) δ 151.65, 145.24, 131.99, 123.37, 115.46, 113.84, 84.89, 30.61, 9.74.

(1*S*,3*R*,3'*R*)-3,3'-diethyl-3*H*,3'*H*-1,1'-spirobi[isobenzofuran]-7,7'-diol (*S*,*R*,*R*-4-7) from 4-6b



Spiroketal **(*S*,*R*,*R*)-4-6b** (20.9mg, 0.04mmol) and MeOH (200 μ L) were added to a vial. Solution was cooled to 0°C, and then acetyl chloride (8.0 μ L, 0.11mmol) was added slowly. Reaction mixture was warmed to room temperature. After 3h, reaction mixture was diluted with EtOAc, and treated with a saturated solution of NaHCO₃ (1 mL). After separating layers, the aqueous fraction was extracted three times with EtOAc. Combined organic was washed with brine, dried with Na₂SO₄, and purified by FCC (SiO₂, 5%→40% EtOAc in hexanes) to obtain diol **4-7** (11.6mg, 98% yield 1.3:3.6:4.5 dr **(*R*,*S*,*R*)-4-7:(*R*,*R*,*R*)-4-7:(*S*,*R*,*R*)-4-7**).

(1*R*,3*S*,3'*S*)-3,3'-diethyl-3*H*,3'*H*-1,1'-spirobi[isobenzofuran]-7,7'-diol (*R*,*S*,*S*-4-7) from 4-6c



Spiroketal **(*R*,*S*,*S*)-4-6c** (54mg, 0.11mmol), Pd/C (22mg, 0.022mmol), NaHCO₃(84mg, 1mmol) and methanol (2mL) were added to a round bottom flask charged with nitrogen before purging with hydrogen balloon twice. After 2h at room temperature, reaction mixture was filtered

through syringe filter and concentrated *in vacuo* to obtain (**R,S,S**)-**4-7** (32 mg, 93% yield, d.r. = 7:1) as white solid. Spectral properties described above.

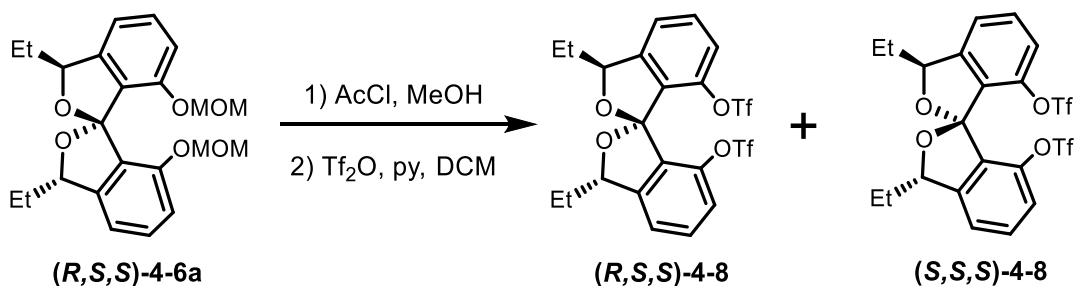
Diol equilibration studies

The isomeric ratio of the diols was variable, because epimerization happens in silica-containing solutions and the d.r. is dependent on the solvent. Most solvents, such as EtOAc/Hexanes mixtures slightly favor the (**S,S,S**)-**4-7** isomer. Curiously, SiO₂ in PhMe lightly favors equilibration towards the (**R,S,S**)-**4-7** isomer, this is not unreasonable given that the gas phase free energy difference between diastereomers is small.

A vial was charged with a 2.9:1 (**S,S,S**)-**4-7**:(**R,S,S**)-**4-7** mixture (300mg), PhMe (3mL), and SiO₂ (3.0g). After stirring at room temperature for 4 days, the diol mixture was recovered quantitatively by filtration and concentration *in vacuo*, with a 1:2.4 (**S,S,S**)-**4-7**:(**R,S,S**)-**4-7** d.r.. Similarly, a vial was charged with a 1:2.4 (**S,S,S**)-**4-7**:(**R,S,S**)-**4-7** mixture (100mg), EtOAc (0.5mL), hexanes (0.5mL), and SiO₂ (1.0g). After stirring at room temperature for 2 days, the diol mixture was recovered quantitatively by filtration and concentration *in vacuo*, with a 1.2:1 (**S,S,S**)-**4-7**:(**R,S,S**)-**4-7** d.r..

(**1S,3S,3'S**)-3,3'-diethyl-3H,3'H-1,1'-spirobi[isobenzofuran]-7,7'-diyl

bis(trifluoromethanesulfonate) ((**S,S,S**)-**4-8**) from (**R,S,S**)-**4-6a**



The (*R,S,S*)-**4-8**:(*S,S,S*)-**4-8** ratio was mostly conserved during the triflation, so the product ratio depended on the d.r. of the diol used. An (*S,S,S*)-**4-8**-selective preparation is described next. Spiroketal (*R,S,S*)-**4-6a** (12.57g, 7.0mmol) and methanol (160mL) were cooled to 0°C before dropwise addition of acetyl chloride (1.0mL, 14.1mmol). Reaction mixture was then warmed to room temperature. After for 6h, the volatiles were removed *in vacuo*, and the crude was purified by FCC (SiO₂, 30%→40% EtOAc in hexanes). Purified diol, DCM (150mL), and pyridine (12.5mL, 165.3mmol) were cooled to 0°C before addition of trifluoromethanesulfonic anhydride (12.0mL, 71.5mmol) over 30min. Reaction mixture was then warmed to room temperature. After 1h, a saturated aqueous solution of NaHCO₃ (150mL) was added. After separating the layers, the aqueous phase extracted with DCM twice. Combined organic was dried over Na₂SO₄ and concentrated *in vacuo*. Crude was purified by a short column (SiO₂, 10% EtOAc in hexanes) to afford a mixture of triflates as an oil which solidified on cooling (15.8g, 1:2.6:4.7 d.r. of (*S,R,S*)-**4-8**:(*R,S,S*)-**4-8**:(*S,S,S*)-**4-8**, 49.6% yield of desired (*S,S,S*)-**4-8**, 27.1% yield of (*R,S,S*)-**4-8**).

The ditriflates can be separated by FCC (SiO₂, 4% EtOAc in hexanes), but for convenience we chose to do a chemical resolution (*vide infra*). The spectral characteristics of the isolated ditriflates are shown below:

(*1R,3S,3'S*)-3,3'-diethyl-3H,3'H-1,1'-spirobi[isobenzofuran]-7,7'-diyl

bis(trifluoromethanesulfonate) ((*R,S,S*)-4-8**)**

¹H NMR (400 MHz, CDCl₃) δ 7.53 (t, *J* = 7.9 Hz, 2H), 7.30 (d, *J* = 8.5 Hz, 4H), 5.36 (dd, *J* = 8.5, 4.0 Hz, 2H), 2.05 (m, *J* = 15.0, 7.5, 4.0 Hz, 2H), 1.97 – 1.82 (m, 2H), 1.11 (t, *J* = 7.4 Hz, 6H).

¹⁹F NMR (376 MHz, CDCl₃) δ -74.57.

¹³C NMR (100 MHz, CDCl₃) δ 147.80, 144.92, 132.21, 129.82, 122.91, 120.81, 119.72, 119.13, 116.54, 113.33, 83.64, 27.39, 10.05.

ESI-HRMS Calcd. for C₂₁H₁₉F₆O₈S₂⁺ 577.0426 [M+H]⁺, found 577.0415.

IR (powder): ν_{max} = 2975, 2878, 1470, 1419, 1204, 1137, 936, 896, 848 cm⁻¹

(1*S*,3*S*,3'*S*)-3,3'-diethyl-3*H*,3'*H*-1,1'-spirobi[isobenzofuran]-7,7'-diyl

bis(trifluoromethanesulfonate) ((*S,S,S*)-4-8)

¹H NMR (400 MHz, CDCl₃) δ 7.51 (t, *J* = 7.9 Hz, 2H), 7.29 (d, *J* = 7.5 Hz, 2H), 7.23 (d, *J* = 8.2 Hz, 2H), 5.38 (dd, *J* = 7.2, 4.5 Hz, 2H), 2.07 – 1.81 (m, 4H), 1.06 (t, *J* = 7.4 Hz, 6H)

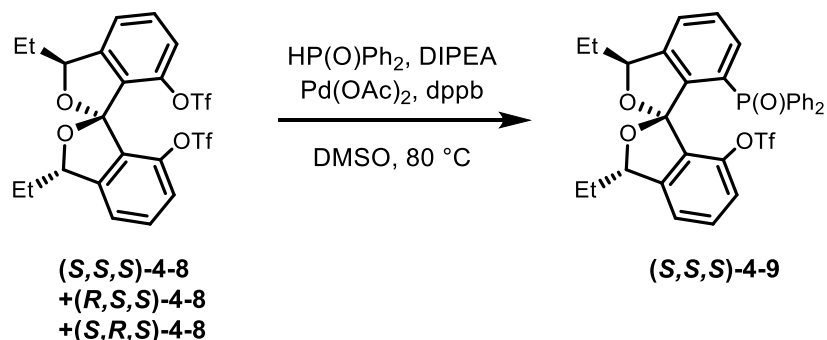
¹⁹F NMR (376 MHz, CDCl₃) δ -74.58.

¹³C NMR (100 MHz, CDCl₃) δ 147.33, 144.73, 132.07, 130.30, 122.92, 121.21, 119.74, 119.62, 119.60, 116.55, 114.51, 113.37, 84.77, 30.09, 9.45.

ESI-HRMS Calcd. for C₂₁H₁₉F₆O₈S₂⁺ 577.0426 [M+H]⁺, found 577.0418.

IR (powder): ν_{max} = 2973, 2880, 1470, 1422, 1207, 1137, 935, 852, 749 cm⁻¹

(1*S*,3*S*,3'*S*)-7'-(diphenylphosphoryl)-3,3'-diethyl-3*H*,3'*H*-1,1'-spirobi[isobenzofuran]-7-yl trifluoromethanesulfonate ((*S,S,S*)-4-9)



A flask in the glovebox was charged with a 1:2.6:4.7 mixture of ditriflates (*S,R,S*)-4-8:(*R,S,S*)-4-8:(*S,S,S*)-4-8 (12.624g, 21.86mmol), palladium(II) acetate (245mg, 1.09mmol), 1,4-Bis(diphenylphosphino)butane (466mg, 1.09mmol), and diphenylphosphine oxide (4.861g, 24.04mmol). The flask was taken outside the glovebox, and DMSO (85mL) and N,N-Diisopropylethylamine (9.5mL, 54.64mmol) were added. Reaction mixture was then stirred at room temperature for 1h, before being heated to 80°C. After 8h, reaction mixture was cooled to room temperature and partitioned between EtOAc (260mL) and a half saturated aqueous solution of NaHCO₃ (260mL). After separating the layers, the aqueous phase was extracted with EtOAc twice. Combined organic was washed with brine, dried over Na₂SO₄, and concentrated *in vacuo*. Crude was purified by FCC (SiO₂, 10 → 50% EtOAc in hexanes) to yield two fractions. At 10% EtOAc in hexanes, a mixture of (*S,R,S*)-4-8 and (*R,S,S*)-4-8 was obtained (1:4.2 d.r., 3.88g of useful (*R,S,S*)-4-8, 99.0% recovery based on starting (*R,S,S*)-4-8). At 50% EtOAc in hexanes, a mixture of epimeric product (*S,R,S*)-4-9 and desired phosphine oxide (*S,S,S*)-4-9 was obtained (1:12.6 dr, 7.34g of desired (*S,S,S*)-4-9, 93.8% yield based on starting (*S,S,S*)-4-8).

The desired product was further purified by two recrystallizations from cyclohexane with excellent recovery. The first recrystallization of 5.71g of the product mixture gave 5.33g of a 1:26 mixture of epimeric product (*S,R,S*)-**4-8** and desired phosphine oxide (*S,S,S*)-**4-8**, respectively (97% recovery of product). Chiral HPLC analysis showed that the desired product was enantioenriched to >99% ee. A second recrystallization of 5.02g of this mixture produced 4.58g of almost pure (*S,S,S*)-**4-8** (1:65 with respect to (*S,R,S*)-**4-8**) (93% recovery of product), as a white foam.

¹H NMR (500 MHz, CDCl₃) δ 7.52 – 7.42 (m, 4H), 7.42 – 7.31 (m, 4H), 7.27 – 7.21 (m, 2H), 7.21 – 7.10 (m, 4H), 7.02 (dd, *J* = 13.9, 7.5 Hz, 1H), 6.41 (dd, *J* = 7.1, 1.5 Hz, 1H), 5.56 (dd, *J* = 7.1, 4.7 Hz, 1H), 5.28 (dd, *J* = 7.2, 5.0 Hz, 1H), 1.92 (m, *J* = 13.5, 6.3 Hz, 3H), 1.83 (m, *J* = 14.3, 7.2 Hz, 1H), 1.06 (t, *J* = 7.4 Hz, 3H), 0.99 (t, *J* = 7.4 Hz, 3H).

¹³C NMR (126 MHz, CDCl₃) δ 148.85, 146.47, 146.40, 144.19, 141.69, 141.64, 133.80, 133.77, 133.70, 132.93, 132.51, 132.14, 132.07, 131.68, 131.55, 131.53, 131.31, 131.25, 131.20, 131.18, 131.01, 130.94, 128.59, 128.49, 128.22, 128.19, 128.12, 128.09, 127.40, 125.38, 125.36, 121.89, 120.41, 119.34, 118.47, 116.80, 116.25, 85.27, 83.49, 30.60, 29.71, 26.90, 9.88, 9.66.

¹⁹F NMR (471 MHz, CDCl₃) δ -75.05.

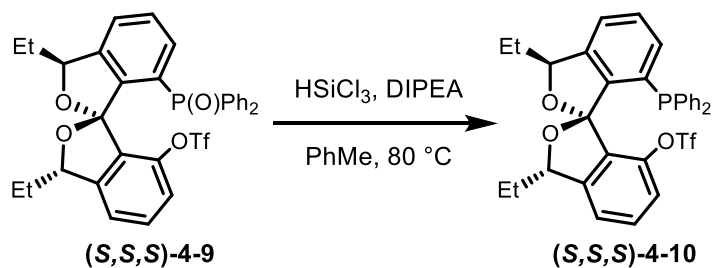
³¹P NMR (202 MHz, CDCl₃) δ 28.57.

ESI-HRMS Calcd. for C₃₂H₂₉F₃O₆PS⁺ 629.1375 [M+H]⁺, found 629.1366.

IR (powder): ν_{max} = 2934, 1419, 1210, 1194, 1140, 931 cm⁻¹

[α]_D: -70.8 (c = 1.0 in DCM)

(1*S*,3*S*,3'*S*)-7'-(diphenylphosphanyl)-3,3'-diethyl-3*H*,3'*H*-1,1'-spirobi[isobenzofuran]-7-yl trifluoromethanesulfonate ((*S,S,S*)-4-10)



Phosphine oxide (**(*S,S,S*)-4-9**) (4.95g, 7.88mmol), PhMe (80mL), and Diisopropylethylamine (55mL, 316.8mmol) were cooled to 0°C before addition of trichlorosilane (12.5mL, 126.1mmol) over 10min. The flask was sealed with a glass stopper and heated to 80°C. After 20h, the mixture was cooled to room temperature and quenched carefully by transferring it to a flask containing a saturated aqueous solution of NaHCO₃ (120mL) at 0°C, with diethyl ether washings. Crude was filtered through Celite with diethyl ether washings, and the filtrate was dried over Na₂SO₄ and concentrated *in vacuo*. Crude was purified by FCC (SiO₂, 5% EtOAc in hexanes) to afford (**(*S,S,S*)-4-10**) (3.89g, 80.7% yield) as white foam.

¹H NMR (500 MHz, CDCl₃) δ 7.32 (t, *J* = 7.5 Hz, 1H), 7.29 – 7.20 (m, 6H), 7.17 (d, *J* = 7.5 Hz, 1H), 7.13 (td, *J* = 7.5, 1.5 Hz, 2H), 7.07 (td, *J* = 7.5, 2.0 Hz, 2H), 6.89 (dd, *J* = 7.4, 4.6 Hz, 1H), 6.85 (td, *J* = 7.9, 1.4 Hz, 2H), 6.62 (d, *J* = 8.1 Hz, 1H), 5.35 (td, *J* = 6.8, 4.6 Hz, 2H), 1.96 (m, *J* = 16.9, 14.0, 5.9 Hz, 2H), 1.87 (m, *J* = 14.2, 7.2, 4.6 Hz, 2H), 1.06 (t, *J* = 7.3 Hz, 3H), 1.00 (t, *J* = 7.3 Hz, 3H).

¹³C NMR (126 MHz, CDCl₃) δ 147.39, 147.37, 144.53, 143.68, 143.62, 142.55, 142.35, 137.03, 136.93, 135.49, 135.41, 133.96, 133.94, 133.63, 133.49, 133.46, 133.33, 132.58, 132.56, 132.42, 131.46, 129.59, 128.42, 128.20, 128.17, 128.12, 128.00, 127.95, 122.04, 120.56, 119.35, 118.87, 116.81, 116.51, 116.49, 84.66, 84.61, 84.05, 30.47, 29.70, 9.64, 9.43.

^{19}F NMR (471 MHz, CDCl_3) δ -74.90.

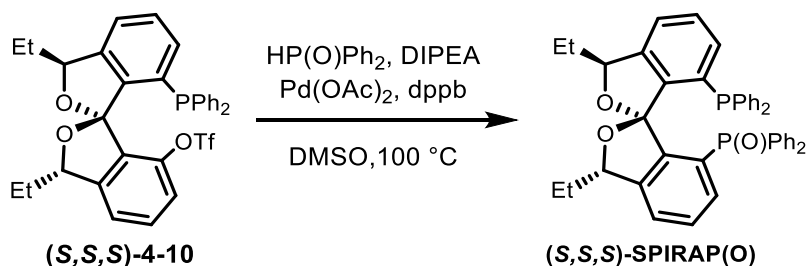
^{31}P NMR (202 MHz, CDCl_3) δ -18.88.

ESI-HRMS Calcd. for $\text{C}_{32}\text{H}_{29}\text{F}_3\text{O}_5\text{PS}^+$ 613.1425 $[\text{M}+\text{H}]^+$, found 613.1419.

IR (powder): ν_{max} = 2970, 1738, 1421, 1211, 1140, 943 cm^{-1}

$[\alpha]_{\text{D}}$: -44.0 (c = 1.0 in DCM)

((*1S,3S,3'S*)-7'-(diphenylphosphanyl)-3,3'-diethyl-3H,3'H-1,1'-spirobi[isobenzofuran]-7-yl)diphenylphosphine oxide ((*S,S,S*)-SPIRAP(O))



A flask in the glovebox was charged with phosphine (*S,S,S*)-4-10 (3.89g, 6.35mmol), palladium(II) acetate (71.3mg, 0.32mmol), 1,4-Bis(diphenylphosphino)butane (135.4mg, 0.32mmol), and diphenylphosphine oxide (2.57g, 12.7mmol). The flask was taken outside the glovebox, and DMSO (25 mL) and N,N-Diisopropylethylamine (5.5mL, 31.56mmol) were added. Reaction mixture was then stirred at room temperature for 1h before being then heated to 100°C. After 2h, reaction mixture was cooled down to room temperature and partitioned between EtOAc (160mL) and a half saturated aqueous solution of NaHCO_3 (160mL). After separating the layers, the aqueous phase was extracted with EtOAc twice. Combined organic was washed with brine,

dried over Na₂SO₄, and concentrated *in vacuo*. Crude was purified by FCC (SiO₂, 20 → 30% EtOAc in hexanes) to yield (*S,S,S*)-SPIRAP(O) (3.95g, 93.5% yield) as white foam.

¹H NMR (700 MHz, CDCl₃) δ 7.45 (td, *J* = 6.3, 2.6 Hz, 1H), 7.41 – 7.29 (m, 6H), 7.29 – 7.13 (m, 13H), 7.07 (td, *J* = 7.3, 2.1 Hz, 2H), 7.02 (td, *J* = 7.7, 1.7 Hz, 2H), 6.87 (dd, *J* = 7.5, 4.8 Hz, 1H), 6.71 (dd, *J* = 13.9, 7.5 Hz, 1H), 5.35 (t, *J* = 5.2 Hz, 1H), 4.71 (dd, *J* = 8.2, 3.8 Hz, 1H), 1.93 (m, *J* = 14.8, 7.5, 3.8 Hz, 1H), 1.79 (m, *J* = 14.0, 6.9 Hz, 1H), 1.72 (m, *J* = 11.4, 3.4 Hz, 1H), 1.64 (m, *J* = 14.3, 7.4 Hz, 1H), 0.86 (t, *J* = 7.3 Hz, 3H), 0.75 (t, *J* = 7.3 Hz, 3H).

¹³C NMR (176 MHz, CDCl₃) δ 146.70, 146.55, 146.26, 146.24, 146.21, 146.19, 144.53, 144.51, 144.50, 143.64, 143.60, 138.60, 138.53, 136.55, 136.48, 134.76, 134.17, 134.16, 134.06, 133.46, 133.42, 133.40, 133.24, 133.13, 133.05, 132.87, 132.36, 132.31, 131.56, 131.51, 131.08, 131.07, 131.03, 131.01, 130.99, 130.93, 128.79, 128.29, 128.22, 127.95, 127.93, 127.89, 127.86, 127.81, 127.76, 127.74, 127.72, 127.65, 127.27, 124.65, 124.64, 121.46, 118.68, 84.29, 83.26, 83.21, 29.93, 29.54, 9.85, 8.82.

³¹P NMR (283 MHz, CDCl₃) δ 28.63, -18.52.

ESI-HRMS Calcd. for C₄₃H₃₉O₃P₂⁺ 665.2374 [M+H]⁺, found 665.2366.

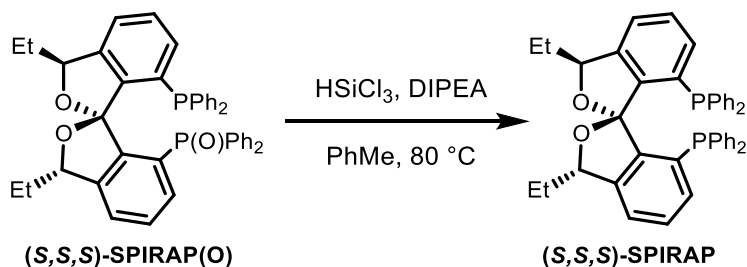
IR (powder): ν_{max} = 2964, 1434, 1336, 1214, 998, 915, 696 cm⁻¹

[α]_D: -93.3 (c = 1.0 in CHCl₃)

Crystallographic data: CCDC **1812181** contains the supplementary crystallographic data of (*S,S,S*)-SPIRAP(O). These data can be obtained free of charge from The Cambridge Crystallographic Data Centre via www.ccdc.cam.ac.uk/data_request/cif

((1*S*,3*S*,3'*S*)-3,3'-diethyl-3*H*,3'*H*-1,1'-spirobi[isobenzofuran]-7,7'-

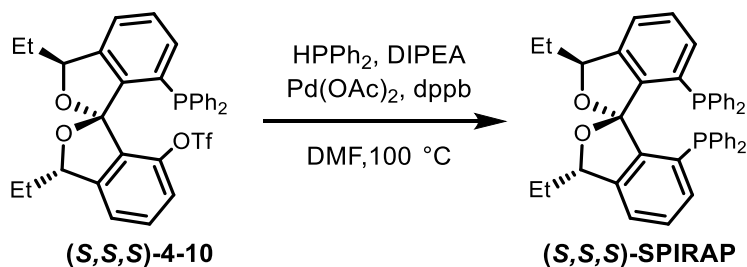
diyl)bis(diphenylphosphane) ((*S,S,S*)-SPIRAP) from phosphine oxide (*S,S,S*)-SPIRAP(O)



Phosphine oxide (*S,S,S*)-SPIRAP(O) (106mg, 0.159 mmol), PhMe (1.6mL), and diisopropylethylamine (1.1mL, 6.3mmol) were cooled to 0°C before dropwise addition of trichlorosilane (0.25mL, 2.5mmol). The flask was sealed with a glass stopped and heated to 80°C. After 20h, reaction mixture was cooled to room temperature and quenched carefully by transferring it to a flask containing a saturated aqueous solution of NaHCO₃ (5mL) at 0°C, with diethyl ether washings. Crude was filtered through Celite with diethyl ether washings, and the filtrate was dried over Na₂SO₄, and concentrated *in vacuo*. Crude mixture was purified by FCC (SiO₂, 5% EtOAc in hexanes) to afford (*S,S,S*)-SPIRAP (58.2mg, 56% yield) as white foam. The yield for this reaction was variable, with a 2.9g scale giving 35% yield due to the formation of an epimeric (*S,R,S*)-SPIRAP trichlorosilane adduct as the major component of the mixture, which can be cleanly converted to its free phosphine by stirring in isopropanol with traces of acetyl chloride. For this reason, we developed a direct method of obtaining (*S,S,S*)-SPIRAP from monophosphine (*S,S,S*)-4-10. Spectral properties described below.

((1*S*,3*S*,3'*S*)-3,3'-diethyl-3*H*,3'*H*-1,1'-spirobi[isobenzofuran]-7,7'-

diyl)bis(diphenylphosphane) ((*S,S,S*)-SPIRAP) from phosphine (*S,S,S*)-4-10



A Schlenk flask was charged with palladium(II) acetate (36.6mg, 0.163mmol) and 1,4-Bis(diphenylphosphino)butane (76.6mg, 0.180mmol). DMF (3.0mL) and diisopropylethylamine (1.8mL, 10.3mmol) were added. Solution was stirred at room temperature. After 1h, diphenyl phosphine (850 μ L, 4.89mmol) was added. After 5min, phosphine (*S,S,S*)-4-10 (1.000g, 1.632mmol) was added as a solution in DMF (3.5mL, including washings). The sealed flask was heated to 100°C. After 24h, volatiles were removed under N₂ flow. Crude was purified by FCC (SiO₂, 0 → 15% → 30% DCM in hexanes), and the product was then washed with hexanes to yield (*S,S,S*)-SPIRAP (977mg, 92.3% yield) as white solid.

¹H NMR (700 MHz, CDCl₃) δ 7.30 (t, J = 7.5 Hz, 2H), 7.23 (tq, J = 13.7, 7.6 Hz, 10H), 7.17 – 7.10 (m, 4H), 7.06 (td, J = 7.5, 1.8 Hz, 4H), 6.89 (dd, J = 7.5, 4.5 Hz, 2H), 6.83 (t, J = 7.4 Hz, 4H), 4.96 (dd, J = 6.8, 4.3 Hz, 2H), 1.86 (m, J = 14.6, 7.3, 4.1 Hz, 2H), 1.76 (m, J = 14.3, 7.2 Hz, 2H), 0.87 (t, J = 7.3 Hz, 6H).

¹³C NMR (176 MHz, CDCl₃) δ 145.51, 145.49, 145.36, 145.34, 144.09, 144.07, 144.05, 144.03, 138.22, 138.15, 136.81, 136.74, 134.11, 133.99, 133.72, 133.71, 133.13, 133.02, 132.59, 132.48, 129.12, 128.23, 128.02, 127.98, 127.93, 127.85, 127.82, 127.76, 121.54, 118.55, 83.29, 83.25, 29.76, 9.32.

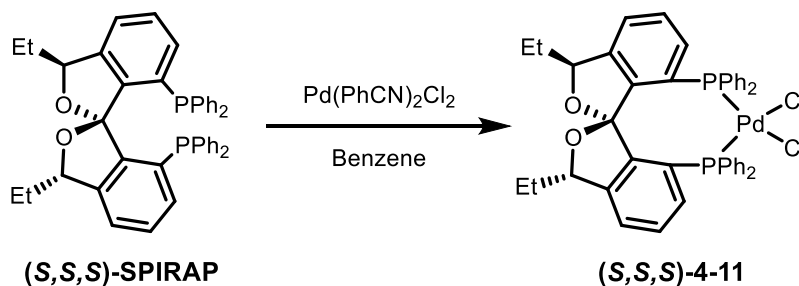
^{31}P NMR (283 MHz, CDCl_3) δ -18.71.

ESI-HRMS Calcd. for $\text{C}_{43}\text{H}_{39}\text{O}_2\text{P}_2^+$ 649.2425 $[\text{M}+\text{H}]^+$, found 649.2417.

IR (powder): ν_{max} = 2970, 1739, 1433, 1365, 1217, 696 cm^{-1}

$[\alpha]_{\text{D}}$: -227.4 ($c = 1.0$ in CHCl_3)

[[*(1S,3S,3'S)*-3,3'-diethyl-3H,3'H-1,1'-spirobi[isobenzofuran]-7,7'-diyl]bis(diphenylphosphane)]palladium(II) chloride (*(S,S,S)*-4-11)



Diphosphine *(S,S,S)*-SPIRAP (8.0mg, 0.012mmol), bis(benzonitrile)palladium(II) chloride (4.7mg, 0.012mmol), and benzene (0.82mL) were stirred at room temperature. After 6h, the complex was precipitated upon addition of hexanes as an orange solid, which was collected by filtration and washed with hexanes. The solid was redissolved in DCM for collection, and the volatiles were evaporated *in vacuo* to yield pure complex *(S,S,S)*-4-11 as a yellow-orange solid (9.9mg, 97% yield).

^1H NMR (700 MHz, CDCl_3) δ 7.77 (dd, $J = 12.3, 7.4$ Hz, 4H), 7.57 (s, 4H), 7.48 – 7.40 (m, 2H), 7.35 (d, $J = 7.8$ Hz, 6H), 7.24 – 7.17 (m, 4H), 7.09 (d, $J = 7.8$ Hz, 4H), 6.88 (d, $J = 7.5$ Hz, 2H), 3.75 (dd, $J = 9.9, 4.3$ Hz, 2H), 1.80 (m, 2H), 1.72 – 1.62 (m, 2H), 0.99 (t, $J = 7.4$ Hz, 6H).

^{13}C NMR (176 MHz, CDCl_3) δ 147.30, 147.26, 137.91, 137.87, 135.23, 135.16, 134.24, 134.18, 133.99, 133.93, 131.75, 131.39, 130.52, 130.30, 129.46, 129.41, 128.02, 127.95, 126.64, 126.33, 125.54, 125.42, 125.31, 116.26, 83.57, 30.49, 11.27.

^{31}P NMR (283 MHz, CDCl_3) δ 32.83.

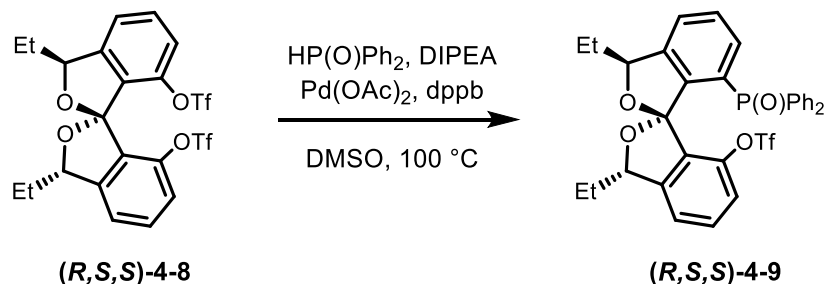
ESI-HRMS Calcd. for $\text{C}_{43}\text{H}_{38}\text{ClO}_2\text{P}_2\text{Pd}^+$ 789.1070 $[\text{M}-\text{Cl}]^+$, found 789.1076.

IR (powder): ν_{max} = 2225, 1435, 1095, 998, 921 727, 688 cm^{-1}

$[\alpha]_{\text{D}}$: +10.9 ($c = 0.5$ in CHCl_3)

Synthesis of diphosphine (*R,S,S*)-SPIRAP and Pd(II) complex

(*1R,3S,3'S*)-7'-(diphenylphosphoryl)-3,3'-diethyl-3H,3'H-1,1'-spirobi[isobenzofuran]-7-yl trifluoromethanesulfonate ((*R,S,S*)-4-9)



Recovered (*R,S,S*)-4-8 (from the coupling of (*S,S,S*)-4-8 to diphenylphosphine oxide) was recrystallized from cyclohexane. A flask in the glovebox was charged with ditriflate (3.946g, 6.85mmol), palladium(II) acetate (154mg, 0.68mmol), 1,4-Bis(diphenylphosphino)butane (321mg, 0.75mmol), and diphenylphosphine oxide (2.768g, 13.69mmol). The flask was taken outside the glovebox, and DMSO (27mL) and N,N-Diisopropylethylamine (4.8mL, 27.59mmol)

were added. Reaction mixture was then stirred at room temperature for 1h, before being heated to 100°C. After 24h, reaction mixture was cooled to room temperature and partitioned between EtOAc (60mL) and a half saturated aqueous solution of NaHCO₃ (60mL). After separating the layers, the aqueous phase was extracted with EtOAc twice. Combined organic was washed with brine, dried over Na₂SO₄, and concentrated *in vacuo*. Crude was purified by FCC (SiO₂, 5 → 40% EtOAc in hexanes). At 5% EtOAc in hexanes, some impure starting material was recovered (100.9mg). At 40% EtOAc in hexanes, the desired product (**R,S,S**)-**4-9** was obtained as white foam (4.081g, 94.8% yield).

¹H NMR (401 MHz, CDCl₃) δ 7.51 – 7.28 (m, 13H), 7.15 (dd, *J* = 10.0, 8.0 Hz, 2H), 7.06 (dd, *J* = 13.8, 7.5 Hz, 1H), 5.33 (dd, *J* = 8.2, 4.0 Hz, 1H), 5.14 (dd, *J* = 10.0, 3.5 Hz, 1H), 2.03 (m, *J* = 14.9, 7.4, 4.1 Hz, 1H), 1.88 (m, *J* = 14.4, 7.3 Hz, 1H), 1.70 (m, *J* = 15.0, 7.5, 3.7 Hz, 1H), 1.60 – 1.44 (m, 1H), 1.08 (t, *J* = 7.4 Hz, 3H), 0.53 (t, *J* = 7.4 Hz, 3H).

³¹P NMR (162 MHz, CDCl₃) δ 29.90.

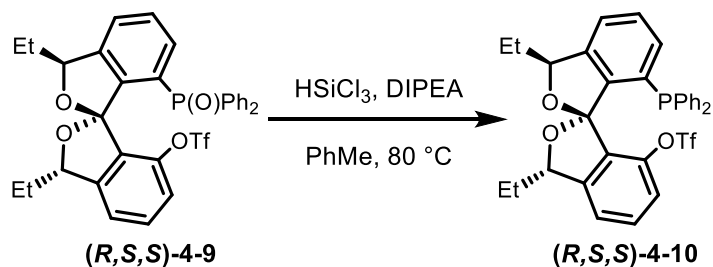
¹⁹F NMR (377 MHz, CDCl₃) δ -75.08.

ESI-HRMS Calcd. for C₃₂H₂₉F₃O₆PS⁺ 629.1375 [M+H]⁺, found 629.1372.

IR (powder): ν_{max} = 2970, 1738, 1419, 1214, 1141, 930, 695 cm⁻¹

[α]_D: -46.3 (c = 1.0 in CHCl₃)

(1*R*,3*S*,3'*S*)-7'-(diphenylphosphanyl)-3,3'-diethyl-3*H*,3'*H*-1,1'-spirobi[isobenzofuran]-7-yl trifluoromethanesulfonate ((*R,S,S*)-4-10)



Phosphine oxide (**(*R,S,S*)-4-8**) (2.00g, 3.18mmol), PhMe (32mL), and Diisopropylethylamine (22.2mL, 127.3mmol) were cooled to 0°C before addition of trichlorosilane (6.80mL, 50.9mmol) over 10min. The flask was sealed with a glass stopper and heated to 80°C. After 16h, the mixture was cooled to room temperature and quenched carefully by transferring it to a flask containing a saturated aqueous solution of NaHCO₃ (70mL) at 0°C, with diethyl ether washings. Crude was filtered through Celite with diethyl ether washings, and the filtrate was dried over Na₂SO₄ and concentrated *in vacuo*. Crude was purified by FCC (SiO₂, 5% EtOAc in hexanes) to afford (**(*R,S,S*)-4-10**) (870mg, 44.6% yield, 66.1% BRSM) as white foam. Starting material was recovered at 50% EtOAc in hexanes (311mg).

¹H NMR (500 MHz, CDCl₃) δ 7.32 (t, *J* = 7.5 Hz, 1H), 7.29 – 7.20 (m, 6H), 7.17 (d, *J* = 7.5 Hz, 1H), 7.13 (td, *J* = 7.5, 1.5 Hz, 2H), 7.07 (td, *J* = 7.5, 2.0 Hz, 2H), 6.89 (dd, *J* = 7.4, 4.6 Hz, 1H), 6.85 (td, *J* = 7.9, 1.4 Hz, 2H), 6.62 (d, *J* = 8.1 Hz, 1H), 5.35 (td, *J* = 6.8, 4.6 Hz, 2H), 1.96 (m, *J* = 16.9, 14.0, 5.9 Hz, 2H), 1.87 (m, *J* = 14.2, 7.2, 4.6 Hz, 2H), 1.06 (t, *J* = 7.3 Hz, 3H), 1.00 (t, *J* = 7.3 Hz, 3H).

¹³C NMR (126 MHz, CDCl₃) δ 147.39, 147.37, 144.53, 143.68, 143.62, 142.55, 142.35, 137.03, 136.93, 135.49, 135.41, 133.96, 133.94, 133.63, 133.49, 133.46, 133.33, 132.58, 132.56, 132.42,

131.46, 129.59, 128.42, 128.20, 128.17, 128.12, 128.00, 127.95, 122.04, 120.56, 119.35, 118.87, 116.81, 116.51, 116.49, 84.66, 84.61, 84.05, 30.47, 29.70, 9.64, 9.43.

^{19}F NMR (471 MHz, CDCl_3) δ -74.90.

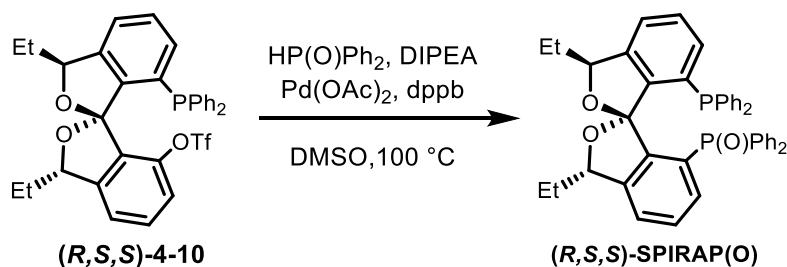
^{31}P NMR (202 MHz, CDCl_3) δ -18.88.

ESI-HRMS Calcd. for $\text{C}_{32}\text{H}_{29}\text{F}_3\text{O}_5\text{PS}^+$ 613.1425 $[\text{M}+\text{H}]^+$, found 613.1419.

IR (powder): ν_{max} = 2968, 1469, 1421, 1211, 1140, 1009, 962, 926, 848, 743 cm^{-1}

$[\alpha]_{\text{D}}$: +47.6 ($c = 1.0$ in CHCl_3)

((*1R,3S,3'S*)-7'-(diphenylphosphanil)-3,3'-diethyl-3H,3'H-1,1'-spirobi[isobenzofuran]-7-yl)diphenylphosphine oxide ((*R,S,S*)-SPIRAP(O))



A flask in the glovebox was charged with phosphine (*R,S,S*)-**4-10** (83mg, 0.14mmol), palladium(II) acetate (1.52mg, 0.007mmol), 1,4-Bis(diphenylphosphino)butane (2.89mg, 0.007mmol), and diphenylphosphine oxide (54.8mg, 0.271mmol). The flask was taken outside the glovebox, and DMSO (540 μL) and N,N-Diisopropylethylamine (100 μL , 74.4mmol) were added. Reaction mixture was then stirred at room temperature for 1h before being then heated to 100°C. After 3h, reaction mixture was cooled down to room temperature and partitioned between EtOAc (1mL) and a half saturated aqueous solution of NaHCO_3 (1mL). After separating the layers, the

aqueous phase was extracted with EtOAc twice. Combined organic was washed with brine, dried over Na₂SO₄, and concentrated *in vacuo*. Crude was purified by FCC (SiO₂, 35% EtOAc in hexanes) to yield (***R,S,S***-SPIRAP(O)) (84.8mg, 94% yield) as white foam.

¹H NMR (500 MHz, CDCl₃) δ 7.54 – 7.16 (m, 20H), 7.16 – 7.00 (m, 5H), 6.95 (dd, *J* = 13.9, 7.5 Hz, 1H), 5.19 (dd, *J* = 9.9, 3.5 Hz, 1H), 5.11 (dd, *J* = 10.1, 3.5 Hz, 1H), 1.81 (m, 1H), 1.73 – 1.62 (m, 1H), 1.55 (m, 1H), 1.40 (m, 1H), 0.83 (t, *J* = 7.4 Hz, 3H), 0.45 (t, *J* = 7.4 Hz, 3H).

³¹P NMR (202 MHz, CDCl₃) δ 29.82, -22.07.

¹³C NMR (126 MHz, CDCl₃) δ 148.72, 148.49, 147.11, 147.09, 147.04, 147.02, 144.48, 142.80, 142.74, 138.82, 138.71, 137.86, 137.75, 135.25, 135.22, 135.04, 134.93, 134.21, 134.10, 133.59, 133.55, 133.44, 132.83, 132.68, 132.59, 132.52, 131.97, 131.89, 131.16, 131.13, 131.10, 131.08, 130.47, 130.33, 128.67, 128.21, 128.11, 128.08, 128.03, 128.01, 127.97, 127.90, 127.81, 127.45, 126.62, 124.66, 124.64, 121.61, 110.00, 83.37, 82.38, 28.03, 28.00, 27.32, 10.88, 10.59.

ESI-HRMS Calcd. for C₄₃H₃₉O₃P₂⁺ 665.2374 [M+H]⁺, found 665.2370.

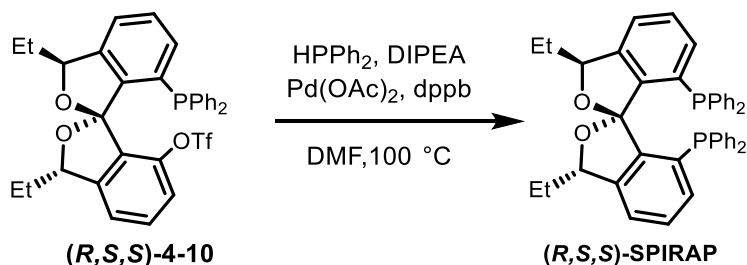
IR (powder): ν_{max} = 2969, 2842, 1435, 1217, 1007, 973, 917, 741, 694 cm⁻¹

[α]_D: -45.8 (c = 1.0 in CHCl₃)

Crystallographic data: CCDC 1812182 contains the supplementary crystallographic data of (***S,R,R***-SPIRAP(O)) made by using (***R***)-**4-2a**. These data can be obtained free of charge from The Cambridge Crystallographic Data Centre via www.ccdc.cam.ac.uk/data_request/cif

((1*R*,3*S*,3'*S*)-3,3'-diethyl-3*H*,3'*H*-1,1'-spirobi[isobenzofuran]-7,7'-

diyl)bis(diphenylphosphane) ((*R,S,S*)-SPIRAP) from phosphine (*R,S,S*)-4-10



A Schlenk flask was charged with palladium(II) acetate (21.9mg, 0.097mmol) and 1,4-Bis(diphenylphosphino)butane (46.0mg, 0.107mmol). DMF (1.9mL) and diisopropylethylamine (1.04mL, 5.97mmol) were added. Solution was stirred at room temperature. After 1h, diphenyl phosphine (510 μ L, 2.92mmol) was added. After 5min, phosphine (**(*R,S,S*)-4-10**) (596mg, 0.97mmol) was added as a solution in DMF (2.0mL, including washings). The sealed flask was heated to 100°C. After 16h, volatiles were removed under N₂ flow. Crude was purified by FCC (SiO₂, 30% → 40% DCM in hexanes) and the product was washed in hexanes to yield (**(*R,S,S*)-SPIRAP**) (551mg, 87% yield) as white solid.

¹H NMR (500 MHz, CDCl₃) δ 7.37 (t, $J = 7.5$ Hz, 2H), 7.31 – 7.14 (m, 14H), 7.06 – 6.92 (m, 10H), 5.15 (dd, $J = 10.1, 3.5$ Hz, 2H), 1.70 (m, 2H), 1.30 (m, 2H), 0.66 (t, $J = 7.3$ Hz, 6H).

³¹P NMR (202 MHz, CDCl₃) δ -20.99.

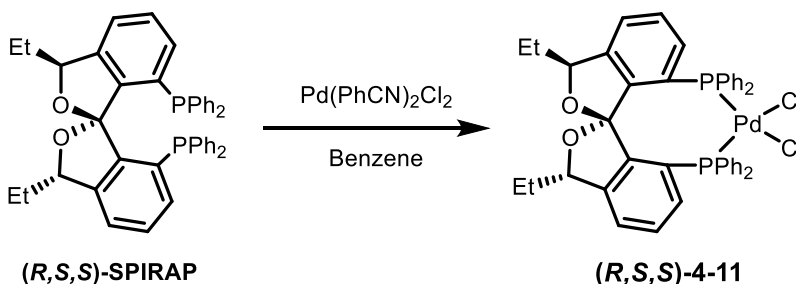
¹³C NMR (126 MHz, CDCl₃) δ 145.38, 145.15, 144.72, 144.69, 144.65, 138.28, 138.18, 137.55, 137.44, 134.73, 134.14, 134.05, 133.97, 132.98, 132.90, 132.83, 132.15, 132.12, 131.98, 131.95, 129.28, 128.22, 128.19, 128.17, 128.14, 128.11, 128.09, 128.04, 128.02, 128.00, 127.97, 127.95, 127.57, 121.73, 117.51, 82.84, 27.88, 10.77.

ESI-HRMS Calcd. for C₄₃H₃₉O₂P₂⁺ 649.2425 [M+H]⁺, found 649.2421.

IR (powder): ν_{\max} = 3067, 2969, 2845, 1434, 1274, 1005, 969, 917, 741, 694 cm^{-1}

$[\alpha]_{\text{D}}$: +203.8 ($c = 1.0$ in CHCl_3)

[[*(1R,3S,3'S)*-3,3'-diethyl-3H,3'H-1,1'-spirobi[isobenzofuran]-7,7'-diyl]bis(diphenylphosphane)]palladium(II) chloride (*(R,S,S)*-4-11)



Diphosphine **(*R,S,S*)-SPIRAP** (12.0mg, 0.018mmol), bis(benzonitrile)palladium(II) chloride (7.1mg, 0.018mmol), and benzene (1.2mL) were stirred at room temperature. After 16h, the complex was precipitated upon addition of hexanes as an orange solid, which was collected by filtration and washed with hexanes. The solid was redissolved in DCM for collection, and the volatiles were evaporated *in vacuo* to yield pure complex **(*R,S,S*)-4-11** as a yellow-orange solid (14.0mg, 92% yield).

$^1\text{H NMR}$ (500 MHz, CDCl_3) δ 7.80 (ddd, $J = 12.3, 6.6, 2.7$ Hz, 4H), 7.65 – 7.51 (m, 4H), 7.41 (dd, $J = 12.8, 7.9$ Hz, 2H), 7.36 (d, $J = 2.6$ Hz, 6H), 7.24 (t, $J = 7.8$ Hz, 2H), 7.21 – 7.14 (m, 2H), 7.05 (ddd, $J = 18.8, 9.1, 4.8$ Hz, 6H), 4.71 (dd, $J = 9.8, 4.0$ Hz, 2H), 1.50 (m, 2H), 0.94 (t, $J = 7.3$ Hz, 6H), 0.84 (m, 2H).

$^{31}\text{P NMR}$ (202 MHz, CDCl_3) δ 33.38.

^{13}C NMR (126 MHz, CDCl_3) δ 148.22, 148.16, 140.26, 140.19, 135.74, 135.64, 134.11, 134.03, 133.87, 133.78, 132.70, 132.19, 130.83, 130.25, 129.57, 129.50, 128.23, 128.13, 128.08, 128.03, 127.88, 127.46, 125.78, 125.42, 124.17, 113.55, 80.36, 24.97, 10.80.

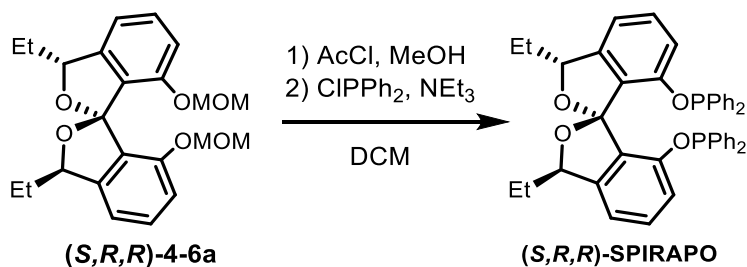
ESI-HRMS Calcd. for $\text{C}_{43}\text{H}_{39}\text{O}_2\text{P}_2\text{Pd}^+$ 755.1460 $[\text{M}-2\text{Cl}+\text{H}]^+$, found 755.1438.

IR (powder): ν_{max} = 2970, 1738, 1435, 1092, 998, 969, 912, 740, 688 cm^{-1}

$[\alpha]_{\text{D}}$: +27.1 ($c = 1.0$ in CHCl_3)

Synthesis of diphosphinite (*S,R,R*)-SPIRAPO

(((*1S,3R,3'R*)-3,3'-diethyl-3H,3'H-1,1'-spirobi[isobenzofuran]-7,7'-diyl)bis(oxy))bis(diphenylphosphane) ((*S,R,R*)-SPIRAPO)



Spiroketal (*S,R,R*)-**4-6a** (40mg, 0.10mmol) and methanol (1.0mL) were cooled to 0°C before dropwise addition of acetyl chloride (14 μL , 0.20mmol). Reaction mixture was then warmed to room temperature. After for 6h, the volatiles were removed in vacuo. The crude diol and 4-Dimethylaminopyridine (1.2mg, 0.01mmol) were dissolved into DCM (1.0mL) at room temperature before addition of triethylamine (0.13mL, 1.0mmol) and chlorodiphenylphosphine (46 μL , 0.25mmol) over 30min. After 12h, volatiles were removed *in vacuo*, and the crude was

purified by FCC (SiO₂ treated with 5% TEA, 4%→ 9% EtOAc in hexanes) to afford (**S,R,R**)-**SPIRAPO** (34mg, 56% yield) and (**R,R,R**)-**SPIRAPO** (17mg, 26% yield) as white foams.

For purified (**S,R,R**)-**4-12**

¹H NMR (399.54 MHz, CDCl₃) δ 7.31-7.21 (m, 12H), 7.14 (t, J = 7.4 Hz, 2H), 7.06 (m, 6H), 6.97 – 6.90 (m, 4H), 6.86 – 6.81 (m, 2H), 5.26 (dd, J = 8.2, 4.2 Hz, 2H), 1.57 (m, 2H), 1.41 (m, 2H), 0.87 (t, J = 7.4 Hz, 6H)

¹³C NMR (100 MHz, CDCl₃) δ 152.36, 152.27, 146.31, 140.11, 139.92, 139.88, 139.72, 130.73, 130.59, 130.49, 129.74, 129.63, 129.52, 128.89, 128.39, 128.31, 128.25, 128.18, 115.33, 115.17, 115.09, 114.69, 82.94, 28.02, 10.25

³¹P NMR (161.75 MHz, CDCl₃) δ 105.24

ESI-HRMS Calcd. for C₄₃H₃₉O₄P₂⁺ 681.2317 [M+H]⁺, found 681.2316.

[α]_D: -80.7 (c = 1.25 in THF)

For purified (**R,R,R**)-**4-12**

¹H NMR (500 MHz, CDCl₃) δ 7.34 – 7.19 (m, 12H), 7.15 (t, J = 7.7 Hz, 2H), 7.13 – 6.99 (m, 6H), 6.97 (t, J = 7.4 Hz, 4H), 6.71 (d, J = 7.5 Hz, 2H), 4.78 (dd, J = 7.2, 4.5 Hz, 2H), 1.89 – 1.72 (m, 4H), 0.99 (t, J = 7.4 Hz, 6H).

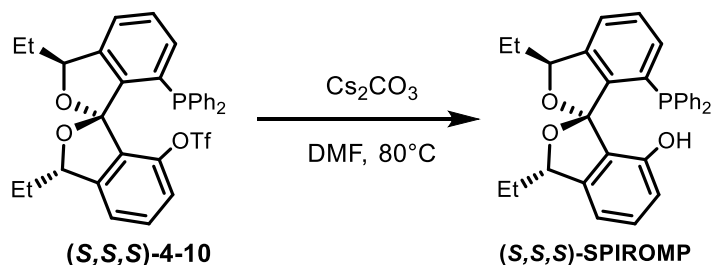
¹³C NMR (126 MHz, CDCl₃) δ 145.83, 130.82, 130.63, 130.47, 130.46, 129.75, 129.61, 129.57, 129.06, 128.23, 128.17, 115.11, 114.72, 84.21, 30.06, 9.74.

³¹P NMR (202 MHz, CDCl₃) δ 104.37.

[α]_D: -14.8 (c = 5.25 in THF)

Synthesis of monophosphine (*R,S,S*)-SPIROMP and (*S,S,S*)-SPIROMP

(*1S,3S,3'S*)-7'-(diphenylphosphanyl)-3,3'-diethyl-3H,3'H-1,1'-spirobi[isobenzofuran]-7-ol
(*(S,S,S)*-SPIROMP)



Hydrolysis based on a modified reported procedure.^[3] Triflate (*S,S,S*)-4-10 (300mg, 0.49mmol), wet Cs_2CO_3 (800mg, 2.45mmol), and DMF (8.0mL) were added to a flask. Reaction mixture was heated to 80°C. After 8h, reaction mixture was filtered through Celite and then purified by FCC (SiO_2 , 20% \rightarrow 25% EtOAc in hexanes) to obtain (*S,S,S*)-SPIROMP (224mg, 95% yield) as white solid.

^1H NMR (500 MHz, CDCl_3) δ 7.32 (t, $J = 7.5$ Hz, 1H), 7.26 (m, 5H), 7.16 – 7.06 (m, 4H), 7.04 (t, $J = 7.6$ Hz, 1H), 6.93 (dd, $J = 7.3, 4.4$ Hz, 1H), 6.86 (t, $J = 7.7$ Hz, 2H), 6.73 (d, $J = 7.4$ Hz, 1H), 6.10 (d, $J = 7.9$ Hz, 1H), 5.42 (t, $J = 5.4$ Hz, 1H), 5.24 (dd, $J = 7.9, 4.3$ Hz, 1H), 4.13 (s, 1H), 2.04 – 1.77 (m, 4H), 1.11 (t, $J = 7.4$ Hz, 3H), 0.99 (t, $J = 7.4$ Hz, 3H).

^{31}P NMR (202 MHz, CDCl_3) δ -18.74.

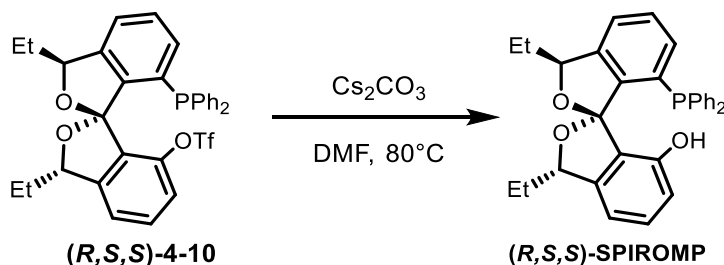
^{13}C NMR (126 MHz, CDCl_3) δ 151.04, 145.19, 145.17, 143.40, 143.35, 142.91, 142.71, 137.32, 137.22, 135.46, 135.38, 134.29, 134.27, 133.86, 133.68, 133.63, 133.53, 133.46, 133.38, 131.46, 129.56, 128.40, 128.16, 128.11, 127.88, 127.82, 126.08, 126.05, 122.12, 116.75, 116.73, 114.46, 113.09, 85.38, 85.32, 83.73, 30.96, 29.54, 10.04, 9.14.

ESI-HRMS Calcd. for $C_{31}H_{30}O_3P^+$ 481.1933 $[M+H]^+$, found 481.1934.

IR (powder): ν_{\max} = 3306, 2962, 1606, 1474, 1297, 1005, 927, 741, 692 cm^{-1}

$[\alpha]_D$: -3.7 ($c = 1.0$ in $CHCl_3$)

(*R,S,S*)-7'-(diphenylphosphanyl)-3,3'-diethyl-3H,3'H-1,1'-spirobi[isobenzofuran]-7-ol
((*R,S,S*)-SPIROMP)



Triflate (**(*R,S,S*)-4-10**) (112mg, 0.18mmol), wet Cs_2CO_3 (300mg, 0.92mmol), and DMF (3.0mL) were added to a flask. Reaction mixture was heated to 80°C. After 8h, reaction mixture was filtered through Celite and then purified by FCC (SiO_2 , 20% EtOAc in hexanes) to obtain (**(*R,S,S*)-SPIROMP**) together with an impurity (90.1mg, 1:11.6 impurity:product). The product was further purified by recrystallization from cyclohexane (35mg, 40% yield).

1H NMR (401 MHz, $CDCl_3$) δ 7.37 (t, $J = 7.5$ Hz, 1H), 7.32 – 7.16 (m, 8H), 7.02 (m, 5H), 6.79 (d, $J = 7.4$ Hz, 1H), 6.47 (d, $J = 8.0$ Hz, 1H), 5.41 (dd, $J = 6.7, 4.0$ Hz, 1H), 5.24 (dd, $J = 9.6, 3.9$ Hz, 1H), 4.24 (s, 1H), 2.07 (m, 1H), 1.90 – 1.77 (m, 2H), 1.77 – 1.66 (m, 1H), 1.00 (t, $J = 7.4$ Hz, 3H), 0.83 (t, $J = 7.4$ Hz, 3H).

^{31}P NMR (162 MHz, $CDCl_3$) δ -23.06.

^{13}C NMR (101 MHz, $CDCl_3$) δ 150.95, 145.81, 143.90, 143.84, 142.99, 142.72, 137.33, 137.20, 136.59, 136.45, 135.30, 134.12, 133.91, 133.70, 132.98, 132.80, 131.38, 130.09, 128.51, 128.18,

128.11, 127.81, 125.98, 125.95, 122.30, 115.57, 114.87, 113.10, 84.39, 84.34, 81.67, 81.63, 27.94, 27.64, 27.59, 10.70, 9.24

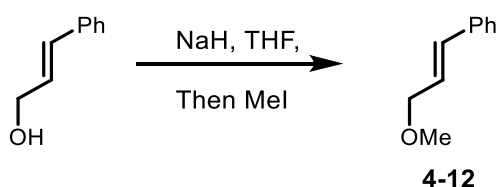
ESI-HRMS Calcd. for $C_{31}H_{30}O_3P^+$ 481.1933 $[M+H]^+$, found 481.1929.

IR (powder): $\nu_{\max} = 3326$ (br), 2959, 2853, 1604, 1473, 1295, 1005, 922, 740, 696 cm^{-1}

$[\alpha]_D$: +13.2 (c = 1.0 in $CHCl_3$)

Asymmetric hydroarylation of methylated cinnamyl alcohol

Preparation of substrate - (*E*)-(3-methoxyprop-1-en-1-yl)benzene



Alkenyl ether (**4-15**) was prepared according a reported procedure^[4] A flask was charged with a suspension of NaH (60%, prewashed with hexanes, 520mg, 21.7mmol) and THF (30mL) before addition of cinnamyl alcohol (1.4mL, 10.87mmol). After stirring at room temperature for 100min, methyl iodide (2.0mL, 32.6mmol) was added at room temperature. After 3h, reaction mixture was filtered through a SiO_2 pad, with 50% EtOAc in hexanes elution. The filtrate was concentrated *in vacuo* and purified by FCC (SiO_2 , 5% EtOAc in hexanes) to afford the desired product (1.52g, 94.4% yield) as a colorless oil. Spectral properties match those reported in literature.

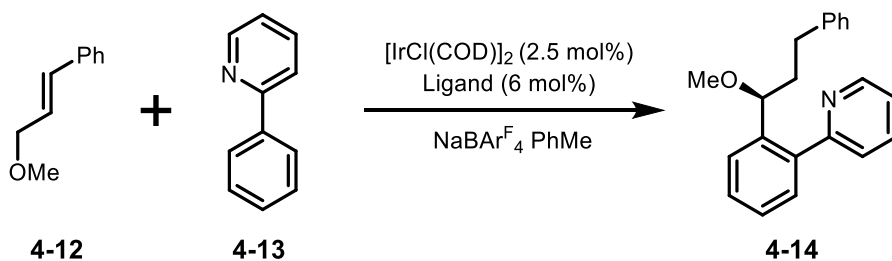
¹H NMR (400 MHz, Chloroform-*d*) δ 7.38 (dd, $J = 8.3, 1.5$ Hz, 1H), 7.31 (dd, $J = 8.4, 6.7$ Hz, 1H), 7.26 – 7.20 (m, 1H), 6.28 (dt, $J = 16.0, 6.0$ Hz, 1H), 4.09 (dd, $J = 6.0, 1.5$ Hz, 1H), 3.38 (d, $J = 0.5$ Hz, 2H).

¹³C NMR (100 MHz, cdcl₃) δ 136.70, 132.40, 128.52, 127.63, 126.44, 125.94, 73.07, 57.96.

IR (film): $\nu_{\max} = 3026, 2924, 2820, 1494, 1449, 1379, 1190, 1119, 965, 734, 691$ cm⁻¹

Hydroarylation procedure

(*S*)-2-(2-(1-methoxy-3-phenylpropyl)phenyl)pyridine



Hydroarylations were carried out according to a recently reported procedure.^[5] Bis(1,5-cyclooctadiene)diiridium(I) dichloride (3.3mg, 0.0049 mmol) and (*S,S,S*)-**SPIRAP** (7.6mg, 0.012mmol) were added to a Schlenk tube strictly under nitrogen. PhMe (330 μ L) was added and the mixture was stirred at room temperature. After 20min, sodium tetrakis[3,5-bis(trifluoromethyl)phenyl]borate (18.1mg, 0.0196mmol) was added. After 15min, 2-phenylpyridine **4-13** (30 μ L, 0.21mmol) and alkenyl ether **4-12** (30 μ L, 0.196mmol) were added. Reaction mixture was then heated to 70°C. After 24h, reaction mixture was cooled to room temperature. Volatiles were removed *in vacuo* and the crude was purified by FCC (10% EtOAc in

hexanes) to obtain pure product **4-14** (56.9mg, 96% yield, 95.4% ee) as colorless oil that solidifies on cooling.

¹H NMR (500 MHz, CDCl₃) δ 8.59 – 8.51 (m, 1H), 7.63 (td, *J* = 7.7, 5.3 Hz, 2H), 7.46 (dt, *J* = 8.2, 4.3 Hz, 1H), 7.35 (d, *J* = 4.3 Hz, 2H), 7.19 (ddt, *J* = 26.8, 14.7, 7.7 Hz, 5H), 7.11 – 7.04 (m, 2H), 4.45 (dd, *J* = 8.4, 4.2 Hz, 1H), 3.17 (s, 3H), 2.75 (m, 1H), 2.65 (m, 1H), 2.02 (m, 2H).

¹³C NMR (126 MHz, CDCl₃) δ 159.28, 149.05, 142.02, 140.75, 140.19, 136.06, 129.41, 128.73, 128.52, 128.18, 127.06, 126.16, 125.50, 123.99, 121.63, 78.18, 56.57, 39.61, 32.20.

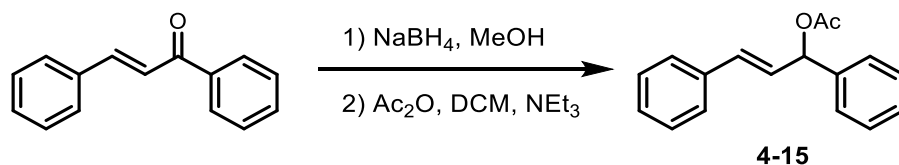
ESI-HRMS Calcd. for C₂₁H₂₂NO⁺ 304.1701 [M+H]⁺, found 304.1696.

IR (film): ν_{max} = 2924, 1585, 1425, 1100, 1022, 747, 698 cm⁻¹

SFC (Chiralpak OD-H, 92:8 CO₂/isopropanol, 3.5 ml/min, 40°C, 120 bar back pressure), t_r = 7.4 min (minor, *R*), 7.9 min (major, *S*)

Asymmetric allylic alkylation of chalcone derivatives

Preparation of substrate - (*E*)-1,3-diphenylallyl acetate



(*E*)-1,3-diphenylallyl acetate was synthesized following a slightly modified reported procedure.^[2] (*E*)-chalcone (988mg, 4.74mmol) and methanol (12mL) were cooled to 0°C before portionwise addition of sodium borohydride (365mg, 9.66mmol). Reaction mixture was then warmed to room temperature. After 1h, reaction mixture was partitioned between EtOAc (30mL)

and water (30mL). After separating the layers, the aqueous solution was extracted with EtOAc twice. Combined organic was washed with brine, dried over Na₂SO₄, and concentrated *in vacuo*. The allylic alcohol was acetylated without further purification as follows. 4-Dimethylaminopyridine (58.8mg, 48.1mmol), DCM (30mL), and triethylamine (1.7mL, 12.2mmol) were added to the crude. Reaction mixture was cooled to 0°C before dropwise addition of acetic anhydride (1.1mL, 11.6mmol). Reaction mixture was warmed to room temperature and stirred overnight. Water (30mL) was added, and after separating the layers, the aqueous solution was extracted with DCM twice. Combined organic was washed with brine, dried over Na₂SO₄, and concentrated *in vacuo*. Pure product **4-15** (841.2mg, 70.3% yield) was obtained after purification by FCC (SiO₂, 10 → 20% EtOAc in hexanes). Spectral properties match those reported in literature.

¹H NMR (400 MHz, CDCl₃) δ 7.49 – 7.13 (m, 10H), 6.65 (d, *J* = 15.8 Hz, 1H), 6.46 (d, *J* = 6.9 Hz, 1H), 6.36 (dd, *J* = 15.7, 6.8 Hz, 1H), 2.15 (s, 3H).

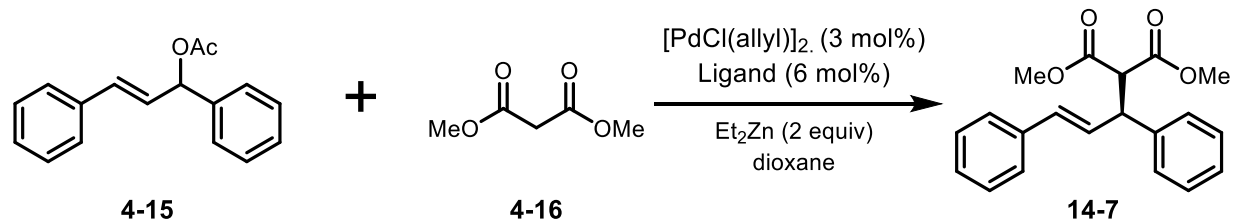
¹³C NMR (100 MHz, CDCl₃) δ 169.97, 139.20, 136.14, 132.56, 128.59, 128.54, 128.45, 128.39, 128.29, 128.13, 128.02, 127.47, 127.01, 126.66, 76.10, 21.32.

IR (film): ν_{\max} = 3029, 1734, 1495, 1370, 1227, 1017, 962, 743, 694 cm⁻¹

For (*S,R,R*)-**SPIRAP** – No product observed.

Asymmetric allylic alkylation procedure

Dimethyl (*S,E*)-2-(1,3-diphenylallyl)malonate



The asymmetric alkylation was performed following a modified reported procedure.^[6] (*E*)-1,3-diphenylallyl acetate (49.3mg, 0.195mmol) **4-15** and 1,4-dioxane (1mL) were stirred at room temperature. In a separate flask, allylpalladium(II) chloride dimer (1.8mg, 0.0049mmol), (*S,S,S*)-**SPIRAP** (7.6mg, 0.012mmol), and 1,4-dioxane (1mL) were stirred for 1h at room temperature. The catalyst solution was transferred to the substrate flask by syringe with dioxane washings (1mL). In another flask, dimethyl malonate **4-16** (45μL, 0.39mmol) and 1,4-dioxane (1mL) were cooled to 0°C, and then treated with a 1 M solution of diethylzinc in hexanes (390μL, 0.39mmol). The substrate flask was cooled with an ice bath while the reagent solution was slowly transferred via syringe with dioxane washings (1mL). Reaction mixture was then warmed to room temperature. After 90min, reaction mixture was diluted with EtOAc (5mL) and quenched with a saturated aqueous solution of NH₄Cl (5mL). After separating the layers, the aqueous solution was extracted with EtOAc twice. Combined organic was washed with brine, dried over Na₂SO₄, and concentrated *in vacuo*. Crude was purified by FCC (SiO₂, gradient 0 → 10% EtOAc in hexanes) to afford pure product **4-17** (59.8mg, 94% yield, 96.6% ee) as colorless oil. Spectral properties match those reported in literature.

¹H NMR (400 MHz, CDCl₃) δ 7.41 – 7.18 (m, 10H), 6.51 (d, *J* = 15.7 Hz, 1H), 6.37 (dd, *J* = 15.7, 8.6 Hz, 1H), 4.30 (dd, *J* = 10.9, 8.5 Hz, 1H), 3.99 (d, *J* = 10.8 Hz, 1H), 3.73 (s, 3H), 3.54 (s, 3H).

^{13}C NMR (100 MHz, CDCl_3) δ 168.20, 167.78, 140.20, 136.84, 131.85, 129.14, 128.74, 128.49, 127.89, 127.59, 127.18, 126.40, 57.67, 52.63, 52.46, 49.22.

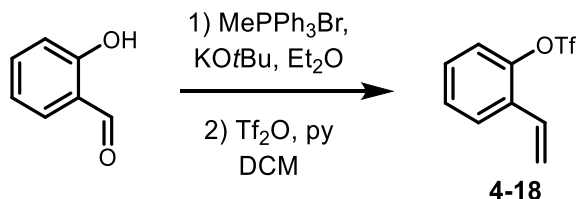
IR (film): ν_{max} = 3316 (br), 3026, 2861, 1494, 1091, 945, 733, 691 cm^{-1}

HPLC (Chiralpak AD column, 95:5 hexanes/isopropanol, 1.0 ml/min), t_r = 12.6 min (minor, *R*), 17.1 min (major, *S*)

For (*R,S,S*)-SPIRAP – 98% yield, 86% ee

Asymmetric Heck reaction of 2-vinylphenyl triflate with norbornene

Substrate synthesis



2-vinylphenyl trifluoromethanesulfonate was synthesized following a two-step procedure reported elsewhere.^[8] Methyltriphenyl-phosphonium bromide (3.52g, 9.85mmol) and diethyl ether (60mL) were cooled to 0°C before the addition of $\text{KO}t\text{-Bu}$ (2.16g, 19.25mmol). After 15min, a solution of salicylaldehyde (1mL, 9.38mmol) in diethyl ether (30mL) was added. Reaction mixture was then warmed to room temperature. After 16h, a saturated aqueous solution of NH_4Cl (30mL) was added. After separating the layers, the aqueous solution was extracted with diethyl ether twice. Combined organic was washed with brine, dried over Na_2SO_4 , and concentrated *in vacuo*. Crude was purified by FCC (SiO_2 , gradient 5 \rightarrow 15% EtOAc in hexanes) to afford unreacted starting

material (141mg, 12% recovery) and pure 2-vinylphenol (942 mg, 84% yield) as light yellow liquid.

Vinylphenol (767mg, 6.38mmol), DCM (18mL), and pyridine (1mL, 12.77mmol) were cooled to 0°C before the dropwise addition of trifluoromethanesulfonic anhydride (1.3mL, 7.66mmol). Reaction mixture was then warmed to room temperature. After 13h, reaction mixture was filtered with DCM washings, concentrated *in vacuo*, and purified by FCC (SiO₂, hexanes) to afford 2-vinyltriflate (1.427g, 89% yield) as colorless liquid.

¹H NMR (401 MHz, CDCl₃) δ 7.69 – 7.59 (m, 1H), 7.39 – 7.15 (m, 3H), 6.92 (dd, *J* = 17.5, 11.1 Hz, 1H), 5.84 (d, *J* = 17.5 Hz, 1H), 5.48 (d, *J* = 11.0 Hz, 1H).

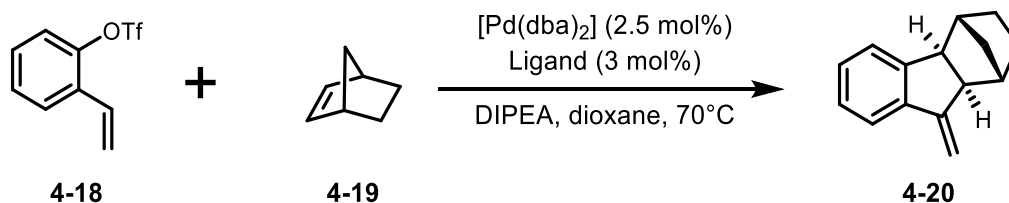
¹³C NMR (101 MHz, CDCl₃) δ 146.82, 131.01, 129.23, 128.81, 128.35, 127.21, 121.62, 120.15, 118.58, 116.97.

¹⁹F NMR (377 MHz, CDCl₃) δ -73.64.

IR (film): ν_{\max} = 1419, 1207, 1137, 1077, 886, 792, 760 cm⁻¹

Asymmetric Heck reaction

(1*S*,4*R*,4*aS*,9*aR*)-9-methylene-2,3,4,4*a*,9,9*a*-hexahydro-1*H*-1,4-methanofluorene



The asymmetric Heck reaction was performed following a modified reported procedure.^[7] Bis(dibenzylideneacetone)palladium(0) (4.7mg, 0.0082mmol), (*S,S,S*)-**SPIRAP(O)** (6.5mg, 0.0098mmol) were added to a Schlenk tube strictly under nitrogen. 1,4-dioxane (320 μ L) was added, and the mixture was stirred at room temperature. After 30min, 2-vinyltriflate **4-18** (60 μ L, 0.32mmol), norbornene (122.1mg, 1.30mmol), and diisopropylethylamine (110 μ L, 0.63mmol) were added and then the mixture was heated to 70°C. After 20h, reaction mixture was concentrated *in vacuo* and purified through a short pipette column (SiO₂) with hexanes elution to afford pure product **4-20** (63.7mg, 99% yield, 95% ee)

¹H NMR (400 MHz, CDCl₃) δ 7.50 – 7.39 (m, 1H), 7.29 – 7.12 (m, 3H), 5.51 (d, *J* = 2.4 Hz, 1H), 5.03 (d, *J* = 2.0 Hz, 1H), 3.06 (d, *J* = 7.0 Hz, 1H), 2.83 (d, *J* = 7.0 Hz, 1H), 2.36 – 2.20 (m, 2H), 1.61 (m, *J* = 18.4, 15.4, 11.6, 5.7 Hz, 2H), 1.41 (m, *J* = 18.9, 9.0, 2.4 Hz, 2H), 1.09 – 0.92 (m, 2H).

¹³C NMR (100 MHz, CDCl₃) δ 154.44, 148.89, 142.58, 128.54, 126.57, 125.09, 119.95, 102.93, 52.20, 52.01, 44.59, 42.49, 32.33, 29.36, 28.62.

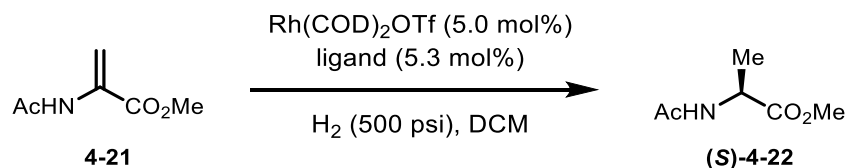
IR (film): ν_{\max} = 2948, 2868, 1635, 1471, 868, 782, 756, 730 cm⁻¹

SFC (Chiralpak OJ-H, 99:1 CO₂/isopropanol, 3.5 ml/min, 40°C, 120 bar back pressure), *t*_r = 3.5 min (minor, (*1R,4S,4aR,9aS*)), 3.8 min (major, (*1S,4R,4aS,9aR*))

For (*R,S,S*)-**SPIRAP(O)** – 96% yield, -86% ee (enantiomer of **20**)

Asymmetric hydrogenation of acrylate derivatives

Methyl acetyl-*L*-alaninate



The asymmetric hydrogenation of acetamidoacrylic esters was based on a reported procedure.^[8] (*S,R,R*)-SPIRAPO (11.2mg, 0.016mmol) and Rh(COD)₂OTf (7.0mg, 0.015mmol) were measured and packed into a Schlenk tube in the glovebox before the addition of dry DCM (3.0mL) to make a stock solution. Methyl 2-acetamidoacrylate (28.6mg, 0.20mmol) was added to the flask before addition of the stock solution (2.0mL). The reaction flask was placed into the hydrogenation apparatus before purging with N₂ and H₂, and the reaction was stirred under 500 psi H₂ for 3h. Volatiles were removed *in vacuo*, and the crude was purified by FCC (SiO₂, 20% EtOAc in hexanes) to afford methyl acetyl-*L*-alaninate (*S*)-4-22 (25.3mg, 87% yield, 91% ee) as clear oil.

¹H NMR (400 MHz, CDCl₃) δ 6.02 (s, 1H), 4.58 (p, *J* = 7.3 Hz, 1H), 3.74 (s, 3H), 2.00 (s, 3H), 1.38 (d, *J* = 7.1 Hz, 3H).

¹³C NMR (100 MHz, CDCl₃) δ 173.62, 169.52, 52.46, 48.00, 23.15, 18.55.

IR (film): ν_{\max} = 3282, 2955, 1739, 1652, 1533, 1436, 1372, 1207, 1160, 1058, 733, 607 cm⁻¹

GC conditions 1:

Rt- bDExsm column (df = 0.25 μ m, 0.25 mm i.d. \times 30 m, fused silica capillary column); carrier gas, He (flow 1.5 mL/min); injection temp, 230 $^{\circ}$ C; initial column temperature, 70 $^{\circ}$ C; progress rate, 2 $^{\circ}$ C /min; final column temperature, 90 $^{\circ}$ C); t_r = 28.9 min (minor, *R*), 29.3 min (major, *S*)

GC conditions 2

Rt- bDExsm column (df = 0.25 μ m, 0.25 mm i.d. \times 30 m, fused silica capillary column); carrier gas, He (flow 1.5 mL/min); injection temp, 230 $^{\circ}$ C; initial column temperature, 70 $^{\circ}$ C; progress rate, 2 $^{\circ}$ C /min; final column temperature, 110 $^{\circ}$ C); t_r = 48.7 min (major, *R*), 51.2 min (minor, *S*)

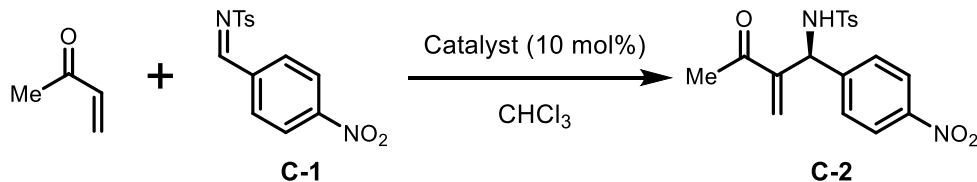
For (*S*)-**SDPO** – 85% yield, 94% ee (*S*)-**4-22**

For (*S*)-**BINAPO** – 84% yield, -91% ee (*R*)-**4-22**

For (*R,R,R*)-**SPIRAPO** – 85% yield, -93% ee (*R*)-**4-22**

Asymmetric Baylis-Hillman reaction of methyl vinyl ketone and an aromatic tosylimine

(*S*)-4-methyl-N-(2-methylene-1-(4-nitrophenyl)-3-oxobutyl)benzenesulfonamide



The asymmetric Baylis-Hillman reaction was performed following a reported procedure.^[9] Imine **C-1** (48mg, 0.16mmol), catalyst (*S,S,S*)-**SPIROMP** (7.9mg, 0.02mmol), activated 3Å MS, and CHCl₃ (820μL) were added to a Schlenk tube. Mixture was cooled to -78°C, then 3-Buten-2-one (41μL, 0.50mmol) was added before warming the reaction to -10°C. After 5 days, volatiles were removed *in vacuo*, and the crude was purified by FCC (SiO₂, 20→40% EtOAc in hexanes) to afford sulfonamide (*S*)-**C-2** (50.2mg, 85% yield, 83% ee).

¹H NMR (500 MHz, CDCl₃) δ 8.10 – 8.01 (m, 2H), 7.64 (d, *J* = 8.0 Hz, 2H), 7.34 (d, *J* = 8.5 Hz, 2H), 7.24 (d, *J* = 8.0 Hz, 2H), 6.13 (s, 1H), 6.08 (s, 1H), 5.93 (d, *J* = 9.3 Hz, 1H), 5.32 (d, *J* = 9.4 Hz, 1H), 2.41 (s, 3H), 2.15 (s, 3H).

¹³C NMR (126 MHz, CDCl₃) δ 198.72, 147.18, 146.15, 145.42, 143.81, 137.36, 129.63, 127.23, 127.17, 123.61, 58.95, 26.17, 21.51.

SFC (Chiralpak IA, 70:30 CO₂/isopropanol, 3.5 ml/min, 40°C, 120 bar back pressure), *t_r* = 4.0 min (major *S*), 4.6 min (minor, *R*)

For (*R,S,S*)-**SPIROMP** – 6.8% yield, -71.8% ee (*R*)-**C-2**

Computational models and analysis

Quantum chemical calculations were performed using the Q-Chem 4.3 package.^[10] Geometry optimizations were evaluated using the B97-D density functional.^[11] For compounds not containing transition metals, double- ζ - quality basis set with polarization functions was used on all atoms, 6-31G**.^[12,13] For Pd-complexes, the LANL2DZ basis set was used of Pd, P, and Cl atoms, while 6-31G** was used on all other atoms.^[14-16] Pictorial representations of we made in Discovery Studio 4.1 Visualizer.^[17] The electronic Gibbs free energy values were obtained from single point calculatings using the ω B97X-D exchange functional.^[18] The final Gibbs free energy values were obtained by correcting the electronic free energy with the enthalpic and entropic contributions from vibrations, rotations, and translations at 298 K. These frequency computations were performed using the B97-D functional. For the enthalpic and entropic corrections to the free energies from the harmonic oscillator approximation, all frequencies below 50 cm⁻¹ were treated as if they were 50 cm⁻¹.

Cartesian coordinates for starting geometries, transition states, and products are described below.

43 • Diol (S,S,S)-4-7

C	-3.16660418	2.51676888	1.21187067
C	-3.47220673	1.73275471	0.08830678
C	-2.53030555	0.80808774	-0.40577742
C	-1.30924670	0.68440827	0.27839571
C	-1.01430839	1.47044495	1.39556754
C	-1.93172027	2.40595904	1.88125011
C	-0.12997580	-0.19398482	-0.05346636
O	0.70580487	-0.09105548	1.11598208
C	0.39861682	1.13963116	1.82881223
C	-0.37560667	-1.64951697	-0.36454275
C	0.38034724	-2.02588796	-1.47838614
C	1.15869767	-0.80975373	-1.93518700
O	0.51272696	0.29807553	-1.24524866
C	-1.16867638	-2.57630232	0.33225338
C	-1.19723175	-3.90426804	-0.13963789
C	-0.43227714	-4.27249729	-1.25731951
C	0.37379853	-3.34325761	-1.94429854
O	-1.91800076	-2.25264222	1.42462945
O	-2.84906405	0.06926319	-1.50667348
C	3.41783300	0.38462186	-1.92406340
C	2.65144451	-0.89646971	-1.56304832
C	2.84936369	1.86763352	1.78200466
C	1.39725415	2.25469900	1.46328589
H	-3.91142875	3.22728152	1.57364590
H	-4.43155190	1.82694792	-0.41941506
H	-1.70717902	3.02792390	2.74812206
H	0.47683546	0.90246922	2.90277633
H	1.05154092	-0.60576479	-3.01314195
H	-1.82004054	-4.63174383	0.37983659
H	-0.47177422	-5.30695997	-1.60170327
H	0.96516968	-3.64555388	-2.80885692
H	-1.80138354	-1.30443316	1.61090982
H	-2.08996952	-0.49764490	-1.72910958
H	4.47230619	0.31117324	-1.62012042
H	3.38544103	0.57146204	-3.00921822
H	2.96579672	1.24714660	-1.41595888
H	2.71218848	-1.09304024	-0.48259783
H	3.08175872	-1.76942095	-2.08222447
H	3.54273745	2.67255686	1.49694678
H	2.97854259	1.66895187	2.85785605
H	3.12365368	0.95793215	1.23163953
H	1.28101785	2.46614191	0.38996576
H	1.10629563	3.16536281	2.01307874

43

• Diol (R,S,S)-4-7

C	-3.76748275	-3.51818612	3.74134222
C	-4.04786752	-4.32271515	2.62564730
C	-3.45630547	-4.03988022	1.37903507
C	-2.58731767	-2.93968672	1.29453362
C	-2.33080690	-2.13637533	2.40609471
C	-2.90764851	-2.40726314	3.65048742
C	-1.75263192	-2.46918854	0.12313126
O	-1.33419260	-1.15283165	0.52609458
C	-1.39749492	-1.02425722	1.97727821
C	-2.41852000	-2.41568750	-1.22378468
C	-1.76340458	-3.25381099	-2.12681959
C	-0.58568313	-3.88561829	-1.41845772
O	-0.63347975	-3.35355276	-0.06748417
C	-3.54783541	-1.66657797	-1.59694885
C	-4.04281795	-1.82777312	-2.90574637
C	-3.39386045	-2.69531117	-3.79983007
C	-2.24066834	-3.41529605	-3.43270641
O	-4.17439363	-0.80788731	-0.74398872
O	-3.76646128	-4.84404146	0.31544995
C	0.53095627	-6.03436956	-0.60243733
C	-0.65273218	-5.42162842	-1.36568745
O	-0.95554273	1.48604679	1.79257206
C	-1.88902753	0.38542121	2.32117428
H	-4.24178652	-3.75594205	4.69457540
H	-4.73073494	-5.16856809	2.70062728

H	-2.70758831	-1.77956704	4.51933719
H	-0.38105357	-1.17187408	2.38584392
H	0.37166407	-3.57603345	-1.87653534
H	-4.92315513	-1.26253861	-3.20950163
H	-3.79409634	-2.80270317	-4.80896192
H	-1.74017002	-4.07168318	-4.14457134
H	-3.59982713	-0.69337294	0.03439360
H	-3.42615899	-4.43070991	-0.49806151
H	0.44644039	-7.12979398	-0.55685303
H	1.48529960	-5.78251220	-1.09156344
H	0.55748647	-5.64086814	0.42266486
H	-1.60205125	-5.70440808	-0.88514505
H	-0.68313979	-5.79451996	-2.40318202
H	-1.34103428	2.48445362	2.04502104
H	0.05015853	1.38430648	2.22935637
H	-0.86048987	1.41117827	0.70081747
H	-2.90513296	0.50713752	1.90944932
H	-1.98200101	0.45008968	3.41754948

85 • Diphosphine (S,S,S)-SPIRAP

85

C	-7.90764641	4.02001391	-0.83380907
C	-8.73687968	2.88382919	-0.82809801
C	-8.19982073	1.57815228	-0.84935829
C	-6.79307735	1.47712345	-0.87837356
C	-5.96971226	2.60520309	-0.86840526
C	-6.51019265	3.89422007	-0.85036631
C	-5.90792373	0.25061771	-0.97713722
O	-4.59106596	0.73441794	-0.67744595
C	-4.52621460	2.16693643	-0.88023199
C	-6.17256176	-0.96590450	-0.11275732
C	-6.08335956	-2.10139521	-0.92085989
C	-5.80582018	-1.68030128	-2.34138947
O	-5.97863626	-0.24283852	-2.32359121
C	-6.42856914	-1.05256265	1.27216854
C	-6.58147584	-2.35190383	1.80273633
C	-6.48332319	-3.49521836	0.98946764
C	-6.23375823	-3.38431127	-0.38623589
P	-6.78078390	0.48213066	2.26531693
C	-6.98264883	-0.23098775	3.97005112
C	-5.93078373	-0.39357444	4.89360778
C	-6.17654444	-0.95213631	6.15720737
C	-7.47150586	-1.36450667	6.50908669
C	-8.52607438	-1.20765798	5.59522774
C	-8.28407762	-0.63542328	4.33831026
C	-5.11365286	1.28903301	2.37946729
C	-3.89754775	0.59604254	2.21516053
C	-2.67533597	1.27755487	2.29588594
C	-2.65390580	2.66017617	2.54586685
C	-3.85990152	3.35978388	2.70811059
C	-5.08302591	2.67798932	2.61664993
P	-9.24673037	0.05359405	-0.62106436
C	-10.95981583	0.77002223	-0.64094337
C	-11.42747123	1.34630849	0.56147976
C	-12.71456381	1.89554698	0.63696180
C	-13.56372506	1.85516235	-0.48138255
C	-13.11358046	1.27113343	-1.67522810
C	-11.81748872	0.73823713	-1.75841582
C	-9.13924589	-0.77089700	-2.27768337
C	-9.37509966	-2.15997856	-2.32426442
C	-9.29822771	-2.85484377	-3.54094681
C	-8.96937924	-2.16851902	-4.72072830
C	-8.72122194	-0.78601403	-4.68035743
C	-8.80806051	-0.09071416	-3.46615752
C	-4.09030743	-1.53863732	-4.22412336
C	-4.38555316	-2.04782917	-2.80522051
C	-2.36275746	1.96149457	-2.21138747
C	-3.80347831	2.49280888	-2.20007364
H	-8.36371906	5.01127638	-0.81735828
H	-9.81679996	3.01756759	-0.79335127
H	-5.86560702	4.77455090	-0.83789391
H	-3.96614341	2.57700505	-0.02528605
H	-6.55538974	-2.07544920	-3.04544850

H	-6.79072764	-2.47799627	2.86382364
H	-6.60982679	-4.48034059	1.44186675
H	-6.17110686	-4.26957097	-1.02086764
H	-4.92247659	-0.08204485	4.62077012
H	-5.35450550	-1.07121192	6.86539243
H	-7.65843792	-1.80122674	7.49143592
H	-9.53596752	-1.52224537	5.86359684
H	-9.10645234	-0.50624819	3.63096079
H	-3.91734998	-0.47097711	1.99572448
H	-1.74025911	0.73275036	2.15605383
H	-1.70158551	3.18961372	2.60643515
H	-3.84960055	4.43542765	2.89213393
H	-6.02140882	3.22693431	2.71661133
H	-10.77256313	1.37381334	1.43531412
H	-13.05766320	2.34635264	1.56983298
H	-14.56961448	2.27340596	-0.42041490
H	-13.76841783	1.23629022	-2.54772753
H	-11.46941555	0.29827418	-2.69309161
H	-9.59714548	-2.69919218	-1.40145400
H	-9.48293789	-3.93011735	-3.56527841
H	-8.89936938	-2.70873016	-5.66628152
H	-8.45468321	-0.25169991	-5.59363251
H	-8.59199231	0.97630720	-3.42701153
H	-3.07018880	-1.80464183	-4.53924995
H	-4.19382515	-0.44556076	-4.25707290
H	-4.79867957	-1.96941946	-4.94991582
H	-4.27968607	-3.14500505	-2.75648042
H	-3.67935161	-1.61255768	-2.08224141
H	-1.86467047	2.17860027	-3.16798376
H	-2.36715602	0.87370143	-2.05587264
H	-1.77079779	2.41772489	-1.40197647
H	-3.81717628	3.58735788	-2.33851580
H	-4.38677856	2.04683405	-3.01971212

• **Diphosphine (S,R,R)-SPIRAP**

85

P	-0.78415159	20.90796583	8.41079710
P	1.44835665	20.43430813	5.41165053
O	-1.04984959	17.26105507	7.80678199
O	-0.30266885	17.20831307	5.55590269
C	-1.66600258	20.13399215	9.84495430
C	-1.09623503	20.30205435	11.12593669
H	-0.18905620	20.89924711	11.23977342
C	-1.68127432	19.70405196	12.25082947
H	-1.23242863	19.84458927	13.23547462
C	-2.83319146	18.91319687	12.10660070
H	-3.28284917	18.43739840	12.97944197
C	-3.39766703	18.73140872	10.83504215
H	-4.28555929	18.10901962	10.71593561
C	-2.81978708	19.33731675	9.71008592
H	-3.24943097	19.17805742	8.72261144
C	-1.31874942	22.68327129	8.50317996
C	-2.15880668	23.20666114	9.50525908
H	-2.57059359	22.54357470	10.26624302
C	-2.46775272	24.57630343	9.52951042
H	-3.11890619	24.96770466	10.31330913
C	-1.95381877	25.43645292	8.54770159
H	-2.19874538	26.49952954	8.56664662
C	-1.12030554	24.92154126	7.54042534
H	-0.71441795	25.58191739	6.77222087
C	-0.79722161	23.55870422	7.52324894
H	-0.14376871	23.16803974	6.74064575
C	-1.77123850	20.30637233	6.95544366
C	-2.80272911	21.06589082	6.36246850
H	-3.08520489	22.01858200	6.80791271
C	-3.46127534	20.62695103	5.20081197
H	-4.25336544	21.24283339	4.77186890
C	-3.10603661	19.41576269	4.58694232
H	-3.60632120	19.08016497	3.67733792
C	-2.08213158	18.66129965	5.16631175
C	-1.43572263	19.09156420	6.32870521
C	-0.45011830	18.01137998	6.73664555
C	-0.01387803	16.65003924	8.61711635
H	0.13910922	15.60870864	8.27088828

C	-0.45802469	16.64005166	10.08296308
H	0.37627309	16.23896695	10.68282052
H	-0.62826443	17.67615770	10.40413394
C	-1.72308853	15.79686732	10.30075393
H	-2.53627035	16.17476779	9.66774796
H	-2.05086861	15.85060209	11.34866297
H	-1.54480759	14.74088983	10.04150267
C	-1.47175595	17.35675891	4.71104185
H	-2.16325425	16.51494294	4.91083434
C	-1.03798088	17.32672629	3.24210820
H	-0.32112489	18.14124582	3.07505656
H	-1.92853948	17.53369087	2.62476451
C	-0.41765011	15.97954802	2.84489722
H	0.44671025	15.76284502	3.48662920
H	-0.07162089	16.00354784	1.80182159
H	-1.14707909	15.16104056	2.95664787
C	0.94298216	18.32973076	7.24450786
C	1.21184547	17.48143543	8.32188346
C	2.45775386	17.49231728	8.95504196
H	2.66414729	16.83238112	9.79920224
C	3.43127793	18.38740700	8.48397498
H	4.41276123	18.42395247	8.95938475
C	3.15621713	19.24681701	7.40628079
H	3.92190114	19.94425583	7.06981299
C	1.90162380	19.23810159	6.76101811
C	2.81885080	21.67689055	5.55692059
C	2.79328531	22.52623338	6.68689579
H	2.02042159	22.38908734	7.44513480
C	3.76034101	23.52640402	6.84830858
H	3.73045732	24.16933122	7.72956545
C	4.75869560	23.70602320	5.87560954
H	5.50681619	24.49082982	5.99685308
C	4.78771088	22.87115013	4.74871476
H	5.56366650	23.00082813	3.99221152
C	3.82783956	21.85817009	4.59107684
H	3.86448584	21.20608385	3.71875756
C	1.88737349	19.49699309	3.87551629
C	1.54939669	20.08168870	2.63484725
H	1.08602933	21.07010352	2.61118928
C	1.78783169	19.39689245	1.43513121
H	1.52278789	19.86110757	0.48379392
C	2.34942177	18.10985989	1.45932229
H	2.52195944	17.57094257	0.52651538
C	2.67936470	17.51833252	2.68790860
H	3.10922365	16.51603927	2.71429402
C	2.45247597	18.20612908	3.88879625
H	2.69521526	17.73460756	4.83950101

• **Pd(II) complex (S,S,S)-4-11**

88

C	-7.31325408	4.25310845	-0.85667450
C	-8.28059072	3.24108705	-0.78570509
C	-7.93246512	1.87306479	-0.83350841
C	-6.56592680	1.55823475	-0.95121539
C	-5.60241497	2.57883528	-0.94677030
C	-5.95192899	3.92821540	-0.91974585
C	-5.80235929	0.25904828	-1.18699475
O	-4.46953808	0.56102088	-0.74196306
C	-4.22397977	1.97335870	-0.96471382
C	-6.20460791	-1.08161074	-0.61060131
C	-6.05771916	-2.04471358	-1.61904520
C	-5.60278464	-1.37020693	-2.88440487
O	-5.81246810	0.03811196	-2.61280113
C	-6.63842165	-1.45885458	0.66281852
C	-6.96377874	-2.81704924	0.88649366
C	-6.79154084	-3.77349867	-0.12268943
C	-6.32587692	-3.39353971	-1.39253495
P	-7.16546413	-0.32380265	2.05888680
C	-6.38682904	-1.09286747	3.59038195
C	-5.26550328	-1.93255208	3.47963304
C	-4.61203625	-2.37426697	4.64162253
C	-5.07302815	-1.97280590	5.90407583
C	-6.19098177	-1.12829268	6.00673118

C	-6.85107267	-0.68525327	4.85272282
C	-6.31391949	1.34702163	2.09853202
C	-4.91584006	1.43367961	2.21162113
C	-4.32023188	2.68131853	2.44001535
C	-5.11800771	3.83205463	2.56350910
C	-6.51389486	3.73556724	2.46194299
C	-7.11631737	2.48903229	2.23762135
P	-9.32435365	0.62351327	-0.51425630
C	-10.85596410	1.64584230	-0.88476260
C	-11.49617429	2.29316183	0.18570072
C	-12.57591914	3.14907211	-0.06982510
C	-13.02373340	3.34333004	-1.38745467
C	-12.39005938	2.68140842	-2.45046109
C	-11.29882039	1.83342641	-2.20215958
C	-9.21260266	-0.65364489	-1.87287261
C	-9.67151795	-1.95567625	-1.61016789
C	-9.64592498	-2.90995223	-2.63764062
C	-9.18516828	-2.56198054	-3.91757950
C	-8.73835520	-1.25492923	-4.17440044
C	-8.73901121	-0.29827514	-3.14835466
C	-3.68605429	-0.95947120	-4.51823506
C	-4.13283724	-1.66674286	-3.23085743
C	-2.09229412	1.54184743	-2.30938289
C	-3.46371114	2.23190164	-2.27740697
H	-7.63113301	5.29610331	-0.82964156
H	-9.32554374	3.52692046	-0.68616545
H	-5.18618099	4.70481481	-0.92297706
H	-3.62679775	2.32103147	-0.10691819
H	-6.25369424	-1.62320374	-3.73470222
H	-7.37771482	-3.11556068	1.84997212
H	-7.05021874	-4.81325055	0.07980392
H	-6.21410856	-4.12622044	-2.19246212
H	-4.90604542	-2.24554626	2.49992378
H	-3.74420512	-3.02994199	4.55429657
H	-4.56605695	-2.31945358	6.80584430
H	-6.55951071	-0.82137195	6.98620323
H	-7.73243805	-0.05189617	4.93020940
H	-4.30415581	0.53726095	2.12415480
H	-3.23524151	2.75288559	2.53166522
H	-4.65058437	4.80083117	2.74651897
H	-7.13567811	4.62582302	2.56091574
H	-8.20055590	2.39269092	2.17264325
H	-11.16611965	2.10027636	1.20617408
H	-13.07863312	3.64599650	0.76096440
H	-13.87133813	4.00200992	-1.58288924
H	-12.74445882	2.81979047	-3.47295034
H	-10.80667392	1.31362397	-3.02367618
H	-10.05101401	-2.20698801	-0.62018825
H	-9.99229999	-3.92407491	-2.43553562
H	-9.17475736	-3.30658540	-4.71542256
H	-8.37837332	-0.98053258	-5.16723401
H	-8.34911614	0.70243305	-3.32788003
H	-2.62954037	-1.16867867	-4.74107223
H	-3.81063922	0.12672242	-4.41717802
H	-4.29200442	-1.29308113	-5.37578636
H	-4.02572267	-2.75960897	-3.33513720
H	-3.51816056	-1.35346984	-2.37499949
H	-1.57366928	1.73804862	-3.25933052
H	-2.21227782	0.45618507	-2.19819514
H	-1.45092205	1.89990159	-1.48809403
H	-3.34567476	3.32363939	-2.38362073
H	-4.09554755	1.88395096	-3.10589737
Pd	-9.49227147	-0.41132773	1.63300775
Cl	-9.77093887	-1.66774910	3.69369728
Cl	-11.80753886	-0.89597443	1.04150558

• Pd(II) complex (S,R,R)-4-11

88

P	-0.90564579	21.52013263	8.07779970
P	2.16806278	20.99025472	6.47176278
O	-0.95078418	17.50092404	7.78344443
O	0.26231649	17.41601059	5.76324743
C	-1.35079455	20.49334597	9.58341307
C	-0.57239852	20.59778059	10.74756900

H	0.32824982	21.20966943	10.74427984
C	-1.00182537	19.95375836	11.91884091
H	-0.40280373	20.03804863	12.82624115
C	-2.20318614	19.22714287	11.92942193
H	-2.54124877	18.74478364	12.84790900
C	-2.96190689	19.10416717	10.75368338
H	-3.87973749	18.51560037	10.75070386
C	-2.52681182	19.72004304	9.57191755
H	-3.09627699	19.60549305	8.65032876
C	-2.07811039	22.99178613	8.10870204
C	-3.31591521	22.94245564	8.76589386
H	-3.59917440	22.05709976	9.33400277
C	-4.17452960	24.05232766	8.71015458
H	-5.13153366	24.01991386	9.23297052
C	-3.79997274	25.19919794	7.99340370
H	-4.46757351	26.06118174	7.95464202
C	-2.55672563	25.24404137	7.34024500
H	-2.25008198	26.14192128	6.80217674
C	-1.69126862	24.14455192	7.40367756
H	-0.70195011	24.18974647	6.94644487
C	-1.57184049	20.51924643	6.61029570
C	-2.57753439	21.10411717	5.80966925
H	-2.97380301	22.08201989	6.07103630
C	-3.07103039	20.46494859	4.66402478
H	-3.84502743	20.95527900	4.07220695
C	-2.56317241	19.21849103	4.27200935
H	-2.92556535	18.71775093	3.37372654
C	-1.57076247	18.63761675	5.06063761
C	-1.07849215	19.26307605	6.21933342
C	-0.13644549	18.24956101	6.86830331
C	-0.07712602	16.73118240	8.64616236
H	0.10333090	15.74710319	8.17271379
C	-0.73048509	16.54030308	10.01427912
H	-0.04073392	15.93589047	10.62676931
H	-0.82197094	17.52233748	10.49259318
C	-2.10007994	15.85181375	9.91914806
H	-2.78224143	16.45923472	9.30961356
H	-2.54365684	15.72250480	10.91712146
H	-2.00967130	14.85971302	9.44853023
C	-0.88281105	17.30245735	4.88677719
H	-1.54157975	16.50154626	5.27534765
C	-0.42867905	16.94448117	3.47329937
H	0.18390921	17.76809073	3.08736338
H	-1.32969555	16.88069572	2.84074421
C	0.34796931	15.61851467	3.43331392
H	1.24046857	15.68523157	4.07080849
H	0.66520449	15.37840211	2.40785480
H	-0.27268430	14.78792381	3.80501582
C	1.13189910	18.52477805	7.66037711
C	1.19002909	17.54924819	8.66917596
C	2.27780561	17.44768145	9.53640179
H	2.29901847	16.68787867	10.31862176
C	3.32751412	18.37020794	9.39845726
H	4.17769098	18.34332250	10.08059748
C	3.27809876	19.35584370	8.40480813
H	4.06599659	20.10605994	8.34966042
C	2.19103983	19.42625597	7.50254438
C	3.92621206	21.18316787	5.83375426
C	4.73532032	20.05528789	5.61476928
H	4.40086149	19.06761642	5.93196298
C	5.98559189	20.21054947	4.99472612
H	6.61778244	19.33673683	4.82913123
C	6.41732724	21.48311330	4.59112502
H	7.39053821	21.60109094	4.11210904
C	5.60085671	22.60498736	4.81000651
H	5.93869160	23.59742811	4.50950412
C	4.35332156	22.45948237	5.43211456
H	3.72870756	23.32718987	5.63638208
C	1.27434986	20.86034865	4.82956477
C	0.32560267	21.84322627	4.51388123
H	0.02905756	22.56109464	5.27864226
C	-0.22383937	21.89327637	3.22490956
H	-0.97091852	22.65059116	2.98586328
C	0.19392073	20.97612557	2.24997567
H	-0.22438864	21.02116090	1.24349056

C	1.16460265	20.01004349	2.56315947
H	1.50269242	19.30654444	1.80090692
C	1.70385045	19.94474043	3.85490949
H	2.45924527	19.19958720	4.09994906
Pd	1.30592700	22.42607994	8.12900717
Cl	3.54114409	23.30447829	8.48135910
Cl	0.51438352	23.78480381	9.99552640

• Pd(II) complex of SDP 4-23

80

P	-1.03083899	21.55173105	7.79536988
P	2.06039684	20.97466813	6.28960293
C	-0.98767733	17.27059421	7.80515386
C	0.48969899	17.27541403	5.72945301
C	-1.17251147	20.64137704	9.42161851
C	-0.19336920	20.85507908	10.40490781
H	0.61803050	21.55401082	10.21023899
C	-0.28099594	20.16741362	11.62413992
H	0.48626648	20.32328689	12.38278033
C	-1.34406614	19.28218619	11.86419547
H	-1.40668141	18.74883844	12.81411744
C	-2.33370203	19.08793244	10.88660721
H	-3.16603158	18.40732435	11.07224498
C	-2.24948386	19.76984386	9.66351473
H	-3.00405613	19.60940129	8.89232618
C	-2.37400534	22.87238890	7.79650815
C	-3.56310989	22.72329959	8.52344495
H	-3.71042163	21.85588468	9.16493512
C	-4.55644256	23.71238959	8.43701482
H	-5.47684825	23.60433495	9.01278008
C	-4.36292258	24.83628667	7.61966909
H	-5.13549755	25.60405963	7.55576632
C	-3.16798370	24.98138634	6.89472715
H	-3.00368192	25.86401401	6.27527072
C	-2.16904360	24.00423565	6.98807280
H	-1.21825627	24.12638373	6.46826680
C	-1.62995039	20.35434238	6.43789451
C	-2.64632130	20.85252935	5.59049559
H	-3.12033800	21.80180167	5.82533229
C	-3.04515981	20.17503217	4.43248802
H	-3.83436917	20.59829226	3.80963759
C	-2.40782050	18.98468165	4.06529556
H	-2.67452727	18.46637950	3.14288064
C	-1.41241163	18.47079658	4.89864663
C	-1.03002399	19.11722531	6.09778147

C	-0.10218013	18.16784479	6.86441945
C	-0.05474690	16.79733495	8.94048947
H	0.37345269	15.80353583	8.72388060
H	-0.57529273	16.72957884	9.90688781
C	-0.63511182	17.19009738	4.67484001
H	-1.27933528	16.31149857	4.84780952
H	-0.24920012	17.11921210	3.64696471
C	1.00587261	18.64190236	7.78981086
C	1.03784974	17.84420493	8.95626251
C	1.99605847	18.04206580	9.95188413
H	1.98724353	17.42729632	10.85311158
C	2.95104882	19.05776303	9.78535274
H	3.69259476	19.25349626	10.56049546
C	2.94764391	19.84151370	8.62623437
H	3.66787028	20.65294431	8.51999286
C	1.99414993	19.62085026	7.60270120
C	3.86625655	20.99920877	5.76514979
C	4.66533426	19.85186794	5.90938651
H	4.28271740	18.98077970	6.44009574
C	5.96281023	19.83578595	5.37245063
H	6.58357362	18.94597223	5.48890700
C	6.45521834	20.95915690	4.69154949
H	7.46505963	20.94742688	4.27859857
C	5.64944659	22.10042277	4.54584606
H	6.03219412	22.97969317	4.02645439
C	4.35337044	22.12513843	5.07908614
H	3.73494920	23.01604166	4.99246844
C	1.26700022	20.62682274	4.62312530
C	0.22470765	21.47042040	4.21311281
H	-0.15955015	22.21140280	4.91352790
C	-0.31141761	21.34152882	2.92477727
H	-1.13177921	21.98861599	2.61432776
C	0.20582017	20.38124490	2.04238014
H	-0.21157895	20.28179575	1.03935322
C	1.27360231	19.55993966	2.44232346
H	1.69727208	18.83230403	1.74860401
C	1.81829993	19.69351626	3.72706708
H	2.68292733	19.09902480	4.02175109
Pd	1.08559651	22.67095635	7.60769297
Cl	3.20684563	23.84515231	7.63532991
Cl	0.23715372	24.18187929	9.32889567
H	1.36983928	17.77012854	5.30232504
H	0.80322027	16.29761799	6.12167921
H	-1.44210045	16.44644670	7.23832794
H	-1.79714027	17.87613280	8.22169960

Energy values and geometric parameters are described in the following tables.

Table C.1. Calculated energy values for the described geometries.

	G_e^a (kcal/mol)	H_{vib}^b (kcal/mol)	S_{vib}^b (kcal/mol)	G_{corr}^c (kcal/mol)
Diol (S,S,S)-4-7	-650274.0	230.2	148.1	-650088.0
Diol (R,S,S)-4-7	-650273.2	230.1	147.5	-650087.0
Diphosphine (S,S,S)-SPIRAP	-1565059.2	450.3	245.8	-1564682.1
Diphosphine (S,R,R)-SPIRAP	-1565058.5	449.8	238.7	-1564679.8
Pd(II) complex ((S,S,S)-4-11)	-1243189.9			
Pd(II) complex ((S,R,R)-4-11)	-1243184.6			
Pd(II) complex of SDP (4-23)	-1099473.7			

^a Gas-phase electronic energy (ω B97X-D/SMD/6-31G**). ^b Vibrational, rotational, and translational entropic and enthalpic contributions (B97-D/6-31G**) at 298K. ^c Corrected free energy values at 298K. Pd(II) complexes vibrational, rotational, and translational contributions to the total free energy were not calculated.

Table C.2. Geometrical parameters for SPIRAP Pd-complexes.

	α ($^\circ$) ^a	β ($^\circ$) ^a	τ_4 ^b	τ_4' ^c	Bite angle ($^\circ$) ^d
(S,S,S)-4-11	173.8	169.9	0.11	0.13	94.4
(S,R,R)-4-11	174.8	172.8	0.09	0.09	95.3
4-23	174.7	169.2	0.11	0.13	94.2

^a Largest angles at Pd. ^b geometry index parameter, calculated from: $\tau_4 = -0.00709\alpha - 0.00709\beta + 2.55$; ^[19] ^c geometry index parameter, calculated from $\tau_4' = -0.00399\alpha - 0.01019\beta + 2.55$; ^[20] ^d P-Pd-P angle.

X-Ray crystallography studies

(*S,S,S*)-SPIRAP(O) – CCDC Number: 1812181

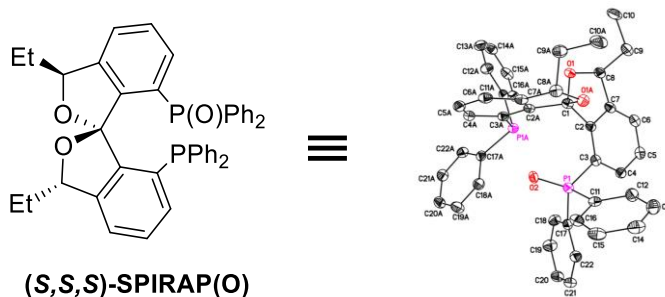


Table C.3. Crystal data and structure refinement for aa1711:

Identification code	aa1711
Empirical formula	C ₄₃ H ₃₈ O ₃ P ₂
Formula weight	664.67
Temperature	85(2) K
Wavelength	1.54184 Å
Crystal system, space group	Hexagonal, P6(4)
Unit cell dimensions	a = 15.22339(13) Å alpha = 90 deg.
	b = 15.22339(13) Å beta = 90 deg.
	c = 12.75692(12) Å gamma = 120 deg.
Volume	2560.35(5) Å ³
Z, Calculated density	3, 1.295 Mg/m ³
Absorption coefficient	1.472 mm ⁻¹
F(000)	1053
Crystal size	0.190 x 0.150 x 0.100 mm
Theta range for data collection	3.352 to 69.236 deg.
Limiting indices	-18<=h<=17, -18<=k<=18, -15<=l<=15
Reflections collected / unique	39371 / 3173 [R(int) = 0.0574]
Completeness to theta = 67.684	100.00%
Absorption correction	Semi-empirical from equivalents
Max. and min. transmission	1.00000 and 0.82517
Refinement method	Full-matrix least-squares on F ²
Data / restraints / parameters	3173 / 1 / 224
Goodness-of-fit on F ²	1.109
Final R indices [I>2sigma(I)]	R1 = 0.0342, wR2 = 0.0865
R indices (all data)	R1 = 0.0343, wR2 = 0.0866
Absolute structure parameter	-0.130(18)
Extinction coefficient	0.0089(6)
Largest diff. peak and hole	0.191 and -0.227 e.Å ⁻³

(S,R,R)-SPIRAP(O) – CCDC: 1812182

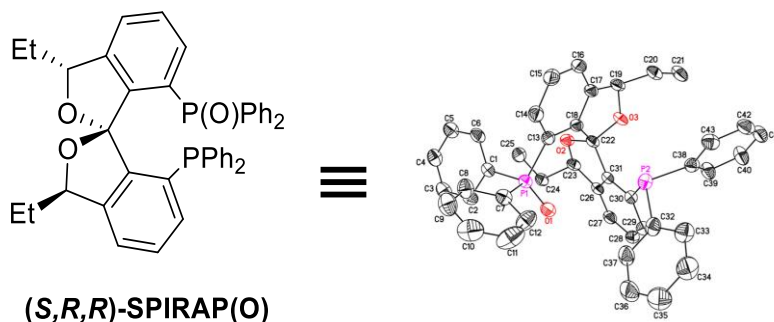


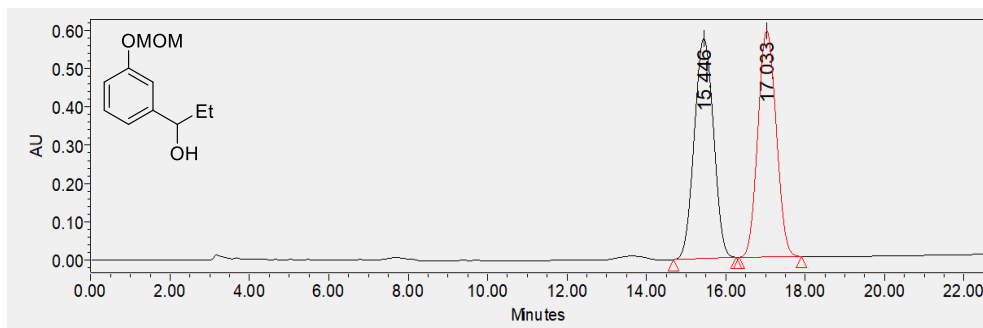
Table C.4. Crystal data and structure refinement for aa2393:

Identification code	aa2393
Empirical formula	C ₄₃ H ₃₈ O ₃ P ₂
Formula weight	664.67
Temperature	225(2) K
Wavelength	1.54178 Å
Crystal system, space group	Monoclinic, P2(1)
Unit cell dimension	a = 10.01060(10) Å alpha = 90 deg.
	b = 31.3874(3) Å beta = 90.2490(10) deg.
	c = 11.24650(10) Å gamma = 90 deg.
Volume	3533.69(6) Å ³
Z, Calculated density	4, 1.249 Mg/m ³
Absorption coefficient	1.422 mm ⁻¹
F(000)	1400
Crystal size	0.12 x 0.04 x 0.04 mm
Theta range for data collection	2.816 to 69.327 deg.
Limiting indices	-12 ≤ h ≤ 11, -37 ≤ k ≤ 38, -13 ≤ l ≤ 13
Reflections collected / unique	54487 / 12761 [R(int) = 0.0529]
Completeness to theta = 67.679	100.00%
Absorption correction	Semi-empirical from equivalents
Max. and min. transmission	1.00000 and 0.59423
Refinement method	Full-matrix least-squares on F ²
Data / restraints / parameters	12761 / 1 / 870
Goodness-of-fit on F ²	1.048
Final R indices [I > 2σ(I)]	R1 = 0.0481, wR2 = 0.1318
R indices (all data)	R1 = 0.0509, wR2 = 0.1375
Absolute structure parameter	0.048(15)
Extinction coefficient	n/a
Largest diff. peak and hole	0.776 and -0.350 e.Å ⁻³

HPLC, SFC, and GC traces

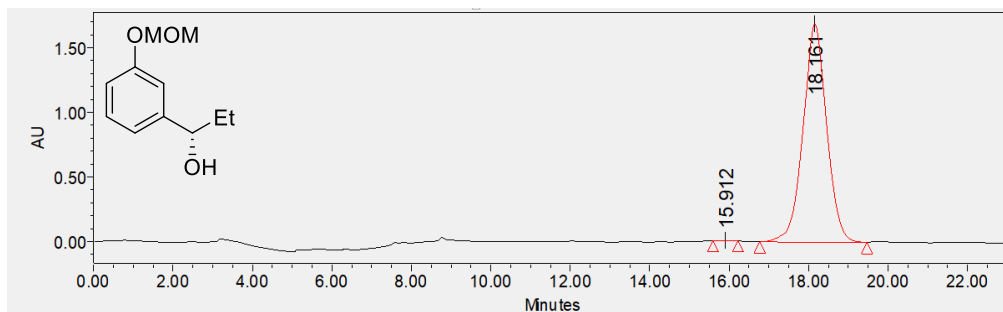
1-(3-(methoxymethoxy)phenyl)propan-1-ol (4-2a)

Racemic



Retention Time [min]	% Area
15.446	50.56
17.033	49.44

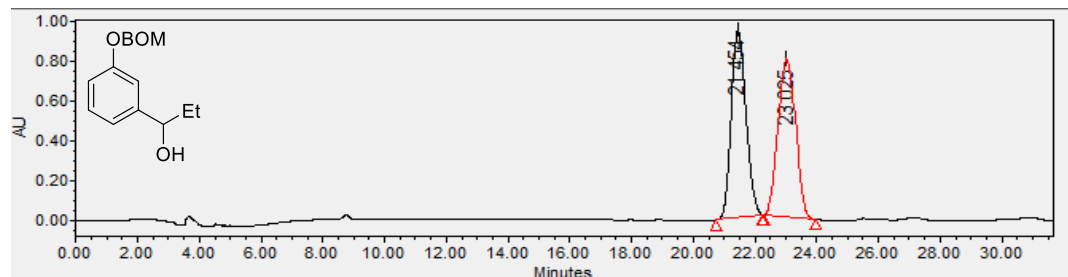
(S)-4-2a



Retention Time [min]	% Area
15.912	0.09
18.161	99.91

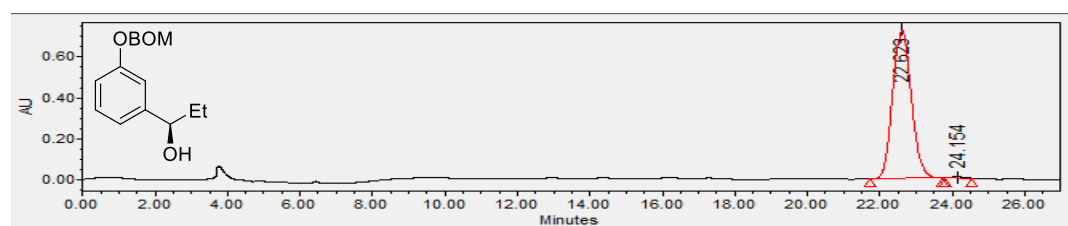
1-(3-((benzyloxy)methoxy)phenyl)propan-1-ol (4-2b)

Racemic



Retention Time [min]	% Area
21.454	49.87
23.025	50.13

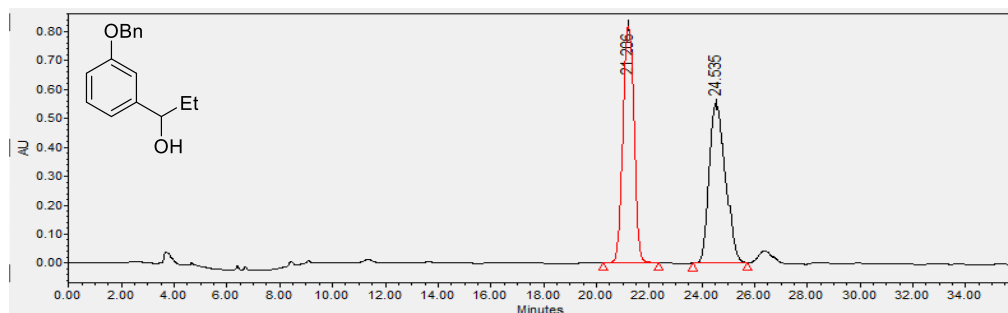
(*R*)-4-2b



Retention Time [min]	% Area
22.623	99.43
24.154	0.57

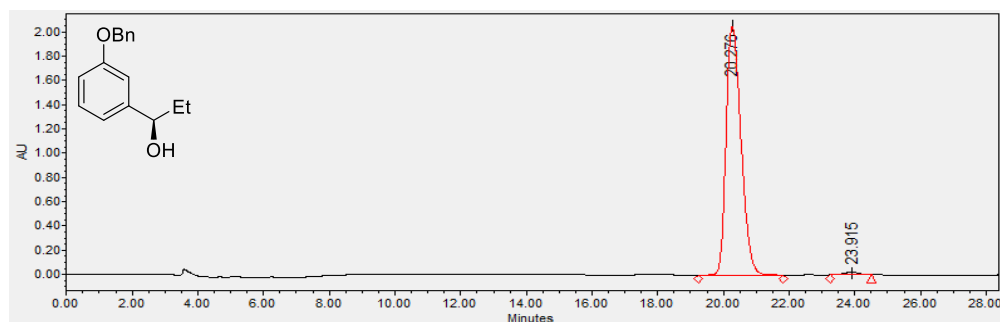
1-(3-(benzyloxy)phenyl)propan-1-ol (4-2c)

Racemic



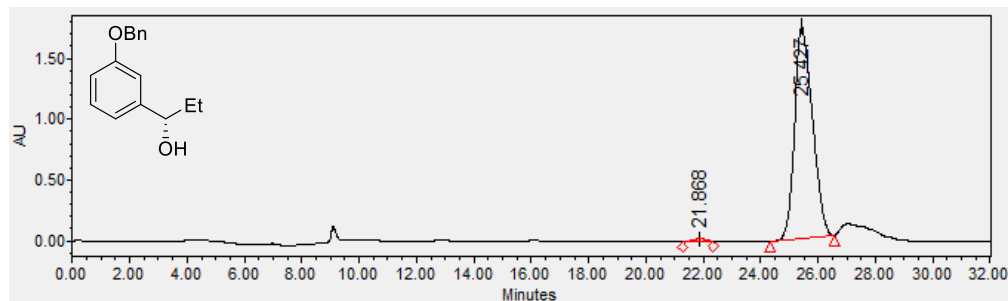
Retention Time [min]	% Area
21.206	50.43
24.535	49.57

(*R*)-4-2b



Retention Time [min]	% Area
20.276	98.91
23.915	1.09

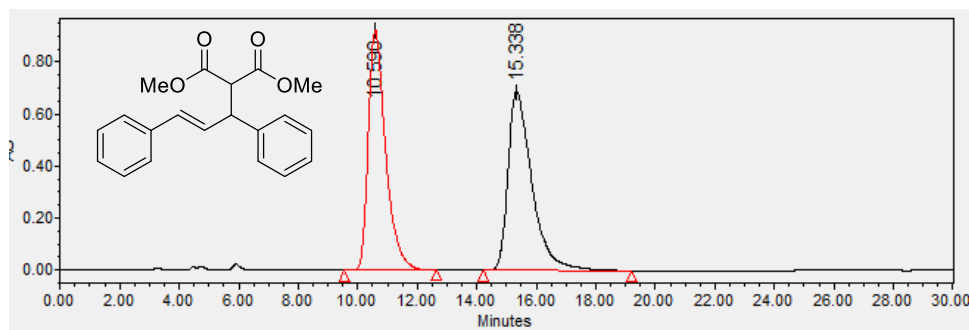
(S)-4-2b



Retention Time [min]	% Area
21.868	0.86
25.427	99.14

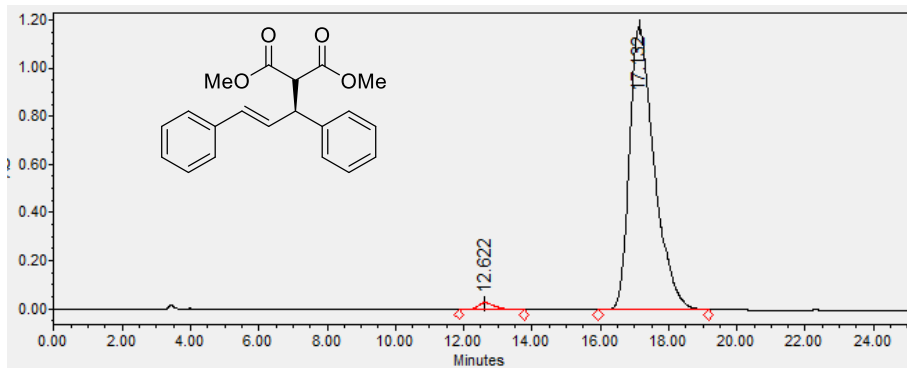
Dimethyl (*E*)-2-(1,3-diphenylallyl)malonate (4-17)

Racemic



Retention Time [min]	% Area
10.590	49.39
15.338	50.61

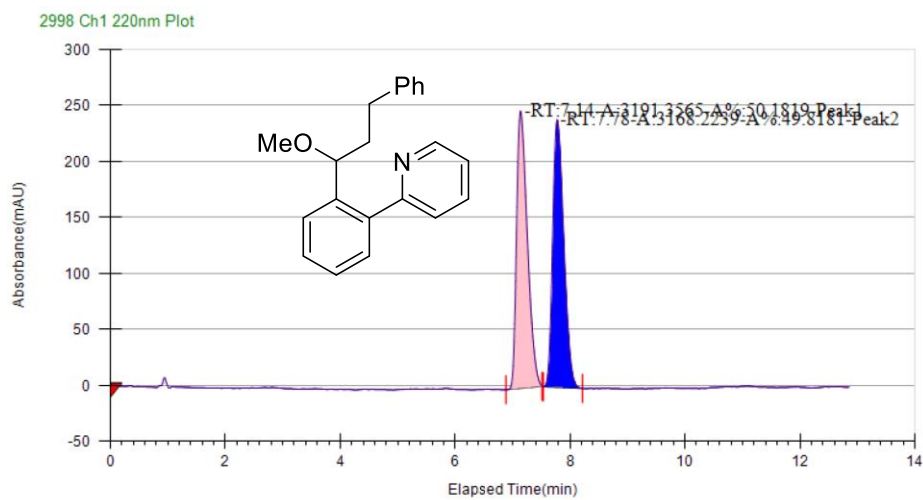
Using (*S,S,S*)-SPIRAP



Retention Time [min]	% Area
12.622	1.71
17.132	98.29

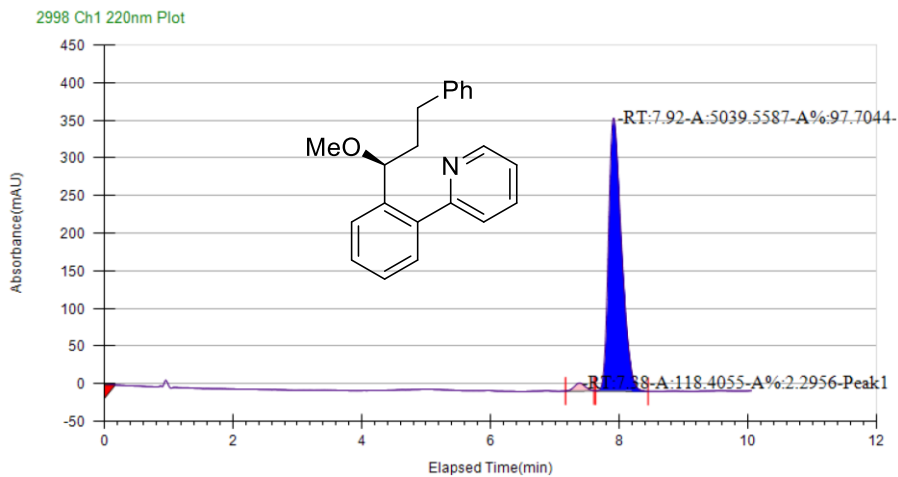
2-(2-(1-methoxy-3-phenylpropyl)phenyl)pyridine (4-14)

Racemic



Retention Time [min]	% Area
7.14	50.18
7.78	49.82

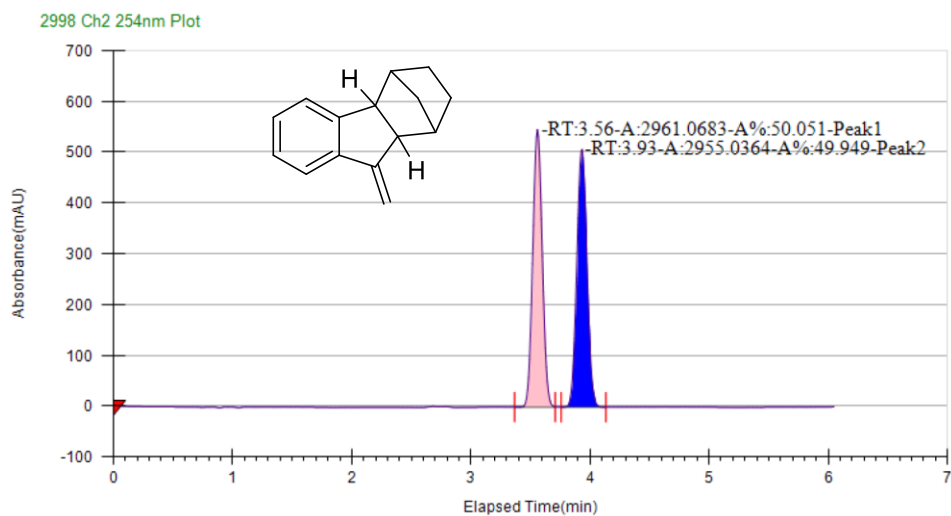
Using (S,S,S)-SPIRAP



Retention Time [min]	% Area
7.38	2.30
7.92	97.70

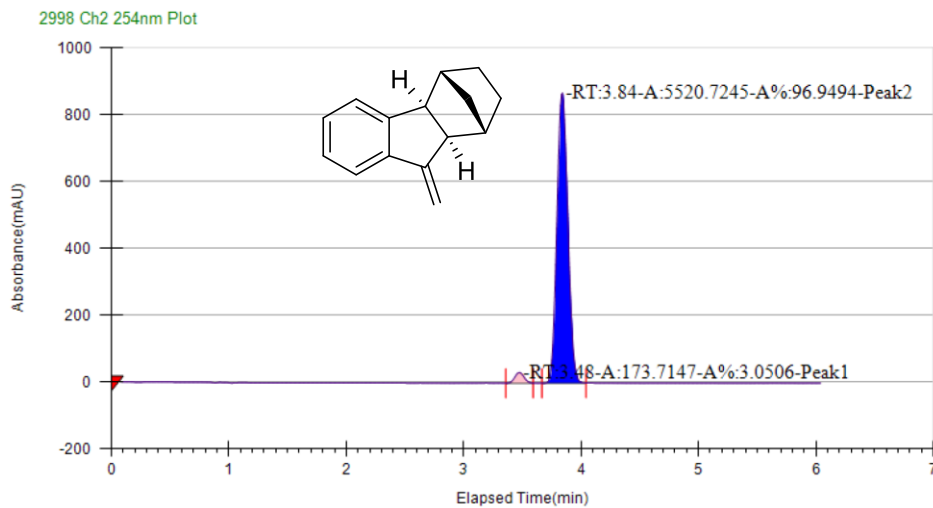
9-methylene-2,3,4,4a,9,9a-hexahydro-1H-1,4-methanofluorene (4-20)

Racemic



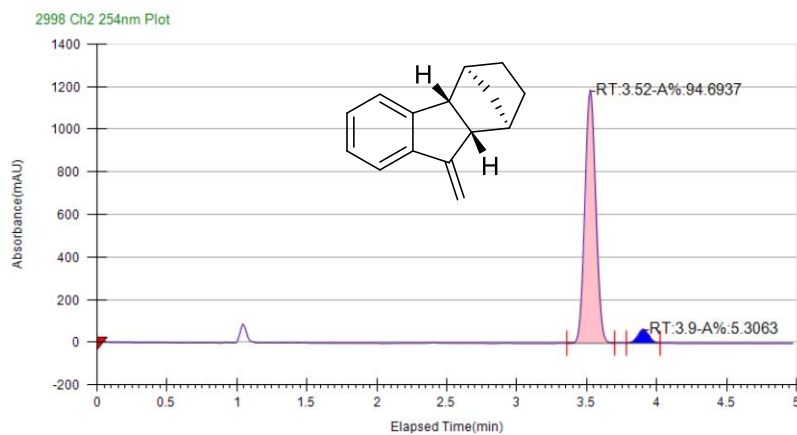
Retention Time [min]	% Area
3.56	50.05
3.93	49.95

Using (*S,S,S*)-SPIRAP(O)



Retention Time [min]	% Area
3.48	3.05
3.84	96.95

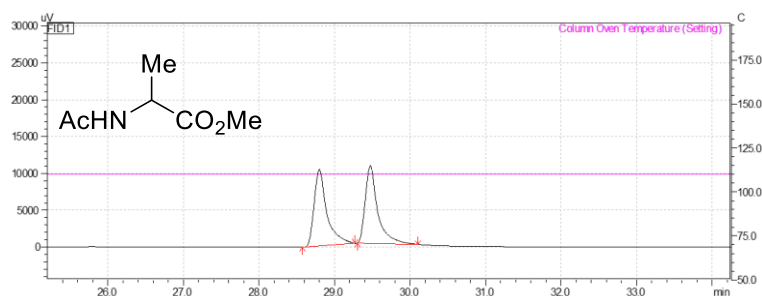
Using (*R,S,S*)-SPIRAP(O)



Retention Time [min]	% Area
3.52	94.69
3.90	5.31

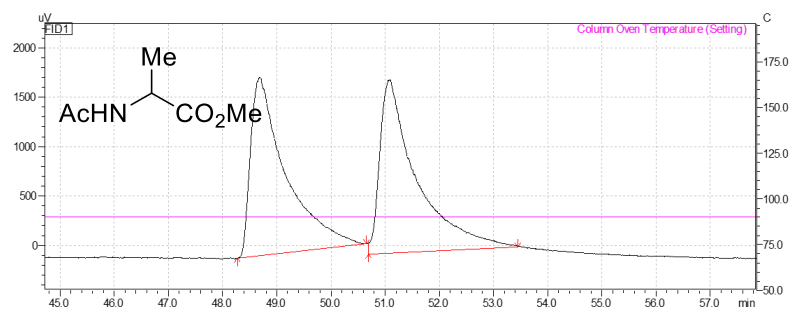
Methyl acetylalaninate (4-22)

Racemic (GC conditions 1)



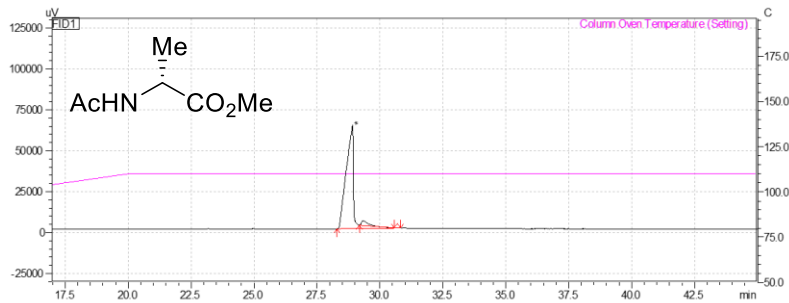
Retention Time [min]	% Area
28.800	50.176
29.476	49.824

Racemic (GC conditions 2)



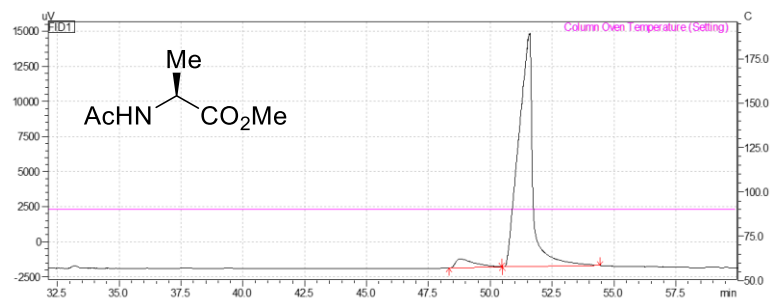
Retention Time [min]	% Area
48.687	49.415
51.078	50.585

With (*R,R,R*)-SPIRAPO (GC conditions 1)



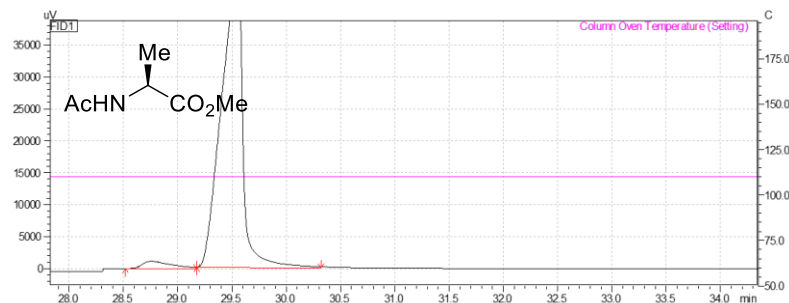
Retention Time [min]	% Area
28.914	96.449
29.344	3.551

With (*S,R,R*)-SPIRAPO (GC conditions 2)



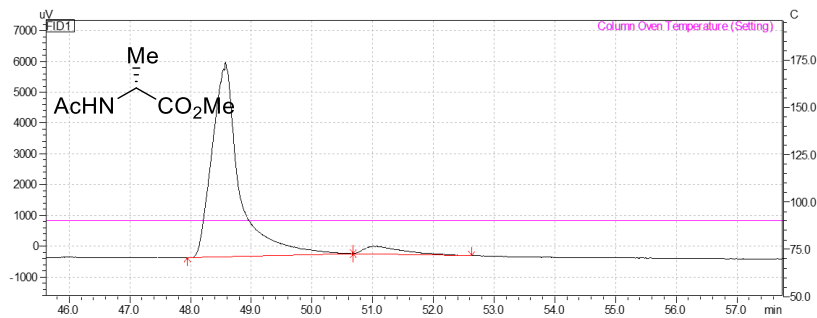
Retention Time [min]	% Area
48.776	4.785
51.595	95.215

With (*S*)-SDPO (GC conditions 1)



Retention Time [min]	% Area
28.753	3.256
29.553	96.744

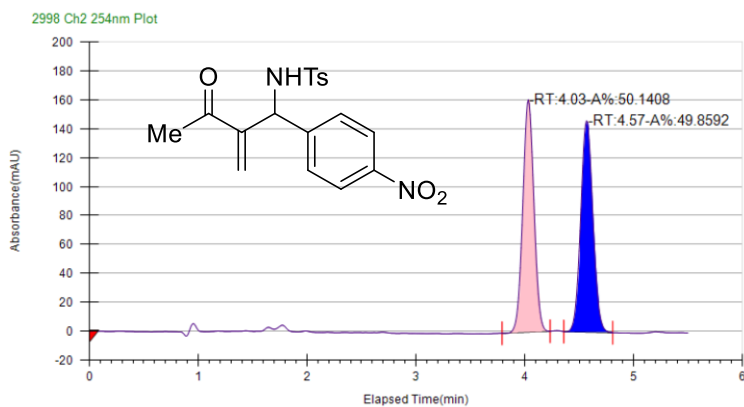
With (S)-BINAPO (GC conditions 2)



Retention Time [min]	% Area
48.576	94.717
51.020	5.283

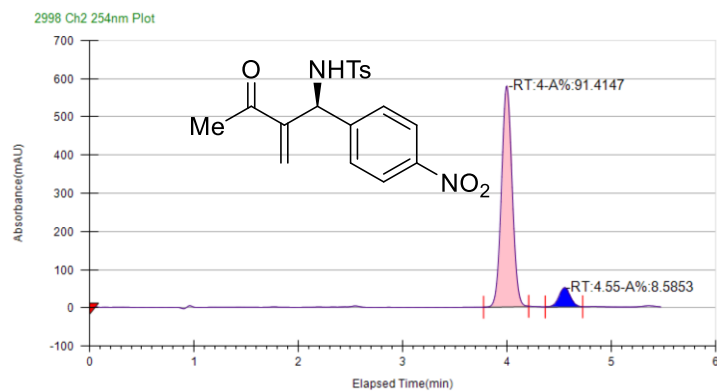
4-methyl-N-(2-methylene-1-(4-nitrophenyl)-3-oxobutyl)benzenesulfonamide (C-2)

Racemic



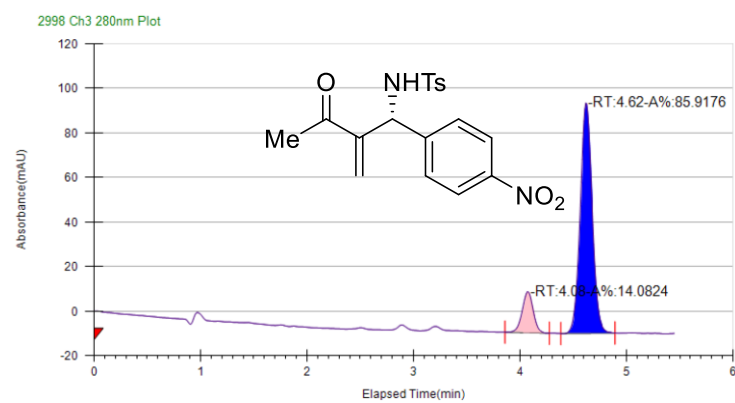
Retention Time [min]	% Area
4.03	50.14
4.57	49.86

Using (*S,S,S*)-SPIROMP



Retention Time [min]	% Area
4.00	91.41
4.55	8.59

Using (*R,S,S*)-SPIROMP



Retention Time [min]	% Area
4.08	14.08
4.62	85.92

References

- [1] K. Soai, S. Yokoyama, T. Hayasaka, *J. Org. Chem.* **1991**, *56*, 4264–4268.
- [2] M. C. Wang, Y. H. Wang, G. W. Li, P. P. Sun, J. X. Tian, H. J. Lu, *Tetrahedron Asymmetry* **2011**, *22*, 761–768.
- [3] A. E. Green, V. Agouridas, E. Deniau, *Tetrahedron Lett.* **2013**, *54*, 7078–7079.
- [4] R. Matsubara, T. F. Jamison, *Chem. - An Asian J.* **2011**, *6*, 1860–1875.
- [5] Y. Ebe, M. Onoda, T. Nishimura, H. Yorimitsu, *Angew. Chem., Int. Ed.* **2017**, *56*, 5607–5611.
- [6] J. H. Xie, H. F. Duan, B. M. Fan, X. Cheng, L. X. Wang, Q. L. Zhou, *Adv. Synth. Catal.* **2004**, *346*, 625–632.
- [7] J. Hu, H. Hirao, Y. Li, J. Zhou, *Angew. Chem., Int. Ed.* **2013**, *52*, 8676–8680.
- [8] R. Guo, T. T. L. Au-Yeung, J. Wu, M. C. K. Choi, A. S. C. Chan, *Tetrahedron Asymmetry* **2002**, *13*, 2519–2522.
- [9] S. Takizawa, K. Kiriyama, K. Ieki, H. Sasai, *Chem. Commun.* **2011**, *47*, 9227–9229.
- [10] Y. Shao, Z. Gan, E. Epifanovsky, A. T. B. Gilbert, M. Wormit, J. Kussmann, A. W. Lange, A. Behn, J. Deng, X. Feng, et al., *Mol. Phys.* **2015**, *113*, 184–215.
- [11] A. D. Becke, *J. Chem. Phys.* **1997**, *107*, 8554–8560.
- [12] P. C. Hariharan, J. A. Pople, *Theor. Chim. Acta* **1973**, *28*, 213–222.
- [13] M. M. Francl, W. J. Pietro, W. J. Hehre, J. S. Binkley, M. S. Gordon, D. J. DeFrees, J. A. Pople, *J. Chem. Phys.* **1982**, *77*, 3654–3665.
- [14] P. J. Hay, W. R. Wadt, *J. Chem. Phys.* **1985**, *82*, 299–310.
- [15] W. R. Wadt, P. J. Hay, *J. Chem. Phys.* **1985**, *82*, 284–298.
- [16] P. J. Hay, W. R. Wadt, *J. Chem. Phys.* **1985**, *82*, 270–283.
- [17] Discovery Studio 4.1 Visualizer: Accelrys Software Inc. San Diego, USA, **2015**.
- [18] J. Da Chai, M. Head-Gordon, *J. Chem. Phys.* **2008**, *128*, 084106.
- [19] L. Yang, D. R. Powell, R. P. Houser, *Dalt. Trans.* **2007**, *0*, 955–964.
- [20] A. Okuniewski, D. Rosiak, J. Chojnacki, B. Becker, *Polyhedron* **2015**, *90*, 47–57.

APPENDIX D

Experimental Information for Chapter 5, Section 5.2

(Adapted from:

Supporting information for: Tay, J. H.; Argüelles, A. J.; DeMars, M.; Zimmerman, P. M.; Sherman, D.; Nagorny, P. *J. Am. Chem. Soc.* **2017**, *139*, 8570.)

The experimental work was done by Dr. Tay Rosenthal while the computational studies were done by me. A complete account of the experiments, including the synthesis of substrates as well as characterization data can be found in the supplementary information for reference [1].

Computational Studies

All quantum chemical calculations were performed using the Q-Chem 4.3 package.^[2] Geometry optimizations were evaluated using the B97-D density functional^[3,4] using the double- ζ - quality basis set with polarization functions on all atoms, 6-31G**.^[5,6] Pictorial representations of important stationary points were generated in Discovery Studio 4.1 Visualizer.^[7]

For the growing string reaction path optimizations, between 7-15 nodes were used, including the end points. In the initial phase, termed growth phase, new nodes were added when the perpendicular gradient magnitude on the frontier node was less than 0.10 Hartree/Å for double-ended strings, or when the RMS gradient was less than 0.005 Hartree/Å for single-ended strings. Additionally, an initial maximum optimization step size of 0.1 Å-radians was used. When the total perpendicular gradient magnitude over all nodes, F , reached a value of less than 0.3, the climbing

image search was initiated. When $F < 0.1$, or when the node of highest energy had a RMS gradient below double the nodal convergence criterion and $F < 0.2$, the exact transition state search was initiated. The string is considered fully converged when an RMS gradient < 0.0005 Hartree/Å was obtained for the node representing the transition state. Further detail regarding the growing string implementation developed in the Zimmerman group can be found in the references.^[8-11]

The electronic Gibbs free energy values of all stationary points were computed through solvent corrected (dichloromethane) single point energies using the SMD model.^[12] For these calculations the ω B97X-D exchange functional^[13] was employed with a 6-31G** basis set. The final Gibbs free energy values were obtained by correcting the electronic free energy with the enthalpic and entropic contributions from vibrations, rotations, and translations at 298.15 K. These frequency computations were performed using the B97-D functional and 6-31G** basis set. For the enthalpic and entropic corrections to the free energies from the harmonic oscillator approximation, all frequencies below 50 cm^{-1} were treated as if they were 50 cm^{-1} .

A model system consisting of diphenyl hydrogen phosphate (**DPPA**); 2,3,4-Tri-*O*-methyl- α -D-6-deoxyglucopyranosyl trichloroacetimidate **5-9A** and 2,4-*syn*-pentadiol (**X-3**) was utilized to explore various pathways leading to the overall conversion of the sugar donor to the respective *O*-glycoside. Single-ended growing string calculations were performed on optimized starting materials or intermediates as the fixed nodes with varying driving coordinates according to the pathways explored. To account for variation in conformations and binding complexes, the most stable conformations were sampled for the growing string calculations. These were obtained in part by manually sampling relevant torsions and angles of approach, and also by using an algorithm which allowed a thorough conformational analysis by ranking a vast number of unique conformers generated by the systematic variation of the torsional angles.^[14] In the latter approach, 10,000

configurations were sampled and the lowest 100 energy structures at the semi-empirical PM6 level of theory were further investigated.

The interaction between **DPPA** and **5-9A** is estimated to be favorable (~0.6 kcal/mol), due to the formation of a hydrogen bond between the acidic proton of **DPPA** and the basic nitrogen of **5-9A**. An S_N2-like displacement of the trichloroacetimide moiety was modeled and found to be facile (**TS1**: 12.1 kcal/mol barrier). This was confirmed experimentally by the instantaneous formation of β-phosphates upon mixing donor **A** with phosphoric acids (**R**)-**5-6f** (*cf.* SI-8). Following the exothermic release of trichloroacetamide (**TCA**), β-phosphate **X-4** would bind to the diol **X-3** (**5-9C** to **5-9D**). Subsequently, a second S_N2-like displacement of the phosphate may occur to yield α-*O*-glycoside **α-5-9F**, with an estimated barrier of 20.7 kcal/mol (**TS2**). This double displacement mechanism supports the α-selectivity observed for the reaction of donor **A** with **6-dEB** catalyzed by a phosphoric acid. The increased β preference of glycosylations with fucose, or with the less reactive **7** may be due to a competing phosphate anomerization of the β-phosphate to the more stable α-form. A computed ΔG of 0.7 kcal/mol has been calculated between the β-phosphate **X-4** and the more stable α anomer **X-5**. This difference could be easily enhanced by the introduction of bulky groups in the phosphate. This hypothesis is backed-up by the fact that mostly α-phosphate is formed when benzyl protected 6-deoxyfucose-α-trichloroacetimidate is treated with various CPAs. Additionally, an analogous uncatalyzed S_N2-like reaction of the α-trichloroacetimidate **5-9A** with diol **X-3** to afford the β-glycoside (**β-5-9F**) was modelled but found to be high in energy (**TS3**: 34.8 kcal/mol barrier).

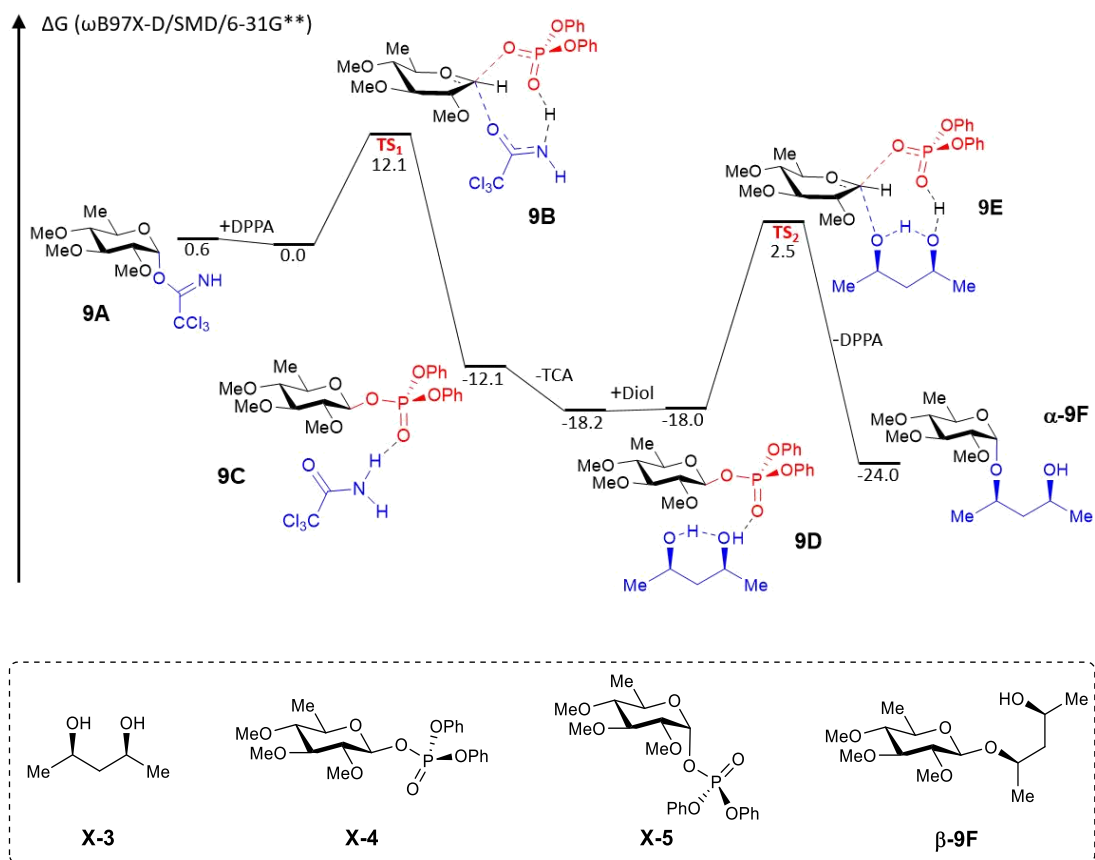


Figure D.1. Energy diagram for the CPA-catalyzed glycosylation of 1,3-diols.

A summary of calculated values, including solvent corrected single point electronic energies, as well as enthalpic and entropic corrections associated with vibrational, rotational, and translational energy at 298.15 K are provided below.

Table D.1. Calculated energy values for the described geometries.

	G_{SMD} (kcal/mol) ^a	H_{vrt} (kcal/mol) ^b	S_{vrt} (cal/mol.K) ^b	G_{corr} (kcal/mol) ^c
DPPA	-694020.3	139.1	124.1	-693918.2
6-deoxyglucose α -donor 5-9A	-1406312.9	197.2	158.6	-1406163.0
Diol	-218452.9	110.6	89.3	-218368.9
α -donor 5-9A bound to DPPA	-2100349.7	337.5	233.7	-2100081.8
TS1: formation of β -phosphate	-2100336.1	336.7	236.1	-2100069.7
β -phosphate bound to TCA	-2100363.5	338.5	235.6	-2100095.2
β -phosphate	-1103956.6	303.2	191.9	-1103710.6
TCA	-996395.8	33.4	90.4	-996389.3
β -phosphate bound to diol X-3	-1322424.8	415.7	235.9	-1322079.4
TS2: formation of α -glycoside α-5-9F	-1322401.9	414.1	238.5	-1322058.9
α -glycoside α-5-9F bound to DPPA	-1322436.3	415.7	230.5	-1322089.2
α -glycoside α-5-9F	-628393.9	274.5	160.6	-628167.3
α -phosphate- 5-5	-1103958.0	303.4	190.6	-1103711.4
TS3: direct formation of β -glycoside β-5-9F	-1624742.1	305.9	206.6	-1624497.8

^aGas-phase electronic energy (ω B97X-D/SMD/6-31G**). ^bVibrational, rotational, and translational entropic and enthalpic contributions (B97-D/6-31G**) at 298K. ^cCorrected free energy values at 298K.

Cartesian coordinates for starting geometries, transition states, and products are described below.

28

• **DPPA**

C	-4.10738	1.21178	1.67082
C	-4.32407	0.40975	2.80231
C	-3.77138	-0.88019	2.85779
C	-3.01683	-1.37353	1.78490
C	-2.81599	-0.55925	0.66357
C	-3.34328	0.73714	0.59343
O	-2.02978	-1.09985	-0.36745
P	-2.48372	-1.12452	-1.93683
O	-4.11105	-1.20952	-1.89617
C	-4.74524	-2.28253	-1.23677
C	-4.44406	-3.61239	-1.55857
C	-5.13723	-4.63529	-0.89293
C	-6.11810	-4.32673	0.06254
C	-6.40610	-2.98501	0.36196
C	-5.71568	-1.95070	-0.28444
O	-2.35275	0.40615	-2.47481
O	-1.72116	-2.13225	-2.71372
H	-4.52731	2.21742	1.62366
H	-4.91706	0.78782	3.63560
H	-3.93622	-1.51166	3.73162
H	-2.59989	-2.37938	1.78978
H	-3.16652	1.35198	0.28709
H	-3.67775	-3.82513	-2.30196
H	-4.91016	-5.67542	-1.12977
H	-6.65609	-5.12708	0.57176
H	-7.16379	-2.74004	1.10724
H	-5.89945	-0.90333	-0.05226
H	-1.69489	0.41669	-3.18923

38

• **6-deoxyglucose α -donor 5-9A**

C	0.26331	-2.70561	-3.31594
C	1.12486	-1.77389	-2.39151
C	0.83283	0.14105	-0.91748
C	0.33207	-0.32343	0.47132
C	-1.20020	-0.21179	0.56065
C	-1.65131	1.19601	0.13065
C	-1.06267	1.58149	-1.24497
N	2.36918	-1.86436	-2.14021
C	-2.04257	-1.77266	2.17369
C	2.07803	-1.79458	1.15846
C	-3.74677	1.73744	1.15641
C	-1.32763	3.03770	-1.60114
O	0.31367	-0.82195	-1.91049
O	0.38560	1.41030	-1.25398
Cl	-0.43047	-1.72338	-4.67684
Cl	1.26779	-4.04275	-4.02500
Cl	-1.07781	-3.44810	-2.34439
O	0.70994	-1.66051	0.76014
O	-1.64413	-0.42623	1.90142
O	-3.07072	1.25688	-0.00736
H	1.92592	0.15063	-0.98444
H	0.76753	0.37456	1.21284
H	-1.65073	-0.94539	-0.12914
H	-1.29475	1.92492	0.88367
H	-1.50169	0.91534	-2.00422
H	2.79942	-2.65433	-2.62207
H	-2.41131	-1.78202	3.20887
H	-2.85860	-2.08785	1.49598
H	-1.19903	-2.47153	2.06930
H	2.20614	-2.83794	1.47562
H	2.76376	-1.58656	0.32023
H	2.30963	-1.12408	2.00779
H	-4.81851	1.73866	0.91373
H	-3.55537	1.08962	2.02465

H	-3.43061	2.77024	1.40149
H	-2.41087	3.21272	-1.58701
H	-0.84385	3.69992	-0.86778
H	-0.93211	3.26546	-2.59995

19

• **Diol X-3**

C	-1.90604	5.13988	-2.86560
O	-1.03433	5.00926	-1.74314
H	-0.13388	4.97374	-2.11551
C	-3.32347	4.83513	-2.37409
H	-3.57045	5.47818	-1.51755
H	-3.38942	3.78583	-2.04874
H	-4.05911	5.00882	-3.17400
H	-1.88167	6.18177	-3.25720
C	-1.49941	4.20385	-4.02516
H	-1.40502	3.17658	-3.63674
C	-0.19029	4.60734	-4.71435
H	-2.29241	4.20422	-4.79085
O	0.86545	4.51270	-3.72293
H	-0.28433	5.66112	-5.04361
C	0.14135	3.72443	-5.92298
H	1.65118	4.93464	-4.10026
H	0.22125	2.67401	-5.60777
H	1.09954	4.02732	-6.37481
H	-0.64019	3.80687	-6.69373

66

• **α -donor 5-9A bound to DPPA**

C	0.20014	-3.68847	-2.17462
C	1.45109	-2.75959	-1.97865
C	1.95514	-0.45788	-1.29579
C	1.70857	-0.34102	0.22655
C	0.35316	0.31857	0.52848
C	0.21117	1.61296	-0.28992
C	0.41719	1.32464	-1.79111
N	2.67172	-3.14982	-1.99431
C	-0.41053	-0.34124	2.69788
C	3.01837	-1.95136	1.42345
C	-1.19956	3.16568	0.85928
C	0.41680	2.58828	-2.63940
O	1.02355	-1.52249	-1.79205
O	1.70825	0.68639	-2.01543
Cl	-0.82839	-3.04214	-3.51532
Cl	0.68364	-5.39093	-2.58748
Cl	-0.72791	-3.70318	-0.62129
O	1.75210	-1.62756	0.83731
O	0.27212	0.64394	1.91764
O	-1.09631	2.16743	-0.15844
H	2.97533	-0.76155	-1.51920
H	2.49557	0.31909	0.62587
H	-0.46119	-0.36771	0.23788
H	0.98719	2.32784	0.04023
H	-0.37618	0.63726	-2.12701
H	2.75953	-4.14764	-2.18184
H	-0.39999	0.02272	3.73460
H	-1.45957	-0.45301	2.36377
H	0.09102	-1.31916	2.63788
H	2.90794	-2.95579	1.85355
H	3.82628	-1.95838	0.67661
H	3.27418	-1.23282	2.22192
H	-2.23772	3.52501	0.83729
H	-0.96239	2.75199	1.85075
H	-0.51896	4.01494	0.65318
H	-0.54700	3.09854	-2.51914
H	1.22323	3.26245	-2.31442

H	0.56987	2.33738	-3.69751
H	3.77943	2.57352	-1.94413
H	3.24927	3.82152	0.16536
C	4.12552	2.21740	-0.97675
C	3.82646	2.89686	0.20982
O	5.06918	0.41577	-2.16132
C	4.86249	1.02311	-0.92609
O	5.66205	-1.35575	-3.90524
H	9.48795	1.80251	-4.54860
C	4.25870	2.39257	1.44861
C	9.25651	1.49085	-3.52924
P	5.71233	-1.07931	-2.44921
H	7.86954	-0.07196	-4.15692
C	8.35111	0.43901	-3.32472
C	5.31525	0.51208	0.30156
H	4.01628	2.91774	2.37246
C	9.86459	2.13513	-2.44028
H	10.57007	2.94918	-2.60974
C	5.00541	1.20656	1.48279
C	8.05517	0.05341	-2.00895
O	5.02558	-2.09699	-1.43403
H	4.11374	-2.47109	-1.73639
C	9.55973	1.72790	-1.13181
H	5.88621	-0.41081	0.33982
O	7.18404	-1.01247	-1.72634
C	8.64914	0.68522	-0.90880
H	5.35215	0.80523	2.43608
H	10.02494	2.22438	-0.27907
H	8.38800	0.36158	0.09757

H	-1.88409	3.45216	-1.58610
H	-0.20750	3.85319	-1.10060
H	-0.56343	3.40185	-2.79515
H	7.19760	0.60233	2.70564
H	9.55958	-0.23773	2.71147
C	7.61998	0.10376	1.83434
C	8.93864	-0.36349	1.82328
O	5.51803	0.42260	0.79545
C	6.81992	-0.04918	0.68984
O	3.46327	1.76472	0.14547
H	5.96063	5.58130	1.90826
C	9.46615	-0.97820	0.67471
C	6.48928	4.85769	1.28462
P	4.66169	1.08284	-0.47816
H	4.66446	3.95746	0.49268
C	5.75241	3.96661	0.49234
C	7.32849	-0.67300	-0.46376
H	10.49708	-1.33498	0.66603
C	7.89375	4.82659	1.28078
H	8.45847	5.52484	1.89958
C	8.65592	-1.12721	-0.46141
C	6.44247	3.03342	-0.29804
O	4.42390	0.03979	-1.57461
H	3.47896	-1.31136	-1.88742
C	8.56732	3.88906	0.47956
H	6.69472	-0.78048	-1.34062
O	5.76677	2.13208	-1.12718
C	7.84430	2.98445	-0.31043
H	9.05555	-1.60286	-1.35936
H	9.65747	3.85130	0.47767
H	8.33958	2.22538	-0.91466

• **TS₁: formation of β -phosphate X-4**

66

C	0.96082	-3.58642	-2.70683
C	1.63722	-2.19861	-2.33866
C	1.47117	0.53729	-1.05649
C	1.02428	-0.03347	0.27739
C	-0.51054	-0.00491	0.43605
C	-1.01112	1.39719	0.05016
C	-0.61260	1.75035	-1.39429
N	2.95567	-2.18029	-2.17045
C	-1.16009	-1.61306	2.08987
C	2.77819	-1.44631	1.15690
C	-2.98067	1.97495	1.28565
C	-0.82511	3.21339	-1.74598
O	0.84652	-1.24255	-2.24242
O	0.82160	1.46016	-1.68150
Cl	0.08183	-3.38131	-4.26952
Cl	2.14111	-4.97564	-2.88195
Cl	-0.19486	-3.98835	-1.37775
O	1.49690	-1.34320	0.50643
O	-0.87357	-0.24174	1.78910
O	-2.43117	1.47683	0.05781
H	2.46353	0.35351	-1.46312
H	1.45156	0.67721	1.01056
H	-0.96096	-0.75050	-0.24025
H	-0.56437	2.13623	0.74173
H	-1.15374	1.08516	-2.08030
H	3.48671	-3.03535	-2.28628
H	-1.51015	-1.63079	3.13095
H	-1.95745	-2.00129	1.42967
H	-0.26419	-2.24208	1.98227
H	2.81979	-2.46204	1.57217
H	3.59866	-1.30463	0.44436
H	2.87695	-0.70456	1.96421
H	-4.06927	2.00314	1.14211
H	-2.72546	1.31763	2.12928
H	-2.61401	2.99801	1.49418

• **β -phosphate X-4 bound to TCA**

66

C	1.43608	-3.62307	-1.86648
C	1.89092	-2.13674	-2.23136
C	2.46391	0.93530	-0.42405
C	1.90763	0.14628	0.76743
C	0.36770	0.04724	0.63978
C	-0.28758	1.39451	0.23279
C	0.48667	2.09748	-0.90688
N	3.20988	-1.97316	-2.42871
C	-1.34408	-1.12341	1.85825
C	2.59595	-1.78467	2.01629
C	-2.00070	0.58546	-1.28226
C	-0.03644	3.50140	-1.17677
O	1.02606	-1.28238	-2.40309
O	1.87039	2.21146	-0.50240
Cl	1.30874	-4.52277	-3.44568
Cl	2.62109	-4.49629	-0.78418
Cl	-0.16544	-3.59904	-1.05352
O	2.52336	-1.14116	0.74299
O	-0.11445	-0.39507	1.91379
O	-1.68703	1.25416	-0.05378
H	2.29998	0.37833	-1.35724
H	2.16142	0.69230	1.69464
H	0.16886	-0.70977	-0.13531
H	-0.25112	2.05064	1.11546
H	0.43587	1.48126	-1.82189
H	3.89211	-2.66377	-2.13873
H	-1.50416	-1.53609	2.86446
H	-2.18865	-0.47453	1.58181
H	-1.27636	-1.95569	1.13337
H	3.18904	-2.69629	1.86431
H	3.10160	-1.13536	2.75665
H	1.59811	-2.04174	2.39793
H	-3.07457	0.36020	-1.23710

H	-1.80828	1.23165	-2.15706
H	-1.43911	-0.35291	-1.41947
H	-1.10695	3.44889	-1.41576
H	0.09043	4.12162	-0.27774
H	0.51194	3.96711	-2.00532
H	5.31053	-1.00083	0.95968
H	5.31798	-3.51284	0.94690
C	5.70102	-1.56023	0.11403
C	5.69574	-2.96161	0.08597
O	6.21627	0.53974	-0.97770
C	6.18377	-0.87128	-1.00396
O	3.87072	1.14944	-0.21213
H	3.11407	6.33217	0.20221
C	6.14954	-3.65259	-1.05020
C	3.33380	5.70111	-0.65957
P	4.85692	1.26298	-1.49729
H	4.70507	4.39693	0.42874
C	4.22609	4.62855	-0.52099
C	6.64186	-1.53497	-2.14767
H	6.13066	-4.74213	-1.06906
C	2.72077	5.95838	-1.89614
H	2.02612	6.79281	-1.99736
C	6.62065	-2.93841	-2.16501
C	4.48778	3.82978	-1.63690
O	4.28441	0.74675	-2.77824
H	3.54701	-1.03645	-2.67420
C	2.99661	5.13714	-3.00114
H	6.98797	-0.95479	-3.00118
O	5.42456	2.77831	-1.49071
C	3.88591	4.05890	-2.87864
H	6.96763	-3.47065	-3.05101
H	2.51925	5.33138	-3.96230
H	4.10827	3.39712	-3.71370

• **β-phosphate X-4**

57

C	1.47686	0.75613	-0.54949
C	0.60932	0.36618	0.66051
C	-0.86324	0.73514	0.37630
C	-1.00333	2.18097	-0.14281
C	-0.02545	2.43035	-1.31339
C	-2.31227	-0.66424	1.67322
C	1.61514	-1.41230	1.91546
C	-3.20561	2.99100	0.33325
C	-0.03058	3.87609	-1.79068
O	1.31546	2.12708	-0.87737
O	0.67970	-1.03657	0.89632
O	-1.64261	0.59582	1.56532
O	-2.32105	2.42003	-0.63392
H	1.23038	0.11893	-1.41848
H	0.95245	0.94565	1.53535
H	-1.24101	0.06490	-0.41801
H	-0.74835	2.88240	0.67379
H	-0.30064	1.75337	-2.14541
H	-2.86896	-0.63841	2.62029
H	-3.02397	-0.80577	0.83778
H	-1.59549	-1.49908	1.68004
H	1.58628	-2.50732	1.97100
H	2.63833	-1.09617	1.67030
H	1.32055	-0.98370	2.89173
H	-4.17177	3.12707	-0.17215
H	-3.32455	2.33247	1.20662
H	-2.83489	3.97659	0.67644
H	-1.04481	4.14323	-2.11254
H	0.27303	4.54316	-0.96980
H	0.66921	4.00183	-2.62746
H	5.88937	-0.68770	1.84259
H	5.50414	-2.78178	3.18841

C	5.35922	-1.54314	1.42541
C	5.13228	-2.71296	2.16536
O	5.15204	-0.29037	-0.59106
C	4.87463	-1.46944	0.11407
O	2.84662	0.58362	-0.19009
H	3.87327	4.69951	2.16014
C	4.42318	-3.78431	1.59845
C	4.58426	4.10683	1.58268
P	3.97372	0.52854	-1.37607
H	3.10237	3.44143	0.12093
C	4.14125	3.41933	0.44265
C	4.17544	-2.53079	-0.47725
H	4.24466	-4.68940	2.17989
C	5.92851	4.03547	1.98240
H	6.26372	4.57291	2.87011
C	3.94646	-3.68810	0.28134
C	5.06969	2.66273	-0.28189
O	3.51296	0.01787	-2.68842
C	6.84073	3.27102	1.23707
H	3.81621	-2.43553	-1.50109
O	4.65564	1.99732	-1.45701
C	6.41426	2.57513	0.09569
H	3.39641	-4.51772	-0.16427
H	7.88625	3.21279	1.54245
H	7.09661	1.96801	-0.49663

• **TCA**

9

O	-1.30869	-1.27960	-1.52241
C	-0.73985	-1.86867	-2.42298
H	0.40827	-3.12783	-1.31179
Cl	-2.13744	-0.13582	-4.08638
N	0.17868	-2.85558	-2.25794
Cl	-1.85601	-3.01396	-4.69634
C	-1.05625	-1.54373	-3.95653
H	0.63350	-3.31513	-3.03440
Cl	0.50310	-1.20288	-4.86013

• **β-phosphate X-4 bound to diol X-3**

76

C	1.84302	0.53432	-1.24980
C	0.92078	-0.16624	-0.24088
C	-0.54694	0.13892	-0.60910
C	-0.76878	1.65713	-0.76925
C	0.27196	2.24318	-1.75070
C	-2.01106	-1.60483	0.10919
C	1.95007	-2.06691	0.79893
C	-3.07259	2.14640	-0.33068
C	0.19068	3.75726	-1.87658
O	1.60229	1.92888	-1.26381
O	1.12007	-1.57864	-0.26196
O	-1.40662	-0.34856	0.42637
O	-2.05504	1.94070	-1.31085
H	1.72489	0.10685	-2.25769
H	1.12443	0.25008	0.76135
H	-0.77719	-0.32768	-1.58127
H	-0.63706	2.14752	0.21551
H	0.12061	1.76035	-2.73134
H	-2.63151	-1.88121	0.97357
H	-2.65198	-1.52127	-0.78780
H	-1.24973	-2.38109	-0.06622
H	2.04668	-3.14903	0.64218
H	2.94739	-1.60767	0.78349
H	1.47461	-1.87953	1.77921
H	-3.97791	2.43674	-0.88180
H	-3.26267	1.23505	0.25601

H	-2.79514	2.96284	0.36503
H	-0.81712	4.03330	-2.21019
H	0.38792	4.22750	-0.90129
H	0.93235	4.11962	-2.60111
H	5.39579	0.50424	1.55101
H	5.23222	-1.21380	3.36711
C	5.40841	-0.55875	1.31973
C	5.31564	-1.53097	2.32696
O	5.66692	-0.02911	-1.03343
C	5.51082	-0.98166	-0.01108
O	3.19937	0.35082	-0.80056
H	3.40260	3.49806	2.85006
C	5.32618	-2.89790	2.00320
C	4.23258	3.30114	2.17005
P	4.45214	0.80499	-1.72611
H	2.94930	2.85612	0.45665
C	3.96344	2.94961	0.83857
C	5.52788	-2.33651	-0.35770
H	5.25190	-3.64732	2.79169
C	5.55633	3.39895	2.63008
H	5.75462	3.67151	3.66718
C	5.43336	-3.29642	0.66132
C	5.04507	2.69662	-0.01433
O	4.32097	0.63573	-3.19810
C	6.62389	3.15058	1.75188
H	5.61117	-2.62176	-1.40450
O	4.80474	2.34829	-1.35910
C	6.37257	2.79276	0.41851
H	5.44179	-4.35559	0.40139
H	7.65327	3.22564	2.10379
H	7.17857	2.57496	-0.28022
H	0.77238	-2.39868	-2.50333
H	3.12086	-2.16792	-2.14734
H	-1.76265	-2.56004	-2.71620
H	0.46166	-0.24397	-4.16246
O	-0.44336	-0.56372	-3.96612
O	2.20676	-0.75051	-4.34317
C	0.83784	-2.62252	-3.57847
C	3.32888	-2.58446	-3.14278
C	-1.68886	-2.59821	-3.81342
H	3.04308	-0.34220	-4.03368
H	0.77617	-3.71774	-3.69541
H	-2.53992	-2.04830	-4.23975
H	4.30479	-2.21414	-3.49054
C	-0.37397	-1.96659	-4.27286
C	2.21477	-2.17753	-4.11527
H	3.37582	-3.68058	-3.05535
H	-1.74663	-3.64949	-4.13319
H	-0.27272	-2.10035	-5.36969
H	2.38706	-2.66468	-5.09418

• **TS₂: formation of α -glycoside α -9F**

76

C	1.26956	1.61067	-1.65837
C	0.52545	0.73608	-0.68413
C	-0.93888	1.19047	-0.53350
C	-0.92647	2.68732	-0.18160
C	-0.17351	3.51796	-1.24489
C	-2.26913	-0.68969	0.09941
C	1.28432	-1.44626	-0.08258
C	-2.88332	3.20403	1.11090
C	0.18899	4.91426	-0.76595
O	1.09747	2.90155	-1.71070
O	0.64517	-0.61640	-1.07743
O	-1.56764	0.48383	0.53198
O	-2.22882	3.26424	-0.16353
H	2.17487	1.26615	-2.14478
H	1.03046	0.91899	0.27947

H	-1.47422	1.04078	-1.48528
H	-0.42905	2.80970	0.80059
H	-0.80352	3.55151	-2.14574
H	-2.73839	-1.11597	0.99636
H	-3.05322	-0.42922	-0.63591
H	-1.58505	-1.42166	-0.35498
H	1.40073	-2.43633	-0.53838
H	2.26920	-1.04341	0.18565
H	0.65019	-1.51869	0.81781
H	-3.79404	3.81019	1.01426
H	-3.13767	2.17039	1.38382
H	-2.24156	3.63353	1.90297
H	-0.73483	5.42525	-0.46855
H	0.86406	4.85200	0.09974
H	0.68020	5.48544	-1.56458
H	4.85598	-0.88050	2.17764
H	3.85864	-3.09634	2.82902
C	4.65441	-1.65063	1.43406
C	4.09331	-2.88767	1.78332
O	5.52715	-0.16988	-0.24868
C	4.95166	-1.38747	0.08758
O	3.34399	1.24582	-0.10411
H	4.41067	5.63850	1.70158
C	3.82713	-3.85227	0.79688
C	5.10151	4.82321	1.47728
P	4.51971	0.93375	-1.00920
H	4.01981	4.16562	-0.30125
C	4.87709	4.01506	0.35355
C	4.69083	-2.34306	-0.90869
H	3.39059	-4.81309	1.07487
C	6.20532	4.58703	2.31336
H	6.37531	5.21866	3.18657
C	4.12877	-3.57581	-0.54697
C	5.77035	2.96969	0.07258
O	4.28216	0.51250	-2.45442
C	7.08760	3.53421	2.02189
H	4.92016	-2.09308	-1.94317
O	5.59393	2.19159	-1.06914
C	6.87352	2.71891	0.90016
H	3.92443	-4.32016	-1.31852
H	7.94453	3.34383	2.67055
H	7.53585	1.88924	0.65724
H	0.66742	0.10119	-5.90071
H	2.82742	-1.18939	-6.50917
H	-1.44532	1.44155	-5.34813
H	0.95328	0.13848	-3.41018
O	0.26116	0.87973	-3.34025
O	2.37037	-0.47226	-3.94873
C	1.28891	0.94929	-5.56780
C	3.42096	-0.33829	-6.14251
C	-0.82210	2.27211	-4.98647
H	3.09014	-0.27359	-3.27894
H	1.45262	1.60698	-6.43461
H	-1.36443	2.78423	-4.17765
H	4.36018	-0.72090	-5.71833
C	0.52201	1.73978	-4.49125
C	2.64085	0.41643	-5.06410
H	3.66075	0.32229	-6.99038
H	-0.66630	2.98572	-5.80849
H	1.15265	2.57932	-4.14980
H	3.24652	1.26218	-4.69619

• **α -glycoside α -9F bound to DPPA**

76

C	0.92283	1.79659	-1.16778
C	0.70724	0.29456	-0.86890
C	-0.78742	-0.04651	-0.97656

C	-1.59267	0.91134	-0.08129
C	-1.29048	2.38038	-0.43383
C	-1.89361	-2.12200	-1.39739
C	1.63426	-1.81999	-1.67090
C	-3.57610	-0.06086	0.83060
C	-1.98024	3.35814	0.50818
O	0.13380	2.61066	-0.31457
O	1.55243	-0.39430	-1.78856
O	-1.00601	-1.40018	-0.54614
O	-2.99813	0.68143	-0.24293
H	1.96255	2.07526	-0.96663
H	1.04207	0.10143	0.16287
H	-1.10535	0.08761	-2.02350
H	-1.28410	0.74505	0.96672
H	-1.60465	2.55863	-1.47579
H	-1.99113	-3.13021	-0.97080
H	-2.88450	-1.64144	-1.44698
H	-1.48657	-2.20506	-2.42388
H	2.59337	-2.09872	-2.12574
H	1.60675	-2.12855	-0.61699
H	0.80574	-2.31154	-2.20496
H	-4.64806	-0.15466	0.60705
H	-3.12341	-1.06233	0.91659
H	-3.45264	0.46735	1.79530
H	-3.06485	3.19367	0.46886
H	-1.62740	3.19798	1.53806
H	-1.75889	4.39469	0.21856
H	3.97430	2.17646	0.41278
H	2.47894	2.53528	2.37500
C	3.54200	1.33081	0.94042
C	2.70022	1.51926	2.04704
O	4.61610	-0.27326	-0.58797
C	3.79258	0.02374	0.49269
O	4.14825	1.95209	-1.96330
H	7.98020	4.29719	-0.05812
C	2.14322	0.42339	2.72454
C	7.96482	3.20854	-0.12614
P	4.75736	0.58611	-1.98920
H	6.53778	3.16377	-1.77832
C	7.16132	2.59016	-1.09553
C	3.27043	-1.08246	1.18057
H	1.48728	0.58271	3.58076
C	8.74546	2.43592	0.74860
H	9.37012	2.92281	1.49836
C	2.44688	-0.87913	2.29647
C	7.14861	1.18991	-1.16904
O	4.33372	-0.39646	-3.15081
C	8.71933	1.03479	0.65729
H	3.50791	-2.08320	0.82393
O	6.38472	0.54007	-2.15314
C	7.91534	0.40187	-0.30210
H	2.03266	-1.74204	2.81941
H	9.32045	0.43018	1.33780
H	7.86727	-0.68273	-0.38703
H	0.52179	2.49202	-5.07890
H	2.01061	1.31360	-6.87182
H	-0.70668	4.18214	-3.45604
H	1.66619	0.64425	-3.53418
O	0.62729	1.99005	-2.54865
O	2.25150	0.53317	-4.32044
C	1.45462	2.86094	-4.62121
C	2.90528	1.65830	-6.33235
C	0.25394	4.37965	-2.95602
H	3.48262	-0.05795	-3.64102
H	1.73054	3.79387	-5.13762
H	0.07264	4.54680	-1.88725
H	3.69985	0.90897	-6.45652
C	1.20055	3.19034	-3.14323
C	2.58771	1.84942	-4.85055
H	3.24525	2.60782	-6.77193

H	0.69473	5.28851	-3.39372
H	2.16627	3.38421	-2.64878
H	3.48152	2.21210	-4.31746

• **α -glycoside α -9F**

48			
C	0.69310	1.98582	-1.31233
C	0.68359	0.44556	-1.14161
C	-0.75412	-0.08825	-0.99956
C	-1.52925	0.71049	0.06699
C	-1.39866	2.23212	-0.16528
C	-0.80807	-2.38958	-1.68417
C	2.70452	-0.02425	-2.33336
C	-3.33923	-0.65817	0.86369
C	-2.01345	3.04657	0.96604
O	-0.00187	2.60888	-0.24311
O	1.29281	-0.22352	-2.24467
O	-0.75085	-1.46020	-0.59811
O	-2.92465	0.41345	0.01535
H	1.71897	2.38459	-1.23420
H	1.23168	0.21993	-0.20723
H	-1.27631	0.03726	-1.96470
H	-1.10911	0.46802	1.06165
H	-1.88928	2.47348	-1.12195
H	-0.90506	-3.38692	-1.23257
H	-1.68902	-2.19512	-2.32488
H	0.09989	-2.34530	-2.30383
H	3.05208	-0.63930	-3.17138
H	2.95654	1.02937	-2.54487
H	3.20519	-0.33556	-1.39762
H	-4.43607	-0.69402	0.80194
H	-2.91038	-1.61954	0.54380
H	-3.04315	-0.47152	1.91415
H	-3.06328	2.75208	1.08958
H	-1.47164	2.85665	1.90475
H	-1.96061	4.12067	0.74007
H	-0.42446	3.08538	-5.06313
H	1.05443	2.48512	-7.20798
H	-1.60049	4.27112	-3.05936
H	0.90618	0.94949	-4.05338
O	0.16010	2.26125	-2.58893
O	1.22896	1.05466	-4.96722
C	0.54669	3.41367	-4.65931
C	1.96603	2.60647	-6.60355
C	-0.60977	4.58695	-2.70051
H	0.76418	4.40967	-5.07882
H	-0.63019	4.66010	-1.60605
H	2.69857	1.85340	-6.92645
C	0.45123	3.57208	-3.13907
C	1.63304	2.41285	-5.12135
H	2.38074	3.60999	-6.78104
H	-0.38572	5.57809	-3.12340
H	1.44207	3.89048	-2.75776
H	2.55008	2.61574	-4.52225

• **α -phosphate X-5**

57			
C	-0.24524	1.72159	-1.85611
C	0.34892	1.20370	-0.52633
C	0.63420	-0.30706	-0.60560
C	-0.61617	-1.05506	-1.11153
C	-1.15699	-0.42079	-2.41088
C	2.39226	-0.90709	0.89958
C	1.34838	3.18560	0.36803
C	-0.48588	-3.32814	-0.35234

C	-2.49752	-1.00821	-2.83189
O	-1.36996	1.01060	-2.24156
O	1.55093	1.88088	-0.18972
O	0.97952	-0.81892	0.68249
O	-0.31062	-2.41150	-1.43482
H	-0.53430	2.77849	-1.79492
H	-0.42278	1.36775	0.25017
H	1.44750	-0.47959	-1.32922
H	-1.40298	-1.00122	-0.33402
H	-0.40577	-0.57305	-3.20138
H	2.52409	-1.36661	1.88956
H	2.87274	-1.53929	0.13154
H	2.86429	0.08615	0.87934
H	2.33718	3.53851	0.68727
H	0.94838	3.88860	-0.37939
H	0.67348	3.13374	1.24248
H	-0.29017	-4.32934	-0.76118
H	0.20589	-3.11344	0.47526
H	-1.52306	-3.29203	0.03415
H	-2.38561	-2.09199	-2.96147
H	-3.25450	-0.81333	-2.05764
H	-2.83325	-0.55913	-3.77632
H	3.90082	1.07997	-5.97134
H	5.79193	2.03382	-7.31737
C	4.00845	2.15480	-6.10632
O	2.00384	2.44164	-4.81875
C	5.06374	2.69970	-6.85259
O	0.77734	1.58645	-2.91434
C	3.08199	3.02152	-5.51516
H	3.65529	-2.12141	-3.63708
C	5.18588	4.09078	-6.99745
H	2.63984	0.11572	-4.02344
P	1.82545	2.76653	-3.22282
C	3.95946	-1.27945	-3.01406
C	3.38232	-0.02009	-3.24160
H	5.35839	-2.44082	-1.83494
C	3.18083	4.41301	-5.64990
C	4.24586	4.94170	-6.39443
H	6.00933	4.50896	-7.57729
C	4.91377	-1.45947	-2.00184
O	1.44706	4.14833	-2.83371
C	3.76597	1.05966	-2.42883
H	2.44227	5.05119	-5.16799
O	3.27198	2.35518	-2.57678
C	5.28993	-0.36608	-1.20404
C	4.71605	0.89445	-1.41096
H	6.02914	-0.49396	-0.41225
H	4.33570	6.02314	-6.50366
H	4.98170	1.75271	-0.79598

• **TS3: direct formation of β -glycoside β -9F from α -donor 9A**

57

C	0.18417	-3.63388	-3.10233
C	0.92248	-2.41207	-2.34934
C	1.24394	0.27515	-0.54510

C	0.50716	-0.14507	0.72777
C	-1.02167	0.06764	0.61034
C	-1.31433	1.45375	0.01084
C	-0.62421	1.59768	-1.35510
N	2.23908	-2.42859	-2.23480
C	-2.10451	-1.29628	2.25220
C	1.99584	-1.78077	1.66455
C	-3.43128	2.25686	0.79353
C	-0.73427	2.99188	-1.94935
O	0.10072	-1.56194	-1.93703
O	0.81904	1.30019	-1.27448
Cl	-0.76927	-2.96206	-4.49767
Cl	1.31108	-4.93661	-3.77191
Cl	-0.94117	-4.43406	-1.92052
O	0.73599	-1.50352	1.04725
O	-1.61964	0.00602	1.90012
O	-2.70308	1.61630	-0.25758
H	1.78118	-0.48072	-1.09048
H	0.86382	0.51588	1.54035
H	-1.43242	-0.70080	-0.06398
H	-0.94736	2.23888	0.69955
H	-1.03235	0.83112	-2.02681
H	2.65867	-3.25347	-2.65864
H	-2.62286	-1.18160	3.21378
H	-2.81657	-1.66882	1.49392
H	-1.27888	-2.01710	2.34968
H	1.92370	-2.80338	2.05530
H	2.82774	-1.73781	0.94471
H	2.19843	-1.08093	2.49644
H	-4.47222	2.31769	0.44924
H	-3.37443	1.68123	1.72876
H	-3.04884	3.27978	0.97377
H	-1.79726	3.24151	-2.05427
H	-0.25489	3.72723	3.28529
H	-0.25411	3.02989	-2.93606
H	5.56720	1.07669	-0.57853
H	4.62606	2.77708	1.09124
H	6.43752	-0.76225	-2.22254
H	3.25974	-1.58183	-1.55454
O	4.00676	-0.94002	-1.08893
O	2.90412	0.87755	0.19728
C	4.78549	1.31985	-1.31673
C	3.89632	3.08841	0.33018
C	5.59429	-0.53150	-2.89049
H	3.38505	-0.00379	-0.15293
H	5.19616	2.07312	-2.00522
H	5.28530	-1.45766	-3.39498
H	2.98749	3.44137	0.83637
C	4.42666	0.02982	-2.07997
C	3.56330	1.92785	-0.60113
H	4.32243	3.92123	-0.24929
H	5.92698	0.19062	-3.65215
H	3.57478	0.23975	-2.75529
H	2.83306	2.25516	-1.35622

References

- [1] J. H. Tay, A. J. Argüelles, M. D. Demars, P. M. Zimmerman, D. H. Sherman, P. Nagorny, *J. Am. Chem. Soc.* **2017**, *139*, 8570–8578.
- [2] Y. Shao, Z. Gan, E. Epifanovsky, A. T. B. Gilbert, M. Wormit, J. Kussmann, A. W. Lange, A. Behn, J. Deng, X. Feng, et al., *Mol. Phys.* **2015**, *113*, 184–215.
- [3] A. D. Becke, *J. Chem. Phys.* **1997**, *107*, 8554–8560.
- [4] S. Grimme, *J. Comput. Chem.* **2006**, *27*, 1787–1799.
- [5] P. C. Hariharan, J. A. Pople, *Theor. Chim. Acta* **1973**, *28*, 213–222.
- [6] M. M. Francl, W. J. Pietro, W. J. Hehre, J. S. Binkley, M. S. Gordon, D. J. DeFrees, J. A. Pople, *J. Chem. Phys.* **1982**, *77*, 3654–3665.
- [7] Discovery Studio 4.1 Visualizer: Accelrys Software Inc. San Diego, USA, **2015**.
- [8] P. M. Zimmerman, *J. Chem. Phys.* **2013**, *138*, 184102.
- [9] P. M. Zimmerman, *Mol. Simul.* **2015**, *41*, 43–54.
- [10] P. M. Zimmerman, *J. Comput. Chem.* **2015**, *36*, 601–611.
- [11] P. M. Zimmerman, *J. Chem. Theory Comput.* **2013**, *9*, 3043–3050.
- [12] A. V. Marenich, C. J. Cramer, D. G. Truhlar, *J. Phys. Chem. B* **2009**, *113*, 6378–6396.
- [13] J.-D. Chai, M. Head-Gordon, *J. Chem. Phys.* **2008**, *128*, 084106.
- [14] N. M. O’Boyle, M. Banck, C. A. James, C. Morley, T. Vandermeersch, G. R. Hutchison, *J. Cheminform.* **2011**, *3*, 33.

APPENDIX E

Experimental Information for Chapter 5, Section 5.3

Computational Studies

All quantum chemical calculations were performed using the Q-Chem 4.3 package.^[1] Geometry optimizations were evaluated using the B3LYP-D3 density functional^[2,3] using the double- ζ - quality basis set with polarization functions on all atoms, 6-31G**.^[4,5] Pictorial representations of important stationary points were generated in Discovery Studio 4.1 Visualizer.^[6]

For the growing string reaction path optimizations, between 7-15 nodes were used, including the end points. In the initial phase, termed growth phase, new nodes were added when the perpendicular gradient magnitude on the frontier node was less than 0.10 Hartree/Å for double-ended strings, or when the RMS gradient was less than 0.005 Hartree/Å for single-ended strings. Additionally, an initial maximum optimization step size of 0.1 Å-radians was used. When the total perpendicular gradient magnitude over all nodes, F , reached a value of less than 0.3, the climbing image search was initiated. When $F < 0.1$, or when the node of highest energy had a RMS gradient below double the nodal convergence criterion and $F < 0.2$, the exact transition state search was initiated. The string is considered fully converged when an RMS gradient < 0.0005 Hartree/Å was obtained for the node representing the transition state. Further detail regarding the growing string implementation developed in the Zimmerman group can be found in the references.^[7-10]

The electronic Gibbs free energy values of all stationary points were computed through solvent corrected (dichloromethane) single point energies using the SMD model.^[11] For these calculations the ω B97X-D3 exchange functional^[12] was employed with a 6-31G** basis set. The final Gibbs free energy values were obtained by correcting the electronic free energy with the enthalpic and entropic contributions from vibrations, rotations, and translations at 298.15 K. These frequency computations were performed using the B3LYP-D3 functional and 6-31G** basis set. For the enthalpic and entropic corrections to the free energies from the harmonic oscillator approximation, all frequencies below 50 cm⁻¹ were treated as if they were 50 cm⁻¹.

A model system consisting of biphenyl hydrogen phosphate (**BPA**), enol ether **5-15b**, and diol **5-16a** was utilized to explore various pathways that lead to formation either C2 glycosides **5-17a** or C3 glycosides **5-18a**. Both the direct addition of diol **16a** to enol ether **5-15b** (concerted and uncatalyzed pathways), as well as mechanisms mediated by axial phosphate **5-20a** and equatorial phosphate **5-20b**. To account for variation in conformations and binding complexes, the most stable conformations were sampled for the growing string calculations. These were obtained in part by manually sampling relevant torsions and angles of approach, and also by using an algorithm which allowed a thorough conformational analysis by ranking a vast number of unique conformers generated by the systematic variation of the torsional angles.^[13]

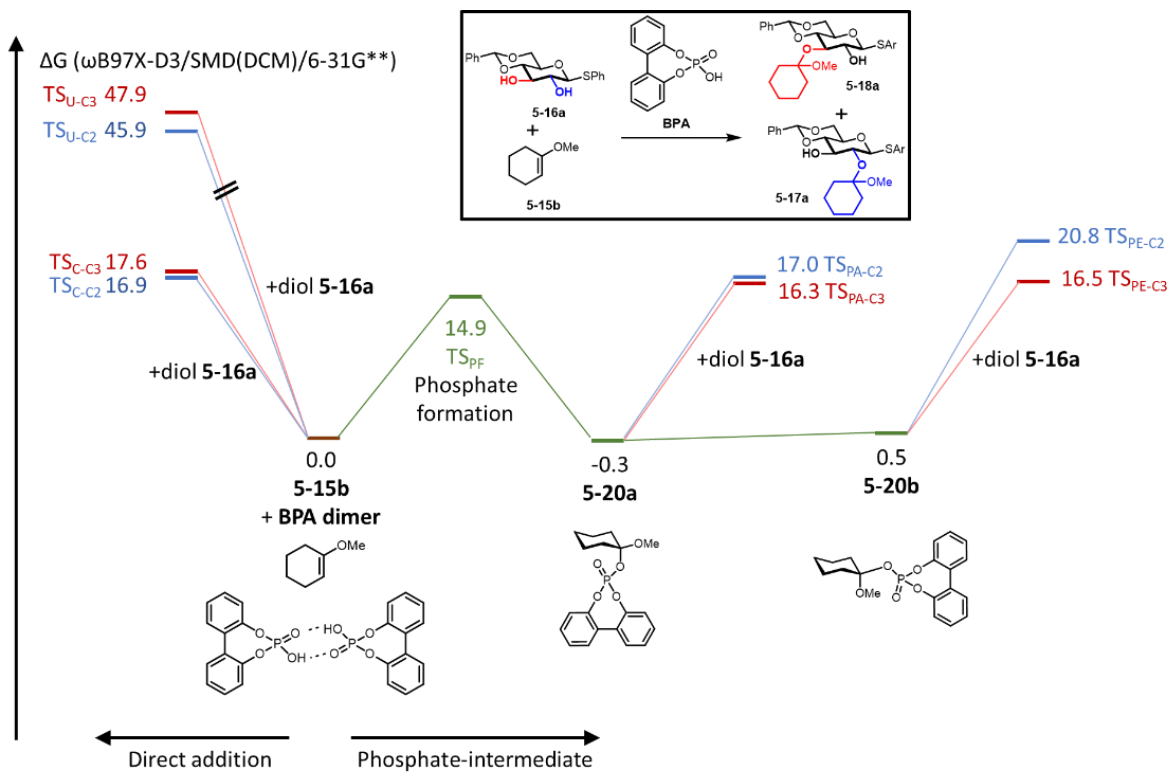


Figure E.1. Energy diagram for the CPA-catalyzed intermolecular acetalization of 6-deoxyglucose-derived 2,3-diols.

A summary of calculated values, including solvent corrected single point electronic energies, as well as enthalpic and entropic corrections associated with vibrational, rotational, and translational energy at 298 K are provided below.

Table E.1. Calculated energy values for the BPA-catalyzed acetalization of diols.

	G_{SMD} [kcal/mol]^a	S_{vrt} [cal/mol]^b	H_{vrt} [kcal/mol.K]^b	G_{corr} [kcal/mol]^c
BPA	-693422.0	113.1	128.3	-693327.4
BPA dimer	-1386862.3	176.6	257.5	-1386657.5
Diol 5-16a	-947766.9	152.8	242.5	-947570.0
Enol 5-15b	-219113.8	86.4	118.3	-219021.2
Enol 5-15b +diol 5-16a complex	-1166892.4	194.1	362.8	-1166587.5
Enol 5-15b + BPA complex	-912550.3	154.3	248.3	-912348.0
Enol 5-15b + diol 5-16a + BPA complex	-1860334.0	255.9	493.0	-1859917.2
Axial phosphate 5-20a	-912556.7	148.1	249.2	-912351.6
Equatorial phosphate 5-20b	-912555.7	148.4	249.1	-912350.8
Axial phosphate 5-20a + diol 5-16a	-1860336.4	252.1	493.2	-1859918.4
Equatorial phosphate 5-20b + diol 5-16a	-1860334.5	250.6	493.6	-1859915.6
TS_{U-C2}	-1166847.0	195.6	360.0	-1166545.3
TS_{U-C3}	-1166845.4	191.0	359.1	-1166543.3
TS_{C-C2}	-1860321.1	248.0	490.6	-1859904.4
TS_{C-C3}	-1860319.0	255.8	491.5	-1859903.7
TS_{PF}	-912538.5	151.3	247.3	-912336.4
TS_{PA-C2}	-1860321.5	247.5	491.0	-1859904.3
TS_{PA-C3}	-1860322.0	251.3	491.9	-1859905.0
TS_{PE-C2}	-1860315.9	255.2	491.4	-1859900.5
TS_{PE-C3}	-1860322.9	250.5	492.8	-1859904.8

^aGas-phase electronic energy (ω B97X-D3/SMD/6-31G**). ^bVibrational, rotational, and translational entropic and enthalpic contributions (B97-D/6-31G**) at 298K. ^cCorrected free energy values at 298K.

To probe the theoretical equilibrium constant for phosphate formation from enol ether **5-15b** and BPA, relevant geometries were reoptimized without dispersion (B3LYP/6-61g**). A summary of calculated values, including solvent corrected single point electronic energies, as well as enthalpic and entropic corrections associated with vibrational, rotational, and translational energy at 298 K for these geometries are provided below.

Table E.2. Calculated energy values geometries reoptimized without dispersion corrections.

	G_{SMD} [kcal/mol]^a	S_{vrt} [cal/mol]^b	H_{vrt} [kcal/mol.K]^b	G_{corr} [kcal/mol]^c
BPA	-693422.0	113.2	128.3	-693327.5
BPA dimer	-1386885.0	173.3	256.2	-1386680.5
BPA + enol ether 5-15b complex	-912549.1	153.3	247.3	-912347.6
Enol ether 5-15b	-219113.8	86.7	118.2	-219021.4
Axial phosphate 5-20a	-912567.5	150.4	248.5	-912363.8
Equatorial phosphate 5-20b	-912567.4	150.2	248.6	-912363.6

^aGas-phase electronic energy (ω B97X-D3/SMD/6-31G**). ^bVibrational, rotational, and translational entropic and enthalpic contributions (B97-D/6-31G**) at 298K. ^cCorrected free energy values at 298K.

Cartesian coordinates for starting geometries, transition states, and products are described below.

• **BPA**

26

H -5.73139141 -0.46670236 0.98367596
C -6.28016398 -0.34924933 0.05465183
C -7.67291908 -0.34938804 0.06344181
H -8.20629545 -0.48240391 0.99930266
C -8.38159393 -0.16679134 -1.12626098
H -9.46697664 -0.15868364 -1.12514023
C -7.69135592 0.00730018 -2.32323415
H -8.20397197 0.14469402 -3.26870075
C -6.30136442 -0.00457525 -2.31435416
O -5.64469980 0.06211448 -3.54816638
C -5.55858758 -0.17643182 -1.13782247
H -3.91975793 -1.87026301 0.17544770
H -1.44498084 -1.89677610 0.19427455
C -3.36430934 -1.13598641 -0.40004011
C -1.97254597 -1.15576411 -0.39798376
C -4.08111809 -0.19697680 -1.15796233
C -1.26125955 -0.23239636 -1.16690520
H -0.17599274 -0.24295083 -1.17120586
C -3.33804147 0.71585561 -1.92497421
C -1.94757064 0.70584186 -1.93556625
O -3.98354542 1.73233722 -2.63458624
H -1.42793533 1.44173357 -2.53844644
P -4.87526444 1.42498931 -3.95216081
O -5.66213799 2.59024164 -4.38850767
O -3.86287028 0.82009783 -5.04737300
H -3.81959983 1.41968359 -5.80582350

• **BPA dimer**

52

H -5.32892985 -0.85420909 -1.28047371
C -6.13555259 -1.43708757 -1.71343674
C -7.20799086 -1.83332005 -0.91850698
H -7.22375888 -1.57199351 0.13473974
C -8.26622681 -2.55053718 -1.47991429
H -9.10949020 -2.85863508 -0.86995850
C -8.24028230 -2.87101182 -2.83474932
H -9.03742928 -3.43345033 -3.30787037
C -7.15879207 -2.47322379 -3.61232181
O -7.14228475 -2.92974448 -4.93606147
C -6.07755336 -1.74857677 -3.08293863
H -3.44017013 -1.81801048 -2.43870421
H -1.52781751 -0.98007029 -3.76208865
C -3.60994463 -1.37729772 -3.41587383
C -2.53299939 -0.91020796 -4.16557501
C -4.92418681 -1.31145054 -3.90547711
C -2.74463553 -0.35827906 -5.43139126
H -1.90927967 0.01210191 -6.01703795
C -5.09648062 -0.76633387 -5.18731851
C -4.03682349 -0.28605231 -5.94749496
O -6.38809439 -0.62764005 -5.70192758
H -4.25115367 0.14079923 -6.92064201
P -7.14989837 -1.96048235 -6.21746262
O -8.63031006 -1.47576531 -6.41679910
O -6.49716367 -2.63570414 -7.37822793
H -8.72251943 -0.96833323 -7.28660788
H -6.93329658 -2.57049560 -8.93922133
O -8.51204319 -0.25371768 -8.71738570
O -7.17681296 -2.20581361 -9.84447963
O -6.06971448 0.07642575 -9.31562032
P -7.46237330 -0.66427660 -9.69353118
H -4.08887339 -1.46836524 -8.70292095
C -3.95274700 -0.98117491 -9.66229554
C -4.96087799 -0.15221535 -10.13864158
O -7.72408952 -0.25929964 -11.22756490
H -9.40713308 1.45645949 -12.08849189

C -7.35673416 0.98892095 -11.74005161
H -2.02149102 -1.82319172 -10.08676286
C -2.81549809 -1.17525679 -10.44369479
C -8.38496706 1.79295783 -12.21917380
C -4.90034854 0.47842992 -11.39011404
C -6.00226532 1.34050725 -11.88007376
C -8.07932331 2.98802219 -12.86583819
H -8.87955663 3.61595289 -13.24415423
C -5.72747321 2.55322091 -12.53322681
C -6.74514750 3.36614032 -13.02549363
H -4.69176051 2.85927084 -12.63993197
H -6.49655839 4.29697736 -13.52514674
C -2.71360783 -0.55310820 -11.69039169
C -3.74621658 0.25663288 -12.15778138
H -1.83599951 -0.71329964 -12.30868047
H -3.68015254 0.70530221 -13.14411031

• **Diol 5-16a**

45

C -7.29651667 -1.31448222 0.81837879
C -7.98754074 -2.09282284 -0.28440331
C -7.06281363 -2.14358202 -1.51236149
C -6.57340081 -0.73589698 -1.90192975
O -5.94313222 -0.09301983 -0.79699281
C -6.85222916 0.05465533 0.28963297
C -6.17915759 0.81666871 1.42601337
O -8.17258277 -1.10347960 1.91704525
O -8.28118838 -3.39917087 0.16716387
O -7.83009700 -2.74549014 -2.54279022
O -7.08985259 0.89280752 2.51959277
C -7.51919326 -0.38738269 2.95288106
C -8.47320549 -0.23357327 4.11351334
C -8.41123471 0.88863526 4.94420240
C -9.27142680 0.99617290 6.03755489
C -10.19206651 -0.01714808 6.30922112
C -10.25153176 -1.13970151 5.48102712
C -9.39521846 -1.24985090 4.38621044
S -5.37689753 -0.85758397 -3.28070381
C -5.65005586 0.71334987 -4.10153448
C -5.77015171 0.73544399 -5.49561940
C -5.94782039 1.95018769 -6.15812593
C -6.02809551 3.14093406 -5.43479268
C -5.91438094 3.11525033 -4.04326835
C -5.71007377 1.90958786 -3.37286690
H -6.40656700 -1.87897753 1.14259853
H -8.90500698 -1.55309692 -0.57148429
H -6.18917484 -2.75800830 -1.24307106
H -7.42656084 -0.14140270 -2.25889460
H -7.74895973 0.61119923 -0.02374349
H -5.24911020 0.29987368 1.71117037
H -5.93578638 1.84069450 1.13427888
H -8.62755967 -3.87745338 -0.59991894
H -7.26428961 -2.83454555 -3.32312113
H -6.62461716 -0.96723140 3.25487759
H -7.69868056 1.67432062 4.72137952
H -9.22376797 1.87399549 6.67533510
H -10.86131705 0.06766032 7.16050744
H -10.96887342 -1.92957770 5.68425938
H -9.44361774 -2.11075150 3.72868611
H -5.73599933 -0.19382200 -6.05595162
H -6.04050749 1.96107849 -7.24017870
H -6.17815245 4.08320995 -5.95285366
H -5.97120329 4.03916745 -3.47529194
H -5.59709400 1.88583865 -2.29430173

• **Enol 5-15b**

20

C -6.80079762 0.42751417 -0.14966134
 C -7.63890678 1.46015848 -0.32995077
 C -9.12870080 1.34668009 -0.10083277
 C -9.59755304 -0.11255455 -0.01418213
 C -8.65989437 -0.92417927 0.88668052
 C -7.23904099 -0.94024910 0.30725694
 O -5.44745358 0.44127260 -0.36194305
 C -4.86880165 1.63947490 -0.85111904
 H -7.26382914 2.42741931 -0.64689313
 H -9.40452319 1.87659839 0.82460790
 H -9.66598172 1.86392361 -0.90680577
 H -10.62854586 -0.15891046 0.35472645
 H -9.59752655 -0.55465739 -1.01958191
 H -8.64013974 -0.47052421 1.88628973
 H -9.02445593 -1.95006985 1.01008562
 H -6.51570126 -1.30847035 1.04420925
 H -7.18069818 -1.63034222 -0.54619994
 H -5.00144135 2.46940393 -0.14391093
 H -3.80321296 1.43813059 -0.97501294
 H -5.30119527 1.92952135 -1.81851267

• **Enol 5-15b + diol 5-16a complex**

65

C -9.74084568 -4.35471810 5.17475708
 C -9.31491299 -4.14791691 6.48804807
 C -8.16883300 -3.38945899 6.73258915
 C -7.45002614 -2.84086829 5.67035035
 C -7.87778418 -3.04586705 4.35505939
 C -9.02534072 -3.80689818 4.11031112
 C -7.06988614 -2.51306888 3.19816090
 O -7.93438913 -2.24265302 2.10407192
 C -7.16832847 -1.83208872 0.97918507
 C -6.40968616 -0.54772309 1.34343719
 C -5.55109808 -0.82022360 2.57522745
 O -6.37911537 -1.34110279 3.60914174
 C -8.03883974 -1.56437182 -0.23112682
 C -7.10524800 -1.10177964 -1.35976969
 C -6.30016965 0.13184098 -0.91087423
 O -5.56343010 -0.13488276 0.26992608
 O -7.94117058 -0.80578276 -2.46692956
 O -8.75477702 -2.72812867 -0.59944679
 H -6.32628636 -3.25993516 2.86411459
 S -5.15530308 0.74596134 -2.21549281
 C -3.91717472 -0.55792384 -2.23168001
 C -3.88242497 -1.48856534 -3.27596134
 C -2.88242219 -2.46206746 -3.31241894
 C -1.92043535 -2.51497089 -2.30276181
 C -1.95966714 -1.59194774 -1.25459461
 C -2.94975796 -0.61077267 -1.21856510
 H -10.63332705 -4.94158748 4.97688947
 H -9.87345889 -4.57493257 7.31603665
 H -7.83438206 -3.22168321 7.75230046
 H -6.56321957 -2.24459545 5.85273231
 H -9.35453695 -3.95465158 3.08752110
 H -6.43724604 -2.60948690 0.72401478
 H -7.14237083 0.23832021 1.58262013
 H -4.75417132 -1.52882282 2.30498220
 H -5.09369363 0.09639372 2.95422886
 H -8.73793302 -0.74398415 0.00129492
 H -6.40291999 -1.91844577 -1.58224968
 H -6.99902872 0.97080019 -0.76543539
 H -7.36820204 -0.56238764 -3.20808277
 H -9.15969083 -2.53183483 -1.45735510
 H -4.63530294 -1.44842690 -4.05677761
 H -2.86292093 -3.18258361 -4.12445599

H -1.14435490 -3.27388352 -2.33140539
 H -1.21408368 -1.63213483 -0.46588151
 H -2.99217432 0.10684295 -0.40793610
 H -7.96300927 -4.44843718 -2.04581129
 H -7.62339036 -4.85776275 0.50729193
 H -5.94024849 -4.03407173 -3.29913918
 O -4.95893649 -4.53293642 1.03701279
 H -2.98702633 -4.37047623 0.37332304
 C -7.37373005 -5.33068901 -2.31140060
 C -6.88367454 -5.58267106 0.14286347
 H -3.39168313 -3.65401499 1.95931886
 C -5.59892586 -4.85225569 -0.13814091
 C -5.16379109 -4.53423891 -1.36717200
 H -4.22702115 -4.00987863 -1.50945301
 H -7.82781924 -5.78948129 -3.19699409
 C -3.74202738 -3.80759565 0.93687283
 H -8.43311573 -6.64379950 -0.93656068
 C -5.93375541 -4.89474026 -2.61564804
 C -7.41230784 -6.28820266 -1.11388556
 H -6.70820268 -6.29471280 0.95727558
 H -3.89007891 -2.83854664 0.44443279
 H -5.40585276 -5.69633475 -3.15636474
 H -6.79691274 -7.17293560 -1.32641094

• **Enol 5-15b + BPA complex**

46

C -7.06528773 0.37142474 -0.01831926
 C -8.08905411 1.06263490 -0.52882087
 C -9.44643715 0.43622205 -0.74400357
 C -9.38870521 -1.09813260 -0.72450403
 C -8.55702116 -1.59294979 0.46447279
 C -7.11385335 -1.07672280 0.37881989
 O -5.79532703 0.88979949 0.20607679
 C -5.46703601 2.14624567 -0.39599969
 H -7.98321657 2.11658284 -0.75969108
 H -10.13392939 0.79174274 0.03874823
 H -9.86953541 0.78433807 -1.69511299
 H -10.40272511 -1.51112253 -0.68434575
 H -8.93285809 -1.45508857 -1.65753174
 H -9.01185049 -1.23273615 1.39300547
 H -8.55653288 -2.68723459 0.51211166
 H -6.60493165 -1.19361552 1.34143341
 H -6.53447715 -1.65765549 -0.35230632
 H -6.05268616 2.96215019 0.03288239
 H -4.40860101 2.31024873 -0.18969341
 H -5.63802220 2.09745551 -1.47654916
 H -5.03797963 4.55777559 2.94324643
 O -6.06138288 0.57324548 5.16653164
 O -6.57674544 2.77248446 3.96933274
 C -5.98978611 4.48995064 2.42853343
 H -5.36678364 0.92166176 1.84474304
 H -5.60168120 6.07568355 1.02856787
 P -6.25852538 1.17596070 3.84250801
 C -6.90870073 3.53505768 2.85913361
 C -6.31528978 5.33042239 1.36591397
 O -5.08341957 0.99637837 2.79392194
 C -8.16870062 3.38840249 2.24976577
 C -7.55455552 5.20025084 0.73276626
 O -7.51881621 0.64614380 2.94611327
 C -9.16825472 2.40889562 2.73520015
 H -7.80981459 5.83948576 -0.10659419
 C -8.46290289 4.24034162 1.17166660
 C -8.81504988 1.10588060 3.12479244
 H -10.83123063 3.75624455 2.53369679
 C -10.52996390 2.75028219 2.80827440
 C -9.76104078 0.19151850 3.58109754
 H -9.42373434 -0.79669960 3.87260813
 C -11.48887179 1.84030394 3.24603432

H -9.41608574 4.12652748 0.66404922
C -11.10363761 0.55695565 3.63920494
H -12.53181804 2.13737628 3.29399829
H -11.84328054 -0.15544724 3.99123063

• **Enol 5-15b + diol 5-16a + BPA complex**

91

C -11.51825289 -1.87746686 1.63570700
C -12.25713675 -1.68248938 2.80479329
C -11.67786558 -1.01538109 3.88622486
C -10.37113249 -0.53485766 3.79714412
C -9.63575099 -0.72034183 2.62374717
C -10.20969372 -1.40248225 1.54635914
C -8.22596509 -0.19144529 2.51435626
O -7.93708994 0.02692366 1.15046597
C -6.61944542 0.55365882 0.96447370
C -6.51884295 1.85501802 1.75596683
C -6.82369562 1.57373490 3.21761235
O -8.12790460 0.99661046 3.28734270
C -6.38970078 0.82446714 -0.50659214
C -5.11363848 1.67054073 -0.72654599
C -5.05615053 2.87091591 0.25227887
O -5.23749636 2.44298148 1.60603081
O -5.04388521 2.10704925 -2.07124520
O -6.32246775 -0.40653999 -1.20051472
H -7.49389166 -0.92139290 2.91348125
S -3.52726385 3.86512500 0.14839224
C -2.28644852 2.58335015 0.33878930
C -1.44526600 2.27522324 -0.73659043
C -0.46523124 1.29116406 -0.59657999
C -0.33455451 0.59829056 0.60764816
C -1.18172656 0.89711052 1.67738323
C -2.14944513 1.89326070 1.55193169
H -11.96103017 -2.39981009 0.79202981
H -13.27645341 -2.05185651 2.87362701
H -12.24822174 -0.86164076 4.79797435
H -9.92638383 0.01148956 4.62074907
H -9.63092989 -1.53878373 0.63963429
H -5.86853151 -0.16496572 1.33208202
H -7.28981891 2.53365258 1.37859542
H -6.06342267 0.89853404 3.64229875
H -6.84566985 2.49279752 3.80658812
H -7.23510986 1.41630835 -0.86262896
H -4.24605009 1.02720330 -0.55356180
H -5.84575781 3.58714042 -0.01978353
H -5.81792610 2.67945875 -2.21915623
H -6.62060472 -0.21922508 -2.10315738
H -1.57771829 2.79390501 -1.68023122
H 0.18372833 1.05548572 -1.43510495
H 0.42070228 -0.17534155 0.71133703
H -1.08588599 0.35631206 2.61476065
H -2.81485369 2.12934940 2.37419252
O -9.06128767 5.17829221 -0.92104956
O -10.16979744 3.64478689 -2.52261280
H -10.13092587 4.93589195 3.49980789
H -11.98075446 3.36640736 3.99380320
H -6.86425493 6.55346665 -1.14106562
H -10.01858130 2.93397206 -3.19285513
C -10.35913366 4.13003865 2.80909770
C -11.40293019 3.25031814 3.08240412
C -7.02427478 6.18683138 -0.13388044
C -8.15937308 5.43078386 0.13445429
H -5.20530086 6.98407982 0.68794142
C -6.11198548 6.42524201 0.89214080
C -8.42754242 4.89107789 1.39857609
C -9.58896297 4.00803898 1.64321400
C -11.69895133 2.21915341 2.19026033
H -12.48570365 1.50584668 2.40990043

P -8.88545705 3.72163623 -1.58817136
C -6.35517700 5.91467162 2.16941573
C -7.50264145 5.16749784 2.41773236
C -9.92106101 2.96690420 0.76084207
C -10.95145988 2.07471888 1.02417590
H -5.63556989 6.07584126 2.96448170
H -7.67443640 4.73840480 3.39917900
H -11.12502571 1.25356938 0.34205500
O -7.59174266 3.44115107 -2.25429351
O -9.11590579 2.70119605 -0.35398500
H -11.60844370 -0.95713688 -4.03753413
H -7.21894886 2.38570493 -4.47420075
H -9.43220795 -1.17021390 -2.50166865
H -11.60327454 0.91548453 -5.56912729
C -11.83573446 0.02400899 -3.60122788
H -12.92467355 0.09083940 -3.50633262
C -6.95922929 1.32358783 -4.48642327
H -11.58629085 -0.57616622 -1.51421859
C -11.31846986 1.13030408 -4.53170978
H -7.14504209 0.89294596 -5.47697935
H -5.91546852 1.20944136 -4.19810253
C -9.64834679 -0.10328985 -2.35589795
C -9.80863538 1.27972913 -4.46024087
C -9.06376154 0.65565911 -3.51945180
C -11.15866162 0.13281123 -2.23114803
H -9.32351869 1.80601162 -5.27559404
O -7.70615865 0.62378259 -3.48506530
H -9.12573348 0.18677682 -1.43880792
H -11.81776916 2.07929608 -4.28298992
H -11.33495353 1.13901331 -1.83200334

• **Axial phosphate 5-20a**

46

C -6.91181663 0.79044834 0.98138860
C -8.24799421 0.32328627 1.56153070
C -8.09282224 -0.92771862 2.43327209
C -7.41173637 -2.06027500 1.65231185
C -6.06250323 -1.60387460 1.07989027
C -6.20396301 -0.33623456 0.22183183
O -7.17561968 1.93418087 0.23865080
C -6.10391640 2.48393097 -0.53750366
H -8.89585169 0.11070094 0.70312986
H -7.49884915 -0.68351390 3.32003147
H -9.07838596 -1.24652488 2.79029039
H -7.26907379 -2.93529501 2.29679778
H -8.06630955 -2.37629550 0.82719829
H -5.37231763 -1.39407712 1.90469807
H -5.61111706 -2.39992460 0.47690787
H -5.22059567 0.00974998 -0.10800085
H -6.80448540 -0.54172671 -0.67277252
H -6.45047255 3.46603025 -0.86122419
H -5.20048390 2.61430167 0.06381242
H -5.89216147 1.86755943 -1.41905781
O -5.13347101 1.89347825 4.29707678
O -5.33454411 3.63894106 2.41234855
H -7.70449842 2.00488878 8.03312377
H -8.93020361 4.14441065 8.28798336
H -4.06948928 -0.45025118 4.16636309
H -8.69845152 1.14881025 2.11300745
C -7.92689853 2.61282342 7.16130748
C -8.61110696 3.81782671 7.30324766
C -4.95022525 -0.43341046 4.79794601
C -5.63055088 0.77038597 4.95652089
H -4.91360459 -2.52501552 5.29495611
C -5.42966803 -1.57925529 5.42822705
C -6.78305200 0.87714139 5.74897418
C -7.49300607 2.16646388 5.90388616
C -8.87359682 4.60719867 6.18134799

H -9.40335156 5.54890742 6.28506621
P -5.93039632 2.41876169 2.97966394
C -6.58341614 -1.50847091 6.21295080
C -7.24405264 -0.29288625 6.37456919
C -7.77224529 2.98208846 4.79512119
C -8.45389086 4.18733243 4.92043653
H -6.97457057 -2.40219730 6.68901229
H -8.15490563 -0.24431106 6.96299084
H -8.64871453 4.76886607 4.02627220
O -5.96585405 1.10113679 2.08146720
O -7.46810971 2.53626788 3.51112983

• **Equatorial phosphate 5-20b**

46

C -7.73248847 -0.02484694 -1.14496832
C -8.94345743 0.79996147 -0.70713739
C -8.88976635 1.08170986 0.80122963
C -8.76602469 -0.21289025 1.61603651
C -7.55425417 -1.03786042 1.15702940
C -7.62367520 -1.32770410 -0.34841433
O -6.61915530 0.81387674 -1.03383802
C -5.33212830 0.22874247 -1.24456361
H -8.96677674 1.72592944 -1.28370118
H -8.02625100 1.72570567 1.00429194
H -9.78440039 1.63974217 1.09838545
H -8.68603317 0.01415989 2.68528930
H -9.67862217 -0.81218490 1.48704556
H -6.63413754 -0.48171353 1.37589084
H -7.49569749 -1.98223691 1.70950923
H -6.76022352 -1.90278336 -0.69411408
H -8.51158467 -1.92648316 -0.57787028
H -4.64813310 1.06280343 -1.40841182
H -5.00103498 -0.34008743 -0.36745968
H -5.32287501 -0.41136289 -2.13050701
O -8.33983307 -0.48787261 -4.99497965
O -8.81233302 1.70676175 -3.72828672
H -5.34041931 -0.17420757 -8.41864388
H -4.62048175 2.15507087 -8.84439445
H -8.79017344 -2.97636590 -4.55804550
H -9.84296109 0.22997250 -0.96372988
C -5.39015091 0.56301098 -7.62315793
C -4.99285728 1.87588051 -7.86374503
C -7.87693596 -2.81857119 -5.12049730
C -7.47920800 -1.51197780 -5.38545853
H -7.41955424 -4.90191145 -5.39230435
C -7.11027924 -3.88087286 -5.59395511
C -6.30816813 -1.22248726 -6.10603785
C -5.88785141 0.17090940 -6.37088322
C -5.09092728 2.83325224 -6.85174265
H -4.79377502 3.86039614 -7.03822730
P -7.94145439 0.52215743 -3.79424670
C -5.94950841 -3.62624475 -6.32770736
C -5.55647086 -2.31309905 -6.57415128
C -5.96239479 1.15404496 -5.37119786
C -5.57853190 2.47085043 -5.59770719
H -5.34658417 -4.44926091 -6.69871906
H -4.64225120 -2.11637550 -7.12539932
H -5.66837610 3.18463016 -4.78697189
O -7.87840922 -0.47383735 -2.54327605
O -6.35815613 0.78982762 -4.08419609

• **Axial phosphate 5-20a + diol 5-16a**

91

C -8.76498896 0.75995036 2.15765354
C -9.59690914 0.93425295 3.43030219
C -9.38117130 -0.17045138 4.47335599

C -9.51140591 -1.56977784 3.85949547
C -8.58411461 -1.72176548 2.64747206
C -8.87279506 -0.65503265 1.58421834
O -9.18001537 1.76456648 1.28513598
C -8.58038043 1.78368136 -0.01265588
H -10.63930370 0.93350679 3.09268630
H -8.39020757 -0.06455174 4.91611586
H -10.10550869 -0.03647870 5.28482685
H -9.27012731 -2.32414327 4.61678900
H -10.55169560 -1.74843603 3.55058632
H -7.54418523 -1.61574486 2.97183640
H -8.68324181 -2.71635974 2.19931735
H -8.18165601 -0.75548027 0.74306514
H -9.89370829 -0.76051033 1.19748092
H -8.84666952 2.74691919 -0.44720665
H -7.48992516 1.71342879 0.05428253
H -8.96522486 0.97733306 -0.64751532
O -7.14061129 3.37220200 3.38131955
O -6.50011452 1.39215143 4.81133056
H -3.80185016 6.31510506 2.27620815
H -1.58816081 5.76786254 3.23919268
H -9.21258256 4.19827863 2.13350246
H -9.40108001 1.92698717 3.84632868
C -3.56784188 5.29209490 2.55309210
C -2.32501843 4.98341934 3.09856996
C -8.30079711 4.59966264 1.71096225
C -7.08450967 4.19880506 2.25439986
H -9.26242597 5.76151010 0.18209951
C -8.31423910 5.45597910 0.61351402
C -5.85427592 4.65621556 1.75749826
C -4.55461533 4.30699835 2.37672016
C -2.03692927 3.67169423 3.47671443
H -1.08229114 3.41750495 3.92323946
P -6.54202514 1.86951624 3.40802025
C -7.10829135 5.90137945 0.06853456
C -5.90127968 5.50703544 0.63841055
C -4.23759513 3.00480021 2.79201533
C -2.99776417 2.67598552 3.32169044
H -7.10904351 6.55062804 -0.80138536
H -4.96427016 5.84288321 0.20716835
H -2.81089555 1.65916855 3.63908341
O -7.31055866 0.92691412 2.38591771
O -5.15499708 1.96004708 2.58708458
H -1.03991962 -1.38438684 6.16690475
H -2.55495162 0.17142605 7.18211109
H -3.62508984 -1.63435420 6.25386778
H -4.76698811 -3.57981249 5.26259892
C -1.20076544 -0.82658858 5.23165435
H -0.29156335 -0.88194211 4.62871242
S -3.09315028 -5.21633329 3.61790652
O -2.27253978 -2.81773740 4.37234660
O -1.44294035 0.56009556 5.49657814
C -2.63740299 0.75935973 6.24740853
H -0.77916326 -3.61428463 2.67713340
H -0.71085210 2.57679588 6.83615389
C -3.67285073 -1.09588294 5.29293027
C -2.40708140 -1.40702150 4.49680623
C -3.35220209 -3.41223628 3.63618969
C -1.91546545 -5.40361665 2.28507488
C -4.71911000 -3.09071660 4.27526613
C -0.88539949 -4.48403253 2.03899717
C -1.69907345 3.02449749 6.82292818
C -2.81154992 2.22979102 6.53469895
O -3.76303374 0.29972886 5.52840315
H -2.83385017 -7.25466425 1.66688973
O -6.10181431 -1.38261935 5.17635559
C -2.02742453 -6.55020936 1.48647139
H -6.57160060 -3.28698251 3.82418824
C -4.87374554 -1.58162259 4.50592969
H -0.99255773 5.00772278 7.26630065

C -1.86068646 4.39060885 7.05242491
C 0.00021598 -4.70474626 0.98360672
C -4.08849776 2.79867171 6.50774295
H 0.78838503 -3.98249693 0.79070681
H -2.48614151 -0.92941236 3.50676136
H -4.94802878 2.18219942 6.27822168
H -6.25110384 -0.41624827 5.20670027
O -5.73839858 -3.56452312 3.41687007
H -3.34717952 -3.05096631 2.59770939
C -1.11824416 -6.77558594 0.45437795
C -0.10686685 -5.84985749 0.19257526
C -3.13224755 4.96582892 6.99757482
C -4.24397655 4.16591601 6.73030798
H -1.21314928 -7.66797888 -0.15762584
H -4.87969252 -1.07891291 3.52427071
H -3.25552409 6.03193489 7.16409549
H 0.59206008 -6.02095527 -0.62046654
H -5.23722958 4.60309506 6.68001538

• **Equatorial phosphate 5-20b + diol 5-16a**

91

C -7.36262029 -0.49902034 -0.32184092
C -8.77034383 0.07010446 -0.18057868
C -9.16583617 0.14902121 1.30305748
C -9.05549875 -1.22140799 1.98004730
C -7.63909389 -1.79155374 1.82532581
C -7.24823925 -1.87249802 0.34107667
O -6.49382526 0.46780364 0.17151620
C -5.11993745 0.10972842 0.29567081
H -8.80789011 1.05765879 -0.64444166
H -8.51793009 0.87420523 1.80899315
H -10.19311746 0.52272298 1.37706141
H -9.32949258 -1.14631362 3.03823785
H -9.77397705 -1.90670868 1.51477761
H -6.92551868 -1.15369426 2.36353778
H -7.57326551 -2.79058853 2.27021033
H -6.23661602 -2.26469787 0.20528181
H -7.93042704 -2.53704483 -0.19329725
H -4.58343489 1.04399987 0.46619905
H -4.95005078 -0.56292288 1.14413794
H -4.74666207 -0.35880560 -0.62094563
O -6.55507271 1.03142143 -3.57224512
O -7.24661761 -1.32953308 -4.23668793
H -9.19398007 4.74959235 -3.87235803
H -11.24907400 4.42482284 -5.20634178
H -4.52114565 1.79633385 -2.19542681
H -9.45521239 -0.59489475 -0.70752823
C -9.60193346 3.75228526 -4.00200103
C -10.75497482 3.56823862 -4.75897268
C -5.38343608 2.43425390 -2.04031282
C -6.56113574 2.13122111 -2.71230809
H -4.43226692 3.76606330 -0.64808469
C -5.34637764 3.52996267 -1.18345382
C -7.71399105 2.92076830 -2.59550974
C -8.92492970 2.67114336 -3.41052319
C -11.26299976 2.28207222 -4.94840092
H -12.16068351 2.12131170 -5.53676122
P -7.40852930 -0.29856768 -3.18643890
C -6.49218933 4.30818567 -1.00529421
C -7.65504649 4.00845072 -1.70820776
C -9.45238325 1.38873189 -3.63640592
C -10.61205350 1.18841795 -4.38372521
H -6.48048191 5.14948163 -0.31994040
H -8.54669135 4.61100376 -1.56608935
H -11.01067486 0.18786097 -4.50767526
O -6.96850676 -0.76567306 -1.74896459
O -8.92008254 0.26657286 -3.00332399
H -13.33702776 -0.36044027 -2.58981217

H -12.09706434 -0.47538898 -0.52463431
H -10.91490444 -1.08542572 -2.40639747
H -9.75176872 -1.60248180 -4.41797141
C -13.60980960 -1.41323287 -2.41313441
H -14.60359076 -1.59267492 -2.82909148
S -11.26576823 -2.22531946 -6.81286440
O -12.37463669 -1.95596083 -4.41354305
O -13.67949336 -1.70005652 -1.01514659
C -12.42778183 -1.51972343 -0.36704612
H -14.06987123 -2.58731574 -5.99863487
H -12.76697962 0.24741364 1.66920936
C -11.24291972 -2.12816990 -2.28212535
C -12.55549607 -2.31596345 -3.04514009
C -11.40434601 -2.78466350 -5.08329882
C -12.66077712 -3.07195916 -7.55281979
C -10.04721668 -2.65293338 -4.37179663
C -13.92485360 -3.09324484 -6.94638478
C -12.75262049 -0.78225631 2.01685090
C -12.58902548 -1.81966569 1.09778127
O -11.44307770 -2.39213847 -0.89731986
H -11.48889692 -3.70198904 -9.24831965
O -8.96318201 -2.84627244 -2.20849656
C -12.47266988 -3.70307974 -8.78924879
H -8.28212877 -2.87320878 -5.09025173
C -10.18905530 -3.03058722 -2.88317083
H -13.01206901 -0.25360963 4.08860492
C -12.89156783 -1.06477816 3.37684924
C -14.97975297 -3.76280525 -7.56650281
C -12.57558913 -3.14573569 1.54061650
H -15.95392593 -3.78540054 -7.08593654
H -12.87780127 -3.36446542 -2.95340325
H -12.43483759 -3.93928022 0.81525028
H -8.26551116 -3.16882412 -2.79967796
O -9.04441079 -3.46081080 -4.95489782
H -11.74541299 -3.82903306 -5.08960186
C -13.54155013 -4.34514984 -9.41486296
C -14.79560276 -4.38428053 -8.80319453
C -12.86923160 -2.38835654 3.81815043
C -12.71225230 -3.42823740 2.89783554
H -13.38695815 -4.83185020 -10.37360599
H -10.51496150 -4.08194607 -2.81091984
H -12.97135770 -2.61027441 4.87640064
H -15.62303962 -4.89556600 -9.28629430
H -12.69276770 -4.45890340 3.23977256

• **TS_{U-C2}**

65

C -8.370396 -5.575241 5.292173
C -8.555836 -5.075632 6.582951
C -8.129980 -3.783182 6.892701
C -7.518502 -2.992566 5.919236
C -7.333724 -3.491362 4.626783
C -7.760301 -4.787297 4.316440
C -6.629421 -2.669350 3.572157
O -7.182508 -2.970518 2.307261
C -6.498427 -2.259005 1.271245
C -6.639586 -0.757603 1.556717
C -6.088149 -0.460439 2.946242
O -6.750544 -1.292822 3.894788
C -7.082968 -2.534479 -0.091727
C -6.390839 -1.650475 -1.166300
C -6.447316 -0.167547 -0.723089
O -5.939453 0.026725 0.601977
O -6.989803 -1.873469 -2.369615
O -6.926651 -3.884273 -0.492661
H -5.549252 -2.921499 3.545957
S -5.557189 0.980442 -1.846479
C -3.927684 0.240449 -1.965346

C -3.398022 -0.031153 -3.233144
C -2.105831 -0.541492 -3.363204
C -1.340138 -0.807923 -2.228169
C -1.871202 -0.551205 -0.961738
C -3.150838 -0.015128 -0.825206
H -8.704183 -6.579034 5.042752
H -9.031809 -5.690097 7.342589
H -8.276446 -3.387653 7.893958
H -7.190640 -1.985422 6.148371
H -7.623007 -5.159961 3.306627
H -5.429798 -2.531017 1.276739
H -7.714003 -0.514701 1.546802
H -5.000497 -0.640048 2.950727
H -6.271856 0.575493 3.239177
H -8.152925 -2.258477 -0.075590
H -5.315527 -1.934354 -1.140051
H -7.492062 0.176769 -0.790167
H -6.059865 -1.189885 -3.888574
H -6.990302 -3.787932 -1.462343
H -4.007599 0.127694 -4.116909
H -1.706486 -0.747060 -4.352835
H -0.338315 -1.215444 -2.328626
H -1.281511 -0.759326 -0.072926
H -3.566074 0.190803 0.154111
H -8.672531 0.065147 -6.387014
H -8.739519 -4.561975 -5.275626
H -9.416043 -2.146554 -5.235705
H -6.289929 0.406840 -6.423957
C -8.235345 0.444848 -5.452341
H -8.427652 1.522168 -5.431494
C -7.973773 -4.496614 -4.499175
H -9.971407 0.010069 -4.206002
C -6.717656 0.200685 -5.437795
H -8.434801 -4.322938 -3.525949
H -7.367654 -5.398954 -4.484827
C -8.784797 -1.773484 -4.410668
C -6.327271 -1.223967 -4.985189
C -7.391535 -2.188535 -4.733201
C -8.911344 -0.253817 -4.268002
H -5.493405 -1.680711 -5.518989
O -7.048786 -3.428769 -4.825525
H -9.074282 -2.281356 -3.490291
H -6.259786 0.894686 -4.726834
H -8.427082 0.017009 -3.325627

• TS_{U-C3}

65

C -6.626335 -5.871218 5.312893
C -7.819057 -5.631531 6.000811
C -8.504469 -4.432135 5.804296
C -8.007739 -3.472751 4.919403
C -6.819420 -3.712483 4.228841
C -6.130091 -4.913173 4.430205
C -6.283899 -2.744680 3.205254
O -6.615871 -3.265617 1.928163
C -6.091298 -2.435793 0.884925
C -6.655319 -1.028385 1.046783
C -6.346861 -0.512218 2.448732
O -6.832065 -1.458319 3.405271
C -6.459522 -3.022347 -0.479932
C -5.930940 -2.031740 -1.546335
C -6.368658 -0.578775 -1.247471
O -6.073936 -0.159386 0.079990
O -6.472679 -2.436410 -2.796391
O -5.991551 -4.289062 -0.641935
H -5.180873 -2.675372 3.272398
S -5.626388 0.634885 -2.415698
C -3.876861 0.333933 -2.135793

C -3.095353 -0.204685 -3.164931
C -1.729837 -0.416718 -2.968928
C -1.142918 -0.109013 -1.741371
C -1.923329 0.419881 -0.711113
C -3.284460 0.652895 -0.905808
H -6.082919 -6.798998 5.468150
H -8.208639 -6.375188 6.689475
H -9.430107 -4.242548 6.339592
H -8.531277 -2.536865 4.760293
H -5.203678 -5.094727 3.891375
H -4.992902 -2.394788 0.971751
H -7.749896 -1.071201 0.922220
H -5.259426 -0.370562 2.553776
H -6.846542 0.436990 2.654957
H -7.566903 -2.940703 -0.550634
H -4.833506 -2.092031 -1.544742
H -7.450081 -0.505160 -1.446365
H -6.103382 -1.851704 -3.473722
H -6.693384 -5.097056 -1.799756
H -3.558685 -0.464160 -4.112275
H -1.130460 -0.834182 -3.772081
H -0.081794 -0.281364 -1.587711
H -1.470234 0.659744 0.246831
H -3.896870 1.064236 -0.114025
H -10.474439 -6.010655 -1.837742
H -7.286663 -6.710218 2.024059
H -9.256071 -6.118642 0.746747
H -8.951866 -5.609174 -3.695043
C -10.034704 -5.006659 -1.930080
H -10.771985 -4.384606 -2.449799
C -6.461169 -6.633956 1.312252
H -10.704556 -4.431066 0.047790
C -8.742153 -5.089535 -2.755281
H -6.012851 -5.636367 1.341758
H -5.729105 -7.418634 1.502821
C -8.740979 -5.276632 0.256548
C -7.624191 -5.828632 -2.011294
C -7.697264 -5.954461 -0.585850
C -9.772885 -4.444419 -0.529482
H -7.156140 -6.681182 -2.507108
O -6.910943 -6.855342 -0.045304
H -8.273713 -4.691519 1.052444
H -8.395968 -4.084251 -3.016572
H -9.448291 -3.401224 -0.598865

• TS_{C-C2}

91

C -7.444034 -5.157386 6.163946
C -7.134182 -5.292410 7.518660
C -6.304360 -4.354654 8.135896
C -5.784703 -3.286973 7.403715
C -6.097763 -3.149725 6.047965
C -6.927641 -4.090717 5.429089
C -5.502178 -2.025102 5.234791
O -6.408833 -1.672927 4.202133
C -5.860451 -0.643983 3.385791
C -5.577532 0.576613 4.266125
C -4.633463 0.162720 5.388579
O -5.221957 -0.930969 6.089222
C -6.814477 -0.258780 2.276525
C -6.249519 0.955878 1.504131
C -5.881654 2.091597 2.491061
O -4.992466 1.619664 3.505283
O -7.256309 1.352857 0.590336
O -7.013097 -1.367935 1.413613
H -4.552796 -2.345326 4.760257
S -5.182754 3.599016 1.742797
C -3.866184 3.002070 0.681498

C -3.673573 3.685742 -0.523924
C -2.651035 3.294284 -1.385254
C -1.827581 2.214486 -1.061255
C -2.018079 1.539931 0.146900
C -3.020130 1.940346 1.031314
H -8.091062 -5.882377 5.678248
H -7.537524 -6.123624 8.089964
H -6.062370 -4.452735 9.190217
H -5.145824 -2.550837 7.877657
H -7.171399 -3.971023 4.379048
H -4.912069 -0.983163 2.935106
H -6.529769 0.905097 4.713109
H -3.656125 -0.115678 4.962471
H -4.485885 0.970138 6.108259
H -7.770120 0.055174 2.731047
H -5.338438 0.633159 0.982831
H -6.816889 2.450264 2.951701
H -6.909887 2.025842 -0.053537
H -7.609686 -1.025930 0.736155
H -4.328421 4.499045 -0.812782
H -2.520226 3.832233 -2.319180
H -1.039692 1.902928 -1.741010
H -1.374206 0.706130 0.413463
H -3.151006 1.438553 1.982753
O -8.127231 4.001262 -3.131124
O -6.660195 2.801190 -1.534810
H -12.220948 3.963073 -1.182220
H -12.246624 3.002181 1.102084
H -8.254637 5.384564 -5.298414
H -8.099109 1.892336 -1.980192
C -11.312020 3.955306 -0.587215
C -11.325148 3.410198 0.696057
C -9.090171 5.572405 -4.633034
C -9.095296 4.945485 -3.388747
H -10.146313 6.884588 -5.969332
C -10.149558 6.400918 -4.997041
C -10.145298 5.147243 -2.471599
C -10.141144 4.501783 -1.139144
C -10.153443 3.401144 1.459179
H -10.155777 2.988506 2.463940
P -6.924698 4.233468 -1.995910
C -11.212845 6.601126 -4.113802
C -11.201263 5.985594 -2.864451
C -8.967951 4.458966 -0.358732
C -8.976160 3.921869 0.927242
H -12.041344 7.245704 -4.391314
H -12.013924 6.163618 -2.166289
H -8.048185 3.930808 1.482468
O -5.849529 5.133173 -2.471528
O -7.804513 5.020666 -0.830287
H -6.359544 1.246423 -3.807461
H -11.018049 -0.036481 -0.773720
H -6.314977 0.086727 -1.517577
H -8.654803 1.980904 -4.306395
C -7.080459 0.493983 -4.146844
H -6.929949 0.366247 -5.224220
C -10.194094 0.040272 -0.062745
H -5.788764 -1.171279 -3.586438
C -8.505419 0.986384 -3.885051
H -9.964916 1.076000 0.186566
H -10.405736 -0.536462 0.835253
C -7.031072 -0.656081 -1.900378
C -8.806725 1.090806 -2.365367
C -8.353288 -0.047523 -1.601835
C -6.813511 -0.827129 -3.420644
H -9.827584 1.405686 -2.151661
O -9.004666 -0.591470 -0.627752
H -6.893906 -1.577397 -1.330279
H -9.234067 0.307515 -4.346374
H -7.480797 -1.613863 -3.795492

• TS_{C-C3}

91

C -9.055553 -5.027503 4.671664
C -9.389272 -4.394568 5.870975
C -8.869575 -3.131158 6.156916
C -8.022354 -2.498146 5.246961
C -7.695195 -3.128756 4.043277
C -8.201954 -4.402165 3.764979
C -6.776092 -2.464754 3.045418
O -7.193864 -2.840218 1.743168
C -6.385711 -2.240548 0.744997
C -6.441813 -0.717691 0.894828
C -5.994903 -0.359130 2.307128
O -6.817971 -1.061033 3.233064
C -6.873318 -2.634903 -0.631542
C -6.131156 -1.816332 -1.695134
C -6.022473 -0.314006 -1.391445
O -5.576915 -0.100077 -0.053384
O -6.732359 -1.996630 -2.967350
O -6.632235 -4.006166 -0.901926
H -5.728793 -2.803682 3.179405
S -4.865862 0.555477 -2.526035
C -3.454692 -0.554557 -2.464471
C -3.016081 -1.167088 -3.646867
C -1.935370 -2.051614 -3.620496
C -1.301486 -2.349391 -2.412664
C -1.736648 -1.739431 -1.233072
C -2.795494 -0.831881 -1.256144
H -9.451861 -6.013163 4.446494
H -10.054385 -4.882935 6.577366
H -9.129463 -2.633461 7.086512
H -7.628065 -1.510196 5.453503
H -7.956804 -4.875228 2.820354
H -5.333771 -2.557011 0.860222
H -7.478289 -0.377941 0.746233
H -4.933000 -0.629922 2.429625
H -6.110674 0.707271 2.511172
H -7.951558 -2.436330 -0.701803
H -5.108140 -2.207320 -1.706091
H -6.995029 0.168711 -1.568909
H -7.310181 -2.780959 -2.924078
H -7.468332 -4.343624 -1.346598
H -3.530872 -0.953729 -4.578396
H -1.593492 -2.514093 -4.542441
H -0.468066 -3.045461 -2.391566
H -1.240305 -1.959962 -0.292422
H -3.139795 -0.356672 -0.345831
O -9.621916 -3.500811 -4.404943
O -9.145886 -6.016559 -4.270025
H -13.972273 -2.693957 -5.504570
H -15.259830 -4.761341 -5.948737
H -8.569720 -1.201181 -3.960804
H -7.102392 -6.223219 -2.143633
C -13.659926 -3.633440 -5.058577
C -14.379160 -4.798332 -5.314820
C -9.645427 -1.187669 -3.850306
C -10.343245 -2.378706 -4.038285
H -9.771055 0.912415 -3.417200
C -10.327834 -0.008212 -3.566425
C -11.750135 -2.409679 -3.979214
C -12.511093 -3.649302 -4.251522
C -13.955237 -6.013400 -4.770347
H -14.505805 -6.927124 -4.974945
P -9.510528 -4.847259 -3.429408
C -11.722096 -0.018787 -3.480985
C -12.416055 -1.208992 -3.689377
C -12.112492 -4.882521 -3.708023
C -12.818489 -6.055339 -3.966526
H -12.268124 0.892000 -3.254645

H -13.499963 -1.226979 -3.619383
H -12.459103 -6.979338 -3.527844
O -8.678987 -4.469347 -2.213287
O -11.047979 -4.920879 -2.831773
H -3.311941 -7.213313 -1.312204
H -4.165790 -4.050161 -4.840120
H -3.326394 -5.179493 -2.943859
H -5.537688 -8.163570 -0.971109
C -4.002378 -6.671858 -0.650060
H -3.751489 -6.971805 0.372670
C -5.244967 -3.907633 -4.770809
H -2.782330 -4.844922 -0.596325
C -5.461984 -7.072907 -0.934852
H -5.505330 -2.941893 -4.334529
H -5.723712 -4.041243 -5.737966
C -4.099115 -4.759491 -2.274579
C -6.046513 -6.510698 -2.245457
C -5.368418 -5.318168 -2.807698
C -3.801585 -5.164488 -0.827463
H -6.063345 -7.244387 -3.062760
O -5.837988 -4.955390 -3.941392
H -4.060542 -3.679483 -2.426737
H -6.089861 -6.737862 -0.104719
H -4.482182 -4.625830 -0.164875

• **TS_{PF}**

46

C -6.904353 0.318007 0.104449
C -7.787890 1.202274 -0.673043
C -9.199014 0.654789 -0.957628
C -9.754494 -0.099906 0.255769
C -8.823194 -1.257787 0.621894
C -7.421929 -0.750176 1.008764
O -5.647127 0.516999 -0.091582
C -4.640207 -0.001795 0.826096
H -7.257958 1.558391 -1.561730
H -9.841735 1.499647 -1.221253
H -9.176877 -0.014824 -1.827768
H -9.839013 0.579380 1.110886
H -10.756549 -0.480170 0.035953
H -9.220357 -1.830681 1.464877
H -8.745640 -1.950520 -0.226553
H -7.444282 -0.263877 1.994309
H -6.695522 -1.565883 1.075731
H -3.703920 0.418072 0.464725
H -4.894857 0.371155 1.818647
H -4.608495 -1.092790 0.782699
O -7.361987 3.639459 3.812865
O -8.104978 3.515854 1.367397
H -10.913611 3.907252 6.614294
H -13.075949 4.063234 5.415732
H -5.249737 3.311550 5.261979
H -7.912671 2.112962 -0.028049
C -11.006463 3.508661 5.608353
C -12.220509 3.603161 4.930761
C -6.161266 3.056023 5.788969
C -7.371167 3.143584 5.103268
H -5.203879 2.587890 7.655004
C -6.147946 2.655294 7.123544
C -8.590648 2.825764 5.730188
C -9.877880 2.930679 5.006699
C -12.326031 3.125477 3.623138
H -13.264612 3.209481 3.083144
P -7.665379 2.663908 2.515620
C -7.345355 2.338932 7.769331
C -8.549697 2.423333 7.074172
C -10.013286 2.442582 3.694381
C -11.219373 2.547936 3.003584

H -7.340555 2.018965 8.806794
H -9.483048 2.157830 7.562005
H -11.271154 2.179062 1.985331
O -6.574075 1.636753 2.339653
O -8.957648 1.777164 3.105472

• **TS_{PA-C2}**

91

C -8.128880 -0.514834 3.071984
C -8.612479 0.034127 4.372189
C -8.207291 -0.756180 5.627949
C -8.112430 -2.260766 5.351580
C -7.057835 -2.506878 4.266682
C -7.413550 -1.812697 2.942105
O -8.687759 0.043358 2.051441
C -8.309681 -0.322649 0.696907
H -9.705412 0.055121 4.257020
H -7.240574 -0.406552 5.989724
H -8.933433 -0.537317 6.415768
H -7.826347 -2.784255 6.269648
H -9.089396 -2.664586 5.045291
H -6.104609 -2.109280 4.613775
H -6.928832 -3.574130 4.062514
H -6.515370 -1.693842 2.323234
H -8.117057 -2.437770 2.366968
H -8.823621 0.394053 0.060776
H -7.230541 -0.218781 0.600121
H -8.649721 -1.338565 0.479815
O -6.935109 3.440867 2.361504
O -6.243068 2.277179 4.481814
H -4.364936 7.144111 1.576671
H -2.644414 7.538563 3.313235
H -8.443275 3.094289 0.327688
H -8.291662 1.081731 4.439488
C -4.003719 6.317776 2.180783
C -3.039173 6.538728 3.162202
C -7.588753 3.721473 0.097262
C -6.662726 3.965509 1.110122
H -8.131684 4.098747 -1.950434
C -7.411220 4.290947 -1.161553
C -5.535242 4.781000 0.898080
C -4.541672 5.038677 1.966736
C -2.589737 5.479291 3.954922
H -1.840477 5.647666 4.722501
P -6.019567 2.237024 2.996073
C -6.301108 5.104229 -1.400257
C -5.380824 5.340744 -0.381029
C -4.071562 3.997392 2.783578
C -3.108162 4.199811 3.766075
H -6.147267 5.544400 -2.380353
H -4.505208 5.952448 -0.576636
H -2.786165 3.348632 4.358535
O -6.215083 0.911489 2.285230
O -4.507461 2.701712 2.547895
H 0.397096 0.283322 3.438427
H -0.178126 -0.874102 1.381428
H -1.933243 0.009080 2.579607
H -3.720183 0.970618 3.979407
C 0.295926 -0.697251 3.931274
H 0.991417 -0.740701 4.772255
S -3.064255 1.538474 6.784253
O -1.513337 0.188620 5.235994
O 0.635119 -1.762350 3.045614
C -0.243835 -1.834364 1.931577
H -3.811327 -0.592831 8.643478
H 2.256110 -2.823335 1.554882
C -2.036971 -0.939512 3.133952
C -1.147624 -0.883897 4.382405

C -2.849568 0.056724 5.695334
C -4.594269 1.144364 7.633184
C -3.836952 0.022124 4.515047
C -4.681692 0.037643 8.487378
C 1.522677 -3.345196 0.950260
C 0.175671 -2.983390 1.046029
O -1.589085 -2.024216 2.327149
H -5.653358 2.800798 6.754485
O -4.343393 -1.089311 2.382349
C -5.706351 1.975218 7.453886
H -5.578487 0.750239 4.976482
C -3.499225 -1.105953 3.520655
H 2.957617 -4.658656 0.032098
C 1.910186 -4.378684 0.097444
C -5.884256 -0.255410 9.127454
C -0.779257 -3.657467 0.278653
H -5.949692 -1.123029 9.777300
H -1.232324 -1.847905 4.908933
H -1.821957 -3.372312 0.364635
H -4.869193 -0.260168 2.372913
O -5.160321 -0.141433 4.972076
H -2.980277 -0.851185 6.304087
C -6.899437 1.689435 8.117156
C -6.995953 0.571701 8.947058
C 0.956142 -5.053975 -0.665993
C -0.388228 -4.690552 -0.572936
H -7.761021 2.332632 7.962230
H -3.617873 -2.077840 4.023539
H 1.258634 -5.859518 -1.328820
H -7.930507 0.345348 9.452836
H -1.135612 -5.213968 -1.162316

• **TS_{PA-C3}**

91

C -9.222764 0.108577 2.740904
C -9.520101 0.739620 4.059804
C -9.525019 -0.212445 5.267921
C -9.979918 -1.626212 4.888817
C -9.030785 -2.193757 3.828990
C -9.048970 -1.357447 2.543473
O -9.491153 0.884097 1.742257
C -9.183045 0.478194 0.381470
H -10.498919 1.218577 3.920056
H -8.516682 -0.275110 5.680086
H -10.166632 0.219658 6.041108
H -9.974141 -2.267367 5.775836
H -11.014397 -1.611508 4.513333
H -8.012259 -2.190751 4.219656
H -9.290508 -3.223652 3.566329
H -8.150204 -1.548890 1.951659
H -9.904813 -1.644906 1.910325
H -9.423378 1.344673 -0.229418
H -8.118754 0.254682 0.332972
H -9.797462 -0.376983 0.092760
O -6.900036 3.245058 2.480001
O -6.498007 1.857464 4.518653
H -3.474143 6.162216 1.733471
H -1.647403 6.000236 3.400586
H -8.537668 3.497667 0.541685
H -8.802330 1.556250 4.209980
C -3.314669 5.236232 2.277759
C -2.287368 5.143010 3.214816
C -7.547207 3.855870 0.282399
C -6.544950 3.756177 1.246348
H -8.049175 4.500307 -1.709343
C -7.268332 4.425532 -0.957826
C -5.243396 4.234933 1.008276
C -4.177680 4.155039 2.035130

C -2.089619 3.954453 3.919725
H -1.301747 3.873463 4.661509
P -6.317927 1.808549 3.024724
C -5.980709 4.894310 -1.226642
C -4.989406 4.799149 -0.252608
C -3.966075 2.981882 2.777117
C -2.930234 2.866165 3.696536
H -5.747652 5.327497 -2.194834
H -3.985013 5.146714 -0.469875
H -2.793651 1.927055 4.217825
O -6.902439 0.624516 2.263421
O -4.754702 1.862218 2.525864
H -1.656384 -1.879782 6.577607
H -2.939882 -0.071854 7.679159
H -4.175053 -1.727729 6.224602
H -5.573180 -3.117952 4.205867
C -1.535198 -1.187097 5.730402
H -0.553119 -1.349863 5.280577
S -3.748643 -4.448806 2.486895
O -2.763891 -2.697496 4.227404
O -1.571718 0.177920 6.162463
C -2.809586 0.540890 6.765401
H -1.033450 -3.296359 2.716017
H -0.697988 2.045940 7.576698
C -3.977181 -1.012001 5.410921
C -2.666117 -1.369706 4.726516
C -3.709250 -2.749683 3.144840
C -2.305329 -4.461903 1.427406
C -5.139451 -2.325608 3.580347
C -1.104713 -3.823822 1.773456
C -1.599508 2.641390 7.476070
C -2.786258 2.024609 7.068046
O -3.903003 0.315518 5.906888
H -3.321360 -5.656843 -0.052277
O -6.350679 -0.776733 4.971623
C -2.387612 -5.175736 0.224440
H -6.068311 -1.187260 2.290977
C -5.093840 -1.028833 4.390212
H -0.647458 4.492161 8.023023
C -1.573932 4.016087 7.716684
C -0.013557 -3.882638 0.905766
C -3.950311 2.787524 6.907206
H 0.908753 -3.376023 1.175400
H -2.492046 -0.660458 3.901634
H -4.856819 2.323598 6.534500
H -6.428516 0.206800 5.013765
O -5.961124 -2.147885 2.435870
H -3.384029 -2.080691 2.335410
C -1.280807 -5.252543 -0.621360
C -0.092974 -4.599680 -0.288273
C -2.733351 4.777150 7.554733
C -3.917373 4.159652 7.152598
H -1.355587 -5.809072 -1.550977
H -4.830392 -0.235253 3.679440
H -2.710638 5.847181 7.732983
H 0.762497 -4.649622 -0.953849
H -4.816810 4.747713 7.002399

• **TS_{PE-C2}**

91

C -9.997069 -2.125650 -2.601961
C -9.411997 -1.571839 -1.354981
C -9.654289 -2.534789 -0.163277
C -11.105168 -3.026885 -0.109165
C -11.518740 -3.660770 -1.443487
C -11.409160 -2.606631 -2.582259
O -9.165878 -2.397547 -3.528569
C -9.568969 -2.746081 -4.892269

H -8.356431 -1.361452 -1.519326
H -8.976573 -3.392426 -0.262032
H -9.380937 -2.013870 0.758334
H -11.235612 -3.739327 0.711711
H -11.770571 -2.179480 0.102691
H -10.882634 -4.525240 -1.670604
H -12.550685 -4.021882 -1.414310
H -11.735149 -2.987910 -3.549368
H -12.046957 -1.763193 -2.318777
H -8.707605 -2.459225 -5.488128
H -9.774379 -3.817751 -4.930767
H -10.428376 -2.137646 -5.170924
O -6.077948 1.315892 -4.505271
O -8.106541 1.562589 -2.992745
H -2.219053 0.124578 -2.438388
H -2.445288 0.161529 0.029447
H -5.714244 1.115745 -7.045330
H -9.933227 -0.619618 -1.204653
C -3.194765 -0.004484 -1.980253
C -3.324243 0.025900 -0.592827
C -4.983419 0.549803 -6.478736
C -5.088472 0.544271 -5.089562
H -3.882625 -0.163946 -8.181059
C -3.960315 -0.163848 -7.098255
C -4.184703 -0.174941 -4.286196
C -4.311658 -0.167524 -2.812688
C -4.587860 -0.091102 -0.010468
H -4.701275 -0.043983 1.067981
P -7.411967 0.577938 -3.886193
C -3.047402 -0.883011 -6.324526
C -3.162668 -0.884792 -4.935892
C -5.569716 -0.315307 -2.202126
C -5.711986 -0.258415 -0.817618
H -2.254947 -1.450665 -6.802263
H -2.469397 -1.464621 -4.334449
H -6.706711 -0.333197 -0.391851
O -8.224370 -0.141182 -4.933184
O -6.677049 -0.610410 -2.976371
H -14.871367 3.522981 -1.850631
H -13.549288 3.897791 0.203234
H -12.395323 3.097459 -1.844715
H -11.268116 1.868653 -3.984836
C -15.025094 2.493167 -1.489860
H -16.020713 2.159042 -1.794491
S -13.134070 0.295109 -5.676879
O -13.907921 1.534524 -3.437484
O -14.970399 2.426418 -0.064827
C -13.710772 2.835307 0.459894
H -15.845243 0.408511 -4.581620
H -13.815481 4.695104 2.481191
C -12.585372 2.076170 -1.476547
C -13.928971 1.580929 -2.014956
C -12.976560 0.547577 -3.874031
C -14.496616 -0.872346 -5.664787
C -11.539987 0.936682 -3.471971
C -15.718321 -0.560317 -5.051336
C -13.797848 3.673170 2.850998
C -13.744929 2.611272 1.949119
O -12.634395 2.063980 -0.048883
H -13.373231 -2.359234 -6.742023
O -10.239909 1.594513 -1.463931
C -14.323904 -2.120421 -6.275535
H -9.795566 0.192367 -4.167260
C -11.470915 1.149173 -1.941038
H -13.860567 4.254194 4.924670
C -13.822671 3.423569 4.226113
C -16.746952 -1.503908 -5.036177
C -13.717448 1.296615 2.426039
H -17.688712 -1.262179 -4.551989
H -14.110560 0.575781 -1.600344

H -13.663924 0.483418 1.711154
H -9.501726 1.555493 -2.127506
O -10.680261 -0.125418 -3.858790
H -13.228083 -0.415985 -3.405482
C -15.366053 -3.048385 -6.278385
C -16.576732 -2.745360 -5.652929
C -13.787126 2.112288 4.699320
C -13.731806 1.047998 3.794453
H -15.227475 -4.012651 -6.759890
H -11.719550 0.166608 -1.492306
H -13.793793 1.918715 5.768268
H -17.384752 -3.472439 -5.647592
H -13.700097 0.025316 4.159373

• TS_{PE-C3}

91

C -5.472703 -0.298291 0.587954
C -6.571789 0.626635 0.924165
C -6.781608 0.551694 2.465926
C -6.978772 -0.897634 2.923004
C -5.823685 -1.796467 2.463507
C -5.644235 -1.731465 0.909581
O -4.378819 0.233536 0.214177
C -3.210393 -0.538073 -0.189518
H -6.330831 1.631364 0.580083
H -5.914568 1.006776 2.950899
H -7.650760 1.166696 2.714693
H -7.060012 -0.936799 4.015168
H -7.919517 -1.286589 2.514415
H -4.890776 -1.490939 2.954904
H -6.001416 -2.842278 2.730240
H -4.815711 -2.353988 0.573016
H -6.565788 -2.052793 0.410035
H -2.556674 0.197852 -0.646426
H -2.770080 -1.001481 0.695186
H -3.504713 -1.275983 -0.935248
O -7.630348 1.018506 -1.972308
O -6.074847 -0.691766 -2.993024
H -8.992302 3.043476 -5.921941
H -8.109448 1.945342 -7.911426
H -8.651456 2.408585 -0.104572
H -7.463059 0.248037 0.415217
C -8.723039 1.997214 -5.861505
C -8.219803 1.371423 -6.997456
C -9.149655 2.568122 -1.053812
C -8.724244 1.824916 -2.158559
H -10.496994 4.071013 -0.318159
C -10.174621 3.500184 -1.183749
C -9.313374 2.015517 -3.425495
C -8.832675 1.315571 -4.637544
C -7.826360 0.033749 -6.945600
H -7.412169 -0.453184 -7.823141
P -7.437788 -0.610991 -2.343589
C -10.784793 3.691278 -2.424779
C -10.354482 2.954338 -3.522819
C -8.460016 -0.039189 -4.621781
C -7.955516 -0.675583 -5.754269
H -11.594576 4.403766 -2.536287
H -10.829912 3.095079 -4.487920
H -7.664616 -1.716807 -5.672299
O -7.784888 -1.417140 -1.133282
O -8.624014 -0.783930 -3.463398
H -4.474914 6.030465 -1.625690
H -3.540565 4.565639 0.044735
H -3.538440 3.668149 -2.145593
H -3.719040 2.712574 -4.543581
C -5.438152 5.536204 -1.427107
H -6.243135 6.257247 -1.581725

S -5.550470 4.201707 -6.284082
O -5.436695 4.695130 -3.685081
O -5.518209 5.103687 -0.065490
C -4.542635 4.133959 0.238835
H -7.479303 5.581582 -4.512694
H -6.440483 4.851274 2.088339
C -4.545653 3.263805 -1.950154
C -5.594402 4.318198 -2.326260
C -5.700922 3.593229 -4.572328
C -7.180205 4.889961 -6.533200
C -4.743841 2.406447 -4.298832
C -7.923354 5.471480 -5.494727
C -5.692864 4.188649 2.507921
C -4.659802 3.726179 1.690827
O -4.679344 2.964801 -0.553434
H -7.176354 4.340448 -8.618662
O -3.981203 0.945903 -2.492500
C -7.744980 4.795525 -7.813332
H -5.725615 0.743452 -4.658578
C -4.819276 2.039880 -2.797937
H -6.554588 4.166780 4.480689
C -5.748401 3.802995 3.850346
C -9.236556 5.883251 -5.723224
C -3.692257 2.865657 2.221069
H -9.813835 6.295754 -4.900639
H -6.592287 3.887387 -2.149007
H -2.903553 2.495480 1.573469
H -4.527299 0.185200 -2.784943
O -5.050869 1.287587 -5.101748
H -6.733098 3.243975 -4.438796
C -9.046494 5.239891 -8.040600
C -9.806451 5.766958 -6.991982
C -4.772374 2.960116 4.381912
C -3.743229 2.487433 3.561531
H -9.477234 5.147012 -9.033595
H -5.853763 1.759288 -2.595119
H -4.813668 2.668612 5.427023
H -10.829308 6.086309 -7.165374
H -2.981835 1.827818 3.967684

• **BPA no dispersion reoptimized without dispersion**

26

H -5.72378886 -0.46097378 0.97187728
C -6.27774776 -0.34909621 0.04514956
C -7.66996351 -0.35391065 0.06373547
H -8.19575597 -0.48341738 1.00451089
C -8.38558143 -0.18028019 -1.12254759
H -9.47098589 -0.17828749 -1.11434828
C -7.70317932 -0.00337390 -2.32419697
H -8.22694310 0.12960973 -3.26425872
C -6.31218969 -0.00297626 -2.32514193
O -5.65949834 0.08317706 -3.55931810
C -5.56178462 -0.17587792 -1.15132593
H -3.92160443 -1.85697409 0.18995159
H -1.45146796 -1.88746378 0.21946043
C -3.36602425 -1.12979584 -0.39419638
C -1.97406430 -1.15199715 -0.38405130
C -4.08083428 -0.19893688 -1.16691151
C -1.25597207 -0.23840341 -1.15784006
H -0.17058602 -0.25086785 -1.15762860
C -3.32864658 0.70655164 -1.93405126
C -1.93716477 0.69480497 -1.93609801
O -3.96459781 1.72686105 -2.64486517
H -1.41070724 1.42673786 -2.53851201
P -4.87163292 1.43929943 -3.95439259
O -5.64106726 2.62213221 -4.37368356
O -3.87912897 0.82706185 -5.06332905

H -3.83533270 1.42594696 -5.82240819

• **BPA dimer reoptimized without dispersion**

52

H -6.14870047 -1.60584753 -0.40100539
C -6.86034705 -1.71491215 -1.21330380
C -8.22601209 -1.63372637 -0.95425060
H -8.57306249 -1.47632195 0.06211431
C -9.14312422 -1.74150214 -2.00137801
H -10.20902518 -1.67364075 -1.80784075
C -8.68803173 -1.93386129 -3.30404324
H -9.37229957 -2.02945819 -4.13963103
C -7.32062934 -2.01610270 -3.54535059
O -6.90944798 -2.31108885 -4.84864198
C -6.37095455 -1.91010899 -2.51582100
H -4.51371830 -3.25850943 -1.07363840
H -2.07609510 -3.38474708 -1.46029066
C -4.07271022 -2.73439493 -1.91577902
C -2.70043110 -2.81176966 -2.13867656
C -4.91542005 -2.01017499 -2.77561537
C -2.13319794 -2.16448717 -3.23822664
H -1.06477006 -2.22422374 -3.42009069
C -4.31268410 -1.37279691 -3.87236571
C -2.94386989 -1.44116291 -4.11019807
O -5.08194354 -0.56284614 -4.71315019
H -2.53628857 -0.92031693 -4.96946987
P -6.12226468 -1.23208460 -5.75460760
O -7.09902912 -0.05301646 -6.06691670
O -5.48944616 -1.92106728 -6.91772681
H -7.14085739 0.20286137 -7.05446072
H -5.72001684 -1.80536456 -8.43135007
O -7.11568875 0.51295636 -8.54763682
O -5.87809312 -1.61276118 -9.41867406
O -5.16790580 0.78633800 -10.13474467
P -6.39738039 -0.15820781 -9.67058882
H -2.72709437 -0.04370109 -10.25705199
C -3.15324298 0.13720108 -11.23765010
C -4.47937268 0.54776471 -11.32672433
O -7.24659424 -0.36572844 -11.02414713
H -9.59120550 0.66365215 -11.32593651
C -7.52442566 0.71879836 -11.86233696
H -1.37041120 -0.34366849 -12.33740637
C -2.40487909 -0.02133369 -12.40195384
C -8.84655073 1.14122071 -11.95287711
C -5.09854975 0.81278192 -12.55922996
C -6.50280825 1.27808472 -12.64694248
C -9.18163490 2.15416842 -12.84891729
H -10.21115113 2.49007782 -12.92199425
C -6.87152170 2.29884191 -13.53945547
C -8.19050091 2.73260276 -13.64384857
H -6.09989748 2.76775738 -14.14216259
H -8.44185191 3.52833676 -14.33808839
C -2.99111854 0.23107193 -13.64376873
C -4.32014542 0.64010565 -13.71596094
H -2.41734190 0.10057232 -14.55590124
H -4.78108586 0.81423003 -14.68318622

• **BPA + enol ether 5-15b complex reoptimized without dispersion**

46

C -7.20366235 0.28765183 -0.24973137
C -8.34822476 0.80794667 -0.70830923
C -9.50324835 -0.05747667 -1.15510041
C -9.09414838 -1.52320530 -1.36062391
C -8.21905666 -2.00911469 -0.19995831

C -6.92723390 -1.18510689 -0.11175724
O -6.09901916 1.03255287 0.14135196
C -6.13588616 2.44779121 -0.05306579
H -8.48894262 1.88265768 -0.75887608
H -10.31241626 0.00115493 -0.41100557
H -9.92803627 0.34703414 -2.08317891
H -9.98627128 -2.15075848 -1.46426549
H -8.52957651 -1.61436950 -2.29799461
H -8.77396571 -1.90644462 0.74138903
H -7.97406119 -3.07067461 -0.31168767
H -6.42208166 -1.36529556 0.84282873
H -6.21936758 -1.48863640 -0.89597944
H -6.90312646 2.91571247 0.57250045
H -5.15332835 2.81838900 0.23967299
H -6.32287295 2.67966094 -1.10667773
H -4.57396808 3.74376066 3.60446557
O -5.26015922 -0.80844677 4.72331112
O -5.83429990 1.66531762 4.44308185
C -5.64340415 3.81462232 3.43822517
H -5.34100682 0.59147108 1.60948175
H -5.60249572 5.79817667 2.60866520
P -5.71695752 0.19251332 3.75109271
C -6.44623110 2.73664905 3.80786345
C -6.22643627 4.95576742 2.89106139
O -4.84717140 0.34192927 2.43314304
C -7.84391569 2.76472284 3.64655608
C -7.61069239 5.00996981 2.71203749
O -7.20478880 0.00971580 3.09465020
C -8.70460137 1.63729987 4.07560509
H -8.07273381 5.89281401 2.28117535
C -8.40264313 3.92584982 3.08456400
C -8.35124204 0.29953187 3.83111696
H -10.20941659 2.89196269 4.95939045
C -9.92385376 1.86881791 4.73462894
C -9.16406437 -0.76125104 4.21949155
H -8.83820260 -1.77279211 4.00386359
C -10.74955157 0.81774781 5.12462743
H -9.47670643 3.96316387 2.93121681
C -10.36935723 -0.50100748 4.86802448
H -11.68219315 1.02755881 5.63885771
H -11.00488035 -1.32558413 5.17530125

- **Enol ether 5-15b reoptimized without dispersion**

20

C -6.80016768 0.42382097 -0.15738892
C -7.63802951 1.45669281 -0.33782435
C -9.12776226 1.34700051 -0.10744730
C -9.60083810 -0.10995372 -0.00540928
C -8.65770648 -0.92587151 0.88597016
C -7.23845517 -0.94345508 0.30215553
O -5.44615898 0.44142905 -0.36789645
C -4.86810141 1.64392328 -0.84511579
H -7.26025005 2.42309327 -0.65550435
H -9.40371970 1.89025098 0.81034894
H -9.66425151 1.85603159 -0.91940540
H -10.62686374 -0.14896010 0.37818008
H -9.62015162 -0.55677071 -1.00854424
H -8.63284055 -0.47988295 1.88897857
H -9.02380715 -1.95178371 1.00584128
H -6.51442291 -1.31041079 1.03934693
H -7.18128926 -1.63828138 -0.54783995
H -5.00644815 2.46753445 -0.13233396
H -3.80156383 1.44555797 -0.96470234
H -5.29557192 1.94017509 -1.81215914

- **Axial phosphate 5-20a reoptimized without dispersion**

46

C -7.04042421 0.17232605 -1.10419642
C -8.17419654 1.07100221 -0.60403125
C -9.46110266 0.29126580 -0.30755975
C -9.20557172 -0.87777557 0.65445757
C -8.09850785 -1.79806029 0.12299388
C -6.80474192 -1.02331440 -0.17280282
O -5.93182706 0.99593012 -1.28833886
C -4.67996646 0.37106345 -1.57963066
H -7.80183448 1.54393209 0.31247692
H -10.20605794 0.97650438 0.11178117
H -9.88162215 -0.08588100 -1.24714039
H -8.90952899 -0.48376741 1.63725487
H -10.12703708 -1.45026535 0.81277474
H -7.88308029 -2.59832167 0.84028004
H -8.43715641 -2.28179502 -0.80063881
H -6.38301151 -0.62169434 0.75709921
H -6.05862071 -1.69026607 -0.61440941
H -4.00856907 1.17884827 -1.87497888
H -4.26466659 -0.13180922 -0.69846539
H -4.76760265 -0.33816683 -2.40726826
O -8.35915572 -0.87153268 -4.67287139
O -8.56625356 1.50983370 -3.72397236
H -6.14734962 -1.10774018 -8.67378427
H -5.47126588 1.10144513 -9.55731781
H -8.76583721 -3.28741299 -3.89293627
H -8.34906853 1.85958953 -1.33798769
C -6.01371187 -0.27101943 -7.99515035
C -5.64021350 0.97490982 -8.49246144
C -7.98008990 -3.22183859 -4.63745370
C -7.62010898 -1.96551608 -5.11738694
H -7.62077136 -5.33780087 -4.75698262
C -7.34099533 -4.35740424 -5.13002360
C -6.62314549 -1.80225224 -6.09492606
C -6.25061043 -0.46947873 -6.62477036
C -5.49730437 2.06021730 -7.62527918
H -5.21191069 3.03500194 -8.00833954
P -7.71830552 0.30642312 -3.76029806
C -6.34481103 -4.22787392 -6.09977299
C -5.99384782 -2.96537187 -6.57013464
C -6.09591878 0.64146374 -5.77991673
C -5.72717523 1.89370280 -6.26121626
H -5.83701158 -5.10728598 -6.48332444
H -5.20552468 -2.86245183 -7.30943458
H -5.62269406 2.71330137 -5.55908156
O -7.40303057 -0.46540032 -2.39790034
O -6.22745302 0.47358628 -4.40027329

- **Equatorial phosphate 5-20b reoptimized without dispersion**

46

C -7.65461191 0.01223339 -1.06411186
C -8.94319792 0.75642452 -0.70525401
C -9.02383023 1.02874963 0.80469243
C -8.87737148 -0.26072952 1.62347467
C -7.58557482 -1.00580536 1.25442940
C -7.51009160 -1.28203260 -0.25509734
O -6.60739581 0.92287036 -0.89647611
C -5.27049287 0.43389222 -1.01777925
H -8.98494406 1.68311155 -1.28004717
H -8.22947987 1.73204022 1.08136793
H -9.97641223 1.52053600 1.03138586
H -8.88994298 -0.03630937 2.69636344
H -9.73916692 -0.91535374 1.42952606
H -6.72014516 -0.40403538 1.55996124
H -7.51729729 -1.95411613 1.79972981
H -6.57995153 -1.78968358 -0.52658647
H -8.32744351 -1.94610597 -0.55618859

H -4.63648440 1.31984062 -1.08134469
H -4.97192896 -0.15297328 -0.14115803
H -5.14048050 -0.16061202 -1.92607784
O -8.28415850 -0.52336327 -4.90458776
O -8.64341413 1.70783341 -3.68050693
H -5.50480470 -0.16821938 -8.52616447
H -4.71118697 2.13691659 -8.94060588
H -8.78111158 -3.02215797 -4.57309100
H -9.78668149 0.13422065 -1.02525138
C -5.47392594 0.54808313 -7.71103541
C -5.03433877 1.84844163 -7.94520702
C -7.89722586 -2.85538549 -5.17868081
C -7.47937544 -1.54610684 -5.40122738
H -7.51288348 -4.93289086 -5.57436606
C -7.18812652 -3.91139351 -5.74644025

C -6.35152907 -1.24989461 -6.18659958
C -5.90938135 0.14169925 -6.43873090
C -5.02345062 2.78098731 -6.90578121
H -4.68807376 3.79786107 -7.08419233
P -7.79888011 0.50398643 -3.74765286
C -6.06413692 -3.64985450 -6.53242604
C -5.65552168 -2.33595282 -6.74426177
C -5.88496004 1.10335510 -5.41541103
C -5.45207878 2.40748865 -5.63377253
H -5.50229817 -4.46758103 -6.97289808
H -4.76940852 -2.13356916 -7.33798043
H -5.45601875 3.10534660 -4.80390943
O -7.69061979 -0.45096959 -2.46914627
O -6.22493104 0.72533564 -4.11482268

References

- [1] Y. Shao, Z. Gan, E. Epifanovsky, A. T. B. Gilbert, M. Wormit, J. Kussmann, A. W. Lange, A. Behn, J. Deng, X. Feng, et al., *Mol. Phys.* **2015**, *113*, 184–215.
- [2] A. D. Becke, *J. Chem. Phys.* **1997**, *107*, 8554–8560.
- [3] S. Grimme, *J. Comput. Chem.* **2006**, *27*, 1787–1799.
- [4] P. C. Hariharan, J. A. Pople, *Theor. Chim. Acta* **1973**, *28*, 213–222.
- [5] M. M. Francl, W. J. Pietro, W. J. Hehre, J. S. Binkley, M. S. Gordon, D. J. DeFrees, J. A. Pople, *J. Chem. Phys.* **1982**, *77*, 3654–3665.
- [6] Discovery Studio 4.1 Visualizer: Accelrys Software Inc. San Diego, USA, **2015**.
- [7] P. M. Zimmerman, *J. Chem. Phys.* **2013**, *138*, 184102.
- [8] P. M. Zimmerman, *J. Comput. Chem.* **2013**, *34*, 1385–1392.
- [9] P. M. Zimmerman, *J. Comput. Chem.* **2015**, *36*, 601–611.
- [10] P. M. Zimmerman, *J. Chem. Theory Comput.* **2013**, *9*, 3043–3050.
- [11] A. V. Marenich, C. J. Cramer, D. G. Truhlar, *J. Phys. Chem. B* **2009**, *113*, 6378–6396.
- [12] J. Da Chai, M. Head-Gordon, *J. Chem. Phys.* **2008**, *128*, 084106.
- [13] N. M. O’Boyle, M. Banck, C. A. James, C. Morley, T. Vandermeersch, G. R. Hutchison, *J. Cheminform.* **2011**, *3*, 33.

APPENDIX F

Experimental Information for Chapter 5, Section 5.4

General information

Proton, carbon, and deuterium NMR spectra were recorded on Varian VNMRS-700 (700 MHz), Varian VNMRS-500 (500 MHz), Varian INOVA 500 (500 MHz) or Varian MR400 (400 MHz). ^1H NMR chemical shifts (δ) are reported in parts per million (ppm) relative to tetramethylsilane with the solvent resonance employed as the internal standard (C_6D_6 , δ 7.16 ppm; CD_2Cl_2 δ 5.32 ppm; CDCl_3 , δ 7.24 ppm).

Computational Studies

All quantum chemical calculations were performed using the Q-Chem 4.3 package.^[1] Geometry optimizations were evaluated using the B97-D density functional^[2,3] using the double- ζ - quality basis set with polarization functions on all atoms, 6-31G**.^[4,5] Pictorial representations of important stationary points were generated in Discovery Studio 4.1 Visualizer.^[6]

For the growing string reaction path optimizations, between 7-15 nodes were used, including the end points. In the initial phase, termed growth phase, new nodes were added when the perpendicular gradient magnitude on the frontier node was less than 0.10 Hartree/Å for double-ended strings, or when the RMS gradient was less than 0.005 Hartree/Å for single-ended strings. Additionally, an initial maximum optimization step size of 0.1 Å-radians was used. When the total

perpendicular gradient magnitude over all nodes, F , reached a value of less than 0.3, the climbing image search was initiated. When $F < 0.1$, or when the node of highest energy had a RMS gradient below double the nodal convergence criterion and $F < 0.2$, the exact transition state search was initiated. The string is considered fully converged when an RMS gradient < 0.0005 Hartree/Å was obtained for the node representing the transition state. Further detail regarding the growing string implementation developed in the Zimmerman group can be found in the references.^[7–10]

The electronic Gibbs free energy values of all stationary points were computed through solvent corrected (dichloromethane) single point energies using the SMD model.^[11] For these calculations the ω B97X-D3 exchange functional^[12] was employed with a 6-31G** basis set. The final Gibbs free energy values were obtained by correcting the electronic free energy with the enthalpic and entropic contributions from vibrations, rotations, and translations at 298.15 K. These frequency computations were performed using the B97-D functional and 6-31G** basis set. For the enthalpic and entropic corrections to the free energies from the harmonic oscillator approximation, all frequencies below 50 cm^{-1} were treated as if they were 50 cm^{-1} .

A model system consisting of biphenyl hydrogen phosphate (**BPA**), 6-deoxyglucose-derived trichloroacetimidate α -**5-19**, and glucose-based diol **5-16b** was utilized to explore the phosphoric acid-catalyzed glycosylation of sugar-derived 2,3-diols. To account for variation in conformations and binding complexes, the most stable conformations were sampled for the growing string calculations. These were obtained in part by manually sampling relevant torsions and angles of approach, and also by using an algorithm which allowed a thorough conformational analysis by ranking a vast number of unique conformers generated by the systematic variation of the torsional angles.^[13] Using the growing string method, pathways for the reaction of BPA with trichloroacetimidate donor α -**5-19** leading to the formation of phosphate β -**5-10b** through S_N2 -like

mechanism were readily found. Following this, the reaction of the phosphate intermediate β -**5-10b** with diol **5-16b** to form C2 and C3 glycosides was evaluated. The lowest reaction pathways calculated for the formation of these glycosides proceeded through a S_Ni mechanism with retention of configuration.

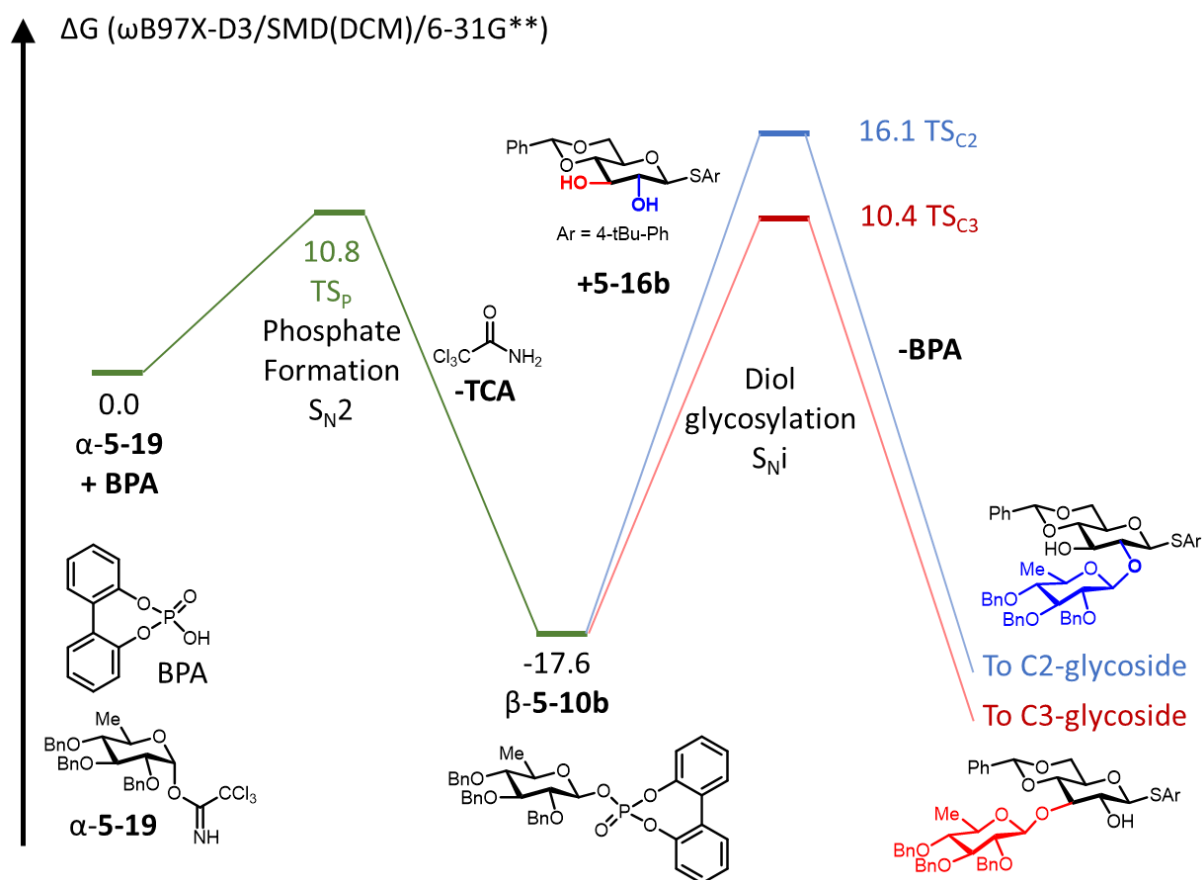


Figure F.1. Energy diagram for the CPA-catalyzed intermolecular glycosylation of 6-deoxyglucose-derived 2,3-diols.

A summary of calculated values, including solvent corrected single point electronic energies, as well as enthalpic and entropic corrections associated with vibrational, rotational, and translational energy at 298 K are provided below.

Table F.1. Calculated energy values for the BPA-catalyzed acetalization of diols.

	GSMD [kcal/mol] ^a	Svrt [cal/mol] ^b	Hvrt [kcal/mol.K] ^b	Gcorr [kcal/mol] ^c
BPA	-693418.0	114.1	126.3	-693325.7
Diol 5-16a	-1046439.2	177.3	310.9	-1046181.1
Trichloroacetimidate donor α-5-19	-1841479.5	217.4	357.7	-1841186.7
Trichloroacetimidate donor α-5-19 + BPA complex	-2534913.6	276.0	484.7	-2534511.2
Trichloroacetamide (TCA)	-996497.9	90.4	33.4	-996491.4
α-phosphate 5-10b	-1538418.7	237.2	450.9	-1538038.5
β-phosphate 5-10b	-1538413.8	238.3	451.2	-1538033.6
β-phosphate 5-10b + diol 5-16a complex	-2584872.8	355.9	764.9	-2584214.0
TS_P	-2534901.7	281.7	484.2	-2534501.5
TS_{C2}	-2584837.9	365.3	760.8	-2584186.0
TS_{C3}	-2584846.5	355.2	760.7	-2584191.7

^aGas-phase electronic energy (ω B97X-D3/SMD/6-31G**). ^bVibrational, rotational, and translational entropic and enthalpic contributions (B97-D/6-31G**) at 298K. ^cCorrected free energy values at 298K.

Cartesian coordinates for starting geometries, transition states, and products are described below.

• **BPA**

26

H -5.72428523 -0.48831442 0.98697438
C -6.28439443 -0.36620410 0.06007891
C -7.68832232 -0.36341207 0.07668617
H -8.21878366 -0.49755063 1.01925451
C -8.40824701 -0.17254738 -1.11938955
H -9.49782706 -0.16110110 -1.11076079
C -7.71851142 0.00685161 -2.33069717
H -8.24375641 0.14914534 -3.27295870
C -6.31717770 -0.00517093 -2.33003536
O -5.65460079 0.06060007 -3.58302558
C -5.56356336 -0.18448078 -1.14510677
H -3.92068644 -1.85692296 0.21829797
H -1.42723110 -1.89050223 0.23304154
C -3.36034227 -1.13416699 -0.37500477
C -1.95668993 -1.15639827 -0.37407259
C -4.08202246 -0.20016108 -1.15752358
C -1.23660574 -0.24141830 -1.16732597
H -0.14707102 -0.25756904 -1.17597693
C -3.32891776 0.71387622 -1.93510103
C -1.92724273 0.69920244 -1.95046188
O -3.97830017 1.76149982 -2.63449179
H -1.40039703 1.42919197 -2.56173595
P -4.87333364 1.44496470 -3.96867356
O -5.65780224 2.62401335 -4.40603117
O -3.84439723 0.82979409 -5.06646961
H -3.81574089 1.43633068 -5.82391071

• **Diol 5-16a**

57

C -7.33779976 -1.23607297 0.64464879
C -8.08925588 -1.94447219 -0.47368577
C -7.20570556 -1.91256272 -1.74361214
C -6.74559910 -0.48708998 -2.10214028
O -6.06662540 0.14906535 -0.96894192
C -6.94991969 0.19377435 0.20955380
C -6.18940012 0.88909710 1.34415808
O -8.18917913 -1.11760538 1.84031500
O -8.35522467 -3.28355554 -0.09013656
O -7.98997612 -2.47519369 -2.79160551
O -7.04761729 0.89542317 2.54309276
C -7.44150612 -0.46599392 2.91823865
C -8.29606823 -0.41841198 4.16241049
C -8.10827481 0.60479936 5.11561960
C -8.86562813 0.61077130 6.30079656
C -9.81001411 -0.40516698 6.54311347
C -9.99633533 -1.42717501 5.59238465
C -9.24181200 -1.43761625 4.40562056
S -5.52476119 -0.49754218 -3.57573424
C -4.27323142 -1.70190155 -2.90094923
C -4.16650647 -2.98338795 -3.46743314
C -3.23382376 -3.90567645 -2.95370350
C -2.39907533 -3.56947855 -1.86519150
C -2.52490866 -2.26953002 -1.31494969
C -3.44381968 -1.33766918 -1.82099451
H -6.42228569 -1.80296167 0.90077082
H -9.02544674 -1.38693508 -0.67695619
H -6.31015482 -2.52489846 -1.53537956
H -7.59699615 0.12577814 -2.44522124
H -7.87142462 0.75245866 -0.02829650
H -5.24947254 0.34102505 1.54303400
H -5.97411616 1.93785742 1.11432044
H -8.73588627 -3.70780785 -0.87565579
H -7.41005272 -2.51969095 -3.57030714
H -6.50704591 -1.05082085 3.06809009
H -7.38232533 1.39022059 4.91599410

H -8.71977921 1.40797242 7.03070074
H -10.39577023 -0.39987963 7.46322708
H -10.72955302 -2.21414322 5.77267898
H -9.38576528 -2.21739498 3.66054499
H -4.80847576 -3.26477323 -4.30253220
H -3.17555835 -4.89327780 -3.40712853
C -1.37047676 -4.54656244 -1.25973357
H -1.89046512 -1.98244992 -0.47607637
H -3.53429962 -0.34832499 -1.37966754
C -1.68825131 -4.76003648 0.25045437
C 0.05762930 -3.93990895 -1.40033357
C -1.37966142 -5.92786426 -1.96115574
H 0.12922647 -2.96515978 -0.89360618
H 0.30961042 -3.79618014 -2.46276161
H 0.79681240 -4.62253163 -0.94947168
H -1.65514036 -3.80892322 0.80403954
H -0.94505652 -5.44333449 0.69321657
H -2.69110948 -5.19771570 0.37830011
H -2.36655707 -6.41182265 -1.88261143
H -0.63498248 -6.58221114 -1.48226105
H -1.12009170 -5.83265090 -3.02764029

• **Trichloroacetimidate donor α -5-19**

68

C 1.45740144 2.59434689 -3.10882893
C 0.75318749 2.34096720 -1.74605697
C -0.65098136 2.96331411 -1.71806237
C -0.62071183 4.41600066 -2.21387691
C 0.07967033 4.52117548 -3.58395033
C -1.69172948 1.74290738 0.23483293
C 1.72353084 0.23920007 -0.85864111
C 0.28497057 5.96605007 -4.03199086
O 1.43235971 3.92246449 -3.49499644
O 0.58066574 0.95482999 -1.48365748
O -1.18431429 3.01171695 -0.34685070
O -1.97305136 4.93386096 -2.43709492
H 1.37299498 2.82342942 -0.96525579
H -1.31453803 2.36854712 -2.36190746
H -0.07662427 5.03930409 -1.48598314
H -0.50267095 3.95658873 -4.32784177
H 0.88134908 6.51228751 -3.28495617
H 0.80565893 5.99420576 -5.00000393
H -0.69598089 6.44980477 -4.12494303
C 1.16610499 -1.09369170 -0.42790821
C 0.85797380 -1.34822081 0.92454706
H 1.10342435 -0.59897113 1.67946149
C 0.22724887 -2.54987494 1.29877336
H -0.00793226 -2.73825993 2.34691724
C -0.11035767 -3.50190750 0.31742647
H -0.60690277 -4.42922136 0.60530378
C 0.19557593 -3.25376569 -1.03622965
H -0.06713261 -3.98576715 -1.80049066
C 0.83353361 -2.05714660 -1.40486542
H 1.05191588 -1.84940301 -2.45151388
C -2.63868287 0.97471526 -0.66448605
C -3.65014710 1.64227041 -1.38982926
H -3.72163948 2.72791020 -1.32651032
C -4.51834697 0.91968907 -2.22624538
H -5.28433993 1.44520033 -2.79790058
C -4.39357621 -0.48060458 -2.33459264
H -5.06650083 -1.04058643 -2.98508940
C -3.38609374 -1.15038456 -1.61265101
C -2.50425890 -0.42274710 -0.79190969
H -1.69514394 -0.93286298 -0.27156999
H -2.20617998 2.09672240 1.14198418
H -0.84849686 1.09994376 0.52219039
H 2.08846666 0.82574614 0.00285672
H 2.52258885 0.13168408 -1.60823421

C -2.64826414 5.52916723 -1.24593761
C -1.84241508 6.64146823 -0.61494694
C -1.79278199 7.92197980 -1.20792201
H -2.38204256 8.11713326 -2.10592547
C -0.98754863 8.93333798 -0.65450560
H -0.95879444 9.92109417 -1.11643418
C -0.21762115 8.67026532 0.49687232
H 0.40752305 9.45418838 0.92647903
C -0.25415729 7.39317670 1.08896111
H 0.34727983 7.18444228 1.97495630
C -1.06127339 6.38251030 0.53359990
H -1.07682680 5.37921165 0.96075719
H -2.84485768 4.73328406 -0.51646144
H -3.58986952 5.90487133 -1.66893883
H -3.26749951 -2.23029817 -1.70647144
H 2.44047029 -0.86227505 -4.39249822
N 2.31001980 0.09117308 -4.05312143
Cl -0.32732248 0.76541690 -6.71518244
Cl 0.57975728 -1.85375386 -5.69503707
C 1.17402065 0.55659090 -4.39867109
C 0.04659995 -0.17601780 -5.20435677
O 0.73962853 1.79269209 -4.12167922
Cl -1.41587975 -0.31557326 -4.16536102
H 2.50679749 2.27691666 -3.09744401

• **Trichloroacetimidate donor α -5-19 + BPA complex**

94

C 3.07077242 2.81337158 -1.83064999
C 2.32362001 2.24285186 -0.61505065
C 0.91755128 2.86018478 -0.50923418
C 1.01139671 4.39940123 -0.56940472
C 1.88838901 4.90945370 -1.74351689
C -1.11670149 2.34147981 0.84148262
C 2.39711001 0.05984360 0.47048867
C 2.22468769 6.39214746 -1.60585186
O 3.17426750 4.18742699 -1.81343139
O 2.25939666 0.83473168 -0.77593027
O 0.36508181 2.41456438 0.77627004
O -0.31730745 5.04275675 -0.62022161
H 2.92257120 2.51745349 0.26874046
H 0.31089848 2.46118565 -1.33549776
H 1.42932335 4.74934273 0.38428420
H 1.36488022 4.71996398 -2.69200463
H 2.80052077 6.74036235 -2.47502840
H 2.81440049 6.56267877 -0.69239094
C 2.16501290 -1.40326362 0.16060516
C 2.02025403 -2.31002847 1.23437464
H 2.07801981 -1.94259085 2.26079233
C 1.81234129 -3.67881749 0.99146051
H 1.70961870 -4.36748159 1.83079989
C 1.74006201 -4.15956472 -0.33131368
H 1.57755274 -5.22162988 -0.51908626
C 1.87822183 -3.25910043 -1.40519005
H 1.82773912 -3.62077173 -2.43299498
C 2.09129452 -1.88804931 -1.16213187
H 2.19585201 -1.19017556 -1.98821990
C -1.72178391 1.31941325 -0.10818623
C -1.08732195 0.08128378 -0.34251633
H -0.14600057 -0.14018632 0.14707954
C -1.65088645 -0.85709291 -1.22444608
H -1.13924276 -1.80408113 -1.39733430
C -2.86034117 -0.56431988 -1.88776512
H -3.29270836 -1.28632726 -2.58225700
C -3.50694012 0.66395866 -1.64823073
C -2.94191851 1.59994293 -0.76161148
H -3.44426488 2.54907803 -0.58327579
H -1.54237467 3.33656287 0.65400698
H -1.29196972 2.06282186 1.89178158

H 1.66128512 0.42780390 1.20190315
H 3.40696114 0.22873028 0.87538617
C -1.05431023 4.87446886 -1.88669153
C -2.54662873 4.88339238 -1.62989464
C -3.40213665 4.37756233 -2.63274526
H -2.97449225 3.97269874 -3.55243843
C -4.79332514 4.35580834 -2.43811629
H -5.44364120 3.95418461 -3.21599702
C -5.34405504 4.83247921 -1.23158315
H -6.42278347 4.80629446 -1.07365337
C -4.49411825 5.34121749 -0.23138522
H -4.91449140 5.70995686 0.70491695
C -3.10027771 5.37616872 -0.43069710
H -2.43800972 5.76367143 0.34136390
H -0.77743511 3.92831854 -2.37960230
H -0.77299158 5.69944141 -2.56744997
H -4.44161176 0.90094717 -2.15811441
H 3.57639816 -0.13836515 -4.33500408
N 3.56469990 0.61517480 -3.64765344
Cl 1.77921154 -0.10107917 -6.03138794
Cl -0.04913084 0.50643177 -3.78732982
C 2.53229206 1.36272132 -3.76207848
C 1.34346243 1.12260816 -4.76012553
O 2.25906243 2.43542080 -3.04084058
Cl 0.89343978 2.67188847 -5.59208055
H 4.07340025 2.38983118 -1.92269420
H 1.28989281 6.96563527 -1.52996718
H 5.20385060 -5.43897785 -0.09959911
H 7.59635764 -5.80050340 0.58082421
C 5.84235631 -4.59112884 0.14908166
H 4.28343230 -3.10847056 -0.19206892
C 7.18329377 -4.79255028 0.53208056
C 5.31713618 -3.28907702 0.08610029
C 7.99771981 -3.69034071 0.83831967
C 6.13963319 -2.20154455 0.40959201
H 9.04339927 -3.83789112 1.10976362
O 5.45006804 -0.30495679 -2.05720935
H 4.69293030 0.20244846 -2.51224202
C 7.49706587 -2.36659885 0.78035510
O 5.54182437 -0.92128526 0.47812627
P 5.90535683 0.23265786 -0.63560397
C 8.36868771 -1.21292053 1.10642745
O 7.53089120 0.07058925 -0.80900430
H 9.32154296 -2.18553682 2.78056474
O 5.39808671 1.55434491 -0.17195116
C 9.29291259 -1.27835976 2.17752926
C 8.33414534 -0.01433686 0.35087311
C 10.13997889 -0.19995741 2.47870543
C 9.16677088 1.07460196 0.64621627
H 10.83938543 -0.27613079 3.31114676
H 9.09680386 1.96873738 0.02986718
C 10.07563295 0.98193294 1.71383404
H 10.72757594 1.82461144 1.94476802

• **Trichloroacetamide (TCA)**

9

O -1.30869000 -1.27960000 -1.52241000
C -0.73985000 -1.86867000 -2.42298000
H 0.40827000 -3.12783000 -1.31179000
Cl -2.13744000 -0.13582000 -4.08638000
N 0.17868000 -2.85558000 -2.25794000
Cl -1.85601000 -3.01396000 -4.69634000
C -1.05625000 -1.54373000 -3.95653000
H 0.63350000 -3.31513000 -3.03440000
Cl 0.50310000 -1.20288000 -4.86013000

• **α -phosphate 5-10b**

C 2.33289451 1.21322823 -1.00181290
 C 1.22296839 0.99414006 0.04698457
 C 0.15982016 2.09233754 -0.06758692
 C 0.79089662 3.50034090 -0.19720361
 C 2.07174383 3.58945936 -1.07148194
 C -2.05993218 2.42873371 0.97946657
 C 1.26294542 -1.45006847 0.39380444
 C 2.88189747 4.84564085 -0.75695402
 O 2.96734030 2.43736697 -0.84235839
 O 0.57180124 -0.25128371 -0.15531892
 O -0.64276616 2.03572127 1.16044408
 O -0.19260790 4.49403995 -0.67388329
 H 1.69620795 1.04243528 1.04621294
 H -0.47009022 1.85183173 -0.93696504
 H 1.02464049 3.84013713 0.82138301
 H 1.79099744 3.57120096 -2.13435067
 H 3.73789308 4.93967255 -1.44054671
 H 3.25385384 4.80359127 0.27835078
 C 0.26136029 -2.57495441 0.32999226
 C -0.68480538 -2.73463727 1.36462007
 H -0.64455530 -2.07238211 2.23096816
 C -1.68230630 -3.72129287 1.27341621
 H -2.41271801 -3.83401372 2.07521872
 C -1.73756140 -4.56088643 0.14250639
 H -2.50889792 -5.32894395 0.07072394
 C -0.79203022 -4.40956237 -0.89097492
 H -0.83074919 -5.05865170 -1.76695018
 C 0.20330858 -3.41721271 -0.80067501
 H 0.92072892 -3.27097143 -1.60746567
 C -2.84490133 1.45628820 0.11714022
 C -2.59256708 0.06952901 0.18588551
 H -1.78098731 -0.28874239 0.81225193
 C -3.33745423 -0.82576128 -0.59829430
 H -3.12592267 -1.89362218 -0.53752962
 C -4.34132531 -0.34451336 -1.46361176
 H -4.90769309 -1.03947812 -2.08475073
 C -4.59292333 1.03792920 -1.53963985
 C -3.84737617 1.93475144 -0.75099796
 H -4.03537405 3.00529798 -0.82002932
 H -2.11552525 3.44540781 0.56205798
 H -2.43888629 2.44259322 2.01295330
 O 1.97825996 -1.40978125 -2.80491888
 O 1.39960219 0.29518846 -4.67245575
 C 1.30451722 2.58232518 -5.43327101
 C 0.63264489 1.38375223 -5.15029461
 P 1.24737358 -0.15146916 -3.09844640
 H -3.83361180 -2.20624893 -6.26870412
 C -3.10202971 -1.78134442 -5.58141376
 C 0.59646952 3.65373894 -6.00584266
 C -2.42788490 -0.59825631 -5.92495277
 H 1.11195219 4.58863417 -6.22466017
 C -0.75095061 1.21917139 -5.41002969
 C -2.82147518 -2.42576659 -4.35960895
 O 1.73392382 1.18775931 -2.34560921
 C -1.46445369 -0.02972273 -5.05813038
 H -3.33671517 -3.34850009 -4.09288974
 C -1.87633335 -1.87718270 -3.47651044
 C -1.22140150 -0.69231330 -3.83151135
 C -0.77362026 3.51054210 -6.30178455
 O -0.37332186 -0.09030317 -2.87085145
 C -1.43323014 2.30601164 -6.00759850
 H -1.32891580 4.33801707 -6.74231433
 H 1.56228901 -1.22802834 1.43323610
 H 2.15079725 -1.66950477 -0.21724224
 H 3.10422490 0.43211184 -0.95246522
 C -0.64921803 4.32040503 -2.07361564
 C -2.12494107 4.64530933 -2.17875606
 C -2.89557537 4.01469606 -3.17698206

H -2.42797841 3.26871439 -3.81754690
 C -4.25912619 4.32204755 -3.32628355
 H -4.84645239 3.82058251 -4.09687169
 C -4.87056980 5.25033879 -2.46210082
 H -5.93145207 5.48096991 -2.56654594
 C -4.10702547 5.87410113 -1.45479622
 H -4.57778074 6.58869868 -0.77840333
 C -2.73738743 5.57972258 -1.31750618
 H -2.14081870 6.04553941 -0.53499398
 H -0.46637359 3.29453205 -2.43104248
 H -0.05411213 5.00069875 -2.70955107
 H -5.35405162 1.42461509 -2.21867639
 H 2.36695226 2.65204964 -5.20843886
 H -2.49959061 2.20089791 -6.20694358
 H -2.62099997 -0.11181386 -6.88111797
 H -1.65245319 -2.32947701 -2.51500625
 H 2.22800173 5.72390537 -0.86226024

• **β-phosphate 5-10b**

85

C 1.24588822 0.95312557 -0.79668787
 C 0.27467059 1.14859737 0.38067019
 C -0.67028069 2.33112748 0.11249841
 C 0.11727137 3.57574528 -0.34582542
 C 1.05985702 3.20793917 -1.52305984
 C -2.65106602 3.29550201 1.29580395
 C -0.67644437 -0.49490075 1.96964760
 C 1.93695780 4.37692589 -1.96612896
 O 1.95110497 2.14609669 -1.07259596
 O -0.46169673 -0.05936666 0.54865453
 O -1.37989165 2.54564433 1.37905347
 O -0.74491786 4.72301197 -0.66584629
 H 0.89248419 1.38070517 1.26286148
 H -1.38631459 2.02463614 -0.66836787
 H 0.72776612 3.94017543 0.49113262
 H 0.45646424 2.82970067 -2.37301843
 H 2.57832768 4.07490732 -2.80618256
 H 2.57555687 4.69574200 -1.12844688
 C 0.62434931 -0.70757452 2.70487068
 C 1.43509058 -1.82535950 2.41112293
 H 1.08775220 -2.56583220 1.69546434
 C 2.68786543 -1.97499322 3.02665237
 H 3.31199971 -2.83426243 2.77876198
 C 3.14295388 -1.00945984 3.94724016
 H 4.11915136 -1.12360931 4.42044943
 C 2.33948907 0.10662881 4.24909246
 H 2.68953876 0.85832549 4.95780898
 C 1.08655355 0.25826817 3.62510629
 H 0.46271892 1.12914218 3.83753734
 C -3.69189391 2.66962777 0.38012910
 C -4.65853706 3.49807248 -0.22945205
 H -4.61832029 4.57611553 -0.07523248
 C -5.65651657 2.94280945 -1.05150125
 H -6.39373937 3.59599703 -1.51954827
 C -5.68816007 1.55445158 -1.28398981
 H -6.45551624 1.12384447 -1.92878308
 C -4.71710119 0.72482685 -0.68846904
 C -3.72690661 1.27725393 0.14417489
 H -2.95505322 0.64594086 0.58207664
 H -2.45231388 4.33272004 0.99105229
 H -2.99868029 3.29001713 2.34064403
 O 3.52338233 -0.34444316 -2.68004306
 O 1.78334475 -2.07573553 -1.92519166
 C -0.13094092 -2.88843865 -0.72043796
 C 1.24152652 -2.98600613 -0.99109503
 P 2.91347456 -0.96613919 -1.48410276
 H 5.85655501 -6.54415259 -1.46420492
 C 5.43894796 -5.55725135 -1.26541045

C -0.74326799 -3.84701966 0.10409387
C 4.06649798 -5.42060291 -1.00386521
H -1.80898994 -3.77169611 0.31962651
C 2.03947285 -4.02809828 -0.45603096
C 6.27077555 -4.42012457 -1.28470653
O 2.20477639 -0.01076578 -0.37701141
C 3.48793862 -4.15251433 -0.75036229
H 7.33550228 -4.51981495 -1.49385931
C 5.72419145 -3.14970109 -1.03686192
C 4.35265318 -3.03113411 -0.77290375
C 0.02225497 -4.89452044 0.65429470
O 3.86182821 -1.75485677 -0.40986845
C 1.39591868 -4.97684116 0.37739957
H -0.44565282 -5.63339426 1.30442627
H -1.23092788 -1.43372532 1.84771116
H -1.29823913 0.26316110 2.46512651
H 0.69388320 0.60246156 -1.69220749
C -1.61581289 4.57067075 -1.83834528
C -2.67801575 5.65375120 -1.81563278
C -2.69024205 6.67841245 -0.84835632
H -1.89668749 6.71912172 -0.10593430
C -3.72635599 7.63311021 -0.84215403
H -3.72933809 8.41965554 -0.08614802
C -4.75163722 7.57712291 -1.80394516
H -5.55386668 8.31603947 -1.79583693
C -4.73487151 6.56118646 -2.78095252
H -5.52511907 6.50980732 -3.53120987
C -3.70481437 5.60551680 -2.78425750
H -3.70847459 4.80425390 -3.52624701
H -2.11201031 3.58446323 -1.82886560
H -1.00735104 4.63975287 -2.75913274
H -4.72893737 -0.35022886 -0.87508839
H -0.69167165 -2.05321959 -1.12886163
H 1.99875747 -5.77138415 0.81660868
H 3.41658967 -6.29536809 -1.01201524
H 6.33792099 -2.25133371 -1.03703286
H 1.30548091 5.22509738 -2.26683801

• **β -phosphate 5-10b + diol 5-16a complex**

142

C 1.66537861 1.08115438 -1.34260682
C 1.04105116 1.61506354 -0.04370934
C 0.22084416 2.89532934 -0.26999305
C 1.01207168 3.90606115 -1.11980464
C 1.48341179 3.23904844 -2.43528537
C -1.20190985 4.33137244 1.20936193
C 0.31402997 0.33164203 1.94970372
C 2.35235499 4.15840476 -3.29107119
O 2.32919821 2.09236857 -2.08706951
O 0.19057180 0.54227264 0.47354013
O -0.05818936 3.40058938 1.08029391
O 0.25499490 5.14277499 -1.37215247
H 1.86493970 1.84673239 0.64558201
H -0.72418236 2.62710728 -0.76953243
H 1.89000980 4.24790877 -0.56178112
H 0.61090647 2.86290962 -3.00219746
H 2.63908351 3.65465762 -4.22445503
H 3.26381630 4.41722722 -2.73343050
C 1.69039131 -0.13657082 2.36231682
C 2.14856727 -1.41781100 1.98348416
H 1.49754361 -2.07018673 1.40451720
C 3.44126260 -1.84013873 2.33033608
H 3.79209913 -2.82282388 2.01558621
C 4.28751660 -0.99034563 3.07197379
H 5.28987316 -1.32274119 3.34646990
C 3.83740712 0.28703440 3.45578875
H 4.48471444 0.95378417 4.02611733
C 2.54743596 0.71693587 3.08877281

H 2.20950175 1.71896710 3.35772437
C -2.52242609 3.76913939 0.70965074
C -3.49180920 4.64784954 0.17946302
H -3.26638720 5.71092659 0.09887782
C -4.73289637 4.15546151 -0.26488971
H -5.47022027 4.84524732 -0.67724046
C -5.01124007 2.77678569 -0.19380334
H -5.96978097 2.39252530 -0.54529226
C -4.04180567 1.89431876 0.32330802
C -2.80517187 2.38739324 0.77665406
H -2.03837240 1.70737833 1.14246201
H -0.97690259 5.27616085 0.69536852
H -1.23613229 4.51227068 2.29448989
O 4.12498521 -0.19548886 -3.13298054
O 2.44472196 -2.00249510 -2.38715201
C 0.53687194 -2.75820428 -1.12516047
C 1.91077110 -2.85448158 -1.38188817
P 3.46993047 -0.80943747 -1.94691608
H 6.74720169 -6.15896949 -1.38144374
C 6.26112320 -5.18916427 -1.27341133
C -0.05858950 -3.65041696 -0.21755134
C 4.86817736 -5.12730550 -1.09585536
H -1.12527244 -3.57654361 -0.00828976
C 2.73656275 -3.81096104 -0.74031251
C 7.02607336 -4.00596747 -1.32258796
O 2.66482844 0.15925671 -0.92864937
C 4.20158318 -3.88423507 -0.96808265
H 8.10448184 -4.03880947 -1.47042786
C 6.39199892 -2.75902075 -1.19148687
C 5.00461393 -2.72108813 -1.02481679
C 0.72810373 -4.62890913 0.42197411
O 4.41038710 -1.45371288 -0.79028028
C 2.10656335 -4.70137534 0.16348931
H 0.27285573 -5.31858311 1.13220042
H -0.44996371 -0.43370594 2.14307354
H 0.04915765 1.27010743 2.45756722
H 0.90431380 0.58008069 -1.96963155
C -0.91137226 5.02273684 -2.25549685
C -1.73760133 6.29205791 -2.17395378
C -1.30270228 7.43126810 -1.46868873
H -0.33582514 7.41513800 -0.97499924
C -2.11516850 8.57983966 -1.40648734
H -1.76581004 9.45468240 -0.85656308
C -3.36657850 8.60137912 -2.04911952
H -3.99525233 9.49088937 -1.99854268
C -3.80317942 7.46481058 -2.76021617
H -4.77260299 7.47020447 -3.26002212
C -2.99322843 6.31824061 -2.82049837
H -3.34150180 5.43269438 -3.35603118
H -1.53670030 4.16338674 -1.95621572
H -0.56720453 4.85509344 -3.29284833
H -4.24610670 0.82361786 0.36881383
H -0.04538589 -1.98784152 -1.62508013
H 2.72580886 -5.43528151 0.67859475
H 4.27488021 -6.04147440 -1.07338460
H 6.94738938 -1.82559077 -1.21447154
H 1.80555450 5.08318248 -3.51862544
H 5.11161949 1.40292828 -2.62914931
O 5.46404926 2.18735274 -2.16452356
H 1.72685812 7.00745829 -1.81253933
H 3.28785007 7.28742092 -2.62723816
H 1.99199126 8.52009761 -2.73099742
O 3.85835801 2.92695275 0.05899186
C 2.46931361 7.77460386 -2.07254593
H 3.59648562 2.71592279 -0.86098831
H 5.28979951 0.86260355 -0.55418019
C 5.79611100 1.79589222 -0.84261162
H 1.63070389 6.50252389 0.48878178
H 10.39096155 -4.33210443 -4.05182306
H 5.70155164 3.87263040 -0.20620287

H 8.76033151 -2.66132685 -4.95729350
C 5.26997363 2.90473295 0.11067420
C 10.14069995 -3.44163886 -3.47364639
C 9.22755591 -2.49942747 -3.98560402
O 7.71196201 0.38041858 -1.40191774
H 2.45503750 4.67462637 1.93607702
H 11.43163980 -3.95826124 -1.80637407
C 2.69250102 6.45312869 0.72570651
C 10.72631257 -3.23090655 -2.21059287
H 1.07962688 8.59781082 0.24159464
C 8.90673012 -1.34990971 -3.24313483
C 7.29156407 1.58112615 -0.64336318
H 7.86563367 2.45517124 -1.00080799
H 8.18275584 -0.63099266 -3.62253257
C 3.02966135 8.47603758 -0.79840498
C 3.15317391 5.41453982 1.54867853
H 1.45742950 10.00036545 -0.79846124
C 10.40435133 -2.08307591 -1.46133828
C 9.49266887 -1.13748265 -1.97568424
H 10.84344543 -1.91973439 -0.47963815
C 3.58433531 7.39431638 0.15287044
C 1.88558301 9.26599171 -0.09599523
H 3.65460363 10.25691057 -1.88425010
H 4.91506746 8.99737447 -1.80470304
H 9.69311258 1.01148822 -1.54516423
C 9.14077162 0.11280354 -1.19848541
C 4.11271037 9.49355491 -1.23607923
C 5.69785945 2.60591933 1.55205556
H 5.25489424 1.65427165 1.88424675
C 4.53126464 5.29646627 1.81600159
C 4.95909680 7.26397409 0.44684604
H 7.04082080 0.43695283 1.17462644
C 7.59771661 1.33252432 0.84590372
S 5.14167171 3.88395223 2.86295728
H 2.27431658 9.80200836 0.78474721
C 5.43415071 6.22484473 1.27296403
O 7.17468912 2.50649988 1.62516031
H 5.67740156 7.96622520 0.02779606
H 4.55968312 9.99875080 -0.36468976
O 9.45547176 -0.08970621 0.21323164
H 6.49910230 6.13176235 1.48358322
C 9.09698396 1.09354038 1.02964061
H 9.66717253 1.97831533 0.69340412
H 9.36042927 0.84053592 2.06196900

• **TS_p**

94

C 3.294382 2.605560 -1.413501
C 2.332059 2.028264 -0.405132
C 0.977666 2.753482 -0.373544
C 1.203892 4.278132 -0.360361
C 2.220642 4.785895 -1.411451
C -1.141337 2.368923 0.872877
C 2.291090 -0.190608 0.564563
C 2.758799 6.175823 -1.102171
O 3.425629 3.879730 -1.584264
O 2.169087 0.653090 -0.645995
O 0.343221 2.342280 0.882691
O -0.051078 5.031102 -0.531857
H 2.835035 2.215762 0.563351
H 0.382372 2.417338 -1.233216
H 1.540956 4.543702 0.650878
H 1.776736 4.730620 -2.413444
H 3.424627 6.528229 -1.901729
H 3.310215 6.168114 -0.150024
C 2.041301 -1.631531 0.187065
C 1.916821 -2.583137 1.222764
H 1.963263 -2.254476 2.262988

C 1.761681 -3.947364 0.924896
H 1.685358 -4.673606 1.734684
C 1.716206 -4.375360 -0.417238
H 1.604042 -5.434453 -0.652474
C 1.817599 -3.427798 -1.452925
H 1.785502 -3.752106 -2.494094
C 1.981921 -2.061049 -1.155311
H 2.077026 -1.330093 -1.953022
C -1.763654 1.333747 -0.046752
C -1.216509 0.037716 -0.156307
H -0.316900 -0.212638 0.396564
C -1.813862 -0.921518 -0.991648
H -1.367883 -1.912686 -1.075088
C -2.974451 -0.594287 -1.724549
H -3.440685 -1.337349 -2.372844
C -3.527752 0.696603 -1.616004
C -2.923861 1.657276 -0.783865
H -3.352991 2.655041 -0.705876
H -1.485935 3.379843 0.614987
H -1.388362 2.165169 1.925900
H 1.561752 0.161390 1.312159
H 3.306048 -0.063389 0.968826
C -0.675902 4.918677 -1.875455
C -2.185128 4.936498 -1.757341
C -2.948312 4.410110 -2.821520
H -2.440848 3.976004 -3.685082
C -4.352266 4.404544 -2.753775
H -4.932927 3.986794 -3.576755
C -5.005205 4.916579 -1.614784
H -6.093838 4.901154 -1.555243
C -4.246162 5.444602 -0.553057
H -4.746021 5.840377 0.331735
C -2.840173 5.463046 -0.625610
H -2.246373 5.862536 0.194420
H -0.361686 3.987491 -2.372705
H -0.316462 5.766396 -2.486674
H -4.420924 0.960778 -2.183523
H 3.064958 -0.541451 -4.344165
N 3.066537 0.272481 -3.741983
Cl 1.274214 -0.475201 -6.043927
Cl -0.504134 0.297286 -3.803348
C 2.071921 1.147963 -3.822515
C 0.883572 0.829611 -4.825108
O 1.928408 2.190207 -3.154096
Cl 0.458867 2.339418 -5.731081
H 4.026902 1.995393 -1.919616
H 1.906099 6.863671 -1.005833
H 5.365693 -5.258274 -0.292382
H 7.793643 -5.487373 0.313305
C 5.953988 -4.379879 -0.025501
H 4.293807 -2.997925 -0.278918
C 7.315126 -4.507429 0.316729
C 5.343103 -3.113868 -0.024453
C 8.063442 -3.364429 0.647340
C 6.097074 -1.982543 0.322442
H 9.124051 -3.451900 0.886030
O 5.129557 0.007239 -2.052622
H 3.819437 0.305943 -2.998505
C 7.473629 -2.076635 0.652555
O 5.439238 -0.745898 0.451890
P 5.674051 0.438122 -0.702135
C 8.265701 -0.875792 1.007944
O 7.330727 0.401772 -0.859169
H 9.293115 -1.835463 2.643440
O 5.198757 1.740559 -0.075582
C 9.192971 -0.909775 2.076326
C 8.134386 0.341126 0.289092
C 9.951072 0.220722 2.422957
C 8.879019 1.480656 0.635717
H 10.653292 0.169584 3.255737

H 8.734517 2.390284 0.055724
C 9.789381 1.421815 1.703755
H 10.367312 2.306489 1.972940

• **TS_{C2}**

142

C 1.332358 1.509819 -0.840632
C 0.601042 2.161986 0.302950
C -0.170524 3.439121 -0.080132
C 0.621945 4.198476 -1.162165
C 0.751948 3.309537 -2.420664
C -1.386585 5.195317 1.237825
C -0.188008 0.640293 2.133678
C 1.761674 3.836417 -3.433779
O 1.216489 1.902147 -2.063718
O -0.364377 1.131941 0.716366
O -0.322869 4.166079 1.175910
O 0.053469 5.496922 -1.543986
H 1.318789 2.391098 1.104914
H -1.155916 3.134406 -0.467253
H 1.618728 4.451031 -0.785147
H -0.232496 3.128484 -2.874514
H 1.823217 3.175453 -4.308966
H 2.753860 3.912852 -2.967358
C 1.055608 -0.178597 2.365214
C 1.182212 -1.474406 1.816257
H 0.376811 -1.884358 1.206835
C 2.356572 -2.217873 2.010841
H 2.457980 -3.199177 1.552679
C 3.416009 -1.675528 2.763097
H 4.331282 -2.251776 2.900627
C 3.298236 -0.388291 3.324147
H 4.113885 0.032991 3.913780
C 2.121601 0.359395 3.121516
H 2.024703 1.356246 3.554592
C -2.781970 4.673495 0.941483
C -3.755998 5.568963 0.446929
H -3.484263 6.606300 0.252074
C -5.065539 5.124938 0.190227
H -5.807100 5.826104 -0.194205
C -5.409751 3.777726 0.413669
H -6.422081 3.428955 0.206847
C -4.440085 2.879874 0.901875
C -3.134049 3.324765 1.173113
H -2.377146 2.628369 1.531082
H -1.134795 6.032534 0.571201
H -1.310658 5.538242 2.280712
O 4.061933 -0.866327 -2.998674
O 2.836515 -2.953088 -2.205524
C 1.310171 -4.182190 -0.814215
C 2.624645 -3.958747 -1.258112
P 3.606230 -1.552225 -1.722734
H 7.912371 -6.216165 -2.314255
C 7.281387 -5.379583 -2.011082
C 1.037563 -5.244326 0.064535
C 5.940413 -5.608750 -1.657827
H 0.017959 -5.414039 0.412517
C 3.697098 -4.787615 -0.837046
C 7.810018 -4.073575 -1.965840
O 2.814977 -0.796925 -0.671909
C 5.091753 -4.541678 -1.277553
H 8.853707 -3.886837 -2.215725
C 6.989447 -3.000676 -1.579625
C 5.642240 -3.235152 -1.267396
C 2.084659 -6.084832 0.493176
O 4.870341 -2.161699 -0.805286
C 3.395820 -5.854336 0.043078
H 1.881847 -6.907634 1.179032

H -1.103692 0.049988 2.270217
H -0.204985 1.526947 2.787272
H 1.795387 0.490450 -0.754749
C -1.276605 5.463312 -2.186348
C -1.953925 6.812093 -2.049970
C -1.338184 7.915367 -1.427737
H -0.319673 7.821158 -1.062524
C -2.040500 9.128439 -1.282904
H -1.554787 9.976497 -0.798606
C -3.358030 9.247509 -1.760683
H -3.901720 10.185629 -1.644514
C -3.972233 8.147427 -2.393742
H -4.993163 8.231237 -2.767652
C -3.273286 6.937883 -2.537593
H -3.759565 6.080834 -3.007547
H -1.908872 4.690999 -1.716811
H -1.147755 5.206149 -3.253671
H -4.700849 1.834319 1.070885
H 0.524105 -3.518662 -1.170709
H 4.216371 -6.485165 0.386190
H 5.526706 -6.617452 -1.690413
H 7.370506 -1.989574 -1.474300
H 1.445531 4.840604 -3.751501
H 4.706908 0.580661 -2.520488
O 4.968318 1.516156 -2.253146
H 1.755386 9.071338 -0.771767
H 1.756563 7.767119 -1.996984
H 2.294714 9.418618 -2.437444
O 3.310234 2.611197 -0.607136
C 2.294784 8.659295 -1.640425
H 3.491335 2.274607 -1.530760
H 4.994343 0.425178 -0.491800
C 5.358034 1.381416 -0.895076
H 1.652250 7.003143 0.099032
H 11.741041 -3.235385 -3.730188
H 5.143618 3.481335 -0.313689
H 9.875216 -1.953715 -4.801899
C 4.653150 2.518071 -0.104617
C 11.195232 -2.482400 -3.160083
C 10.149327 -1.758371 -3.765146
O 7.613726 0.458039 -1.305742
H 1.781898 5.097394 1.644005
H 12.332333 -2.798179 -1.338630
C 2.634450 6.631310 0.378327
C 11.529170 -2.234750 -1.815215
H 4.006449 9.935698 0.164303
C 9.445184 -0.787991 -3.031842
C 6.846652 1.490862 -0.597275
H 7.242061 2.487731 -0.871677
H 8.619225 -0.243193 -3.485228
C 3.752317 8.285127 -1.267838
C 2.699780 5.542770 1.265875
H 4.465870 10.341567 -1.519125
C 10.826294 -1.264890 -1.076541
C 9.780631 -0.538694 -1.683162
H 11.071705 -1.075753 -0.033888
C 3.801410 7.178299 -0.196901
C 4.489504 9.552711 -0.748831
H 4.427136 8.561497 -3.334965
H 3.956123 6.877127 -2.949204
H 9.376543 1.557622 -1.163691
C 9.030733 0.529258 -0.921063
C 4.460045 7.777169 -2.560479
C 4.808367 2.229151 1.393741
H 4.410329 1.238723 1.661378
C 3.944159 4.988275 1.597799
C 5.049598 6.645348 0.209782
H 6.621163 0.263758 1.169312
C 7.012532 1.266266 0.927562
S 3.965490 3.430976 2.605004

H 5.541975 9.327071 -0.515654
C 5.131474 5.562657 1.102708
O 6.266009 2.296488 1.679330
H 5.969017 7.065415 -0.198511
H 5.514333 7.527800 -2.365751
O 9.209995 0.329687 0.514922
H 6.093533 5.130539 1.375654
C 8.491869 1.352593 1.303232
H 8.880030 2.361166 1.071204
H 8.672693 1.107049 2.354860

• **TS_{C3}**

142

C 1.797558 1.701300 -0.524595
C 1.113567 2.141332 0.737966
C 0.335614 3.456464 0.561185
C 1.278994 4.434962 -0.169549
C 1.517962 3.899770 -1.601447
C -1.081468 4.857655 2.084328
C 0.026947 0.803907 2.545508
C 2.626630 4.612193 -2.359681
O 1.897489 2.415454 -1.583874
O 0.244184 1.023468 1.078833
O -0.018190 3.843347 1.917362
O 0.790213 5.811287 -0.230512
H 1.886683 2.307366 1.507791
H -0.571523 3.273355 -0.037706
H 2.229207 4.511646 0.373927
H 0.570508 3.879442 -2.158350
H 2.757982 4.181457 -3.361888
H 3.566556 4.530670 -1.797232
C 1.305007 0.644694 3.332097
C 2.334999 -0.193186 2.850843
H 2.245914 -0.660359 1.872286
C 3.501423 -0.380682 3.611677
H 4.306959 -0.992511 3.224095
C 3.628033 0.231686 4.874720
H 4.533087 0.072066 5.460932
C 2.607268 1.075062 5.355022
H 2.712268 1.568030 6.322468
C 1.455815 1.298254 4.575401
H 0.670899 1.971030 4.926200
C -2.425477 4.459599 1.496404
C -3.355894 5.481296 1.203835
H -3.078513 6.522082 1.369717
C -4.624649 5.164724 0.687723
H -5.334334 5.963614 0.469234
C -4.973164 3.821894 0.445339
H -5.954035 3.575229 0.037731
C -4.047558 2.799652 0.729524
C -2.782659 3.113925 1.259456
H -2.064476 2.320702 1.461769
H -0.746028 5.818768 1.669525
H -1.137060 4.957445 3.177912
O 5.344552 -1.233376 -1.557591
O 3.054657 -1.198099 -2.668995
C 0.707212 -0.781127 -2.956773
C 1.761293 -1.703679 -2.835562
P 3.880899 -1.453023 -1.229508
H 3.815680 -6.878738 -4.571444
C 3.771084 -6.076890 -3.834224
C -0.597209 -1.229919 -3.224046
C 2.725452 -5.139735 -3.881938
H -1.411882 -0.510252 -3.314279
C 1.538161 -3.097444 -3.002427
C 4.769663 -5.967984 -2.845890
O 3.237437 -0.682416 -0.096630
C 2.646875 -4.080267 -2.946333

H 5.589579 -6.685736 -2.810781
C 4.712046 -4.927975 -1.902051
C 3.656826 -4.003349 -1.955514
C -0.844925 -2.608143 -3.377804
O 3.539725 -3.057281 -0.928398
C 0.214872 -3.523348 -3.271410
H -1.855270 -2.966730 -3.574835
H -0.563259 -0.122801 2.539034
H -0.575924 1.631746 2.943304
H 2.081040 0.635409 -0.622270
C -0.444797 6.045143 -1.009361
C -0.961237 7.432853 -0.687684
C -0.123650 8.429210 -0.142354
H 0.915673 8.194936 0.075230
C -0.641593 9.707830 0.139763
H 0.009924 10.468081 0.572256
C -1.990023 10.006086 -0.134252
H -2.387882 10.997565 0.084669
C -2.824229 9.017494 -0.692812
H -3.870132 9.240184 -0.907185
C -2.312482 7.736695 -0.966242
H -2.965519 6.964271 -1.375208
H -1.207444 5.290996 -0.752856
H -0.216369 5.956525 -2.087893
H -4.307913 1.757714 0.539867
H 0.934835 0.279895 -2.870445
H 0.029672 -4.592013 -3.382119
H 1.964914 -5.203759 -4.660827
H 5.465614 -4.820403 -1.124084
H 2.358226 5.674251 -2.451648
H 4.380320 1.920150 -0.759652
O 3.973171 2.487742 -0.062428
H 2.615647 -3.887827 2.071183
H 2.379977 -3.065920 3.637244
H 1.841982 -4.764237 3.425913
O 6.129215 1.014337 -0.558552
C 2.620783 -4.029227 3.162438
H 5.879762 0.089002 -0.882274
H 5.744095 3.309078 0.567213
C 5.048053 2.512240 0.892596
H 4.653516 -3.743220 1.130867
H 1.315922 9.376931 4.018818
H 5.164651 0.348859 1.176880
H 0.541460 7.641083 2.382785
C 5.815319 1.157279 0.809537
C 1.807027 8.403473 3.975894
C 1.368985 7.428664 3.059102
O 3.988796 4.166374 2.388848
H 6.290843 -2.063882 0.369061
H 3.228313 8.860489 5.551675
C 5.264370 -3.233864 1.872101
C 2.881116 8.112062 4.838019
H 4.333612 -5.830315 1.899086
C 2.000805 6.174829 3.005366
C 4.627741 2.825100 2.312213
H 3.941198 2.070043 2.725819
H 1.654155 5.420554 2.310520
C 4.008985 -4.539249 3.658316
C 6.186441 -2.271359 1.431421
H 3.532258 -6.642812 3.273595
C 3.514716 6.856469 4.786538
C 3.079207 5.880497 3.864721
H 4.344904 6.631474 5.451429
C 5.089331 -3.519825 3.246265
C 4.313867 -5.915775 2.996426
H 3.151829 -5.471734 5.430000
H 3.674543 -3.783882 5.693114
H 3.052308 3.709882 4.199812
C 3.713785 4.508728 3.809756
C 3.932672 -4.731910 5.193534

C 7.061895 1.260150 1.716209
H 7.737701 2.050221 1.341752
C 6.945201 -1.556002 2.376198
C 5.887962 -2.813244 4.174712
H 6.580184 3.659586 2.719866
C 5.935955 2.869277 3.147196
S 8.166078 -0.274970 1.805143
H 5.290011 -6.300098 3.334034
C 6.803043 -1.829762 3.747798

O 6.623623 1.575172 3.099865
H 5.783236 -3.000164 5.242073
H 4.890208 -5.096105 5.600200
O 4.932758 4.521855 4.603824
H 7.388306 -1.266383 4.472581
C 5.621099 3.214746 4.599149
H 4.980621 2.440260 5.047515
H 6.531918 3.351826 5.191368

References

- [1] Y. Shao, Z. Gan, E. Epifanovsky, A. T. B. Gilbert, M. Wormit, J. Kussmann, A. W. Lange, A. Behn, J. Deng, X. Feng, et al., *Mol. Phys.* **2015**, *113*, 184–215.
- [2] A. D. Becke, *J. Chem. Phys.* **1997**, *107*, 8554–8560.
- [3] S. Grimme, *J. Comput. Chem.* **2006**, *27*, 1787–1799.
- [4] P. C. Hariharan, J. A. Pople, *Theor. Chim. Acta* **1973**, *28*, 213–222.
- [5] M. M. Francl, W. J. Pietro, W. J. Hehre, J. S. Binkley, M. S. Gordon, D. J. DeFrees, J. A. Pople, *J. Chem. Phys.* **1982**, *77*, 3654–3665.
- [6] Discovery Studio 4.1 Visualizer: Accelrys Software Inc. San Diego, USA, **2015**.
- [7] P. M. Zimmerman, *J. Chem. Phys.* **2013**, *138*, 184102.
- [8] P. M. Zimmerman, *J. Comput. Chem.* **2013**, *34*, 1385–1392.
- [9] P. M. Zimmerman, *J. Comput. Chem.* **2015**, *36*, 601–611.
- [10] P. M. Zimmerman, *J. Chem. Theory Comput.* **2013**, *9*, 3043–3050.
- [11] A. V. Marenich, C. J. Cramer, D. G. Truhlar, *J. Phys. Chem. B* **2009**, *113*, 6378–6396.
- [12] J. Da Chai, M. Head-Gordon, *J. Chem. Phys.* **2008**, *128*, 084106.
- [13] N. M. O’Boyle, M. Banck, C. A. James, C. Morley, T. Vandermeersch, G. R. Hutchison, *J. Cheminform.* **2011**, *3*, 33.

APPENDIX G

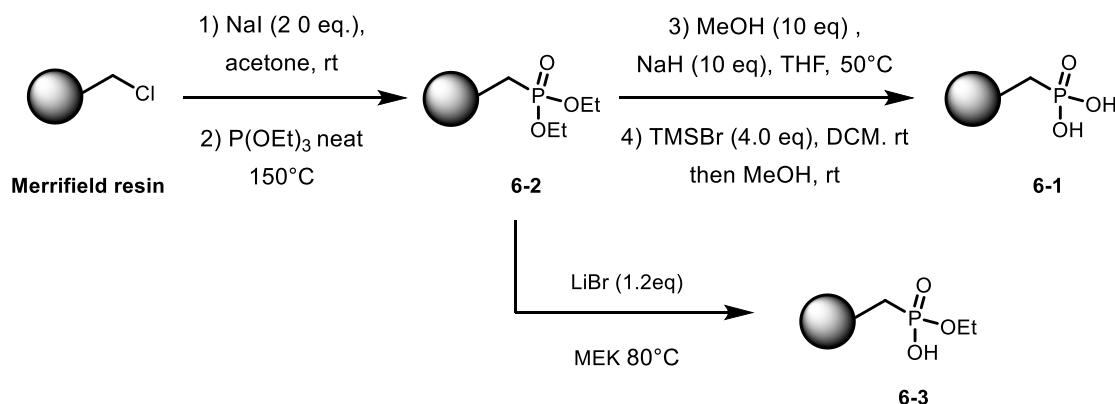
Experimental Information for Chapter 6

General information

Unless otherwise stated, all reagents were purchased from commercial suppliers and used without further purification. All reactions were carried out under an atmosphere of nitrogen in flame- or oven-dried glassware with magnetic stirring, unless otherwise noted. Air-sensitive reagents and solutions were transferred via syringe or cannula and were introduced to the apparatus through rubber septa. Reactions were cooled via external cooling baths: ice water (0 °C), dry ice-acetone (-78 °C), or Neslab CB 80 immersion cooler (-20 to -60 °C). Heating was achieved by the use of a silicone bath with heating controlled by an electronic contact thermometer. Deionized water was used in the preparation of all aqueous solutions and for all aqueous extractions. Solvents used for extraction and column chromatography were ACS or HPLC grade. Tetrahydrofuran (THF), dichloromethane (DCM), toluene and diethyl ether (Et₂O) were filtered through a column (Innovative Technologies) of activated alumina under nitrogen atmosphere. Reactions were monitored by thin layer chromatography on silica gel precoated glass plates (0.25 mm, SiliCycle, SiliaPlate). Visualization was accomplished by irradiation with UV light at 254 nm or by staining with potassium permanganate (KMnO₄) or cerium ammonium molybdenate (CAM). Purification of the reactions mixtures was performed by flash chromatography using SiliCycle SiliaFlash P60 (230-400 mesh) silica gel. Powdered 4 Å molecular sieves were pre-activated before the use. Proton, carbon, and deuterium NMR spectra were recorded on Varian VNMRS-700 (700 MHz),

Varian VNMRS-500 (500 MHz), Varian INOVA 500 (500 MHz) or Varian MR400 (400 MHz). ^1H NMR chemical shifts (δ) are reported in parts per million (ppm) relative to tetramethylsilane with the solvent resonance employed as the internal standard (C_6D_6 , δ 7.16 ppm; CD_2Cl_2 δ 5.32 ppm; CDCl_3 , δ 7.24 ppm). Data are reported as (br = broad, s = singlet, d = doublet, t = triplet, q = quartet, qn = quintet, sext S4 = sextet, m = multiplet; coupling constant(s) in Hz; integration). Slight shape deformation of the peaks in some cases due to weak coupling (e.g. aromatic protons) is not explicitly mentioned. The diastereomeric ratio of product mixtures were analyzed using a Shimadzu RP-HPLC with Waters Nova-Pak C18 column (60Å, 4 μm , 3.9 x 150mm).

Preparation of phosphonic acid-functionalized resin



Merrifield resin (200-400mesh, 1.3 mmol/g, 2.0g), and NaI (780mg, 2.0equiv), were put in in a flask. N_2 -sparged acetone (5mL) was then added to the flask, and the suspension was stirred in the dark at rt. After 15h, the resin was filtered and washed with: 1) acetone; 2) water; 3) acetone; and finally, 4) DCM, and was then dried *in vacuo*. The iodinated resin was then put in a flask and $\text{P}(\text{OEt})_3$ (9.0mL, 20equiv) was added. The suspension was heated at 150°C for 2d. Following this, the resin was filtered and then washed with: 1) DCM; 2) acetone; 3) water; 4) acetone; and finally, 5) THF. In another flask, NaH (1.0g of 60% dispersion, washed with hexanes prior to use, 10equiv)

was suspended in THF (25mL), and MeOH (1mL, 10equiv) was added. This suspension was stirred at rt for 30min, and then added to the diethyl phosphonate-functionalized resin. The suspension was stirred at 50° for 16h, then the solid was filtered and washed with: 1) MeOH; 2) acetone; 3) water; 4) acetone; and finally, 5) DCM, and was then dried *in vacuo*. The capped diethyl phosphonate-functionalized resin could now be treated either with LiBr (1.2equiv) in MEK for 16h at 80°C, then filtered and washed with 1) 1M HCl_(aq); 2) 1:1 THF: 1M HCl_(aq); 3) THF; and finally, 4) DCM to give the solid-supported ethyl hydrogen benzylphosphonate **6-3**; or, continuing this example, it could be suspended in DCM (20mL), then treated with TMSBr (1.4mL, 4.0equiv) at rt for 3h, then treated with MeOH (20mL) and stirred at rt for 16h. The phosphonate diacid-functionalized resin **6-1** is then filtered and washed with 1) MeOH; 2) acetone; 3) water; 4) acetone; and finally, 5) DCM, before being dried *in vacuo* (1.904g, light beige solid).

Each phosphorous-containing synthesized resin was characterized by NMR by putting a substantial amount of resin (30-50mg) in an NMR tube, and then swelling the resin with CDCl₃ for 15min before acquiring the spectra.

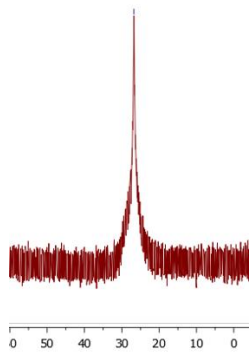
³¹P Gel NMR

6-1: 29.9 ppm

6-2: 26.7 ppm

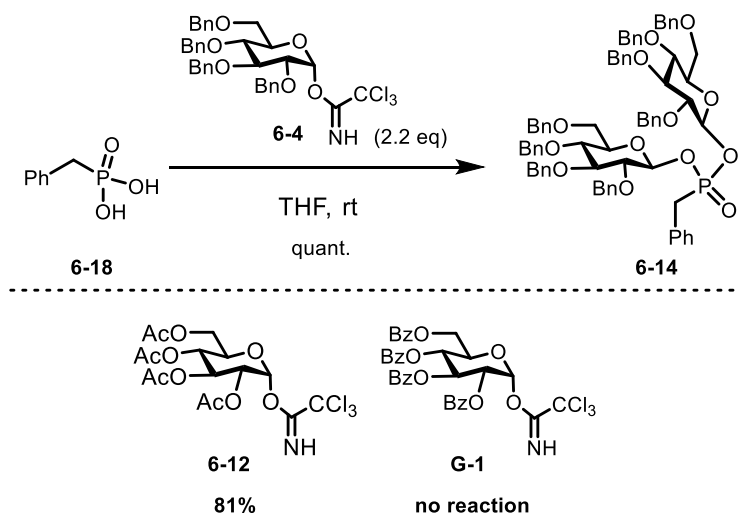
6-3: 28.5 ppm

Example ^{31}P Gel NMR spectra for 6-2:



Preparation of soluble glycosyl phosphonates

A. Using trichloroacetimidate donors:

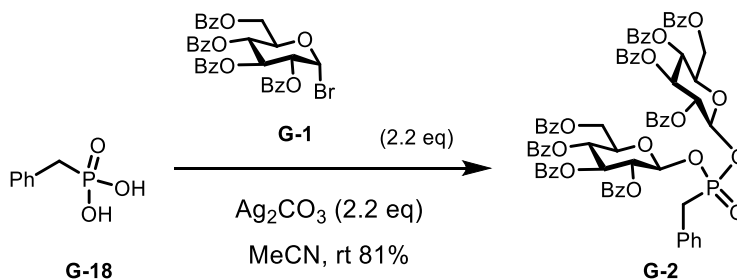


Benzyl phosphonic diacid **6-18** (20mg, 0.12mmol) and trichloroacetimidate donor **6-4** (175mg, 2.2 equiv) were stirred in THF (0.6mL) at rt for 12h. Then the mixture was purified using a short silica column, using 0.5:9.5 EtOAc:Hexanes to elute residual trichloroacetimidate and then 1:1 to give the product **6-14** (132mg, quant.).

$^{31}\text{P-NMR}$: 25.9 ppm

This protocol also works for peracetylated trichloroacetimidate **6-12** (81% yield, $^{31}\text{P-NMR}$: 26.7ppm), but does not proceed with perbenzoylated trichloroacetimidate **G-1**.

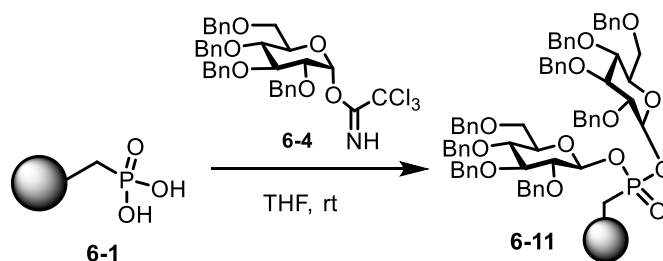
B. Using bromide donors:



Benzyl phosphonic acid (8mg) **6-18**, perbenzoylated bromide donor **G-1** (67mg, 2.2equiv), and Ag_2CO_3 (28.2mg, 2.2equiv) were stirred in MeCN (0.5mL) for 12h at rt. The product was directly purified using a short column and eluting first with 1:9 EtOAc/Hexanes and then with 3:7 EtOAc:Hexanes to afford the product **G-2** (50mg, 81% yield).

$^{31}\text{P-NMR}$: 27.7 ppm

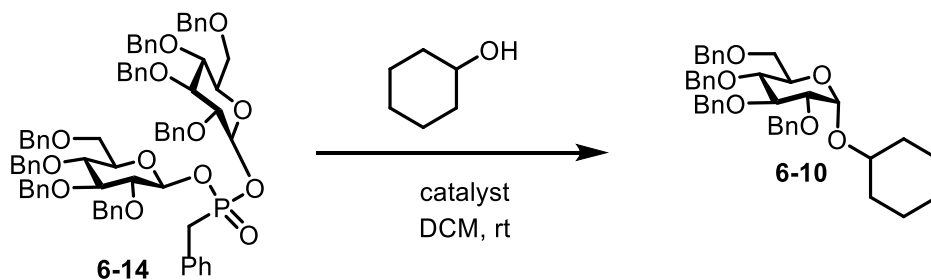
Preparation of solid-supported glycosyl phosphonates



Phosphonic diacid-containing resin **6-1** (200mg) was stirred with trichloroacetimidate donor **6-4** (198mg) in DCM (2mL) at rt. After 30min, the resin was filtered and washed with DCM, to give 324mg of glycosyl phosphonate-functionalized resin **6-11**. The loading could also be

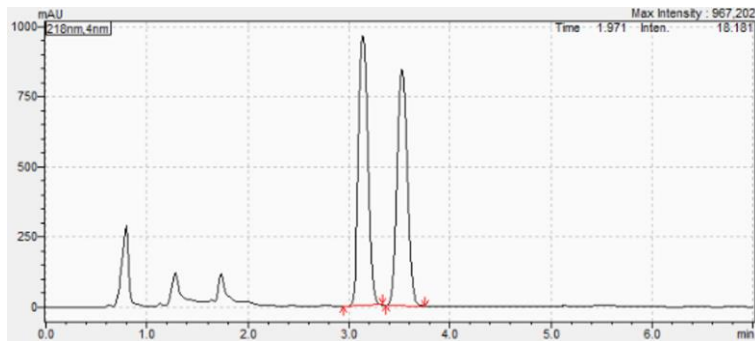
performed in other solvents besides DCM, such as THF and PhMe, with no difference in the outcome, although the reaction did not work in more polar solvents such as MeCN.

General procedure for glycosylation with soluble glucosyl phosphonates



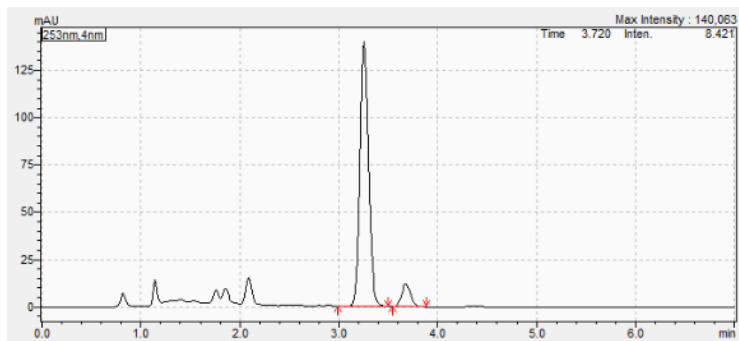
Stirred glucosyl benzylphosphonate **6-14** and cyclohexanol in DCM for 15min, then added catalyst (0.5equiv). After 1-2h, the mixture was filtered through a silica plug, eluting with 1:3 EtOAc:Hexanes, then concentrated, redissolved in 1mL MeCN, and analyzed by RP-HPLC (Nova-Pak C18, 95% MeCN, $t_R=3.1$ min for α and, $t_R=3.5$ min for β). Examples of HPLC traces:

Unselective glycosylation (Using Fe(III) triflate): 1.1 α : β



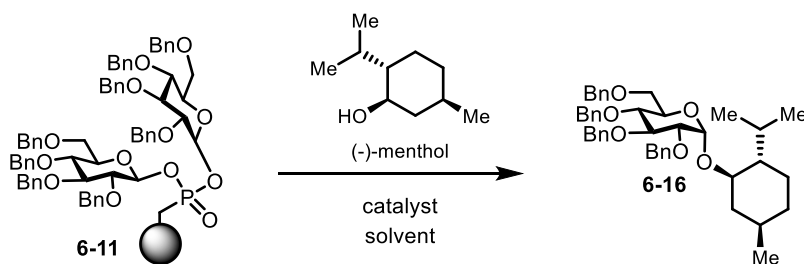
Retention Time [min]	% Area
3.142	52.1
3.526	47.9

α -selective glycosylation (Using Fe(III) chloride): 10.6:1 α : β



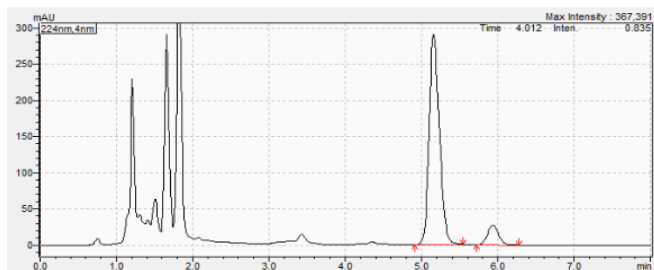
Retention Time [min]	% Area
3.257	91.4
3.684	8.6

General procedure for glycosylation with solid-supported phosphonates



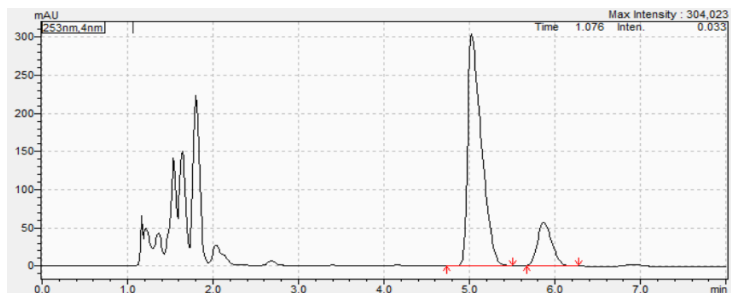
Stirred glucosyl phosphonate-containing resin **6-11** and (-)-menthol in solvent for 15min, then added catalyst (0.2-0.5 equiv calculated from amount of sugar that was loaded on the resin). After 1-2h, the mixture was filtered through a silica plug, eluting with 1:3 EtOAc:Hexanes, then concentrated, redissolved in 1mL MeCN and analyzed by RP-HPLC (Nova-Pak C18, 97% MeCN t_R =5.2 min for α and , t_R =6.0 min for β). Examples of HPLC traces:

α -selective glycosylation (Using Fe(III) chloride and excess acceptor) in 1,4-dioxane: 10.0:1 α : β



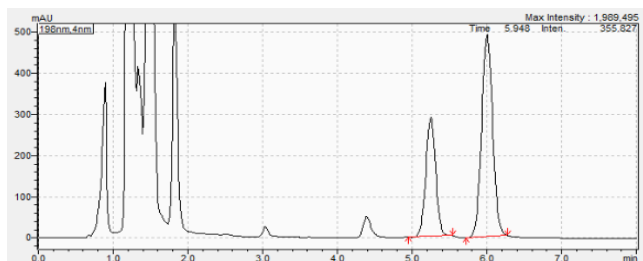
Retention Time [min]	% Area
5.159	90.9
5.937	9.1

α -selective glycosylation (Using Fe(III) chloride and limiting acceptor) in PhMe: 5.1:1 α : β



Retention Time [min]	% Area
5.033	83.6
5.872	16.4

β -selective glycosylation (Using Fe(III) chloride) in MeCN: 1:1.9 α : β



Retention Time [min]	% Area
5.248	34.4
6.002	65.6

APPENDIX H

Experimental Information for Chapter 7

Computational Studies

All quantum chemical calculations were performed using the Q-Chem 4.3 package.^[1] Geometry optimizations were evaluated using the B97-D density functional^[2,3] using the double- ζ - quality basis set with polarization functions on all atoms, 6-31G**.^[4,5] Pictorial representations of important stationary points were generated in Discovery Studio 4.1 Visualizer.^[6]

For the growing string reaction path optimizations, between 7-15 nodes were used, including the end points. In the initial phase, termed growth phase, new nodes were added when the perpendicular gradient magnitude on the frontier node was less than 0.10 Hartree/Å for double-ended strings, or when the RMS gradient was less than 0.005 Hartree/Å for single-ended strings. Additionally, an initial maximum optimization step size of 0.1 Å-radians was used. When the total perpendicular gradient magnitude over all nodes, F , reached a value of less than 0.3, the climbing image search was initiated. When $F < 0.1$, or when the node of highest energy had a RMS gradient below double the nodal convergence criterion and $F < 0.2$, the exact transition state search was initiated. The string is considered fully converged when an RMS gradient < 0.0005 Hartree/Å was obtained for the node representing the transition state. Further detail regarding the growing string implementation developed in the Zimmerman group can be found in the references.^[7-10]

The electronic Gibbs free energy values of all stationary points were computed through solvent corrected (dichloromethane) single point energies using the SMD model.^[11] For these calculations the ω B97X-D3 exchange functional^[12] was employed with a 6-31G** basis set. The final Gibbs free energy values were obtained by correcting the electronic free energy with the enthalpic and entropic contributions from vibrations, rotations, and translations at 298.15 K. These frequency computations were performed using the B97-D functional and 6-31G** basis set. For the enthalpic and entropic corrections to the free energies from the harmonic oscillator approximation, all frequencies below 50 cm⁻¹ were treated as if they were 50 cm⁻¹.

A model system consisting of biphenyl hydrogen phosphate (**BPA**) and truncated mupirocin **7-6** was utilized to explore various pathways leading to the intramolecular epoxide opening to either the *exo*-product **7-7** or the *endo*-product **7-8**. Single-ended growing string calculations were performed on optimized **7-6** (phosphate intermediate pathway), **7-7** (concerted *exo*-pathway), and **7-8** (concerted *endo*-pathway) as the fixed nodes with varying driving coordinates according to the pathways explored. To account for variation in conformations and binding complexes, the most stable conformations were sampled for the growing string calculations. These were obtained in part by manually sampling relevant torsions and angles of approach, and also by using an algorithm which allowed a thorough conformational analysis by ranking a vast number of unique conformers generated by the systematic variation of the torsional angles.^[13]

A summary of calculated values, including solvent corrected single point electronic energies, as well as enthalpic and entropic corrections associated with vibrational, rotational, and translational energy at 298 K are provided below.

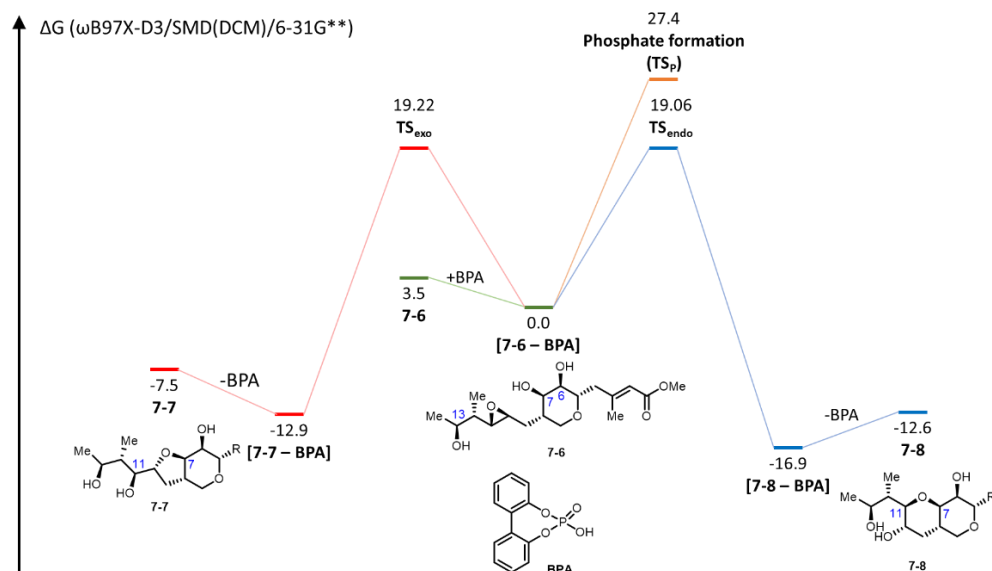


Figure H.1. Energy diagram for the intramolecular ERO of a truncated mupirocin model.

Table H.1. Calculated energy values of relevant geometries for the intramolecular ERO of **7-6**.

	G _{SMD} [kcal/mol] ^a	H _{vrt} [kcal/mol] ^b	S _{vrt} [cal/mol.K] ^b	G _{corr} [kcal/mol] ^c
BPA	-693279.38	124.90	113.94	-693188.43
Truncated mupirocin 7-6	-771958.45	308.30	180.35	-771703.89
7-6 BPA complex	-1465259.56	435.04	238.69	-1464895.66
<i>Exo</i> -product 7-7	-771972.45	309.58	174.45	-771714.85
7-7 BPA complex	-1465274.50	436.72	237.76	-1464908.64
<i>Endo</i> -product 7-8	-771977.47	309.49	174.55	-771720.00
7-8 BPA complex	-1465279.88	435.93	230.46	-1464912.63
Concerted <i>endo</i> cyclization TS _{<i>endo</i>}	-1465239.96	433.97	237.38	-1464876.73
Concerted <i>exo</i> cyclization TS _{<i>exo</i>}	-1465241.98	433.19	227.42	-1464876.57
TS for phosphate formation from 7-6 TS _P	-1465230.80	434.597	242.335	-1464868.42

^a Gas-phase electronic energy (ω B97X-D/SMD/6-31G**). ^b Vibrational, rotational, and translational entropic and enthalpic contributions (B97-D/6-31G**) at 298K. ^c Corrected free energy values at 298K.

Cartesian coordinates for starting geometries, transition states, and products are described below.

26 • BPA

H -5.72428523 -0.48831442 0.98697438
C -6.28439443 -0.36620410 0.06007891
C -7.68832232 -0.36341207 0.07668617
H -8.21878366 -0.49755063 1.01925451
C -8.40824701 -0.17254738 -1.11938955
H -9.49782706 -0.16110110 -1.11076079
C -7.71851142 0.00685161 -2.33069717
H -8.24375641 0.14914534 -3.27295870
C -6.31717770 -0.00517093 -2.33003536
O -5.65460079 0.06060007 -3.58302558
C -5.56356336 -0.18448078 -1.14510677
H -3.92068644 -1.85692296 0.21829797
H -1.42723110 -1.89050223 0.23304154
C -3.36034227 -1.13416699 -0.37500477
C -1.95668993 -1.15639827 -0.37407259
C -4.08202246 -0.20016108 -1.15752358
C -1.23660574 -0.24141830 -1.16732597
H -0.14707102 -0.25756904 -1.17597693
C -3.32891776 0.71387622 -1.93510103
C -1.92724273 0.69920244 -1.95046188
O -3.97830017 1.76149982 -2.63449179
H -1.40039703 1.42919197 -2.56173595
P -4.87333364 1.44496470 -3.96867356
O -5.65780224 2.62401335 -4.40603117
O -3.84439723 0.82979409 -5.06646961
H -3.81574089 1.43633068 -5.82391071

• Truncated mupirocin 7-6
55

C 30.46969421 82.65695276 81.87093348
C 29.31945566 82.36830261 80.98829127
C 28.19469668 83.11508470 80.86386709
C 27.11437851 82.66829940 79.90198393
C 25.75056866 82.47698501 80.57583024
C 24.64738105 82.12760823 79.54463137
C 23.32645641 81.80750548 80.26937525
C 23.54187039 80.73370825 81.36544576
C 23.85756170 79.33977800 80.77047134
C 22.87357544 78.94783680 79.68801136
C 23.20734392 79.04765479 78.25374782
C 22.17549447 79.36792245 77.17434054
C 22.02790869 78.18620134 76.17461356
C 21.14442686 78.53744447 74.97397423
C 27.89468888 84.37860880 81.63211101
C 24.68462653 81.20938530 82.28385867
C 32.61517540 81.85908811 82.49565071
O 31.43082470 81.69002873 81.68851281
O 30.61118571 83.58413098 82.66103862
O 25.88667475 81.41431785 81.53515823
O 22.88044945 83.05809002 80.83931021
O 24.46392775 83.16204946 78.57959183
O 23.16257774 77.75236548 78.92973295
C 22.59806715 80.68617289 76.49103974
O 21.42182629 77.06038279 76.81007174
H 29.41064052 81.46076086 80.38995242
H 26.96742499 83.43296792 79.12174697
H 27.39609710 81.72579715 79.40767635
H 25.44930384 83.40697710 81.09350950
H 24.96641800 81.23246879 78.99282473
H 22.59479175 81.46511518 79.51860358
H 22.61167610 80.66575587 81.95787173
H 24.87571520 79.34024572 80.35730700
H 23.83512000 78.59473685 81.58237906
H 21.81240921 79.05322427 79.95709932
H 24.23568197 79.33952868 78.00318402

H 21.18663417 79.48932851 77.64790948
H 23.04522723 77.93021653 75.80591269
H 20.98347196 77.63668003 74.36582859
H 21.61527963 79.30851310 74.34962310
H 20.16505974 78.90277786 75.31963254
H 27.40314093 85.11387247 80.97452186
H 28.79214143 84.80731414 82.08582055
H 27.17939643 84.14617209 82.43907514
H 24.38304372 82.14604018 82.78582502
H 24.92287912 80.44836367 83.04007014
H 32.36270286 81.82172969 83.56536579
H 33.09267376 82.82658933 82.28360509
H 21.94598440 82.95236423 81.06706051
H 23.93027887 83.83763248 79.03369032
H 21.79437927 81.06711385 75.84829254
H 23.48634881 80.51607046 75.86159940
H 22.85765329 81.46710154 77.22149745
H 21.91824578 76.91472027 77.63566925
H 33.27664289 81.02875646 82.22271214

• 7-6 BPA complex
81

C -5.93507924 -0.41246604 -0.92033089
C -5.22771240 -1.51682474 -1.73059982
C -4.06639864 -0.81569852 -2.46609831
O -3.13022686 -0.22467236 -1.56048179
C -3.68699417 0.70884724 -0.62265652
C -4.92551016 0.14755375 0.11178278
O -4.44483263 -0.85073416 1.01079272
C -3.97646939 2.08703404 -1.29732141
C -4.16461822 3.18640160 -0.27511002
C -2.88986993 3.74526299 0.30313056
C -5.42229060 3.55747290 0.08000265
C -5.78977190 4.54488448 1.11500340
O -5.06641806 5.31370963 1.73572944
O -7.17126857 -0.78486157 -0.31535505
C -6.97560062 -3.30106929 -1.93173900
C -6.15987032 -2.28218661 -2.69745666
C -7.37742244 -4.63989756 -2.40126346
C -8.62634401 -5.31020559 -1.80230227
C -8.25027968 -6.42551788 -0.79155183
O -7.52005219 -5.85655656 0.33337976
O -6.22848464 -4.48171745 -1.50735397
O -7.15475813 4.49222308 1.32009588
C -7.65126232 5.40971201 2.31901037
C -9.45827685 -7.14592718 -0.19766037
C -9.52547463 -5.82082720 -2.94258314
H -6.20883957 0.39634834 -1.61903347
H -4.78175356 -2.23004436 -1.02236522
H -4.47988000 -0.05699340 -3.16391120
H -3.48447473 -1.53989761 -3.05428465
H -2.89362528 0.84295552 0.12523638
H -5.41726002 0.96811876 0.66252031
H -5.19931974 -1.33108965 1.39490158
H -3.10609307 2.30909486 -1.93387240
H -4.85966220 2.00686118 -1.94544785
H -2.36988587 4.33163109 -0.47410013
H -3.06740748 4.38897870 1.16833157
H -2.21192401 2.91977231 0.57215977
H -6.26599094 3.06598328 -0.40781260
H -7.59816518 -2.87882080 -1.14248394
H -6.84113580 -1.58252916 -3.20947459
H -5.56437046 -2.80518405 -3.46360004
H -7.08624306 -4.97250824 -3.40592057
H -9.17723437 -4.55347962 -1.21965026
H -7.58291455 -7.15200644 -1.28824971
H -8.32722054 -4.93887918 1.21578814
H -6.81242033 -5.28941948 -0.07103061

H -8.72422323 5.20175529 2.39736001
H -7.14742140 5.24381699 3.28201790
H -7.47643789 6.44919455 2.00652345
H -9.12282900 -7.85014175 0.57599619
H -10.14303772 -6.41923160 0.26573944
H -10.00351992 -7.70598553 -0.96921461
H -10.49694957 -6.15687665 -2.56014680
H -9.70505572 -5.01976070 -3.67454841
H -9.04794149 -6.66263204 -3.46950130
O -7.36531001 -3.42321469 3.84487199
O -6.65134363 -2.85696903 1.45970694
H -7.99510846 0.31839256 6.40298188
H -7.46640555 2.42897833 5.18574034
H -8.18159028 -5.45946973 5.21893418
H -6.97806411 -1.50527504 0.32270418
C -8.05348718 0.35447229 5.31482471
C -7.75159859 1.53660429 4.62749937
C -8.57655877 -4.51777459 5.59795708
C -8.26424398 -3.33590802 4.91953279
H -9.62325453 -5.37774951 7.28108783
C -9.37160480 -4.45887793 6.75059478
C -8.73215049 -2.07374540 5.35131063
C -8.40830293 -0.82447728 4.62369688
C -7.79743639 1.56837895 3.22377458
H -7.55554010 2.47913568 2.67651266
P -7.85798098 -3.11507228 2.31778549
C -9.84021791 -3.21911311 7.21473859
C -9.52437288 -2.04581799 6.51945653
C -8.45380102 -0.75325851 3.21466361
C -8.15411641 0.41555838 2.50996672
H -10.46079050 -3.16806439 8.10981309
H -9.90440996 -1.08359619 6.86423496
H -8.18030333 0.39840005 1.42219910
O -8.82804314 -4.26292183 1.82993444
O -8.89810177 -1.87387466 2.47916123

• **Exo-product 7-7**

55

C -4.77009321 -0.96377823 -0.40117379
C -3.50004789 -1.80177314 -0.46332413
C -2.65499626 -1.29277927 -1.63082172
O -2.35868009 0.10263204 -1.42906488
C -3.49052184 0.96790935 -1.23841644
C -4.45515644 0.49582478 -0.11117274
O -3.79792143 0.66833625 1.14214846
C -4.22935774 1.19971294 -2.59114496
C -5.42888388 2.11470139 -2.47821251
C -5.13621765 3.50870655 -1.98438081
C -6.65731810 1.62469841 -2.78358834
C -7.94568074 2.34894716 -2.70672735
O -8.15205016 3.50257136 -2.35009589
O -5.54242625 -1.60664763 0.62494515
C -5.41249647 -3.04388936 0.37065702
C -4.08881232 -3.22000817 -0.45226648
C -6.64210875 -3.58099825 -0.39570170
C -8.02686961 -3.42559645 0.29144146
C -8.66016059 -1.99748514 0.27701728
O -8.16549538 -1.13934124 1.30254459
O -6.38969076 -4.96198403 -0.71886635
O -8.95292380 1.50540816 -3.11059533
C -10.27807901 2.07917141 -3.06860223
C -8.58581370 -1.31342467 -1.09862817
C -8.04069424 -3.98937275 1.72323969
H -5.31173593 -1.02288477 -1.36457208
H -2.94474147 -1.60684634 0.46538374
H -3.18674375 -1.46251074 -2.58776338
H -1.67587854 -1.78663318 -1.69138523
H -3.04829817 1.91483700 -0.90099103

H -5.37784444 1.10133427 -0.15802835
H -4.32838171 0.17500612 1.78868715
H -3.48446857 1.63970472 -3.27366977
H -4.53476285 0.23233561 -3.01383374
H -4.27474416 3.92381560 -2.53245968
H -6.00235844 4.16852106 -2.07815861
H -4.83947543 3.46819156 -0.92280653
H -6.73522401 0.59161404 -3.12544975
H -5.35138227 -3.52386770 1.35889048
H -4.32793514 -3.56294287 -1.47013632
H -3.42097262 -3.96219405 0.00304146
H -6.67278587 -3.07738874 -1.37282490
H -8.69016501 -4.04370842 -0.33712471
H -9.72301146 -2.15130637 0.52781223
H -7.20220209 -1.08952698 1.14036238
H -6.42808342 -5.45513579 0.11623654
H -10.95160639 1.27986188 -3.39743970
H -10.52384981 2.40405800 -2.04771982
H -10.34219268 2.94752059 -3.73980512
H -9.18764518 -0.39648118 -1.09500702
H -7.55120017 -1.02252898 -1.33114460
H -8.94846391 -1.97307409 -1.90349558
H -9.07108242 -4.02544842 2.10457662
H -7.63735468 -5.01419639 1.77805579
H -7.46451310 -3.33966692 2.39435971

• **7-7 BPA complex**

81

C -4.90139140 -1.10555506 -0.61101869
C -3.87262091 -1.99993154 -1.28578414
C -2.90647637 -1.09357226 -2.05380040
O -2.31800410 -0.12581900 -1.15977133
C -3.23366705 0.66954471 -0.39321320
C -4.24863851 -0.19291236 0.42092031
O -3.51039606 -0.89669991 1.41355239
C -3.92647231 1.73910723 -1.31032164
C -5.05740550 2.46193787 -0.61612044
C -4.64376776 3.40736755 0.48082037
C -6.33505135 2.13475182 -0.94140806
C -7.56195786 2.55712526 -0.23528159
O -7.70086866 3.46810544 0.57484924
O -5.88504264 -2.02650685 -0.09426216
C -6.05528939 -3.07040113 -1.14025541
C -4.78277767 -2.98795850 -2.03733672
C -7.36198398 -2.78640894 -1.90883342
C -8.62854712 -2.74396231 -0.99617201
C -9.30387967 -4.13722980 -0.87737203
O -8.33176833 -5.19670133 -0.74520279
O -7.46619348 -3.71651779 -2.98848221
O -8.58558786 1.71487753 -0.59102735
C -9.83559534 1.92233851 0.11000713
C -10.33193588 -4.20701217 0.25825226
C -9.62554755 -1.70054445 -1.53999403
H -5.40540110 -0.47956149 -1.36573753
H -3.31436420 -2.50929200 -0.48723351
H -3.44428871 -0.59622142 -2.88520141
H -2.05613589 -1.64428959 -2.47616984
H -2.59895353 1.17972910 0.34301963
H -4.99587134 0.47057144 0.88307890
H -4.14230449 -1.26128721 2.05353350
H -3.13960943 2.44337126 -1.62070412
H -4.29975601 1.24243951 -2.21592449
H -3.99579763 4.19385434 0.05921052
H -5.50007058 3.87170852 0.97669353
H -4.02946567 2.86778823 1.22119490
H -6.49715387 1.40776058 -1.73864679
H -6.13915140 -4.02051901 -0.60092035
H -5.06038580 -2.59999837 -3.02890006

H -4.32289781 -3.97360888 -2.17811721
H -7.23922131 -1.79759469 -2.38393598
H -8.31171483 -2.43061643 0.00859549
H -9.79923602 -4.34455692 -1.83948048
H -7.96510827 -5.14120983 0.16270286
H -7.57761777 -4.58006695 -2.54353063
H -10.55128236 1.24988556 -0.37471243
H -9.71462108 1.65942822 1.17029406
H -10.15416804 2.97002318 0.02761396
H -10.76033680 -5.21809519 0.30110459
H -9.84771335 -3.98800372 1.21994294
H -11.14936240 -3.48732299 0.10644813
H -10.53871285 -1.65812868 -0.92938235
H -9.17049074 -0.69932659 -1.54444768
H -9.91202599 -1.95684202 -2.57225520
O -6.63402354 -3.75372839 4.23416413
O -5.47874006 -3.00671531 2.20011961
H -8.13422273 0.08655804 6.25658716
H -7.67270268 2.15854742 4.95083093
H -7.49583500 -5.74988218 5.63212553
H -5.55640860 -2.65374948 1.23466068
C -7.99162134 0.03468339 5.17672796
C -7.72594659 1.19581142 4.44204331
C -8.04388560 -4.83211145 5.83996718
C -7.72504756 -3.68095236 5.11394635
H -9.29914835 -5.66811254 7.38618960
C -9.04480895 -4.77262599 6.81878533
C -8.38757083 -2.45007695 5.32524933
C -8.06438048 -1.22869013 4.55037185
C -7.52294779 1.12435212 3.05354043
H -7.33256974 2.02935504 2.47937861
P -6.87363102 -3.64438428 2.62727204
C -9.71524051 -3.56292325 7.06161138
C -9.38915011 -2.42159326 6.32008842
C -7.85672545 -1.26708962 3.15467316
C -7.58716691 -0.11770765 2.40374893
H -10.49915721 -3.51160629 7.81757107
H -9.92402725 -1.48592009 6.48582712
H -7.45493151 -0.21223383 1.32743749
O -7.32526887 -4.87547170 1.91882646
O -8.01821529 -2.47797317 2.46653894

• **Endo-product 7-8**

55

C -5.68748840 -0.49279435 -0.10390782
C -4.73698579 0.60444261 -0.60538368
C -3.41591345 0.50743580 0.16989836
O -2.83627319 -0.80366748 0.03517658
C -3.67763483 -1.85078928 0.56690883
C -5.01887479 -1.87694597 -0.21134149
O -4.78720712 -2.24440014 -1.57111266
C -3.84519886 -1.77903118 2.10594050
C -2.52625527 -1.56233954 2.81848029
C -1.44035284 -2.55386645 2.48990659
C -2.40412199 -0.50513298 3.65902604
C -1.19967152 -0.12678244 4.43171445
O -0.10300732 -0.67275776 4.45088551
O -6.90079648 -0.52481667 -0.84778609
C -7.64984749 0.71743505 -0.86704020
C -6.75573081 1.90754837 -1.29951468
C -5.45260528 1.95196763 -0.47784657
C -8.85221537 0.42222254 -1.79572652
C -8.46404923 0.42230635 -3.30121535
O -7.19963146 -0.20468375 -3.58045229
O -7.53240435 3.09858575 -1.10973749
O -1.48213434 0.99527284 5.17358583
C -0.38413878 1.48245549 5.97529307
C -9.54646735 -0.24269236 -4.16439048

C -10.03645811 1.36879271 -1.52255094
H -5.92354230 -0.28292142 0.95912342
H -4.53637580 0.40750715 -1.67082443
H -3.58109788 0.74887498 1.23500795
H -2.66772858 1.20615954 -0.22871656
H -3.13561509 -2.77264244 0.31646040
H -5.68864665 -2.64299282 0.20617752
H -4.01595081 -1.72495156 -1.85476415
H -4.56354133 -0.99943587 2.39400063
H -4.27772660 -2.74675464 2.41511501
H -1.07085856 -2.34391741 1.47309204
H -0.60144785 -2.49254341 3.18782968
H -1.85415973 -3.57560111 2.47730341
H -3.26502404 0.15062809 3.80430265
H -8.01145771 0.93058464 0.15837291
H -6.49119196 1.76225335 -2.35924911
H -4.81599152 2.77980390 -0.83466244
H -5.70187226 2.15069586 0.57868311
H -9.16376074 -0.60362536 -1.53332918
H -8.36470105 1.47924715 -3.61192070
H -6.93469276 -0.71840432 -2.79479122
H -7.03086918 3.81985374 -1.51774151
H -0.76763730 2.37380830 6.48469552
H -0.06984187 0.72066592 6.70319639
O 4.75946662 1.73467834 5.33830168
H -9.22036333 -0.25299983 -5.21361799
H -9.69604394 -1.28395810 -3.83827251
H -10.50634777 0.29112730 -4.09990013
H -10.93690715 1.02458086 -2.04949002
H -10.26255097 1.39934857 -0.44609381
H -9.79833746 2.38996580 -1.84559835

• **7-8 BPA complex**

81

C -5.84381390 -0.21018497 -0.38739799
C -5.06182232 0.99675055 -0.92226540
C -3.62233825 0.92700879 -0.40332480
O -3.00161135 -0.31615545 -0.79194826
C -3.67327829 -1.47517619 -0.25433710
C -5.13246090 -1.51892360 -0.77767843
O -5.14770757 -1.70724550 -2.19467794
C -3.56003061 -1.58310221 1.28848673
C -2.14870014 -1.31523250 1.77176998
C -1.07487197 -2.17219341 1.15457838
C -1.94950440 -0.31366728 2.66420576
C -0.65075135 0.12360977 3.22263379
O 0.46720768 -0.31745742 2.98468980
O -7.17896973 -0.25676545 -0.90078886
C -7.97532458 0.94536780 -0.67126073
C -7.21068858 2.18169560 -1.21459409
C -5.82004643 2.27954198 -0.57089884
C -9.32485970 0.62682736 -1.35204944
C -9.25462227 0.65398890 -2.90127805
O -8.03177046 0.02816013 -3.43191535
O -7.94458990 3.39171789 -1.04623848
O -0.86737718 1.16308729 4.09546393
C 0.32831584 1.70142878 4.70048319
C -10.44183159 -0.05820618 -3.55039915
C -10.44968751 1.55089033 -0.84619935
H -5.90004476 -0.12949370 0.71567748
H -5.03129457 0.91561342 -2.02131839
H -3.59727900 1.04219997 0.69472850
H -3.00606757 1.71920621 -0.84844820
H -3.13699852 -2.32163686 -0.70410566
H -5.66746868 -2.37875585 -0.34815275
H -4.46745927 -1.10916727 -2.54841988
H -4.26415882 -0.90431595 1.78804427
H -3.85893322 -2.61272545 1.55317168

H -0.92273094 -1.83963099 0.11475898
H -0.12548404 -2.09354647 1.69048943
H -1.40825433 -3.22198008 1.11258915
H -2.81572704 0.24667278 3.02059485
H -8.12756466 1.06728203 0.41794877
H -7.04796749 1.98097693 -2.27662220
H -5.30361975 3.16042649 -0.97134835
H -5.91361653 2.39520909 0.52255750
H -9.55927355 -0.40808702 -1.04827701
H -9.22257953 1.70117611 -3.23199330
H -7.50839354 -0.33766877 -2.67841064
H -8.18609553 3.67597880 -1.95169074
H -0.01686571 2.48330132 5.38649208
H 0.87442259 0.91702697 5.24334990
H 0.99206066 2.12274846 3.93151636
H -10.32631972 -0.05465010 -4.64278541
H -10.49291207 -1.10163403 -3.20424652
H -11.38468522 0.44716283 -3.29879574
H -11.42407793 1.23283522 -1.24066944
H -10.49909851 1.51727127 0.25177036
H -10.25867389 2.58881607 -1.14284792
O -5.55129267 3.60086762 -3.57022194
O -6.60822885 1.66036553 -4.75215962
H -2.19988844 5.52754494 -5.92991549
H -1.68416091 4.28866707 -8.03174227
H -6.16145978 5.15297189 -1.55013434
H -7.21774587 0.99927366 -4.21742639
C -2.96263702 4.90956487 -6.40490583
C -2.67364571 4.20744063 -7.58079961
C -5.56115411 5.65541113 -2.30833037
C -5.22805690 4.96349473 -3.47697463
H -5.38513566 7.53452142 -1.25774542
C -5.13083926 6.98224445 -2.16298892
C -4.51600500 5.56302066 -4.53792561
C -4.22721289 4.81764149 -5.78472547
C -3.65228248 3.38737203 -8.16569069
H -3.43211606 2.83080017 -9.07716935
P -6.84641785 3.20165856 -4.50574101
C -4.38469214 7.59712956 -3.18221962
C -4.09042393 6.89612488 -4.35864076
C -5.19542160 3.99424198 -6.40655958
C -4.91945050 3.28128276 -7.57698052
H -4.05098348 8.62917118 -3.06962990
H -3.54667218 7.38238629 -5.16933208
H -5.70376308 2.66230330 -8.00988132
O -8.15953275 3.65109041 -3.94716033
O -6.51100427 3.94877236 -5.91837538

• **TS_{endo}**

81

C -5.784503 -0.542422 -0.295462
C -5.002851 0.678860 -0.829826
C -3.567008 0.637611 -0.278634
O -2.904142 -0.593512 -0.606897
C -3.563179 -1.749069 -0.043414
C -4.997929 -1.837668 -0.613709
O -4.960208 -2.062090 -2.023796
C -3.505847 -1.787330 1.504802
C -2.123369 -1.458402 2.032421
C -1.003567 -2.314945 1.501786
C -1.985332 -0.414765 2.887847
C -0.721487 0.082220 3.476908
O 0.416117 -0.337827 3.303093
O -7.123489 -0.642835 -0.784797
C -8.178903 1.418189 -0.809187
C -6.974827 2.080794 -1.309136
C -5.687766 2.024593 -0.516354
C -9.339776 0.883672 -1.596965

C -9.069513 0.602821 -3.102538
O -7.806822 -0.063680 -3.306086
O -7.835099 3.235216 -1.161759
O -1.000997 1.153430 4.290287
C 0.152871 1.753151 4.918797
C -10.171267 -0.275572 -3.706113
C -10.569882 1.807122 -1.402956
H -5.885562 -0.437413 0.796287
H -4.937585 0.588953 -1.927146
H -3.572452 0.792638 0.815127
H -2.966182 1.435804 -0.733140
H -2.989847 -2.597391 -0.439289
H -5.531172 -2.695367 -0.178028
H -4.263733 -1.479855 -2.368137
H -4.248191 -1.108596 1.946201
H -3.787379 -2.812657 1.802331
H -0.804740 -2.020304 0.458190
H -0.083915 -2.194446 2.079811
H -1.312499 -3.372894 1.486000
H -2.878187 0.138731 3.184997
H -8.315846 1.461525 0.273950
H -6.767042 1.868042 -2.355375
H -5.045809 2.849753 -0.860400
H -5.866275 2.147494 0.564026
H -9.556682 -0.078805 -1.101922
H -9.047117 1.572756 -3.621855
H -7.132851 -0.624579 -1.784608
H -7.989199 3.559003 -2.212665
H -0.241855 2.565650 5.539320
H 0.686714 1.014302 5.533315
H 0.845602 2.143397 4.159222
H -9.935343 -0.470013 -4.760473
H -10.217060 -1.239776 -3.176750
H -11.156695 0.207836 -3.650257
H -11.472145 1.323166 -1.798486
H -10.733709 2.028816 -0.338605
H -10.407724 2.754830 -1.933518
O -5.412572 3.808923 -3.584005
O -6.664525 1.902361 -4.708239
H -2.523442 5.753224 -6.514673
H -2.513186 4.664112 -8.757872
H -5.575234 5.325407 -1.447694
H -7.250214 0.592302 -3.808784
C -3.396915 5.199329 -6.859847
C -3.391707 4.582070 -8.117087
C -5.095603 5.813062 -2.294282
C -5.035476 5.150240 -3.526809
H -4.633642 7.631683 -1.224084
C -4.585129 7.113534 -2.182603
C -4.516029 5.782053 -4.681732
C -4.512208 5.107581 -6.000389
C -4.511919 3.851844 -8.543036
H -4.511873 3.360585 -9.516548
P -6.816367 3.367591 -4.368971
C -4.024009 7.746689 -3.302589
C -4.004377 7.088245 -4.537823
C -5.630548 4.373958 -6.461709
C -5.635081 3.746249 -7.712711
H -3.625689 8.758446 -3.219063
H -3.609651 7.589836 -5.422182
H -6.521053 3.189468 -8.013229
O -8.016076 3.851214 -3.534384
O -6.801678 4.337221 -5.699353

• **TS_{exo}**

81

C -5.019010 -0.843776 -0.623416
C -4.116971 -1.892251 -1.279148

C -3.096899 -1.112529 -2.139860
O -2.343612 -0.172146 -1.363747
C -3.116818 0.749354 -0.573138
C -4.150498 0.019498 0.312793
O -3.433036 -0.746458 1.268482
C -3.770325 1.854537 -1.483625
C -4.830563 2.644465 -0.746465
C -4.319019 3.551195 0.341645
C -6.138447 2.393287 -1.016272
C -7.307594 2.827646 -0.223155
O -7.372277 3.706745 0.629581
O -6.125181 -1.434509 0.038416
C -6.178422 -3.356192 -1.323540
C -4.940916 -2.932825 -2.080910
C -7.527285 -3.063560 -1.795138
C -8.733014 -2.981969 -0.836658
C -9.335159 -4.385712 -0.557789
O -8.249803 -5.364968 -0.400386
O -7.123442 -4.401096 -2.304863
O -8.379414 2.029982 -0.552450
C -9.571909 2.249040 0.238190
C -10.264271 -4.446522 0.650702
C -9.799470 -2.019355 -1.388444
H -5.455421 -0.198485 -1.399404
H -3.571175 -2.400960 -0.471049
H -3.645679 -0.602556 -2.959093
H -2.349003 -1.778115 -2.593359
H -2.381781 1.220990 0.091980
H -4.801569 0.758665 0.806793
H -4.070162 -1.217824 1.838427
H -2.956825 2.509038 -1.831588
H -4.209539 1.371112 -2.366645
H -3.641884 4.302065 -0.098829
H -5.127509 4.057489 0.875643
H -3.712042 2.966432 1.053030
H -6.373941 1.693050 -1.818850
H -6.070437 -3.902504 -0.386274
H -5.241321 -2.526299 -3.060003
H -4.317114 -3.820763 -2.258847
H -7.560658 -2.336215 -2.614492
H -8.350138 -2.574767 0.106048
H -9.866643 -4.729375 -1.459070
H -7.757457 -5.116153 0.474571
H -7.553927 -5.048135 -1.452148
H -10.342604 1.618578 -0.220132
H -9.393002 1.944125 1.279004
H -9.863764 3.307926 0.213997
H -10.605905 -5.482017 0.786829
H -9.762984 -4.113715 1.568896
H -11.146741 -3.811458 0.485594
H -10.641969 -1.938275 -0.688888
H -9.370042 -1.014762 -1.520789
H -10.185221 -2.368527 -2.359685
O -6.665569 -3.790088 4.138258
O -5.331958 -2.734707 2.232445
H -8.405749 -0.113640 6.317585
H -7.833805 2.062186 5.242828
H -7.661509 -5.881358 5.241521
H -5.781007 -1.899040 0.854683
C -8.169861 -0.072294 5.253684
C -7.846765 1.148622 4.647559
C -8.242319 -4.986729 5.462143
C -7.844358 -3.776759 4.877394
H -9.653599 -5.965673 6.771872
C -9.348585 -5.020637 6.320327
C -8.547444 -2.570833 5.131543
C -8.167486 -1.277176 4.516776
C -7.521896 1.193094 3.281086
H -7.239842 2.131366 2.803521
P -6.643798 -3.441792 2.525187

C -10.056550 -3.839237 6.595699
C -9.655693 -2.636206 6.004179
C -7.844418 -1.200125 3.145700
C -7.529697 0.012797 2.521841
H -10.921934 -3.856731 7.258616
H -10.213167 -1.717831 6.194048
H -7.300772 0.009966 1.458780
O -7.050026 -4.651782 1.704416
O -7.912543 -2.365463 2.377601

• TS_P

81

C 30.511550 84.528693 81.481703
C 29.332561 84.094506 80.709292
C 28.045190 84.261972 81.099361
C 26.927373 83.725569 80.235638
C 26.152067 82.601070 80.931492
C 24.908532 82.169333 80.115618
C 24.230714 80.940086 80.747394
C 25.239782 79.816912 81.082469
C 25.730965 79.056998 79.812583
C 24.607761 78.366114 79.117644
C 24.015277 78.881655 77.871868
C 22.552401 78.627818 77.451824
C 22.395464 77.252261 76.741412
C 20.941810 76.795692 76.649166
C 27.622381 84.916375 82.396078
C 26.432236 80.429991 81.835044
C 32.883159 84.594887 81.452111
O 31.658686 84.223248 80.785472
O 30.528817 85.074404 82.580393
O 27.045820 81.483182 81.086207
O 23.595619 81.385680 81.960176
O 23.973287 83.233349 79.957971
O 25.051280 77.948362 77.362608
C 22.054115 79.774076 76.551099
O 23.199082 76.240576 77.413349
H 29.539443 83.595889 79.761768
H 26.192740 84.519387 80.025258
H 27.312053 83.344338 79.276874
H 25.806240 82.940589 81.926702
H 25.257409 81.894431 79.105858
H 23.461310 80.574513 80.057157
H 24.738737 79.092485 81.737731
H 26.224606 79.766759 79.134480
H 26.470295 78.308780 80.132569
H 24.361573 77.353720 79.419698
H 24.352258 79.902091 77.652990
H 21.967123 78.609661 78.379577
H 22.843110 77.333129 75.738131
H 20.894188 75.809849 76.168372
H 20.345319 77.505995 76.059317
H 20.519241 76.718232 77.660485
H 26.550867 85.162910 82.376887
H 28.214574 85.815070 82.603457
H 27.803821 84.230679 83.238915
H 26.056340 80.816806 82.798951
H 27.216867 79.682168 82.022253
H 32.975980 84.067255 82.412684
H 32.906515 85.677869 81.646017
H 22.916490 80.715607 82.150721
H 23.459162 83.228754 80.786077
H 20.990448 79.645720 76.309014
H 22.620566 79.806149 75.606562
H 22.169582 80.743641 77.057272
H 24.502575 77.062782 77.343471
H 33.689740 84.303838 80.768133
O 21.034524 77.102247 81.998062

O 21.996838 76.171516 79.799401
H 22.226819 75.285730 85.986504
H 23.483559 73.142931 85.757014
H 20.009615 79.455780 82.454679
H 22.794165 76.131798 78.329624
C 22.777567 75.065444 85.069745
C 23.477407 73.860473 84.937042
C 20.609006 79.089029 83.287677
C 21.237202 77.843531 83.165075
H 20.267611 80.789406 84.579623
C 20.754839 79.819016 84.475949
C 22.040214 77.306069 84.196584
C 22.748162 76.016162 84.027507

C 24.164216 73.578747 83.745670
H 24.714816 72.642819 83.638620
P 22.272441 77.165870 80.906830
C 21.524097 79.296738 85.528785
C 22.156977 78.055682 85.386629
C 23.455812 75.711562 82.838174
C 24.152803 74.504631 82.694843
H 21.641103 79.862344 86.453755
H 22.782748 77.662186 86.189232
H 24.686792 74.319222 81.763305
O 22.615171 78.611488 80.575984
O 23.581502 76.660231 81.830213

References

- [1] Y. Shao, Z. Gan, E. Epifanovsky, A. T. B. Gilbert, M. Wormit, J. Kussmann, A. W. Lange, A. Behn, J. Deng, X. Feng, et al., *Mol. Phys.* **2015**, *113*, 184–215.
- [2] A. D. Becke, *J. Chem. Phys.* **1997**, *107*, 8554–8560.
- [3] S. Grimme, *J. Comput. Chem.* **2006**, *27*, 1787–1799.
- [4] P. C. Hariharan, J. A. Pople, *Theor. Chim. Acta* **1973**, *28*, 213–222.
- [5] M. M. Francl, W. J. Pietro, W. J. Hehre, J. S. Binkley, M. S. Gordon, D. J. DeFrees, J. A. Pople, *J. Chem. Phys.* **1982**, *77*, 3654–3665.
- [6] Discovery Studio 4.1 Visualizer: Accelrys Software Inc. San Diego, USA, **2015**.
- [7] P. M. Zimmerman, *J. Chem. Phys.* **2013**, *138*, 184102.
- [8] P. M. Zimmerman, *J. Comput. Chem.* **2013**, *34*, 1385–1392.
- [9] P. M. Zimmerman, *J. Comput. Chem.* **2015**, *36*, 601–611.
- [10] P. M. Zimmerman, *J. Chem. Theory Comput.* **2013**, *9*, 3043–3050.
- [11] A. V. Marenich, C. J. Cramer, D. G. Truhlar, *J. Phys. Chem. B* **2009**, *113*, 6378–6396.
- [12] J. Da Chai, M. Head-Gordon, *J. Chem. Phys.* **2008**, *128*, 084106.
- [13] N. M. O’Boyle, M. Banck, C. A. James, C. Morley, T. Vandermeersch, G. R. Hutchison, *J. Cheminform.* **2011**, *3*, 33.